OFFICE OF NAVAL RESEARCH

FINAL REPORT

FOR

CONTRACT N00014-91-J-1656
R&T CODE 413h007---05

ELECTRICAL MICROENGINEERING OF REDOX ENZYMES

ADAM HELLER
Department of Chemical Engineering
The University of Texas at Austin
Austin, Texas 78712-1062

MARCH 31, 1994

Results of the work on Contract N00014-91-J-1656, R&T Code 413h007---05, are reported in the enclosed 20 papers. These include summaries in three invited articles "Electrical Wiring of Redox Enzymes" (Accounts of Chemical Research, 1990, *23*, 128-134), "Electrical Connection of Enzyme Redox Centers to Electrodes", (J.Phys.Chem. 1992, *96*, 3579-3587), and "Electron Conducting Adducts of Water Soluble Redox Polyelectrolytes and Enzymes, Katakis, I., Vreeke, M., Ye, L., Aoki, A. and Heller, A. ("Advances in Molecular & Cell Biology", Bengt Danielsson (Ed.) JAI Press Inc., (1993)).

The key results were the following:

- Enzymes made of electrically insulating proteins were made electron conducting through incorporation of electron relaying redox centers. The redox centers were covalently bound to amino acids of proteins, particularly to lysine amines,[1,2] or to peripheral oligosaccharides of glycoproteins, of enzymes. When peripherally bound, the redox functions were attached to the ends of flexible spacer chains, that were long enough to allow deep penetration of the redox functions into the protein shell.[3]

- Reaction centers of enzymes were electrically "wired", i.e. electrically connected, through redox macromolecules to electrodes.[4-9] Wiring was effective when the redox macromolecules were water soluble and formed electrostatic adducts with the enzymes.[4,10] The adducts of enzymes and polymers were crosslinked with water soluble crosslinkers, to form electron conducting hydrogels. Electrons from reaction

centers of enzymes were routed via polymer skeletons of these hydrogels to electrodes. Because water soluble substrates and products of the enzyme permeated rapidly through the hydrogel, the turnover of the gel-bound enzymes was not limited by diffusion of substrates or products into or from the gel. When the electron transfer from the enzyme to the redox polymer was sufficiently rapid and when the hydrogels' electron diffusion coefficients approached $\sim 10^{-8} cm^2 sec^{-1}$, substrates were electrooxidized and electroreduced at high rates.[6,11] The current densities on semi-infinite planar electrodes reached $2 mA/cm^2$. For 7μm carbon fiber microelectrodes, where the electron diffusion through the polymer was radial, the current densities reached $10 mA/cm^2$.[12,13]

- The wired enzyme electrodes efficiently transduced fluxes of biochemicals into electrical currents. Based on such transduction, biosensors for a wide range of biochemicals and hydrogen peroxide were built. FAD, FMN,[14,15] heme[16] and PQQ[10] enzymes were directly electrically connected to electrodes. The turnover of NADH and NADPH dependent enzymes was observed through translation of NADH and NADPH fluxes to hydrogen peroxide through their homogeneous, n-methylphenazonium, catalyzed reaction with dissolved molecular oxygen. The hydrogen peroxide formed was detected through its electrocatalytic reduction to water with wired horseradish peroxidase.[16]

- The current densities of the hydrogel-wired enzyme electrodes depended on the electron diffusion coefficients in the hydrogels. High electron diffusion coefficients were observed when chain segments of the crosslinked redox polymer in the gel were fluid, i.e. mobile. Fluidity of the chain segments led to electron transferring collisions between the segments. Such collisions shorted the otherwise tortuous route of electrons through backbones of folded polymer chains. The electron diffusion coefficients depended on the charge of the redox polymers, on the ionic strength of the solutions and on the degree of crosslinking of the polymers. High charge density of the redox polymer and low ionic strength led to stretched redox polymer segments that, when colliding, effectively transferred electrons. Screening of the charge by counterions caused random folding of the stretched polymer segments and reduced the frequency of electron transferring collisions between chain segments of neighboring polymer molecules. Excessive crosslinking immobilized the segments and reduced the electron diffusion coefficients.[17]

- Sequential reactions of multiple enzymes were coupled within individual hydrogel layers and also between different layers of hydrogels. Thus, using hydrogels made with both an enzyme hydrolyzing a substrate to an electrooxidizable product, and the product electrooxidation catalyzing enzyme, the turnover of hydrolytic enzymes was transduced to an electrical current.[18] Hydrolytic reactions were also carried out in overcoatings of wired enzyme layers in bilayer gels. In reaction sequences involving three sequential enzyme-catalyzed reactions in gels,

fluxes of biochemicals were still efficiently transduced into electrical currents, proving that in gels the coupling of reactions can be efficient.[18]

- The selectivity of the wired enzyme electrodes was enhanced through use of redox polymers that were tailored to have redox potentials within the narrow window where oxygen was not electroreduced and common interferants were not electrooxidized.[19] Electrooxidizable interferant-produced currents were eliminated through enzymatic oxidation of the ensemble of common interferants by hydrogen peroxide in a non-wired peroxidase containing layer. Hydrogen peroxide was produced within the peroxidase containing layer through enzymatic reaction of glucose (or lactate) with dissolved oxygen.[20]

Industrial Activity:

The wired enzyme transducers proved to be of industrial interest. A venture has acquired the wired enzyme technology from the University of Texas, is developing enzyme microelectrodes and is marketing the technology. A one year option has been acquired by a major producer of biosensors. Three additional companies had wired enzyme biosensor projects in the reporting period.

Patents:

A patent application entitled "Biosensors Based on Chemically Modified Enzymes" has been filed.

1. Electrical Wiring of Redox Enzymes, Heller, A., Accounts of Chemical Research, *23*, 128 (1990).

2. Electrical Communication Between Graphite Electrodes and Glucose Oxidase/Redox Polymer Complexes, Pishko, M.V., Katakis, I., Lindquist, S.-E., Heller, A., Degani, Y., Mol.Cryst.Liq.Cryst., *190*, 221 (1990).

3. Electron Transfer Between Glucose Oxidase and Electrodes via Redox Mediators Bound with Flexible Chains to the Enzyme Surface, Schuhmann, W.; Ohara, T.; Heller, A.; Schmidt, H.-L., J.Am.Chem.Soc., *113*, 1394-1397 (1991).

4. Electrical Connection of Enzyme Redox Centers to Electrodes, Heller, A. Feature Article, J.Phys.Chem., *96*, 3579-3587 (1992).

5. Cross-Linked Redox Gels Containing Glucose Oxidase for Amperometric Biosensor Applications, Gregg, B. A., and Heller, A., Anal.Chem. *62*, 258 (1990).

6. Redox Polymer Films Containing Enzymes. 1. A Redox-Conducting Epoxy Cement: Synthesis, Characterization, and Electrocatalytic Oxidation of Hydroquinone, Gregg, B. A. and Heller A., J.Phys.Chem., *95*, 15, 5970-5975 (1991).

7. Redox Polymer Films Containing Enzymes. 2. Glucose Oxidase Containing Enzyme Electrodes, Gregg. B. A. and Heller, A., J.Phys.Chem. *95*, 15, 5976-5980 (1991).

8. Amperometric Biosensors based on 3-Dimensional Hydrogel-Forming Epoxy Networks, Heller, A., Maidan, R., Wang, D. L., Sensors and Actuators, *13*, 180-183 (1993).

9. Direct Electrical Communication between Graphite Electrodes and Surface Adsorbed Glucose Oxidase/Redox Polymer Complexes, Pishko, M.V., Katakis, I., Lindquist, S.-E., Ye, L., Gregg, B. A., and Heller, A., Angewandte Chemie Intl.Ed., *29*, 1,82 (1990).

10. Electron Conducting Adducts of Water Soluble Redox Polyelectrolytes and Enzymes, Katakis, I., Vreeke, M., Ye, L., Aoki, A. and Heller, A. "Advances in Molecular & Cell Biology", Bengt Danielsson (Ed.) JAI Press Inc., (1993).

11. High Current Density "Wired" Quinoprotein Glucose Dehydrogenase, Ye, L., Hammerle, M., Olsthoorn, A. J. J., Schuhmann, W., Schmidt-H.-L., Duine, J. A., Heller, A., Anal.Chem. *65*, 238-241 (1993).

12. Amperometric Glucose Microelectrodes Prepared through Immobilization of Glucose Oxidase in Redox Hydrogels, Pishko, M. V.; Michael, A.C.; Heller, A. Anal.Chem. *63*, 2268-2272 (1991).

13. SECM 24. Enzyme Microelectrodes for the Measurement of Hydrogen Peroxide at Surfaces, Horrocks, B. R., Schmidtke, D., Heller, A., Bard, A. J. Anal. Chem. *65*. 3605-14 (1993).

14. L-α-Glycerophosphate and L-Lactate Electrodes Based on the Electrochemical "Wiring" of Oxidases, Katakis, I., and Heller, A., Anal.Chem., *64*, 1008-1013 (1992).

15. Miniaturized Flexible Amperometric Lactate Probe, Wang, D. L., Heller, A., Anal.Chem. *65*, 1069-1073 (1993).

16 Hydrogen Peroxide and ß-Nicotinamide Adenine Dinucleotide Sensing Amperometric Electrodes Based on Electrical Connection of Horseradish Peroxidase Redox Centers to Electrodes through a Three-Dimensional Electron Relaying Polymer Network, Vreeke, M; Maidan, R.; Heller, A. Anal.Chem. *64*, 3084-3090 (1992).

17. Electron Diffusion Coefficients in Hydrogels formed of Crosslinked Redox Polymers. Aoki, A., Heller, A., J.Phys.Chem. *97*, 11014-11019 (1993).

18. Bienzyme Sensors based on "Electrically Wired" Peroxidase, Ohara, T. J., Vreeke, M. S., Battaglini, F., Heller, A., Electroanalysis, W. Simon Memorial Issue, *5*, 825-831 (1993).

19. Glucose Electrodes based on Crosslinked $[Os(bpy)_2Cl]^{+/2+}$ Complexed Poly(1-Vinylimidazole) Films, Ohara, T. J., Rajagopalan, R., Heller, A. Anal.Chem. *65*, 3512-3517 (1993).

20. Elimination of Electrooxidizable Interferant-Produced Currents in Amperometric Biosensors, Maidan, R.; Heller, A. Anal.Chem. *64*, 2889-2896 (1992).

ELECTRON CONDUCTING ADDUCTS OF WATER-SOLUBLE REDOX POLYELECTROLYTES AND ENZYMES

Ioanis Katakis, Mark Vreeke, Ling Ye, Atsushi Aoki and Adam Heller

Department of Chemical Engineering, The University of Texas at Austin

Austin, TX 78712

Submitted for Publication in BIOCHEMICAL TECHNOLOGY, Advances in Molecular and Cell Biology Series, Proceedings of Mosbach Symposium, JAI Press, Inc., 1993,

ABSTRACT

Biochemical fluxes were transduced to electrical currents through catalytic centers of oxidoreductases, that were electrically connected to electrodes with crosslinked hydrogel forming redox polymers. The enzymes were covalently bound to the hydrogels through which the electrons diffuse. The electron diffusion coefficients, reaching 10^{-8} cm^2sec^{-1} in the redox polymer gels, were high enough to allow efficient collection of the electrons transferred during the electrooxidation or electroreduction of substrates. The adequate electron diffusion through the polymer skeleton of the hydrogel and the rapid diffusion of water-soluble substrates and products in the gels led to high current density enzyme electrodes. These included electrodes with electrically connected flavoenzymes (e.g. sarcosine, glutamate, lactate and glucose oxidases), quinoprotein enzymes (e.g. PQQ glucose dehydrogenase) and heme enzymes (e.g. peroxidases). The peroxidase electrodes were useful in the sensing of NAD(P)H, that reacted with oxygen in the presence of N-methyl phenazonium salts to form $NAD(P)^+$ and H_2O_2.

1. Introduction and Scope

In this chapter, dedicated to Klaus Mosbach on his 60th birthday, we consider the non-diffusional relaying of electrons between redox enzymes and electrodes through hydrogels, built with crosslinked polymer networks. As will be seen, even though these gels contain predominantly water, their 3-dimensional redox-polymer network, to which the enzymes are covalently bound, conducts electrons. Electrochemical biosensors, such as amperometric biosensors based on such gels have some rather unique properties. On the one side, water soluble substrates and products permeate through the hydrogels. On the other, electrons, originating in an oxidizable substrate, or delivered to a reducible substrate, diffuse through the network. Because the electrons are efficiently collected or delivered and because the diffusion of water soluble molecules through the gel does not differ excessively from that through a plain aqueous solution, the current densities flowing through hydrogel-coated electrodes are high. The high current densities translate to substantial sensitivities in the transduction of the flux of biochemicals to electrical currents (1). The group of enzymes that has been electrically connected through electron-conducting hydrogels to electrodes includes now flavoenzymes (2-6), quinoprotein (pyrroloquinoline, PQQ) enzymes (7), and heme peroxidases (8). As will be seen, the hydrogels also allow transduction of NAD(P)H fluxes, after translation to hydrogen peroxide fluxes, to electrical currents (8). We shall review the electron diffusion in redox-polymer skeleton based hydrogels (9), then discuss the electrical connection of flavoenzymes (2-6), heme enzymes (8), PQQ-enzymes (7) via these hydrogels to electrodes.

2. Electron Diffusion in Redox Hydrogels.

Cross-linked redox polymer films in which redox enzymes are immobilized relay electrons between oxidoreductases such as glucose oxidase and electrodes. An effective electron relaying polymer is poly(4-vinylpyridine) partially complexed with osmium

bis(bipyridine) dichloride and quaternized with 2-bromoethylamine (POs-EA) (Figure 1) (4,5). A key parameter in defining the electron relaying behavior of a redox polymer is its electron diffusion coefficient (D_e). We measured D_e for POs-EA, cross-linked with poly(ethylene glycol) diglycidyl ether (PEGDE), using steady state voltammetry at interdigitated array (IDA) electrodes (10-20). De depends on the ionic strength, anion, pH, and degree of cross-linking of POs-EA.

De was measured by the steady state voltammetry at interdigitated array (IDA) electrodes as follows: IDA gold electrodes on glass were fabricated by conventional photolithography and sputter-deposition of gold onto chromium primed glass substrates. The electrodes consisted of 100 (N), 5.0 μm wide fingers (w), separated by 5.0 μm gaps (gap), that were 2.0 mm long. The narrow widths and gaps of the 100 fingers allowed measurement of electron diffusion coefficients, that were much lower than ion diffusion coefficients. When the potential at one of IDA electrode was swept from reducing to oxidizing, while the other electrode was maintained at a reducing potential (generator-collector experiment), an anodic steady state current (I_{ss}) was observed upon redox cycling, because the electrode at the fixed reducing potential generated an oxidizable species. The total charge associated with the redox centers (Q) was obtained by integrating the area of the surface wave voltammogram when the potential of both of the IDA electrodes was scanned (generator-generator experiment). From I_{ss} and Q, D_e is obtained through equation 1 (10-12).

$$D_e = (I_{ss}/Q)\ gap\ (w + gap)\ N/(N-1) \qquad (1)$$

The attractive feature of this technique was that D_e was derived of I_{ss}, Q and the IDA geometry, and did not require knowledge of either the film thickness or of the concentration of the redox species. Furthermore, because the technique was a steady

state method, the current was not affected by diffusion of ions into and out of the redox polymer network, that necessarily takes place in transient experiments.

Typical cyclic voltammograms for POs-EA, cross-linked with 5.0 wt% PEGDE, on IDA electrodes at a 1.0 mV/s scan rate are shown in Figure 2a. The voltammograms in generator-collector experiments (solid line) had a sigmoidal shape; They showed the expected Os^{2+} oxidation at the generator, transport of electrons through the redox polymer (by electron hopping or electron self-exchange between neighboring Os^{3+} and Os^{2+} sites) and re-reduction of Os^{3+} sites at the collector (so called redox cycling). The anodic limiting current was identical with the cathodic one, and the limiting current was independent of scan rate. These results indicated the existence of a linear concentration variation in the $Os^{2+/3+}$ site ratio between the generator and the collector electrodes at the 1.0 mVs^{-1} scan rate, and established that charge transport through the POs-EA polymer limited the current. In contrast, the voltammograms in generator-generator experiment (dotted lines) showed well-defined surface waves. As the voltammetric wave was symmetrical and the peak current was proportional to the scan rate, the total charge of POs-EA polymer coated IDA electrode (Q) could be calculated by integrating the current of the voltammogram. From equation 1, D_e at 0.1 M NaCl was calculated to be 4.8×10^{-9} cm^2s^{-1}. The voltammograms of Figure 2 reveal a strong ionic strength dependence of D_e. When the concentration of NaCl was changed from 0.1 M to 1.0 M, Q was constant but Iss decreased. Moreover, when the potential of one IDA electrode was swept, while the other of IDA electrode was disconnected (generator-open circuit experiment, dashed line), a shoulder, indicating lateral electron diffusion between fingers was seen. This shoulder was sharp in 0.1 M NaCl but had, in 1.0 M NaCl, a diffusional tail, leading us to conclude that D_e of POs-EA decreases upon increasing with the ionic strength. Evidently, dehydration of POs-EA at increasing the ionic strengths made the cross-linked structure more rigid.

Figure 3 presents the pH dependence of D_e for POs-EA cross-linked with 5.0 wt% PEGDE. D_e changes remarkably near pH 4, close to pK_a of the pyridine nitrogen, from 4.5×10^{-9} to 1.6×10^{-8} $cm^2 s^{-1}$. Evidently, the polymer film was swollen and the backbone of the polymer was flexible when the pyridines were protonated at a pH below pK_a, where D_e was high. We conclude that D_e is determined by the degree of swelling of the cross-linked POs-EA polymer. D_e values of the POs-EA polymer at various concentrations of cross-linker are summarized in Table 1. For the network made with 5.0 wt% cross-linker D_e was pH dependent. D_e was, however, almost independent of pH at 25 wt% cross-linker. When the concentration of cross-linker reached 25 wt%, 32 % of the pyridines in the polymer were cross-linked with the diepoxide. Because the polymer could not swell even at low pH, D_e became independent of pH.

We conclude that in cross-linked POs-EA the electron diffusion coefficients increase upon hydration of the network and that electron transport through networks is controlled by segmental motion of the polymer backbone.

3. Electron Connection of Flavoenzyme Redox Centers to Electrodes

We have described previously the synthetic procedure for hydrogel-forming redox polymers (4). Poly(vinyl pyridine) can be derivatized with $Os(bpy)_2Cl_2$ in ethylene glycol or ethanol under reflux. The osmium derivatized polymer can be reacted with bromoethylamine at 60°C. It has been found that the polymer containing a molar substitution ratio near 1:1:3 osmium :ethylamine :non substituted pyridines, meets requirements relevant to enzyme electrodes, such as solubility in water, high charge density, high osmium loading, and crosslinkable side chains. For effective electrical connection of enzyme redox centers the polymer must be flexible so that it can penetrate the proteins. We have found that the polymer POs-EA (Figure 1) electrically "wires" redox enzymes. The hydrogel networks are formed by crosslinking POs-EA at or near ambient temperature and in aqueous solution with the diepoxide polyethylene glycol

diglycidyl ether (PEGDE) (Figure 1b) or a polyfunctional aziridine (PAZ) (Figure 1a). The crosslinker is chosen so as to avoid reaction of amino-acids that are critical for the function of the enzyme.

With polymeric "wires" virtually all flavoproteins, that can transfer one electron at a time from their reduced active centers to an electron acceptor, have been shown to be "wireable" and useful in the construction of enzyme electrodes. Selectivity of the electrodes requires absence of direct electrooxidation of the substrate on the electrode surface itself, or in the redox hydrogel, directly by the oxidized osmium complex, at the applied usually 0.45 V vs. SCE for POs-EA.

High catalytic current density (10^{-4}-10^{-3} Acm^{-2}) enzyme electrodes have been constructed by "wiring" glucose oxidase, lactate, or L-α-glycerophosphate oxidase (4,6); moderate current densities (10^{-6}-10^{-5} A cm^{-2}) resulted form "wiring" glycolate, theophylline, D-amino acid, sarcosine, L-glutamic acid, or cholesterol oxidase. The catalytic currents of L-amino acid and choline oxidase electrodes were very low. For xanthine oxidase the catalytic current was almost indistinguishable from the background current associated with nonenzymatic electrooxidation of xanthine by the oxidized redox polymer.

Examination of the significance of complex formation between the redox polymers and the enzymes on the efficiency of current collection shows that electrostatic complexation is important for efficient communication between the enzymes and the polymers (21), but other kinds of interactions may also be relevant.

Figure 4 shows the response of a sarcosine oxidase electrode and the variation of its current density with the electrode construction parameters. The response of the electrode under anaerobic conditions and under oxygen are shown in Figure 4a. Figure 4b shows the variation of the current density with the enzyme content of the hydrogel. Figure 4c shows that by changing the enzyme content of the gel one can adjust the dynamic range (apparent Michaelis constant, Km) of the sensor. Figure 4(d) shows that increasing the

thickness of the enzyme-polymer film results in an almost linear increase of the maximum current density obtained, up to about 200 μg cm^{-2} loading, where the film thickness reaches about 2 μm. Sarcosine oxidase has been used in bilayer electrodes for the detection of creatine (22). Creatine was converted in an outer creatine amidinohydrolase film into sarcosine, which was sensed by an inner layer of sarcosine oxidase-redox polymer hydrogel. The response of such an electrode is compared to one without the creatine amidinohydrolase in Figure 5. The electrode might be applicable in the direct determination of creatine phosphokinase activity in serum or whole blood.

In some of the flavoenzymes, for example in glycerophosphate oxidase, the semiquinone form of FADH· could not be observed during the normal catalytic cycle when dioxygen was the electron acceptor (23,24). From the efficient electron transfer to Os(III) relays that was observed, it was evident nevertheless that the substrate-reduced enzyme was reoxidized in two sequential electron-proton transfer steps. The rate limiting step in the multistep electron transfer from lactate oxidase to an electrode was the electron transfer between reduced $FADH_2$ centers and Os relays in the hydrogel. Figure 6 shows the pH response of a glucose oxidase electrode. Different pH maxima exist for the redox-hydrogel electrode and the natural enzyme activity. This shift in pH is consistent with the proposal that electron transfer between $FADH_2$ or FADH· and OsIII, which is pH independent, is rate limiting. In the natural enzymatic reaction the pH dependent reduction of O_2 to H_2O_2 is rate limiting.

The key determinants in realization of high current densities are the turnover number and specific activity of the enzyme, and the strength of the complex between the enzyme and the redox polymer (Table 2). In general enzymes with high turnover numbers and high complex formation constants with POs-EA give the highest current densities. The unexpectedly high current density of sarcosine oxidase and low current density of glutamate oxidase show, however, that the two parameters are not the only ones that are important. It is conceivable that the aberrations result from a specific interaction of the

polymer with the catalytically active site of the enzyme. or from particularly deep protein penetration of an electron relay. or from deactivation of the enzyme upon immobilization.

The turnover number and specific activity of the enzyme define the number of electrons produced per unit volume. In extreme cases of low turnover numbers. the volume fraction of protein necessary for the production of a detectable current is so high that the hydrogel no longer contains a high enough density of electron relaying centers and electron diffusion through the film becomes rate limiting. Table 2 shows the strength of the complexes formed between POs-EA and enzymes on a scale built on detection by isoelectric focusing of migration of free enzyme from the complex(21). The values in the table indicate the % enzyme content of the complex when unbound enzyme is first observed. Usually, the higher this number. the stronger the complex. and the stronger the complex. the higher the current density. Formation of a stronger complex can result in a shorter electron transfer distance betweeen the redox center of the enzyme and a relay of the polymer. or an increase in the density of electrically connected enzyme centers in the hydrogel.

4. Electrical Connection of Pyrroloquinoline Quinone Redox Centers

Several groups of quinonprotein enzymes have been isolated and characterized in recent years (25). These enzymes have either pyrroloquinoline quinone (PQQ), topaquinone (TPQ) or tryptophanyl-tryptophan quinone (TTQ) cofactors (26). Glucose dehydrogenase GDH (EC 1.1.99.17), that was successfully wired through the POs-EA based hydrogel (7) belongs to the group of PQQ-containing quinoproteins (27). The apo-enzyme (28) of GDH was reconstituted by incorporating PQQ (27) in the presence of Ca^{2+}(29). PQQ and Ca^{2+} are firmly bound in the reconstitued enzyme. The activity of the reconstituted holo-enzyme, 250 units mg^{-1}, was measured spectrophotometrically by monitoring the decoloration of Wurster's Blue (30). The reconstituted GDH can be stored at 4°C for more than two months without measurable loss of activity.

The dependence of the current density on glucose concentration for POs-EA/PEGDE-wired GDH and similarly wired glucose oxidase (GOX) electrodes is shown in Figure 7. The current density of the GDH electrode substantially exceeded that of the GOX electrode, reaching 1.8 mA cm^{-2} at 70 mM glucose. This current density was about three times higher than that of the electrode made with GOX. The sensitivity of the wired GDH electrode at 5 mM glucose was 165 μA cm^{-2} M^{-1}. The higher current density of the GDH electrode, relative to that of the GOX electrode, derived from the faster rate of electron transfer from the $PQQH_2$ centers than from $FADH_2$ centers to the osmium complex in the redox polymer/enzyme network.

That the 3-dimensional redox network based hydrogel is effective in collecting and carrying electrons from GDH is seen from the fact that in electrode made with the electron shuttling diffusional mediator 1,1'-dimethylferrocene, the current density was only 54 μA cm^{-2} at 4 mM glucose (31), versus 724 μA cm^{-2} for the redox hydrogel at at the same glucose concentration. The current density of the redox-hydrogel based GDH electrode changed relatively little between pH 6.3 and 8.8.

The half-life of the dissolved enzyme in 10 mM HEPES pH 7.3 buffer at room temperature was 5 days (7). The decay of the current of the GDH electrodes in 10 mM glucose at 25°C, pH 7.3 was, however, faster (Fig. 8, open squares), dropping to one half of its initial value in about 8 hours under continuous operation. The operational stability of the "wired" GDH electrode was found to be glucose concentration dependent, the output declining more rapidly at higher glucose concentrations. Fig. 8 shows the rates of decline for GDH electrodes in an electrochemical cell where the glucose concentration was held at 10 mM, and in a flow injection analyser where a computer controlled injection system injected fixed volumes of 10 mM glucose once every 60 minutes. Under the conditions of the experiment, it took less than 3 minutes for the sample to pass through the cell, i.e., the electrode was in 10mM glucose for only 3

minutes each hour. Evidently, the rate of current loss is depended on the amount of glucose electrooxidized (Figure 8).

5. Electrical Connection of Hemeprotein peroxidases

Most peroxidases have catalytic sites containing covalently bound iron porphyrins. In peroxidases the iron heme is positioned close to the surface of the enzyme. The near surface position of the catalytic site allows direct, non-mediated, electroreduction of the enzymes on graphite electrodes and thus the construction of direct H_2O_2 sensors (33,34).

Many diagnostic tests ultimately rely on amperometric of colorimetric detection of H_2O_2. Althougn feasible, enzymatic amperometric H_2O_2 detection is not commercially used. The most common amperometric H_2O_2 assays involve use of a Pt anode held at an oxidizing potential, where not only H_2O_2, but also a variety of interferants are electrooxidized.

Electron conducting POs-EA and PEGDE (Figure 1) redox-hydrogel based H_2O_2 sensors, involving electroreduction of lactoperoxidase (LOP), Arthromyces ramosus peroxidase (ARP), or horseradish peroxidase (HRP) (8). In these, the H_2O_2 fluxes were connected to currents by electrocatalytically reducing H_2O_2 according to the scheme shown in Figure 9. These enzymes were covalently bound to the 3-dimensional redox epoxy based hydrogel Upon such immobilization the ensemble of enzyme molecules in the gel volume was electrically connected to the electrode.

The amperometric measurements were performed in a standard 3-electrode cell, with the working electrode maintained at 0.0V (SCE) and rotated at 1000 RPM. H_2O_2 was catalitically electroreduced at the operating potential. The dependence of the catalytic H_2O_2 electroreduction currents on the H_2O_2 concentration in pH 7.4 phosphate buffer is seen in Figure 10 for four enzymes ARP, LOP, HRP, and periodate-oxidized HRP.

Although immobilization of lactoperoxidase in the redox hydrogel resulted in substantial reduction currents, the currents rapidly decayed when the H_2O_2 concentration exceeded 10μM, because of reversible substrate inhibition of the enzyme (35). Wiring of the peroxidase from Arthromyces ramosus in the electron-conducting hydrogel led to the highest current density > 1mA cm^{-2}. The current density increased linearly with the H_2O_2 concentration from 0.1μM to 500μM. The current was remarkably stable, decaying only a few percent per hour.

The horseradish peroxidase (HRP) containing electrodes did not exhibit either the high current density nor the exceptional linear range of the Arthromyces ramosus peroxidase based electrodes. Nevertheless, when $NaIO_4$ oxidized HRP was used, the sensors' performance improved. The aldehydes formed upon $NaIO_4$ oxidation of HRP sugar residues formed Schiff bases with the POs-EA amines, coupling the enzyme's redox centers with those of the hydrogel and shortening the electron transfer distances. The currents in electrodes modified with hydrogels with $NaIO_4$ oxidized HRP exceeded by a factor of 5 those observed in electrodes with untreated HRP, and the sensitivity reached 1 A M^{-1} cm^{-2}.

The $NaIO_4$ oxidized HRP based electrode was operable at potentials between -0.15V(SCE) and +0.3V(SCE). The wide potential window allowed choice of potentials where non-enzyme specific electrode reaction rates were slow, i.e. where interferant caused currents were low. The useful pH range of the sensors was 3.8 to 9.6, remaining within 10% of the maximum response throughout this range. Transient exposure of the sensors to solutions that were strongly acidic (pH < 3.8) reduced their response, but upon returning to a neutral pH the sensors recovered. Exposure to strong bases (pH > 9.6) caused irreversible decomposition of their gel.

6. Assay of NAD(P)H Through Quantitative Translation to H_2O_2

Quinones and molecules with quinoid structures have been reduced in two electron transfer reactions by NAD(P)H (36-40). Amperometric NAD(P)H sensors based on such reduction have been described by Miller et al (41,42), Gorton et al (43) and Kulys et al (44,45). An example of a water soluble quinoid, that is readily reduced by NAD(P)H is the N-methylphenazonium ion NMP^+ :

$$NAD(P)H + NMP^+ \longrightarrow NAD(P)^+ + NMPH$$

The reduced phenazine, NMPH is reoxidized by molecular oxygen to NMP^+ in the H_2O_2 generating reaction :

$$NMPH + O_2 \longrightarrow NMP^+ + H_2O_2$$

The sum of these reactions is the catalytic reduction of O_2 to H_2O_2 by NAD(P)H:

$$NAD(P)H + O_2 \xrightarrow{NMP+} NAD(P)^+ + H_2O_2$$

Because the reaction is fast and stoichiometric, NAD(P)H sensors based on amperometric assays of the depletion of O_2 (46,47) and the colorimetric assay of the H_2O_2 generated (48-50) have been built.

The translation of NAD(P)H into H_2O_2 through the above reaction sequence allowed the sensing of NAD(P)H with the peroxidase electrodes with 1 A M^{-1} cm^{-2} sensitivity and with a 0.1 to 200 μM linear range, similar to those of the H_2O_2 sensors (8). Figure 11 shows the steady state alcohol response of a sensor with NAD^+/NADH dependent alcohol dehydrogenase, pH 7.4 solution containing 7.1×10^{-6}M N-methylphenazonium methosulfate, 13 units/mL alcohol dehydrogenase and 1.3×10^{-4}M NAD^+. Figure 12 summarizes the electron transfer sequence in the sensing of alcohol.

CONCLUSION

Electrons diffuse in hydrogels built wiht redox polymer skeletons at sufficient rates to allow interception of electrons transferred between oxidoreductases and their substrates. Their .. to electrodes results in the transduction of biochemical fluxes to

electrical currents. Electrical currents are produced by substrates of flavoenzymes, heme enzymes and quinoprotein enzymes. Through catalytic reaction of NAD(P)H with O_2 in an $NAD(P)^+$ and H_2O_2 produsing reaction and electroreduction of H_2O_2 in peroxidase-containing redox hydrogels NAD(P)H concentrations can also be translated to electrical currents.

ACKNOWLEDGMENT

This work is supported by grants from Office of Naval Research. National Science Foundation. the National Institutes of Health Grant No. 1-RO1-DK42015-01. and the Robert A. Welch Foundation.

REFERENCES

(1) Heller, A. (1992). Electrical Connection of Enzyme Redox Centers to Electrodes. J.Phys.Chem. *96*, 3579-3587.

(2) Gregg, B.A. and Heller, A. (1990). Cross-Linked Redox Gels Containing Glucose Oxidase for Amperometric Biosensor Applications. Anal. Chem. *62*, 258-63.

(3) Foulds, N.C. and Lowe, C.R. (1988). Immobilization of Glucose Oxidase in Ferrocene-Modified Pyrrole Polymers. Anal. Chem. *60*, 2473-8.

(4) Gregg, B.A. and Heller, A. (1991). Redox Polymer Films Containing Enzymes. 1. A Redox-Conducting Epoxy Cement: Synthesis, Characterization, and Electrocatalytic Oxidation of Hydroquinone. J. Phys. Chem. *95*, 5970-5.

(5) Gregg, B.A. and Heller, A. (1991). Redox Polymer Films Containing Enzymes. 2. Glucose Oxidase-Containing Enzyme Electrodes. J. Phys. Chem. *95*, 576-80.

(6) Katakis, I. and Heller, A. (1992). L-α-Glycerophosphate and L-Lactate Electrodes Based on the Electrochemical "Wiring" of Oxidases. Anal. Chem. *64*, 1008-13.

(7) Ye, L., Hämmerle, M., Olsthoorn, A.J.J., Schuhmann, W., Schmidt, H.-L., Duine, J.A., Heller, A. (1993). High Current Density "Wired" Quinoprotein Glucose Dehydrogenase Electrode. Anal. Chem., *65*, 238-41.

(8) Vreeke, M., Maidan, R. Heller, A. (1993). Hydrogen Peroxide and β-Nicotinamide Adenine Dinucleotide Sensing Amperometric Electrodes Based on Electrical Connection of Horseradish Peroxidase Redox Centers to Electrodes through a Three-Dimensional Electron Relaying Polymer Network. Anal. Chem. *64*, 3084-90.

(9) Aoki, A. and Adam Heller, A. (1993). Measurement of Electron Diffusion Coefficients in Redox Polymers by Steady State Voltammetry with Interdigitated Array Electrodes. In : Extended Abstracts of the Joint Meeting of the

Electrochemical Society and the Electrochemical Society of Japan. Honolulu, Hawaii.

(10) Chidsey, C.E., Feldman, B.J., Lundgren, C. and Murray, R.W. (1986) Micrometer-Spaced Platinum Interdigitated Array Electrode: Fabrication, Theory, and Initial Use. Anal. Chem. *58*, 601-607.

(11) B.J. Feldman and Royce W. Murray. (1986) Measurement of Electron Diffusion Coefficients through Prussian Blue Electroactive Films Electrodeposited on Interdigitated Array Platinum Electrodes. Anal.Chem. *58*, 2844-2847.

(12) Feldman, B.J. and Murray, R.W. (1987). Electron Diffusion in Wet and Dry Prussian Blue Films on Interdigitated Array Electrodes. Inorg.Chem. *26*, 1702-1708.

(13) Dalton, E.F., Surridge, N.A., Jernigan, J.C., Wilbourn, K.O., Facci, J.S. and Murray, R.W. (1990). Charge Transport in Electroactive Polymers Consisting of Fixed Molecular Redox Sites. Chem.Phys. *141*, 143-157.

(14) Surridge, N.A., Zvanut, M.E., Keene, F.R., Sosnoff, C.S., Silver, M. and Murray, R.W. (1992). Effects of Mixed-Valent Composition and Bathing Environment on Solid-State Electron Self-Exchanges in Osmium Bipyridine Redox Polymer Films. J.Phys.Chem. *96*, 962-970.

(15) Nishihara, H., Dalton, F., Murray, R.W. (1991). Interdigitated Array Electrode Diffusion Measurements in Donor/Acceptor Solutions in Polyether Electrolyte Solvents. Anal.Chem. *63*, 2955-2960.

(16) Kittlesen, G.P., White, H.S., and Wrighton, M.S. (1985) A Microelectrochemical Diode with Submicron Contact Spacing Based on the Connection of Two Microelectordes Using Dissimilar Redox Polymers. J.Am.Chem.Soc. *107*, 7373-7380.

(17) Belanger, D., and Wrighton, M.S. (1987). Microelectrochemical Transistors Based on Electrostatic Binding of Electroactive Metal Complexes in Protonated

Poly(4-vinylpyridine): Devices That Respond to Two Chemical Stimuli. Anal.Chem. *59*. 1426-1432.

(18) Smith. D.K., Lane. G.A., and Wrighton. M.S. (1988). Charge-Transport Properties of an Electrode-Confined Redox Polymer Derived from a Monomer Consisting of a Quinone Flanked by Two Benzylviologen Subunits. J.Phys.Chem. *92*. 2616-2628.

(19) Shu. C.-F., and Wrighton. M.S. (1988). Synthesis and Charge-Transport Properties of Polymers Derived from the Oxidation of 1-Hydro-1'-(6-(pyrrol-1-yl)hexyl)-4,4'-bipyridinium Bis(hexafluorophosphate) and Demonstration of a pH-Sensitive Microelectrochemical Transistor Derived from the Redox Properties of a Conventional Redox Center. J.Phys.Chem. *92*. 5221-5229.

(20) Goss. C.A. and Majda. M. (1991). Lateral Diffusion in Organized Bilayer Assemblies of Electroactive Amphiphiles Influence of the Oxidation State of the Amphiphile Investigated by Steady-State Methods Involving an Interdigitated Miro-Electrode Array Device. J.Electroanal.Chem. *300*. 377-405.

(21) Katakis. I., Davidson, L. and Heller. A. (1993). Oxidoreductase-Redox Polymer Complex Formation and Electron Transfer Efficiency. Submitted.

(22) Motonaka. J., Takabayashi. H., Ikeda, S., Tanaka. N. (1990). Preparation and Properties of a Micro Enzyme Sensor for Creatine. Anal. Lett., *23*, 1981-91.

(23) Claiborne, A. (1986). Studies on the Structure and Mechanism of *Streptococcus faecium* L-α-Glycerophosphate Oxidase. J. Biol. Chem., *261*, 14398-407.

(24) Jacobs. N.J. and VanDemark, P.J. (1960). The Purification and Properties of the α-Glycerophosphate-Oxidizing Enzyme of *Streptococcus Faecalis*". Arch. Biochem. Biophys., *88*, 250-5.

(25) Duine, J.A., Frank, J., and Jongejan, J.A. (1987). Enzymology of Quinoproteins. Adv. Enzymol. *59*. 169-212.

(26) Duine. J.A. (1991). Quinoproteins: Enzymes Containing the Quinonoid Cofactor Pyrroloquinoline Quinone. Topaquinone or Tryptophan-Tryptophan Quinone. Eur. J. Biochem. *200*. 271-284.

(27) Duine. J.A.. Frank. J. and Van Zeeland. J.K. (1979). Glucose Dehydrogenase From *Acinatobactor Calcoacetieus*. FEBS Lett. *108*. 443-446.

(28) Van der Meer. R.A.. Groen. B.W.. Van Kleef. M.A.G.. Frank. J.. Jongejan. J.A., and Duine. J.A. (1990). Isolation. Preparation. and Assay of Pyrroloquinoline Quinone. Meth. Enzymol. *188*. 260-283.

(29) Geiger. O. and Goerisch. H. (1989). Reversible Thermal Inactivation of the Quinoprotein Glucose Dehydrogenase from *Acinatobacter Calcoacetieus* . Biochem. J. *261*. 415-21.

(30) Dokter. P.. Frank. J. and Duine. J.A. (1986). Purification and Characterization of Quinoprotein Glucose Dehydrogenase From *Acinatobacter Calcoacetieus* L.M.D.79.41. Biochem. J. *239*. 163-167.

(31) D'Costa. E.J., Higgins. I.J. and Turner. A.P.F. (1986). "Quinoprotein Glucose Dehydrogenase and Its Application in an Amperometric Glucose Sensor", Biosensors *2*. 71-87.

(32) Maehly, A.C. (1955). Plant Peroxidase. Meth. Enzymol., *2*, 801-13.

(33) Kulys, J.J., and Schmid, R.D. (1990). Mediatorless Peroxide electrode and Preparation of Bienzyme Sensors", Bioelectrochem. Bioenerg., *24*, 305-11.

(34) Jonsson-Pettersson, G. (1991). Reagentless Hydrogen Peroxide and Glucose Sensors Based on Peroxidase Immobilized on Graphite Electrodes. Electroanalysis, *3*, 741-50.

(35) Polis, D. and Shmukler, H.W. (1955). Lactoperoxidase. Meth. Enzymol. *2*, 813-7.

(36) Kitani, A., So, Y.-H. and Miller,L.L. (1981). An Electrochemical study of the Kinetics of NADH being Oxidized by Diimines Derived from Diaminobenzine and Diaminopyrimidines. J. Am. Chem. Soc., *103*, 7636-41.

(37) Itoh, S., Kinugawa, M., Mita, N. and Ohshiro, Y. (1989). Efficient NAD^+ Regeneration System with Heteroaromatic o-Quinones and Molecular Oxygen. J. Chem. Soc. Chem. Commun., 694-5.

(38) Ottaway, J.H. (1966). Some Rate Constants for the Phenazine Methosulfate-Catalysed Oxidation of Reduced Nicotinamide-Adenine Dinucleotide. Biochem. J., *99*, 253-56.

(39) Jones, J.B. and Taylor, K.E. (1976). Nicotinamide coenzyme regeneration. Flavin mononucleotide (riboflavin phosphate) as an efficient, economical, and enzyme-compatible recycling agent. Can. J. Chem., *54*, 2969-73.

(40) Tse, D.C.-S. and Kuwana, T. (1978). Electrocatalysis of Dihydronicotinamide Adenosine Diphosphate with Quinones and Modified Quinone Electrodes. Anal. Chem., *50*, 1315-18.

(41) Degrand, C. and Miller, L.L. (1980). An Electrode Modified with Polymer Bound Dopamine which Catalyzes NADH Oxidation. J. Am. Chem. Soc., *102*, 5728-32.

(42) Fukui, M., Kitani, A., Degrand, C. and Miller, L.L. (1982) Propogation of a Redox Reaction Through a Quinoid Polymer Film on an Electrode. J. Am. Chem. Soc., *104*, 28-33.

(43) Gorton, L., Csoregi, E., Dominguez, E., Emneus, J., Jonsson-Pettersson, G., Marko-Varga, G. and Persson, B. (1991). Selective Detection in Flow Analysis Based on the Combination of Immobilized Enzymes and Chemically Modified Electrodes. Chim. Acta, *250*, 203-48.

(44) Cenas, N.K., Kanapieniene, J.J., and Kulys, J.J. (1985). Electrocatalytic Oxidation of NADH on Carbon Black Electrodes. J. Electroanal. Electrochem., *189*, 163-69.

(45) Kulys, J.J. (1986) Enzyme Electrodes Basd on Organic Metals. Biosensors, *2*, 3-13.

(46) Polster, J. and Schmidt, H.L. (1989). Determination of Dehydrogenase Substrates by Clark Type Oxygen Electrodes and Photosensitized Coenzyme Oxidation. Talanta, *36*, 864-66.

(47) Huck, H., Schelter-Graf, A., Danzer, J., Kirch, P. and Schmidt, H.L. (1984). Bioelectrochemical Detection systems for substrates of Dehydrogenases. Analyst, *109*, 147-50.

(48) Williams, D.C. III and Seitz, R.W. (1976). Automated Chemiluminescence Method for Determining the Reduced Form of Nicotinamide Adenine Dinucleotide Coupled to the Measurement of Lactate Dehydrogenase Activity. Anal. Chem., *48*, 1478-81.

(49) European Patent Application, *111*, Issue 9, 1988, EP 285998.

(50) European Patent Application, *112*, Issue 13, 1988, EP 317070.

FIGURE CAPTIONS

Figure 1. Structure of the water soluble, enzyme complexing redox "wire" POs-EA. m=1, n=1, p=3 or 2. The polymer-enzyme complexes are crosslinked with either : (a) a polyfunctional aziridine (PAZ), or (b) poly(ethylene glycol) diglycidyl ether (PEGDE) to yield hydrogel-forming networks.

Figure 2. Ionic strength dependence of cyclic voltammograms for POs-EA cross-linked with 5.0 wt% PEGDE coated on IDA electrodes, at an $Os^{3+/2+}$ site coverage of $\Gamma = 1.93 \times 10^{-8}$ mol cm^{-2} in 20 mM phosphate buffer at pH 7.0 and at 1.0 mV s^{-1} scan rate. Generator-collector (solid line), generator-open circuit (dashed line), generator-generator (dotted line) voltammograms are shown for (a), 0.1 M; (b), 1.0 M NaCl.

Figure 3. pH dependence of the electron diffusion coefficient of POs-EA cross-linked with 5.0 wt% PEGDE, $\Gamma = 4.35 \times 10^{-9}$ mol cm^{-2} in 20 mM phosphate buffer containing 0.1 M NaCl at 2.0 mV s^{-1} scan rate.

Figure 4. (a) Dependence of the current density of a sarcosine oxidase electrode on sarcosine concentration. Open circles, Ar atmosphere; solid circles, O_2 atmosphere; glassy carbon electrode; 20 weight % enzyme; 200 µg cm^{-2} loading; 0.45 V (SCE); pH 7.2 phosphate buffer, 0.1 M NaCl; 1000 rpm; 22°C. (b) Dependence of the maximum current density of sarcosine oxidase electrodes on the enzyme content of the hydrogel at 150 µg cm^{-2} loading. Conditions same as above. Jmax determined from Eadie-Hofstee plots. (c) Dependence of the apparent Michaelis constants of sarcosine oxidase electrodes on the enzyme content of the hydrogel. (d) Dependence of the maximum current density of sarcosine electrodes made with 20 weight % enzyme on the thickness of the hydrogel-films.

Figure 5. Response of a bilayer sarcosine - creatine amidinohydrolase electrode (open circles) to creatine. The solid circles show the creatine-response of a sarcosine electrode made without the hydrolase. The hydrogel-forming polymer contained 26 % sarcosine oxidase, 20% PAZ crosslinker, and 54% POs-EA. Loading was 50 μg cm^{-2} .The bilayer electrode had an exterior film of 40 μg of creatine amidinohydrolase (0.5 units) crosslinked with PAZ and poly(vinyl pyridine) quaternized with bromoethylamine.

Figure 6. pH dependence of the glucose-produced current of a glassy carbon electrode, modified with the hydrogel formed of glucose oxidase, POs-EA and PEGDE under argon (open circles) and of a hydrogen peroxide detecting platinum electrode modified with the same gel, except for having the POs-EA analog without the osmium complex under oxygen (solid circles). 10% weight glucose oxidase, 80 μg cm^{-2} loading.

Figure 7. Comparison of the current output and the sensitivity for GDH and GOX electrodes. Open square: GDH electrode; Solid diamonds: GOX electrode. 0.4 V (SCE); 1000 rpm; air atmosphere.

Figure 8. Time dependence of the output of GDH electrode at 0.4 V (SCE). Continuous operation at constant 10 mM glucose concentration (open squares) and in a flow injection analyzer where 30 second 10 mM glucose pulses were injected once per hour (solid diamonds).

Figure 9. Scheme of cathodic assay of hydrogen peroxide using POs-EA-based electron conducting hydrogels to which a peroxidase is covalently bound. $Os^{2+/3+}$ denotes gel-bound redox centers.

Figure 10. Amperometric response of peroxide sensing cathodes built with different peroxidases covalently bound to electron conducting hydrogels based on POs-EA. Closed circles. HRP: open circles. $NaIO_4$ oxidized HRP: squares. LOP: triangles. ARP.

Figure 11. Steady state alcohol response for alcohol dehydrogenase with the "wired" peroxidase cathode. 0 V (SCE); 1000 rpm; pH 7.4 phosphate buffer.

Figure 12. Electron transfer sequence in the transduction of the concentration dependent alcohol flux to a cathodic current. Even though 7 electron transfer steps are involved in the transduction, these are so efficient that the current represents about 10% of the electron pairs transferred in the oxidation of ethanol to acetaldehyde.

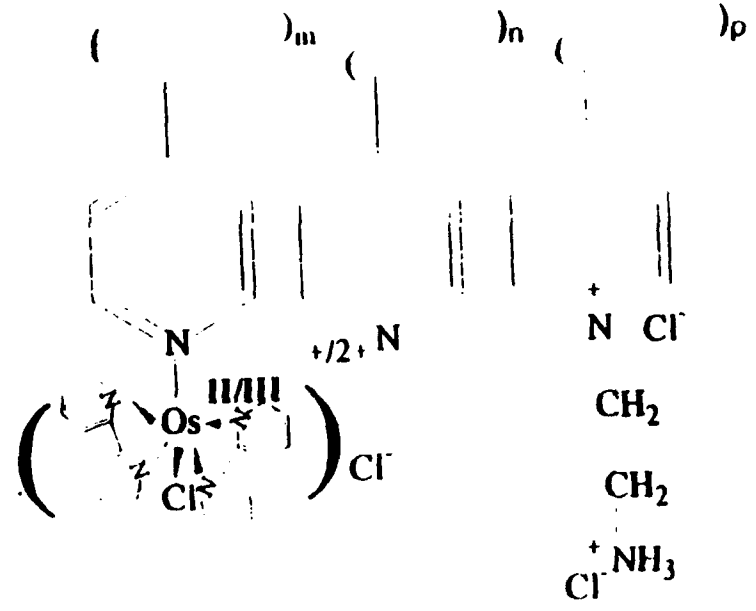

PAZ

(a)

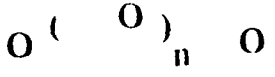

PEGDE

(b)

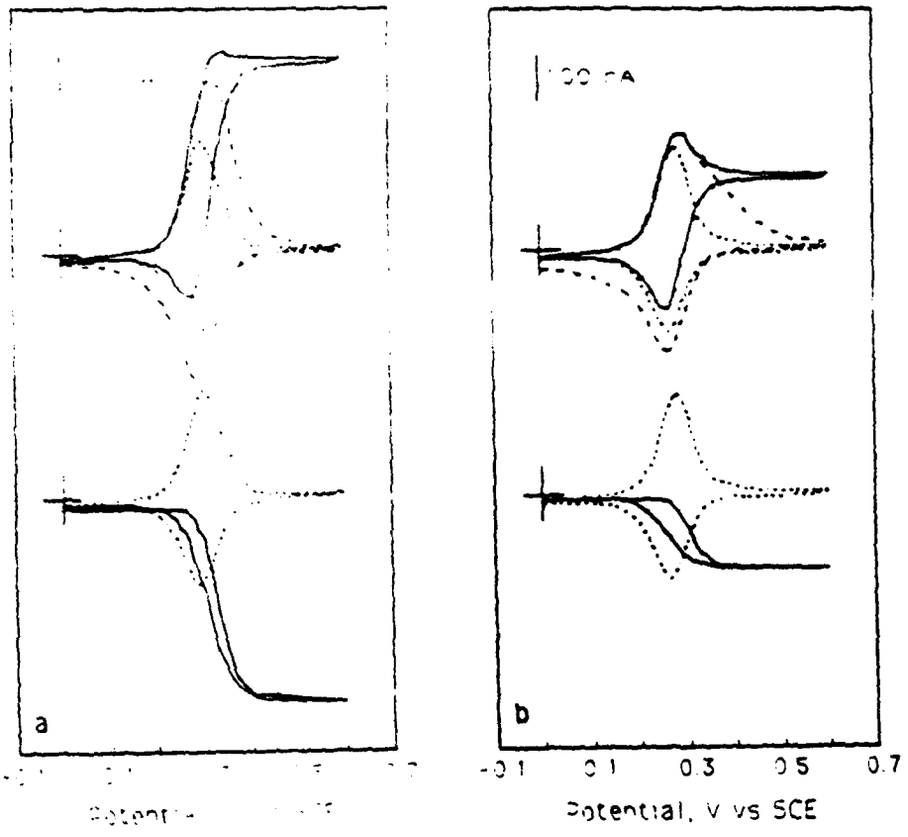
100 nA
a
b
-0.1
0.1
0.3
0.5
0.7
Potential, V vs SCE

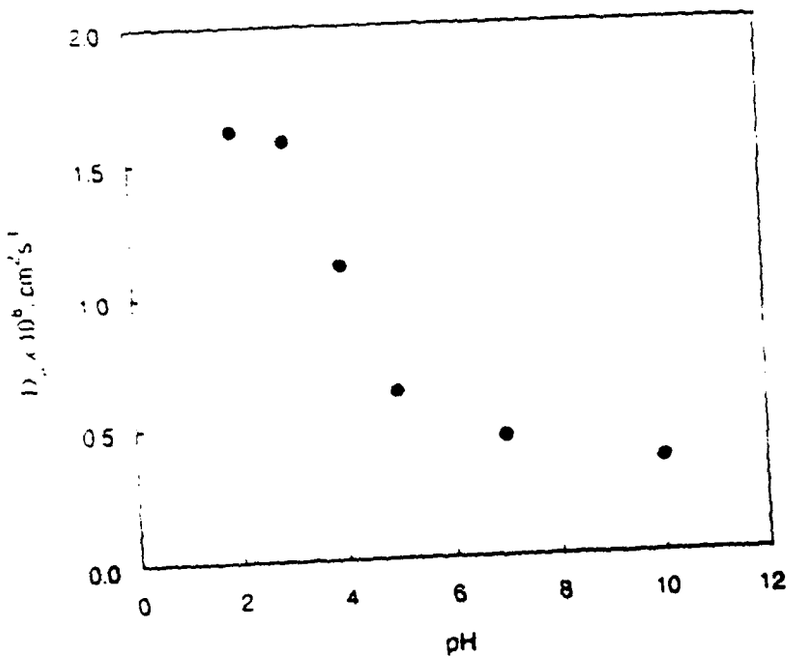
2.0
1.5
1.0
0.5
0.0
0
2
4
6
8
10
12
pH

(a)

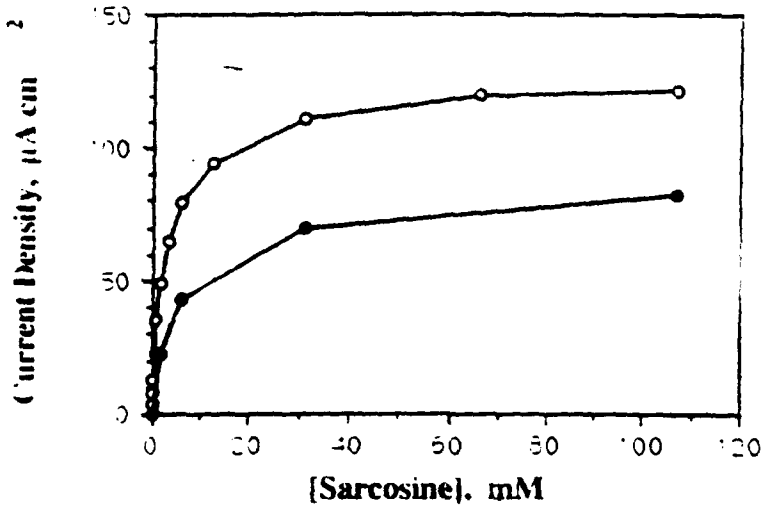
Current Density, μA cm
0
50
100
150
0
20
40
60
80
100
120
[Sarcosine], mM

(b)

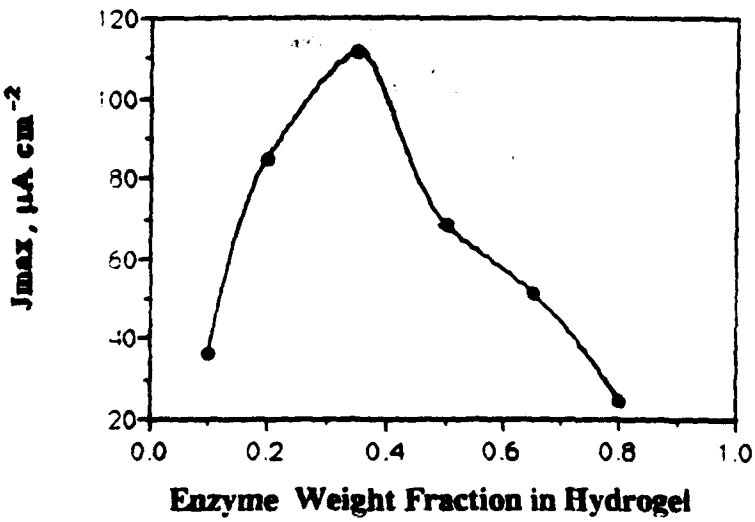
Jmax, μA cm-2
20
40
60
80
100
120
0.0
0.2
0.4
0.6
0.8
1.0
Enzyme Weight Fraction in Hydrogel

(c)

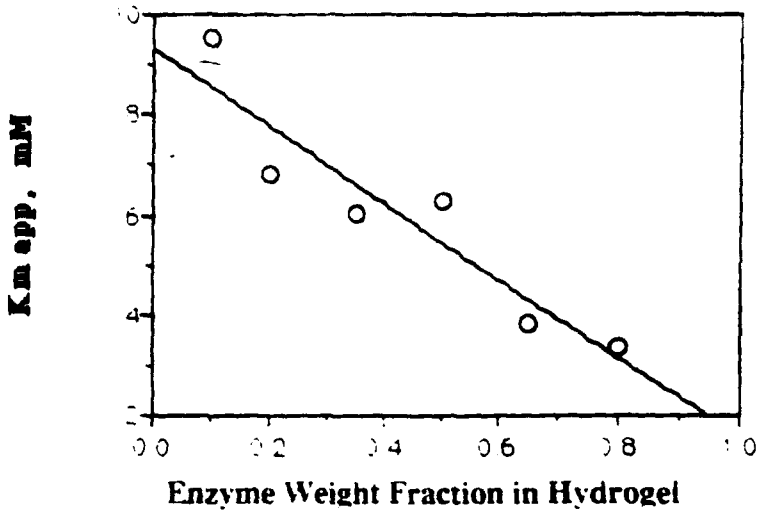
Km app, mM
8
6
4
0.0
0.2
0.4
0.6
0.8
1.0
Enzyme Weight Fraction in Hydrogel

(d)

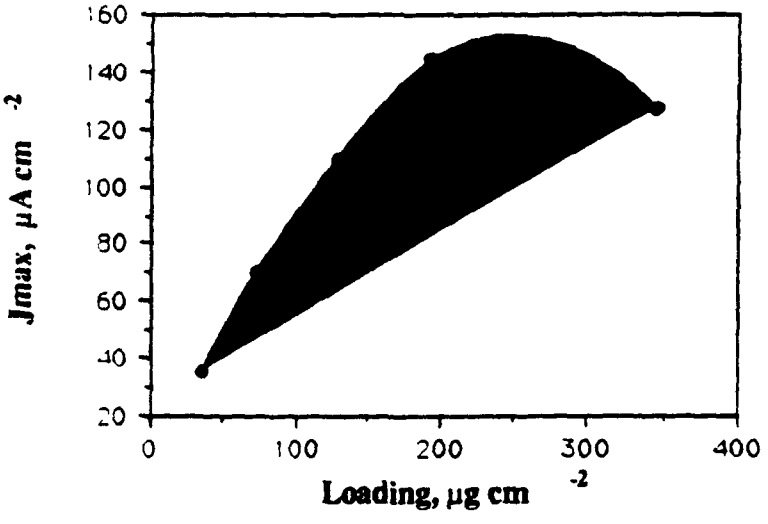
Jmax, μA cm -2
160
140
120
100
80
60
40
20
0
100
200
300
400
Loading, μg cm -2

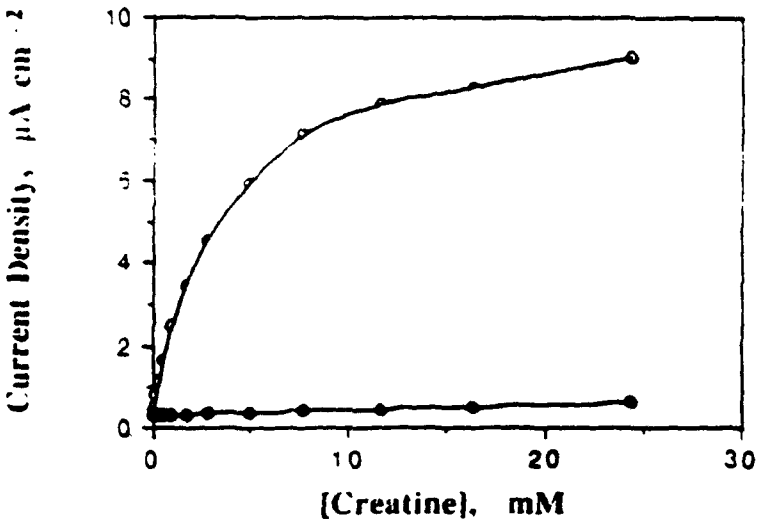
Current Density, μA cm⁻²
10
8
6
4
2
0
0
10
20
30
[Creatine], mM

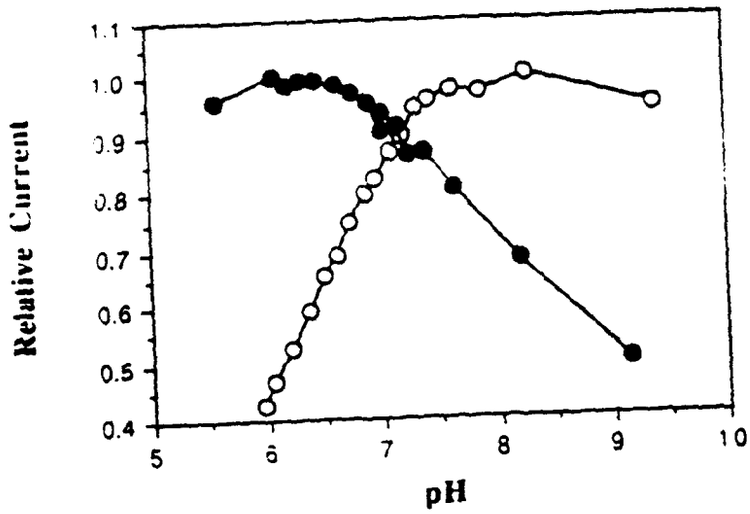
Relative Current
1.1
1.0
0.9
0.8
0.7
0.6
0.5
0.4
5
6
7
8
9
10
pH

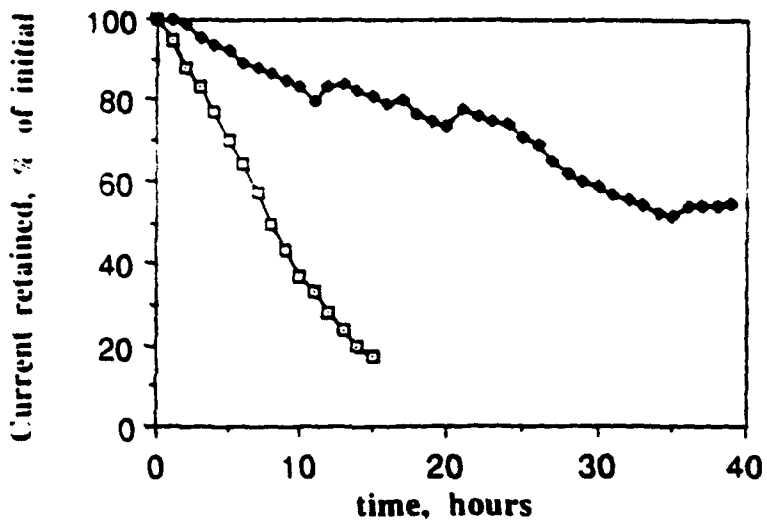
Current retained, % of initial
100
80
60
40
20
0
0
10
20
30
40
time, hours

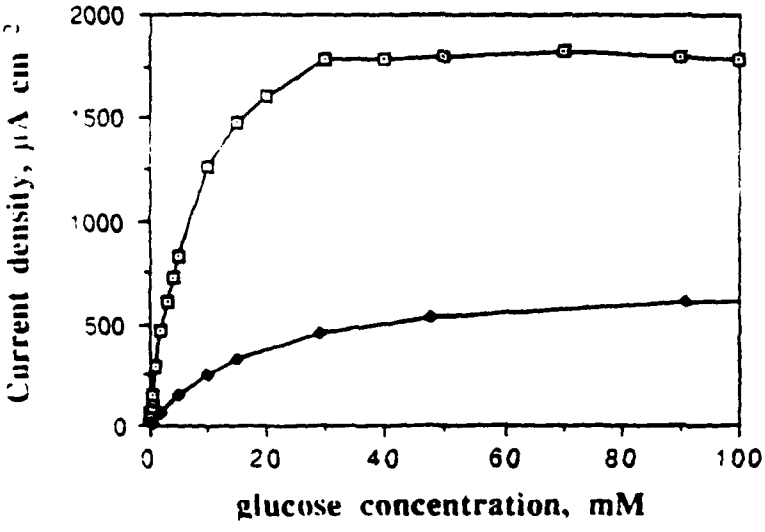
Current density, μA cm
2000
1500
1000
500
0
0
20
40
60
80
100
glucose concentration, mM

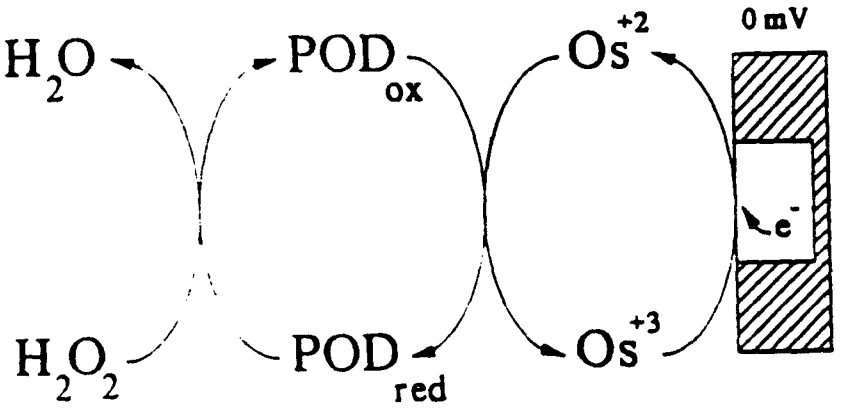
H_2O
POD_{ox}
Os^{+2}
0 mV
e^-
H_2O_2
POD_{red}
Os^{+3}

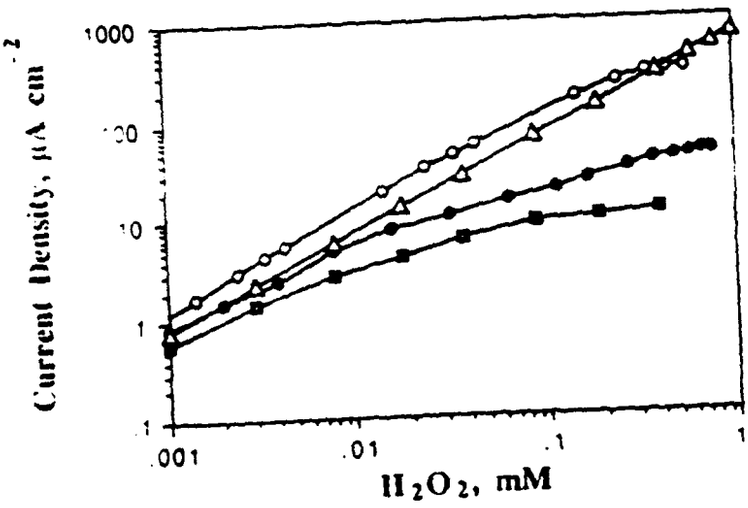
Current Density, μA cm-2
1000
100
10
1
.1
.001
.01
.1
1
H2O2, mM

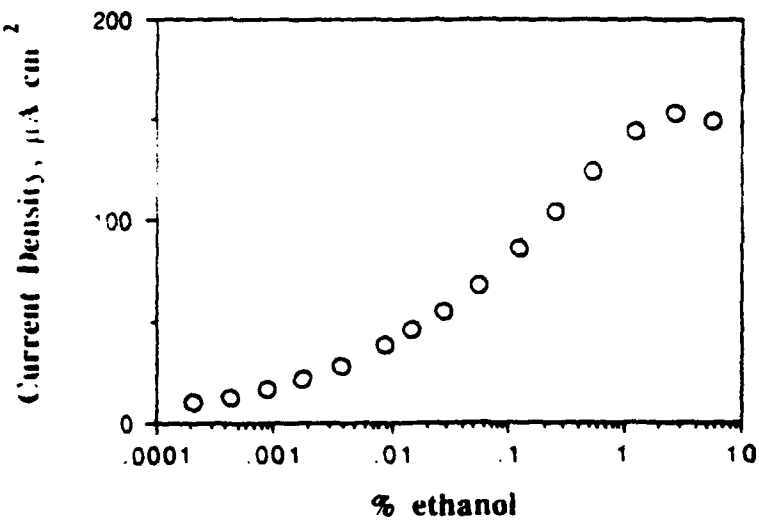
Current Density, μA cm⁻²
200
100
0
.0001
.001
.01
.1
1
10
% ethanol

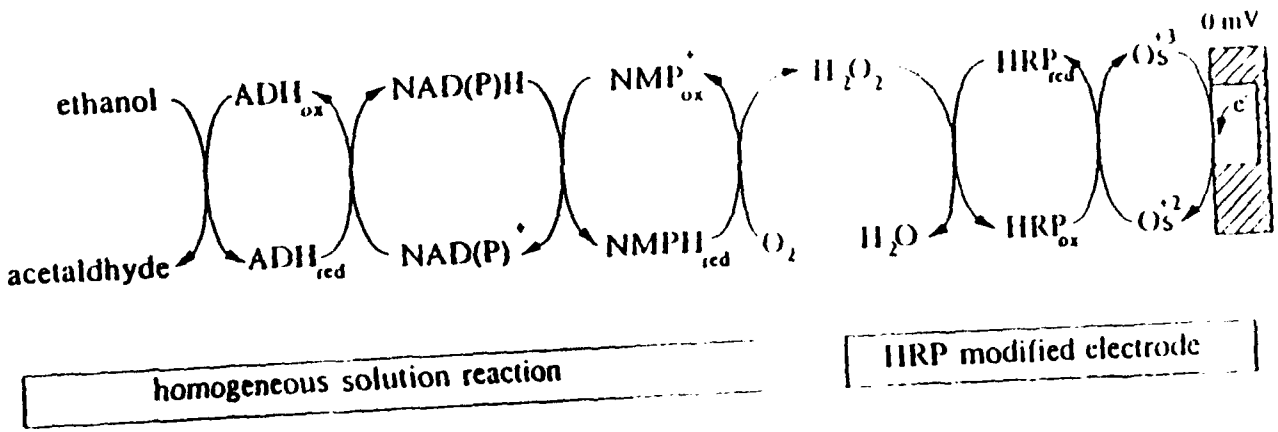
ethanol
acetaldhyde
ADH ox
ADH red
NAD(P)H
NAD(P)+
NMP+ ox
NMPH red
O2
H2O2
H2O
HRP red
HRP ox
Os+3
Os+2
e-
0 mV
homogeneous solution reaction
HRP modified electrode

Table 1. Effect of the Extent of Cross Linking on the Electron Diffusion Coefficient (D_e)

Cross linker wt%	D_e, $cm^2 s^{-1}$ pH 3.0	pH 7.0
5	1.6×10^{-8}	4.5×10^{-9}
25	4.2×10^{-9}	3.2×10^{-9}

Table 2. Response of "Wired" Flavin Oxidase Electrodes and its Relationship to Kinetics of the Enzyme, Strength of Enzyme-Polymer complex and Crosslinker Used‡

ENZYME *	Highest Current Density ($\mu A\ cm^{-2}$)	% Enzyme Content of Complex at Saturation**	Turnover Number (s^{-1})	Crosslinker***
GOx	290	73	203	PEGDE
LOx	120	>68	144	PEGDE,PAZ
GPO	83	81	30	PEGDE
GLUx	6.5	75	79	PEGDE
SOx	90	73	14	PAZ
THOx	2	>56	?	PAZ
CHOx	1	62	8	PEGDE
DAAOx	7	86	3.5	PAZ

‡ Electrodes so constructed as to be kinetically limited and have 0.1 ± 0.02 units immobilized

* Abbreviations : GOx, glucose oxidase; LOx, lactate oxidase; GPO, L-α-glycerophosphate oxidase; GLUx, L-glutamate oxidase; SOx, sarcosine oxidase; THOx, theophyline oxidase; CHOx, cholesterol oxidase; DAAOx, D-amino acid oxidase

** As determined by isoelectric focusing experiments.

*** PAZ : polyfunctional aziridine, PEGDE : poly(ethylene glycol) diglycidyl ether.

Reprinted from Analytical Chemistry, 1993, 65.

Glucose Electrodes Based on Cross-Linked $[Os(bpy)_2Cl]^{+/2+}$ Complexed Poly(1-vinylimidazole) Films

Timothy J. Ohara, Ravi Rajagopalan, and Adam Heller*

Department of Chemical Engineering, University of Texas at Austin, Austin, Texas 78712-1062

Enzyme electrodes based on a redox hydrogel formed upon complexing water-soluble poly(1-vinylimidazole) (PVI) with $[Os(bpy)_2Cl]^+$ and cross-linked with water-soluble poly(ethylene glycol) diglycidyl ether (molecular weight 400, peg 400) are described. The properties of the electrodes depended on their polymers' osmium content, the extent of cross-linking, the pH, and the ionic strength in which they were used. The redox hydrogels' electron diffusion coefficients (D_e) increased with osmium content of their polymers. The D_e values were 1.5×10^{-6}, 1.3×10^{-6}, and 4.3×10^{-9} cm²/s for PVI_3-Os, PVI_5-Os, and PVI_{10}-Os, respectively, the subscripts indicating the number of monomer units per osmium redox center. D_e decreased with increasing ionic strength and increased upon protonation of the polymer. In glucose electrodes, made by incorporating into their films glucose oxidase (GOX) through covalent bonding in the cross-linking step, glucose was electrooxidized at >150 mV (SCE). The characteristics of these electrodes depended on the GOX concentration, film thickness, O_2 concentration, pH, NaCl concentration, and electrode potential. The steady-state glucose electrooxidation currents were independent of the polymers' osmium content in the studied (3–10 monomer units per osmium center) range. Electrodes containing 39% GOX reached steady-state glucose electrooxidation current densities of 400 μA/cm² and, when made with thick gel films, were selective for glucose in the presence of physiological concentrations of ascorbate and acetaminophen.

INTRODUCTION

Redox hydrogel films are unique both in having adequate electron diffusion coefficients (i.e., not rate limiting) and in being permeable to water-soluble substrates and products of enzymatic reactions.[1] When a cross-linked redox polymer network electrically "wires" an enzyme that is covalently bound to it, then the gel and the current-collecting metal form enzyme electrodes. Such electrodes are potentially useful in applications where release of diffusional mediators from the electrodes is to be avoided and where small size is important.[2] Here we show that hydrogels, based on the $Os(bpy)_2Cl^{+/2+}$ complex of poly(1-vinylimidazole) (PVI) (Figure 1) termed PVI-Os, are adequate electron conductors and that electrons originating in the redox site of glucose oxidase (GOX) are transferred through the gel's polymer network to electrodes. The hydrogels are made by cross-linking poly-

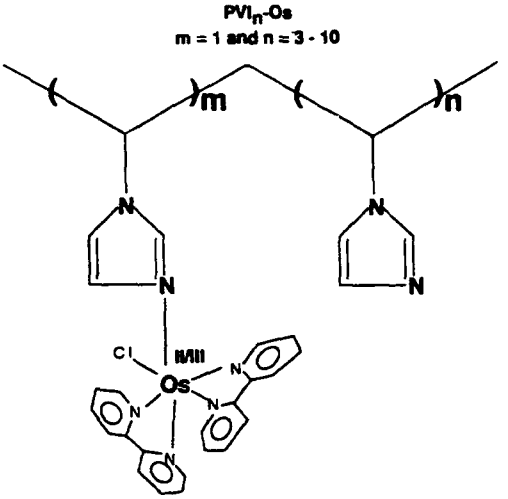

Figure 1. Chemical structure of $Os(bpy)_2Cl$ complexed with poly(1-vinylimidazole).

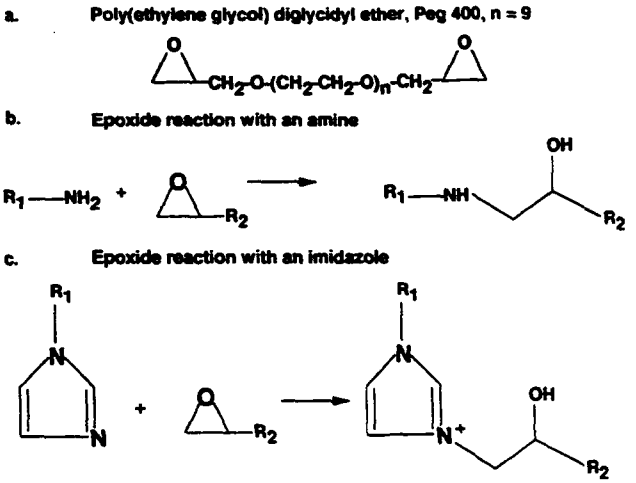

Figure 2. (a) Chemical structure of the diepoxide cross-linking agent. (b) General reaction of an epoxide with an amine. (c) General reaction of an epoxide with an imidazole.

(ethylene glycol) diglycidyl ether (peg 400, Figure 2a) with PVI_n-Os and GOX.

A reference polymer with which the PVI_n-Os polymers is compared is poly(4-vinylpyridine) (PVP) complexed with $Os(bpy)_2Cl$ (POs) and partially quaternized with bromoethylamine (POs-EA).[3] POs is only marginally soluble in water except at high osmium loading. POs-EA is, however, water soluble and easy to cross-link with diepoxides such as peg 400, which binds POs-EA amines and lysyl functions of enzyme proteins (Figure 2b).[4] The resulting redox hydrogel adheres well to the electrodes. In contrast with the PVP-

(1) Heller, A. *J. Phys. Chem.* **1992**, *96*, 3579–3587.
(2) Pishko, M. V.; Michael, A. C.; Heller, A. *Anal. Chem.* **1991**, *63*, 2268–2272.
(3) Gregg, B. A.; Heller, A. *J. Phys. Chem.* **1991**, *95*, 5970–5975.
(4) Gregg, B. A.; Heller, A. *J. Phys. Chem.* **1991**, *95*, 5976–5980.

0003-2700/93/0365-3512$04.00/0

derived polymers, the PVI_n-Os polymers are highly water soluble and do not require quaternization with bromoethylamine for easy cross-linking with water-soluble diepoxides (Figure 2c). The redox potential of PVI_n-Os is 200 mV (SCE) vs 280 mV (SCE) for POs or POs-EA. Because the redox potential of the resulting enzyme electrode is also lower, currents resulting from electrooxidation of some interferants are reduced.

EXPERIMENTAL SECTION

Chemicals. 1-Vinylimidazole (Aldrich), K_2OsCl_6 (Johnson Matthey), 2,2′-bipyridine (Aldrich), (sodium 4-(2-hydroxyethyl)-1-piperazineethanesulfonate) (Na-HEPES; Aldrich), poly(ethylene glycol) diglycidyl ether (Polysciences, peg 400, catalog No. 08210), and glucose oxidase (EC 1.1.3.4) from *Aspergillus niger* (type X-S, 198 units) were used as received. 2,2′-azobis(isobutyronitrile) (AIBN, Polysciences) was purified by double recrystallization from methanol and stored at −20 °C. $Os(bpy)_2Cl_2$ was prepared by a reported procedure.[5]

Poly(1-vinylimidazole) (PVI). Bulk polymerization of PVI was carried out by heating 6 mL of 1-vinylimidazole and 0.5 g of AIBN at 70 °C for 2 h under Ar. A dark yellow precipitate formed soon after heating. After the reaction mixture was allowed to cool, the precipitate was dissolved in methanol and added dropwise to a strongly stirred solution of acetone. The filtered precipitate was a pale yellow hygroscopic solid. The molecular weight of the polymer was found, by HPLC analysis using a Synchrom Catsec 300 column with 0.1% trifluoroaccetic acid and 0.2 M NaCl as the elutant, to be ~7000. The flow rate in the molecular weight determination was 0.4 mL/min, and poly(2-vinylpyridine) was used as the standard.

PVI_n-Os, n = 3, 5, 10. Osmium-derivatized polymers were prepared by a procedure similar to that of Forster and Vos,[6] where the appropriate amount of $Os(bpy)_2Cl_2$ was refluxed with PVI in ethanol for 3 days. The elemental analyses were as follows. Calcd for $[PVI_3\text{-}Os] \cdot 3H_2O$, $C_{35}Cl_2H_{34}N_{10}Os{\cdot}3H_2O$: C, 46.2; H, 4.4; N, 15.4; Os, 20.9. Found: C, 46.4; H, 4.2; N, 15.3; Os, 18.4. Calcd for $[PVI_5\text{-}Os] \cdot 5H_2O$, $C_{45}Cl_2H_{46}N_{14}Os{\cdot}5H_2O$: C, 47.7; H, 5.0; N, 17.3; Os, 16.8. Found: C, 48.2; H, 4.5; N, 16.2; Os, 15.4. Calcd for $[PVI_{10}\text{-}Os]{\cdot}10H_2O$, $C_{70}Cl_2H_{76}N_{24}Os{\cdot}10H_2O$: C, 49.6; H, 5.7; N, 19.9; Os, 11.2. Found: C, 51.1; H, 5.2; N, 18.7; Os, 11.0. The three osmium-derivatized polymers are referred to as PVI_3-Os, PVI_5-Os, and PVI_{10}-Os, where the subscript represents the number of vinylimidazole units per $Os(bpy)_2Cl$.

Electrodes. Rotating disk electrodes were prepared by embedding vitreous carbon rods (3-mm diameter, V-10, Atomergic) in a Teflon shroud using a low-viscosity epoxy (Polysciences, Catalog No. 01916). Electrodes were prepared by syringing a 2-μL aliquot of 5 mg/mL^{-1} PVI_n-Os solution onto the electrode surface (0.071 cm^2). Next, a 2-μL volume of a 4 mg/mL^{-1} (10 mM HEPES, pH = 8.1) solution of glucose oxidase was added onto the electrode and stirred with a syringe needle. In the final step, 1.2 μL of a 2.5 mg/mL solution of peg 400 was added to the electrode and stirred. The electrode was allowed to cure for at least 48 h under vacuum.

Measurements. Electrochemical measurements were performed with a Princeton Applied Research 175 universal programmer, a Model 173 potentiostat, and a Model 179 digital coulometer. The signal was recorded on a Kipp and Zonen X–Y–Y' recorder. Rotating disk electrode experiments were performed with a Pine Instruments AFMSRX rotator with an MSRS speed controller. The three -electrode cell contained 0.1 M NaCl buffered with phosphate (20 mM, pH = 7.2). The current responses of the glucose electrodes were found to have a sigmoidal dependence on potential reaching a plateau in oxidation current at potentials of ≥300 mV (SCE). In the constant-potential experiments, the working electrode was poised at 0.4 V (SCE) well in the plateau of glucose electrooxidation. The chronoamperometric measurements were performed with a Princeton Applied Research Model 273 potentiostat. The potential was initially held at 0.0 V (SCE) for 15 s and then stepped to 0.8 V for 0.3 s. The slopes of the resulting i vs $t^{-1/2}$ plots were unaffected upon varying the residence time (0.1–0.5 s). Three hundred data points were recorded. The reported values are averages of either four or five measurements.

RESULTS AND DISCUSSION

Cyclic Voltammetry of PVI_n-Os-Peg 400-Coated Electrodes. The effect of the extent of cross-linking on the electrochemical behavior of PVI_n-Os (n = 3, 5, 10) films cross-linked with 5–20% peg 400 was determined for electrodes in which the quantity of redox polymer was held constant, with the films cured for >48 h. Coulometry (by cyclic voltammetry at 1 mV/s) showed that ~50% of the osmium was immobilized and that it did not vary with the extent of cross-linking. The cross-linked films adhered well to the vitreous carbon electrodes and retained ~95% of their electroactive osmium when soaked in a stirred phosphate buffer at room temperature for 72 h.

The separation of the oxidation and the reduction peaks (ΔE_p) of the voltammograms at a 100 mV/s scan rate remained constant at ~100 mV through the cross-linking range studied. This contrasts to the results from POs-EA films, where ΔE_p increased with cross-linker (peg 400) concentration, suggesting better electron diffusion kinetics in PVI_n-Os films.[3]

The peak width at half-height (E_{fwhm}) (for the oxidation wave measured at 1 mV/s) increased with the extent of cross-linking from 60 to 110 mV for PVI_n-Os (n = 3, 5, 10). While in the POs-EA system the E_{fwhm} of the oxidation peak was narrower than that of the reduction peak, in the PVI_n-Os-peg 400 systems the two were precisely equal.[3]

Diffusion Coefficients. $D_eC_p^2$ values (D_e being the electron diffusion coefficient and C_p the concentration of the redox couple in the film) were measured for the cross-linked films by potential step chronoamperometry.[7] C_p values were calculated by dividing the moles of electroactive osmium complex (found by cyclic voltammetry at 1 mV/s) by the film thickness. Since all electrodes were prepared with the same amount of osmium redox polymer, they were assumed to have the same film thickness of 0.7 μm based on a density of 1 g/cm^3. There was substantial scatter in the data, suggesting that there was no discernible trend in the dependence of $D_eC_p^2$ on cross-linking (Table I). D_e was, however, higher in the PVI_5-Os polymer films than in the cross-linked POs-EA films by a factor of 5.[3] D_e was higher and nearly identical for PVI_3-Os and PVI_5-Os films and lower for PVI_{10}-Os films.

Effects of Ionic Strength and pH on the Electron Diffusion Coefficients. As seen in Figure 3, $D_eC_p^2$ decreased with increasing NaCl concentration through the 88–2000 mM range. Specifically, $D_eC_p^2$ decreased by ~50% when the NaCl concentration was raised from 88 to 1000 mM NaCl. The anions screen the cationic charges on the polymer and thereby reduce the electrostatic repulsion that straightens the chains. When the electrostatic repulsion is reduced, the chains assume an entropically favored randomly coiled configuration, i.e., the chains, which are reasonably straight at low ionic strength, ball up. When the chains are straight, most of their redox

(5) Lay, P. A.; Sargeson, A. M.; Taube, H. *Inorg. Synth.* **1986**, *24*, 291–299.

(6) Forster, R. J.; Vos, J. G. *Macromolecules* **1990**, *23*, 4372–4377.

(7) Murray, R. W. In *Electroanalytical Chemistry*; Bard, A. J., Ed.; Marcel Dekker: New York, 1984; pp 191–368.

Table I. Effects of the Extent of Cross-Linking and Redox Site Density on $D_eC_p^2$

% peg 400	PVI_3-Os	PVI_5-Os	PVI_{10}-Os
	$D_eC_p^2$ ($\times 10^{16}$ mol^2 cm^{-4} s^{-1})		
20.0	18.7	15.3	1.21
16.7	26.6	7.65	3.46
9.1	38.2	11.3	9.92
4.8	36.0	5.60	3.51
avg $D_eC_p^2$	30.0 ± 9.0	9.96 ± 4.27	4.52 ± 3.75
	D_e ($\times 10^8$ cm^2 s^{-1})		
20.0	0.85	2.34	0.11
16.7	1.29	0.86	0.25
9.1	1.46	1.55	0.68
4.8	2.28	0.57	0.68
avg D_e	1.47 ± 0.60	1.33 ± 0.79	0.43 ± 0.29

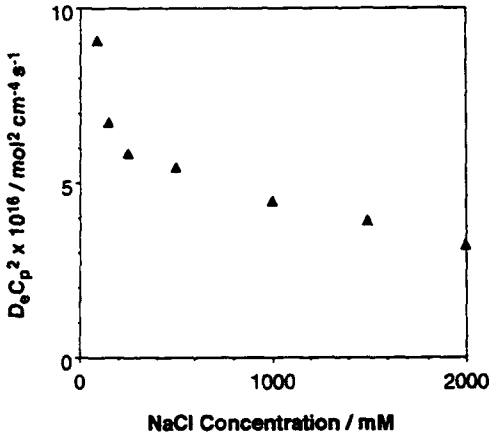

Figure 3. Dependence of $D_eC_p^2$ on the concentration of NaCl for electrodes coated with cross-linked PVI_{10}-Os film with 9.1% peg 400.

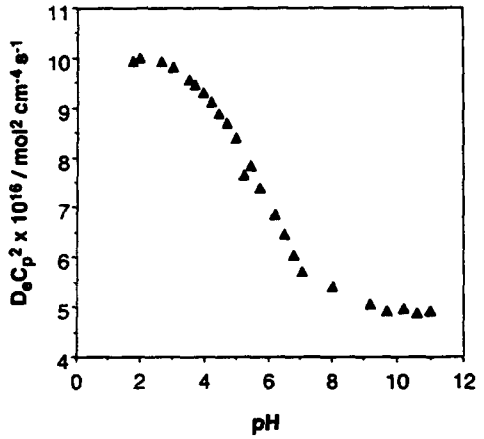

Figure 4. Dependence of $D_eC_p^2$ on the pH for an electrodes coated with PVI_{10}-Os with 9.1% peg 400.

centers are exposed and electrons are transferred through collisions between segments of neighboring chains. When the chains ball up, only their exposed, i.e., surface, redox centers transfer electrons in collisions and D_e is reduced. Even though C_p increases with ionic strength, the loss in D_e is so great that $D_eC_p^2$ is also reduced.[8]

Figure 4 shows the pH dependence of $D_eC_p^2$ in 0.2 M NaCl. The observed decrease in $D_eC_p^2$ at pH = 4 coincides with the pK_a of PVI.[9] As the PVI is deprotonated the repulsive forces within the network are decreased and the mobility of chain segments, which apparently control electron transport, diminish. The pH dependence of D_e was similar to that observed in the POs-EA-peg 400 system[3,10] where charging of the network facilitated electron transfer. In PVI_n-Os networks swelling at low pH should decrease C_p. Nevertheless, the increase in D_e was so large that $D_eC_p^2$ still increased.

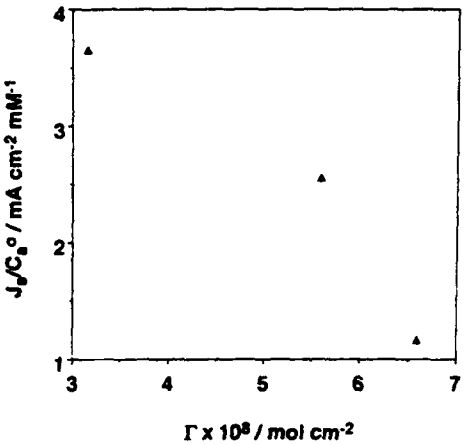

Figure 5. Benzoquinone permeation current density per millimolar concentration as a function of surface coverage. The benzoquinone concentration was 1.1 mM and the scan rate used was 5 mV/s. Gold electrode area was 0.071 cm^2, and the reduction currents were measured at −0.5 V (SCE).

Permeability of PVI_n-Os-Peg 400 Hydrogels. Permeability of the hydrogels to water-soluble substrates and products is important in biosensor applications. For the analysis of permeability, *p*-benzoquinone was chosen as a model compound because of its known electrochemistry and its nonionic nature. The diffusional and kinetic characteristics of benzoquinone partitioning through an electrode film has been analyzed by Saveant et al.,[11] who measured limiting current densities for rotating disk electrodes and obtained Koutecky–Levich plots for polymer film electrodes. Benzoquinone is reduced at pH = 7 at ~0.2 V negative of the redox potential of PVI_n-$Os^{II/III}$, i.e., at a potential where benzoquinone cannot be catalytically reduced by PVI_n-Os^{II}. The benzoquinone electroreduction current densities were measured as a function of osmium loading (Figure 5). The current densities decreased upon increasing osmium loading more rapidly than they did in POs-EA films. A cross-linked PVI_3-Os film having 6.6×10^{-8} mol/cm^2 osmium sites reached a current density of 1.2 mA/cm^2 at 1 mM benzoquinone, while a POs-EA film with 9.7×10^{-8} mol/cm^2 Os sites had a current density of 2 mA/cm^2 at 1 mM benzoquinone.[3] Apparently, ethylamine groups in POs-EA films loosen the cross-linked structure.

Steady-State Amperometric Glucose Response of Cross-Linked PVI_n-Os Films Containing GOX. The steady-state electrooxidation current was measured at 1000 rpm as a function of the amount of enzyme in the films at 48 mM glucose concentration, well above the K_m of the electrodes (Figure 6). In electrodes prepared with a fixed amount of 10 μg of PVI_n-Os (n = 3, 5, 10), 12% peg 400 (by weight), and 0.5–8 μg of GOX, the current densities did not vary with the osmium content of the polymers, the sensor response being controlled by the amount of enzyme. The currents were highest in electrodes containing 8 μg of GOX, corresponding to 39 wt %. In a series of electrodes made with 39% GOX

(8) Degani, Y.; Heller, A. *J. Am. Chem. Soc.* **1989**, *111*, 2357–2358.
(9) Tan, J. S.; Sochor, A. R. *Polym. Prepr.* **1979**, *20*, 15–18.
(10) Aoki, A.; Heller, A. *J. Phys. Chem.*, in press.
(11) (a) Andrieux, C. P.; Haas, O.; Saveant, J. M. *J. Am. Chem. Soc.* **1986**, *108*, 8175–8182. (b) Andrieux, C. P.; Saveant, J. M. *J. Electroanal. Chem.* **1982**, *134*, 163–166. (c) Andrieux, C. P.; Dumas-Bouchiat, J. M.; Saveant, J. M. *J. Electroanal. Chem.* **1982**, *131*, 1–35. (d) Andrieux, C. P.; Dumas-Bouchiat, J. M.; Saveant, J. M. *J. Electroanal. Chem.* **1984**, *169*, 9–21. (e) Ledy, J.; Bard, A. J.; Maloy, J. T.; Saveant, J. M. *J. Electroanal. Chem.* **1985**, *187*, 205–227.

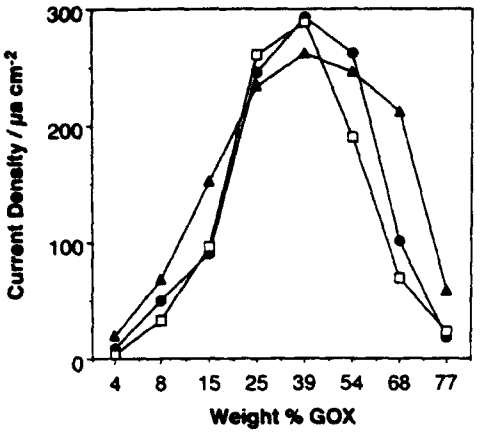

Figure 6. Dependence of the limiting catalytic current density on the GOX weight fraction for PVI_n-Os [n = 3 (circles), 5 (squares), 10 (triangles)] cross-linked with 12% peg 400; 48 mM glucose, 1000 rpm, 20 mM phosphate, pH = 7.2, air.

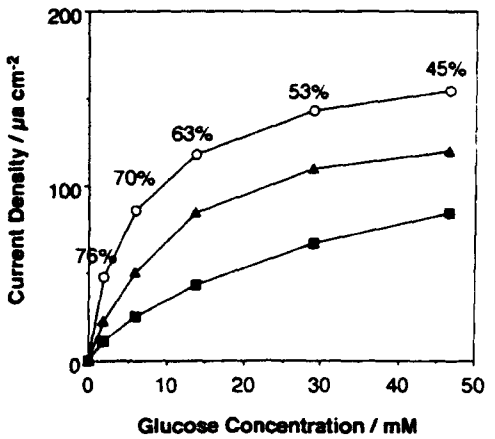

Figure 7. Dependence of the steady-state current density on the glucose concentration for the same electrode under N_2 (circles), air (triangles), and O_2 (squares). Electrode coated with 10 μg of PVI_3-Os, 8 μg of GOX, and 2.5 μg of peg 400; at 1000 rpm.

and cross-linker concentrations varying between 2 and 22%, the highest current densities were observed in electrodes made with 12% cross-linker. Above 68% enzyme content, the current densities are highest for PVI_{10}-Os, the polymer having the lowest density of redox centers. Evidently, electron-transferring collisions of chains, not electron hopping between neighboring sites, now limit the transport of electrons.

Glucose Diffusion through Cross-Linked Films. Increasing the rotation rate from 100 to 2500 rpm at 10 and 48 mM glucose concentrations did not substantially affect the glucose electrooxidation currents. At 1 mM glucose concentration under a nitrogen atmosphere, the current decreased only by 14% when the rotation rate was reduced from 2500 to 100 rpm. As will be discussed later, this was not the case when the solution was O_2 saturated. The absence of greater dependence of current density on rotation rate suggests that the currents were controlled primarily by a process within the films and not by mass transport to the films at >1 mM glucose. Thus, from the measured 1.2 mA/cm² current density for benzoquinone, and assuming that glucose and benzoquinone permeation rates do not differ greatly, one can conclude that, unless limited by the activity of the enzyme, the current density is limited either by the rate of electron transfer to the redox polymer from the enzyme's $FADH_2$ centers or by electron diffusion through the cross-linked polymer.

O_2 Effects on Glucose Response. The steady-state glucose response is shown in Figure 7 for a typical cross-linked electrode (10 μg of PVI_3-Os, 8 μg of GOX, and 2.5 μg of peg 400) under N_2, air, and O_2 at 1000 rpm. Evidently, O_2 competes effectively with PVI_3-Os in the oxidation of $FADH_2$ centers.

At 48 mM glucose, the glucose electrooxidation current decreased by 45% when the bubbled gas was switched from N_2 to O_2. At 2 mM glucose, the decrease was 76%. Apparently, at high glucose concentrations the O_2 flux is consumed in the outer layer of the film, while a substantial inbound glucose flux survives oxidation by O_2 and penetrates the film. Consistently, the loss in current upon switching the atmosphere from N_2 to O_2 was reduced not only at high glucose concentrations but also when thicker cross-linked films were employed or when the films were heavily loaded with GOX. Furthermore, upon decreasing the O_2 flux through stopping the 1000 rpm rotation of the electrodes, the O_2-associated loss diminished (Figure 8). The glucose electrooxidation current at >6 mM glucose was greater when the electrode rotation was stopped because of the decrease in O_2 flux (Figure 9). Below 6 mM glucose the behavior was, however, normal;

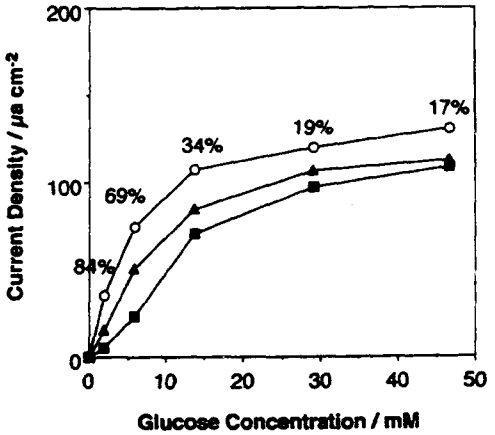

Figure 8. Dependence of the steady-state current density on the glucose concentration under N_2 (circles), air (triangles), and O_2 (squares). Electrode coated as in Figure 7. Stagnant solution (no rotation).

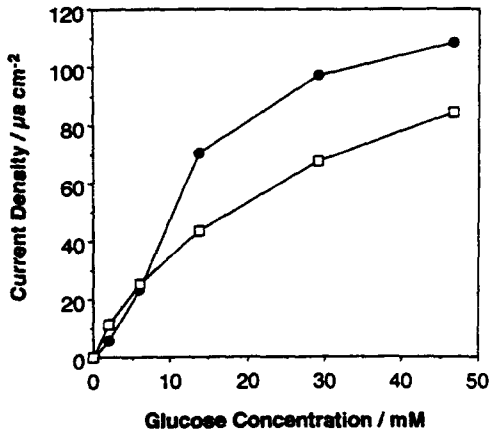

Figure 9. Dependence of the steady-state current density on the glucose concentration under O_2 at 1000 rpm (squares) and under stagnant conditions (circles). Electrode coated as in Figure 7.

i.e., the currents were higher for the rotating electrode, being dominated by glucose flux.

Dependence of the Glucose Response on Film Thickness. Electrodes with films having 1.1×10^{-9}–9.7×10^{-8} mol/cm² electroactive osmium were studied. For this experiment, all electrodes were prepared with a constant percentage of PVI_3-Os (49%), GOX (39%), and peg 400 (12%). A plot of the steady-state glucose electrooxidation current at 48 mM as a function of the amount of osmium in the enzyme/polymer

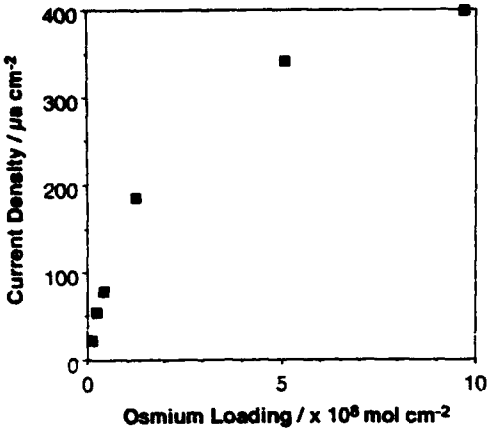

Figure 10. Dependence of the limiting catalytic current density on the amount of electroactive osmium in the enzyme/polymer film. Electrodes were prepared with a constant percentage of PVI_5-Os (49%), GOX (39%), and peg 400 (12%). Conditions as in Figure 6 with 48 mM glucose.

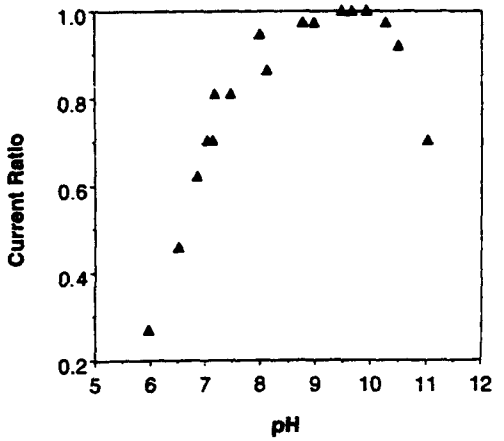

Figure 11. Dependence of the steady-state current density on pH. Electrode coated with 10 μg of PVI_5-Os, 8 μg of GOX, and 2.5 μg of peg 400. Conditions as in Figure 6.

film is shown in Figure 10. The current density increased with the amount of osmium in the enzyme/polymer film. The trend seen in Figure 10 is similar to that observed for POs-EA.[4]

pH and NaCl Concentration Dependence of the Glucose Electrooxidation Currents. The dependence of the current density on pH is shown in Figure 11. As in the case of POs-EA,[12] the catalytic current peaked at and was nearly independent of pH from pH = 7.5 to pH = 10, in contrast with the GOX-catalyzed oxidation of glucose by O_2, where a narrow pH optimum near 5.5 has been observed. Current was lost irreversibly at pH >10.

The dependence of the current density on NaCl concentration is shown in Figure 12 for a 10 mM phosphate buffer solution (pH = 7.2). The highest glucose current is observed at 0 mM NaCl with an onset in current loss occurring at 100 mM NaCl. As discussed earlier, at high NaCl concentration, the charge on the cationic polymer is screened. This causes coiling of the redox polymer, prevents its conforming to the oppositely charged enzyme surface, and results in poor electron transfer from the enzyme to the redox polymer. A decrease in current with ionic strength has been reported earlier for a similar system.[8]

Selectivity against Interferants. Glucose sensors are often insufficiently selective when operated at potentials where urate, ascorbate, and acetaminophen are also electrooxidized. The resulting errors can be reduced by membranes that preferentially transport glucose. Examples of such membranes are cellulose acetate[13] and Nafion.[14] The effects of interferants can also be reduced by poising the electrodes at more negative potentials, where the rate of interferant electrooxidation is reduced.[15] Since the redox potential of PVI_n-Os is cathodic relative to that of POs-EA by 80 mV, the PVI_n-Os electrodes are more selective. When required, glucose selectivity can be further improved by nonelectrochemical catalytic preoxidation of the interferants by H_2O_2 in an outer film of horseradish peroxidase.[16]

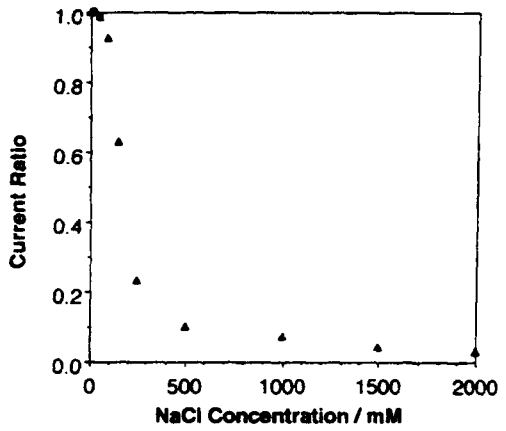

Figure 12. Dependence of the steady-state current density on NaCl concentration. Electrode coated with 10 μg of PVI_5-Os, 8 μg of GOX, and 2.5 μg of peg 400. Conditions as in Figure 6.

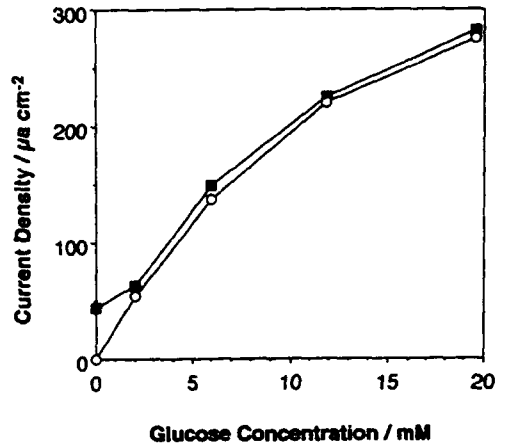

Figure 13. Dependence of the steady-state current density on glucose concentration in the presence of 0.1 mM ascorbate (squares) and without ascorbate (circles). Electrode coated with 40 μg of PVI_5-Os, 32 μg of GOX, and 10 μg of peg 400.

Figure 13 shows a glucose calibration curve for a thick-film electrode (prepared with 560 μg/cm² PVI_5-Os, 450 μg/cm² GOX, and 140 μg/cm² peg 400) in the absence and presence of 0.1 mM ascorbate. Although in the absence of glucose the ascorbate electrooxidation current was high, this current was small with >2 mM glucose. The current was increased by the 0.1 mM ascorbate at 6 mM glucose by 9%, corresponding to a +0.5 mM error in the glucose reading. The error was further reduced when the glucose concentration was increased. Thus, at 20 mM glucose, the error was only 2%. The error reported represents the change in overall net oxidation current when ascorbate is added.

(12) Katakis, I.; Heller, A. *Anal. Chem.* **1992**, *64*,1008–1013.

(13) Lobel, E.; Rishpon, *J. Anal. Chem.* **1981**, *53*, 51–53.

(14) Bindra, D. S.; Wilson, G. S. *Anal. Chem.* **1989**, *61*, 2566–2570.

(15) Cass, A. E. G.; Davis, G.; Francis, G. D.; Hill, H. A. O.; Aston, W. J.; Higgins, I. J.; Plotkin, E. V.; Scott, L. D. L.; Turner, A. P. F. *Anal. Chem.* **1984**, *56*, 667–671.

(16) Maidan, R.; Heller, A. *Anal. Chem.* **1992**, *64*, 2889–2896.

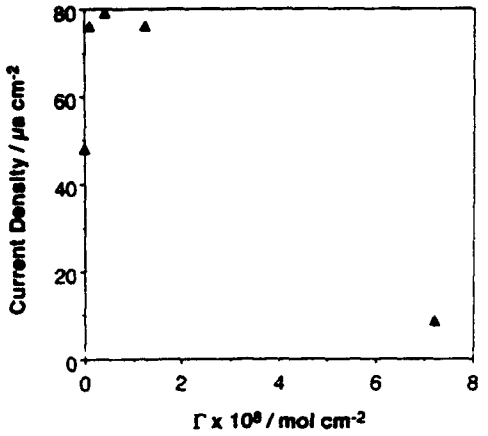

Figure 14. Dependence of the steady-state oxidation current of 0.1 mM ascorbate film thickness. Electrodes prepared with PVI_5-Os (49%), GOX (39%), and peg 400 (12%). Conditions as in Figure 6.

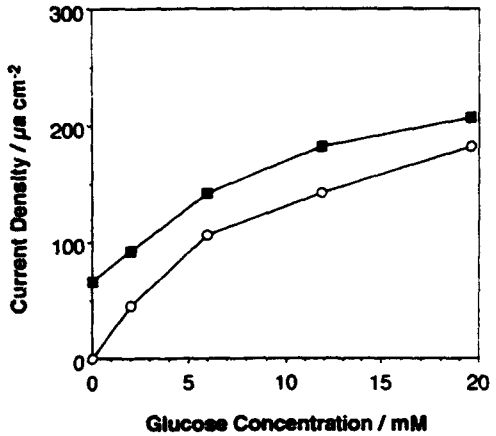

Figure 15. Dependence of the steady-state current density on glucose concentration in the presence of 0.1 mM ascorbate (squares) and without ascorbate (circles). Electrode coated with 10 μg of PVI_5-Os, 8 μg of GOX, and 2.5 μg of peg 400.

When the glucose electrodes were made with thick PVI_5-Os films, the ascorbate- and acetaminophen-caused currents decreased in the absence of glucose. Figure 14 shows the change in ascorbate current with film thickness. Interferants can be electrooxidized either at the electrode surface (I_{surf}), at osmium redox sites (I_{Os}), or at both. Reduction in interference with increasing film thickness is interpreted as resulting from a lesser flux of ascorbate to the carbon surface (i.e., from reduced I_{surf}) and/or from a decrease in ascorbate oxidation at the outer osmium sites, because of slow electron diffusion. Because both ascorbate and $FADH_2$ are oxidized by a limited number of Os^{III} sites, I_{Os} decreases upon increasing the glucose concentration. At 0 mM glucose, the concentration of Os^{III} sites is the highest and I_{Os} is largest. Upon increasing the glucose concentration, I_{Os} decreases. Note that if ascorbate rather than a $FADH_2$ center is oxidized by an Os^{III} center, then the glucose electrooxidation current (I_G) is decreased and the increase in I_{Os} is offset by the decrease in I_G.

In thin-film electrodes the situation is quite different. The glucose response is shown in Figure 15 for an electrode with a thin film (140 μg/cm² PVI_5-Os, 110 μg/cm² GOX, 35 μg/cm² peg 400) in the absence and in the presence of 0.1 mM ascorbate. The ascorbate-related current increment is large, doubling the current at 6 mM glucose. Evidently, in thin-film electrodes I_{surf} introduces a large error. The oxidation of ascorbate is strongly rotation rate dependent, in contrast with the glucose electrooxidation rate, which is nearly independent of the rotation rate.

Thick-film PVI_n-Os-based glucose electrodes were also selective against acetaminophen. The glucose response curve with 1 mM acetaminophen was similar to that shown for 0.1 mM ascorbate. The addition of urate caused, however, an initial increase in oxidation current, followed by a rapid decay. Cyclic voltammetry confirmed urate electrooxidation by Os^{III} sites and a resulting loss in the surface density of these sites.

CONCLUSIONS

The poly(vinylimidazole)-derived redox polymers PVI_n-Os form with GOX, upon cross-linking with a water-soluble diepoxide, hydrogels that are permeable to glucose and through which electrons diffuse. The polymer is simpler and easier to make than the earlier reported poly(vinylpyridine)-derived POs-EA and does not require modification with primary amine for cross-linking with a diepoxide at ambient temperature in an aqueous solution. Electrons diffuse through the gel through a chain flexing dependent mechanism; i.e., the rate of electron diffusion is not controlled by hopping between neighboring redox sites within chains, but by collisions between segments of redox polymer chains. Amperometric glucose sensors made with thick PVI_n-Os- and GOX-based gels are reasonably selective in their glucose response in the presence of the electroxidizable interferants ascorbate and acetaminophen.

ACKNOWLEDGMENT

We acknowledge support of this work by the Office of Naval Research, The National Science Foundation, The National Institutes of Health, and the Robert A. Welch Foundation. We especially thank Ioanis Katakis and Dr. Nigel Surridge for insightful comments.

RECEIVED for review April 28, 1993. Accepted September 15, 1993.•

• Abstract published in *Advance ACS Abstracts*, October 15, 1993.

Reprinted from The Journal of Physical Chemistry, 1993, 97.

Electron Diffusion Coefficients in Hydrogels Formed of Cross-Linked Redox Polymers

Atsushi Aoki and Adam Heller*

Department of Chemical Engineering, The University of Texas at Austin, Austin, Texas 78712-1062

*Received: January 13, 1993; In Final Form: July 7, 1993**

The apparent electron diffusion coefficient (D_e) for the redox polymer POs-EA, an ethylamine quaternized poly(4-vinylpyridine) complex of $[Os(bpy)_2Cl]^{+/2+}$ (bpy = 2,2′-bipyridine) chloride, has been measured by steady-state voltammetry at interdigitated array (IDA) electrodes. In cross-linked POs-EA D_e decreased upon deprotonation of the pyridine rings at pH ≥ 4, upon increasing the ionic strength, and upon replacing the well-hydrated chloride counterion by the less-hydrated perchlorate counterion. In moderately cross-linked POs-EA (5 wt % cross-linker) D_e increased from 4.5×10^{-9} to 1.6×10^{-8} cm^2 s^{-1} when the pyridine rings were protonated, but in highly cross-linked POs-EA (25 wt % cross-linker), where the motion of the chain segments was restricted, D_e was independent of pH. The results suggest that D_e increases with the hydration of the cross-linked redox polymer.

Introduction

The transport of electrons and ions through redox polymers has been the subject of intensive study during the past two decades.[1] A subgroup of these materials, consisting of redox hydrogels formed by cross-linking water-soluble redox polymers, is of particular interest in the context of biosensors.[2-5] When redox enzymes are integrated in the cross-linked polymer, electrons are transported via the redox polymer network between the enzymes' reactive centers and electrodes. An example of a cross-linkable enzyme-connecting redox polymer is poly(4-vinylpyridine) partially complexed with osmium bis(2,2′-bipyridine)chloride and partially quaternized with 2-bromoethylamine, (designated POs-EA).[2] The dynamic electron-relaying properties of this polymer are of importance in defining its current carrying capacity from enzyme redox centers to electrodes. Realization of high-current density electrodes, made with thick, enzyme-loaded hydrogel films, requires that both electron transport and substrate/product mass transport be rapid. Water-soluble substrates and products permeate usually rapidly through the hydrogels, where their solubilities and diffusion coefficients approach those in water. The electron diffusion coefficients in diepoxide-cross-linked polycationic POs-EA hydrogels depend on the pH, on the nature of the counterion and on the ionic strength of the contacting aqueous solution. Specifically, electron diffusion increases when the polymer network is charged by protonation of its free pyridines and decreases either if Cl^-, a hydrophilic counterion, is replaced by ClO_4^-, a less hydrophilic counterion, or when the ionic strength is raised.

Transport of electrons, i.e., self-exchange between identical redox centers of POs-EA, involves both charge propagation along the polymer's backbone (through σ and other chemical bonds) and collisions between segments of the folded polymer. The colliding segments may be spatially in each other's proximity, even if separated by a long sequence of bonds. When propagating along bonds in chains, electrons hop between neighboring redox sites, traversing occasionally cross-linker segments. Such hopping, while possible, results in a much longer path and in a more resistive route than the combination of hopping between neighboring redox sites of chains and electron-transferring collisions between redox polymer segments. Electron transport involving both σ bonds and hopping through space together accounts better for observed electron-transfer rates in proteins than either electron transfer exclusively along tortuous σ-bond sequences or exclusively along the shortest route where electrons propagate by jumping across spaces between protein segments.[6] Because the rate of electron transport along bonds of a polymer's backbone decays relatively slowly with distance, but the tortous electron route is long, while the rate of electron transport between chains decay rapidly with distance, but the electron route is short, an optimum must exist where the resistances along the backbone and collision routes are equal. Segmental motion of the polycationic polymer backbone involves significant displacement of anions.[7] The balance between electron routing along redox polymer chains and routing between chains depends on the flexibility of the redox polymer backbone,[8] the nature of the redox centers,[9] and their density.[10]

The transport of electrons through redox polymers is measured by their apparent electron diffusion coefficients, D_e, which can be measured by transient[7,8,11] and steady-state[9,10,12-16] electrochemical methods. The transient methods included cyclic voltammetry,[7] chronoamperometry,[2f,7] chronocoulometry,[8] and pulse techniques.[11] Because of the macroscopic movement of counterions into and out of the polymer films upon oxidation or reduction, interpretation of the measurements requires separation of the electronic and ionic components of the measured response. Andrieux and Savéant have shown that the mobility and concentration of the counterion do indeed affect the transient response in films that are highly redox site loaded and that the lesser the mobility or concentration of the counterion, the more the transient current is affected by ion migration.[17] The need for sorting out the response component resulting from macroscopic ion migration is avoided in steady-state measurements; sandwich,[9] rotating ring-disk,[12] and interdigitated array (IDA) electrodes[13-16] were all used for such measurements. As shown by Savéant,[18] even though the current response does not depend in these measurements on the diffusion coefficient of the mobile counterion, it still depends on microscopic counterion displacement. Steady-state voltammetry is, nevertheless, the method of choice for measuring D_e in redox polymers. Furthermore, steady-state voltammetry with IDA electrodes allows direct measurement of D_e and has the advantage of not requiring knowledge of the film thickness or of the concentration of the redox centers in the polymer.[13] If the spacings between the fingers are narrowed to micron dimensions and the arrays are made with a large number ($\sim 10^2$) of fingers, then D_e can be measured accurately even if it is much smaller than the coefficient of diffusion of ions in liquid solutions. For this reason, we chose for measurements of D_e the IDA-based method of Murray and co-workers[13] in our

* Abstract published in *Advance ACS Abstracts*, September 15, 1993.

0022-3654/93/2097-11014$04.00/0

SCHEME I

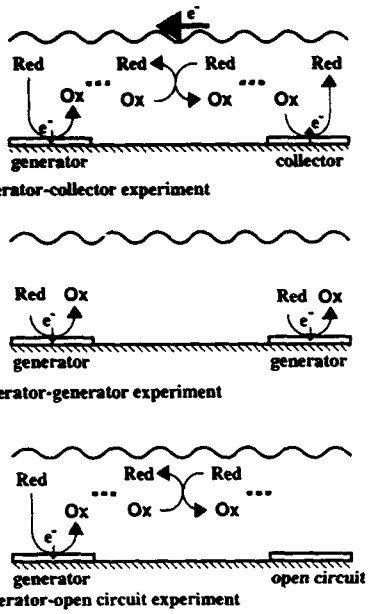

films made by cross-linking the water soluble POs-EA with water soluble poly(ethylene glycol)diglycidyl ether (PEGDE).[2]

The principle of steady-state voltammetry with IDA electrodes is shown in Scheme I. In the generator–collector experiment (Scheme IA), the potential of the electrode on the left—the generator—is swept from reducing to oxidizing. The collector (on the right) is maintained at a fixed sufficiently reducing potential to collect the electron vacancies produced at the generator. The steady-state concentration profile of redox sites through the zone between the generator and the collector depends on the potential at which the generator is poised.

The total charge (Q) of the electroactive centers is obtained in a generator–generator experiment, shown in Scheme IB. Here, the potential is swept at both electrodes so that the polymer is first fully reduced then fully oxidized. Integration of the voltammogram yields the charge Q. Once Q is known D_e is calculated by eq 1,[13] where I_{SS} is the steady-state anodic current

$$D_e = \frac{I_{ss}}{\omega Q} gap(w + gap)\frac{N}{N-1} \qquad (1)$$

plateau reached in the generator–collector experiment, i.e., the current flowing when the oxidizing potential on the generator is sufficient to cause the current to be limited by electron diffusion to the collector; ω is a correction factor for microscopic counterion displacement;[18] N is the number of fingers; w and gap are the finger and gap widths, respectively. Equation 1 was derived assuming a linear concentration gradient between the generator and the collector electrodes. Microscopic counterion displacement and dependence of the local polymer fluidity on oxidation state[19] may distort the linearity. Simulations by Fritsch-Faules and Faulkner[19] and Goss and Majda[16] suggest nonlinearity. Fritsch-Faules and Faulkner,[20] who experimentally observed linear concentration profiles in quaternized poly(4-vinylpyridine), i.e., a poly(4-vinylpyridinium) matrix with dissolved $Fe(CN)_6^{3-/4-}$, on individually addressable electrodes in microelectrode arrays, explained the linearity by diffusion of $Fe(CN)_6^{3-/4-}$ through the contacting solution. Diffusion of $Fe(CN)_6^{3-/4-}$ in the polymer itself could not account for the linearity observed.[20] Here we shall not attempt to account for actual or possible nonlinearity in the concentration profile. Rather we consider the D_e values that we derive as an average for the concentrations of reduced or oxidized centers between the generator and collector electrodes. These are likely to differ at different points. For this average concentration we calculate, from I_{SS}, Q and the geometry, a value of the apparent D_e.

The values of the apparent D_e that we obtain in hydrogels may be compared with values obtained by Murray et al.[9] for electropolymerized $Os(bpy)_2(vpy)_2^{2+/3+}$ (bpy = 2,2′-bipyridine, vpy = 4-vinylpyridine) and $Os(vbpy)_3^{2+/3+}$ (vbpy = 4-methyl-4′-vinyl-2,2′-bipyridine). These osmium complexes had, respectively, two or three vinyl groups, causing extensive cross-linking and formation of rigid matrixes. Our D_e values may also be compared with those of Oh and Faulkner,[8] who studied poly(4-vinylpyridine)-based systems with both electrostatically held and coordinatively attached redox centers and estimated the concentration of redox centers in their dry polymers by chronocoulometry. Our study of effects of the ionic strength on D_e follows work by Anson and Savéant,[21] who showed that in polymers that were highly loaded with ions and had lower dielectric constants, ionic association lowered D_e. Study of the POs-EA/PEGDE hydrogel by steady-state voltammetry at IDA electrodes shows that protonation of the backbone and presence of the hydrophilic Cl^- counterion—both of which lead to hydration—increase the apparent D_e. High NaCl concentrations and presence of the relatively hydrophobic ClO_4^- counterion decrease the apparent D_e. Overall, our findings agree with the suggestion that D_e is enhanced when motion of segments of a redox polymer allows collisional electron transfer between segments. Such electron-transferring collisions evidently shunt the longer, equally significant, tortous routes involving redox-site to redox-site hopping of electrons along the backbone of redox polymers.

Experimental Section

Chemicals. POs-EA was prepared as described.[2f] The polymer consisted of 50 kDa poly(4-vinylpyridine) (PVP) partially complexed with $Os(bpy)_2Cl_2$ (Os) and quaternized with 2-bromoethylamine (EA). The PVP/Os/EA ratio was 6:1:1.2. Thus, 63% of the pyridine group were not quaternized. The diepoxide used for cross-linking the POs-EA was poly(ethylene glycol) diglycidyl ether (Polyscience, PEG400). The experiments were performed in a (pH = 7.0) 20 mM phosphate buffer solution with 0.1 M NaCl. All chemicals were reagent grade and were used without further purification.

Apparatus. A Pine Instruments RDE-4 bipotentiostat with a x–y–y' Kipp and Zonnen recorder was used. The single-compartment water-jacketed electrochemical cell had Pt auxiliary and saturated calomel electrode (SCE) reference electrodes. The experiments were carried out under N_2 at room temperature (20 ± 1 °C).

IDA Electrodes. The IDA electrodes were fabricated by conventional photolithography using liftoff of a positive photoresist (Hoechst, AZ 1350J-SF). Gold was sputter-deposited onto the chromium-primed glass substrate with the patterned resist as described earlier.[20,22] The IDA consisted of 100 (N), 2.0-mm-long, 5.0-μm-wide fingers (w), separated by 5.0-μm gaps (gap). Except for the finger area the electrodes were coated with the photoresist. For quality control, cyclic voltammograms for 2.0 mM ferrocenecarboxylic acid were obtained at a 5.0 mV/s scan rate. The voltammogram shape, the steady-state current, and the collection efficiency were as predicted by theory.[23]

After the test, IDA electrodes were prepared by pipetting premixed solutions of 20 μL of POs-EA (5.0 mg/mL) and 2.5 μL of PEGDE (2.0 mg/mL) onto both the finger and the internal gap areas and allowing the water to evaporate at room temperature. The electrodes were then left to cure in air at ambient temperature for 24 h.

Three experiments were performed on the POs-EA/PEGDE coated IDA electrodes (Scheme I). In the generator–collector experiments (Scheme IA), cyclic voltammograms were obtained by scanning the potential of the generator from 0.0 (SCE) to 0.6 V (SCE) at various scan rates, while maintaining the potential

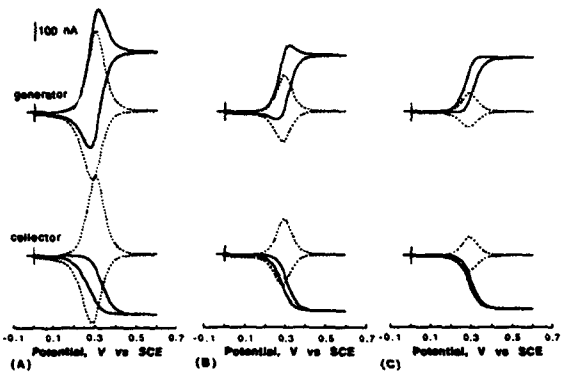

Figure 1. Scan rate dependence of the cyclic voltammograms for POs-EA cross-linked with 5.0 wt % PEGDE coated on IDA electrodes, at an $[Os(bpy)_2vpyCl]^{+/2+}$ site coverage of $\Gamma = 9.60 \times 10^{-9}$ mol cm^{-2} in 20 mM phosphate buffer at pH 2.89 containing 0.1 M NaCl. Generator–collector (solid line), generator–generator (dotted line) voltammograms are shown for (A), 5.0; (B), 2.0; (C), 1.0 mV s^{-1} scan rates.

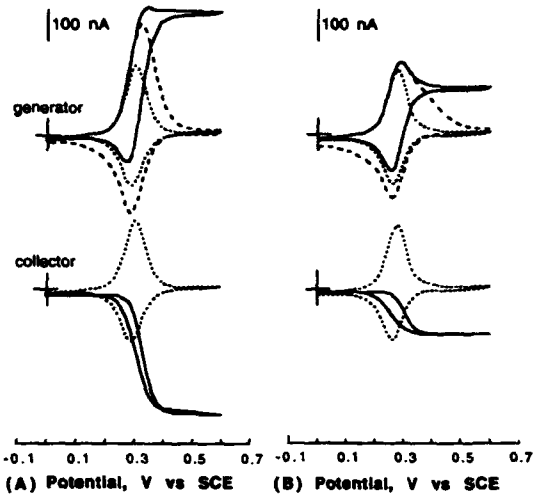

Figure 2. Ionic strength dependence of cyclic voltammograms for POs-EA cross-linked with 5.0 wt % PEGDE coated on IDA electrodes, at an $[Os(bpy)_2vpyCl]^{+/2+}$ site coverage of $\Gamma = 1.93 \times 10^{-8}$ mol cm^{-2} in 20 mM phosphate buffer at pH 7.0 and at 1.0 mV s^{-1} scan rate. Generator–collector (solid line), generator–open circuit (dashed line), generator–generator (dotted line) voltammograms are shown for (A), 0.1 M; (B), 1.0 M NaCl.

of the collector at 0.0 V (SCE). In the generator–generator experiments (Scheme IB), the voltammograms were obtained by scanning the potentials of both IDA electrodes from 0.0 V (SCE) to 0.6 V (SCE) at various scan rates. In the generator–open circuit experiment (Scheme IC), the voltammogram was obtained by scanning the potential of the generator from 0.0 V (SCE) to 0.6 V (SCE), while the other IDA electrode was disconnected.

Results and Discussion

Electrochemical Behavior. Figure 1 shows the cyclic voltammograms for POs-EA, cross-linked with 5.0 wt% PEGDE, at various scan rates. The voltammograms of the generator–collector experiments are shown as solid lines and those of the generator–generator experiments are represented by dotted lines. The voltammograms of the generator–generator experiments (dotted line) exhibited well-defined surface waves at both IDA electrodes. The waves were almost symmetrical and the peak currents were nearly proportional to the scan rate. Cyclic voltammetry confirmed that the $[Os(bpy)_2vpyCl]^+$ centers were completely oxidized both on the fingers and in the internal gaps. The charge (Q) of the POs-EA polymer coated IDA electrodes was calculated by integrating the currents of the voltammograms of the generator–generator experiments which equalled 9.26 μC and corresponded to an $[Os(bpy)_2vpyCl]^{+/2+}$ coverage of 9.60×10^{-9} mol cm^{-2} at all scan rates.

The voltammograms of the generator–collector experiments (solid lines) show that a steady-state current was reached at 0.6 V (SCE). The generator voltammograms differed from those of the collector in that the collector voltammograms were sigmoidal at all of the scan rate. The shapes of the generator voltammograms changed with the scan rate, while the generator current equalled, at a given potential, the sum of the collector current of the generator–collector experiment and the current of the generator–generator experiment. Thus, when the peak current in the generator–generator experiment reached a substantial fraction of the steady-state current, the generator voltammogram of the generator–collector experiments also showed a peak (Figure 1A,B). However, when the peak current of the generator–generator experiment was small relative to the steady-state current, the generator voltammogram had a sigmoidal shape (Figure 1C). The steady-state current was that expected for $[Os(bpy)_2vpyCl]^+$ oxidation at the generator, transport of electrons through the redox polymer and rereduction of $[Os(bpy)_2vpyCl]^{2+}$ sites at the collector. The anodic limiting current was identical to the cathodic one, and the limiting current was independent of scan rate. The observed hysteresis between forward and backward potential sweeps at the collector electrode was caused by the insufficiency of time for establishment of steady-state concentration profiles at the applicable scan rates and the hysteresis decreased when the scan rate was slower. The results show the existence of a steady-state $Os^{II+/III+}$ concentration profile between the generator and the collector electrodes and establish that charge transport through the POs-EA polymer limits the current. The steady-state current is expected, however, to be affected by microscopic counterion displacement[18] and to be slightly in excess of the electron diffusion current. According to Savéant's theory,[18] the value of the correction factor ω is 1.114 for $[Os(bpy)_2vpyCl]^{+/2+}$ and a monovalent counterion, such as Cl^- or ClO_4^-. However, the theory assumes that the only mobile ion in the film is the counterion and that the electroneutrality of the film is maintained only by the counterion. This assumption is valid only for perfect Donnan exclusion of ions from the film. In a well-hydrated open-network redox hydrogel, the supporting electrolyte permeates the film and allows the concentrations of the ions in the bulk of the solution and the hydrogel to approach each other. Thus, in swollen hydrogels microscopic counterion transport should affect the current less than predicted by Savéant's theory, and that ω in eq 1 should approach 1.0. For $\omega = 1$, the calculated value of D_e is 1.6×10^{-8} cm^2 s^{-1} at pH 2.89. As pointed out earlier, we do not account for spatial nonlinearity of the concentration profile of $Os^{II+/III+}$ caused by the variation in polymer fluidity with the oxidation state of the redox centers in the gaps between the microanodes and microcathodes,[19] and the calculated D_e value represents on average for the polymer between the generator and the collector.

Effect of the Ionic Strength and the Anionic Species on D_e. The voltammograms of Figure 2 show that D_e depends strongly on ionic strength. When the concentration of NaCl was raised from 0.1 to 1.0 M, Q remained constant but I_{SS} decreased. Moreover, in the generator–open circuit experiment (dashed line), a shoulder, indicating lateral electron diffusion between the fingers (Scheme IC) was seen. This shoulder is a consequence of the distance between two fingers (15 μm) being much larger than the film thickness. While the shoulder was sharp in 0.1 M NaCl, a diffusional tail was observed in 1.0 M NaCl. D_e decreased logarithmically with the NaCl concentration above 0.1 M NaCl (Figure 3A). Below 0.1 M NaCl, where the ionic strength was controlled by the 20 mM phosphate concentration and not by the NaCl concentration, D_e was constant. Earlier results obtained by transient methods suggested that D_e slightly increases with ionic strength at a constant density of redox sites in film.[2f,7b] The effective density of redox sites would, however, change if the

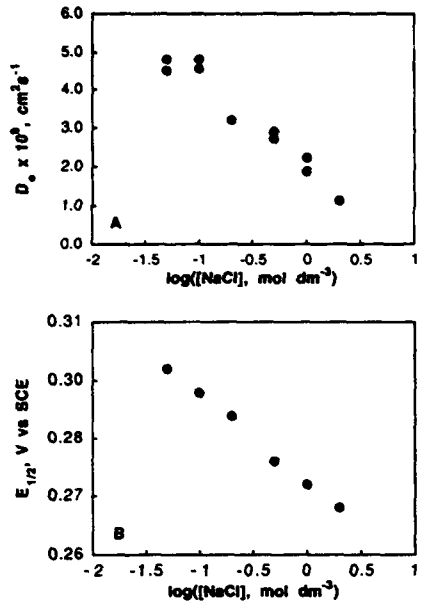

Figure 3. Effect of the ionic strength on the electron diffusion coefficient (A) and the half-wave potential of the POs-EA polymer (B). The conditions are the same as in Figure 2.

change in ionic strength greatly perturbs the microscopic routes of electron transfer, e.g., by changing the local dielectric constant of spaces between colliding cationic chains segments and thus the electrostatic repulsion between these. Since steady-state voltammetry using IDA electrodes defines apparent average D_e values for the actual system, without adjustment for redox site concentrations, the variation in the effective density of redox sites is intrinscally accounted for. Furthermore, the macroscopic ion migration effects that cannot be ignored at low ionic strengths in the transient measurements does not affect the steady-state measurements, where there is no net movement of ions into or out of the films. The observed decrease of D_e with increasing ionic strength may be caused by association between $[Os(bpy)_2vpyCl]^{+/2+}$ centers and chloride counterions. For Nafion films with only electrostatically bound $Os(bpy)_3^{2+/3+}$ ion, Anson and Savéant[21] suggested a model involving, at high ionic strengths, charge propagation by dissociation of ion pairs, electron transfer, and association of pairs. This model is applicable for low dielectric constant domains in the interior of Nafion. Association of ions in POs-EA is uncertain, but is suggested by the fact that the polymer is soluble in 0.1 M NaCl yet precipitates from 1.0 M NaCl. Association of ions would explain the decrease by 20 mV/decade in the apparent half-wave potential of $Os^{II+/III+}$ upon increasing the NaCl concentration (Figure 3B).[2b,f,24] A 59 mV/decade slope was measured by Anson et al. and was explained as resulting from Donnan exclusion.[25] Because the swollen cross-linked POs-EA hydrogel is more easily permeated by both anions and cations than Anson's ion-exchange resins, that were designed to exclude either anions or cations, these Donnan exclusions were incomplete at best in our hydrogel.

Figure 4 shows the cyclic voltammograms at the IDA collector electrodes at 0.1 M NaCl (A) and 0.1 M $NaClO_4$ (B). When the hydrated chloride anion was replaced by the hydrophobic perchlorate anion that is not hydrated,[7b] the peak current decreased and a diffusional tail appeared in the generator–generator experiment. In the generator–collector experiment the steady-state current decreases. Both indicate sluggish electron transport.[7b,8,9g] Because the Stokes radius of the chloride anion is almost identical with that of perchlorate anion,[26] the polymer structure need not be changed for geometrical considerations upon substitution of the anions. Therefore, the distance between the $Os^{2+/3+}$ sites should be the same with either chloride or perchlorate as the counterion in the polymer. The anion changes,

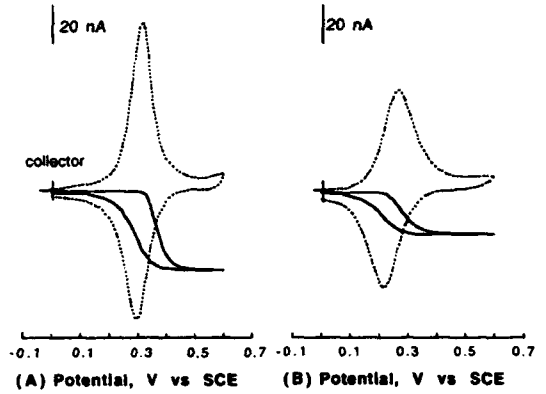

Figure 4. Anion dependence of the cyclic voltammograms at the collector electrode for POs–EA cross-linked with 5.0 wt % PEGDE, at an $[Os(bpy)_2vpyCl]^{+/2+}$ site coverage of $\Gamma = 4.01 \times 10^{-9}$ mol cm^{-2} in 20 mM phoshate buffer at pH 7.0 and at 2.0 mV s^{-1} scan rate. Generator–collector (solid line) and generator–generator (dotted line) voltammograms are shown for (A), 0.1 M NaCl; (B), 0.1 M $NaClO_4$.

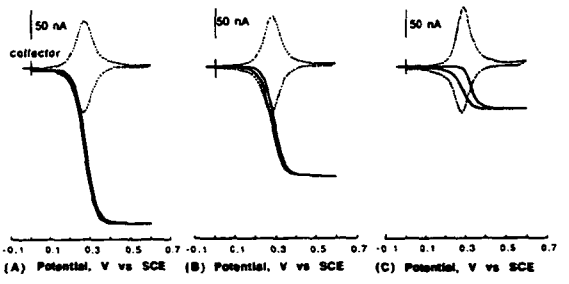

Figure 5. pH dependence of the cyclic voltammograms at the collector for POs-EA cross-linked with 5.0 wt % PEGDE, at an $[Os(bpy)_2vpyCl]^{+/2+}$ site coverage of $\Gamma = 4.35 \times 10^{-9}$ mol cm^{-2}, in 20 mM phosphate buffer containing 0.1 M NaCl, and at 2.0 mV s^{-1} scan rate. Generator–collector (solid line), generator–generator (dotted line) voltammograms are shown for pH (A), 2.0; (B), 4.0; (C), 7.0.

however, the nature of the polymer, because hydrophobic interactions are enhanced by the perchlorate anion. Oh and Faulkner[8] reported that the water content in a redox polymer film with perchlorate was reduced relative to that with chloride. Upon replacement of Cl^- by ClO_4^- the half-wave potential of POs-EA in 0.1 M perchlorate was shifted cathodically by 40 mV to 0.245 V (SCE). This shift resulted from a change in the equilibrium constant for pairing of $[Os(bpy)_2vpyCl]^{+/2+}$ cation and the anion or from a related change in the solubility of the oxidized redox polymer.[24d,27,28] In the ClO_4^- system ion pairing is enhanced, causing POs-EA, which is soluble in 0.1 M NaCl, to precipitate in 0.1 M $NaClO_4$.

Dependence of D_e on pH. Figure 5 shows the pH dependence of the cyclic voltammograms for the collector. The steady-state current decreased with increasing pH, while the total charge remained constant. The dependence of D_e on pH for POs-EA cross-linked with 5.0 wt % PEGDE is shown in Figure 6. D_e increased from 4.5×10^{-9} to 1.6×10^{-8} cm^2 s^{-1} when the pH was lowered from 7.0 to the pK_a of pyridine.[2f] The protonated and positively charged gel visibly expanded. Although the expansion decreased the concentration of the Os sites, segmental motion of the polymer was facilitated and D_e increased.

The voltammograms in the generator–generator experiments (Figure 5, dotted lines) also changed with pH. The peak currents increased with pH and the peaks' width at half-height narrowed with increasing pH. The values of the peak currents and the peak widths at half-height are summarized in Table I. At pH 2.0 the peak current and the peak width in the anodic voltammetric wave were identical with their theoretical values.[29] However, the anodic peak current and the peak width deviated from their theoretical values at high pH. This deviation is explained by interaction between the redox species, as observed earlier in other

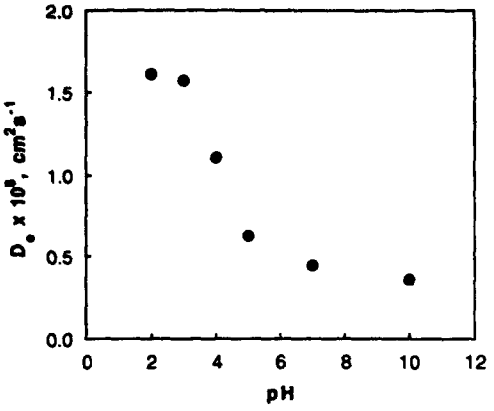

Figure 6. pH dependence of the electron diffusion coefficient of POs-EA cross-linked with 5.0 wt % PEGDE. $\Gamma = 4.35 \times 10^{-9}$ mol cm^{-2}, 20 mM phosphate buffer containing 0.1 M NaCl, 2.0 mV s^{-1} scan rate.

TABLE I: pH Dependence of the Peak Current and the Peak Width at Half-Height of the Anodic and the Cathodic Waves

	peak current, nA		peak width, mV	
pH	anodic	cathodic	anodic	cathodic
2.0	80	72	90	95
4.0	84	72	85	95
5.0	88	68	80	90
7.0	100	72	75	90
theoretical	80[a]		90.6	

[a] Value calculated from $\Gamma = 4.35 \times 10^{-9}$ mol cm^{-2}, $v = 2.0$ mV s^{-1}.

TABLE II: Effect of the Extent of Cross-Linking on the Electron Diffusion Coefficient

	D_e, cm^2 s^{-1}	
cross-linker, wt %	pH 3.0	pH 7.0
5	1.6×10^{-8}	4.5×10^{-9}
25	4.2×10^{-9}	3.2×10^{-9}

polymers.[1,30-32] When the pyridine nitrogen of the POs-EA polymer is protonated and the polymer is swollen at pH 2.0, the distance between Os sites is large and the sites do not interact. Because at pH > 4 the pyridine nitrogens are not protonated, the polymer is less swollen and the distance between the Os sites is small enough for the sites to interact. No interaction is seen, however, at pH 2, because at this pH the oxidized redox polymer is well swollen.

The D_e values for the POs-EA polymer at various cross-linker concentrations are summarized in Table II. When the network was made with 5.0 wt % cross-linker the network could swell at low pH and D_e was pH dependent. D_e was, however, almost independent of pH for the polymer made with 25 wt % cross-linker. When the concentration of the cross-linker was 25 wt %, 32 % of the pyridines in the polymer were cross-linked with the diepoxide. At such extreme cross-linking the polymer did not swell even at low pH, and the electron-transfer affecting segmental motion of the polymer backbone was restricted.

Conclusions

D_e decreases with increasing ionic strength because of enhanced association between $[Os(bpy)_2vpyCl]^{+/2+}$ and the chloride counterion. D_e also decreases when the hydrated chloride ion is replaced by the hydrophobic perchlorate ion. Lowering the pH causes swelling of the cross-linked POs-EA films yet increases D_e, probably because of enhancement of electron-transferring collisions between chain segments. D_e is independent of pH when POs-EA films are highly cross-linked and the segmental motion is limited.

Acknowledgment. This work was supported by the National Institutes of Health (No. 1 R01 DK42015-01A1), Office of Naval Research and the Welch Foundation. We thank D. Isamu Uchida and Dr. Tomokazu Matsue for the photomask, Ioanis Katakis for the POs-EA polymer used. We are grateful to Dr. Sten-Eric Lindquist and Timothy J. Ohara for their helpful comments.

References and Notes

(1) Murray, R. W. In *Electroanalytical Chemistry*; Bard, A. J., Ed.; Marcel Dekker: New York, 1984; pp 191–368.

(2) (a) Degani, Y.; Heller, A. *J. Am. Chem. Soc.* **1989**, *111*, 2357. (b) Pishko, M. V.; Katakis, I.; Lindquist, S.-E.; Heller, A. *Mol. Cryst. Liq. Cryst.* **1990**, *190*, 221. (c) Pishko, M. V.; Katakis, I.; Lindquist, S.-E.; Ye, L.; Gregg, B. A.; Heller, A. *Angew. Chem., Int. Ed. Engl.* **1990**, *29*, 82. (d) Heller, A. *Acc. Chem. Res.* **1990**, *23*, 128. (e) Gregg, B. A.; Heller, A. *Anal. Chem.* **1990**, *62*, 258. (f) Gregg, B. A.; Heller, A. *J. Phys. Chem.* **1991**, *95*, 5970. (g) Gregg, B. A.; Heller, A. *J. Phys. Chem.* **1991**, *95*, 5976. (h) Pishko, M. V.; Michael, A. C.; Heller, A. *Anal. Chem.* **1991**, *63*, 2268. (i) Maidan, R.; Heller, A. *J. Am. Chem. Soc.* **1991**, *113*, 9003. (j) Katakis, I.; Heller, A. *Anal. Chem.* **1992**, *64*, 1008. (k) Heller, A. *J. Phys. Chem.* **1992**, *96*, 3579.

(3) (a) Hale, P. D.; Inagaki, T.; Karan, H. I.; Okamoto, Y.; Skotheim, T. A. *J. Am. Chem. Soc.* **1989**, *111*, 3482. (b) Hale, P. D.; Boguslavski, L. I.; Inagaki, T.; Lee, H. S.; Skotheim, T. A.; Karan, H. I.; Okamoto, Y. *Mol. Cryst. Liq. Cryst.* **1990**, *190*, 251. (c) Hale, P. D.; Boguslavski, L. I.; Inagaki, T.; Karan, H. I.; Lee, H. S.; Skotheim, T. A.; Okamoto, Y. *Anal. Chem.* **1991**, *63*, 677.

(4) Foulds, N. C.; Lowe, C. R. *Anal. Chem.* **1988**, *60*, 2437.

(5) Bartlett, P. N.; Tebbutt, P.; Whitaker, R. G. *Prog. Reaction Kinetics* **1991**, *16*, 55.

(6) (a) Beratan, D. N.; Onuchic, J. N.; Hopfield, J. J. *J. Chem. Phys.* **1987**, *86*, 4488. (b) Onuchic, J. N.; Beratan, D. N. *J. Chem. Phys.* **1990**, *92*, 722. (c) Betts, J. N.; Beratan, D. N.; Onuchic, J. N. *J. Am. Chem. Soc.* **1992**, *114*, 4043.

(7) (a) Lyons, M. E. G.; Fay, H. G.; Vos, J. G.; Kelly, A. J. *J. Electroanal. Chem.* **1988**, *250*, 207. (b) Forester, R. J.; Kelly, A. J.; Vos, J. G.; Lyons, M. E. G. *J. Electroanal. Chem.* **1989**, *270*, 365. (c) Forster, R. J.; Vos, J. G. *Macromolecules* **1990**, *23*, 4372. (d) Forster, R. J.; Vos, J. G.; Lyons, M. E. G. *J. Chem. Soc., Faraday Trans.* **1991**, *87*, 3761. (e) Forster, R. J.; Vos, J. G.; Lyons, M. E. G. *J. Chem. Soc., Faraday Trans.* **1991**, *87*, 3769. (f) Forster, R. J.; Vos, J. G. *J. Electrochem. Soc.* **1992**, *139*, 1503.

(8) (a) Oh, S.-M.; Faulkner, L. R. *J. Electroanal. Chem.* **1989**, *269*, 77. (b) Oh, S.-M.; Faulkner, L. R. *J. Am. Chem. Soc.* **1989**, *111*, 5613. (c) Faulkner, L. R. *Electrochim. Acta* **1989**, *34*, 1699.

(9) (a) Pickup, P. G.; Murray, R. W. *J. Am. Chem. Soc.* **1983**, *105*, 4510. (b) Pickup, P. G.; Kutner, W.; Leidner, C. R.; Murray, R. W. *J. Am. Chem. Soc.* **1984**, *106*, 1991. (c) Jernigan, J. C.; Chidsey, C. E. D.; Murray, R. W. *J. Am. Chem. Soc.* **1985**, *107*, 2824. (d) Jernigan, J. C.; Murray, R. W. *J. Am. Chem. Soc.* **1987**, *109*, 1738. (e) White, B. A.; Murray, R. W. *J. Am. Chem. Soc.* **1987**, *109*, 2576. (f) Jernigan, J. C.; Surridge, N. A.; Zvanut, M. E.; Silver, M.; Murray, R. W. *J. Phys. Chem.* **1989**, *93*, 4260. (g) Dalton, E. F.; Murray, R. W. *J. Phys. Chem.* **1991**, *95*, 6383.

(10) Facci, J. S.; Schmehl, R. H.; Murray, R. W. *J. Am. Chem. Soc.* **1982**, *104*, 4959.

(11) (a) Feldman, B. J.; Feldberg, S. W.; Murray, R. W. *J. Phys. Chem.* **1987**, *91*, 6558. (b) Licht, S.; Cammarata, V.; Wrighton, M. S. *Science* **1988**, *243*, 1176. (c) Cammarata, V.; Talham, D. R.; Crooks, R. M.; Wrighton, M. S. *J. Phys. Chem.* **1990**, *94*, 2680. (d) Licht, S.; Cammarata, V.; Wrighton, M. S. *J. Phys. Chem.* **1990**, *94*, 6133.

(12) Chen, X.; He, P.; Faulkner, L. R. *J. Electroanal. Chem.* **1987**, *222*, 223.

(13) (a) Chidsey, C. E. D.; Feldman, B. J.; Lundgren, C.; Murray, R. W. *Anal. Chem.* **1986**, *58*, 601. (b) Feldman, B. J.; Murray, R. W. *Anal. Chem.* **1986**, *58*, 2844. (c) Feldman, B. J.; Murray, R. W. *Inorg. Chem.* **1987**, *26*, 1702. (d) Dalton, E. F.; Surridge, N. A.; Jernigan, J. C.; Wilbourn, K. O.; Facci, J. S.; Murray, R. W. *Chem. Phys.* **1990**, *141*, 143 (e) Surridge, N. A.; Zvanut, M. E.; Keene, F. R.; Sosnoff, C. S; Silver, M.; Murray, R. W. *J. Phys. Chem.* **1992**, *96*, 962.

(14) Nishihara, H.; Dalton, F.; Murray, R. W. *Anal. Chem.* **1991**, *63*, 2955.

(15) (a) Kittlesen, G. P.; White, H. S.; Wrighton, M. S. *J. Am. Chem. Soc.* **1985**, *107*, 7373. (b) Belanger, D.; Wrighton, M. S. *Anal. Chem.* **1987**, *59*, 1426. (c) Smith, D. K.; Lane, G. A.; Wrighton, M. S. *J. Phys. Chem.* **1988**, *92*, 2616. (d) Shu, C.-F.; Wrighton, M. S. *J. Phys. Chem.* **1988**, *92*, 5221.

(16) Goss, C. A.; Majda, M. *J. Electroanal. Chem.* **1991**, *300*, 377.

(17) Andrieux, C. P.; Savéant, J. M. *J. Phys. Chem.* **1988**, *92*, 6761.

(18) (a) Savéant, J. M. *J. Electroanal. Chem.* **1988**, *242*, 1. (b) Savéant, J. M. *J. Electroanal. Chem.* **1987**, *238*, 1.

(19) Fritsch-Faules, I.; Faulkner, L. R. *J. Electroanal. Chem.* **1989**, *263*, 237.

(20) Fritsch-Faules, I.; Faulkner, L. R. *Anal. Chem.* **1992**, *64*, 1118.

(21) (a) Anson, F. C.; Blauch, D. N.; Savéant, J. M.; Shu, C.-F. *J. Am. Chem. Soc.* **1991**, *103*, 1922. (b) Savéant, J. M.; *J. Phys. Chem.* **1988**, *92*, 4526. (c) Savéant, J. M. *J. Phys. Chem.* **1988**, *92*, 1011.

(22) Aoki, A.; Matsue, T.; Uchida, I. *Anal. Chem.* **1990**, *62*, 2206.
(23) (a) Aoki, K.; Morita, M.; Niwa, O.; Tabei, H. *J. Electroanal. Chem.* **1988**, *256*, 269. (b) Niwa, O.; Morita, M.; Tabei, H. *Anal. Chem.* **1990**, *62*, 447. (c) Aoki, K. *J. Electroanal. Chem.* **1990**, *284*, 35.
(24) (a) Inzelt, G. *Electrochim. Acta* **1989**, *34*, 83. (b) Inzelt, G.; Szabo, L.; Chambers, J. Q.; Day, R. W. *J. Electroanal. Chem.* **1988**, *242*, 265. (c) Inzelt, G.; Bacskai, J.; Chambers, J. Q.; Day, R. W. *J. Electroanal. Chem.* **1986**, *201*, 301. (d) Inzelt, G.; Szabo, L. *Electrochim. Acta* **1986**, *31*, 1381.
(25) Naegeli, R.; Redepenning, J.; Anson, F. C. *J. Phys. Chem.* **1986**, *90*, 6227.
(26) Marcus, Y. *Ion Solvation*; Wiley: New York, 1985.
(27) Oosawa, F. *Polyelectrolytes*; Marcel Dekker: New York, 1971.
(28) Rice, S. A.; Nagasawa, M.; Morawetz, H. *Polyelectrolyte Solutions, Molecular Biology International Series*; Academic Press: London, 1961; Vol. 2.
(29) Bard, A. J.; Faulkner, L. R. *Electrochemical Methods*; Wiley: New York, 1980; Chapter 10.
(30) Ikeda, T.; Leidner, C. R.; Murray, R. W. *J. Electroanal. Chem.* **1982**, *138*, 343.
(31) Andrieux, C. P.; Haas, O.; Savéant, J.-M. *J. Am. Chem. Soc.* **1986**, *108*, 8175.
(32) Chidsey, C. E. D.; Murray, R. W. *J. Phys. Chem.* **1986**, *90*, 1479.

Sensors and Actuators B, 13–14 (1993) 180–183

Amperometric biosensors based on three-dimensional hydrogel-forming epoxy networks

Adam Heller, Ruben Maidan and DanLi Wang

Department of Chemical Engineering, The University of Texas at Austin, Austin, TX 78712-1062 (USA)

1. Introduction

Proteins and glycoproteins of enzymes behave with respect to electron transport, but not ion transport, as good electrical insulators. We have shown that these insulators can be made sufficiently electron conducting to allow the flow of a current between reaction centers of redox enzymes and electrodes equaling or exceeding the current associated with the turnover of the enzymes. In order for such a current to flow it is necessary to introduce into the enzyme proteins or glycoproteins fast electron-relaying centers, so as to reduce the electron transfer distances [1, 2].

2. Methods of introducing fast electron relays into enzymes

There are three ways by which fast electron relays can be introduced into an enzyme: (a) covalent bonding of relays to the enzyme's protein [3–5]; (b) covalent bonding through a sufficiently long and flexible tether to a peripheral oligosaccharide of a glycoprotein enzyme [6]; (c) forming complexes between enzyme proteins and redox macromolecules [1, 7].

2.1. Covalent attachment of electron relays to enzyme proteins

Relays can be attached to lysine amines of enzyme proteins through carbodiimide coupling with carboxylic acid derivatives of relays [3, 4]. The resulting enzymes can be directly and continuously electrooxidized if reduced by their substrates. The relay-modified enzymes retain most of their activity and selectivity. For example, glucose oxidase can be chemically modified by covalent attachment of 13 ± 2 electron-relaying ferrocenes to its protein. The $FADH_2$ centers of the modified enzyme are electrooxidizable in the absence of diffusional mediators.

2.2. Covalent attachment of tethered electron relays to oligosaccharides on the periphery of enzymes

Periodate oxidation of surface oligosaccharides on enzymes produces aldehydes. These form Schiff bases with electron relays that are attached through tethers to terminal amines. The Schiff bases can then be reduced with sodium borohydride to form hydrolytically stable secondary amines. Investigation of tethered ferrocenes as relays shows that efficient electron relaying requires sufficiently long tethers for the relay to reach the midpoint between the reactive centre of the redox enzyme and its periphery. When the tethers are too short electron relaying is inefficient; and after a certain length, further lengthening of the tether does not improve the electron-relaying efficiency. For glucose oxidase the required tether has 11–13 carbon atoms or carbon and nitrogen atoms [6].

2.3. Electron relaying through water-soluble redox macromolecules. Electron transport in enzymes: redox polymer conjugates

Interaction between water-soluble biomolecules is common in nature forming the basis for immune reactions, DNA replication and recognition systems. Water-dissolved enzyme molecules can be designed to couple to appropriately designed water-soluble redox macromolecules. The binding may involve hydrophobic, ionic or hydrogen bonding interactions. The redox molecule and the enzyme protein interpenetrate in the coupling reaction. As a result, redox centers of the enzymes are brought into electrical contact with those of the electron-relaying redox macromolecules [1, 7].

The enzyme-complexing redox macromolecules are polyelectrolytes with fast, nitrogen-complexed $[Os(bpy)_2Cl]^{+/2+}$ redox centers. The backbones can be based on poly(vinyl pyridine) or other polymers having $Os^{2+/3+}$ complexing functions. An example of such a macromolecule is shown in Fig. 1.

2.4. Simple biosensors based on complexes of redox enzymes and redox macromolecules

When an enzyme-binding redox macromolecule is adsorbed on or attached to an electrode surface, it will complex dissolved enzymes and electrically connect these [7]. Thus amperometric biosensors can be made in a process involving two adsorption and rinsing steps. Such biosensors have a rise time shorter than 1 s.

0925-4005/93/$6.00

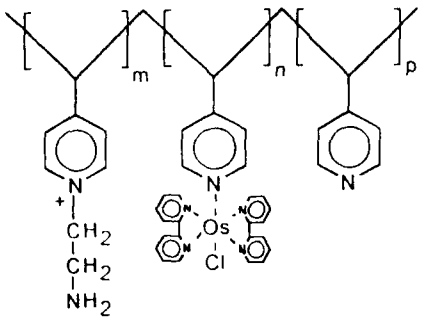

n = 1, m ≈ 4, p ≈ 1.2

Fig. 1. Example of an electron-relaying, enzyme-complexing redox macromolecule.

A simple biosensor can be made by adsorbing a polymer similar to that shown in Fig. 1, but with a methyl group substituting for the ethylamine, on a carbon electrode, rinsing and complexing the enzyme to transiently non-adsorbed segments of the electrode-adsorbed redox macromolecule. For such complexing, the redox macromolecule must be long because a sufficient number of adsorbed segments is needed in order to avoid desorption; yet most of its segments must be 'in solution', i.e., transiently desorbed, so as to complex and penetrate the enzyme protein [1].

3. Crosslinked 3D electron-transporting enzyme redox polymer networks: electrical 'wiring' of enzymes

The enzyme redox polymer adducts of Section 2.4 can be crosslinked if the polymer of Fig. 1 is an amine, or if its segments are modified with carboxylic acid functions.

In the first case, the amines of the redox polymer and of the enzyme can be crosslinked with a bi-functional crosslinker, such as a diepoxide. In the second case the carboxylic acids can be esterified to form reactive *N*-hydroxysuccinimides. The latter react with lysine amines of the enzyme, the enzyme acting as a crosslinker of the redox macromolecule [8].

3.1. Enzyme-wiring redox epoxy hydrogel networks

The redox polyamines of Section 3 can be crosslinked with a water-soluble diepoxide, such as polyethylene glycol diglycidyl ether, that does not complex either the enzyme or the redox macromolecule [9, 10]. This is important because complexing of either component can lead to the break up of the complex in which the enzyme is 'wired'. The polyethylene glycol diglycidyl ethers used are of 400–600 daltons. Their chains are flexible and well hydrated. With both the enzyme and the redox polymer being water soluble, a hydrogel is formed upon crosslinking. This hydrogel is not only permeable to the substrate and the product of the enzyme-catalyzed redox reaction, but also has an electron-transporting polymer network. Consequently, the substrate and product diffuse easily to and from the network-bound enzyme, while the network electrically connects the redox centers of the bound enzymes to electrodes. The current densities and sensitivities of the resulting biosensors are high: current densities in excess of 10^{-3} A cm^{-2} are observed and sensitivities reach 0.1 A cm^{-2} M^{-1}.

3.2. Miniaturization of amperometric biosensors

The enzymes in the redox epoxy hydrogels are well 'wired', i.e., the electrons associated with their turnover are efficiently collected at the electrodes. In Faraday cages we have observed the turnover of as few as 300 enzyme molecules.

In practical applications biosensors must, however, function in an environment with electromagnetic noise. The noise equivalent currents in our laboratory are near 10^{-11} A. Thus, unless the biosensors are operated in Faraday cages, the currents must exceed 10^{-10} A. For this reason our practical microsensor tips are miniaturized to 7 μm diameter, but not less. Electron transport to these tips is radial and current densities in excess of 3 mA cm^{-2} are observed at high substrate (e.g. glucose) concentrations [11].

4. Elimination of interferants

Biosensors are only imperfectly selective, because non-enzyme-catalyzed electrode reactions may also take place. Thus, on anodes poised positive of the redox potential of the enzyme-wiring, redox macromolecule biological fluid constituents such as urate, ascorbate and acetaminophen may also be electrooxidized. Their electrooxidation currents add to and distort the true, substrate-associated current.

To eliminate the electrooxidizable interferants we use the very fact that they are easy to oxidize. Specifically, the interferants are rapidly oxidized by hydrogen peroxide in the presence of horseradish peroxidase. Thus ascorbate, urate, acetaminophen and other interferants are quantitatively eliminated in immobilized horseradish peroxidase overlayers on enzyme electrodes that are electrically insulated from the sensing layer. The fluid reaching the sensing layer is stripped of all interferants, while species detected such as lactate or glucose are not oxidized [12].

5. Miniature flexible physiological lactate sensor

The concepts of 3D wired enzyme hydrogels and interference elimination have been implemented in biosensors of which a miniature physiological lactate sensor is an example. The sensor is 0.3 mm in diameter, consisting of 300–500 carbon fiber tips [13]. The fibers are epoxy-embedded and are contained in a 0.3 mm diameter biocompatible polyimide tubing. The ensemble of epoxy-embedded fiber tips is coated with the redox epoxy hydrogen containing lactate oxidase. This sensing layer is then coated with an electrically insulating layer made of poly(vinyl-imidazole), crosslinked with ethylene glycol diglycidyl ether. The top overlayer contains two co-immobilized enzymes: glucose oxidase and horseradish peroxidase (Fig. 2).

The physiological fluid, e.g. blood, contains glucose and oxygen. Glucose is oxidized by oxygen in the glucose oxidase and horseradish peroxidase containing overlayer in a reaction generating gluconolactone and hydrogen peroxide. The hydrogen peroxide generated oxidizes the horseradish peroxidase, that, in turn, oxidizes and eliminates all the electrooxidizable interferants, but not lactate. The sensing layer sees, therefore, a preoxidized stream from which the interferants are stripped. The electrode is then overcoated with a biocompatible film. The electrode's sensitivity is 2.5×10^{-2} A cm^{-2} M^{-1}. It can be stored at 4 °C for four months with no measurable change. Its 10–90% rise time is 1 min. If periodically recalibrated, the electrode can be used for 10^3 lactate measurements.

Acknowledgements

The work was supported by the National Institutes of Health, National Science Foundation, Office of Naval Research and Robert A. Welch Foundation.

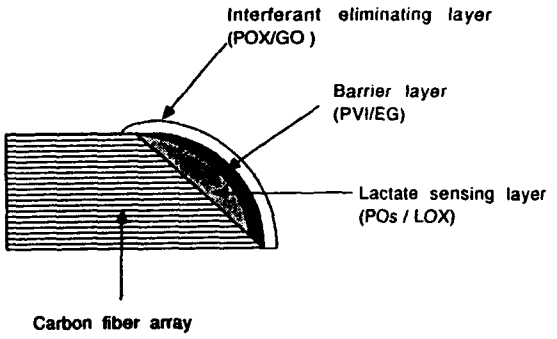

Fig. 2. Schematic drawing of the 0.3 mm diameter flexible physiological lactate sensor.

References

1 A. Heller, Electrical connection of enzyme redox centers to electrodes, *J. Phys. Chem.*, *96* (1992) 3579–3587.
2 A. Heller, Electrical wiring of redox enzymes, *Acc. Chem. Res.*, *23* (1990) 128–134.
3 Y. Degani and A. Heller, Direct electrical communication between chemically modified enzymes and metal Electrodes. I. Electron transfer from glucose oxidase to metal electrodes via electron relays, bound covalently to the enzyme, *J. Phys. Chem.*, *291* (1987) 1285–1289.
4 Y. Degani and A. Heller, Direct electrical communication between chemically modified enzymes and metal electrodes. II. Methods for bonding electron-transfer relays to glucose oxidase and D-amino-acid oxidase, *J. Am. Chem. Soc.*, *110* (1988) 2615–2620.
5 A. Heller and Y. Degani, Direct electrical communication between modified enzymes and metal electrodes. III. Electron-transfer relay modified glucose oxidase and D-amino-acid oxidase, in G. Dryhurst and K. Niki (eds.), *Redox Chemistry and Interfacial Behaviour of Biological Molecules, Proc 3rd Int. Symp. Redox Mechanisms and Interfacial Properties of Molecules of Biological Importance, Honolulu, HI, USA*, 1987, Plenum, New York, 1988, pp. 151–171.
6 W. W. Schuhmann, T. Ohara, A. Heller and H.-L. Schmidt, Electron transfer between glucose oxidase and electrodes via redox mediators bound with flexible chains to the enzyme surface, *J. Am. Chem. Soc.*, *113* (1991) 1394–1397.
7 M. V. Pishko, I. Katakis, S.-E. Lindquist, L. Ye, B. A. Gregg and A. Heller, Direct electrical communication between graphite electrodes and surface adsorbed glucose oxidase/redox polymer complexes, *Angew. Chem., Int. Ed. Engl.*, *29* (1990) 82–84.
8 B. A. Gregg and A. Heller, Cross-linked redox gels containing glucose oxidase for amperometric biosensor applications, *Anal. Chem.*, *62* (1990) 258–263.
9 B. A. Gregg and A. Heller, Redox polymer films containing enzymes. 1. A redox-conducting epoxy cement: synthesis, characterization, and electrocatalytic oxidation of hydroquinone, *J. Phys. Chem.*, *95* (1991) 5970–5975.
10 B. A. Gregg and A. Heller, Redox polymer films containing enzymes. 2. Glucose oxidase containing enzyme electrodes, *J. Phys. Chem.*, *95* (1991) 5976–5980.
11 M. V. Pishko, A. C. Michael and A. Heller, Amperometric glucose microelectrodes prepared through immobilization of glucose oxidase in redox hydrogels, *Anal. Chem.*, *63* (1991) 2268–2272.
12 R. Maidan and A. Heller, Elimination of electrooxidizable interferants in glucose electrodes, *J. Am. Chem. Soc.*, *113* (1991) 9003–9004.
13 DanLi Wang and A. Heller, 0.3 mm diameter flexible amperometric lactate probe, *Anal. Chem.*, in press.

Biography

Adam Heller received his M.Sc. (chemistry and physics, 1957) and Ph.D. (chemistry, 1961) from the Hebrew University, Jerusalem, where he studied under E. D. Bergmann. Following postdoctoral work at U.C. Berkeley and at Bell Laboratories, he joined GTE Laboratories where he became Manager of Exploratory Research in 1970. In 1975 he returned to ATT Bell Laboratories,

heading from 1977 until 1988 the Electronic Materials Research Department. He was appointed to the Ernest Cockrell, Sr. Chair in Engineering at the University of Texas at Austin in 1988.

Dr Heller is best known for pioneering the direct electrical connection of redox centers of enzymes to electrodes and the associated direct amperometric biosensors (1987–1992), the first efficient hydrogen-generating solar cells (1980) and electrical power-producing photoelectrochemical cells (1978), the first paper on the lithium-thionyl chloride battery used in pacemakers and personal computers, on which 1800 papers were subsequently published by others and which is manufactured worldwide (1972), the introduction of electrochemistry in oxyhalides (1966), and inorganic liquid lasers (1964).

Dr Heller received the 1978 Battery Research Award of the Electrochemical Society, was named Guest Professor at the Collège de France in 1982, received the David C. Grahame Physical Electrochemistry Award of the Electrochemical Society in 1987, was elected to the U.S. National Academy of Engineering in 1987, received the Vittorio De Nora Gold Medal of the Electrochemical Society in 1988 and was awarded the title of Doctor honoris causa by Uppsala University in Sweden in 1991.

Reprinted from Analytical Chemistry, 1992, 64.

Hydrogen Peroxide and β-Nicotinamide Adenine Dinucleotide Sensing Amperometric Electrodes Based on Electrical Connection of Horseradish Peroxidase Redox Centers to Electrodes through a Three-Dimensional Electron Relaying Polymer Network

Mark Vreeke, Ruben Maidan, and Adam Heller*

Department of Chemical Engineering and Materials Science and Engineering Center, The University of Texas at Austin, Austin, Texas 78712-1062

Hydrogen peroxide is efficiently electroreduced at an electrode modified with a hydrophilic, permeable film of horseradish peroxidase (HRP) covalently bound to a 3-dimensional epoxy network having polyvinyl pyridine (PVP)-complexed $[Os(bpy)_2Cl]^{2+/2+}$ redox centers. The sensitivity of the resulting H_2O_2 cathode at 0.0 V (SCE) is 1 A cm^{-2} M^{-1}. Its current increases linearly with H_2O_2 concentration in the 1×10^{-7}–2×10^{-4} M range. Related NAD(P)H cathodes are based on stoichiometric homogeneous reduction of O_2 to H_2O_2 by NADH or NAD(P)H. The reduction involves two known steps. In the first step, NAD(P)H transfers two electrons and a proton to a dissolved quinoid. The quinoids are typically derived of phenazines; however phenothiazine and phenoxazine derivatives are also useful. In the second step, two electrons and a proton are transferred from the reduced quinoid to O_2. This reaction produces H_2O_2 and the original quinoid. Because the two reactions are quantitative, the sensitivity and the linear range of the resulting NADH and NADPH electrodes are identical with those of the H_2O_2 electrode, 1 A cm^{-2} M^{-1} and 1×10^{-7}–2×10^{-4} M, respectively.

INTRODUCTION

Selective electrooxidation of NADH and NADPH cofactors (reaction 1) of enzymes allows, in principle, amperometric assay of a substantial number of biochemicals. When the

$$NAD(P)H \rightarrow NAD(P)^+ + 2e^- + H^+ \qquad (1)$$

electrooxidation products are the cofactors NAD^+ or $NADP^+$, these can be enzymatically rereduced and electrocatalytic enzyme electrodes can be made. The reversible potential of the NADH/NAD^+ couple is −0.56 V (SCE) at pH 7.[1] Because, the reaction involves the concerted transfer of two electrons and a proton, it is usually slow, proceeding at practical rates on most electrodes only at high overpotentials. At these high overpotentials reaction products of NADH and other constituents of biological fluids that are also electrooxidized interfere with the amperometric assays of NAD(P)H.[2,3] Following Elving's definition of this problem,[4-6] several groups, particularly those of Miller,[7] Gorton,[11] and Kulys,[12,13] developed electrodes on which reaction 1 proceeds rapidly at low overpotentials. The most successful electrodes, of which Gorton's phenoxazine-derivative and Kulys' phenazine-based electrodes are examples,[11-16] utilize electrode-bound, electrode-adsorbed, or freely diffusing mediators having quinoid structures in their oxidized state. The quinoids effectively catalyze reaction 1 at potentials near 0.0 V (SCE).

Here we consider a more complex but nevertheless very fast and efficient set of coupled reactions for the amperometric assay of NAD(P)H. The first is a homogeneous solution reaction, exemplified by (2), where, as in the electrode

$$PMS^+ + NADH \rightarrow PMSH + NAD^+ \qquad (2)$$

reactions of Miller, Kulys, and Gorton, two electrons and a proton are transferred from NAD(P)H to a quinoid mediator. A particularly effective mediator is the water-soluble 5-methylphenazonium cation (PMS^+) which is quantitatively reduced by NAD(P)H to 5-methylphenazine (PMSH). PMSH is next reoxidized to PMS^+ by dissolved molecular oxygen which is, in turn, reduced to H_2O_2 (reaction 3). With reactions

$$PMSH + O_2 + H^+ \rightarrow PMS^+ + H_2O_2 \qquad (3)$$

2 and 3 being quantitative, each mole of NAD(P)H produces 1 mol of H_2O_2. H_2O_2 is then assayed through electroreduction on the "wired" peroxidase electrode (reaction 4). Several

$$H_2O_2 + 2e^- + 2H^+ \rightarrow 2H_2O \qquad (4)$$

previously reported detection schemes for NADH and NADPH have utilized reactions 2 and 3, amperometrically sensing the depletion of oxygen[17,18] or spectrophotometrically mea-

(1) Clark, W. M. *Oxidation-Reduction Potentials of Organic Systems*; William and Wilkins: Baltimore, 1960.
(2) Moiroux, J.; Elving, P. J. *Anal. Chem.* **1979**, *51*, 346–50.
(3) Blaedel, W. J.; Jenkins, R. A. *Anal. Chem.* **1975**, *47*, 1337–43.
(4) Samec, Z.; Elving, P. J. *J. Electroanal. Chem. Interfacial Electrochem.* **1983**, *144*, 217–34.
(5) Elving, P. J.; Bresnahan, W. T.; Moiroux, J.; Samec, Z. *Bioelectrochem. Bioenerg.* **1982**, *9*, 365–78.
(6) Moiroux, J.; Elving, P. J. *J. Am. Chem. Soc.* **1980**, *102*, 6533–8.
(7) Degrand, C.; Miller, L. L. *J. Am. Chem. Soc.* **1980**, *102*, 5728–32.
(8) Kitani, A.; So, Y. H.; Miller, L. L. *J. Am. Chem. Soc.* **1981**, *103*, 7636–41.
(9) Fukui, M.; Kitani, A.; Degrand, C.; Miller, L. L. *J. Am. Chem. Soc.* **1982**, *104*, 28–33.
(10) Lau, N. K.; Miller, L. L. *J. Am. Chem. Soc.* **1983**, *105*, 5271–84.
(11) Gorton, L.; Csoregi, E.; Domingues, E.; Emneus, J.; Jonsson-Petterson, G.; Marko-Varga, G.; Persson, B. *Anal. Chim. Acta* **1991**, *250*, 203–48.
(12) Cenas, N. K.; Kanapieniene, J. J.; Kulys, J. J. *J. Electroanal. Chem. Interfacial Electrochem.* **1985**, *189*, 163–9.
(13) Kulys, J. J. *Biosensors* **1986**, *2*, 3–13.
(14) Gorton, L.; Torstensson, A.; Jaegfeldt, H.; Johansson, G. *J. Electroanal. Chem. Interfacial Electrochem.* **1984**, *161*, 103–20.
(15) Persson, B.; Gorton, L. *J. Electroanal. Chem. Interfacial Electrochem.* **1990**, *292*, 115–38.
(16) Bremle, G.; Persson, B.; Gorton, L. *Electroanalysis* **1991**, *3*, 77–86.
(17) Polster, J.; Schmidt, H.-L. *Talanta* **1989**, *36*, No. 8, 864–6.

0003-2700/92/0364-3084$03.00/0

Table I. Amperometric H_2O_2 Sensors Based on HRP-Modified Electrodes

electrode surface	mediator or redox matrix	electrode potential[a]	sensitivity (A cm^{-2} M^{-1})	linear range (μM)	comments	ref
glassy carbon	none	0.0	10^{-2}		HRP covalently bound to a hydrophilic epoxy network; polyvinylpyridine-derived polyamine cross-linked with PEGDGE	this work
glassy carbon	polymer I	0.0	1	0.1–100	HRP covalently bound to hydrophilic epoxy network; polymer I crosslinked with PEGDGE	this work
spectrographic graphite	none[c]	0.05	0.175	0.1–500	BSA with glutaraldehyde cross-linking	36
carbon paste	*o*-phenylenediamine[d]	–0.15	NA[b]	3.1–200	butanone peroxide used as the substrate	37
Pt	hexacyanoferrate (0.01 M)[d]	–0.05	*e*	5–1700	HRP immobilized onto a Nylon net	38
$NMP^{+}TCNQ^{-}$	none[f]	0.05	0.168		HRP entrapped with dialysis membrane	39
SnO_2	ferrocenecarboxylic acid[d]	0.2	0.04	0.01–1	HRP immobilized with glutaraldehyde	40
carbon paste	ferrocene[d]	0.05	NA[b]	0.1–10	Nafion coating applied to the electrode to prevent loss of mediator	41
graphite foil	potassium hexacyanoferrate(II)[d]	–0.02[a]	0.03	<600	electrolyte was dioxane with 15% aqueous buffer	42
carbon fiber[g]	none	*h*		40–5000	biotin/avidin complex used to obtain a surface layer of HRP	43
Pt, organic metal, or glassy carbon	potassium ferrocyanide	*i*			membrane with albumin and glutaraldehyde	44
spectrographic graphite or carbon film	hexacyanoferrate(II)[d]	0.0	*e*	0.1–1000	HRP immobilized on arylamino-derivatized controlled-pore glass, packed into a flow-through reactor	45
aminosilylated glassy carbon	hexacyanoferrate(II)[d]	0.0	*i*		glycerophosphate oxidase, HRP, and BSA covalently cross-linked on the glassy carbon surface	46
glassy carbon	hexacyanoferrate(II)[d]	0.0	*i*		albumin, glutaraldehyde, HRP, and oxidase (xanthine, uricase, glucose) matrix held close to the electrode with a dialysis membrane	47
gold or graphite	several[k]	*k*	2.0[j]	0.05–6[j]	HRP free in solution	48

[a] Potential vs SCE. [b] Macroporous electrode. The true surface area is unknown. [c] Uncertainty as to whether the surface species created during electrode pretreatment are mediating. [d] Freely diffusing mediator. [e] Flow system. [f] Probably mediated by the soluble component of the organic metal or the reaction product of the organic metal. [g] Microelectrode. [h] Cyclic voltametry used to provide selective detection of oxygen generated by autocatalytic decomposition of hydrogen peroxide. [i] HRP incorporated into a bienzyme system. [j] Best reported result for ferrocenemonocarboxylic acid. [k] mediators used and redox potential: $[Ru(NH_3)_5py](ClO_4)_3$ = +28, $CpFeC_2B_9H_{11}$ = –8.0, 1,1′-dimethyl-3-(2-aminoethyl)ferrocene = +75, (2-aminoethyl)ferrocene = +185, ferrocenemonocarboxylic acid = +275, (aminomethyl)ferrocene = +309 mV.

suring the H_2O_2 generated.[19-21] We now add to these amperometric reduction of H_2O_2 on peroxidase, electrically connected (wired) through a permeable 3-dimensional redox polymer network to an electrode. Several horseradish peroxidase modified diffusionally mediated and mediatorless type electrodes have been earlier described. Their characteristics are compared with the wired HRP electrode in Table I.

In the wired HRP electrodes electrons from the electrode are relayed to the enzyme through a redox epoxy network to which the enzyme (HRP) is covalently bound. The centers consist of $[Os(bpy)_2Cl]^{3+/2+}$, complexed to polyvinylpyridine. The HRP and the redox polymer are cross-linked into a 3-dimensional epoxy network with a water-soluble diepoxide. In earlier papers we showed that the resulting redox epoxy accepts electrons from substrate-reduced enzymes, relaying these to electrodes.[22,23] Here we show that the network also relays electrons in the reverse direction from the electrode to a bound enzyme. Network-bound HRP is efficiently electroreduced at 0.0 V (SCE), and H_2O_2 is detected with 1 A cm^{-2} M^{-1} sensitivity. Because NAD(P)H concentrations are stoichiometrically translated to H_2O_2 through reactions 2 and 3, these cofactors are also detected at the same potential with the same sensitivity.

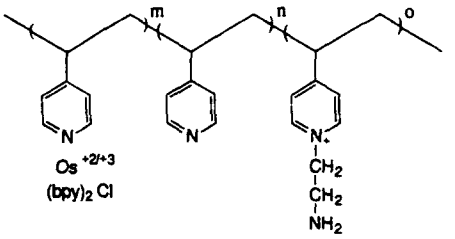

Figure 1. Composition of the electron-relaying redox polymer (m = 1; n = 3.35; o = 0.6). After cross-linking with PEGDGE, it forms a 3-dimensional network that is able to relay electrons to covalently bound HRP. The polymer is referred to as polymer I.

EXPERIMENTAL SECTION

Reagents. Horseradish peroxidase (HRP) E.C. 1.11.1.7 (Sigma P-8375 Type VI, 260 units/mg) was used. Poly(ethylene glycol 600 diglycidyl ether), technical grade (PEGDGE) was purchased from Polysciences (Catalog No. 8211). The osmium redox polyamine (polymer I, Figure 1) was synthesized as described previously.[24] NADH and NADPH were purchased from Sigma (340–110 and N-1630, respectively). 5-Methylphenazonium methyl sulfate was from Aldrich. Other mediators were from Aldrich or Sigma. All chemicals were used as received.

Electrode Construction and Preparation. Rotating disk electrodes were made of a 1-cm length of 3-mm-diameter vitreous

(18) Huck, H.; Schelter-Graf, A.; Danzer, J.; Kirch, P.; Schmidt, H.-L. *Analyst* **1984**, *109*, 147–50.
(19) Williams, D. C., III; Seitz, W. R. *Anal. Chem.* **1976**, *48*, 1478–81.
(20) *Eur. Pat. Appl.* EP 317070, 1989.
(21) *Eur. Pat. Appl.* EP 285998, 1988.
(22) Gregg, B. A.; Heller, A. *J. Phys. Chem.* **1991**, *95*, 5976–80.
(23) Pishko, M. V.; Katakis, I.; Lindquist, S.-E.; Heller, A. *Mol. Cryst. Liq. Cryst.* **1990**, *190*, 221–49.
(24) Gregg, B. A.; Heller, A. *J. Phys. Chem.* **1991**, *95*, 5970–5.

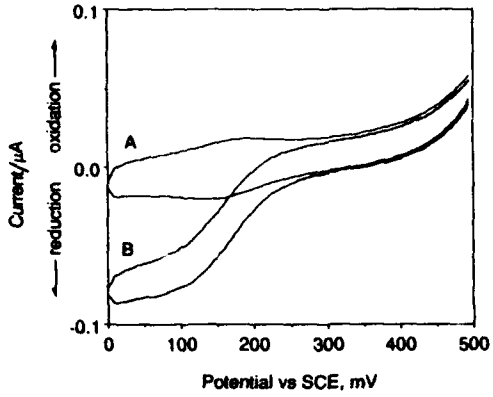

Figure 2. Cyclic voltammogram of a vitreous carbon electrode modified with the Schiff base formed of polyaldehyde–HRP and polymer I *without* $[Os(bpy)_2Cl]^{3+/2+}$ electron-relaying centers, additionally cross-linked with PEGDGE: (A) no H_2O_2; (B) 0.1 mM H_2O_2. Conditions: aerated pH 7 physiological phosphate buffer (PBS) solution; scan rate 2.5 mV s^{-1}; 500 rpm.

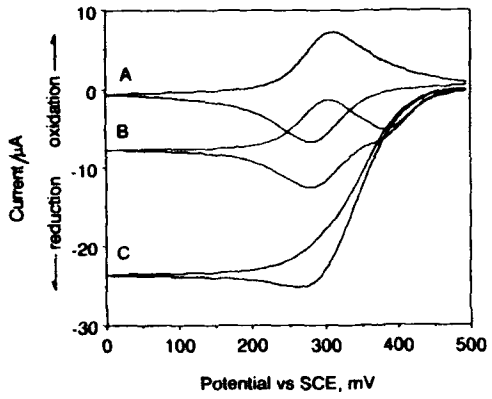

Figure 3. Electrode as in Figure 2, but *with* $[Os(bpy)_2Cl]^{3+/2+}$ electron-relaying centers (polymer I) (1:5 enzyme to polymer I ratio): (A) no H_2O_2; (B) 0.1 mM H_2O_2; (C) 0.5 mM H_2O_2. Conditions for A and B are as in Figure 2. For C the scan rate is 2.5 mV s^{-1}; 2000 rpm.

carbon rods from Atomergic Chemicals Corp. These were press-fitted into one end of a Teflon sleeve. The opposite end of the sleeve had a press-fitted stainless steel rod threaded to match a Pine rotator. Electrical contact between the vitreous carbon and stainless steel rods was made with a silver epoxy Epo-tek H2OE from Epoxy Technology Inc. The electrodes were polished first with 6-μm then with 1-μm diamond suspension, followed by 0.3-μm alumina. The polishing compounds were from Buehler. After each polishing step, the electrodes were sonicated 3–6 min in deionized water.

Enzyme Immobilization. HRP (2 mg) was dissolved in 100 μL of 0.1 M sodium bicarbonate solution. After the addition of 50 μL of 12 mg/mL sodium periodate, the enzyme solution was incubated in the dark for 2.3 h. A 10 mg/mL solution of polymer I was used to dilute aliquots of the enzyme solution to make enzyme: polymer I solutions of various ratios (1:5, 1:10, 1:50, 1:100). A 1-μL loading of enzyme: polymer I solution was applied to the polished vitreous carbon surface. The electrodes were allowed to partially dry for 5–15 min, after which, 1 μL of a 1 mg/mL solution of PEGDGE was applied. The electrodes were then cured in water-saturated air at room temperature for >4 h.

Electrodes were also made by coimmobilizing the $NaIO_4$-oxidized HRP with a polyamine that had no redox centers. This polyamine was obtained by reacting polyvinylpyridine (PVP) (MW 60 000) with 2-bromoethylamine to form the pyridinium-*N*-ethylamine derivative. It is thus similar to polymer I but has no $[Os(bpy)_2Cl]^{3+/2+}$ redox centers. The HRP was cross-linked to the polyamine using PEGDGE through the above described process.

Buffers, Electrodes, and Electrochemical Equipment. The electrodes were operated at room temperature in modified Dulbecco's buffer (PBS) at pH 7.4. Unless otherwise indicated, the solutions were well aerated. All mediator solutions were made daily and protected from light until used. Potentials were referenced to a saturated calomel electrode from EG & G, Catalog No. K0077. A platinum wire was used as the counter electrode. The chronoamperometric experiments were performed on an EG & G potentiostat/galvanostat Model 173 and recorded on a Kipp & Zonen XY recorder Model BD91. The cyclic voltammograms were run on an EG & G potentiostat/galvanostat Model 273A and recorded on a PC with software developed in this lab. The rotator used was a Pine Instruments AFMSRX with the ACMDI 1906C shaft.

RESULTS

H_2O_2 Sensing Electrodes. Electroreduction of H_2O_2 is observed on electrodes modified with HRP immobilized in the epoxy network formed of either the polyamine without $[Os(bpy)_2Cl]^{3+/2+}$ redox centers (Figure 2) or with $[Os(bpy)_2Cl]^{3+/2+}$ redox centers (Figure 3). When there are no $[Os(bpy)_2Cl]^{3+/2+}$ centers in the polymer, reduction takes

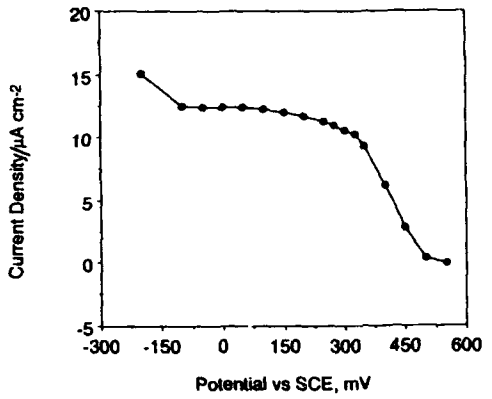

Figure 4. Potential dependence of the steady-state current density for a vitreous carbon electrode modified with PEGDGE-cross-linked HRP–polymer I at 1:5 ratio. Conditions: PBS; 1000 rpm; 1 × 10^{-5} M H_2O_2.

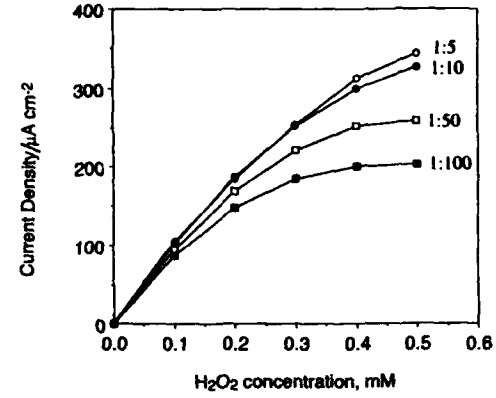

Figure 5. Dependence of the current density on the H_2O_2 concentration for vitreous carbon electrodes modified with PEGDGE-cross-linked HRP–polymer I films. The HRP:polymer I ratios are indicated. Conditions: PBS; 0.0 V (SCE); 1000 rpm.

place at potentials negative of 0.2 V (SCE). In 1 × 10^{-4} M H_2O_2 a ~1 μA cm^{-2} plateau is reached near 0.1 V (SCE). In the redox epoxy network formed by PEGDGE cross-linking of polymer I containing $[Os(bpy)_2Cl]^{3+/2+}$ centers, the current density at 0.0 V (SCE) increases by 2 orders of magnitude to about 100 μA cm^{-2}. Furthermore, H_2O_2 electroreduction is observed already at +0.45 V (SCE) and the steady-state current plateaus at +0.3 V (SCE) (Figure 4).

The dependence of the catalytic H_2O_2 electroreduction current density on the HRP:polymer I ratio in PEGDGE cross-linked films is seen in Figure 5. The current density is nearly independent of the HRP:polymer ratio at low (<1 × 10^{-4} M) H_2O_2 concentration. At higher (>1 × 10^{-4} M) H_2O_2 concen-

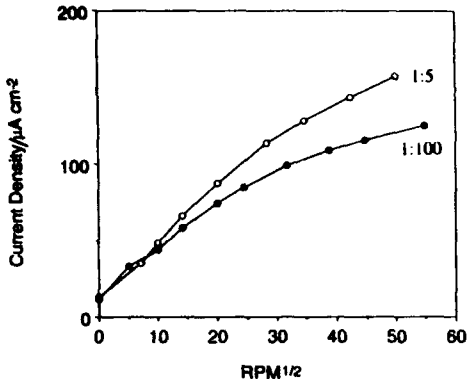

Figure 6. Dependence of the current density on the square root of the angular velocity of PEGDGE-cross-linked 1:5 and 1:100 HRP:polymer I electrodes. Conditions: PBS; 0.0 V (SCE); 0.1 mM H_2O_2.

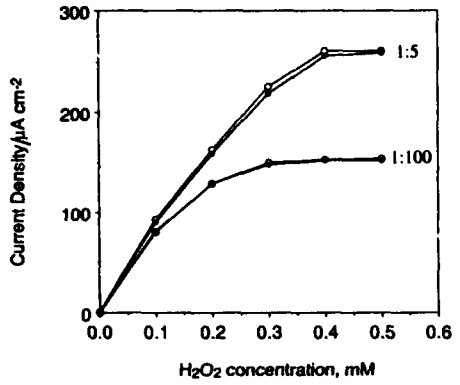

Figure 7. Steady-state calibration curves for PEGDGE-cross-linked 1:5 and 1:100 HRP:polymer I electrodes in air (solid circles) and nitrogen (open circles). Conditions: 0.0 V (SCE); PBS; 500 rpm.

tration the current density increases as the film becomes richer in HRP up to a ratio of 1:5 (Figure 5); the current density then decreases upon further increasing the enzyme content (not shown). The current densities of electrodes with 1:10 and 1:5 (HRP:polymer I) film ratios do not differ greatly. For electrodes with the 1:5 (HRP:polymer I) films the sensitivity in the (0–1) × 10^{-4} M H_2O_2 concentration range is 1 A cm^{-2} M^{-1}; i.e. the current density at 1 × 10^{-4} M H_2O_2 is 100 μA cm^{-2}. When the H_2O_2 concentration exceeds 0.25 mM, the current is time dependent and decays because of (slow) substrate inhibition of HRP. Control electrodes, made with PEGDGE cross-linked films of polymer I without HRP show no measurable H_2O_2 response.

Figure 6 shows Levich plots for 1:100 and 1:5 (HRP:polymer I) electrodes in 1 × 10^{-4} M H_2O_2. Linear dependence of the current density on the square root of the angular velocity is observed only up to about 400 rpm. At higher angular velocities the current densities increase with the HRP content of the films but are not proportional to the HRP content. At 2500 rpm increasing the HRP concentration from 1:100 to 1:5 increases the current density by only 30%.

The insensitivity of the electrodes to the partial pressure of oxygen is seen in Figure 7. There is no measurable difference between the calibration curves of the 1:100 (HRP:polymer I) electrode in nitrogen-purged or air-saturated solutions. For the 1:5 (HRP:polymer I) electrode there appears to be a marginal difference, with the readings in air exceeding those in nitrogen by less than 2%.

The dynamic range of the 1:5 (HRP:polymer I) electrode is seen in Figure 8. The current density increases linearly with H_2O_2 concentration over a range of 3 orders of magnitude from about 1 × 10^{-7} to 1 × 10^{-4} M (correlation coefficient

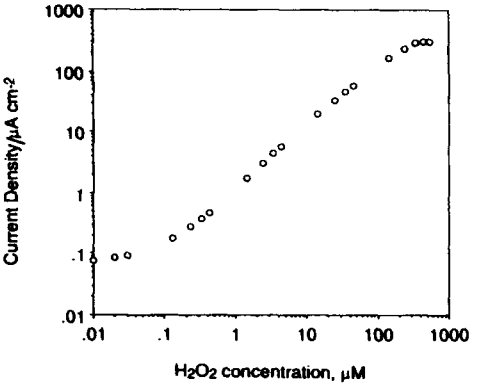

Figure 8. Dynamic range of the 1:5 HRP:polymer I electrode. Steady-state measurements were at 0.0 V (SCE) and 1000 rpm with PBS.

0.997; slope 1 A cm^{-2} M^{-1}). At 10^{-5} M H_2O_2 the 0–95% rise time is 2 min. At lower concentrations the rise times are longer. Following an H_2O_2 injection raising the concentration from 0.0 to 1 × 10^{-7} M, the rise time is about 10 min. The noise equivalent H_2O_2 concentration is 3 nM; i.e. at 1 × 10^{-6} M H_2O_2 the signal to noise ratio is 3. The background current, measured after the electrode was allowed to stabilize for 30 min, is 70 nA cm^{-2}.

NAD(P)H Sensing Electrodes Derived of HRP Wired to a 3-Dimensional Redox Polymer Network. The wired HRP electrodes are insensitive to NAD(P)H; i.e. the background current at 0.0 V (SCE) does not change when either cofactor is added. However, if 1-methoxy-5-methylphenazonium methyl sulfate (I, cation), 5-methylphenazonium methyl sulfate (II, cation), Meldola's blue (III, cation), Nile blue (IV, cation), toluidine blue O (V, cation), methylene blue (VI, cation), thionine (VII), flavin mononucleotide (VIII), 4,5-dihydro-4,5-dioxo-1*H*-pyrrolo[2,3-*f*]quinoline-2,7,9-tricarboxylic acid (PQQ) (IX), or methylene violet (Bernthsen) (X) is added, an NAD(P)H concentration dependent cathodic current is observed. The structures of these heterocyclic quinoids are shown in Figure 9. The relative effectiveness of these mediators in the H_2O_2-forming reaction is in the order of their listing, the phenazonium derivatives and Meldola's blue being the most effective and flavin mononucleotide, PQQ, and methylene violet the least. Addition of any of the mediators at <1.0 μM concentration does not produce a current response.

The dependence of the steady-state current density on the NADH concentration for aerated solutions containing 1.6 μM 5-methylphenazonium methyl sulfate is seen in Figure 10. The dependence is linear through the 1–100 μM NADH concentration range and the slope, i.e. sensitivity, is 1 A cm^{-2} M^{-1}, similar to that for H_2O_2. Corresponding results for NADPH are seen for the 1:5 electrode in Figure 11. The linear range for NADPH is from 1 to 200 μM, and the sensitivity is again 1 A cm^{-2} M^{-1}. The equilibration times for steady-state measurements depend on the concentration of the mediator; a higher mediator concentration results in acceleration of the H_2O_2 production. Typically, the 0–95% rise time of the current following an NADH injection was 5–7 min at 3.3 μM 5-methylphenazonium methyl sulfate concentration.

As expected from reaction 3, electroreduction currents were observed only in aerated or oxygenated solutions. The current did not increase when O_2 rather than air was bubbled through the solution. When the solutions were purged of oxygen by bubbling with N_2, the current reversed; i.e. an electrooxidation current was observed in the PMSH (PMS^+ and NADH) containing solution. Electrooxidation of PMSH proceeded on glassy carbon electrodes whether or not these were modified

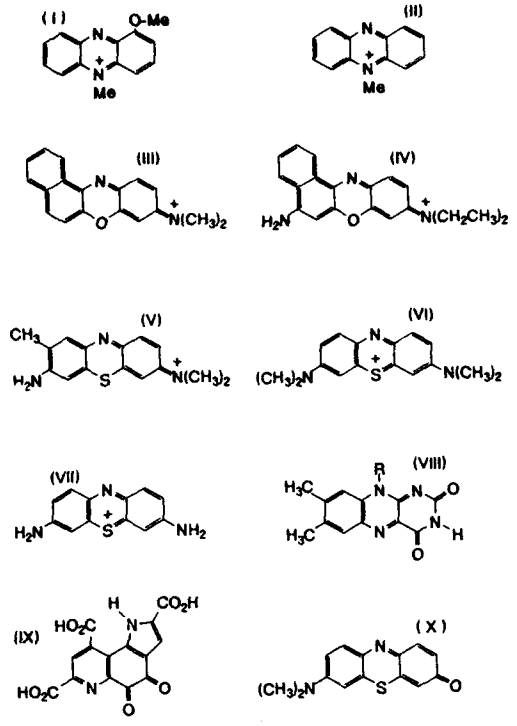

Figure 9. Structures of the mediators which are able to catalytically cycle through reactions 2 and 3. Note the central quinoidal structure stabilized by the adjacent aromatic rings: cation of 1-methoxy-5-methylphenazonium methyl sulfate (I); cation of 5-methylphenazonium methyl sulfate (II); cation of Meldola's blue (III); cation of Nile blue (IV); cation of toluidine blue O (V); cation of methylene blue (VI); thionine (VII); flavin mononucleotide (VIII); 4,5-dihydro-4,5-dioxo-1*H*-pyrrolo[2,3-*f*]quinoline-2,7,9-tricarboxylic acid (PQQ) (IX); methylene violet (Bernthsen) (X).

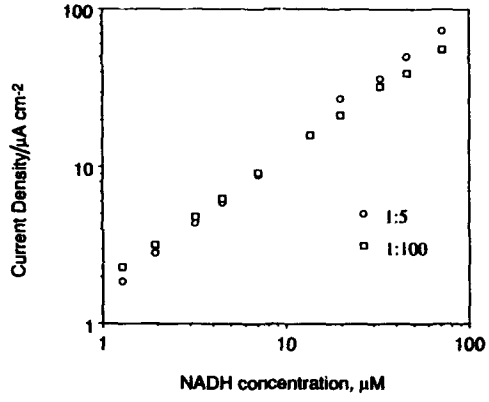

Figure 10. Dependence of the steady-state electrocatalytic reduction current density on the NADH concentration for PEGDGE-cross-linked 1:5 and 1:100 HRP:polymer I film-modified vitreous carbon electrodes. Conditions: 0.0 V (SCE), 1000 rpm, 1.6 μM 5-methylphenazonium methyl sulfate (PMS^+); PBS.

with HRP-containing films. Even minimal aeration of the PMSH solutions reversed the current, but only on HRP-modified electrodes.

Light Effects. PMS^+ solutions strongly absorb $\lambda < 480$ nm light. It has been reported that the mechanism of reduction of heterocyclic quinoid dyes by NADH can involve their excited states.[17,25] Furthermore, the oxidant of the NADH-reduced quinoid dye may not be ground-state (triplet) oxygen but excited (singlet) oxygen, formed through energy transfer from the excited dye in its triplet state. Thus, as a precaution, the effect of 0.2 mW cm^{-2} 4100 K color temperature "cool-white" fluorescent on the rise time of the current

(25) Julliard, M.; Le Petit, J. *Photochem. Photobiol.* **1982**, *36*, 283–90.

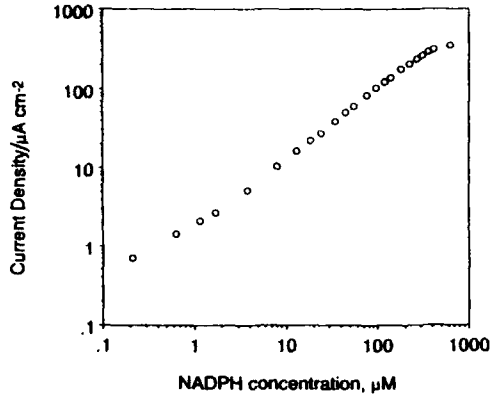

Figure 11. Dependence of the steady-state electrocatalytic reduction current density on the NADPH concentration for the 1:5 electrode of Figure 10. Conditions were as in Figure 10, except that the 5-methylphenazonium methyl sulfate concentration was 4.7 μM.

was checked. Control experiments with PMS^+ (1×10^{-5} M) show that the current is not changed when the electrode is operated in the dark or with the above ambient irradiance. It was also noted, however, that PMS^+ measurably photodecomposed even at low irradiance by the ambient light.

DISCUSSION

HRP-Based Hydrogen Peroxide Sensing Electrodes. Table I compares H_2O_2 electrodes based on direct, diffusionally mediated, and redox polymer-relayed electroreduction of HRP. Comparison of the electrodes shows that the wiring of HRP to an electrode, i.e. its covalent binding to a hydrophilic 3-dimensional electron-relaying redox network, increases sensitivity. In the absence of osmium-complex relays the observed sensitivity, 1×10^{-2} A cm^{-2} M^{-1}, is 2 orders of magnitude lower than that in their presence (Figures 2 and 3). In the first case only redox centers of HRP molecules actually contacting the electrode surface may be electroreduced. These redox centers produce the redox wave in Figure 2. In contrast, most HRP molecules in the films, the thickness of which is $\simeq 10^{-4}$ cm, are electrically accessible when electrons are relayed through $[Os(bpy)2Cl]^{3+/2+}$ centers complexed to the polyvinylpyridine backbone in polymer I. Electrooxidation of HRP in the electron-relaying epoxy network starts at +0.45 V, i.e. 0.18 V positive of the +0.27-V redox potential of the $[Os(bpy)_2Cl]^{3+/2+}$ centers. This implies that oxidized HRP accepts electrons from the network even when the ratio of the reduced to oxidized centers is only about 1:1000.

The optimal HRP:polymer I ratio in the film (Figure 5) is near 1:5. At higher enzyme content, the electron-relaying capacity of the films is diminished by the nonrelaying HRP in the network. The network, with an electron diffusion coefficient below 10^{-8} cm^2 s^{-1},[24] does not transport or transfer electrons to the bound enzyme molecules fast enough to match their turnover rate at optimal (10^{-4} M) substrate concentration. Had the electron transport through the polymer been faster, still higher current densities might have been realized. That the electrodes are limited by the rate of electron transfer either through the network or from the network to the enzyme is seen in the Levich plots of Figure 6. These show normal solution mass transfer limited kinetics of the substrate, characterized by linear dependence of the current density on the square root of the angular velocity, only at low angular velocities. At high angular velocities where the kinetics does not depend linearly on substrate mass transport and depends only weakly on enzyme content, the characteristics are dominated by transport of either electrons or substrate through the film. Previous work with glucose oxidase

containing redox epoxy films suggests electron transfer or transport limitation.[24]

Reduction of Heterocyclic Quinoids by Two Electron Plus Proton Transfer from NAD(P)H. The earlier results of Miller, Gorton, Kulys, and their colleagues[26-31] show that NAD(P)H is rapidly and cleanly oxidized to $NAD(P)^+$ by transferring two electrons plus a proton to any of a variety of dissolved or electrode-surface-bound quinoids, including native quinoids on oxidized graphite (reaction 5). 5-Methylphenazonium derivatives and Meldola's blue and its derivatives are particularly fast two electron plus proton acceptors from NAD(P)H. The homogeneous bimolecular two electron proton transfer rate from NADH to PMS^+ (reaction 2) is 3.8×10^3 M^{-1} s^{-1} at 25 °C.[32]

$$\text{quinoid}_{ox} + NAD(P)H \rightarrow \text{quinoid}_{red} + NAD(P)^+ \quad (5)$$

Oxidation of PMSH by O_2 (reaction 3), whereby PMS^+ is recovered and H_2O_2 is produced, has a bimolecular homogeneous rate constant of 1.8×10^2 M^{-1} s^{-1} in water at 25 °C.[32] Thus in an aqueous solution in equilibrium with air ($\simeq 2.5 \times 10^{-4}$ M O_2), the oxidation of PMSH is rapid. Indeed, the related reaction of dihydrophenazine and O_2 in an organic solvent (reaction 6) has been considered as an industrial process for the production of H_2O_2.[33]

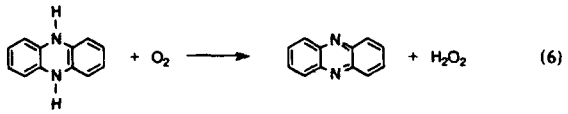

(6)

The rates of reactions 2 and 3 and H_2O_2 diffusion may all slow the response, i.e. rise time, of the NAD(P)H sensor. At low NADH concentration (0.1 μM) the calculated rate from reaction 2 and inherent diffusion-controlled transport of H_2O_2 are limiting factors of the electrode's kinetics. At higher NADH concentration (100 μM) and at low PMS^+ concentrations (1.6 μM) reaction 3 limits the electrode's response. The calculated H_2O_2 formation rates through reaction 3 and experimental sensor rise times are of the same order of magnitude.

The variation of current with concentration, and the 1 A cm^{-2} M^{-1} sensitivity, for NADH (Figure 10) and NADPH (Figure 11) through their 1×10^{-7} to 2×10^{-4} M concentration range are identical to those of H_2O_2 (Figure 8). We infer from the identical sensitivities and dynamic ranges that the homogeneous two electron and proton transfer reactions proceed either at or very close to unit current efficiency, i.e. that NAD(P)H produces a stoichiometric amount of H_2O_2 through reactions 2 and 3. The actual mechanism of H_2O_2 production involves more steps than represented by equations 2 and 3.

Interferences. Schmidt et al. suggested that "Reduction of the oxygen proceeds by a complex sequence of reactions, producing among other intermediates the superoxide radical ion, which leads to hydrogen peroxide and this in turn is capable of oxidizing methylene blue and so a stoichiometric production of hydrogen peroxide is not observed".[17] The disparity probably results from the higher dye concentrations employed by Schmidt et al. At a high dye concentration the rates of side reactions, particularly between the reduced dye and H_2O_2, are increased. At the NAD(P)H and mediator concentrations employed here we observe only the stoichiometric reaction 7. As is evident from reaction 3, the assay

$$NAD(P)H + H^+ + O_2 \rightarrow NAD(P)^+ + H_2O_2 \quad (7)$$

requires that the solutions be aerated. A decrease in O_2 partial pressure will slow reaction 3. Nevertheless, even in this case the ultimate steady-state current will not change, because reaction 3 is irreversible. The high bimolecular rate constant (1.8×10^2 M^{-1} s^{-1}) for PMSH oxidation by O_2 usually ensures a rapid reaction in air-exposed solutions. When the oxygen concentration is only $^1/_{10}$th of that in a well-aerated solution (a typical value at 25 °C being 0.25 mM), the half-life of PMSH is 154 s, assuming a pseudo-first-order reaction in PMSH.

HRP-catalyzed reactions may cause severe interference by a number of interferants. H_2O_2-oxidized HRP may be reduced by any of a number of hydrogen donors. Such reduction will cause loss of catalytic current. Addition of 0.1 mM ascorbate, a common component of biological samples, will reduce the cathodic current by over 50%. Current will also be lost if NAD(P)H directly reduces H_2O_2-oxidized HRP. This reaction is actually observed in our experiments as a dip in the current from the electrodes when NAD(P)H is initially injected into a solution with a substantial H_2O_2 concentration already present. Once the NAD(P)H reacts to form H_2O_2 and $NAD(P)^+$, the current recovers. The ultimate current is not lowered, because reactions occurring at the electrode surface do not change the bulk solution concentrations, the bulk H_2O_2 concentration being reached through the homogeneous solution reactions 2 and 3. Beyond organic hydrogen donors, H_2O_2 itself is oxidized by HRP to O_2 and water.[34] Fortunately, the latter reaction is not fast.

CONCLUSIONS

In contrast with redox centers of flavoprotein enzymes like glucose oxidase, that do not communicate directly with carbon electrodes on which the enzymes are adsorbed, redox centers of directly absorbed horseradish peroxidase do communicate electrically with carbon electrodes.[35,36] The maximum current

(26) Murray, R. W. In *Electroanalytical Chemistry*; Bard, A. J., Ed.; Marcel Dekker: New York; Vol. 13, pp 191–238.
(27) Albery, W. J.; Bartlett, P. N.; Cass, A. E. G. *Phil. Trans. R. Soc. London B* **1987**, *316*, 107–19.
(28) Albery, W. J.; Bartlett, P. N. *J. Chem. Soc., Chem. Commun.* **1984**, 234–6.
(29) Itoh, S.; Kinugawa, M.; Mita, N.; Ohshiro, Y. *J. Chem. Soc., Chem. Commun.* **1989**, 694–5.
(30) Yabuki, S.; Mizutani F.; Asai, M. *Biosensors Bioelectron.* **1991**, *6*, 311–5.
(31) Kimura, Y.; Niki, K. *Anal. Sci.* **1985**, *1*, 271–4.
(32) Halaka, F. G.; Babcock, G. T.; Dye, J. L. *J. Biol. Chem.* **1982**, *257*, No. 3, 1458–61.
(33) *Encyclopedia of Chemical Technology*, 3rd ed.; Kirk, J. R., Othmer, D. F., Eds.; John Wiley and Sons: New York, 1981; Vol. 13, pp 16–22.
(34) Brill, A. S. *Comprehensive Biochemistry*; Elsevier: Amsterdam, 1966; pp 447–79.
(35) Yaropolov, A. I.; Malovik, V.; Varfolomeev, S. D.; Berezin, I. V. *Dokl. Akad. Nauk. USSR* **1979**, *249* (6), 1399–401.
(36) Jonsson, G.; Gorton, L. *Electroanalysis* **1989**, *1*, 465–8.
(37) Wang, J.; Frieha, B.; Naser, N.; Romero, E. G.; Wollenberger, U.; Ozsoz, M.; Evans, O. *Anal. Chim. Acta* **1991**, *254*, 81–8.
(38) Cosgrove, M.; Moody, G. J.; Thomas, J. D. R. *Analyst* **1988**, *113*, 1811–5.
(39) Kulys, J. J.; Samalius, A. S.; Svirmickas, G.-J. S. *FEBS Lett.* **1980**, *114*, 7–10.
(40) Tatsuma, T.; Okawa, Y.; Watanabe, T. *Anal. Chem.* **1989**, *61*, 2352–5.
(41) Sanchez, P. D.; Ordieres, A. J. M.; Garcia, A. C.; Blanco, P. T. *Electroanalysis* **1991**, *3*, 281–5.
(42) Schubert, F.; Saini, S.; Turner, A. P. F. *Anal. Chim. Acta* **1991**, *245*, 133–8.
(43) Pantano, P.; Morton, T. H.; Kuhr, W. G. *J. Am. Chem. Soc.* **1991**, *113*, 1832–3.
(44) Kulys, J. J.; Pesliakiene, M. V.; Samalius, A. S. *Bioelectrochem. Bioenerg.* **1981**, *8*, 81–8.
(45) Lundback, H.; Olsson, B. *Anal. Lett.* **1985**, *18* (B7), 871–89.
(46) Kojima, J.; Morita, N.; Takagi, M. *Anal. Sci.* **1988**, *4*, 497–500.
(47) Kulys, J. J.; Laurinavicius, V.-S. A.; Pesliakiene, M. V.; Gureviciene, V. V. *Anal. Chim. Acta* **1983**, *148*, 13–8.

density does not exceed, however, in the absence of a diffusional mediator or of nondiffusing electron-relaying centers, the current density associated with the turnover of the enzyme layer directly contacting the electrode surface. Oxidized horseradish peroxidase molecules, that are remote from the electrode surface, do not accept electrons from electrodes unless the electrons are relayed through redox centers in the polymer. The current density is increased by 2 orders of magnitude when the HRP molecules bound throughout the thick film are connected to the electrode through its 3-dimensional electron-relaying network. The sensitivity of the resulting amperometric H_2O_2 sensor is 1 A cm^{-2} M^{-1} at 0.0 V (SCE), and its dynamic range is 1×10^{-7}–2×10^{-4} M H_2O_2.

Two electron plus proton transfer from NAD(P)H to quinoids produces stoichiometric concentrations of H_2O_2. With NADH and NAD(P)H stoichiometrically translated to H_2O_2, their concentrations can be amperometrically assayed at wired horseradish peroxidase cathodes poised at 0.0 V (SCE) (Figure 12). The sensitivities and dynamic ranges of these cathodes are identical with those of H_2O_2 cathode, 1 A cm^{-2} M^{-1} through the 1×10^{-6}–10^{-4} M concentration range.

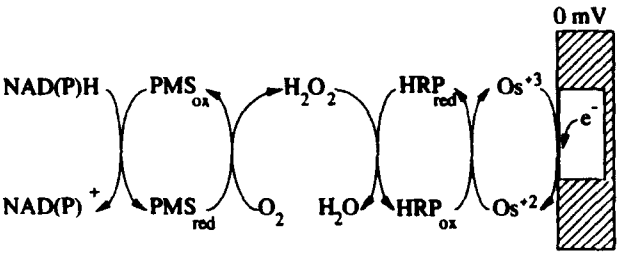

Figure 12. Cycles of the proposed NADH (and NADPH) cathodes.

Although the assay of these cofactors requires molecular oxygen, the electrodes are not excessively sensitive to variations in O_2 partial pressure because the quinoid-catalyzed NAD(P)H reactions with O_2 are irreversible.

ACKNOWLEDGMENT

The work described was supported by the Office of Naval Research, by the National Science Foundation, and by the Welch Foundation.

RECEIVED for review April 21, 1992. Accepted September 28, 1992.

(48) Frew, J. E.; Harmer, M. A.; Allen, H.; Hill, O.; Libor, S. I. *J. Electroanal. Chem. Interfacial Electrocem.* **1986**, *201*, 1–10.

Reprinted from Analytical Chemistry, 1992, *64*.

L-α-Glycerophosphate and L-Lactate Electrodes Based on the Electrochemical "Wiring" of Oxidases

Ioanis Katakis and Adam Heller*

The University of Texas at Austin, Department of Chemical Engineering, Austin, Texas 78712

The title electrodes were constructed by colmmobilizing the respective FAD oxidases on solid electrode surfaces with a poly(vinyl pyridine) polymer which was N-derivatized with bromoethylamine and $Os(bpy)_2Cl_2$. The redox-polymer–enzyme hydrogels were cross-linked on the electrode surface using poly(ethylene glycol) diglycidyl ether. As in the case of glucose oxidase, the redox polymer acts as an electron relaying "wire" transferring electrons directly from the enzymes' $FADH_2$ centers to the electrode. This transfer competes with the natural process of reoxidation of $FADH_2$ by molecular oxygen. The variation of the response of these electrodes with the atmosphere (N_2 or air), pH, and substrate concentration was determined. The pH profile of the electrocatalytic current differs from that of the activity of the free enzymes, exhibiting a broader maximum, shifted to higher pH values. The observed sensitivities and linear ranges are respectively 2×10^{-2} A M^{-1} cm^{-2} and 2.7 mM for L-α-glycerophosphate, and 0.3 A M^{-1} cm^{-2} and 0.2 mM for L-lactate that may be compared to 2×10^{-2} A M^{-1} cm^{-2} and 10 mM for glucose. The 0–90% response time for all electrodes is 1 s or less.

INTRODUCTION

In contrast with low molecular weight polymers that diffusionally mediate electron transfer from the enzymes' active center[1-3] to electrodes, high molecular weight polymers can be designed to complex with redox enzyme proteins and to nondiffusionally relay electrons from the enzyme redox centers to electrodes. In these complexes, the oxidized redox polymers compete efficiently with oxygen in the oxidation of substrate-reduced enzyme redox centers.[4-6] The high molecular weight redox polymers connect the enzyme redox centers to electrodes only when they (a) are adsorbed on the electrodes and (b) have long nonabsorbed segments extended into the solution that complex and penetrate enzyme proteins. These superficially contradictory requirements are met by making the molecular weight high enough so that even though most segments are most of the time unadsorbed, i.e. in solution, there is always a sufficient number of segments adsorbed to make their simultaneous desorption statistically improbable. In the special case of cross-linkable enzyme-complexing polymers, three-dimensional, enzyme-incorporating hydrophilic networks of molecular weights greatly exceeding those of either the constituent redox polymer or the enzyme can be

0003-2700/92/0364-1008$03.00/0

formed on electrode surfaces.[7-11]

We show here that in addition to redox centers of glucose oxidase[11] also redox centers of glycerophosphate oxidase, and lactate oxidase can be electrochemically connected to electrodes through cross-linked redox polymer–enzyme hydrophilic epoxy networks and characterize the resulting glycerol 3-phosphate and lactate electrodes.

EXPERIMENTAL SECTION

Chemicals. L-α-Glycerol phosphate oxidase (GPO) (L-α-glycerophosphate: oxygen oxidoreductase, EC 1.1.3.21), from *Aerococcus viridans*, and lactate oxidase (LOX) (L-lactate: oxygen oxidoreductase, former EC 1.1.3.2), from *Pediococcus* species, were purchased from Genencor Int (representatives of Toyo Jozo) and were used without purification. Glucose oxidase (GOX) (D-glucose: oxygen oxidoreductase, EC 1.1.3.4), from *Aspergillus niger*, and peroxidase (Donor: H_2O_2 oxidoreductase, EC 1.11.1.7), from horseradish, were purchased from Sigma (Catalog Nos. G-7141 and P-8250, respectively) and were also used without purification. L-Lactic acid and D,L-α-glycerophosphate were also purchased from Sigma. D-Glucose was purchased from J. T. Baker. All other chemicals (phenol, o-dianisidine, 4-aminoantipyrine) were of reagent grade or better and were purchased either from Sigma or Aldrich. Water used was NANOpure, and the buffer most commonly employed was 33 mM phosphate, 0.15 M NaCl at pH 7.15 (to be referred to as STD buffer). The redox polymer (linear PVP of approximately 50 kDa N-derivatized with $Os(bpy)_2Cl_2$ and bromoethylamine as reported earlier) had an approximate equivalent MW per osmium center of 1510 as determined by elemental analysis and UV spectrophotometry.[11] The diepoxide used was poly(ethylene glycol) diglycidyl ether purchased from Polysciences (Catalog No. 08210).

Electrodes. Modified electrodes were glassy-carbon disks, 3 mm in diameter (V-10 grade vitreous carbon from Atomergic). The glassy-carbon rods were encased in Teflon cylinders with deaerated slow-setting epoxy (Armstrong), and the Teflon cylinder was fitted on an AFMSRX rotator (Pine Instruments).

All electrodes were treated by polishing on three grits of sand paper and then successively on four grades of alumina (20, 5, 1, 0.3 μm) with sonication and thorough washing with NANOpure water between grades. Background scans for every electrode were taken at 1000, 500, and 100 mV s^{-1} in STD buffer to make sure the voltammograms were featureless. The electrodes were subsequently washed and stored in a desiccator until use. The average capacitance of the GC electrodes in STD buffer was 29 ± 5 $\mu F/cm^{-2}$.

The modification procedure was similar to that reported earlier.[11] Elecrodes were prepared either by depositing the components sequentially and mixing on the electrode surface, or (in the case of diffusion studies) from a common mix of enzyme, polymer, and cross-linker when reproducibility was important. The weight ratios of enzyme protein to nonenzymatic material (contaminants from the enzyme isolation process) to polymer were 1:3:5 for LOX and 1.5:0.5:5 for GPO electrodes, so as to keep the operation of the electrodes in the kinetically limited regime (see Discussion) and/or to keep the observed current densities at saturating substrate concentrations similar for both types of electrodes. The mixtures contained 6% (per weight) of cross-linker. For a typical electrode a total of about 8 μg of material yielding a geometric surface coverage of 130 μg cm^{-2} was applied on the surface. The dry thickness of such electrodes was about 0.8 μm as determined by profilometry and SEM. The electrodes were left to cure in a desiccator for 24 h under reduced pressure. Before use they were washed by incubation in STD buffer for at least 8 h (in a 2-mL volume) under vigorous stirring. The solutions in which the electrodes were washed were assayed for enzymatic activity and protein content (see below). There was no effort made to optimize the immobilization procedure or the current efficiency or the competition with O_2. Rather, the goal was to keep the cross-linking conditions as constant and reproducible as possible. Because the GPO or LOX solutions even in 10 mM HEPES buffer at pH 8.1 are not particularly stable, an effort was made to test all the electrodes during the same 12–24-h period. This requirement was particularly important for the enzymes (other than glucose oxidase) that lost activity during the curing process. The reproducibility of the response of electrodes prepared from the identical enzyme–polymer mixtures was ±10% or better, as evidenced by the scatter in both maximum current density at saturating substrate concentration and the concentration at which half the maximum current density was observed ("apparent K_m" or "half-saturation point").

Electrochemistry. The electrochemical experiments were performed with a Princeton Applied Research 173 potentiostat and a 175 PAR universal programmer equipped with a Model 179 digital coulometer. Signals were recorded on an $X-Y-Y'$ Kipp Zonnen recorder. The chronoamperometric and chronopotentiometric experiments, as well as cyclic voltammetry at less than 1 mV/s were performed with the help of a 273 PAR potentiostat interfaced to an IBM PC. Unless otherwise noted, a single-compartment water-jacketed 100-mL cell was used thermostated at 21.8 ± 0.2 °C, with an aqueous saturated calomel electrode as reference (SCE) and all potentials are reported with respect to this. A platinum wire encased in a heat-shrinkable sleeve with a frit was used as the counter electrode.

Unless otherwise stated, the steady-state current was monitored with the electrodes poised at 0.45 V, where the current no longer varied with potential (the current plateau was reached at about 0.39 V). Concentrations of L-α-glycerophosphate were calculated from the optical rotation of D,L-α-glycerophosphate. For the GOX electrodes, concentrations of D-glucose are reported even though the enzyme only catalyzes the reaction of the D-β-glucose comprising about 60% of the total D-glucose concentration after mutarotation is complete.

Assays. The activity of the enzymes was determined in all cases at 22 ± 1 °C. A series of experiments with a single enzyme normally took about 3–4 days to complete. During this period, the native enzyme stored dissolved in pH 8.1 10 mM HEPES buffer was periodically assayed for loss of activity under the storage conditions. Concentrations of enzyme solutions were determined from the extinction coefficients of bound FAD in GOX and GPO[12-15] (21.6 and 11.3 mM^{-1} cm^{-1}, respectively). For LOX the manufacturer's specification for protein content was accepted. However, after purification of the enzyme through HPLC, it was found that the specific activity and protein content increased 4-fold. For determining the total amount of protein, the Biorad microassay method was used.[16]

The enzyme assays as well as the electrochemical measurements were performed, unless otherwise stated, in STD buffer of pH 7.15. The enzyme assays involved the peroxidase-catalyzed reaction of an oxidizable dye, o-dianisidine in the case of GOX, 4-aminoantipyrine and phenol in the case of GPO, and 4-aminoantipyrine and N,N-dimethylaniline in the case of LOX. Absorbances were measured at 500 nm for the first and 565 nm for the later two, and the known extinction coefficients were used for quantitation.[17] The O_2-saturated total reaction volume was generally about 3 mL, and the dyes, substrate, and peroxidase were present in excess. The mean specific activities of the purified enzymes used were 24 units mg^{-1} for GPO and 108 units mg^{-1} mg for LOX.

RESULTS AND DISCUSSION

Results. Figure 1 shows that lactate and glycerol 3-phosphate, like glucose, are electrocatalytically oxidized at electrodes coated with 3-dimensional redox polymer epoxy networks incorporating the respective oxidases. The two electrodes were made with different enzyme:nonenzymatic material:polymer weight ratios, 1.5:0.5:5 for GPO and 1:3:5 for LOX, so as to make their current densities at high substrate concentrations—where these no longer affect the current—similar. The loading was 100–130 μg cm^{-2} of the enzyme-containing epoxy. The current densities of the resulting electrodes, at high substrate concentrations, were within about 20%. This condition, achieved experimentally by trial and error, represents a specific set of constituent ratios. Comparison of electrodes made with different enzymes must be based on electrodes with similar enzyme to polymer ratios (because the protein is an insulator and electron transport is through the redox polymer) and also with similar current densities, i.e. similar total enzymatic activity. Furthermore,

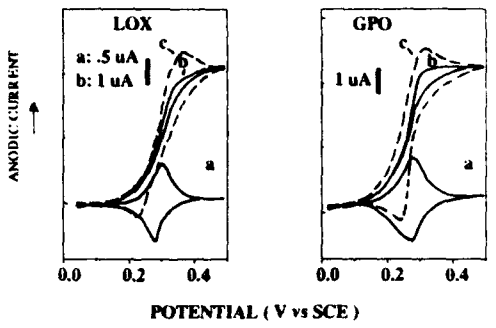

Figure 1. Cyclic voltammograms demonstrating the catalytic nature of the anodic currents and the "threshold" or breakpoint in scan rate for the appearance of reductive waves. Scans: (a) 1 mV s^{-1}, in STD buffer; (b) 1 mV s^{-1} after the introduction of 10 times the half-saturation point substrate concentration; (c) lowest scan rate value where reduction wave appears (GPO, 2 mV s^{-1}; LOX, 5 mV s^{-1}). Electrode construction parameters: typical thickness, 130 μg cm^{-2}. All electrodes had a 3-mm diameter and were rotated at the highest rotation rate for linear E–H plots.

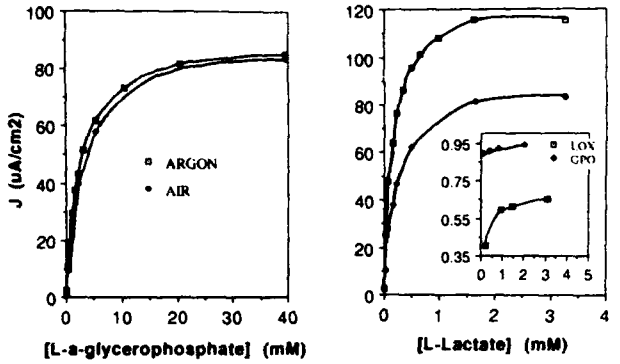

Figure 2. Dependence of the current on substrate concentration. The insert shows the fraction of the current remaining after the argon-purged solution is air saturated as a function of the substrate concentration expressed in multiples of the apparent K_m of the electrodes. Conditions: 130 μg cm^{-2} film thickness; STD buffer; electrodes rotated at 3000 rpm.

the immobilized enzyme activity should be low enough to make the electrodes operate through the widest possible range of substrate concentrations with the turnover of the enzyme being rate limiting.

The voltammograms in the absence of substrate showed 20–25-mV peak to peak separation for either enzyme electrode. The slowest scan rate at which an Os^{3+} reduction wave became observable in the presence of substrate was 2 mV s^{-1} for GPO and 5 mV s^{-1} for LOX.

Figure 2 shows the current density as a function of substrate concentration in argon and in air. Because the electrodes were designed for equal current density and not for optimal electron transfer via the network to the electrode, oxygen competed effectively in the oxidation of the $FADH_2$ centers of LOX.

The pH dependence experiments were conducted in both STD buffer and universal buffer (0.004 M each of sodium citrate, sodium barbitural, potassium phosphate, and boric acid), with the pH being initially at 7.15 and then changed by the dropwise addition of 2 M HCl to about pH 4 and then to pH 10.5 with 2 M NaOH. The electrochemistry of the polymer in this pH range did not exhibit substantial differences. However at the extremes of the pH scale, we did observe changes in the peak separation and the height of the peaks, which were reversible upon pH restoration. Above pH 11, irreversible lowering of peak currents, increase in peak separation (50–100 mV), and diffusional tailing were observed. The changes in current between pH 4 and 10.5 were not totally reversible in GPO and LOX electrodes but were reversible for GOX electrodes up to pH 10.5.

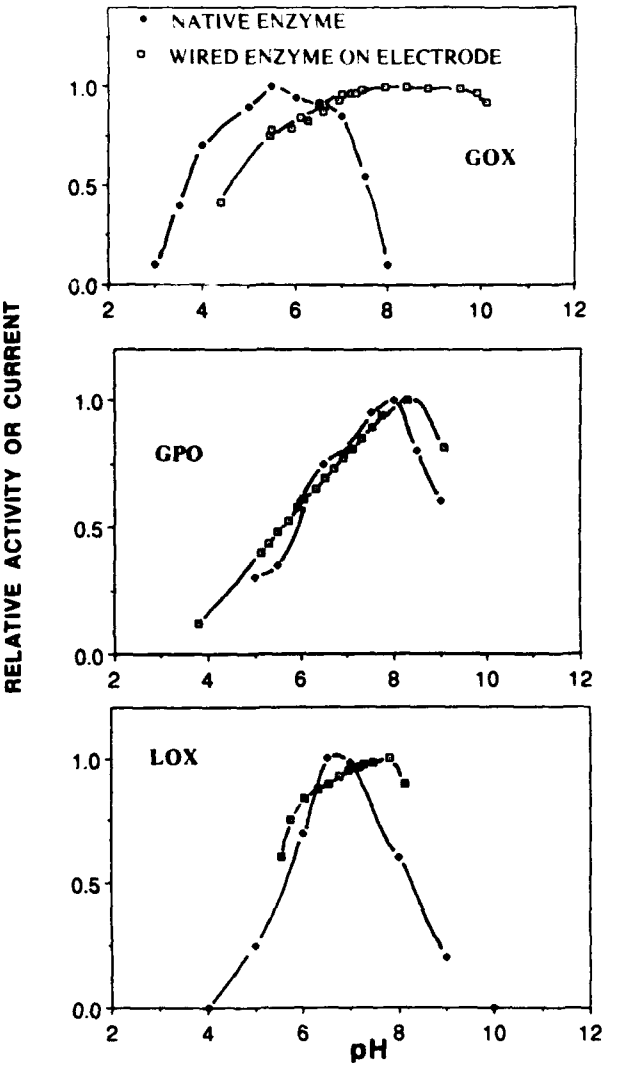

Figure 3. pH dependence of the activity of the native enzymes in solution (♦) and of the response of the electrodes (◇). The electrodes were rotated at 1000 rpm in argon-saturated solutions at saturating substrate concentrations.

Figure 3 shows the pH dependence of the currents under anaerobic conditions at high substrate concentrations, where the current does not increase upon adding substrate. Incorporation of the enzyme in the redox epoxy network broadens the pH domains of maximum response and shifts these domains to higher pH. These effects are observed and are greatest in glucose oxidase, shown for comparison. In glucose electrodes the current remains within 20% of its maximum over the entire pH 6.5–10.5 range, with the maximum being at pH 7.5–9.0. In the case of LOX, the current is within 20% of its maximum over the pH 6.5–8.5 range, the maximum being near pH 8; and in the case of GPO the flat region is at pH 7.5–8.5, peaking at about pH 8.2. The displacement of the pH maxima versus those of the free enzymes is of 3 pH units for GOX, 1.5 units for LOX, and 0.5 units for GPO. These differences in pH dependence will be discussed later.

Figure 4 shows the temperature dependence of the currents. The experiments were conducted at high substrate concentrations under argon. The Arrhenius current plots are reasonably linear through the considered temperature range, and the apparent activation energies are 59 kJ mol^{-1} for GPO and 79 kJ mol^{-1} for LOX electrodes.

Modified Eadie–Hofstee-type plots for the stationary electrode, at 50 rpm rotation and at >3500 rpm, are shown

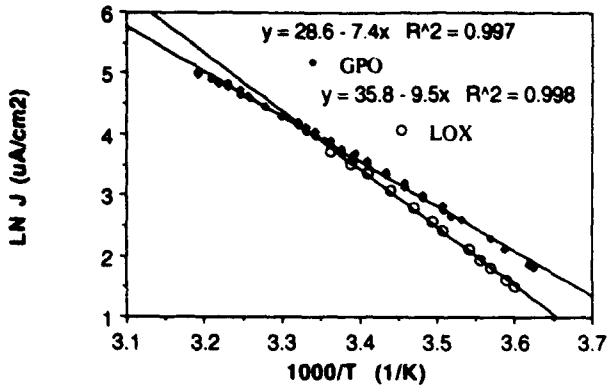

Figure 4. Temperature dependence of the current. Conditions: rotation rate 2000 rpm; film thickness 20 μg cm^{-2}; STD buffer; saturating substrate concentration.

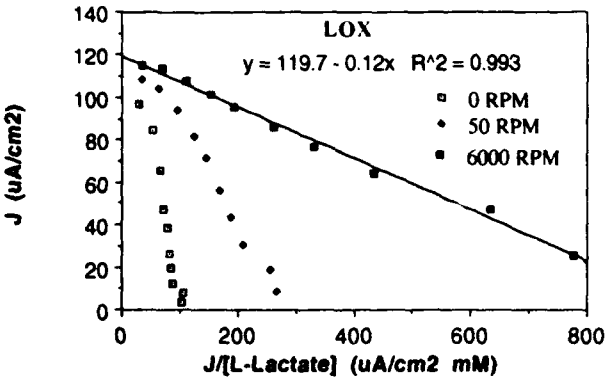

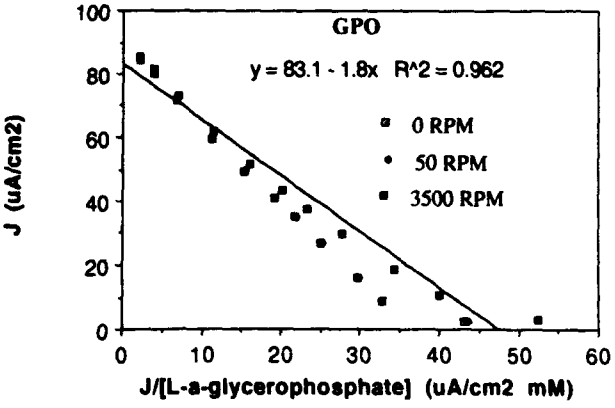

Figure 5. Eadie–Hofstee plots at varying angular velocities. Conditions: STD buffer; 21.7 °C; argon-saturated solution; film thickness 130 μg cm^{-2}.

in Figure 5. The often reported linear dependence is observed in the GPO electrode almost regardless of rotation speed. In the case of the LOX electrode the linearity is observed, however, only at high rotation speed (>4500 rpm).

The film thickness was determined by integrating the area of the quasi-steady-state cyclic voltammogram for each electrode and expressing the thickness as total amount of material per square centimeter. The scan rate was 1 mV s^{-1} for electrodes up to 130 μg cm^{-2} and 0.1 mV s^{-1} for thicker films. A second method for determining film thickness involved double-step chronocoulometry, which was useful up to 130 μg cm^{-2}. In the thinner films the results from such determinations were within 2% of the thicknesses calculated from the amount of polymer deposited on the film and the data from elemental analysis and UV spectrophotometry for

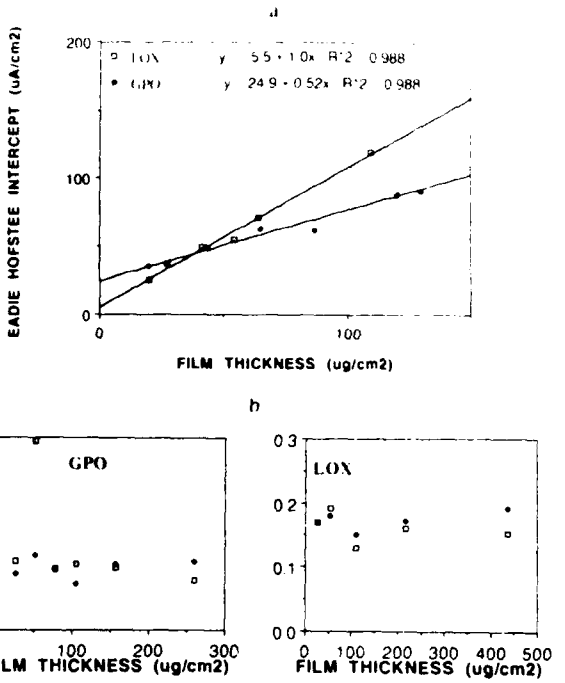

Figure 6. (a) Variation of the intercepts of the modified Eadie–Hofstee plots with film thickness. The intercepts were calculated from plots similar to those in Figure 5 for each electrode. (b) Variation of the slope of the Eadie–Hofstee plots (calculated similarly) with thickness.

the osmium content of the polymer. This indicates that almost all the polymer remains on the surface after immobilization. For thicker films the discrepancy increased to about 20% because of breakdown of the applicability of the methods, and not the loss of polymer after immobilization.

Figure 6 shows the variation of the intercepts of the modified Eadie–Hofstee plots as a function of the thickness of the enzyme-containing redox epoxy network. The electrodes again are designed to have similar current densities at high substrate concentrations where a small change in concentration does not affect the current. The GPO and LOX electrodes Eadie–Hofstee slopes are essentially independent of film thickness, being about 2.5 mM for GPO and 0.18 mM for LOX. The variation of the intercepts, i.e. current densities at infinite substrate concentrations with film thickness, is linear at least through the 0–100 μg cm^{-2} range for LOX-containing redox epoxy networks and at least through the 0–200 μg cm^{-2} for the GPO-containing ones.

GPO electrodes have a much shorter shelf life than GOX electrodes. After 1 month storage at room temperature (~25 °C), the electrodes retained only 10% of their activity, while GOX electrodes, after an initial loss associated with curing of the epoxy network, were stable. When catalase was coimmobilized on the electrode, no substantial improvement was observed. Though dry GPO is quite stable, we observed severe deactivation upon storage in pH 8.1 HEPES buffer. Upon 1 month storage of the [illegible]trodes at room temperature (~25 °C), no current w[illegible]ed.

The response times o[illegible] electrodes were studied by measuring the response of the electrodes to steps in concentration between 0 and 10 times the half-saturation point. The studies were done in a 10-mL cell with the electrode rotating at different rotation rates under a N_2 atmosphere. In all cases the response times decreased with increasing electrode rotation time, to our 4000 rpm limit, when they dropped to 1–2 s. Thus, we were measuring the mixing time not the true response time of the electrodes. (We define response time as the time needed for the response to reach 90% of the saturation current.)

Table I. GPO and LOX Electrode Characteristics

	GPO	LOX
half-saturation point (mM)	2.6 ± 0.3	0.16 ± 0.02
current density at "K_m" (μA cm^{-2})	45 ± 0.5	60 ± 0.3
sensitivity (A M^{-1} cm^{-2})	0.02 ± 0.002	0.3 ± 0.01
half-saturation current/background current ratio	32	43
% current loss at half-saturation in air[a]	8 ± 1	39 ± 5

[a] Comparison between argon- and air-saturated solutions (0 and 0.2 mM [O_2], respectively).

The results summarizing the performance of the "typical" electrode as a sensor are depicted in Table I.

Discussion. In enzyme electrodes with 3-dimensional redox polymer networks complexing, binding, and electrically interconnecting the redox centers to electrodes, the following processes define the observed current:

$$E_{ox} + S \underset{k_{-1}}{\overset{k_1}{\rightleftharpoons}} ES \xrightarrow{k_2} E_r + P \quad (1)$$

$$E_r + 2R_{ox} \xrightarrow{k_3} E_{ox} + 2R_r + 2H^+ \quad (2)$$

$$R_{ox,w} + R_{r,w+1} \xrightarrow{D_{ct}} R_{r,w} + R_{ox,w+1} \quad (3)$$

$$R_r \xrightarrow{\infty} R_{ox} \quad (4)$$

Equation 1 represents in combination with eq 2 the reaction of the enzyme with the substrate (S) by a uni uni uni uni ping pong mechanism, accepted for GPO and GOX.[12,14] The oxidized form of the enzyme (E_{ox}) forms the enzyme–substrate complex (ES) having an equilibrium constant k_{-1}/k_1. The complex dissociates with a rate constant k_2 into the reduced form of the enzyme (E_r) and product (P). At this stage, the enzyme can be reoxidized by oxygen according to

$$E_r + O_2 \xrightarrow{k_0} E_{ox} + H_2O_2$$

Under anaerobic conditions, eq 2 describes the reoxidation process adequately. The reduced enzyme is subsequently oxidized by a sequence of two one-electron transfer steps. The electrons are transferred to the oxidized polymer bound relays (R_{ox}), which are reduced with a rate constant k_3. Finally, electrons transfer through the redox polymer–enzyme network with an overall "electron diffusion coefficient" D_{ct} according to eq 3 which describes the succession of electron-transfer self-exchange reactions between neighboring redox sites (w, w + 1). D_{ct} may increase exponentially with the cube root of concentration of redox centers, if the electron propagation is a percolative, phonon-assisted tunneling process, or quadratically (with the redox center's concentration), if the propagation involves chain segment collisions. The reoxidation of the relay at the electrode surface completing the second part of the catalytic cycle is fast.

An effort has been made to model and simulate this set of equations and solve for the catalytic current. Saveant[18] has solved the general case for a catalytic first-order reaction on a polymer film. Gough[19,20] and others[21-23] have tried in the past to apply this analysis to enzyme electrodes. No analytical solution can be obtained for the general case even when a ping pong mechanism is not involved. However, in order to semiquantitatively interpret the results, we postulate that after applying Aris'[24] analysis to the problem at hand, one can write for the catalytic current

$$j = \frac{\eta j_{max}}{1 + K_{rox}/C_{rt}} - \frac{K_s/a_s}{1 + K_{rox}/C_{rt}} \frac{j}{C_s} \quad (6)$$

where j is the curent density, η is an effectiveness factor, defined as the ratio of the actual current density over the current density that could be obtained under kinetic control, $j_{max} = 2FLk_2C_{Et}$, where F is the Faraday constant, L is the wet film thickness, and C_{Et} is the total enzyme concentration in the film, $K_{rox} = k_2/k_3$, $K_s = (k_2 + k_{-1})/k_1$, a_s is the partition coefficient of the substrate in the film, C_{rt} is the relay concentration in the enzyme–polymer film, and C_s is the substrate concentration in the bulk solution.

Equation 6 looks deceptively simple. This is so because our inability to exactly describe the process has been hidden in the effectiveness factor. Were we able to describe rigorously the coupled processes, η would be the solution of the differential equations describing the reactions of eqs 1–4. In this case η would depend on all the parameters in eq 6, on D_{ct}, and on the diffusion coefficient of the substrate. η cannot assume a closed-form solution unless simplifying assumptions, negating the very purpose of mathematically describing the process, are made. When eq 6 is plotted in the usual Eadie–Hofstee form of j vs j/C_s, the plot is rarely a straight line. Unless there is an unusual coincidence of parameter values, a linear plot is not obtained; i.e. $\eta \neq 1$ unless the current is not limited by either substrate or electron diffusion. Such plots can be used as a semiquantitative diagnostic test for the characterization of immobilized enzymes in general.[25,26] Experimentally, one can distinguish between substrate diffusion limitations and electron diffusion limitations by varying the electrode rotation rate. Above some rotation rate, no external diffusion limitation will prevail. In the absence of internal substrate diffusion limitation and of electron diffusion limitation, the plots become linear at sufficiently high rotation rates. At this point, the current observed is the kinetic current (described by eq 6 when $\eta = 1$). There are additional postulates in eq 6 which will be discussed.

Effectiveness of Electrical Communication via the 3-Dimensional Network. In designing the 3-dimensional enzyme-containing redox polymer network, we seek to transfer electrons from the enzyme redox centers to the network and through the network to the electrode, at rates exceeding the maximum rate of electron transfer from the substrate to the redox centers of the enzyme, i.e. the turnover number of the enzyme. When the transfer of electrons from the substrate to the network is fast enough to maintain a sufficiently high steady-state Os^{2+}:Os^{3+} ratio, i.e. to make the Nernst potential of the film reducing relative to the formal potential, only an oxidation current is observed in slow scan rate cyclic voltammograms. This oxidation current will be maintained until the ratio Os^{2+}:Os^{3+} decreases, because the rate of supply of electrons to the network from the substrate through the enzyme cannot match the rate of oxidation of the network on the electrode. At this point, the Nernst potential of the network will become sufficiently positive for a reduction current to appear at a reducing potential relative to the formal potential of the network. This situation will arise at or above a scan rate related to the turnover rate of the enzyme and its relationship to the efficiency with which electrons are transferred from the enzyme to and through the network. As seen in Figure 1c, for GPO this rate is 2 mV s^{-1} and for LOX it is 5 mV s^{-1}. For glucose electrodes designed to exceed in their enzyme activity (and current density) the LOX and GPO electrodes, critical scan rates are of 20 mV s^{-1}. For the same enzyme concentration in the film, the increasing critical scan rates reflect the increasing turnover numbers for these enzymes and/or the increasing effectiveness of communication via the network.

Under anaerobic conditions both the critical scan rate and the current density reflect qualitatively the relative rates of enzymatic turnover (process described by eq 1) and the effectiveness of communication (process described by eqs 2 and

3). Under aerobic conditions, the current density and the suppression of current relative to anaerobic conditions qualitatively reflect the effectiveness of communication relative to the rate of electron transfer from the enzyme to O_2 (process described by eq 5). As seen in Figure 2, O_2 competes more effectively for reduced LOX electrons than for reduced GPO electrons. This fact may signify a higher k_3 for the GPO than for LOX and/or a higher k_0 for LOX than for GPO (refer to eq 2 and 5).

pH Dependence. The pH dependence of the current in "wired" GOX, LOX, or GPO differs from the pH dependence of the enzyme-catalyzed oxidation of the substrates by O_2; the maxima are shifted to higher pH, and the peaks are broader. These effects might be explained as follows: At higher pH the polyanionic enzyme–polycationic polymer complexes are tighter because the enzyme has a greater net negative charge when its bases are deprotonated and its acids ionized. Because of the tighter binding in the complex, the electron-transfer distances are shorter and the electron-transfer rates faster. The broadening in the pH maxima of the current densities (Figure 3) reflects the balancing of the enhanced electron transfer and the reduced enzyme activity with increasing pH.

A similar argument based on electrostatics accounts for the different pH dependences when eq 2 represents the rate-limiting step of the process. The Os^{3+} relays abstract electrons from either fully reduced ($FADH_2$) or from the ($FADH^{\bullet}$) radical, transiently present because of single electron transfer to Os^{3+}. The pK_a of both of these species is between 6 and 7 in unbound FAD[27] and is also between 6 and 7 for GPO and GOX[15,28] and in FMN-dependent LOX.[29] Thus, above pH 7 the species from which Os^{3+} accepts electrons have a negative charge. The increased electrostatic attraction between the donor and the acceptor at higher pH again shortens the electron-transfer distance and increases the rate of electron transfer. In contrast, higher pH causes a decrease in the rate of the formation of the peroxo adduct[28,30,31] formed upon oxidation of the enzyme by O_2.

Diffusional Effects. As discussed earlier, linearity of Eadie–Hofstee plots is unlikely when $\eta \neq 1$ (eq 6). The condition $\eta = 1$ requires, among other requirements, also that substrate transport to the film not limit the electrode kinetics. When substrate diffusion to the electrode does limit the electrode kinetics, i.e. at sufficiently slow rotation rates, the plots are nonlinear (Figure 5). When the enzyme loading is high and/or when its turnover rate is rapid, mass transport can limit the electrode kinetics even at high rotation rates and the Eadie–Hofstee plots remain nonlinear even for the fastest rotating electrodes (4500 rpm).

When linear, the intercept of the Eadie–Hofstee plots is expected to be proportional to the amount of active enzyme in electrical contact with the electrode. As long as the electrical communication is maintained, the Eadie–Hofstee intercept is expected to be proportional to film thickness. The Eadie–Hofstee slopes should, however, be independent of film thickness when the concentration of polymer and enzyme in the film remain constant. As seen in Figure 6, the slopes are indeed independent of film thickness and the intercepts are proportional to film thickness in both GPO and LOX electrodes. At zero film thickness, the intercepts should, however, be nil. That this is not exactly the case reveals a small systematic error in our estimate of film thickness.

The slope of the Eadie–Hofstee plots represents the apparent K_m of the electrodes and is near 3 mM for the GPO and 0.2 mM for the LOX electrodes analyzed. The slopes, i.e. the apparent K_m values, can be readily varied over a wide range by changing the enzyme:polymer ratio. Though we do not show this in the results, the slopes have been decreased by 1 order of magnitude in both electrodes by increasing the enzyme:polymer ratio. As expected, when the ratio was increased, the Eadie–Hofstee plots became nonlinear even at high electrode rotation rates. Evidently, either diffusional substrate transport or electron diffusion in the electrically insulating enzyme-enriched network and not the enzyme's turnover capacity now controlled the electrode kinetics.

ACKNOWLEDGMENT

We thank Mr. Henry Franklin, director of the Mechanical Engineering Department workshop, for fine craftsmanship in building our apparatus; Dr. Takis Argitis for SEM data; Dr. Danli Wang for sharing preliminary results on the stabilization of LOX; Lois Davidson for the purification of LOX. I.K. thanks Dr. Brian A. Gregg, now at NREL, for guidance. We also thank Dr. Alan Hauser, now at the University of Hawaii, for sharing his painstaking derivation of a model describing the electrode response, and Dr. Adrian Michael, now at the University of Pittsburgh, for a stimulating debate on the process of electron transfer in redox polymer films. We acknowledge support of this work by the Office of Naval Research, The National Science Foundation, and the Welch Foundation.

REFERENCES

(1) Hale, P. D.; Inagaki, T.; Karan, H. I.; Okamoto, Y.; Skotheim, T. A. *J. Am. Chem. Soc.* **1989**, *111*, 3482–3.
(2) Hale, P. D.; Boguslavski, L. I.; Inagaki, T.; Lee, H. S.; Skotheim, T. A.; Karan, H. I.; Okamoto, Y. *Mol. Cryst. Liq. Cryst.* **1990**, *190*, 251–8.
(3) Hale, P. D.; Boguslavski, L. I.; Inagaki, T.; Karan, H. I.; Lee, H. S.; Skotheim, T. A.; Okamoto, Y. *Anal. Chem.* **1991**, *63*, 677–82.
(4) Foulds, N. C.; Lowe, C. R. *Anal. Chem.* **1988**, *60*, 2473–8.
(5) Cenas, N. K.; Pocius, A. K.; Kulys, J. J. *Bioelectrochem. Bioenerg.* **1984**, *12*, 583–91.
(6) Degani, Y.; Heller, A. *J. Am. Chem. Soc.* **1989**, *111*, 2357–8.
(7) Gregg, B. A.; Heller, A. *Anal. Chem.* **1990**, *62*, 258–63.
(8) Pishko, M. V.; Katakis, I.; Lindquist, S.-L.; Ye, L.; Gregg, B. A.; Heller, A. *Angew. Chem., Int. Ed. Engl.* **1990**, *29*, 82–4.
(9) Pishko, M. V.; Katakis, I.; Lindquist, S.-L.; Degani, Y.; Heller, A. *Mol. Cryst. Liq. Cryst.* **1990**, *190*, 221–49.
(10) Gregg, B. A.; Heller, A. *J. Phys. Chem.* **1991**, *95*, 5970–5.
(11) Gregg, B. A.; Heller, A. *J. Phys. Chem.* **1991**, *95*, 5976–80.
(12) Nakamura, S.; Fujuki, S. J. *J. Biochem.* **1968**, *63*, 51–7.
(13) Gibson, Q. H.; Swoboda, B. E. P.; Massey, V. *J. Biol. Chem.* **1964**, *239*, 3927–34.
(14) Jacobs, N. J.; VanDemark, P. J. *Arch. Biochem. Biophys.* **1960**, *88*, 250–5.
(15) Claiborne, A. *J. Biol. Chem.* **1986**, *261* (31), 14398–407.
(16) Bio-Rad Protein Assay. Manufacturer's manual; Bio-Rad: Richmond, CA, 1991.
(17) Finnsugar Biochemicals Inc. *Enzymes for Diagnostic Reagents Technical Information Catalog*; Product No. G-7141; Sigma Chemical Co.: St. Louis, MO, 1991.
(18) Andrieux, C. P.; Dumas-Bouchiat, J. M.; Saveant, J. M. *J. Electroanal. Chem. Interfacial Electrochem.* **1982**, *131*, 1–35.
(19) Leypoldt, J. K.; Gough, D. A. *Anal. Chem.* **1984**, *56*, 2896–904.
(20) Tse, P. H. S.; Leypoldt, J. K.; Gough, D. A. *Biotechnol. Bioeng.* **1987**, *29*, 696–704.
(21) Mell, L. D.; Malloy, J. T. *Anal. Chem.* **1975**, *47* (2), 299–307.
(22) Ikeda, T.; Miki, K.; Senda, M. *Anal. Sci.* **1988**, *4*, 133–8.
(23) Yokoyama, K.; Tamiya, E.; Karube, I. *J. Electroanal. Chem. Interfacial Electrochem.* **1989**, *273*, 107–17.
(24) Aris, R. *Mathematical Theory of Diffusion and Reaction in Permeable Catalysts*; Oxford University Press: London, 1975; pp 348–80.
(25) Engasser, J. M.; Horwath, C. In *Immobilized Enzyme Principles*; Wingard, L. B., Jr., Katchalski-Katzir, E., Goldstein, L., Eds.; Applied Biochemistry and *Bioengineering*; Academic Press Inc.: New York, 1976; Vol. 1, pp 127–200.
(26) Goldstein, L. *Methods Enzymol.* **1976**, *44*, 397–450.
(27) Dryhurst, G. *Electrochemistry of Biological Molecules*; Academic Press: New York, 1977; p 371.
(28) Stankovich, M. T.; Schopfer, L. M.; Massey, V. *J. Biol. Chem.* **1978**, *253* (14), 4971–9.
(29) Stankovich, M.; Fox, B. *Biochemistry* **1983**, *22*, 4466–72.
(30) Ghisla, S.; Massey, V. *Eur. J. Biochem.* **1989**, *181*, 1–17.
(31) Hemmerich, P.; Knappe, W.-R.; Kramer, H. E. A.; Traber, R. *Eur. J. Biochem.* **1980**, *104*, 511–20.

RECEIVED for review October 31, 1991. Accepted February 6, 1992.

Reprinted from The Journal of Physical Chemistry, 1991, 95.

Redox Polymer Films Containing Enzymes. 2. Glucose Oxidase Containing Enzyme Electrodes

Brian A. Gregg*,† and Adam Heller*

Department of Chemical Engineering, University of Texas at Austin, Austin, Texas 78712
(Received: October 30, 1990; In Final Form: April 1, 1991)

Glucose oxidase is covalently bound in a film of cross-linked, redox-conducting epoxy cement on the surface of electrodes. The binding simultaneously immobilizes the enzyme and connects it electrically with the electrode. The effects of cross-linker concentration, film thickness, enzyme concentration, temperature, and oxygen concentration on the steady-state electrocatalytic oxidation of glucose at the redox-epoxy enzyme electrodes are described. The catalytic "reaction layer" extends through the entire film, even for films as thick as ca. 5 μm. The limiting catalytic current density is a function of the enzyme concentration, reaching a maximum near 35 wt % enzyme for films about 1 μm thick. In such films, the activation energy for the electrocatalytic reaction at high glucose concentration is 63 kJ/mol, and the apparent Michaelis constant monotonically decreases with increasing enzyme concentration and increases with increasing oxygen concentration. These results are explained by postulating that in such ~1 μm thick redox-epoxy enzyme films the rate-limiting kinetic step at high substrate concentration is related to electron transfer away from the enzyme active site, a process involving flexing of the cross-linked redox chain segments. This bottleneck may be attributed to the high activity of the enzyme and the small contact area between the redox polymer and the enzyme-active site that is recessed inside the insulating protein shell of the enzyme.

Introduction

The development of enzyme electrodes has reached a point of confluence with recent developments in the field of redox polymer-mediated electrocatalysis. Enzymes have been immobilized in redox polymer films to provide simple and sensitive amperometric biosensors, which no longer require the presence of membranes to contain the enzymes.[1-5] Concurrently, the theoretical and experimental characterization of discrete catalytic species dispersed in redox polymers has progressed.[6-9] It was recognized that some of the characteristics of redox polymers that are desirable in electrocatalytic films, such as chemical inertness and rapid electron self-exchange rates, are not necessarily compatible with catalytic properties that may require the adsorption of species, the accessibility of multiple oxidation states, or the ability to transfer both protons and electrons. Thus, a number of groups have envisioned the dispersion of discrete catalysts in redox polymers to separate and independently optimize the two functions of catalysis and charge transfer to the electrode.

We recently reported the immobilization of glucose oxidase in cross-linked redox polymers and their application as biosensors.[4] The preceding paper in this series[10] reported an improved system for the immobilization of oxidoreductases in redox polymers and described the electrochemical characterization of the pure redox polymer (poly(vinylpyridine) containing complexed $(bpy)_2OsCl$ groups and partially quaternized with bromoethylamine, abbreviated POs–EA). This paper examines the effects of varying cross-linker concentration, film thickness, enzyme concentration, temperature, and oxygen concentration on the steady-state electrochemical response of these glucose oxidase containing redox polymer films. The apparent Michaelis constant and the maximum catalytic current density depend on a number of these variables. One goal of this work is to develop an understanding of the kinetic step(s) that limit(s) the steady-state catalytic current in such enzyme electrodes.

Experimental Section

Chemicals. Glucose oxidase (EC 1.1.3.4) from *Aspergillus niger* (Sigma, catalog no. G-8135), catalase (EC 1.11.1.6) (Sigma, catalog no. C-100) and Na–HEPES (sodium 4-(2-hydroxyethyl)-1-piperazineethanesulfonate) (Aldrich) were used as received. All experiments were performed in aqueous solution containing 100 mM NaCl and 20 mM phosphate at pH 7.1.

Electrodes. Vitreous carbon rotating-disk electrodes (3 mm diameter) were employed for this study. Electrode films were prepared as described previously[10] except that a solution of glucose oxidase (GO) was added to the solution containing the redox polymer, POs–EA, and the diepoxide cross-linking agent, PEG. For example, 5 μL of a 2 mg/mL solution of GO (in 10 mM HEPES, pH 8.2) was added to a mixture of 10 μL of a 4 mg/mL solution of POs–EA (in the same buffer) and 2 μL of a 2.3 mg/mL solution of PEG (polyethylene glycol diglycidyl ether) in water. A 2-μL portion of the resulting mixture was applied to a vitreous-carbon-disk electrode and allowed to dry and set at 37.5 °C for 48 h. The electrodes were then rinsed in H_2O for 10 min to remove salts and unreacted species and then dried at 37.5° for one more hour before use. The resulting films were assumed to contain the same relative amounts of the three components as did the solution, i.e. in this example, 18.3 wt % GO, 8.4 wt % PEG, and 73.3 wt % POs–EA. Solutions with a ratio of GO/POs–EA ≈ 1 or greater tended to precipitate. Even though they were used immediately they still resulted in less uniform electrodes than those from the more dilute solutions. If allowed to go to completion, such precipitation removed all color from the solution; i.e., the precipitate contained all GO and POs–EA.

Unless otherwise noted, all experiments were carried out in a water-jacketed, single-compartment electrochemical cell containing 100 mL of the standard buffer solution at an electrode rotation rate of 1000 rpm. Potentials are reported against the aqueous saturated calomel electrode (SCE).

Results and Discussion

Glucose Oxidase Containing, Cross-Linked Redox Polymer Films, GO/POs–EA/PEG. The immobilization of enzymes in inert polymers has been a subject of extensive research.[11,12]

† Present address: Solar Energy Research Institute, 1617 Cole Blvd., Golden, CO 80401-3393.

(1) Foulds, N. C.; Lowe, C. R. *Anal. Chem.* **1988**, *60*, 2473–2478.
(2) Hale, P. D.; Inagaki, T.; Karan, H. I.; Okamoto, Y.; Skotheim, T. A. *J. Am. Chem. Soc.* **1989**, *111*, 3482–3484.
(3) Pishko, M. V.; Katakis, I.; Lindquist, S.-L.; Ye, L.; Gregg, B. A.; Heller, A. *Angew. Chem., Int. Ed. Engl.* **1990**, *29*, 82–84.
(4) Gregg, B. A.; Heller, A. *Anal. Chem.* **1990**, *62*, 258–263.
(5) Heller, A. *Acc. Chem. Res.* **1990**, *23*, 128–134.
(6) Albery, W. J.; Bartlett, P. N. *J. Electroanal. Chem.* **1982**, *131*, 137–144.
(7) Buttry, D. A.; Anson, F. C. *J. Am. Chem. Soc.* **1984**, *106*, 59–64.
(8) Anson, F. C.; Ni, C.-L.; Saveant, J.-M. *J. Am. Chem. Soc.* **1985**, *107*, 3442–3450.
(9) Lyons, M. E. G.; McCormack, D. E.; Bartlett, P. N. *J. Electroanal. Chem.* **1989**, *261*, 51–59.
(10) Gregg, B. A.; Heller, A. Preceding paper in this journal.
(11) *Methods in Enzymology*; Mosbach, K., Ed.; Academic Press: New York, 1987.

0022-3654/91/2095-5976$02.50/0

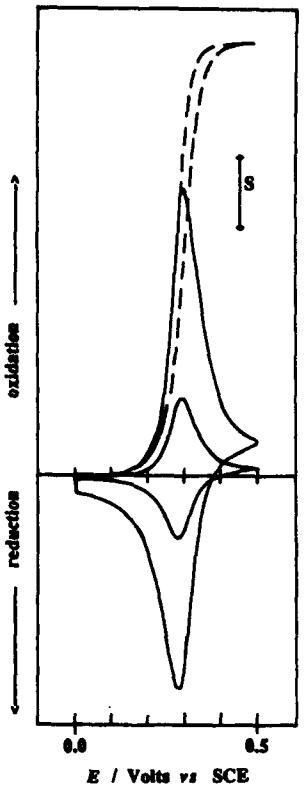

Figure 1. Cyclic voltammograms of a POs–EA/GO/PEG film on a vitreous-carbon-disk electrode. The film contains 36 wt % GO, 5 wt % PEG, the surface coverage of osmium sites is $\Gamma = 3.2 \times 10^{-8}$ mol/cm^2. The solid curves show two scans, at 1 mV/s and 5 mV/s, in the absence of glucose; $S = 28.3$ μA/cm^2. The dashed curve shows a scan at 5 mV/s in the presence of 50 mM glucose; $S = 56.6$ μA/cm^2.

Recently, oxidoreductases were immobilized in electrically active polymers[1-4,13] to establish electrical communication with the enzyme-active site, while at the same time reaping the benefits of enzyme immobilization. Relative to the earlier explored reactions, the network-forming reaction between the poly(ethylene glycol) diglycidyl ether (PEG) and both the primary amines (lysines) on the enzyme surface and the pendant amines on the osmium-containing redox polymer (POs–EA)[10] is simple and gentle. The reaction proceeds at room temperature and neutral pH. It allows the simultaneous immobilization and electrical connection of several enzymes, including glucose oxidase, lactate oxidase, glycerol-3-phosphate oxidase, and D-amino acid oxidase. The resulting enzyme electrodes retain much of the activity and the specificity of the enzymes.[14] Because the cross-linked film is formed on the surface of the electrode, only microgram quantities of enzyme are needed and no further purification of products (e.g., gel chromatography) is required. The procedure reproducibly yields highly permeable, strongly bound, hydrophilic films that may be viewed as enzyme-containing, redox-conducting epoxy cements.

Electrochemical Response of GO/POs–EA/PEG Films. Electrodes with ~1 μm thick films containing two parts by weight POs–EA to one part GO and weight percentages of PEG varying from 1.6% to 18.5% of the total were prepared. At this film thickness and POs–EA/GO ratio the cross-linker concentration had no discernible effect on the electrochemical properties of the enzyme electrodes. The average oxidation peak potential of these electrodes was $E_p = 0.278 \pm 0.003$ mV (SCE). No trend was observed in E_p with PEG concentration, in contrast with that observed for the enzyme-free redox polymer.[10] Most of the enzyme electrodes reported hereafter contained 4–8% PEG by weight.

Cyclic voltammograms of a typical film of GO/POs–EA/PEG in the standard buffer solution are shown in Figure 1. This film contained 36 wt % GO and 5 wt % PEG, while the surface coverage of electroactive osmium centers was $\Gamma = 3.2 \times 10^{-8}$ mol/cm^2. The voltammogram at 1 mV/s and in the absence of glucose exhibits an almost symmetric wave (peak splitting, $\Delta E_p = 10$ mV) indicative of a reversible, surface-bound couple. At 5 mV/s, the peak splitting is substantially increased ($\Delta E_p = 25$ mV) and a tailing of the wave indicates the onset of a diffusional process.[15] Thus, the GO-containing films exhibit slower charge-transfer kinetics than the pure redox polymer films.[10]

Addition of glucose (50 mM) to the buffer solution results in its catalytic electrooxidation (dashed line, Figure 1) according to

$$\text{GO–FAD} + \text{glucose} \rightarrow \text{GO–FADH}_2 + \text{gluconolactone} \quad (1)$$

$$\text{GO–FADH}_2 + 2\ \text{Os(III)} \rightarrow \text{GO–FAD} + 2\ \text{Os(II)} + 2\ \text{H}^+ \quad (2)$$

where GO–FAD represents the oxidized form of the flavin adenine dinucleotide bound to the active site of glucose oxidase and GO–$FADH_2$ represents its reduced form. GO–$FADH_2$ is reoxidized by two osmium(III) centers of the polymer (or by two sequential oxidations by a single osmium(III) center) with the corresponding reduction of the redox polymer centers and the release of two protons. One difference between the kinetics of such an enzyme electrode, constructed from a cross-linked redox polymer, and homogeneous solution kinetics is that the redox sites in the polymer cannot diffuse. Thus, all redox sites are not equivalent: part of the redox centers lie close enough to enzyme-active sites to permit electron transfer from the reduced enzyme to the oxidized redox center (eq 2) within a defined period. The remaining redox centers (except those in contact with the electrode) participate only in electron self-exchange reactions. Thus, after transfer from the enzyme-active site, electrons of the osmium(II) centers "diffuse"[16] through the redox polymer (eq 3) to the electrode. The oxidation

$$\text{Os(II)} + \text{Os(III)} \rightarrow \text{Os(III)} + \text{Os(II)} \quad (3)$$

of Os(II) centers closest to the electrode is expected to be rapid and thus is unlikely to contribute to the observed kinetics.[17] The overall reaction represents the two-electron oxidation of glucose by the electrode, a process that is kinetically forbidden on an unmodified electrode in this potential range.

Glucose Response and Apparent Michaelis Constants of Enzyme Electrodes. The steady-state glucose response curves under nitrogen-, air-, and oxygen-saturated conditions were measured at 1000 rpm and 0.40 V vs SCE, i.e. at a potential on the plateau of the catalytic current response (Figure 1). Figure 2a shows the response curves for electrodes with ~1 μm thick films containing 4.2% GO by weight, a less than optimal fraction of the enzyme. Aliquots of a 1.0 M solution of glucose in the standard buffer were injected into the cell and the steady-state current after stabilization (5–25 s) was recorded as a function of glucose concentration. The electrode current, at moderate glucose concentrations, decreased substantially in the presence of air or pure oxygen because of the competition between the Os(III) centers and O_2 for the reduced form of the enzyme[4] (eqs 2 and 4).

$$\text{GO–FADH}_2 + \text{O}_2 \rightarrow \text{GO–FAD} + \text{H}_2\text{O}_2 \quad (4)$$

The glucose response curves can be described phenomenologically by the Michaelis–Menten equation, expressed here in the Eadie–Hofstee form:[4,18-20]

$$j_m = j_{max} - K_S'(j_m/C^*) \quad (5)$$

(12) Trevan, M. D. *Immobilized Enzymes*; Wiley: New York, 1980.
(13) Foulds, N. C.; Lowe, C. R. *J. Chem. Soc., Faraday Trans. 1* **1986**, *82*, 1259–1264.
(14) Katakis, I.; Gregg, B. A.; Heller, A. Unpublished results.
(15) Murray, R. W. In *Electroanalytical Chemistry*; Bard, A. J., Ed.; Marcel Dekker: New York, 1984; pp 191–368.
(16) Andrieux, C. P.; Dumas-Bouchiat, J. M.; Saveant, J. M. *J. Electroanal. Chem.* **1982**, *131*, 1–35.
(17) Anson, F. C. *J. Phys. Chem.* **1980**, *84*, 3336–3338.
(18) Price, N. C.; Stevens, L. *Fundamentals of Enzymology*; Oxford University Press: Oxford, 1982.
(19) Castner, J. F.; Wingard, L. B., Jr. *Biochemistry* **1984**, *23*, 2203–2210.
(20) Kamin, R. A.; Wilson, G. S. *Anal. Chem.* **1980**, *52*, 1198–1205.

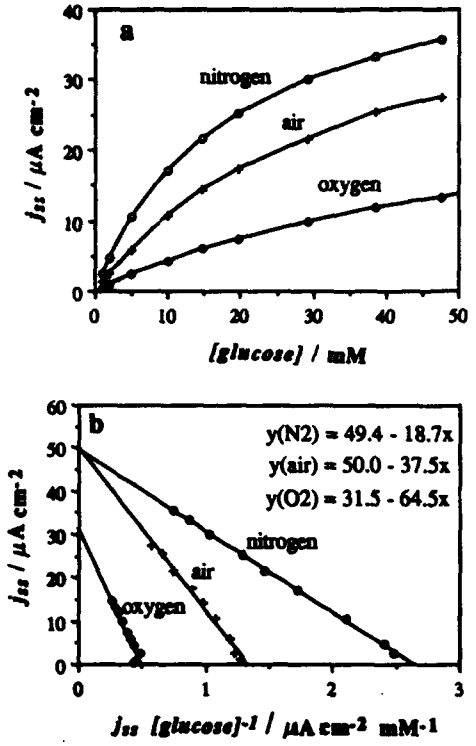

Figure 2. (a) Steady-state glucose response curves under N_2, air, and O_2 for an electrode with 4.2 wt % GO, 7.6 wt % PEG, and $\Gamma = 4.7 \times 10^{-8}$ mol/cm^2. The electrode was held at 0.4 V vs SCE and rotated at 1000 rpm in aqueous buffer at pH 7.1. (b) Data from part a plotted as an Eadie–Hofstee plot (eq 5). The negative of the slope gives the apparent Michaelis constant of the electrode, K_S', and the intercept gives the limiting catalytic current density, j_{max}.

where j_{ss} is the steady-state catalytic current density, j_{max} is the maximum current density under saturating substrate conditions, K_S' is the apparent Michaelis constant (which is not an intrinsic property of the enzyme, but rather of the system as a whole), and C^* is the concentration of glucose in solution. We will show below that consistency with eq 5 does not necessarily imply that the observed process is limited by enzyme kinetics. We employ eq 5 only for a phenomenological description of the electrodes; a detailed kinetic model of these complex systems is beyond the scope of this work. The glucose response data (Figure 2a) were plotted according to eq 5 (Figure 2b) giving straight lines with slopes equal to the negative of the apparent Michaelis constants and intercepts equal to j_{max}. The apparent Michaelis constants increase substantially in the order $(K_S')_{N_2}$ (18.7 mM) < $(K_S')_{air}$ (37.5 mM) < $(K_S')_{O_2}$ (64.5 mM). K_S' and j_{max} characterize the enzyme electrode in a particular environment, not the enzyme itself. K_S' is equal to the substrate concentration that elicits a half-maximal response from the electrode.

Glucose Diffusion through Films. The redox epoxy without the enzyme has an open structure that should make it highly permeable to glucose.[10] Because the permeability is not directly measurable (glucose is not electroactive at the electrode surface), the effect of electrode rotation rate on the catalytic current density at several concentrations of glucose was measured and plotted as a Levich plot (Figure 3).[21] A diffusion-limited process appears in such plots as a straight line passing through the origin with a slope proportional to the $^2/_3$ power of the diffusion coefficient. The absence of a rotation rate dependence in these enzyme electrodes indicates that the kinetic process limiting the current is not glucose transport to the surface of the ~1 μm thick film and that glucose transport to the film surface does not significantly alter the concentration profile of glucose within the electroactive film.[7]

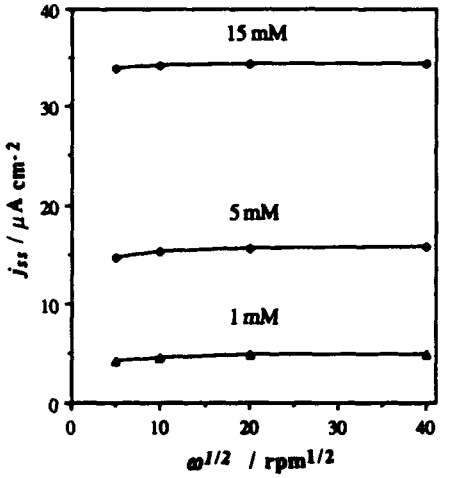

Figure 3. Levich plot for glucose oxidation at several concentrations of glucose for an electrode with 15 wt % GO, 7 wt % PEG, and $\Gamma = 1.1 \times 10^{-6}$ mol/cm^2. $V = 0.4$ V vs SCE.

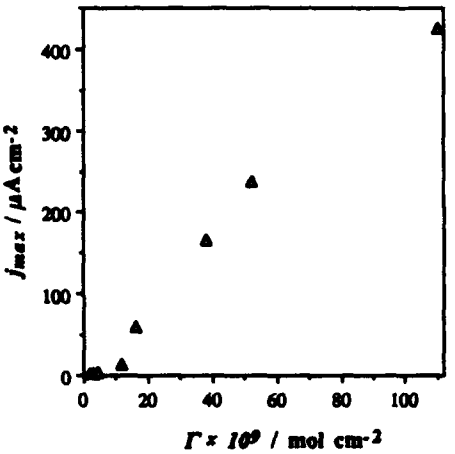

Figure 4. Limiting catalytic current density as a function of surface coverage for electrodes with 18 wt % GO and 8 wt % PEG. [Glucose] = 200 mM; $V = 0.40$ V vs SCE.

Thickness Dependence of Catalytic Current. The increase in limiting catalytic current density in the presence of 200 mM glucose in a series of electrodes of increasing surface coverage of Os(II)/(III) centers (thickness) is shown in Figure 4. These GO/POs–EA/PEG films contained 18 wt % GO and 8 wt % PEG; the surface coverage of osmium centers was varied from $\Gamma = 2.1 \times 10^{-9}$ mol/cm^2 to $\Gamma = 1.1 \times 10^{-7}$ mol/cm^2 by varying the amount and concentration of film-forming solution applied to the electrode. These data show a breakpoint between low and high surface coverages: although the limiting catalytic current density increases approximately linearly with thickness for the thin films, the rate of increase is much less than that for thicker films. The reason for the breakpoint is not clear.

Figure 4 shows that the limiting catalytic current density continues to increase with thickness, even for very thick films. Thus, the electroactive portion of the film, the "reaction layer", extends through the entire film thickness.[16,22] This contrasts with the results described for the electrocatalytic oxidation of hydroquinone on the enzyme-free redox polymer,[10] where the current decreased with increasing film thickness, at least for films thicker than ca. $\Gamma = 1.3 \times 10^{-8}$ mol/cm^2, and the reaction layer constituted only a fraction of the film thickness. In the latter case, the limiting current density was ca. 50 times higher than that for the enzyme-catalyzed reaction in the thickest film shown in Figure 4. These results can be put in perspective by considering the relative density of catalytic sites in the two cases: for hydroquinone

(21) Bard, A. J.; Faulkner, L. R. *Electrochemical Methods*; Wiley: New York, 1980.

(22) Andrieux, C. P.; Haas, O.; Saveant, J.-M. *J. Am. Chem. Soc.* **1986**, *108*, 8175–8182.

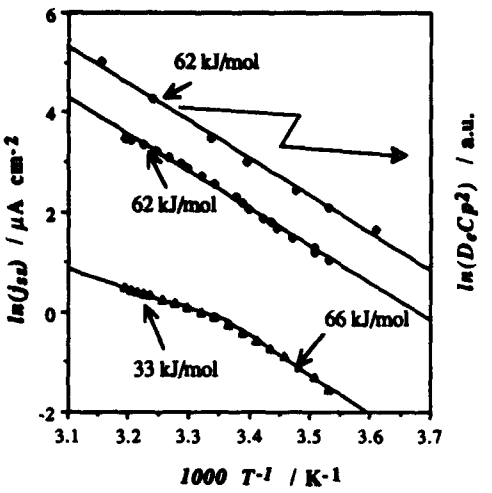

Figure 5. Arrhenius plot of catalytic density for glucose oxidation at [glucose] = 150 mM (♦) and at [glucose] = 2 mM (▲) for an electrode with 4.2 wt % GO, 7.6 wt % PEG, and $\Gamma = 4.7 \times 10^{-8}$ mol/cm². Also shown is the chronoamperometric response, D_eCp^2, for an electrode containing no GO with 9.1 wt % PEG and $\Gamma = 3.7 \times 10^{-8}$ mol/cm² (◇).

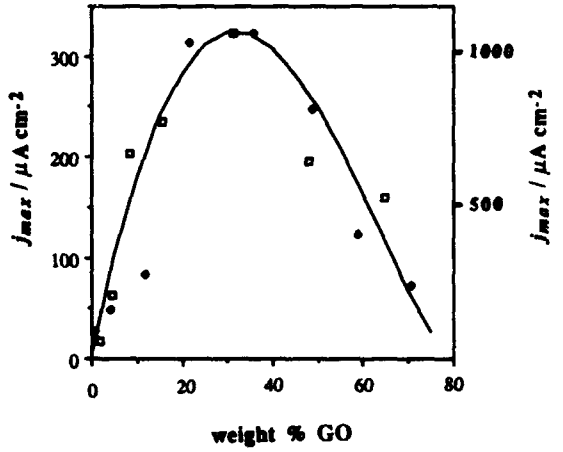

Figure 6. Limiting catalytic current density, j_{max}, as a function of wt % of glucose oxidase, GO, in the film. The total weight of the film components applied to each electrode was approximately 100 μg/cm². The data are from two series of experiments with different batches of GO: j_{max} for the first series (□) is given on the right axis, for the second series (◇) on the left. The curve is an aid to the eye.

oxidation, the catalytic site is the osmium complex, while for glucose oxidation, catalysis takes place at the enzyme-active site. Glucose oxidase is a dimer of molecular weight 160000, or 80000 per active site,[23] while the POs–EA/PEG weight is approximately 1500 per osmium complex. Thus, pure POs–EA/PEG films contain a density of sites active for hydroquinone oxidation (osmium complexes) about 300 times greater than the density of sites active for glucose oxidation (FAD centers) in the films shown in Figure 4. Hence, it is reasonable to expect the "reaction layer" for the enzyme-catalyzed reaction to be much larger, and the current densities smaller, than for the osmium complex catalyzed reaction. The relative rate constants for the two oxidations may also contribute to the relative current densities.

Activation Energies for Electrocatalytic Glucose Oxidation. The change in steady-state electrocatalytic oxidation current with temperature at two concentrations of glucose is shown in Figure 5 as an Arrhenius plot. Also plotted is the temperature dependence of D_e, the "diffusion coefficient" for electrons, for an enzyme-free film of about the same PEG concentration as the enzyme electrode (data taken from ref 10). A ~1 μm thick GO/POs–EA/PEG electrode containing a low concentration of GO (4.2 wt %) was selected for this study to minimize possible enzyme–enzyme interactions. The experiment was carried out under nitrogen where the apparent Michaelis constant of this electrode is 18.7 mM. Thus, the higher concentration of glucose (150 mM ≈ 8 K_S') employed is well into the limiting current region for this electrode, i.e. where the overall electrode reaction is zero order in glucose. The lower concentration of glucose (2 mM ≈ 0.1 K_S') corresponds to the "linear" range of the electrode where the overall electrode reaction is first order in glucose.

The activation energy for the electrocatalytic current, E_{act} = 62 kJ/mol, at high glucose concentration is practically identical with that for charge transfer through the redox polymer. (The average for four electrodes was $E_{act} = 60 \pm 2$ kJ/mol.)[10] For comparison, the activation energy of glucose oxidase itself is reported to be approximately 14 kJ/mol.[24,25] At low glucose concentration, the Arrhenius plot is distinctly curved. It is possible to fit the low concentration result to two activation energies, E_{act} ≈ 66 kJ/mol below room temperature and E_{act} ≈ 33 kJ/mol above room temperature, although this procedure is necessarily inexact. This difference between the low and high glucose regimes has been observed for all thick (>1 μm) film electrodes thus examined. It appears that two separate rate-limiting processes are in balance at low glucose concentrations. The process that limits the low-glucose-concentration current at higher temperatures is distinct from the process that limits the current at high glucose concentration and the process that limits electron diffusion. Thin (<0.1 μm) cross-linked or noncross-linked POs–EA films with adsorbed or bound GO show an activation energy for the electrocatalytic current of ca. 33 kJ/mol, independent of glucose concentration.[26] These data support, but do not prove, the hypothesis that the rate-determining step at high glucose concentration for the ~1 μm thick cross-linked enzyme electrodes is related to electron diffusion through and/or to the redox polymer. An example of such a rate-controlling step might be chain flexing that causes two redox centers to approach each other sufficiently for the electron to be transferred. At low glucose concentration, or for the thin, adsorbed films, the rate-determining step is different.

Catalytic Current and Apparent Michaelis Constant as a Function of Enzyme Loading. Glucose response curves were measured for two series of GO/POs–EA/PEG electrodes containing concentrations of GO varying from 0.9% to 71% by weight. The total weight of the three components applied to the electrode surface was kept approximately constant at about 100 μg/cm² (i.e., if the density is assumed to be 1 gm/cm³, these films are about 1 μm thick). The limiting current densities under nitrogen, obtained from the intercepts of Eadie–Hofstee plots, are plotted against the wt % of GO in the film in Figure 6. The data are from two series of experiments that employed different batches of GO, the first of which produced current densities about 3 times higher than the second. Since we are interested primarily in the variation of j_{max} with % GO, the two series are plotted together in Figure 6 with the axis for the first series 3.3 times that for the second series. Although there is substantial scatter in the data, the trend is clear; j_{max} increases at first with increasing concentration of enzyme, peaks at around 35% GO, and then decreases at higher concentration.

The apparent Michaelis constants under nitrogen of the two sets of electrodes decreased monotonically with increasing concentration of GO (Figure 7, two lower curves). The K_S' for the first set of electrodes were consistently higher than those of the second, as were the j_{max}. The K_S' of the second set of electrodes under air and O_2 (two upper curves, Figure 7) were markedly higher than the K_S' under N_2 and also exhibited an overall decline with increasing concentration of GO.

Kinetic Limitations of Enzyme/Redox Polymer Films. In the absence of a detailed kinetic model for such enzyme electrodes, our discussion of these results must necessarily be somewhat speculative. The results shown in Figures 2, 3, and 5–7 can be

(23) Tsuge, H.; Natsuaki, O.; Ohashi, K. *J. Biochem.* **1975**, *78*, 835–843.
(24) Carvalho, L. B. J.; Melo, E. H. M.; Vaconcelos, A. R. A.; Lira, R. R. *Arq. Biol. Technol.* **1986**, *29*, 525–31.
(25) Ko, J. H.; Byun, S. M. *Taehan Hwahakhoe Chi* **1979**, *23*, 165–74.
(26) Pishko, M. V.; Heller, A. Unpublished results.

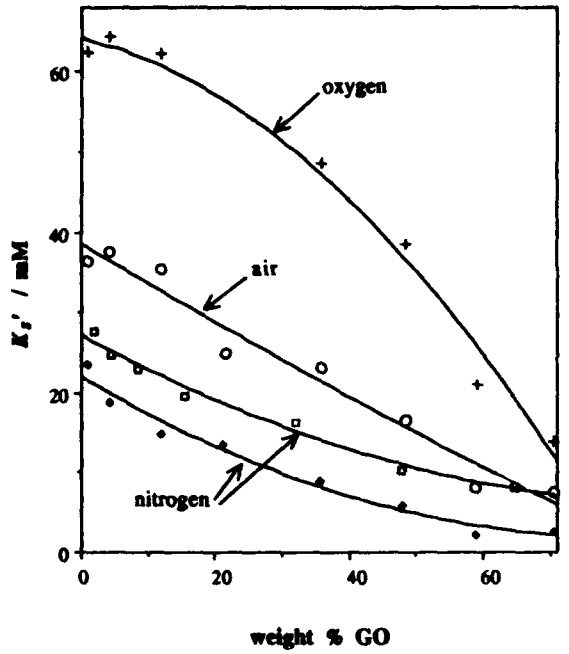

Figure 7. The apparent Michaelis constant, K_S', as a function of wt % glucose oxidase in the film under N_2, air, and O_2. The electrodes are the same as in Figure 6. Both the first (□) and second (◇) series were tested under N_2; only the second series was tested under air (○) and O_2 (+). The curves are only aids to the eye.

explained by assuming that j_{max} is limited by electron "diffusion" through the polymer film and that this limitation becomes more severe at higher enzyme concentration. Thus, the activation energy for electrocatalytic oxidation of glucose at high glucose concentration (Figure 5) is identical with that for electron "diffusion" through the pure redox polymer film.[10] Since O_2 competes with the redox polymer film for electrons (eqs 2 and 4), a greater concentration of substrate is required to reach the half-maximal catalytic current density in the presence of O_2 relative to N_2; i.e., the apparent Michaelis constants increase with oxygen concentration (Figures 2 and 7). If the limitation becomes more severe at higher enzyme concentration, the increase in j_{max} is expected to be at first sublinear, and may eventually decrease, with increasing enzyme concentration (Figure 6). As the catalytic current per enzyme decreases with increasing enzyme concentration, the glucose concentration required to reach half-maximal current per enzyme also decreases, thus K_S' decreases monotonically with increasing enzyme concentration (Figure 7). And finally, Figure 3 is also consistent with a catalytic current limitation caused by electron "diffusion" through the film.

Figure 4, however, shows plainly that the catalytic current density (at least for films of GO ≤ ca. 20 wt %) is not limited by electron "diffusion" *through the bulk film*, even for films many times thicker than those shown in Figures 6 and 7. Such a limitation would result in decreasing catalytic current density with increasing thickness.[16,27,28] We suggest that one possible explanation of these results is that j_{max} may be limited by electron "diffusion" away from the enzyme-active site, rather than by electron "diffusion" through the bulk polymer. Enzyme-active sites are, to some extent, buried inside an insulating protein coating (otherwise they would be directly accessible to planar electrodes and other enzyme-active sites);[5,29-32] thus, the electrical contact area between the redox polymer and the active site may be quite small. Furthermore, glucose oxidase is a highly active enzyme capable of producing larger catalytic currents than most oxidoreductases.[23] Thus, we suggest that the "spreading diffusion" of electrons away from what is essentially a point current source during intermittent contact, rather than the bulk "diffusion" of electrons through the polymer film, may be the factor limiting j_{max} in these enzyme electrodes.

The rate at which electrons "diffuse" away from the enzyme-active site depends upon the local Os(II)/Os(III) concentration gradient. An increase in enzyme concentration will lead to a decrease in steady-state Os(III) concentration as more $FADH_2$ centers come into transient contact with the redox polymer. The resulting decrease in the Os(II)/Os(III) concentration gradient will decrease the rate at which electrons "diffuse" away from the enzyme-active sites and thus should lead to a sublinear increase in electrocatalytic current (Figure 6) and a corresponding decrease in the apparent Michaelis constant (Figure 7) with increasing concentration of enzyme. At very high enzyme concentration the decrease in bulk conductivity caused by the presence of the insulating enzyme in the conducting polymer phase may become the primary limitation to the catalytic current.[33,34]

Conclusions

Glucose oxidase has been simultaneously immobilized on, and electrically connected to, electrodes by binding in an ~1 μm thick cross-linked, redox-conducting epoxy cement. The maximum steady-state current in these modified electrodes is apparently limited by redox polymer kinetics rather than by enzyme kinetics. The most likely source for the kinetic limitation is an electron-transfer process, involving redox polymer chain flexing, that enables the transport of electrons away from the active site of the enzyme. The catalytic current is not limited by diffusion of either electrons or glucose through the bulk of the film; the "reaction layer" extends through the entire film thickness. Control of the limiting current density and the apparent Michaelis constant, i.e. the sensitivity and the dynamic range, of the enzyme electrode is possible by adjusting the concentration of enzyme in the films.

Acknowledgment. Support of this work by the Office of Naval Research and by the Welch Foundation is gratefully acknowledged.

Registry No. Glucose oxidase, 9001-37-0; glucose, 50-99-7.

(27) Andrieux, C. P.; Dumas-Bouchiat, J. M.; Saveant, J. M. *J. Electroanal. Chem.* **1980**, *114*, 159–163.
(28) Andrieux, C. P.; Saveant, J. M. *J. Electroanal. Chem.* **1982**, *134*, 163–166.
(29) Degani, Y.; Heller, A. *J. Phys. Chem.* **1987**, *91*, 1285–1289.
(30) Degani, Y.; Heller, A. In *Redox Chemistry and Interfacial Behavior of Biological Molecules*; Dryhurst, G., Niki, K., Eds.; Plenum Press: New York, 1987.
(31) Degani, Y.; Heller, A. *J. Am. Chem. Soc.* **1988**, *110*, 2615–2620.
(32) Degani, Y.; Heller, A. *J. Am. Chem. Soc.* **1989**, *111*, 2357–2358.
(33) Kirkpatrick, S. *Rev. Mod. Phys.* **1973**, *45*, 574–588.
(34) Carver, M. T.; Hirsch, E.; Wittmann, J. C.; Fitch, R. M.; Candau, F. *J. Phys. Chem.* **1989**, *93*, 4867–4873.

Amperometric Glucose Microelectrodes Prepared through Immobilization of Glucose Oxidase in Redox Hydrogels

Michael V. Pishko, Adrian C. Michael,[1] and Adam Heller*
Chemical Engineering Department, University of Texas at Austin, Austin, Texas 78712

Glucose microelectrodes have been formed with glucose oxidase immobilized in poly[(vinylpyridine)Os(bipyridine)$_2$Cl] derivative-based redox hydrogels on beveled carbon-fiber microdisk (7 μm diameter) electrodes. In the resulting microelectrode, the steady-state glucose electrooxidation current density is 0.3 mA cm^{-2} and the sensitivity is 20 mA cm^{-2} M^{-1}. The current density and sensitivity are 10 times higher than in macroelectrodes made with the same hydrogel. Furthermore, the current is less affected by a change in the partial pressure of oxygen. The higher current density and lower oxygen sensitivity point to the efficient collection of electrons through their diffusion in the redox hydrogel to the electrode surface. These results contrast with those observed for enzyme electrodes based on diffusing mediators, where loss of the enzyme-reduced mediator by radial diffusion to the solution decreases the current densities of microelectrodes relative to similar macroelectrodes.

*To whom correspondence should be addressed.
[1] Current address: Department of Chemistry, University of Pittsburgh, Pittsburgh, PA 15260.

INTRODUCTION

Among the enzyme-based electrochemical biosensors (*1–4*) for the determination of clinical and industrial analytes, the most widely used and studied are those for glucose. Because glucose oxidase transfers electrons to diffusing and nondiffusing mediators, withstands chemical immobilization techniques, and has a high turnover rate ($\sim 10^3$ s^{-1}) at ambient temperature, this enzyme is commonly used in glucose sensors. Miniaturization of glucose sensors is relevant both to the measurement of glucose in small volumes and in vivo, and size is important in monitoring the dynamics of local chemical events in specific regions of an organ. Sensor miniaturization has allowed in vivo measurements of neurotransmitter release from dopaminergic neurons in mammalian brain tissue with microvoltammetric electrodes (*5*). In addition, microsensors with dimensions smaller than their substrate diffusion layer rapidly attain steady-state conditions via radial mass transport, allowing the use of signal-averaging techniques. Glucose microsensors have been made by using glucose oxidase immobilized on microcylinders, microdisks, and microplanar surfaces (*6–17*). These microsensors measure either the change in oxygen partial pressure (*16*), the concentration of evolved

0003-2700/91/0363-2266$02.50/0

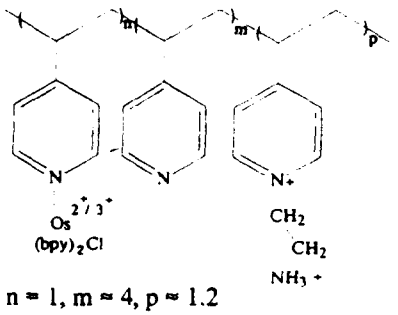

n = 1, m ≈ 4, p ≈ 1.2

Figure 1. Structure of the poly[(vinylpyridine)$Os(bpy)_2Cl^{2+/3+}$]/polyamine used to from the hydrogel redox epoxy.

H_2O_2 (*7–13*), the pH change resulting from the hydrolysis of gluconolactone to gluconic acid (*14*), or the reoxidation of a small diffusing electron shuttle other than O_2 (*6*, *15*, *17*).

Recently, the immobilization of glucose oxidase in redox hydrogels has been reported (*18–20*). Macroelectrodes made with glucose oxidase immobilized in these redox hydrogels show a typical current density of 50 $\mu A/cm^2$ at 5 mM glucose, have good mechanical properties, and are stable when stored. This paper examines the current densities and sensitivities that are reached in enzyme-containing redox hydrogels in the absence of solution mass transport limitations and radial charge diffusion through the enzyme–redox hydrogel network on microelectrodes. The roughly disk-shaped microelectrodes consist of beveled carbon-fiber tips of 7 μm diameter embedded in an insulation material, the overall diameter being less than 20 μm. The microelectrodes are coated with glucose oxidase immobilized in a redox epoxy formed from three components, (a) poly(vinylpyridine)-containing Os(bipyridine)$_2$Cl, partially quaternized with bromoethylamine (*POs-EA*), (*b*) *glucose oxidase, an enzyme* with 15 lysine residues (*21*), and (c) polyethylene glycol diglycidyl ether, a cross-linking agent that reacts with primary amines on both the redox polymer and the enzyme lysine residues.

We find that the redox epoxy hydrogel based glucose microelectrodes exhibit high steady-state current densities (0.3 mA cm^{-2}) and sensitivity (20 mA cm^{-2} M^{-1}) at 5 mM glucose, 10%–90% response times of <5 s, and an approximately linear glucose concentration dependence up to 6 mM. Compared to macroelectrodes with a similar redox epoxy hydrogel coating, the microelectrodes show a 10-fold increase in current density, improved signal to noise ratios, lower glucose detection limits, significantly reduced sensitivity to oxygen, and rapid response to changes in glucose concentration. We attribute these to radial charge transport through the redox network to the microelectrode surface.

EXPERIMENTAL SECTION

Reagents. Glucose oxidase [EC 1.1.3.4] (Type X, 128 units/mg solid) from *Aspergillus niger* (Sigma Chemical Co.), and (polyethylene glycol, MW 400) diglycidyl ether (Polysciences) were used as received. The redox polymer (*19*) shown in Figure 1 was synthesized as previously reported.

Apparatus. An EG&G Princeton Applied Research 273 potentiostat/galvanostat was used for cyclic voltammetry and constant-potential experiments. For the microelectrode experiments, the currents were preamplified by using a Keithley Model 427 current amplifier or a Keithley Model 617 electrometer prior to A/D conversion via the auxiliary input of the potentiostat. An IBM PS/2 Model 80 computer with software developed in house was used for controlling the potentiostat and for data acquisition. All experiments were performed in a Faraday cage. A conventional three-electrode system was used with a Pt-wire counter electrode and a saturated calomel electrode (SCE) as the reference. Vitreous carbon-disk electrodes (3 mm diameter) made by using V-10 vitreous carbon rods (Atomergic Chemetals) were polished on alumina powder suspensions (Buehler) decreasing in particle size from 5 to 0.05 μm.

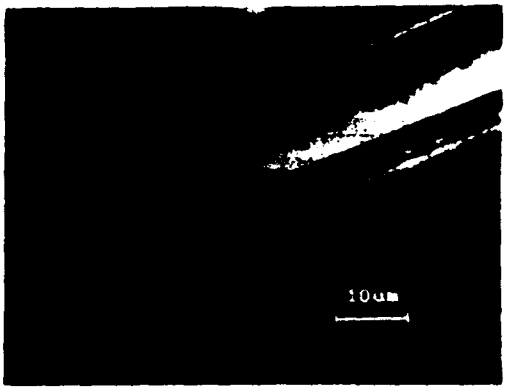

Figure 2. Photograph of a beveled carbon-fiber microelectrode modified with the enzyme-containing redox hydrogel.

A flow cell similar to one described in the literature (*22*) and a rotary injection valve (Beckman) were used for flow injection analysis. The microelectrode was inserted by using a micromanipulator into a 0.75-mm channel located approximately 2 cm from the injection valve. The reference (SCE) and counter (Pt) electrodes were placed approximately 1 cm downstream from the working electrode.

Microelectrode Fabrication. Beveled carbon-fiber microelectrodes were fabricated in a manner similar to the fabrication of electrodes for the in vivo study of neurotransmitters (*5*). A 7-μm carbon fiber (Thornell 300, Union Carbide) was inserted into a 2 mm o.d. Pyrex glass tube. The tube was pulled on a micropipet puller (Narishige Model PB-7) to yield a glass tip of approximately 20 μm o.d. The glass tip was then filled by capillary rise of a low viscosity epoxy (Spurr, Polysciences) and cured at 70 °C for 2 days. The tip was then polished at an angle of 45° with a micropipet beveler (Model BV-10, Sutter Instrument Co.) on an extra-fine diamond abrasive plate to produce an elliptical carbon disk. Electrical contact was established with the carbon fiber by filling the top of the tube with mercury and inserting a stainless steel wire. Similar electrodes have also been made with Pt and Au microwires.

The glucose microelectrode was formed by filling a micropipet with approximately 1 μL of the premixed aqueous solutions of the redox polymer, enzyme, and cross-linker (mass ratio of 1:1:0.4). With gentle air pressure the liquid was ejected from the pipet and allowed to form a droplet on the outer surface of the pipet. Because surface tension caused the droplet to travel several millimeters up the pipet, transfer of the droplet to the microelectrode required contact of the microelectrode with the droplet, while the pipet was used to hold the droplet in place until evaporation of a sufficient amount of water made the droplet too viscous to move. This procedure allowed visible layers of the gel to be attached to the tops of the microelectrodes. Qualitatively thick- or thin-film electrodes were produced by concentrating or diluting the mixture. Thick-film electrodes typically were coated with approximately 1.43 μg of redox polymer, 0.36 units of glucose oxidase, and 0.5 μg of cross-linker. The "thinnest" thin-film electrodes were coated with approximately 0.14 μg of redox polymer, 0.04 units of glucose oxidase, and 0.05 μg of cross-linker. After the mixture droplet dried, the residual film was cured at ambient temperature in air for a minimum of 2 days. Microscopic examination of the microelectrode tips revealed that the film is deposited not only on the beveled tip but also on the glass, to a distance of 10–15 μm away from the tip, as seen on the upper portion of the microelectrode of Figure 2.

RESULTS AND DISCUSSION

Electrochemical Response of Glucose Oxidase Containing Redox Hydrogels on Beveled Carbon-Fiber Microelectrodes. Figure 3a (curve 1) shows a cyclic voltammogram for a thick-film glucose microelectrode in the absence of glucose. The thick-film electrodes exhibit rapid and reversible electron transfer, as indicated by the small difference between the peaks of the reduction and oxidation waves, ΔE_p (<60 mV). The redox centers are attached to the polymer

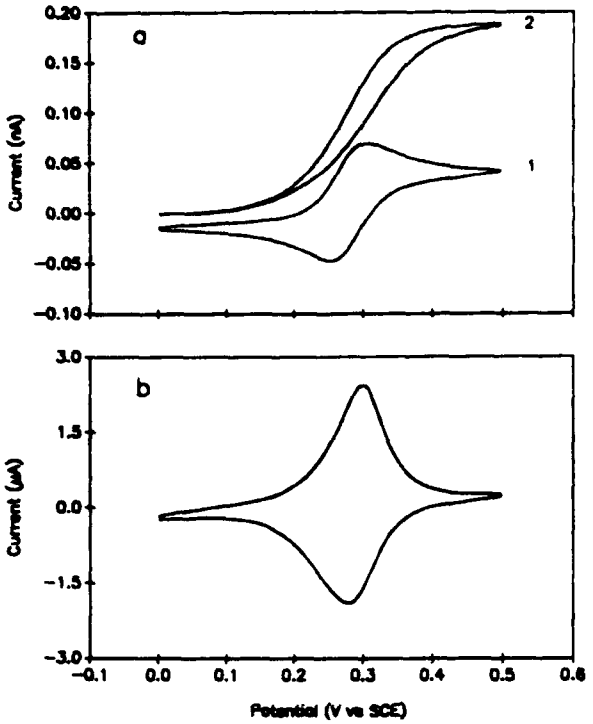

Figure 3. (a) Cyclic voltammograms of a thick-film glucose microelectrode in 0.15 M NaCl, 1 mM NaH_2PO_4, pH 7.4, under N_2, scan rate 5 mV/s: (1) no glucose; (2) 5 mM glucose. (b) Cyclic voltammogram of a redox hydrogel-modified electrode on a 3-mm vitreous carbon disk (macroelectrode), scan rate 5 mV/s, 0.15 M NaCl, 1 mM NaH_2PO_4, pH 7.4, under N_2.

chains and are immobile on a macroscopic scale; thus the current is associated with electron self-exchange between redox centers of different oxidation states. Electron transfer within the film obeys relationships very similar to those for molecular diffusion (*23*), hence the voltammogram in Figure 3a (curve 1) resembles that for a diffusion-controlled process at a microelectrode, revealing the contribution of radial electron transport through the gel to the microelectrode surface. The voltammogram shape approaches that of a steady-state voltammogram, as shown by the small degree of diffusion/depletion tailing and the small oxidation and reduction current peaks. The nonzero current observed at the switching potential (0.5 V) at 5 mV/s sweep rate shows that the film is not completely oxidized at this sweep rate. The near-steady-state current at 0.5 V also shows that the dimension of the electron diffusion layer is greater than the dimension of the microelectrode; i.e. the hydrogel behaves as a semi-infinite solvent volume. The radial electron diffusion through the hydrogel results in an increased flux of electrons to the microelectrode surface. The photograph in Figure 2 shows that the gel thickness and the fiber radius are of similar dimension, suggesting that the redox polymer located on the axial surface of the capillary contributes to the current. Such behavior is not observed at macroelectrodes (3 mm diameter vitreous carbon disk) with similar chemistry and surface coverage, as shown by the voltammogram in Figure 3b, which reveals typical thin-layer behavior. Rapid charge transfer and near-steady-state voltammograms were earlier seen by Murray et al. in the voltammetry of poly$[Os(bpy)_2(vpy)_2]^{2+}$ films containing entrapped polyethylene oxide and of mediators entrapped in films of polyethylene oxide on microelectrodes (*24–26*).

Figure 3a (curve 2) is the voltammogram obtained in the presence of 5 mM glucose, showing the catalytic oxidation of glucose. The current density under cyclic voltammetry conditions in thick-film electrodes at 5 mM glucose concentration

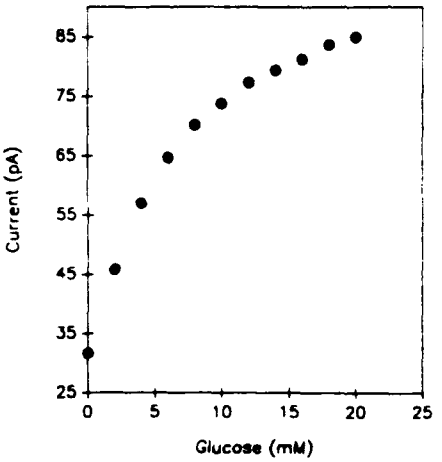

Figure 4. Glucose concentration dependence of the catalytic current for a thin-film glucose microelectrode. Currents determined by cyclic voltammetry from 0.1 to 0.4 V(SCE) in 0.15 M NaCl, 1 mM NaH_2PO_4, pH 7.4, under N_2, scan rate 5 mV/s.

are 0.5 mA cm^{-2} and 0.3 mA cm^{-2} at steady state, a 10-fold increase in current density relative to macroelectrodes with similar surface coverages. Glucose microelectrodes fabricated with thin films also show a current density (50 μA cm^{-2}) higher than that of similar macroelectrodes. Radial mass transport of glucose to the hydrogel is unlikely to be the cause of the enhanced current density given the observed independence of current density on rotation rate for macroelectrodes modified with the redox hydrogel and enzyme (*19*). The elevated current density is surprising considering that the microelectrode cannot oxidize or reduce the entire redox hydrogel at a 5 mV/s sweep rate, because of the distances involved in diffusion to the periphery of the gel. This implies that the redox hydrogel communicates poorly with enzyme molecules immobilized far from the electrode surface. However, the higher current density indicates improved communication as compared to macroelectrodes and can be attributed to the increased flux of electrons via radial diffusion through the hydrogel to the electrode surface from enzyme molecules immobilized close to the electrode surface.

Carbon-fiber microelectrodes of similar dimensions were found to have poor sensitivity to homogeneous catalytic reactions (*27*). Because of the radial diffusion associated with electrodes of this size, diffusing electroactive products (e.g. H_2O_2 or ferrocene derivatives) generated by the catalytic oxidation of glucose by glucose oxidase will rapidly diffuse away from the microelectrode surface, as was observed by Hill et al. (*6*), even if the enzyme is well bound to the electrode surface. However, because the redox hydrogel is a nondiffusing collector of the enzyme-generated current, the current density increases under radial diffusion conditions.

Because an increase in current density upon miniaturization does not imply improvements in sensitivity or detection limits, the sensitivity and signal to noise ratios at various glucose concentrations were investigated. The glucose concentration dependence of the catalytic current, as determined by cyclic voltammetry for a thin-film glucose microelectrode, is shown in Figure 4. The electrode response is approximately linear to 6 mM glucose. The sensitivity is approximately 20 μA cm^{-2} M^{-1} below 6 mM and 6.3 mA cm^{-2} M^{-1} above 10 mM. The signal to noise ratio (S/N) is 550 at 5 mM glucose and 15 at 50 μM glucose. Similar results were obtained for thick-film glucose microelectrodes. Macroelectrodes of similar surface coverage show a sensitivity of 3.2 mA cm^{-2} M^{-1} below 6 mM and 0.7 mA cm^{-2} M^{-1} above 10 mM. S/N is 100 at 5 mM glucose, with S/N dropping to 10 at 50 μM. Miniaturization does result in an increase in sensitivity and improved signal to noise ratios.

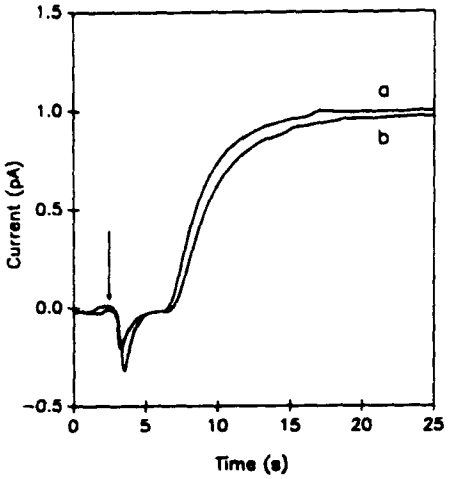

Figure 5. Time-dependent response of a thin-film glucose microelectrode to an increase in glucose from 0 to 5 mM in (a) anaerobic (N_2 purged) and (b) aerated solutions as determined by flow injection analysis. Conditions: applied potential, 0.4 V vs SCE; 0.15 M NaCl, 1 mM NaH_2PO_4, pH 7.4; flow rate, 1 cm/s; 1-mL sample loop. The point of injection is indicated by the arrow. The time necessary for the glucose bolus to reach the electrode is ~2.5 s. The background current (10 pA) was subtracted from the currents shown.

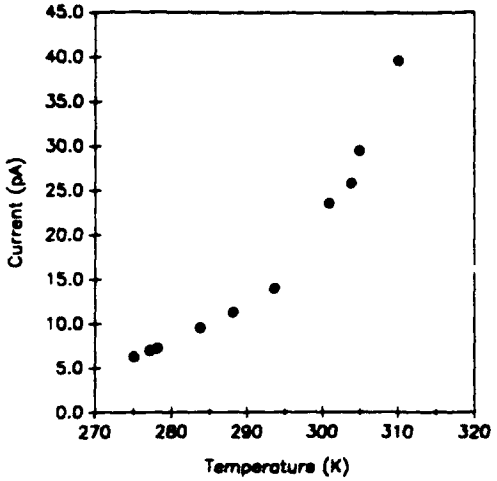

Figure 6. Temperature dependence of the catalytic current as determined by cyclic voltammetry in 5 mM glucose in a thermostated cell. Conditions: electrolyte, 0.15 M NaCl; 1 mM NaH_2PO_4, pH 7.4; under N_2; scan rate, 5 mV/s.

The time response in a flow injection system of a thin-film glucose microelectrode to an increase in glucose concentration from 0 to 5 mM under anaerobic and fully aerated conditions in shown in Figure 5. The $t_{10\%-90\%}$ response time under both conditions is approximately 5 s, only slightly higher than the response time for a surface-adsorbed redox polymer/enzyme complex (*28*, *29*), indicating that the redox hydrogels are nevertheless highly permeable and have fast electrochemistries. The decay time for a concentration change from 5 to 0 mM is approximately 8 s.

Oxygen and Temperature Sensitivity. For in vitro glucose concentration measurements, particularly for the control of blood glucose levels in diabetics, it is desirable that the electrode be insensitive to changes in dissolved oxygen concentration and to changes in temperature. Variations in catalytic current with pO_2 result from the competition between the redox polymer (I) and oxygen (II) in the glucose oxidase catalyzed oxidation of glucose.

(I) β-D-glucose + PVP[Os(bpy)$_2$Cl^{2+}] → gluconolactone + PVP[Os(bpy)$_2$Cl^{2+}]

(II) β-D-glucose + O_2 → gluconolactone + H_2O_2

Oxygen sensitivity can be a problem in glucose sensors based on sensing either hydrogen peroxide or oxygen. To reduce the oxygen sensitivity, catalase has been used to recycle O_2 from H_2O_2 and sensor designs have been employed that allow O_2 to diffuse to the electrode surface axially and radially while glucose can diffuse only axially, resulting in an excess of O_2 compared to glucose at the electrode (*30*, *31*). Electrodes based on fast electron acceptors, such as ferrocenium derivatives, show less O_2 sensitivity, but the natural enzymatic reaction with O_2 still competes with the mediated reaction, leading to some O_2 sensitivity. In the thin-film glucose microelectrode, this sensitivity is small. A change in oxygen concentration from deaerated to completely aerated solutions (~280 μM O_2) produces only a 2% change in the current at 5 mM glucose (Figure 5). The low oxygen sensitivity shows that the oxidation of the $FADH_2$ centers of glucose oxidase by the Os(bpy)$_2$Cl^{2+} centers of the redox hydrogel followed by radial charge transport through the redox hydrogel to the electrode is sufficiently fast to effectively compete with reaction II.

The temperature dependence of the current is characterized by the activation energy of the rate-limiting step in the catalytic electrooxidation of glucose. The temperature dependence of the current was measured in a thermostated cell over a temperature range between 2 and 40 °C (Figure 6). The activation energy for the rate-determining step was determined to be ~35 kJ/mol (as calculated from a linear plot of ln (i/nFA) versus $1/T$). Near room temperature, the change in the catalytic current at 5 mM glucose is of approximately 5%/°C in thin-film electrodes, indicating that accurate glucose concentration measurements require either measurement and compensation for changes in the environmental temperature or a change in the chemical design of the sensor, so as to lower the activation energy by changing the rate-determining step.

CONCLUSIONS

Unlike in diffusionally mediated glucose electrodes, where miniaturization may lead to loss in current density because of loss of enzyme-reduced mediator by radial diffusion, the current density is increased upon miniaturization of electrodes where the enzyme is electrically connected to the microelectrode via a nondiffusing redox hydrogel. Thus, glucose oxidase immobilized in poly[(vinylpyridine)Os(bipyridine)$_2$Cl]-containing redox hydrogels, glucose microelectrodes with current densities and sensitivities 10-fold higher than similar macroelectrodes, have been fabricated on beveled carbon-fiber microelectrodes. The increase in current density, sensitivity, signal to noise ratio, and lower oxygen sensitivity are attributed to the radial diffusion of electrons through the redox hydrogel.

LITERATURE CITED

(1) Wise, D. L., Ed. *Applied Biosensors*; Butterworths: Boston, 1989.
(2) Moebach, K., Ed. *Methods in Enzymology*; Academic Press: New York, 1987; Vol. 137.
(3) Luong, J. H. T.; Mulcandani, A.; Guilbault, G. G. *Trends Biotechnol.* **1988**, *6*, 310.
(4) Hendry, S.; Higgins, I.; Bannister, J. *J. Biotechnol.* **1989**, *15* (3), 229.
(5) Michael, A. C.; Justice, J., Jr. *Anal. Chem.* **1987**, *59* (3), 405.
(6) Hill, H. A. O.; Klein, N. P.; Murthy, A. S. N.; Psaill, I. S. M. *ACS Symp. Ser.* **1989**, *403*, 105.
(7) Shichiri, M.; Kawamori, R.; Goriya, Y.; Yamazaki, Y.; Nomura, M.; Hakui, N.; Abe, H. *Diabetologia* **1983**, *24*, 179.
(8) Sansen, W.; De Wachter, D.; Callewaert, L.; Lambrechts, M.; Claes, A. *Sens. Actuators* **1989**, *B1* (1–6), 298.
(9) Murakami, T.; Nakamoto, S.; Kimura, J.; Kuriyama, T.; Karube, I. *Anal. Lett.* **1986**, *19*, 1973.
(10) Tamiya, E.; Karube, I. *Sens. Actuators* **1988**, *15*, 199.
(11) Gernet, S.; Koudelka, M.; de Rooij, N. F. *Sens. Actuators* **1989**, *17*, 537.
(12) Yamauchi, S. Proceedings of the 3rd International Meeting on Chemical Sensors, Cleveland, OH, Sept 24–26, 1990; p. 13.
(13) Ikariyama, Y.; Shimada, N.; Yamauchi, S. *ACS Symp. Ser.* **1989**, *403*, 96.
(14) Karube, I. *Makromol. Chem., Macromol. Symp.* **1988**, *17*, 419.
(15) Tamiya, E.; Karube, I.; Hattori, S.; Suzuki, M.; Yokoyama, K. *Sens. Actuators* **1988**, *18*, 297.
(16) Suzuki, H.; Tamiya, E.; Karube, I. *Anal. Chem.* **1988**, *60*, 1078.

(17) Yokoyama, K.; Soda, K.; Tamiya, E.; Karube, I. *Anal. Chem. Acta* **1988**, *218*, 137.
(18) Gregg, B.; Heller, A. *J. Phys. Chem.* **1991**, *95*, 5970.
(19) Gregg, B.; Heller, A. *J. Phys. Chem.* **1991**, *95*, 5976.
(20) Gregg, B. A.; Heller, A. *Anal. Chem.* **1990**, *62*, 258.
(21) Frederick, K. R.; Tung, J.; Emerick, R. S.; Masiarz, F. R.; Chamberlin, S. H.; Vasavada, A.; Rosenberg, S.; Chakraborty, S.; Schopter, L. M.; Massey, V. *J. Biol. Chem.* **1990**, *265*, 3793.
(22) Wightman, R. M.; May, L. J.; Baur, J.; Leszczyszyn, D.; Kristensen, E. *ACS Symp. Ser.* **1989**, *403*, 114.
(23) Andrieux, C.; Saveant, J. *J. Electroanal. Chem. Interfacial Electrochem.* **1980**, *111*, 377.
(24) Gang, L.; Reed, R. A.; Kim, M.-H.; Wooster, T. T.; Oliver, B. N.; Egekeze, J.; Kennedy, R. T.; Jorgenson, J. W.; Parcher, J. F.; Murray, R. W. *J. Am. Chem. Soc.* **1989**, *111*, 1614.
(25) Oliver, B. N.; Egekeze, J. O.; Murray, R. W. *J. Am. Chem. Soc.* **1988**, *110*, 2321.
(26) Gang, L.; Longmire, M. L.; Reed, R. A.; Parcher, J. F.; Barbour, C. J.; Murray, R. W. *Chem. Mater.* **1989**, *1*, 58.
(27) Dayton, M. A.; Ewing, A. G.; Wightman, R. M. *Anal. Chem.* **1980**, *52*, 2392.
(28) Pishko, M. V.; Katakis, I.; Lindquist, S.-E.; Heller, A.; Degani, Y. *Mol. Cryst. Liq. Cryst.* **1990**, *190*, 221.
(29) Pishko, M. V.; Katakis, I.; Lindquist, S.-E.; Ye, L.; Gregg, B. A.; Heller, A. *Angew. Chem., Int. Ed. Engl.* **1990**, *29* (1), 82.
(30) Gough, D. *Horm. Metab. Res., Suppl. Ser.* **1988**, No. 20, 30.
(31) Gough, D.; Leypoldt, J.; Armour, J. *Diabetes Care* **1982**, *5*, 190.

RECEIVED for review February 27, 1991. Accepted July 25, 1991. This work is supported by the Office of Naval Research, the Robert A. Welch Foundation, the Texas Advanced Research Project, and the National Science Foundation.

Reprinted from Analytical Chemistry, 1993, 65.

This Research Contribution is in Commemoration of the Life and Science of I. M. Kolthoff (1894–1993).

Scanning Electrochemical Microscopy. 24. Enzyme Ultramicroelectrodes for the Measurement of Hydrogen Peroxide at Surfaces

Benjamin R. Horrocks

Department of Chemistry and Biochemistry, The University of Texas at Austin, Austin, Texas 78712

David Schmidtke and Adam Heller*

Department of Chemical Engineering, The University of Texas at Austin, Austin, Texas 78712

Allen J. Bard*

Department of Chemistry and Biochemistry, The University of Texas at Austin, Austin, Texas 78712

Hydrogen peroxide sensing microelectrodes for scanning electrochemical microscopy (SECM) have been developed and used to measure hydrogen peroxide in the diffusion layer during electrochemical reduction of oxygen on gold and carbon electrodes. These microelectrode biosensors were also used to detect immobilized glucose oxidase through the production of hydrogen peroxide during enzymatic oxidation of glucose. Images of hydrogen peroxide concentration profiles near a platinum microdisk during catalytic decomposition of peroxide and in the diffusion layer of a carbon–platinum composite electrode during oxygen reduction are presented. The factors limiting the spatial resolution (tens of micrometers) and potential applications of the technique are discussed.

INTRODUCTION

In scanning electrochemical microscopy (SECM), an ultramicroelectrode (UME) tip is scanned over the surface of a sample. Topographic and chemical information about the surface and electrochemical processes in the diffusion layer can be obtained from the faradaic current at the UME.[1-3] Commonly, a reversible redox mediator is used and the UME is poised at a potential where the reaction at the tip is diffusion controlled. At such a potential, the tip current is determined by the rate of mass transfer to the tip, which is a known function of the tip-to-sample separation.[4] The current decreases near an insulating surface and increases near a conductor. Insulators, conductors, and samples containing both insulating and conducting regions have been imaged.[5,6] Chemical information about the surface can be obtained by an appropriate choice of mediator. Thus, when the kinetics of regeneration of the mediator at a particular site are slow, the distribution of the slow sites can be mapped.[7,8] Although many chemical systems can be investigated in this way (metals, polymers, semiconductors, oxides, immobilized enzymes),[2,3] the scope of the technique is limited to systems that can be probed by redox mediators. Thus these SECM techniques, like voltammetric methods, have a limited degree of chemical selectivity. Several laboratories have developed potentiometric UME for use in SECM[9,10] and localized measurements of corrosion.[11,12] Potentiometric microelectrodes are also widely used in biology for intracellular measurements of ion concentrations.[13] The use of potentiometry in SECM should allow the monitoring of local pH and halide and alkali metal ion concentrations. In this paper, we show that the scanning tip can be made selective by "electrically wiring" an enzyme to the UME via a cross-linked redox polymer to produce an electrochemical biosensor.

Many different designs for enzyme UMEs have been reported, including physical entrapment on platinum,[14-16] conducting organic salts,[17] covalent attachment using biotin–avidin,[18,19] and immobilization in cross-linked redox polymers.[20] The SECM tips were made by electrically wiring horseradish peroxidase to a carbon electrode via a cross-linked redox polymer (shown in Figure 1).[21,22] The redox polymer

* Author to whom correspondence should be addressed.

(1) Engstrom, R. C.; Pharr, C. M. *Anal. Chem.* **1989**, *61*, 1099A.
(2) Bard, A. J.; Fan, F.-R. F.; Pierce, D. T.; Unwin, P. R.; Wipf, D. O.; Zhou, F. *Science* **1991**, *254*, 68.
(3) Bard, A. J.; Denuault, G.; Lee, C.; Mandler, D.; Wipf, D. O. *Acc. Chem. Res.* **1990**, *23*, 357.
(4) Kwak, J.; Bard, A. J. *Anal. Chem.* **1989**, *61*, 1221.
(5) Lee, C.; Miller, C. J.; Bard, A. J. *Anal. Chem.* **1991**, *63*, 78.
(6) Wipf, D. O.; Bard, A. J.; Tallmann, D. E. *Anal. Chem.* **1993**, *65*, 1373.
(7) Wipf, D. O.; Bard, A. J. *J. Electrochem. Soc.* **1991**, *138*, L4.
(8) Engstrom, R. C.; Small, B.; Kattan, L. *Anal. Chem.* **1992**, *64*, 241.
(9) Denuault, G.; Troise-Frank, M. H.; Peter, L. M. *Faraday Discuss. Chem. Soc.* **1992**, *No. 94*, 23.
(10) Horrocks, B. R.; Mirkin, M. V.; Pierce, D. T.; Bard, A. J.; Nagy, G.; Toth, K. *Anal. Chem.* **1993**, *65*, 1213.
(11) Luo, J. L.; Lu, Y. C.; Ives, M. B. *J. Electroanal. Chem.* **1992**, *326*, 51.
(12) Davis, J. A. *NACE Localized Corros.* **1974**, *3*, 168.
(13) Ammann, D. *Ion Selective Microelectrodes: Principles, Design and Application*; Springer: New York, 1986.
(14) Abe, T.; Lau, Y. Y.; Ewing, A. G. *J. Am. Chem. Soc.* **1991**, *113*, 7421.
(15) Ikariyama, Y.; Yamauchi, S.; Aizawa, M.; Yukiashi, T.; Ushioda, H. *Bull. Chem. Soc. Jpn.* **1988**, *61*, 3525.
(16) Cronenberg, C. C. H.; van den Heuvel, J. C. *Biosens. Bioelectron.* **1991**, *6*, 255.
(17) Kawagoe, J. L.; Niehaus, D. E.; Wightman, R. M. *Anal. Chem.* **1991**, *63*, 2961.
(18) Pantano, P.; Morton, T. H.; Kuhr, W. G. *J. Am. Chem. Soc.* **1991**, *113*, 1832.
(19) Pantano, P.; Kuhr, W. G. *Anal. Chem.* **1993**, *65*, 617, 623.
(20) Pishko, M.; Michael, A. C.; Heller, A. *Anal. Chem.* **1991**, *63*, 2268.
(21) Heller, A. *Acc. Chem. Res.* **1990**, *23*, 128.

0003-2700/93/0365-3605$04.00/0

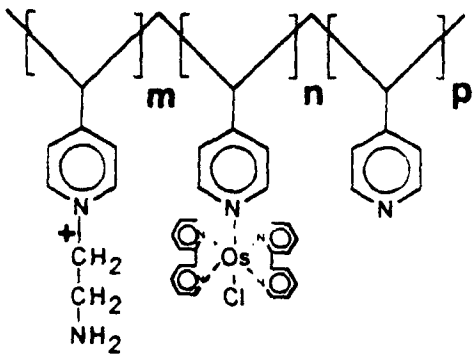

m=1.2, n=1, p=4

(1)

Figure 1. Structure of the osmium redox polymer (1) used in the preparation of the hydrogen peroxide biosensors.

provides an electron diffusion path from the carbon electrode to the reaction center of the enzyme. A cathodic current flows when hydrogen peroxide is reduced to water by the enzyme, the oxidized enzyme is reduced by Os^{2+} centers of the polymer, and the resulting Os^{3+} sites are electroreduced through electron transport via the polymer from the electrode. The advantages of this type of biosensor include high current density and insensitivity to oxygen concentration.[20] We chose a hydrogen peroxide sensing tip because hydrogen peroxide is frequently produced in enzymatic and electrochemial systems through the reduction of oxygen.

The reduction of oxygen on metals has been extensively studied because of its importance as the cathode reaction in fuel cells.[23,24] In protic solvents, the final reduction product can be water or hydrogen peroxide, depending on the electrode material. For an efficient fuel cell, it is desirable that oxygen is reduced directly to water in a four-electron reaction at low overpotential rather than in the two-electron reaction to hydrogen peroxide, and a great deal of effort has been put into designing electrocatalysts to achieve this.[24-26] The activity of these electrodes and the relative contribution of the two-electron and four-electron paths is often examined by rotating ring–disk electrode (RRDE) techniques.[27] In this approach, the disk is fabricated from the catalyst of interest, and a platinum ring is used to detect hydrogen peroxide by amperometric oxidation. Because the reduction of hydrogen peroxide is very sensitive to the cleanliness of the surface,[23,24] H_2O_2 is detected at a platinum ring held at a high positive potential, e.g., +1.0 V, sufficient to oxidize hydrogen peroxide. However, a hydrogen peroxide biosensor is much more selective than a platinum electrode held at +1.0 V and therefore should be applicable to systems where the presence of other electroactive compounds would prevent the use of platinum electrodes.

Hydrogen peroxide is also a byproduct of the reactions of many enzymatic oxidations where the oxidized form of the enzyme is regenerated by reaction of the reduced enzyme with oxygen.[28] Although immobilized oxidoreductases have been studied successfully by SECM with simple redox mediators,[29] it would also be interesting to be able to study these reactions with the usual biological substrate of the enzyme, oxygen.

The aim of this paper is to show that amperometric biosensors can be employed as the tip in SECM. Examples of the information that they can provide in studies of electrochemical and enzymatic oxygen reduction are presented. The advantages and disadvantages of the technique compared to RRDE and simple voltammetric SECM techniques are also discussed. Images of the distribution of catalytic activity on model surfaces are shown, and the technique is compared to other methods of imaging electrochemical activity, such as SECM with voltammetric microelectrodes and fluorescence imaging.[30]

THEORY

As in any scanning probe microscopy, it is necessary to determine the absolute tip-to-sample distance in order to bring the tip close to the surface and to extract quantitative information about concentrations near the surface. In SECM with redox mediators, this is very conveniently done by monitoring the faradaic current at the UME tip as it approaches the surface.[4] This approach is not possible with the biosensor tips used in this paper for two reasons. First, it it undesirable to add a redox mediator to the solution, because this could perturb the chemistry of the system. Second, the rate of diffusion of redox mediators in polymers is slower than in aqueous solutions, and the faradaic current for a redox mediator at the tip may be limited by diffusion through the polymer film. The tip current would therefore be insensitive to the rate of diffusion in the solution and hence to the tip-to-sample distance. However, a modification of the procedure is possible. By applying a high-frequency alternating potential to the tip, the solution resistance between the tip and the auxiliary electrode can be measured. As the tip approaches an insulator, the solution resistance increases because the surface partially blocks some of the pathways for ions to travel between the tip and the auxiliary electrode. A similar effect is applied in scanning ion conductance microscopy.[31] Near a conducting surface, the measured resistance decreases as the tip approaches the surface, because the alternating current can now flow through the conductor; this applies equally whether the conducting sample is used as the auxiliary electrode or is simply left at open circuit. The dependence of the solution resistance on tip-to-surface separation can be calculated with two assumptions: (i) the impedance of the cell can be approximated by a simple series combination of the tip double-layer capacitance and the solution resistance, and (ii) the contribution of the polymer film on the tip to the resistance is either constant or negligible. For a conductive substrate, the measured capacitance will include a contribution from the substrate. At small tip–surface separations, only the part of the substrate underneath the tip is active and the capacitance of this region may be of the same order as the tip double-layer capacitance. However, this effect was found to be within the accuracy of our experimental data and therefore no correction for this effect was applied.

The computation of the solution resistance between a disk electrode and an auxiliary electrode at infinity has been carried out by Newman by solving the Laplace equation for the potential distribution.[32] The equivalent problem for the

(22) Heller, A. *J. Phys. Chem.* **1992**, *96*, 3579.
(23) Hoare, J. P. In *Encyclopedia of Electrochemistry of the Elements*; Bard, A. J., Ed.; Marcel Dekker: New York, 1974; Vol. II, pp 305–337.
(24) Yeager, E. *Electrochim. Acta* **1984**, *29*, 1527.
(25) Karaman, R.; Jeon, S.; Almarsson, O.; Bruice, T. C. *J. Am. Chem. Soc.* **1992**, *114*, 4899.
(26) Collman, J. P.; Denisevich, P.; Konai, Y.; Marroco, M.; Koval, C.; Anson, F. C. *J. Am. Chem. Soc.* **1980**, *102*, 6027.
(27) Durand, R. R., Jr.; Bencosme, C. S.; Collmann, J. P.; Anson, F. C. *J. Am. Chem. Soc.* **1983**, *105*, 2710.
(28) Dixon, M.; Webb, E. C. *Enzymes*; Academic Press: New York, 1979.
(29) Pierce, D. T.; Unwin, P. R.; Bard, A. J. *Anal. Chem.* **1992**, *64*, 1795.
(30) Engstrom, R. C.; Ghaffari, S.; Qu, H. *Anal. Chem.* **1992**, *64*, 2525.
(31) Hansma, P. K.; Drake, B.; Marti, O.; Gould, S. A. C.; Prater, C. B. *Science* **1989**, *243*, 641.
(32) Newman, J. *J. Electrochem. Soc.* **1966**, *113*, 501.

geometry of SECM can be formulated by the following equations.

$$\nabla^2\phi = 0 \quad (1)$$

with the boundary conditions

$$j = -\kappa\nabla\phi \quad \text{in the solution} \quad (2)$$

ϕ = const at a conducting sample–auxiliary electrode (3)

$$\phi = 0 \quad \text{at the tip} \quad (4)$$

$j = 0$ at insulating surfaces and the glass tip sheath (5)

The above equations apply to both dc resistance experiments with a redox couple present and ac experiments in inert electrolyte, as long as ϕ is taken as the alternating part of the potential in the latter case. These equations are strictly analogous to Fick's equation for amperometric SECM at steady state.

$$\nabla^2 c = 0 \quad (6)$$

with the boundary conditions

$$i_T = -nFD\nabla c \quad \text{in the solution} \quad (7)$$

$$c = \text{const} \quad \text{at a conducting sample surface} \quad (8)$$

$$c = 0 \quad \text{at the tip} \quad (9)$$

$i_T = 0$ at insulating surfaces and the glass tip sheath (10)

This analogy has also been pointed out for the calculation of the uncompensated resistance at a UME in bulk solution.[33,34] Using this analogy and normalizing the distance scale by the tip radius, a, we obtain the following expression for the variation of solution resistance with the tip-to-surface separation:

$$R(\infty)/R(d) = i_T(d)/i_{T,\infty} \quad (11)$$

where $i_T(d)$ and $R(d)$ are the feedback current and solution resistance at a normalized tip-to-surface separation of d (in units of tip radius a). This implies that the (decreasing) conductance as the tip approaches an insulator shows the same distance dependence as that of the current in SECM. A similar equivalence exists for the conductance and current with a conductive substrate. Since the distance dependence of the feedback diffusion current is already known,[4] all that remains is to show how the contribution of the solution resistance can be separated from the capacitive contribution to the impedance of the tip.

When the tip–auxiliary electrode cell can be represented by a simple series RC equivalent circuit, the in-phase and quadrature components of the current are

$$i_{0°} = \frac{\omega^2 c_{dl}^2 RV}{1 + \omega^2 c_{dl}^2 R^2} \quad (12)$$

$$i_{90°} = \frac{\omega c_{dl} V}{1 + \omega^2 c_{dl}^2 R^2} \quad (13)$$

where ω, c_{dl}, R, and V are the angular frequency, tip double-layer capacitance, solution resistance, and magnitude of the applied ac voltage, respectively. The normalized solution resistance in eq 11 can then be calculated using

$$\omega c_{dl} R(d) = i_{0°}(d)/i_{90°}(d) \quad (14)$$

After normalizing this by the value of resistance at large distances, $R(\infty)$ (i.e., distances greater than a few radii), a plot of normalized conductance, $R(\infty)/R(d)$, vs distance, d, can be constructed. These data can then be fit to the theory for feedback diffusion in SECM ($i_T(d)/i_{T,\infty}$ vs d) to determine the absolute tip-to-surface distance.

(33) Oldham, K. B. *J. Electroanal. Chem.* **1988**, *250*, 1.
(34) Oldham, K. B. In *Microelectrodes: Theory and Applications*; Montenegro, M. I., Queiros, M. A., Daschbach, J. L., Eds.; Kluwer: Amsterdam, 1991; p 83.

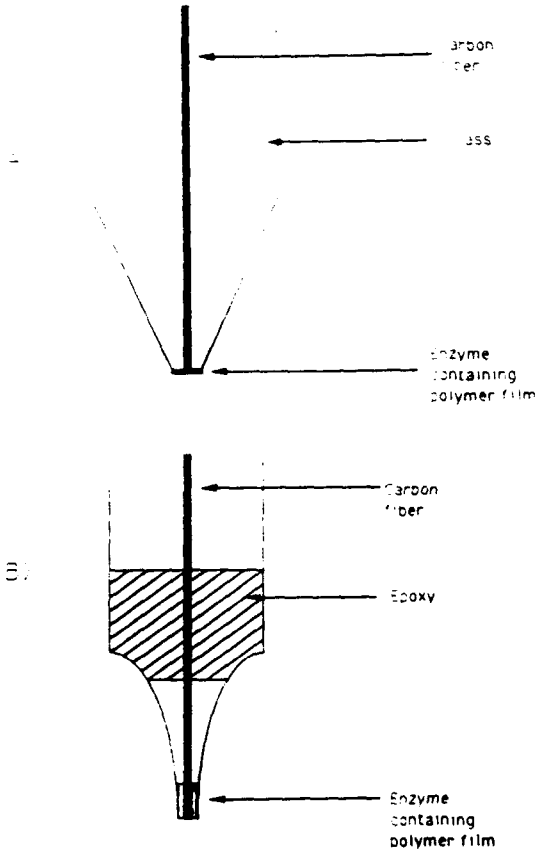

Figure 2. Schematics of the two types (A and B) of hydrogen peroxide sensing microelectrodes used.

EXPERIMENTAL SECTION

Microelectrode Fabrication. Carbon microelectrodes of two different geometries were prepared for use as amperometric biosensors. These are referred to as type A (microdisk) and type B (microcylinder) electrodes.

Type A electrodes (Figure 2A) were prepared by heat sealing 11- or 8-μm-diameter carbon fibers (Amoco Performance Products, Greenville, SC) in 2-mm-o.d. Pyrex capillaries. The tip of the electrode was then beveled to produce an SECM tip, as described previously.[4] The resulting tip geometry was an inlaid microdisk electrode with a ratio of glass sheath diameter to carbon fiber diameter, denoted as RG, of ca. 2–3.

The carbon microdisk was then coated with the electrically wired enzyme. The coating solution contained redox polymer 1, enzyme (horseradish peroxidase), and cross-linker [poly(ethylene glycol) (MW 400) diglycidyl ether] in a weight ratio of 6.2:3.9:1. The tip of the electrode was brought into contact with a drop of the coating solution using a micromanipulator and then withdrawn. The solution was allowed to dry and form a roughly 1-μm-thick film (estimated by optical microscopy) coating the surface of the tip. The film was cured at ambient temperature in air for a minimum of 2 days.

Type B electrodes (Figure 2B) were fabricated in a manner similar to a previously published procedure for glucose-sensing microelectrodes.[20] A 7-μm-diameter carbon fiber was inserted into a 2-mm-o.d. borosilicate glass tube, and the tube was pulled on a micropipet puller (Narishige Model PB-7) to yield a glass tip of approximately 20-μm o.d. The glass tip was then partially filled with a low-viscosity epoxy, leaving a microcylinder as the electrode surface, and was cured at 70 °C overnight. The tip was then polished at an angle of 90° with a micropipet beveler (Model BV-10, Sutter Instrument Co.), first on 1200-grit sand paper and then on an extrafine diamond abrasive plate, to produce a smooth

carbon surface. Electrical contact to the carbon fiber was made by filling the top of the tube with mercury and inserting a stainless steel wire.

The carbon microcylinder was then coated in a manner similar to the microdisk tips. The tip of the microelectrode was pushed into a 1–2-μL drop of the coating solution using a micromanipulator. The mixture was allowed to rise into the glass pipet and coat the fiber. After the mixture dried, the end of the glass micropipet was blocked by the redox polymer film. Again, the film was cured at ambient temperature in air for a minimum of 2 days.

Antimony microdisk electrodes for the measurement of pH near electrode surfaces with the SECM were prepared from antimony shot as described previously.[10] The pH response of each electrode was calibrated using a glass electrode (Orion Research, Model 701A, Boston, MA) in phosphate buffers. The sensitivity of the electrodes was ~50 mV/pH unit, which is typical for polycrystalline antimony.[35]

Platinum microdisk electrodes used for comparison were prepared by sealing platinum wire (Goodfellow Metals Ltd., Cambridge, UK) in glass as described previously.[4] The reference electrode was a silver quasi-reference electrode (AgQRE).

Immobilized Glucose Oxidase. Glucose oxidase was immbolized on a carbon surface using a technique similar to the tip preparation above. The enzyme, redox polymer, and cross-linker [poly(ethylene glycol) (MW 400) diglycidyl ether] were mixed in a weight ratio of 3:7:0.5, and a drop of the solution was applied to the surface of a 3-mm-diameter carbon disk electrode. The mixture was allowed to cure in air at ambient temperature for ~2 days.

Instrumentation. The basic SECM instrument used in this work has been described in detail previously.[36] Briefly, a CE-1000 micropositioning device (Burleigh Instruments, Fishers, NY), connected to a PC via a DAC, controlled the movement of three piezoelectric inchworm motors. The tip was mounted on a three-axis translation stage and could be moved with submicron distance resolution under the control of the PC. The potentials of the tip and, when necessary, the substrate were controlled by a four-electrode EI-400 bipotentiostat (Ensman Instrumentation, Bloomington, IN). The tip and substrate currents were digitized and acquired by the PC using software written in-house (by D. O. Wipf).

Admittance–impedance measurements at UME tips in the SECM were made with a lock-in amplifier (Princeton Applied Research, model 5206, Princeton, NJ). The oscillator output of the lock-in was connected directly to the substrate or to a platinum or silver/silver chloride auxiliary electrode. The tip was held at virtual ground, and the current was measured with a high-frequency current follower. The real and imaginary components of the tip current as measured by the lock-in amplifier were fed into the ADC and collected by the PC.

A high-impedance buffer[10] was used for potentiometric SECM measurements with antimony pH-sensing tips. To avoid problems arising from the interaction of the ground of the EI-400 bipotentiostat and the ground of the high-impedance buffer, the substrate electrode was connected to channel B of the bipotentiostat and an external potential source (PAR 173 potential programmer) was used to run cyclic voltammograms. In this configuration, the reference electrode was at virtual ground and the potential of the tip could therefore be measured with respect to the same reference electrode used by the bipotentiostat. Tip potential and substrate current data were acquired simultaneously by the PC using the SECM software.

Cell and Substrate Electrodes. The cell (volume ca. 4 mL)[10,29] was machined from Teflon material, and the base was threaded to allow easy removal and exchange of different cell bases containing various substrate electrodes.

Glassy carbon substrate electrodes were made by heat-sealing 3-mm-diameter rod directly into a Teflon cell base using standard techniques. Gold substrate electrodes were made by first sealing 450-μm-diameter wire in 2-mm-o.d. soft glass capillaries under vacuum, polishing to expose a cross section, and then inserting them into a hole drilled in the cell base.

Chemicals. Peroxidase (EC 1.11.1.7; Type II, 200 units/mg of solid) from Horseradish (Sigma Chemical Co., St. Louis, MO) and glucose oxidase (EC 1.1.3.4; 122 units/mg of solid) from *Aspergillus niger* were used as received. The cross-linking agent [poly(ethylene glycol) (MW 400) diglycidyl ether] was obtained from Polysciences, and the redox polymer, [poly[(vinylpyridine)-osmium(bipyridine)$_2$Cl] derivatized with bromoethylamine] shown in Figure 1, was synthesized as previously reported.[37] Antimony shot (99.999%) was obtained from Aldrich. Fresh solutions of hydrogen peroxide were made up for each experiment by dilution of a concentrated commercial aqueous solution (30% by volume, Merck). The concentration of the commercial solution was checked by measuring the density. All other reagents were purchased from Aldrich or Sigma.

SECM Experimental Procedure. In general, the experimental procedure involved bringing the biosensor tip close to the sample surface and establishing the distance scale from the solution resistance (type A tips) or by deliberately touching the surface with the tip (type B tips).

For type A tips, the distance calibration was performed in 1 mM KCl. The in-phase and quadrature components of the current were monitored at a frequency of 10 kHz as the tip was pushed toward the surface. The tip was stopped when the real component had decreased by a factor of roughly 2. The tip was then withdrawn a known distance, disconnected from the lock-in amplifier, connected to the bipotentiostat, and held at a potential of −0.1 V vs AgQRE to detect peroxide. Fresh pH 7 phosphate buffer was usually added to the cell at this stage. The tip could then be pushed toward the surface to any desired tip-to-surface separation for imaging or electrochemical generation–detection experiments.

For type B tips, the tip was positioned as close as possible to the surface (~0.1 mm) using a telescopic lens. Next, the tip was connected to the bipotentiostat and very slowly (<0.5 μm/s) pushed toward the surface until a sudden jump in the current indicated that part of the tip was touching the surface. In some experiments, generation of a concentration profile of hydrogen peroxide at the surface aided this step. A gradual increase in tip current due to detection of peroxide was observed as the tip approached the surface, the tip approach was then continued at a slower rate until a sudden increase in the tip current was assumed to indicate electrical contact between tip and surface, and this point was taken as zero tip-to-surface separation. The tip was then withdrawn to the required distance for imaging or electrochemical experiments.

For potentiometric SECM experiments with antimony tips, the antimony tip potential was poised at a value where reduction of oxygen is diffusion controlled, and a current–distance curve corresponding to the case of an insulating substrate was recorded as reported previously.[10] The antimony tip was then reoxidized by returning the tip potential to 0 V for a few seconds to restore the pH function. The tip could then be connected to the high-impedance buffer for potentiometric measurements.

RESULTS

Characterization of Tips. Figure 3 shows a current–concentration calibration for a type B tip. A linear dependence of current on hydrogen peroxide was found up to ~100 μM (inset). If the active area of the tip is taken as roughly the same as the cross-sectional area of the end of the tip, a sensitivity of 0.75 A M^{-1} cm^{-2} is obtained. This is in reasonable agreement with the value of 1 A M^{-1} cm^{-2} found for macroscopic electrodes based on the same enzyme and redox polymer;[38] the discrepancy is mainly due to the uncertainty in the correct value of the area to be used in the calculation. Type B tips exhibited a slowly decaying background current, probably due to the redox process of parts of the polymer in poor electrical communication with the carbon fiber. This current was of the order of 10 pA after a few minutes at the

(35) Glab, S.; Hulanicki, A.; Edwall, G.; Ingman, F. *Crit. Rev. Anal. Chem.* **1989**, *21*, 29.
(36) Wipf, D. O.; Bard, A. J. *J. Electrochem. Soc.* **1991**, *138*, 469.
(37) Gregg, B.; Heller, A. *J. Phys. Chem.* **1991**, *95*, 5976.
(38) Vreeke, M.; Maidan, R.; Heller, A. *Anal. Chem.* **1992**, *64*, 3084.

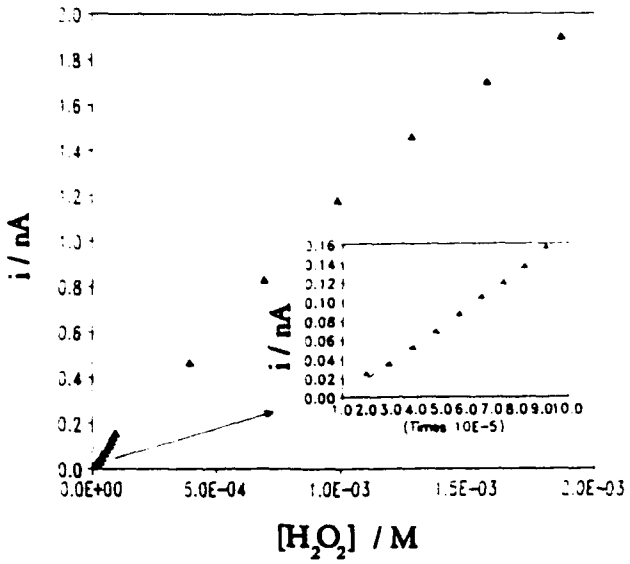

Figure 3. Current vs hydrogen peroxide concentration for a type B tip in 0.2 M pH 7 phosphate buffer. The inset shows the linear region below 100 μM.

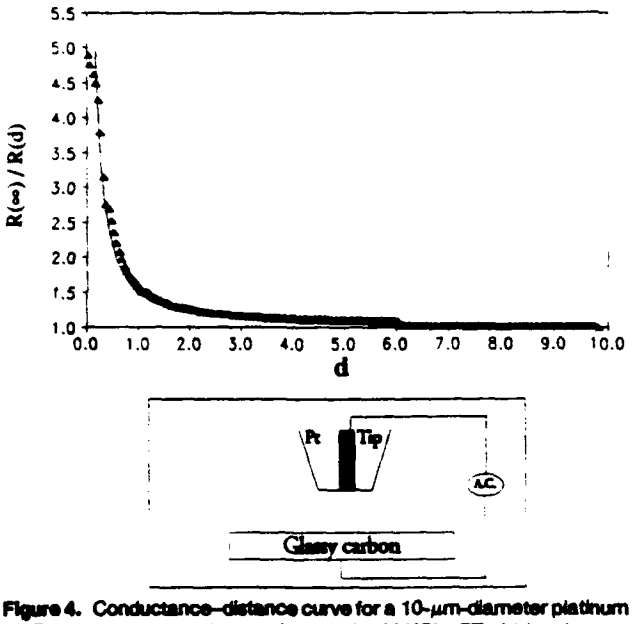

Figure 4. Conductance–distance curve for a 10-μm-diameter platinum UME over a glassy carbon surface in 1 mM KCl. Filled triangles are experiment and line is theory.

potential of −0.1 V vs AgQRE used for peroxide detection. Although type A tips showed smaller background currents, of the order of a few picoamperes, they produced ~10 times less current for a given concentration of peroxide. A crude estimate of the response time of the tips was made by monitoring the current on addition of peroxide to a stirred solution. Both type A and B tips showed similar response times, reaching 80% of the steady current in approximately 1–2 s; these values are close to those reported for glucose microelectrodes of similar design.[20]

Distance Calibration. Figures 4 and 5 show approach curves of conductance against distance for bare platinum UME tips over glassy carbon and Teflon substrates, respectively. These approach curves were recorded in a 1 mM KCl solution, since the UME double-layer capacitance dominates the impedance of the system in solutions of high ionic strength. Although the agreement with theory is excellent, this method of approaching the surface suffers from the limitation that as the tip becomes smaller, the double-layer capacitance decreases, and the relative contribution of the solution

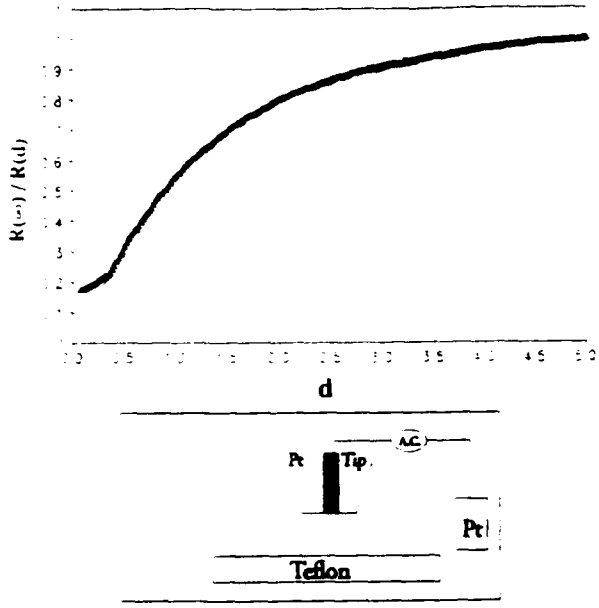

Figure 5. Conductance–distance curve for a 25-μm-diameter platinum UME over a Teflon surface in 1 mM KCl. Filled triangles are experiment and line is theory.

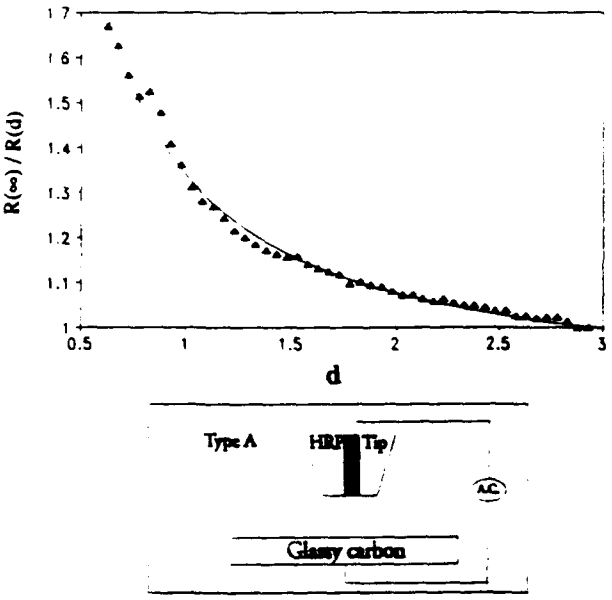

Figure 6. Conductance–distance curve for an 11-μm-diameter type A tip over a glassy carbon surface in 1 mM KCl. Filled triangles are experiment and line is theory.

resistance to the impedance decreases. Moreover, the method of data analysis outlined in the theory section depends on the assumption of a simple RC series equivalent circuit, i.e., with no faradaic process. To some extent these problems can be overcome by the use of low-conductivity solutions and high frequencies so that the contribution of the solution resistance to the impedance is maximized.

The advantage of this method is that it works equally well for insulating and conducting surfaces and could even be used to distinguish regions of different conductivity on a surface in exactly the same way as amperometric SECM. A further advantage is the relative insensitivity to the presence of a thin polymer film on the tip. This is shown in Figure 6, the approach curve for a type A biosensor tip over a glassy carbon surface. The agreement with theory is still sufficiently good to allow calibration of the tip-to-surface distance with an accuracy better than 1 μm. The presence of the polymer film on the tip increased the measured capacitance by a factor of

Table 1. Pathways of Electrochemical Reduction of Oxygen

	reaction	electrode potential/V vs NHE[18]
a	$O_2 + 2H_2O + 4e^- \rightarrow 4OH^-$	+0.401
b	$O_2 + 4H^+ + 4e^- \rightarrow 4H_2O$	+1.229
c	$O_2 + H_2O + 2e^- \rightarrow HO_2^- + OH^-$	−0.065
d	$HO_2^- + H_2O + 2e^- \rightarrow 3OH^-$	+0.867
e	$O_2 + 2H^+ + 2e^- \rightarrow H_2O_2$	+0.67
f	$H_2O_2 + 2H^+ + 2e^- \rightarrow 2H_2O$	+1.77
g	$2H_2O_2 \rightarrow 2H_2O + O_2$	catalyt decomp

~2, possibly due to a change in effective area. No significant difference in resistance between coated and uncoated tips was observed, and therefore, no correction for this was applied. The signal-to-noise ratio for coated electrodes in resistance measurements was poorer than for uncoated ones for reasons that are not clear.

Unfortunately, although type A tips could easily be positioned close to a surface using this method, only ~10% of these tips functioned well as biosensors. The reason for this was the poor adhesion of the polymer to the glass. The swelling of the polymer in solution often resulted in loss of polymer from the tip. For this reason, type B tips were constructed and were found to function as biosensors much more reliably. However, the geometry of these tips does not allow the use of the above theory for the conductance–distance measurement. Instead, the distance was determined by deliberately touching the tip to the conductive surface as described in the Experimental Section. Although this method could be used to calibrate a conductance–distance curve, it was carried out with the tip under potentiostatic control for convenience. This method of distance calibration has several disadvantages, the most obvious being the possibility of damaging the tip, and indeed, it was necessary to use very slow scan rates, 0.5 μm/s or less, when approaching the substrate. Moreover, this method only works with conductive substrates.

Electrochemical Reduction of Oxygen. The mechanism of the electrochemical reduction of oxygen has been intensively studied.[23,24] The reaction is complex, because it involves multiple electron- and proton-transfer reactions and proceeds through a series of high-energy intermediates, e.g., $O_2^{\bullet-}$, and $HO_2^{\bullet}$, with the more stable intermediate H_2O_2 also frequently formed. In aqueous solution, the mechanism depends on electrode material, pH, electrode potential, electrode pretreatment, and purity of the system.[24,39] A few of the processes often found in the main overall reduction are shown in Table 1. Reactions of radical intermediates such as $OH^{\bullet}$, $O_2^{\bullet-}$, and $HO_2^{\bullet}$ are not considered because their lifetimes are too short in aqueous solution to be detected in the SECM experiments reported here. Rotating ring–disk studies have demonstrated the presence of hydrogen peroxide as a stable intermediate.[23,24,39-43] These investigations have shown that, on most electrode materials (other than platinum), the hydrogen peroxide pathway (c–f) accounts for essentially all the current. On platinum electrodes in acidic solutions at low overpotentials, no hydrogen peroxide is detected, leading to the proposal that oxygen is reduced to water without a peroxide intermediate (b) perhaps via dissociative adsorption of oxygen.[23] Alternatively, the intermediates ($O_2^{\bullet-}$, $HO_2^{\bullet}$, or peroxide) may be strongly adsorbed on the surface and reduced to water before they desorb.[24] Furthermore, platinum is known to catalyze the disproportionation of hydrogen peroxide to water and oxygen (g), and therefore, it has been suggested that the rate of hydrogen peroxide decomposition is as fast as its rate of formation. With gold and glassy carbon electrodes, however, hydrogen peroxide is formed as a stable intermediate at any pH.[42,43] Parts A and B of Figure 7 illustrate the results of substrate generation–tip detection experiments using a peroxide-sensing UME tip close to carbon and gold substrate electrodes reducing oxygen in phosphate buffer solutions. The tip potential (with a type A or type B tip) was held constant at −0.1 V vs AgQRE (ca. +0.1 V vs SCE) to detect hydrogen peroxide, and the substrate potential was slowly swept into the region where oxygen is reduced. As the substrate begins to reduce oxygen, for both electrodes at potentials more negative than ca. −0.3 V, the tip current rises because of detection of hydrogen peroxide in the diffusion layer. Eventually, the tip current decreases again as the substrate potential becomes sufficiently negative to reduce the hydrogen peroxide to water. This is clearly seen in the case of glassy carbon (Figure 7A), where two separate, drawn-out waves are seen in the forward scan of the substrate voltammogram corresponding to potentials where the tip current rises and falls. The rise in peroxide detection current on the reverse scan occurs at roughly the same potential (−1 V) as the fall in tip current on the forward scan, confirming the identification of the two waves in the substrate voltammogram as the reduction of oxygen to peroxide and reduction of peroxide to water, respectively. This also shows that the decrease of the peroxide detection current on the forward scan reflects a potential-dependent process and is not due to a slow, time-dependent process, e.g., catalytic decomposition. The time lag for the rise of the tip current on the reverse scan is due to the slow diffusion of oxygen from the bulk solution to the carbon surface, and the slow decay of the tip current at the end of the reverse scan is due to the relaxation of the concentration profile of hydrogen peroxide between the carbon surface and the bulk solution. These results demonstrate that the tip is functioning and are in agreement with previous rotating ring–disk studies on carbon electrodes.[23]

In the case of gold (Figure 7B), the process is more complex. On the forward (0 to −1.7 V) scan, the tip current rises because of the reduction of oxygen to peroxide beginning at ~−0.2 V on the gold substrate (inset on substrate voltammogram). As with carbon, the decrease in tip current at −1.0 V is due to reduction of peroxide to water. The wave for the reduction of peroxide cannot be distinguished on the Au voltammogram, because it merges with the large reduction wave (discussed below) attributed to buffer reduction. However, the tip current does not decrease to zero, but plateaus at ~18 pA beginning at −1.2 V, indicating that peroxide reduction on the gold surface is blocked. Two plausible explanations for this behavior are fouling of the electrode surface or a shift to higher pH at the gold surface, which could reduce the rate of reduction of peroxide. To test this, the pH near the gold surface was directly measured using an antimony tip under the same conditions (Figure 7C). The small apparent rise in pH at −0.3 V in Figure 7C is due to depletion of oxygen, which causes the rest potential of antimony to become more negative. Despite this interference, Figure 7C clearly shows that the pH increases significantly only at potentials more negative than ~−1.5 V (where water reduction occurs) and therefore cannot account for the blocking of peroxide reduction at −1.2 V in Figure 7B. This sharp pH increase does, however, account for the drop in peroxide detection current at −1.5 V, which

(39) Damjanovic, A.; Genshaw, M.; Bockris, J. O'M. *J. Chem. Phys.* **1966**, *45*, 4057.
(40) Damjanovic, A.; Genshaw, M.; Bockris, J. O'M. *J. Electrochem. Soc.* **1966**, *113*, 1107; **1967**, *114*, 466.
(41) Muller, L.; Nekrasov. *J. Electroanal. Chem.* **1965**, *9*, 282.
(42) Genshaw, M. A.; Damjanovic, A. Bockris, J. O'M. *J. Electroanal. Chem.* **1967**, *15*, 163.
(43) Tarasevich, M. R.; Subirov, F. Z.; Mertsalova, A. P.; Burstein, Kh. *Electrokhim.* **1968**, *4*, 432, **1969**, *5*, 608; **1970**, *6*, 1130.

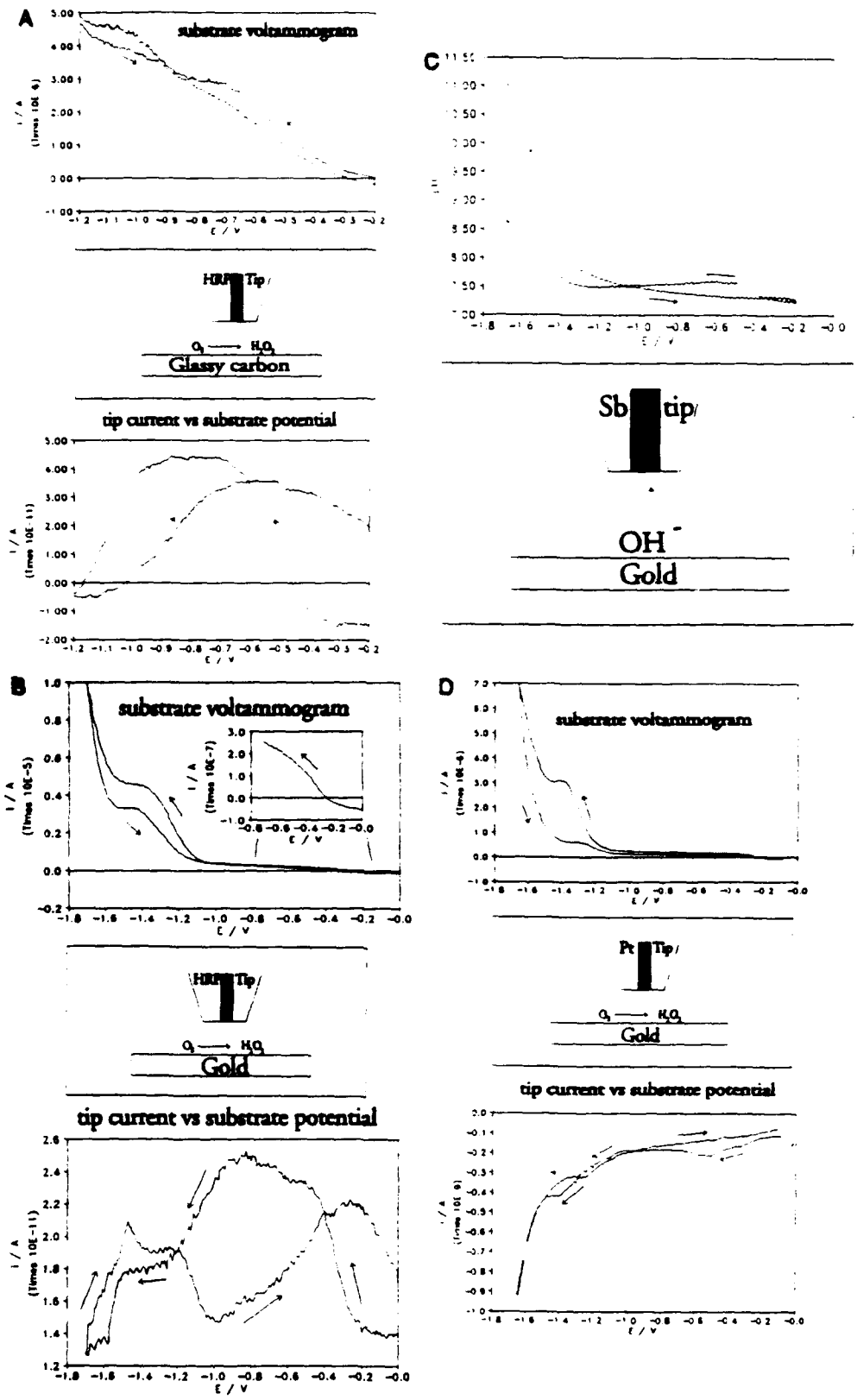

Figure 7. (A) Tip (type A) and substrate (glassy carbon) current as a function of substrate potential during a scan (2 mV/s) with a tip-to-surface distance of 10 μm. (B) (Tip) (type B) and substrate (gold) current as a function of substrate potential during a scan (10 mV/s) with a tip-to-surface distance of ~10 μm. The inset shows the oxygen reduction wave on the forward scan. (C) Tip (20-μm-diameter antimony) potential and substrate (gold) current as a function of substrate potential during a scan (10 mV/s) with a tip-to-surface distance of 10 μm. (D) Tip (10-μm-diameter platinum at +0.7 V) and substrate (gold) current as a function of substrate potential during a scan (10 mV/s) with a tip-to-surface distance of 10 μm. Solutions contained air-saturated 0.2 M pH 7 phosphate buffer, and the reference electrode was a silver wire.

is likely due to deactivation of the enzyme at such a high pH. The pH dependence of a macroscopic horseradish peroxidase electrode is consistent with this interpretation (Figure 8). The peroxide detection current is roughly independent of pH in the range 4.5–7.5. Outside this range, however, the enzyme is deactivated, losing 90% activity by pH 10.5 but recovering on returning to lower pH. The plateau in the tip current in the potential range −1.2 to −1.5 V (Figure 7B)

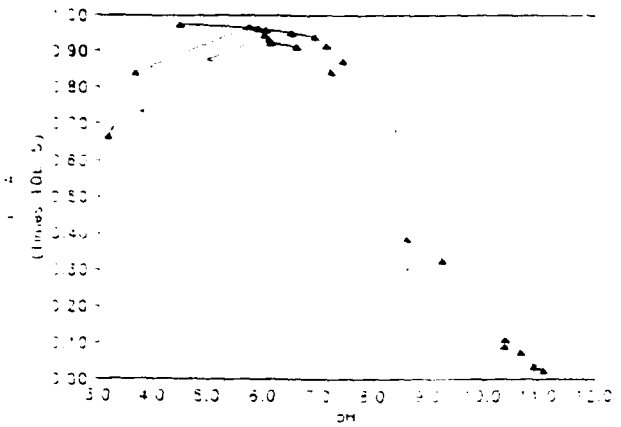

Figure 8. pH dependence of a macroscopic horseradish peroxidase electrode. The electrode used was a 3-mm-diameter glassy carbon disk coated with horseradish peroxidase in redox polymer 1. The solution contained 0.12 mM hydrogen peroxide, and the electrode potential was 0 V vs SCE.

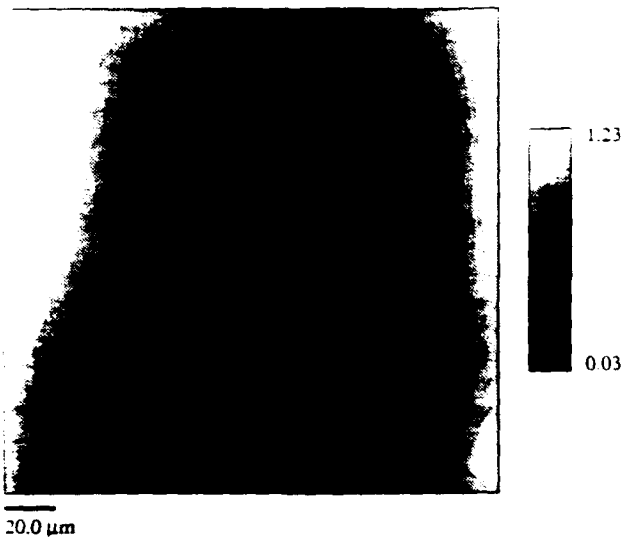

Figure 9. Image of the concentration profile of hydrogen peroxide around a 25-μm-diameter platinum microdisk in a solution of 0.88 mM hydrogen peroxide and 0.2 M pH 7 phosphate buffer.

corresponds to the large reduction wave on the gold substrate. This wave is absent in solutions containing only KCl as electrolyte, but appears on addition of phosphate buffer and is therefore attributed to reduction of buffer anions (e.g., $H_2PO_4^-$) to hydrogen. It is tentatively suggested that the electrode becomes fouled by adsorbed species produced by this reaction and that this inhibits the reduction of peroxide in this potential range, although other mechanisms cannot be ruled out on the basis of the available data. A similar effect has been reported for the reduction of hydrogen peroxide on germanium, and the decrease in reaction rate was interpreted as being due to the adsorption of hydrogen atoms on the active sites for peroxide reduction.[44] During the reverse scan in Figure 7B, the current rises in the range −1.0 to −0.3 V because the potential is no longer sufficient to reduce peroxide, and finally, the tip current falls again at potentials greater than −0.3 V, where oxygen is not reduced, because of diffusion of peroxide away from the surface to the bulk solution. For comparison, the experiment was repeated using a platinum UME as a detector, as shown in Figure 7D. The platinum tip, held at a potential where H_2O_2 oxidation occurs, responds to the production of hydrogen peroxide, but at potentials corresponding to the reduction of the buffer or water; the peroxide detection current is obscured by a large anodic current due to oxidation of hydrogen produced by these processes. The increase in detector current seen at ~−1.2 V confirms the identification of the large plateau in the substrate current at −1.2 to −1.5 V in Figure 7B as the reduction of buffer anions to hydrogen and also demonstrates the selectivity advantage of the biosensor tip, which is almost insensitive to the presence of hydrogen.

Imaging Catalytic Activity. In addition to being a tool for studying reaction mechanisms, SECM can be used to image catalytic activity. This is demonstrated for two systems. Figure 9 shows an image of the hydrogen peroxide detection current over an unbiased platinum microdisk in a solution of hydrogen peroxide. The glass insulator is inert to peroxide, but the platinum surface catalyzes the disproportionation of hydrogen peroxide to oxygen and water, as in Table 1g above. Far from the platinum disk, the peroxide concentration is constant, but decreases as the tip moves over the region near the platinum surface. The image is elongated in a direction perpendicular to the scanning motion of the tip. A possible explanation of this is that the sample surface is tilted with respect to the plane in which the tip was scanned. This results in the tip observing an elliptical section of the concentration profile around the disk. This image was taken with a type B tip, and the poor orientation of the tip and surface could only be avoided by making multiple tip crashes for distance determination. Obviously this procedure is not satisfactory. However, the response of type B tips to peroxide was more stable, and nearly all type B tips prepared had a usable response to peroxide, whereas type A tips did not show a stable response to peroxide for the long periods of time (30 min to 1 h) required to collect these images. Despite the lack of a completely satisfactory distance calibration, type B tips could be used in a qualitative way to image catalytic activity. Figure 10A is an image of the distribution of hydrogen peroxide in the diffusion layer of a glassy carbon electrode which was partially covered with platinum. This surface was prepared by electrodepositing platinum onto a 3-mm-diameter glassy carbon disk from a solution of hexachloroplatinic acid in 0.1 M HCl at a potential of −0.5 V vs Ag/AgCl. This resulted in an uneven distribution of platinum islands partially covering the surface. The platinum deposit was cleaned by potential cycling in 0.5 M H_2SO_4 until the characteristic hydrogen adsorption–desorption peaks were obtained. The dark area in Figure 10A (low tip current) shows a region covered with platinum where oxygen and hydrogen peroxide are reduced to water. The light area is the bare carbon surface where peroxide is a stable intermediate in the reduction of oxygen. A small dark spot visible in the upper right-hand corner of the image suggests the presence of a small, ca. 10-μm, platinum particle. Figure 10B shows an optical micrograph of the surface; unfortunately, it was not possible to determine the part of Figure 10B scanned in Figure 10A because of the lack of structure in the SECM image. However, a comparison with the optical micrograph of the surface shows an important aspect of the technique, that only isolated sinks (or sources) can be resolved. The main platinum region is composed of smaller islands that are so close together that their diffusion layers overlap and are not distinguished in Figure 10A. This limitation is inherent to versions of SECM relying on generation of an electroactive species by the surface under study[10] and to fluorescence imaging[30] where a fluorescence-inducing species is generated, but is less important in feedback SECM experiments where the resolution is determined only by the tip size.[7,8] In comparison with fluorescence imaging, the imaging technique with the enzyme electrode is very slow, requiring 30 min or more to scan a 300-μm by 300-μm region. This is due to the relatively slow, 1–2 s, response time of the

(44) Gerischer, H.; Mindt, W. *Surf. Sci.* 1966, *4*, 440.

discussed in the previous section, the distribution of enzyme in this polymer is quite uniform, in contrast to the observations of Wang and co-workers for the case of glucose oxidase trapped in polypyrrole.[45] Figure 12 shows a scan across the boundary of the polymer–enzyme-coated region and the bare carbon surface, where the current drops to a constant low value over a distance range of roughly 100 μm.

CONCLUSIONS

The utility of horseradish peroxidase microelectrodes in SECM has been demonstrated for mechanistic studies of oxygen reduction and for the detection of immobilized oxidases without the need for artificial redox mediators. For measurements of hydrogen peroxide in the diffusion layer, there are three main advantages over rotating ring–disk techniques. These are the excellent selectivity for hydrogen peroxide over other electroactive compounds, the high sensitivity, and the possibility of imaging distributions of catalytic activity on the surface. However, these sensors have a restricted useful pH range (ca. 4–8); moreover, the substrate generation–tip detection mode of operation is not convenient for quantitative measurements requiring a well-defined collection efficiency or for high-resolution imaging. The sensors have a relatively long response time, which restricts the scanning rate of the tip across the surface and hence increases the time required to obtain an image. This restricts the technique to imaging of steady-state concentration profiles. From the various studies carried out with the tip described here (see, e.g., Figure 10A), we judge the resolution attainable with this technique to be of the order of tens of micrometers.

The technique has promise in the study of enzymatic systems where the presence of many electroactive components could make measurements with platinum or carbon detector electrodes uncertain. In principle, many enzymatic oxidations can be studied without the need to add additional redox mediators (amperometry) or fluorescent dyes (fluorescence imaging).

(45) Yaniv, D. R.; McCormick, L.; Wang, J.; Naser, N. *J. Electroanal. Chem.* **1991**, *314*, 353.

ACKNOWLEDGMENT

The help of Dr. D. O. Wipf in building the high-frequency current follower is gratefully acknowledged. The support of our research by the Office of Naval Research, the National Science Foundation (CHE9214480), the Robert A. Welch Foundation, and the National Institutes of Health is also gratefully acknowledged.

Scientific Parentage of the Author. A. J. Bard, Ph.D. under J. J. Lingane, Ph.D. under I. M. Kolthoff.

LIST OF SYMBOLS

ϕ	electrostatic potential
j	current density, A cm^{-2}
κ	solution conductivity, S cm^{-1}
c	concentration, mol cm^{-3}
$i_T(d)$	SECM feedback current density, A cm^{-1}
D	diffusion coefficient, cm^2 s^{-1}
d	tip-to-surface distance in units of tip radius
a	tip radius, μm
$R(d)$	solution resistance as a function of d
C_{dl}	tip double-layer capacitance
ω	angular frequency of ac voltage
V	magnitude of ac voltage
$i_{0°}$	in-phase component of ac current
$i_{90°}$	quadrature component of ac current

RECEIVED for review June 28, 1993. Accepted September 28, 1993.•

• Abstract published in *Advance ACS Abstracts*, November 1, 1993.

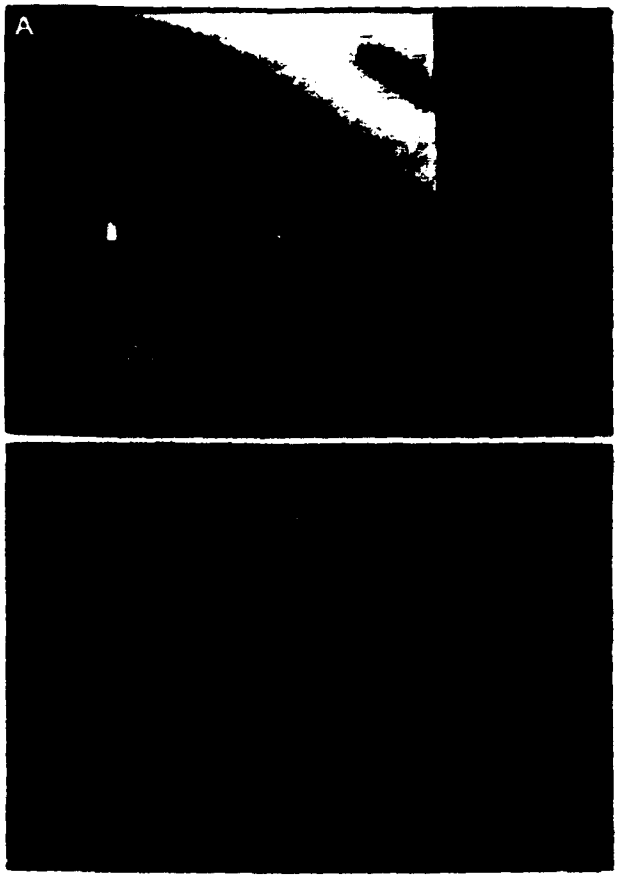

Figure 10. (A) Image of the concentration profile of hydrogen peroxide near the surface of a glassy carbon–platinum composite. The solution contained air-saturated 0.2 M pH 7 phosphate buffer, and the potential of the glassy carbon substrate was −1.0 V vs Ag/QRE. The tip to surface distance was ~20 μm. The white scale bars indicate 25 μm. (B) Optical micrograph of the surface of the glassy carbon–platinum composite from (A). The photograph shows an area ca. 500 μm across. Darker areas are electrodeposited Pt.

tips which necessitates the use of scan rates of 5 μm/s or less. However, the technique does have the ability to provide concentration profiles normal to the surface instead of integrating over a light path.

Enzymatic Oxygen Reduction. Hydrogen peroxide is formed in several oxidase-catalyzed oxidations of substrates by oxygen.[28] A simplified scheme for glucose oxidation catalyzed by glucose oxidase is shown below:

$$GO_{ox} + \beta\text{-D-glucose} \rightarrow GO_{red} + \text{D-gluconolactone} \quad (15)$$

$$GO_{red} + O_2 \rightarrow GO_{ox} + H_2O_2 \quad (16)$$

Therefore an attractive possibility for assaying enzyme activity on a small (length) scale is the measurement of the hydrogen peroxide produced. This is easily done using the peroxide-sensing tips described here. Glucose oxidase was immobilized on a glassy carbon disk (ca. 3-mm diameter) by trapping in the same polymer as used for the tip. The immobilized glucose oxidase was placed in air-saturated pH 7.0 phosphate buffer and 1 mM glucose was added. After allowing the enzyme to generate hydrogen peroxide via reactions 15 and 16 for a few minutes, a quasi-steady-state concentration profile of hydrogen peroxide developed at the surface of the carbon disk. Figure 11 shows an approach curve of tip current against distance over immobilized glucose oxidase in a solution of glucose. The tip current rises slowly over a distance of several hundred micrometers because of

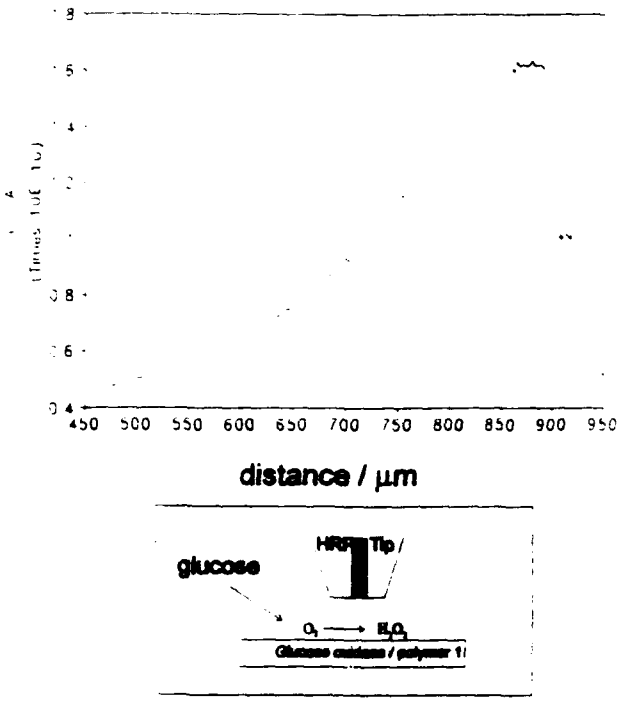

Figure 11. Current–relative distance curve for a type B tip approaching the surface of a glassy carbon disk coated with immobilized glucose oxidase. The solution contained 1 mM glucose and air-saturated 0.2 M pH 7 phosphate buffer. The whole approach curve (limited by the maximum piezo travel of ~475 μm) is shown.

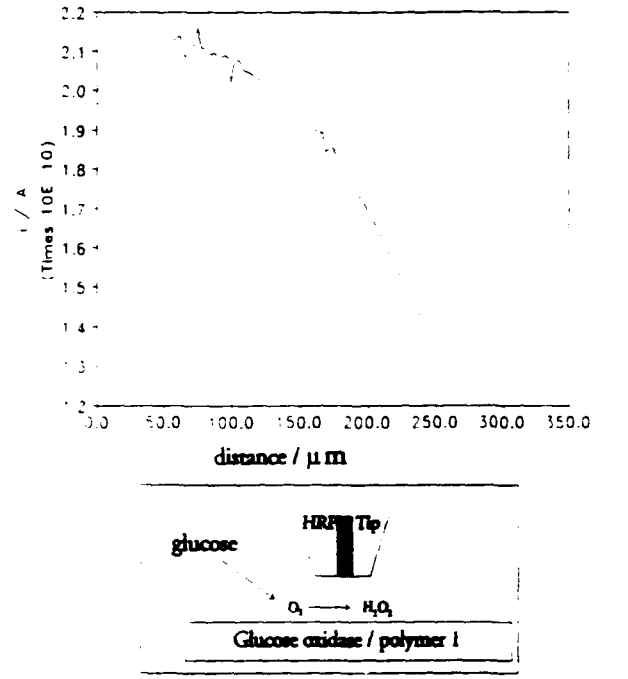

Figure 12. Line scan across the edge of an immobilized glucose oxidase layer. At distances greater than ca. 300 μm, the tip is above a bare carbon surface. The solution contained 1 mM glucose and air-saturated 0.2 M pH 7 phosphate buffer.

the large size of the carbon disk used as substrate. The sharp decrease in tip current is due to the tip blocking diffusion of glucose and oxygen to the immobilized glucose oxidase on the carbon surface under the tip when the tip is close to the surface; the small increase that follows may indicate the tip touched the surface. On scanning the tip over the middle of this surface (not shown), the measured peroxide concentration was constant within ~10%, indicating that, with the proviso

Reprinted from the Journal of the American Chemical Society, 1991, 113.

Electron Transfer between Glucose Oxidase and Electrodes via Redox Mediators Bound with Flexible Chains to the Enzyme Surface

Wolfgang Schuhmann,*,† Timothy J. Ohara,‡ Hans-Ludwig Schmidt,† and Adam Heller*,‡

Contribution from the Department of Chemical Engineering, The University of Texas, Austin, Texas 78712-1062, and Lehrstuhl für Allgemeine Chemie und Biochemie, Technische Universität München, D-8050 Freising-Weihenstephan, FRG. *Received June 6, 1990*

Abstract: Electrical communication between redox centers of glucose oxidase and vitreous carbon electrodes is established through binding to oligosaccharides, at the periphery of the enzyme, ferrocene functions pendant on flexible chains. Communication is effective when the chains are long (>10 bonds), but not when the chains are short (<5 bonds). When attached to long flexible chains, the peripherally bound relays penetrate the enzyme to a sufficient depth to reduce the electron-transfer distances between a redox center of the enzyme and the relay and between the relay and the electrode, thereby increasing the rate of electron transfer.

Introduction

The redox centers of many enzymes are electrically insulated by thick protein or glycoprotein shells, preventing direct electrical communication between the centers and electrodes. The rate of electron transfer[1] between a redox center of an enzyme and an electrode is controlled by (a) the distance between the redox center and the electrode, (b) the potential difference between the redox center and the electrode, and (c) the reorganization energy associated with the electron transfer.[2] For enzymes such as glucose oxidase, with buried redox centers, diffusing redox mediators including O_2/H_2O_2[3] and ferrocene/ferricinium derivatives[4] have been used to shuttle electrons between enzyme redox center and electrodes. Leakage of ferrocene/ferricinium mediators from thin-film enzyme electrodes leads to their deterioration.[5] Leakage can be avoided through the use of soluble diffusing high molecular weight redox mediators, such as ferrocene-derivatized bovine serum albumin[6] and ferrocene bound to high molecular weight poly(ethylene glycol)[7] that can be confined within membranes having sufficiently small pores.

Direct, i.e., not diffusionally mediated, electrical communication between a buried redox center of an enzyme and an electrode can be achieved through insoluble, electrode-attached redox polymers that penetrate the enzyme sufficiently deeply for electron exchange.[8] This route provides the significant advantage of eliminating the need for membrane containing the soluble macromolecular mediator. Yet another way to establish direct electrical communication between a buried redox center of an enzyme and an electrode is through covalently binding to the protein of the enzyme (well below its "periphery") electron relays.[9] For example, in glucose oxidase, a rather rigid glycoprotein with two identical polypeptide chains and a hydrodynamic radius of ~50 Å, the distances involved in electron transfer between the active sites and the electrode are shortened upon binding 12 or more ferrocenecarboxylic acid functions, through amide links, to the enzyme. Replacement of ferrocenecarboxylic acid by ferroceneacetic acid or ferrocenebutanoic acid enhances the kinetics of electron transfer.[9c,d] In the preparation of materials for affinity chromatography, redox-active species of enzymes, such as NAD^+/NADH, are bound to supports with long and flexible spacer chains. Such chains facilitate access of the active species to their specific binding sites.[10]

We report here the modification of glucose oxidase by covalently binding of ferrocene derivatives, via spacer chains of different lengths, to sugar residues on its outer surface. We show that the length of the spacer chain has a crucial influence on the electrooxidation of the enzyme, i.e., on electron transfer from the reduced active site of the enzyme, via the spacer chain attached ferrocenes, to electrodes. This process is rapid only when the spacer chain is sufficiently long to allow the ferrocene to penetrate the enzyme sufficiently to approach the redox center.

Experimental Section

Chemicals. Glucose oxidase type X (EC 1.1.3.4, from *Aspergillus niger*, 128 units mg^{-1}), sodium *m*-periodate, sodium boron hydride, 3-methyl-2-benzothiazolinone hydrazone hydrochloride (MBTH), 1,2-ethylenediamine, 1,3-diaminopropane, 1,6-diaminohexane, 1,8-diaminooctane, 1,10-diaminodecane, and diethylenetriamine were purchased from Sigma; ferrocene carboxaldehyde (98%) was obtained from Aldrich. (Aminoethyl)ferrocene was synthesized according to literature[11] and precipitated as the chloride salt. All other chemicals were of the best available grade and used without further purification. Unless otherwise noted, all experiments were performed at room temperature in a standard aqueous buffer solution containing 100 mM phosphate and 200 mM NaCl at pH 7.2.

Electrodes and Equipment. Electrochemical measurements were performed with an EG&G Princeton Applied Research 175 universal programmer, a Model 173 potentiostat, and a Model 179 digital coulometer. The signal was recorded on a Kipp and Zonen Y-Y-Y′ recorder. Glassy carbon rods (Sigradur, 3-mm diameter) sealed with epoxy resin into glass

† Technische Universität München.
‡ The University of Texas.

(1) Heller, A. *Acc. Chem. Res.* **1990**, *23*, 128.
(2) Marcus, R. M.; Sutin, N. *Biochim. Biophys. Acta* **1985**, *81*, 265.
(3) Clark, L. D., Jr.; Lyons, C. *Ann. N.Y. Acad. Sci.* **1962**, *102*, 29.
(4) (a) Aleksandrovskii, Y. A.; Bezhikina, L. V.; Rodionov, Y. U. *Biokhimiya* **1981**, 708. (b) Kulys, J. J.; Cenas, N. K. *Biochim. Biophys. Acta* **1983**, *744*, 57. (c) Senda, M.; Ikeda, T.; Hiasa, H.; Miki, K. *Anal. Sci.* **1986**, *2*, 501. (d) Cass, A. E. G.; Davis, G.; Green, M. J.; Hill, H. A. O. *J. Electroanal. Chem.* **1985**, *190*, 117. (e) Cass, A. G.; Davis, G.; Francis, G. D.; Hill, H. A.; Aston, W. J.; Higgins, I. J.; Plotkin, E. V.; Scott, L. D. L.; Turner, A. P. F. *Anal. Chem.* **1984**, *56*, 667. (f) Kulys, J. J. *Biosensors*, **1986**, *2*, 3. (g) Albery, W. J.; Bartlett, P. N.; Cass, A. E. G. *Philos. Trans. R. Soc. London B* **1987**, *316*, 107.
(5) Schuhmann, W.; Wohlschlager, H.; Lammert, R.; Schmidt, H.-L.; Loffler, U.; Wiemhofer, H.-D.; Gopel, W. *Sensors Actuators B* **1990**, *1*, 571.
(6) Mizutani, F.; Asai, M. *Denki Kagaku* **1988**, *56*, 1100.
(7) Schuhmann, W., unpublished results.
(8) (a) Degani, Y.; Heller, A. *J. Am. Chem. Soc.* **1989**, *111*, 2357. (b) Gregg, B. A.; Heller, A. *Anal. Chem.* **1990**, *62*, 258. (c) Pishko, M. V.; Katakis, I.; Lindquist, S.-E.; Ye, L.; Gregg, B. A.; Heller, A. *Angew. Chem., Int. Ed. Engl.* **1990**, *39*, 82. (d) Hale, P. D.; Inagaki, T.; Karan, H. I.; Okamoto, Y.; Skotheim, T. A. *J. Am. Chem. Soc.* **1989**, *111*, 3482.
(9) (a) Degani, Y.; Heller, A. *J. Phys. Chem.* **1987**, *91*, 1285. (b) Degani, Y.; Heller, A. *J. Am. Chem. Soc.* **1988**, *110*, 2615. (c) Heller, A.; Degani, Y. In *Redox Chemistry and Interfacial Behavior of Biological Molecules*; Dryhurst, G., Niki, K., Eds.; Plenum Press: New York, 1988; p 151. (d) Bartlett, P. N.; Whitaker, R. G.; Green, M. J.; Frew, J. *J. Chem. Soc., Chem. Commun.* **1987**, 1603.
(10) (a) Mosbach, K.; Guilford, H.; Ohlsson, R.; Scott, M. *Biochem. J.* **1972**, *127*, 627. (b) Schmidt, H.-L.; Grenner, G. *Eur. J. Biochem.* **1976**, *67*, 295. (c) Grenner, G.; Schmidt, H.-L.; Voelkl, W. *Hoppe-Seyler's Z. Physiol. Chem.* **1976**, *357*, 887.
(11) Lednicer, D.; Lindsay, J. K.; Hauser, C. R. *J. Org. Chem.* **1958**, *23*, 653.

0002-7863/91/1513-1394$02.50/0

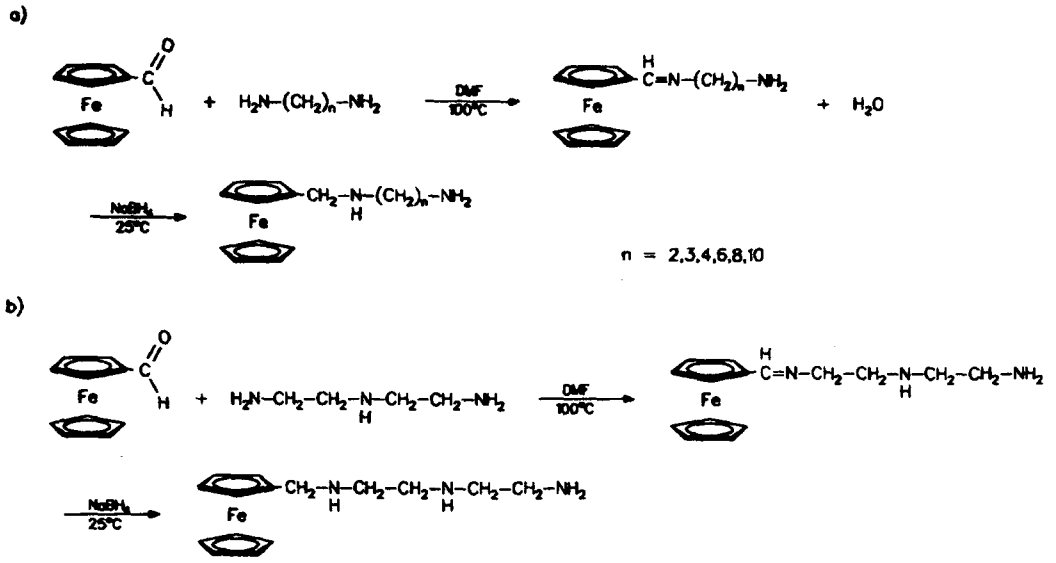

Figure 1. Synthesis of ferrocene amines with spacer chains separating the redox and amine functions.

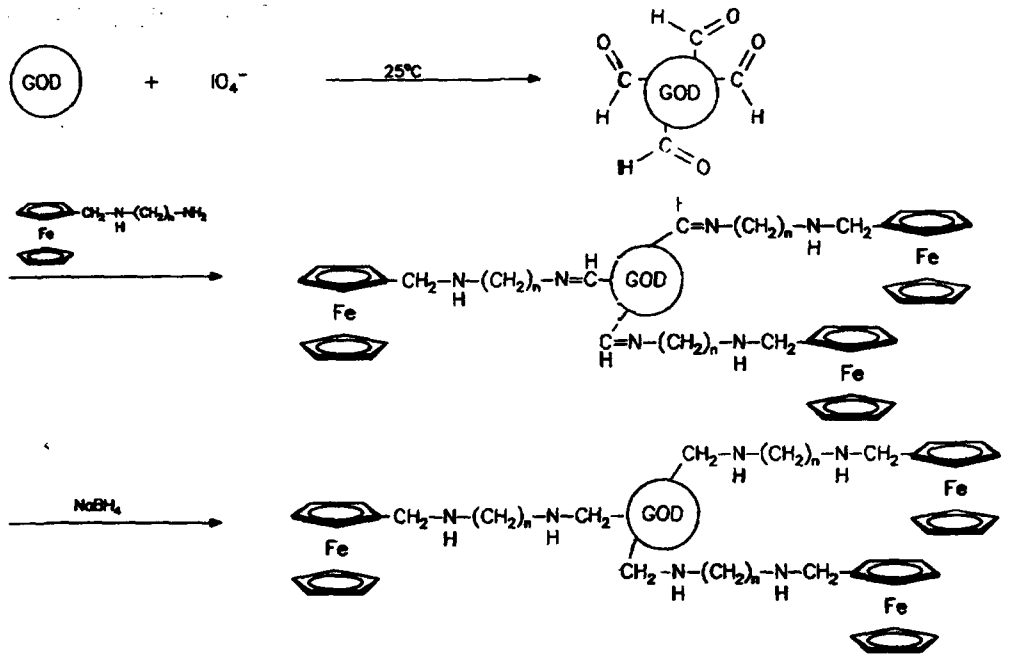

Figure 2. Preparation of glucose oxidase modified by peripherally bound ferrocenes.

were polished prior to use on a polishing cloth sequentially with alumina of decreasing particle size (1, 0.3, 0.5 μm), sonicated, rinsed with distilled water, and then dried in air. A single-compartment electrochemical cell was used with an aqueous KCl/saturated calomel (SCE) reference electrode and a platinum counter electrode. All potentials are referred to this reference electrode (+244 mV vs NHE).

Synthesis of Ferrocene Derivatives. The ferrocene derivatives with different spacer lengths were synthesized as shown in Figure 1. A 4-fold excess of the appropriate diamine was heated in 100 mL of DMF to 100 °C, and 500 mg of ferrocenecarboxaldehyde dissolved in 50 mL of DMF was added dropwise within 1 h to prevent formation of the bridged diferrocene compound. After another hour an excess of sodium borohydride in water was dropped into the solution, and the reaction mixture was stirred for an additional hour at room temperature. The solvent mixture was rotavaporated to dryness and the residue extracted with dichloromethane and separated through a silica column (1.5 cm × 30 cm). A first fraction—the bridged diferrocene—was eluted with dichloromethane, the main fraction with dichloromethane/methanol 10:1. The solvent was evaporated to dryness, the residue dissolved in diethyl ether, and the hydrochloride precipitated by bubbling gaseous hydrochloric acid through the solution. All compounds show the expected ^1H NMR spectra.

Preparation of Ferrocene-Modified Glucose Oxidase. The oxidation of the enzyme-bound sugar residues was performed with sodium *m*-periodate according to established procedures.[12] The ferrocenes were attached to the aldehyde groups formed thus on the outer enzyme surface via Schiff bases, which were reduced with sodium borohydride subsequently (Figure 2). The modified enzyme was isolated from low molecular weight compounds and desalted by gel chromatography (Sephadex G25 equilibrated with water; column 2.5 cm × 20 cm). The volume was reduced by means of ultrafiltration through a membrane (Amicon PM30, MWCO 30000), and the modified enzyme was freeze-dried. To verify that the unreacted ferrocenes were not electrostatically bound to the enzyme, the freeze-dried product was redissolved and extracted with copious amounts of a solution containing 0.1 M phosphate and 0.1 M NaCl at pH 7.1 in an ultrafiltration cell. After refreeze-drying, the electrochemical characteristics of the modified enzyme were unchanged, confirming the absence of noncovalently bound ferrocenes. Determination of the amount of aldehyde groups at the enzyme surface was performed by a procedure of Sawicki et al.[13] The activity of the lyophilized enzymes was determined spectrophotometrically by the *o*-dianisidine/peroxidase assay.[14] The labeling of the enzyme with ferrocenes was

(12) (a) Nakane, P. K.; Kawaoi, A. *J. Histochem. Cytochem.* **1974**, *22*, 1084. (b) Nakamura, S.; Hayashi, S.; Koga, K. *Biochim. Biophys. Acta* **1976**, *445*, 294.

(13) Sawicki, E.; Hauser, T. R.; Stanley, T. W.; Elbert, W. *Anal. Chem.* **1961**, *33*, 93.

Table I. Effect of the Spacer Chain Length on the Catalytic Current of Ferrocene-Modified Glucose Oxidase

no.	compound	bonds	i_{cat},[a] nA	$[Fc]_{rel}$[b]	$i_{cat}/[Fc]_{rel}$	rel enzyme activ $[O_2]$[c]
1	Enz-CH_2-NH-$(CH_2)_2$-NH-CH_2-Fc	7	200	1.50 ± 0.20	400 ± 160	0.27
2	Enz-CH_2-NH-$(CH_2)_3$-NH-CH_2-Fc	8	1010	1.00 ± 0.10	1010 ± 100	0.38
3	Enz-CH_2-NH-$(CH_2)_6$-NH-CH_2-Fc	11	1190	1.00 ± 0.10	1190 ± 120	0.45
4	Enz-CH_2-NH-$(CH_2)_8$-NH-CH_2-Fc	13	2800	1.00 ± 0.10	2800 ± 280	0.41
5	Enz-CH_2-NH-$(CH_2)_{10}$-NH-CH_2-Fc	15	2680	1.00 ± 0.10	2680 ± 270	0.49
6	Enz-CH_2-NH-$(CH_2)_2$-Fc	5	460	0.75 ± 0.25	600 ± 200	0.33
7	Enz-CH_2-NH-$[(CH_2)_2$-NH$]_2$-CH_2-Fc	10	3200	1.00 ± 0.10	3200 ± 320	0.36

[a] Catalytic glucose oxidation current on 3-mm-diameter glassy carbon electrodes at 0.35 V (SCE). [b] Coulometrically determined relative number of ferrocenes per enzyme. [c] Hydrogen peroxide rate of formation, measured relative to the native glucose oxidase rate.

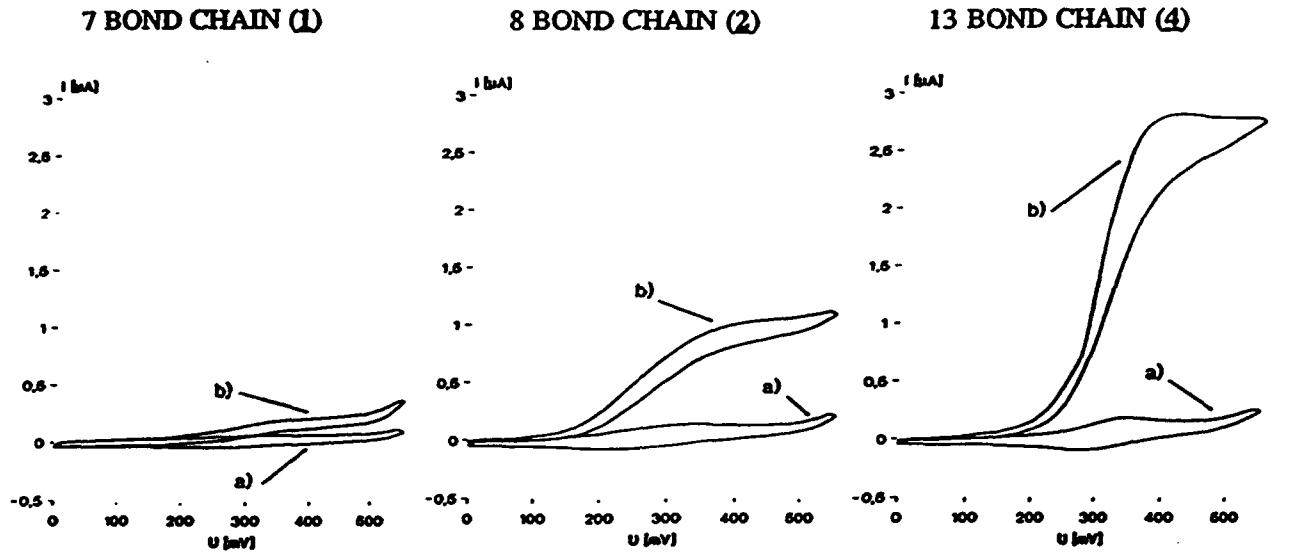

Figure 3. Effect of the chain length connecting peripherally bound ferrocene to glucose oxidase on the electrocatalytic glucose oxidation current. Curves a represent oxidation currents in the absence of glucose; curves b represent currents at 40 mM glucose. All solutions contain 2 mg mL^{-1} of one of the modified enzymes, 0.1 M phosphate buffer (pH 7.2), and 200 units/mL^{-1} catalase; 3-mm-diameter glassy carbon disks; all potentials vs SCE; scan rate 10 mV s^{-1}.

evaluated by atomic absorption spectroscopy and by coulometry.

Results and Discussion

Synthesis of Ferrocene-Labeled Glucose Oxidase. Glucose oxidase (EC 1.1.3.4 from *Aspergillus niger*) is a dimer glycoprotein with a molecular mass of 186 000 daltons. The oligosaccharide chains, which form a hydrophilic periphery, represent ~12% of its weight. Oxidation of these with periodate[12] has been used to provide peripheral aldehyde groups for the immobilization of glycoenzymes to polymeric supports[15] or to electrode surfaces.[16] Analogously, we have now applied this method to bind ferrocene derivatives with different spacer lengths to the surface of glucose oxidase. The periodate oxidation of glucose oxidase was investigated with respect to the number of aldehyde functions obtained and the decrease of enzymatic activity during the reaction. As expected, the aldehyde concentration increased when the reaction times were longer and the enzymatic activity decreased. Optimal results were obtained at a reaction time of 1 h and a periodate concentration of >20 mM, the conditions of our experiments. The number of aldehyde groups, introduced upon oxidation with 20 mM sodium periodate, was determined spectrophotometrically after its reaction with 3-methyl-2-benzothiazolinone hydrazone hydrochloride, following a procedure of Sawicki et al.[13] Assuming that the extinction coefficient reported for the hydrazones of aldehydes formed from mannitol (ϵ = 95 000 L mol^{-1} cm^{-1}) is similar to that of the hydrazones of the oxidized enzyme, we estimate 6.4 aldehyde groups per enzyme molecule.[17] However, because polysaccharides do not react as completely as monosaccharides with this hydrazone, and because the extinction coefficient for the aldehydes derived from mannitol is higher than that of other sugars, this estimate may be low. The functionalized enzyme used for the covalent binding of the different ferrocene compounds showed an activity of 66 units mg^{-1}.

As the rate of electron transfer decays exponentially with the distance of the involved redox centers, a significant influence of the spacer length between enzyme surface and relay on the electron-transfer properties of the modified enzyme in question was expected. To evaluate the effect of chain length on the effectiveness of electron transfer to electrodes, we prepared the series of ferrocene-derivatized enzymes shown in Table I (compounds 1–7). The amino-functionalized ferrocene derivatives have been synthesized through the reaction sequence shown in Figure 1 and purified by column chromatography. Following IO_4^- oxidation of the oligosaccharide residues on the enzyme, the resulting aldehyde groups were reacted with ferrocene amines, to form Schiff bases. These were reduced with $NaBH_4$ to the secondary amines (Figure 2). Binding of amino spacer modified ferrocene derivatives to the surface of the functionalized glucose oxidase did not lead to a further decrease of enzymatic activity (see Table I).

Electrochemical Investigations of Ferrocene-Modified Glucose Oxidase. The results of the electrochemical measurements are summarized in Figure 3 and Table I. The cyclic voltammograms shown in Figure 3 were run at 2 mg mL^{-1} concentration of the

(14) Glucose procedure 541, Sigma Chemical Co., St. Louis, MO.
(15) Royer, G. P. In *Methods in Enzymology, Immobilized Enzymes and Cells*; Colowick, S. P., Kaplan, N. O., Mosbach, K., Eds.; Academic Press: San Diego, CA, 1987; Vol. 135, p 141.
(16) Schuhmann, W.; Kittsteiner, R. *Biosensors Bioelectronics*, in press. Presented at the First World Congress on Biosensors, Singapore, 1990.
(17) Sawicki, E.; Schumacher, R.; Engel, C. R. *Microchem. J.* **1967**, *12*, 377.

Table II. Catalytic Current of Partially Deactivated Ferrocene-Modified Enzymes

no.	compound	bonds	i_{cat},[a] nA	i'_{cat} (deactiv),[b] nA	i''_{cat} (deactiv + native enz),[c] nA
1	Enz-CH_2-NH-$(CH_2)_2$-NH-CH_2-Fc	7	200	120	170
4	Enz-CH_2-NH-$(CH_2)_8$-NH-CH_2-Fc	13	2800	350	470

[a] Catalytic current for modified enzyme from Table I. [b] Catalytic current for modified, then partially deactivated enzyme. [c] Catalytic current of (b) after addition of an equal amount (1 mg mL^{-1}) of native glucose oxidase.

ferrocene-modified enzymes **1**–**7** in 0.1 M phosphate buffer (pH 7.2). The three-electrode cells were equipped with a glassy carbon (3-mm diameter) working electrode, a platinum wire counter electrode, and a KCl-saturated calomel reference electrode. Catalase was added to the solutions (200 units mL^{-1}) to decompose any hydrogen peroxide that might be formed in the presence of residual oxygen. Curve 1 of Figure 3 shows the cyclic voltammograms of a solution of compound **1** in buffer (a) without glucose and (b) with 40 mM glucose. Curves 2 and 3 show the cyclic voltammograms observed under identical conditions for compounds **2** and **4**, respectively. The limiting currents, normalized for the amount of attached ferrocene, increase with chain length (Table I). Notable enhancement of the catalytic current is observed in compound **7**, where i = 6.5 μA, i.e., the current density reaches 90 $\mu A\ cm^{-2}$.

Electron-Transfer Model. A peripherally attached redox mediator may accept electrons through either an intramolecular or an intermolecular process (Figure 4), acting in the latter as a conventional diffusing mediator. For example, mediation by ferrocene-modified albumin has been reported.[6] The dominance of the intramolecular electron-transfer process in the case of enzymes with long chains was established through the following experiment. Enzymes **1** and **4** were partially deactivated by 6 M urea (4 h, 25°) and then separated from the urea by gel-permeation chromatography. Their catalytic currents i' (Table II) were measured at an enzyme concentration of 1 mg mL^{-1} under conditions identical with those for i_{cat} in Table I. Then 1 mg mL^{-1} native glucose oxidase was added, and the catalytic current (i''_{cat}, Table II) was determined. If the process were entirely intermolecular, i''_{cat} would have been equal to or greater than i_{cat}, because the concentration of the electron-transfer mediator is unchanged and both the concentration and relative catalytic activity of the enzyme are increased (note in Table I that **1** and **4** retain, respectively, 0.27 and 0.45 of the native enzyme's activity). If the process were entirely intramolecular, addition of native enzyme would not have changed the catalytic current seen with the deactivated enzyme (i'_{cat}, Table II). Measurement of the catalytic current in the presence of deactivated **1** and **4** with native enzyme added shows that in the case of **1**, where the chain is short, the current approaches i_{cat} for the enzyme prior to deactivation, i.e., that the process of electron transfer either has a substantial intermolecular component or is entirely intermolecular. For compound **4**, made with long chains, i''_{cat}, the current observed with the partially deactivated enzyme plus native enzyme (470 nA), remains much below the 2800-nA catalytic current of the enzyme prior to its partial deactivation and is only marginally higher than the 350-nA current of the partially deactivated enzyme (Table II). This indicates that when the spacer chain is long the process is dominantly intramolecular. We thus conclude that the increase in catalytic currents with increase in chain length (Table I and Figure 3) originates in enhanced intramolecular electron transfer from the enzyme's redox centers to the chain-attached relay and, via the relay, to the electrode. Our observations do not allow us to define the extent of electron transfer by a dynamic process, where the chain-pendant mediator swings "in" and "out" of the enzyme, and a static process, where the relay is reasonably stationary, i.e., is bound by hydrophobic or electrostatic interaction to a specific region in the protein.

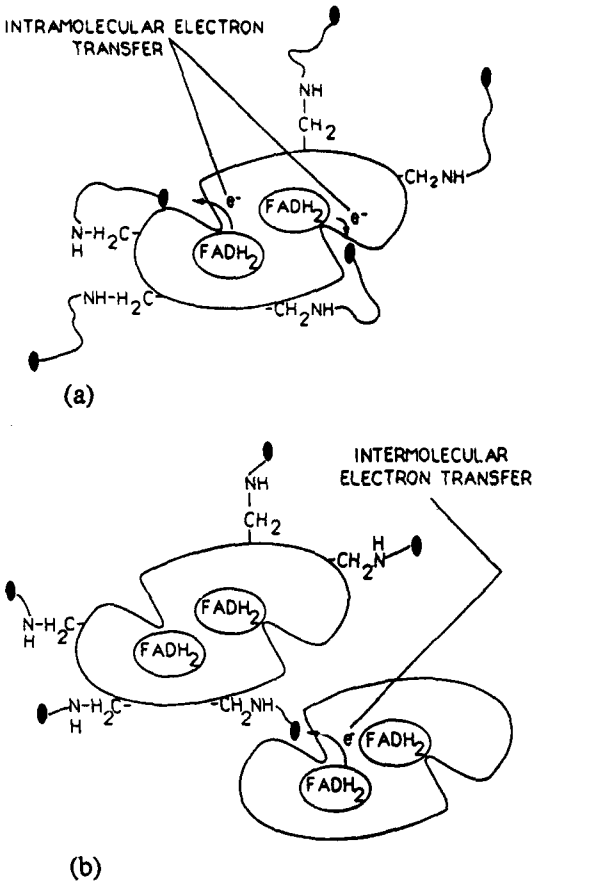

Figure 4. (a) Intramolecular and (b) intermolecular electron transfer via chain-attached mediators.

Acknowledgment. We thank Dr. B. A. Gregg for the preparation of (aminoethyl)ferrocene and many helpful discussions. The work at the University of Texas at Austin is supported by the Office of Naval Research, the Welch Foundation, and the Texas Advanced Research Program. The work at the Technical University of Munich is supported by the Bundesministerium für Forschung und Technologie (BMFT), Projektträger Biotechnologie, FRG. This collaborative study was performed at the University of Texas.

Registry No. **1**, 130859-06-2; **2**, 130859-07-3; **3**, 130859-08-4; **4**, 130859-09-5; **5**, 130859-10-8; **6**, 130859-11-9; **7**, 130859-12-0; FCCH=N$(CH_2)_n$$NH_2$ (n = 2), 130859-13-1; FcCH=N$(CH_2)_n$$NH_2$ (n = 3), 130859-14-2; FcCH=N$(CH_2)_n$$NH_2$ (n = 4), 130859-15-3; FcCH=N$(CH_2)_n$$NH_2$ (n = 6), 130859-16-4; FcCH=N$(CH_2)_n$$NH_2$ (n = 8), 130859-17-5; FcCH=N$(CH_2)_n$$NH_2$ (n = 10), 130859-18-6; FcCH=N$CH_2CH_2NHCH_2CH_2NH_2$, 130859-19-7; 1,2-ethylenediamine, 107-15-3; 1,3-diaminopropane, 109-76-2; 1,6-diaminohexane, 124-09-4; 1,8-diaminooctane, 373-44-4; 1,10-diaminodecane, 646-25 3; diethylenetriamine, 111-40-0; ferrocenecarboxaldehyde, 12093-10-6; glucose oxidase, 9001-37-0.

Reprinted from Accounts of Chemical Research, 1990, 23.

Electrical Wiring of Redox Enzymes

ADAM HELLER

Department of Chemical Engineering, The University of Texas at Austin, Austin, Texas 78712

Received September 29, 1989 (Revised Manuscript Received February 5, 1990)

Relaying of Electrons in Enzymes

This Account describes the chemical modification of regions of large biomolecules, transforming them from electrical insulators to electrical conductors. Redox enzymes are molecules of 40 000 Da (daltons) (e.g., galactose oxidase) to 850 000 Da (e.g., choline dehydrogenase) with one or more redox centers. Their average hydrodynamic diameters range from ~55 to ~150 Å. In the great majority of enzymes, the redox centers are located sufficiently far from the outermost surface (defined by protruding protein or glycoprotein domains) to be electrically inaccessible. Consequently, most enzymes do not exchange electrons with electrodes on which they are adsorbed, i.e., their redox centers are neither electrooxidized at positive potentials nor electroreduced at negative ones. Apparently, part of the protein or glycoprotein shell surrounding the redox centers is there to prevent indiscriminate electron exchange between the different redox macromolecules of living systems. Such exchange would, in the extreme case, lead to an equipotential system, which could not sustain life. Another function of this shell is to stabilize the structure of the enzyme. Because neither function is essential for catalysis, redox enzymes do function when part of the shell is stripped[1,2] or, as we shall see here, when the shell is chemically altered so as to make it electrically conductive.[3-5] Following such alteration, a redox center of an enzyme will directly transfer electrons to an electrode on which the enzyme is adsorbed.[3,4] We call the centers that increase the electron current flowing through their shells by accepting and transferring electrons "electron relays".

The distance dependence of the rate of electron transfer in proteins has been the subject of experimental[7-14] and theoretical[15-21] studies during the past

Adam Heller graduated from the Hebrew University in Jerusalem, where he received his Ph.D. degree in 1961. He joined the University of Texas at Austin in 1988, where he holds the Ernest Cockrell, Sr., Chair in Engineering. Earlier he headed the Electronic Materials Research Department of AT&T Bell Laboratories in Murray Hill, NJ. His accomplishments include construction of the first inorganic liquid laser, codevelopment of the lithium-thionyl chloride battery, demonstration of the first electrical power and hydrogen generating electrochemical solar cell of >10% efficiency, and the direct electrical communication between chemically modified redox enzymes and electrodes. He was elected to the National Academy of Engineering in 1987 and received the Vittorio De Nora Gold Medal of the Electrochemical Society for distinguished contributions to electrochemical technology in 1988.

(1) Nakamura, S.; Hayashi, S.; Koga, K. *Biochem. Biophys. Acta* **1986**, *445*, 294.
(2) Yasuda, Y.; Takahashi, N.; Murachi, T. *Biochemistry* **1971**, *10*, 2624.
(3) Degani, Y.; Heller, A. *J. Phys. Chem.* **1987**, *91*, 1285.
(4) Degani, Y.; Heller, A. *J. Am. Chem. Soc.* **1988**, *110*, 2615.
(5) Heller, A.; Degani, Y. Direct Electrical Communications between Chemically Modified Redox Enzymes and Metal Electrodes: III. Electron Transfer Relay Modified Glucose Oxidase and D-Amino-Acid Oxidase. In *Redox Chemistry and Interfacial Behavior of Biological Molecules*; Dryhurst, G., Niki, K., Eds.; Plenum Publ. Corp.: New York, 1988; p 151–170.
(6) Degani, Y.; Heller, A. *J. Am. Chem. Soc.* **1989**, *111*, 2357.
(7) Lieber, C. M.; Karas, J. L.; Mayo, S. L.; Albin, M.; Gray, H. B. Long Range Electron Transfer in Proteins. XXI. Design of Enzymes and Enzyme Models. *Proceedings of the Robert A. Welch Foundation Conferences on Chemical Research*; The Welch Foundation: Houston, 1987; pp 9–24.
(8) Cowan, J. A.; Gray, H. B. *Chem. Scr.* **1988**, *28A*, 21
(9) Sykes, A. G. *Chem. Soc. Rev.* **1985**, *14*, 283.
(10) Isied, S. S. *Prog. Inorg. Chem.* **1984**, *32*, 443.
(11) Peterson-Kennedy, S. E.; McGourty, J. L.; Ho, P. S.; Sutoris, C. J.; Liang, N.; Zemel, H.; Blough, N. V.; Margoliash, E.; Hoffman, B. M. *Coord. Chem. Rev.* **1985**, *64*, 125.
(12) McLendon, G.; Guarr, T.; McGuire, M.; Simolo, K.; Strauch, S.; Taylor, K. *Coord. Chem. Rev.* **1985**, *64*, 113.

0001-4842/90/0123-0128$02.50/0

decade. Because the process of electron transfer is, in essence, an electron tunneling process,[17] theories predict and experiments show that the rate of electron transfer decays exponentially with distance, when the distance substantially exceeds atomic dimensions (>3 Å). Thus,

$$k_{ET} = 10^{13} e^{-\beta(d-3)} e^{-(\Delta G^\circ + \lambda)^2/4RT\lambda} \quad (1)$$

where k_{ET} is the rate of electron transfer, β is a constant for a given electron donor/acceptor pair in a defined medium, d is the distance between the donor and the acceptor, $-\Delta G^\circ$ is the driving energy, and λ is the Marcus reorganization energy. Most redox enzymes have sufficiently thick protein or glycoprotein shells to make the product $\beta(d - 3)$ large enough to decrease the rate of electron transfer to a negligibly small value for a random encounter between an enzyme and another redox protein or between an enzyme and an electrode.

Function and Design of Electron Relays

Among the several electron-transfer theories, Marcus theory translates the electron-transfer rate into simple chemical terms.[7,16] Electron transfer will take place when both the donor and the acceptor assume structural configurations that require no further reorganization upon electron transfer. The energy invested in order to bring the pair to this structure is the Marcus reorganization energy, denoted by λ. At a given reorganization energy, temperature, and distance and in a given medium, the rate of electron transfer increases when the process is exoergic ($\Delta G < 0$), i.e., the electron hops thermodynamically downhill from a reducing center to an oxidizing center. The difference in the energy of the system is nil for electron transfer between compositionally identical ions in different oxidation states. By measuring the rate of electron transfer within a redox couple, one obtains its "self-exchange rate". A high self-exchange rate is indicative of a small reorganization energy. Couples with small reorganization energies are fast, i.e., exchange electrons rapidly with electrodes. Thus, the best electron relays in biological macromolecules are also fast redox couples. Furthermore, the faster the couple, the greater the allowed distance at which a given current will flow between an electron-donating center of an enzyme and an electron relay based on this couple, and also between the relay and an electrode. This current will increase when the potential difference between the donor and the relay, or between the relay and the electrode, is increased. Usually only one of these two electron hops will be rate controlling.

Of the experimental studies on electron-transfer rates in proteins, those of Gray and colleagues[7,8] are particularly relevant, because they provide quantitative information about the distance dependence at varying reorganization energies and potential differences. For electron transfer between porphyrin-bound Fe^{2+} centers and histidine-bound $[Ru(NH_3)_5]^{3+}$, they find $\beta = 0.91$ Å^{-1}, or a 10-fold decrease in the rate of electron transfer upon each 2.1-Å increase in distance. Thus for a protein and donor–acceptor pair similar to that studied by Gray et al., insertion of a layer of fast relays at half-thickness across a 30-Å-thick protein film on an electrode may increase the current, between a sheet of donors on the solution side of the film and the electrode, by a factor as large as 10^7.

The relationship between d, β, λ, and the potential difference ΔV ($\Delta G = -e\Delta V$) is illuminating. Let us consider a monolayer of a redox enzyme covering an electrode and calculate, from eq 1, some d, λ, and ΔV values required for realizing the full enzyme-turnover-limited current density. Glucose oxidase turns over at ambient temperature at a rate of $\sim 10^2$ s^{-1}, i.e., it produces about 200 transferable electrons/s. Because its radius is ~43 Å, there can be up to 1.7×10^{12} enzyme molecules on the electrode surface. The current density, when all redox centers are electrically well connected to the electrode, may thus reach about 3.4×10^{14} electrons s^{-1} cm^{-2}, or 53 μA cm^{-2}. At a 25-Å distance between the electron-transferring centers and the electrode, it is possible to reach an electron-transfer rate of 200 s^{-1} when $\lambda \leq 1.0$ eV and $\Delta V \leq -0.3$ V, or when $\lambda \leq 0.4$ eV and $\Delta V \leq 0$ V. For $d = 20$ Å, electron transfer will be effective even at $\Delta V = 0.0$ V and $\lambda \leq 0.9$ eV.[7] Thus with a fast relay, having a redox potential substantially oxidizing with respect to the redox potential of glucose oxidase, electron transfer with a typical reorganization energy of 0.5–1 eV may take place across a distance as long as 25 Å. With a fast, moderately oxidizing relay, an electron-transfer distance of 20 Å is realizable.

We can see why small redox proteins, of 2×10^4 daltons or less, with effective hydrodynamic radii of less than ~21 Å can be directly electrooxidized or reduced when adsorbed on electrodes and why glucose oxidase, with 160 000 Da, and a hydrodynamic radius of 43 Å,[1] cannot. Nevertheless, even in small proteins, with redox centers that communicate directly with electrodes, protein orientation is important. By selection of electrode surfaces, or by modification of these with orienting promoters, such as positively charged organic or inorganic molecules or ions, the rate of electron transfer can be enhanced.[22-30] We also see from the relationships why a few large enzymes, after integration of small redox proteins (e.g., cytochrome *c*) into the

(13) Takaka, T.; Takenaka, K.; Kawamura, H.; Beppu, Y. *J. Biochem. (Tokyo)* **1986**, *99*, 833.
(14) Miller, J. R. In *Antennas and Reaction Centers of Photosynthetic Bacteria*: Michel-Beyerle, M. E., Ed.; Springer-Verlag: Berlin, 1985; p 234.
(15) Bixon, M.; Jortner, J. *J. Phys. Chem.* **1986**, *90*, 3795.
(16) Marcus, R. A.; Sutin, N. *Biochim. Biophys. Acta* **1985**, *811*, 265.
(17) DeVault, D. *Quantum Mechanical Tunneling in Biological Systems*, 2nd. ed.; Cambridge Univ. Press: Cambridge, 1984.
(18) Churg, A. K.; Weiss, R. M., Warshel, A.; Takano, T. *J. Phys. Chem.* **1983**, *87*, 1683.
(19) Larson, S. *J. Chem. Soc., Faraday Trans. 2* **1983**, *79*, 1375.
(20) Hopfield, J. J. *Proc. Natl. Acad. Sci. U.S.A.* **1974**, *71*, 3640.
(21) Onuchic, J. N.; Beratan, D. N.; Hopfield, J. J. *J. Phys. Chem.* **1986**, *90*, 3707.
(22) Yeh, P.; Kuwana, T. *Chem. Lett.* **1977**, 1145.
(23) Armstrong, F. A.; Hill, H. A. O.; Walton, N. *Acc. Chem. Res.* **1988**, *21*, 407.
(24) Bowden, E. F.; Hawkridge, F. M.; Blount, N. H. Electrochemical Aspects of Bioenergetics. In *Comprehensive Treatise of Electrochemistry*; Srivanasan, S., et al., Eds.; Plenum: New York, 1985; pp 297.
(25) Lewis, N. S.; Wrighton, M. S. *Science* **1981**, *211*, 944.
(26) Armstrong, F. A.; Lannon, A. M. *J. Am. Chem. Soc.* **1987**, *109*, 7211.
(27) Bancroft, F. E.; Blount, H. N.; Hawkridge, F. M. *Adv. Chem. Ser.* **1982**, *No. 201*, 23.
(28) Bowden, E. F.; Hawkridge, F. M.; Blount, H. N. *Adv. Chem. Ser.* **1982**, *No. 201*, 159.
(29) Castner, J. F.; Hawkridge, F. M. *J. Electroanal. Chem.* **1983**, *143*, 217.
(30) Taniguchi, I. Interfacial Electrochemistry of Promoter Modified Electrodes for Rapid Electron Transfer of Cytochrome *C*. In *Redox Chemistry and Interfacial Behavior of Biological Molecules*; Dryhurst, G., Niki, K., Eds.; Plenum Publ. Corp.: New York, 1988; pp 113–124.

external part of their structure, are directly electrooxidized or reduced on electrodes[31-33] and why most large enzymes, with deep redox centers, are not directly electrooxidized or reduced on electrodes.

Glucose oxidase (GO) (EC 1.1.3.4) is an example of an enzyme of the latter type. This enzyme catalyzes the transfer of electrons from glucose to oxygen, producing gluconolactone and hydrogen peroxide (eq 2 and 3). The process involves the $FAD/FADH_2$ redox cen-

$$\text{glucose} + \text{GO}-\text{FAD} \longrightarrow \text{gluconolactone} + \text{GO}-\text{FADH}_2 \quad (2)$$
$$\text{GO}-\text{FADH}_2 + \text{O}_2 \longrightarrow \text{GO}-\text{FAD} + \text{H}_2\text{O}_2 \quad (3)$$

ters of the enzyme. Glucose cannot be selectively electrooxidized at an electrode on which the enzyme has been adsorbed, because the product $\beta(d - 3)$ is excessive for electron transfer to the electrode. Even at the most anodic potentials that are accessible in aqueous solutions, electrode reaction 4 cannot be driven. Reaction

$$\text{GO–FADH}_2 \rightarrow \text{GO–FAD} + 2\text{H}^+ + 2e^- \quad (4)$$

3 takes place only because oxygen diffuses into the protein, reducing d sufficiently to allow electron transfer. In addition to oxygen, other oxidized members of redox couples can diffuse into enzymes to accept electrons from their redox (e.g., $FADH_2$) centers. One of the first studied may have been methylene blue.[34-36]

The physical parameters that define for enzyme electrodes the effectiveness of bound electron relays consisting of diffusing electron carriers are identical: diffusing species are effective when they need not penetrate the enzyme deeply for electron transfer; and relays are effective when they can accept and transfer electrons across substantial distances. In both cases, we seek high self-exchange rates, though it is also possible to increase the electron-transfer rates by increasing ΔV. The list of effective diffusional electron acceptors and donors includes ferrocene/ferricinium derivatives;[37,38] ruthenium$^{2+/3+}$ ammines;[39] hydroquinones/quinones;[40] reducible and oxidizable components of organic salts;[41,42] and tungsten$^{6+/5+}$ and molybdenum$^{6+/5+}$ octacyanides.[43]

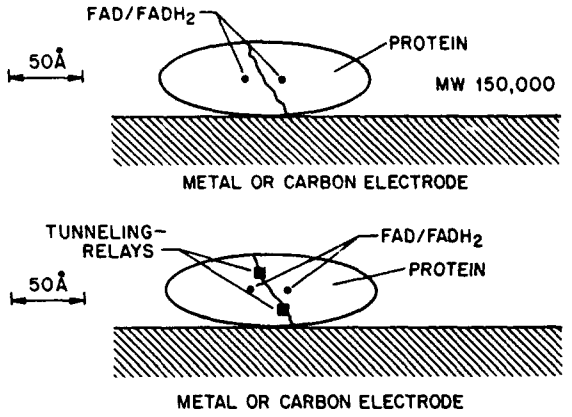

Figure 1. Top: When a native redox enzyme (e.g., glucose oxidase) is adsorbed on an electrode, the electron-transfer distances are excessive for electrical communication between the redox centers and the electrode. Bottom: Flow of electrons through a relay from a redox center of an enzyme (glucose oxidase) to an electrode. A current is observed when the substrate (glucose) transfers a pair of electrons to an FAD center of the enzyme that, in turn, transfers these either to a relay or to a molecular wire, which then transfers the electrons to the electrode.

Bonding of Electron Relays to Enzyme Proteins

Our first study, aimed at establishing that the electrical properties of enzyme proteins can be modified, involved ferrocene/ferricinium carboxylate electron relays (Figure 1).[37,38] Amide links were formed between the carboxylate and part of the 42 lysine amine functions of glucose oxidase through carbodiimide coupling (eq 5).[3,44] The reaction proceeds in an aqueous solution

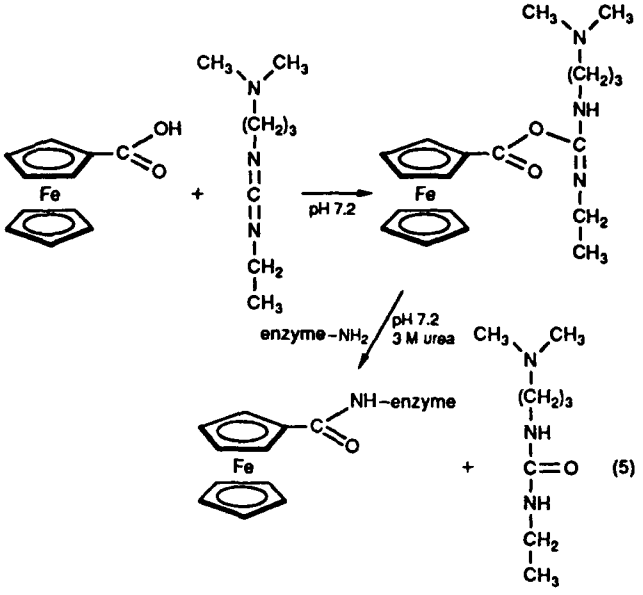

at physiological temperature and pH. In the first experiments, we were unable to reproduce reliably the (occasionally observed) direct electrical communication between the $FAD/FADH_2$ centers of glucose oxidase and metal or graphite electrodes, via the enzyme-bound relays. But after the enzyme protein was reversibly (partially) unfolded by 2–3 M urea, we obtained reproducible results. An average of 12 ferrocene functions could be covalently incorporated in glucose oxidase.[3-5]

(31) Assefa, H.; Bowden, E. F. *Biochem. Biophys. Res. Commun.* **1986**, *139*, 1003.
(32) Cass, A. E. G.; Davis, G.; Hill, H. A. O.; Noncarrow, D. J. *Biochim. Biophys. Acta* **1985**, *828*, 51.
(33) Barker, P. D.; Hill, H. A. O. *Prog. Clin. Biol. Res.* **1988**, *274*, 419–433.
(34) Thunberg, T. *Skand. Arch. Physiol.* **1925**, *46*, 339.
(35) Theorell, H. *Biochem. Z.* **1935**, *78*, 263.
(36) Theorell, H. In *The Enzymes*; Sumner, J. B., Myrback, K., Eds.: Academic: New York, 1951.
(37) Yeh, P.; Kuwana, T. *J. Electrochem. Soc.* **1976**, *123*, 1334.
(38) Cass, A. E. G.; Davis, G.; Green, M. J.; Hill, H. A. O. *J. Electroanal. Chem. Interfacial Electrochem.* **1985**, *190*, 117.
(39) Crumbliss, A. L.; Hill, H. A. O.; Page, D. J. *J. Electroanal. Chem. Interfacial Electrochem.* **1986**, *206*, 327.
(40) Ikeda, T.; Hiasa, H.; Senda, M. Catalytic Oxidation of D-Glucose at an Enzyme-Modified Electrode with Entrapped Mediator. In *Redox Chemistry and Interfacial Behavior of Biological Molecules*, Dryhurst, G., Niki, K., eds.; Plenum Publ. Corp.: New York, 1988; pp 193–201.
(41) Kulys, J. J.; Samalius, A. S.; Svirmickas, G. J. S. *FEBS Lett.* **1980**, *114*, 7.
(42) Albery, W. J.; Bartlett, P. N.; Craston, D. H. *J. Electroanal. Chem. Interfacial Electrochem.* **1985**, *194*, 223.
(43) Taniguchi, I.; Miyamoto, S.; Tomimura, S.; Hawkridge, F. M. *J. Electroanal. Chem. Interfacial Electrochem.* **1988**, *240*, 333.
(44) Hoare, D.; Koshland, D. E. *J. Biol. Chem.* **1967**, *242*, 2247.

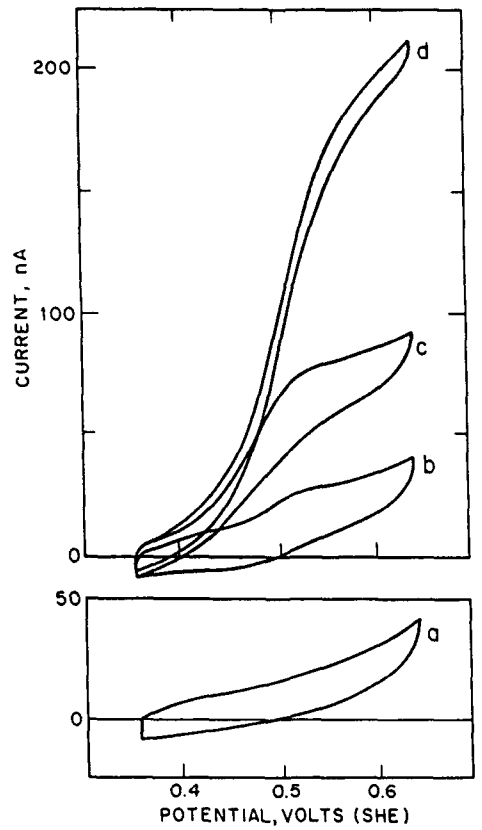

Figure 2. Cyclic voltammograms (current vs potential plots) for electrodes made with (a) native glucose oxidase with or without glucose; (b) glucose oxidase modified by covalent bonding of 12 electron relays per enzyme molecule in the absence of glucose; (c) as in b, but at 0.8 mM glucose; and (d) as in b, but at 5 mM glucose. Scan rate 2 mV/s.

After removal of the urea by gel permeation chromatography, the relay-modified enzyme retained 60% of its activity and communicated electrically with graphite, glassy carbon, gold, and other metals. Communication resulted in a glucose-concentration-dependent current at or above the oxidation potential of the relay (Figures 1 and 2). The current was produced by a sequence of electron-transfer steps: glucose reduced the enzyme's FAD centers to $FADH_2$; the $FADH_2$ centers were reoxidized to FAD upon transferring electrons to the ferricinium relays, reducing these to ferrocene; ferrocene transferred electrons to the electrode and was reoxidized to ferricinium. The greater the number of relays we bound to the enzyme, the better its $FADH_2$ centers communicated with electrodes.[5] This was also the case in D-amino acid oxidase.[4,5] The current in relay-modified glucose oxidase electrodes increased when glucose was added to the solution (Figure 2) but did not change when sucrose, other hexoses, or pentoses were added.[5]

Another effective glucose oxidase bound relay that we and Bartlett and Whitaker[5,45] studied was ferrocene acetic acid, covalently bound to glucose oxidase lysines. In a reaction sequence similar to that shown in eq 5, 21 relays were bound to the enzyme, further enhancing electrical communication.[45] Glucose oxidase was also modified with ruthenium pentaammine relays, bound coordinatively to histidine functions of the enzyme, or to pyridine functions that were covalently bound either to tyrosines by azo links or to lysines through amide links. These relays were less stable than the ferrocenes.[4,5]

(45) Bartlett, P. N.; Whitaker, R. G. *J. Chem. Soc., Chem. Commun.* **1987**, 1603.

Electrical Wiring of Redox Enzymes

When electron relays are bound to an enzyme, the bulk of the enzyme does not become conductive. Rather, electrons are preferentially conducted along routes defined by the relays. As seen earlier, for relays of low reorganization energy and adequate potential difference (between the $FAD/FADH_2$ center and the relay and between the relay and the electrode), electron-transfer distances can be 20–25 Å, and a single relay can be adequate to allow sequential electron hops between the enzyme's redox center and the electrode. Nevertheless, because there are few effective electron-transfer paths even if 12 relays are bound to the enzyme, only when the enzyme tumbles on the surface of the electrode is its charge effectively collected: the enzyme must point a specific zone of its surface to the electrode. When a relay-modified enzyme is covalently bound to an electrode surface in a random fashion, only a small fraction of the enzymes are properly oriented, and the currents are small. Furthermore, in the presence of oxygen, most of the electrons are transferred to it, to produce peroxide, rather than to the electrode.

Our first enzyme electrodes required membranes to contain the freely tumbling enzyme in small volumes near the electrode surface. The membranes needed pores small enough to contain the diffusing enzyme, but large enough to allow in-diffusion of substrate and out-diffusion of product. The membranes required peripheral seals, which increased the manufacturing complexity and cost. Furthermore, in flow systems the membranes limited the rate of substrate transport to, and product transport from, the electrode surface, increasing the time constants. The need for membranes and seals was obviated by wiring the enzyme with an electron-relaying redox polymer, a segment of which was bound to the electrode.[6] Through such wiring the enzyme was electrically connected to the electrode, irrespective of its orientation. The resulting enzyme electrodes were then fast and simple to make.

Our method of wiring enzymes followed one of nature's ways of reducing electron-transfer distances between redox centers of proteins and enzymes. For electron transfer between the redox centers of cytochrome *c* and enzymes such as cytochrome *c* peroxidase or cytochrome *c* oxidase, or between the ferredoxin and ferredoxin NADP reductase, the center-to-center distances are reduced through complexing the redox protein and the redox enzyme. The complexes are often electrostatic,[46-62] forming between enzymes with negatively charged zones and redox proteins with positively charged zones.[46-48]

(46) Koppenol, W. H.; Margoliash, E. *J. Biol. Chem.* **1982**, *257*, 4426.
(47) Salemme, F. R. *Annu. Rev. Biochem.* **1978**, *46*, 299.
(48) Hazzard, J. T.; Moench, S. J.; Erman, J. E.; Satterlee, J. D.; Tollin, G. *Biochemistry* **1988**, *27*, 2002.
(49) Margoliash, E.; Bosshard, H. R. *Trends Biochem. Sci.* **1983**, *8*, 1.
(50) Mochan, E. *Biochem. Biophys. Acta* **1970**, *216*, 80.
(51) Mochan, B. S.; Elliot, W. B.; Nicholls, P. J. *Bioenergetics* **1973**, *4*, 329.
(52) Nicholls, P. *Biochim. Biophys. Acta* **1974**, *346*, 261.
(53) Miller, W. G.; Cusanovich, M. A. *Biophys. Struct. Mech.* **1975**, *1*, 97.
(54) Ng, S.; Smith, M. B.; Smith, H. T.; Millet, F. *Biochemistry* **1977**, *16*, 4975.

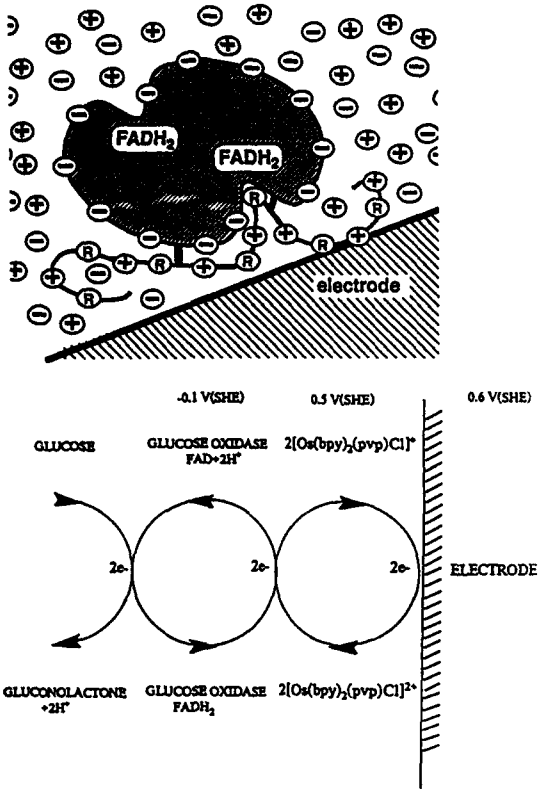

Figure 3. (a) Wiring of a binary redox enzyme. Fast redox centers (R) of a polycation that is electrostatically and covalently bound to the enzyme relay electrons to the electrode, on which a segment of the polycation is adsorbed. Binding of the polycation to the electrode can be electrostatic when the electrode has a negative surface charge. (b) Electron-transfer steps in the electrooxidation of glucose on a wired glucose oxidase electrode.

We also "wired" the enzymes through complexing, but with synthetic, rather than natural, redox macromolecules. The proteins of glucose oxidase, as well as those of other enzymes, have at physiological pH a negative surface charge, because of excess glutamate and aspartate over lysine and arginine. The polyanionic enzymes can be electrostatically complexed with polycationic redox polymers of $\sim 10^5$ Da, typically with 100–200 redox centers and several hundred cationic sites. When segments of the redox polymers fold along the enzyme proteins and penetrate these,[6] electron transfer from the $FADH_2$ center of the enzyme to at least one redox center of the polymer, and via this center to the electrode, becomes possible (Figure 3a). The practicality of such electron transfer was confirmed in our very first (unpublished) experiment, where we complexed glucose oxidase with the copolymer of vinyl-*N*-methylpyridinium chloride and vinylferrocene, a water-soluble redox polycation. We have preferred, however, osmium-based redox polycations over the ferrocenes,[6] because they were shown by Meyer and co-workers to be fast and rugged and to have potentials in the 0.2–0.5-V (SCE) range.[63] Upon complexing commercial 50 000-Da poly(vinylpyridine) with $[Os(2,2'\text{-bipyridine})_2Cl]^{1+/2+}$ and N-methylating part of the uncomplexed pyridine residues, we obtained an effective electron-relaying, stable polycation. After electrostatic complexing with glucose oxidase, the polycation mediated electron transfer from the substrate-reduced ($FADH_2$) centers of the enzyme to electrodes, cycling as shown in Figure 3b. Segments of the polycation were found to adsorb strongly on graphite electrodes,[64] as expected from the earlier work of Oyama and Anson.[65] Because the redox polycations both bind and electrically connect the enzymes with electrodes, the enzyme–electrodes were made simply by dipping abraded, cleaned graphite rods into an aqueous solution of the redox polymer, rinsing, dipping into the enzyme solution, and rinsing again.[64] The current densities were proportional to the concentration of glucose over a broad range, leveling off at 30 $\mu A\ cm^{-2}$ at high (30 mM) glucose concentration. The electrodes were kept in dry air, with little or no change, for 2 days. Their current response was, as expected, rapid: They responded as fast as the fluid changed in the proximity of electrodes in flow systems. In such systems, the current rise times were as short as 0.25 s.

My late teacher of thermodynamics at the Hebrew University, Aharon Katchalsky-Katzir, and his coworkers,[66,67] followed by more recent workers,[68,69] have shown that the structure of a dissolved polyelectrolyte strongly depends on ionic strength. At low ionic strength, electrostatic repulsion between similar charges on a chain tend to straighten it out, even though statistically or entropically the straight-chain configuration is unlikely. At high ionic strength, the charges are screened by counterions and the macromolecules assume entropically more probable coiled configurations. When the redox polymers are coiled, they do not adequately penetrate crevices in enzymes and the electron-transfer distances are not sufficiently reduced for electron transfer. Thus, above 0.5 M NaCl concentration, the flow of current from the substrate-reduced enzyme to the electrode stops, even though the enzyme is still substantially active and continues to transfer electrons to small diffusing mediators in the solution.[6,64] Nevertheless, even at 0.5 M NaCl, the electrostatic redox polycation–enzyme complex does not dissociate, and when an electrode is moved from a glucose solution with 0.5 M NaCl to one with 0.15 M NaCl, the current flows again.

Because the variation in current with ionic strength limits the usefulness of enzyme electrodes to biosensor applications at fixed ionic strength, we added covalent links to the electrostatic complex in order to keep the

(55) Koppenol, W. H.; Vroonland, C. A. J.; Braams, R. *Biochim. Biophys. Acta* **1978**, *503*, 499.
(56) Poulos, T. L.; Kraut, J. *J. Biol. Chem.* **1980**, *255*, 10322.
(57) Simmondsen, R. P.; Weber, P. C.; Salemme, F. R.; Tollin, G. *Biochemistry* **1982**, *21*, 6366.
(58) Poulos, T. L.; Mauk, A. G. *J. Biol. Chem.* **1983**, *258*, 7369.
(59) Erman, J. E.; Vitello, L. B. *J. Biol. Chem.* **1980**, *255*, 6224.
(60) Mauk, M. R.; Reid, L. S.; Mauk, A. G. *Biochemistry* **1982**, *21*, 1843.
(61) Bhattacharrya, A. K.; Meyer, T. E.; Tollin, G. *Biochemistry* **1986**, *25*, 4655.
(62) Hazzard, J. T.; McLendon, G.; Cusanovich, M. A.; Tollin, G. *Biochem. Biophys. Res. Commun.* **1988**, *151*, 429.
(63) Kober, E. M.; Caspar, J. V.; Sullivan, B. P.; Meyer, T. J. *Inorg. Chem.* **1988**, *27*, 4587.
(64) Pishko, M. V.; Katakis, I.; Lindquist, S.-E.; Ye, L.; Gregg, B. A.; Heller, A. *Angew. Chem., Int. Ed. Engl.* **1990**, *29*, 82.
(65) Oyama, N.; Anson, F. C. *J. Am. Chem. Soc.* **1979**, *101*, 3450.
(66) Katchalsky, A. *Pure Appl. Chem.* **1971**, *26*, 327.
(67) Eisenberg, H. *Biological Macromolecules and Polyelectrolytes in Solution*; Clarendon Press: Oxford, 1976.
(68) Nagata, I.; Morawetz, H. *Macromolecules* **1981**, *14*, 87.
(69) Carnie, S. L.; Christos, G. A.; Creamer, T. P. *J. Chem. Phys.* **1988**, *89*, 6484.

enzyme properly wired at high ionic strength. Initially we did so by copolymerizing, at a 20:1 ratio, vinylpyridine with 4-aminostyrene, forming the $[Os(bpy)_2Cl]^{1+/2+}$ complex with about one in six pyridine rings, N-methylating part of the residual rings, diazotizing the aminostyrene functions, and reacting these, at low ionic strength, with tyrosine functions of glucose oxidase, to form azo bonds.[6] Because there are few tyrosines in glucose oxidase, the structure was essentially two dimensional. Three-dimensional wired-enzyme structures, based on cross-linking the redox polymer chains and binding these to glucose oxidase lysine amines, were subsequently designed and synthesized.[70] An example of a polymerization reaction[72] is shown in eq 6. In the resulting network, one pyridine

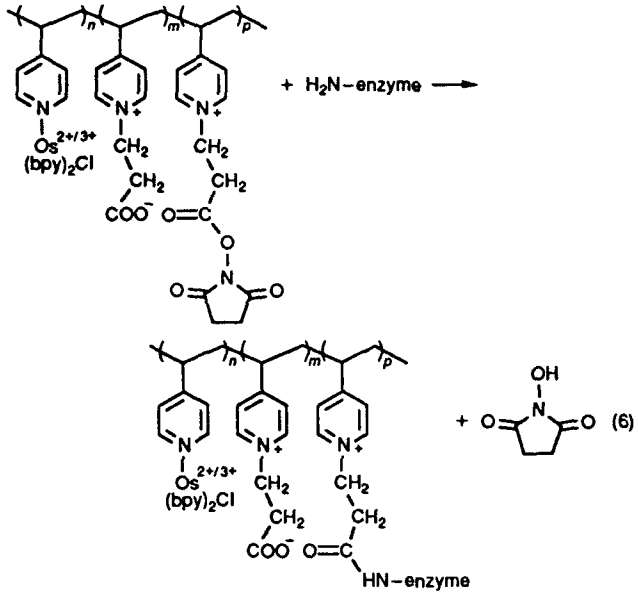

ring in about five carries an $[Os(bpy)_2Cl]^{1+/2+}$ center.

At a sufficiently high redox polymer to enzyme ratio, the wired-enzyme films, of ~1-μm thickness, can still be sufficiently conductive to allow remote enzyme molecules to communicate electrically, via the three-dimensional redox network, with the electrode. We reached in these "thick" films glucose-dependent current densities as high as ~0.5 mA cm^{-2}, showing that at least 10 equivalent enzyme layers communicated electrically with the electrode (Figure 4).[70] The observed electrical communication through these films is consistent with the electrical properties of the pure redox polymer.[71]

Amperometric Biosensors Based on Wired Enzymes

Amperometric biosensors transduce the diffusion-controlled flux of a substrate to an enzyme electrode into an electrical current. Such transducers originated in the work of Clark and Lyons.[73] Updike and Hicks subsequently measured amperometrically hydrogen peroxide formation through reaction 3.[74] Substantially

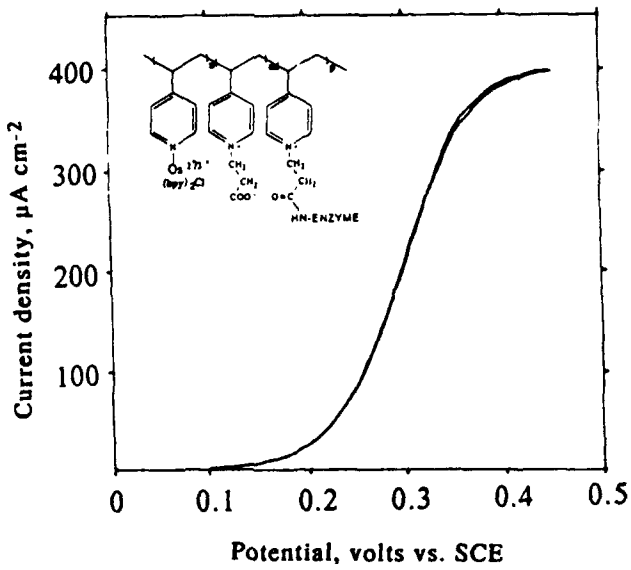

Figure 4. Cyclic voltammogram, showing a 400 μA cm^{-2} glucose diffusion limited current density reached at 40 mM glucose concentration with the wired-enzyme network of eq 6. The scan rate is 5 mV/s.

advanced ex vivo electrodes of these types are now in use, and in vivo electrodes are under development.[75] Amperometric enzyme electrodes based on diffusing redox mediators, including dyes (e.g., methylene blue),[76] ferrocene derivatives,[77] components of conducting organic metals,[78,79] and quinones,[80] have been subject to intensive research. Recently, electrodes based on conducting polypyrroles with ferrocenes also have been reported.[81] Electrodes based on ferrocene derivatives[77] are in commercial production and are used in diverse applications such as monitoring glucose levels in diabetics and food and beverage processing.

Amperometric enzyme electrodes can also be built with relay-modified and redox-polymer-wired enzymes. The relevant issues are manufacturability and cost; response time; reproducibility; selectivity; insensitivity to partial pressure of oxygen; detectivity (ratio of signal to noise (S/N)); output current stability ex vivo; output current stability in vivo; and biocompatibility.

The membraneless glucose electrodes based on three-dimensional wired structures that we are now building are manufacturable at low cost. They respond to a change in glucose concentration in less than 1 s.

(70) Gregg, B. A.; Heller, A. *Anal. Chem.* **1990**, *62*, 258.
(71) Jernigan, J. D.; Surridge, N. A.; Zvanut, M. E.; Silver, M.; Murray, R. W. *J. Phys. Chem.* **1989**, *93*, 4620.
(72) Pollak, A.; Blumenfeld, H.; Max, M.; Baughn, R. L.; Whitesides, G. M. *J. Am. Chem. Soc.* **1980**, *102*, 6324.
(73) Clark, L. D., Jr.; Lyons, C. *Ann. N.Y. Acad. Sci.* **1962**, *102*, 29.
(74) Updike, S. J.; Hicks, G. P. *Nature* **1967**, *214*, 986.
(75) See, for example: (a) Bartlett, P. N.; Whitaker, R. G. *Biosensors 1987/8*, *3*, 359. (b) Scheller, F.; Kirstein, D.; Kirstein, L.; Schubert, F.; Wollenberger, U.; Olsson, B.; Gorton, L.; Johansson, G. *Philos. Trans. R. Soc. London* **1987**, *B316*, 85. (c) *Chemical Sensor Technology*; Seiyama, T., Ed.; Kodansha Ltd. (Tokyo) and Elsevier (Amsterdam), copublishers: 1988; Vol. 1, pp 195–236. (d) McKean, B. D.; Gough, D. *IEEE Trans. Biomed. Eng.* **1988**, *35*, 526. (e) Clark, L. C. *ASAIOJ.* **1987**, *10*, 837.
(76) Silverman, H. P.; Brake, J. M. U.S. Patent 3,506,544, 1970.
(77) Cass, A. E. G.; Davis, G.; Francis, G. D.; Hill, H. A. O.; Aston, W. J.; Higgins, I. J.; Plotkin, E. V.; Scott, L. D. L.; Turner, A. P. F. *Anal. Chem.* **1984**, *56*, 667.
(78) Kulys, J. J. *Biosensors* **1986**, *2*, 3.
(79) Albery, W. J.; Bartlett, P. N.; Cass, A. E. G. *Philos. Trans. R. Soc. London* **1987**, *B316*, 107.
(80) Ikeda, T.; Hamada, H.; Miki, K.; Senda, M. *Agric. Biol. Chem.* **1985**, *49*, 541.
(81) Hale, P. D.; Inagaki, T.; Karan, H. I.; Okamoto, Y.; Skotheim, T. A. *J. Am. Chem. Soc.* **1989**, *111*, 3482.
(82) See, for example: Home, P. D.; Alberti, K. G. M. M. Biosensors in Medicine: The Clinician's Requirements. McCann, J. Exploting Biosensors. In *Biosensors: Fundamentals and Applications*; Turner, A. P. F., Karube, I., Wilson, G. S., Eds.; Oxford Univ. Press: Oxford, 1987; pp 723–746.

Their reproducibility depends on control of (a) the specific activity of the enzyme that is being wired; (b) the ratio of the wiring polymer to the enzyme; and (c) the thickness of the wired-enzyme film. Their selectivity depends on the redox potential of the electron relaying centers. The closer this potential is to the redox potential of the enzyme itself, the lesser the likelihood that a potentially interfering substrate will be spuriously oxidized. Fluctuations in current with partial pressure of oxygen, e.g., oxygen concentration in blood, depend on the ratio of the rate of direct electrooxidation of the $FADH_2$ centers to their rate of oxidation by molecular oxygen, and therefore on the rate of electron transfer to, and the electrical resistance of, the three-dimensional wired-enzyme structure. At high osmium-complex concentrations, and in sufficiently thin layers, the competition is won by electron transfer to the electrode via the osmium centers, and the electrodes are relatively insensitive to oxygen. The signal to noise ratio S/N is, in the absence of interfering substrates, proportional to the number of enzyme molecules that are effectively wired to the electrode surface per unit area. At a film thickness of ~ 1 μm, and at typical blood glucose concentrations ($\sim 10^{-2}$ M), a current density of $\sim 10^{-3}$ A cm^{-2} is achieved. With a low noise potentiostat and only unshielded leads to the biosensor, the noise is less than 10^{-7} A cm^{-2}, i.e., S/N is on the order of 10^4.

The output current stability depends on enzyme durability and on avoiding fouling of the electrodes, primarily by adsorbed proteins. Typical decay rates at 25 °C in the absence of proteins are $\sim 5\%$/day, but are much faster in whole blood. By designing redox polymers that form hydrogels, we are now improving the stability of the bioelectrodes. We are designing relays that are closer in their potential to those of the enzymes, with the objective of further reducing the residual interference by electrooxidizable species such as urate and ascorbate ions. We are also exploring the range of enzymes that can be electrically wired and are building sensors with these. Currently our list includes, in addition to glucose oxidase, the flavo enzymes D-amino acid oxidase, lactate oxidase, and glycerol-3-phosphate oxidase, as well as lipoamide oxidase, through which NAD^+/NADH requiring enzymes are coupled to the electrodes.

The financial support for this research from the Office of Naval Research, the Texas Advanced Research Program, and the Robert A. Welch Foundation is gratefully acknowledged. Harry B. Gray, Heinz Gerischer, and Barry Miller read and improved the manuscript.

Mol. Cryst. Liq. Cryst., 1990, Vol. 190, pp. 221–249
Reprints available directly from the publisher
Photocopying permitted by license only

Printed in the United States of America

Electrical Communication Between Graphite Electrodes and Glucose Oxidase/Redox Polymer Complexes

M. V. PISHKO, I. KATAKIS, S.-E. LINDQUIST and A. HELLER

Department of Chemical Engineering, University of Texas at Austin, Austin, Texas, 78712

and

Y. DEGANI

AT&T Bell Laboratories, Murray Hill, New Jersey 07974

Redox polymers can fold along the glycoproteins of glucose oxidase (MW 160,000) at low electrolyte concentrations and thereby penetrate the enzyme. Upon penetration, the distance between the redox centers of the polymer and the $FADH_2$ centers of the reduced enzyme is reduced sufficiently for electrons to be transferred and, therefore, for the mediated electro-oxidation of glucose on conventional electrodes. At high (1M) electrolyte (NaCl) concentrations the redox polymers coil. Such coiling prevents the penetration of the enzyme by the redox polymers. Consequently, electron transfer does not take place and glucose is not electro-oxidized. When an appropriate polycationic redox polymer is covalently bound to the enzyme, the electro-oxidation of glucose occurs even at high electrolyte concentrations. Electron transfer from the enzyme's $FADH_2$ centers to copolymers of poly(N-methyl-4-vinylpyridinium) chloride with either poly(vinylferrocene), E^o = 0.25V (SCE), or with poly(4-vinylpyridine) complexes of $Os(bpy)_2Cl$, E^o = 0.25V (SCE), or of $Os(4,4'\text{-dimethylbpy})_2Cl$, E^o = 0.15V (SCE) is rapid. The polycationic poly(4-vinylpyridine) complex of $Os(bpy)_2Cl$ can be covalently bound to glucose oxidase by preparing the terpolymer with 4-aminostyrene, diazotization and reaction of the diazonium cations with tyrosine or tryptophane residues of the enzyme. Glucose electrodes made with the redox polymer modified enzyme are relatively stable and sensitive. Furthermore, simple and fast amperometric glucose electrodes can be made by adsorbing either non-quaternized or quaternized poly(vinylpyridine) complexes of $[Os(bipyridine)_2Cl]^{2+}$ (MW 300,000) on graphite, and adsorbing on these polymer films glucose oxidase. These electrodes do not require diffusing redox mediators or membranes to contain the enzyme and the redox polymer. The redox polymer is shown to electrically "wire" the enzyme's redox centers to the electrode. The glucose response of the electrodes is faster than 1 sec; their current increases linearly with glucose concentration through the 0–10 mM range. At 60 mM glucose, their current density is about 20 $\mu A/cm^2$.

INTRODUCTION

Amperometric biosensors based on enzymes bound to electrode surfaces have been the target of substantial research.[1] Oyama and Anson,[2] who investigated a decade ago poly(4-vinylpyridine) (PVP) coated electrodes, found that films of these poly-

mers are strongly adsorbed on pyrolytic graphite and form long-lived, reproducible electrodes with redox couples. The polymer films were made by dipping graphite electrodes into methanol solutions of the polymers and rinsing. They have also prepared and studied electrodes with the N-methylated polycations of PVP (NMPVP) made by reacting the polymer with methyl iodide. Meyer, Murray and their colleagues[3] made PVP and other polypyridine coated metal electrodes by *in situ* electropolymerization of the monomer and by plasma polymerization. Electroactive anions of fast redox kinetics were found to be rapidly reduced and oxidized in these films, as were cations complexed to PVP. The electrochemistry observed was consistent with the physisorption of segments of the macromolecules on graphite. The non-adsorbed segments provided a three-dimensional network into and out of which ions diffused. Thus, complexes of PVP and poly(vinylbipyridine) with ruthenium, iron, osmium and cobalt complexes showed persistent, reproducible and often fast electrochemistries.

In parallel with these studies, the electrochemistry of small redox proteins (such as cytochrome *c*, myoglobin, ferredoxin and phycocyanin) has been studied by Kuwana, Hill, Hawkridge, Blount, Bowden, Armstrong and their colleagues.[4] Although the small proteins were directly electrooxidized/reduced on metal and doped semiconductor electrodes, the rates of the electrode reactions could often be enhanced by "promoters" adsorbed on the electrode surface. These promoters, although electrochemically inert, bind and orient the redox proteins. Prominent among these promoters are compounds of pyridine, such as bipyridine, methyl viologen and bis(4-pyridinethiol). Oxidoreductases, having molecular weights higher by an order of magnitude than redox proteins were usually not directly electrooxidized or reduced even in the presence of promoters. Their lack of direct electrochemistry has been attributed to the thick protein or glycoprotein shells that surround their redox centers. Nevertheless, for one enzyme (cytochrome *c* peroxidase) direct electrochemistry on doped SnO_2 has been reported by Assefa and Bowden.[5]

In earlier work, Degani and Heller, as well as Bartlett *et al.*,[6] covalently bound electron relays to oxidoreductases and showed that the relay modified enzymes communicate directly with gold and carbon electrodes. Furthermore, direct electrical communication between glucose oxidase and graphite electrodes has been established also through electrostatic complexing and through covalent bonding of $Os(bpy)_2Cl$ complexes of N-methylated PVP (bpy = bipyridine) to this enzyme.[7] Recently, we reported that the polycationic $Os(bpy)_2Cl$-PVP complexes, whether N-methylated or not, are strongly adsorbed on graphite, and that the resulting polymer-modified electrodes strongly interact with glucose oxidase, an oxidoreductase that is polyanionic at neutral pH.[8] In the macromolecular complex formed between the redox polymer and enzyme, electrons are transferred from the $FADH_2$ centers of the enzyme, via the redox polymer, to the graphite electrode. Such transfer provides for glucose electrodes that are easy to make. The electrodes are made simply by dipping graphite rods into the redox polymer solution and rinsing, followed by dipping into the enzyme solution and rinsing. Glucose electrodes made by this technique, in contrast with previous ones, require neither membranes to contain the enzyme in the proximity of the conductor nor diffusing mediators to shuttle electrons. Their response times are fast, because the reactant and product

do not have to diffuse through a membrane and because the active layer on the graphite surface is thin.

This paper charts a path to the simultaneous maintenance of stability and achievement of high currents in relay modified enzymes. We find that bonding (covalent or electrostatic) of high molecular weight polycationic redox polymers to negatively charged glucose oxidase results in the establishment of direct electrical communication between the redox centers of the enzyme and carbon or gold electrodes. The degree of modification of the enzyme that is needed in order to establish effective electrical communication is reduced when a redox polymer rather than a group of redox monomers is bound to the enzyme. With a polymer, either electrostatic bonding or covalent bonding of the polymer and the enzyme is sufficient for the establishment of electrical communication. The electron path now consists of an array of redox centers. To improve the intrinsic stability of the redox centers, the earlier used ferrocenes and ruthenium amines were replaced with rugged complexes of osmium. Reduced glucose oxidase transfers electrons at a high rate to the Os complexes.

EXPERIMENTAL

Chemicals

Glucose oxidase (E.C. 1.1.3.4) type X, catalase (E.C. 1.11.1.6), bovine serum albumin (fraction 5) and NaHEPES were purchased from Sigma. The enzymes were used without further purification. $Os(bpy)_2Cl_2$ (bpy = 2,2'-bipyridine) was prepared from K_2OsCl_6 (Aldrich) following a reported procedure.[9] 4-aminostyrene and poly-(4-vinyl pyridine) were purchased from Polysciences. Azobisisobutyronitrile (AIBN), 4-vinylferrocene, acrylamide, acrylic acid, N-vinyl-2-pyrrolidone, glutaraldehyde, and 4-vinylpyridine were purchased from Aldrich. Graphite (HB pencil leads 0.5 or 0.9 mm diameter, and pyrolytic graphite 3mm, 4mm and 6mm diameter) and gold wire (0.5mm diameter) were used as electrodes. Cellulose membranes (Spectra/por 6, 3500 MW cutoff) were purchased from Spectrum, Los Angeles.

Abbreviations for the Redox Polymers

The abbreviations used are listed in Scheme 1.

SYNTHESIS OF REDOX POLYMERS

Copolymer of vinylferrocene and acrylamide: Acrylamide (3.1g) and vinylferrocene (0.5g) were dissolved in 50 mL THF. After degassing with N_2 for 5 min, 35 mg AIBN was added. While under N_2 the solution was stirred in a 50°C water bath for 4 h. The solid product was filtered, washed 3 times with THF and dried in vacuo at ambient temperature.

SCHEME 1

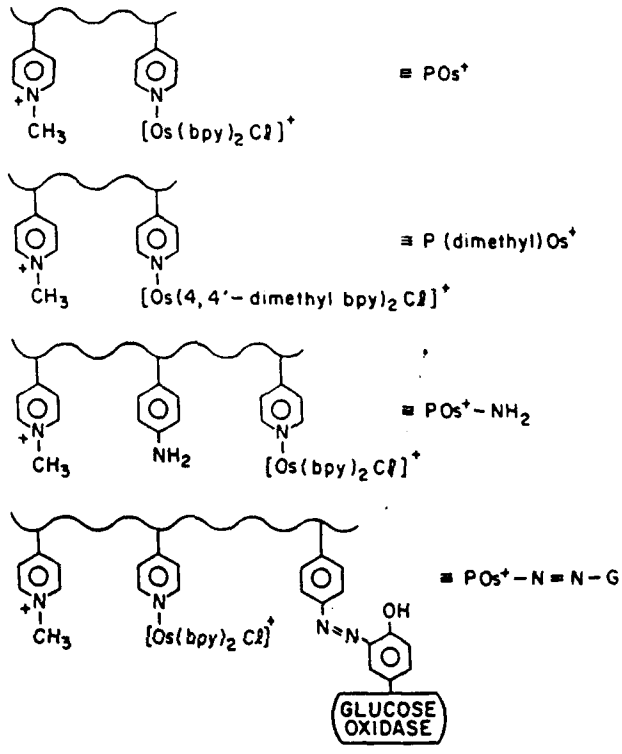

Copolymer of vinylferrocene and acrylic acid: Acrylic acid (5g) and vinylferrocene (1g) were dissolved in 50 mL of benzene. After degassing with N_2 for 5 min, 40 mg AIBN was added. The solution was then refluxed for 2 h and the oily red precipitate was separated by filtration, washed twice with ether, and dried in vacuo at ambient temperature.

Copolymer of vinylferrocene and 4-vinyl-N-methyl pyrdinium chloride: Vinylferrocene (0.5g) and vinylpyridine (8g) were codissolved in 30 mL of benzene. After degassing with N_2 for 5 min, 30 mg AIBN were added and the solution refluxed for 1 h. The viscous orange precipitate was separated by decanting the supernatant solution, washed twice with benzene, dissolved in 30 mL DMF at 120°C, then methylated with 2 mL methyl iodide at reflux. When the methyl iodide was added, a vigorous reaction took place, resulting in the formation of a yellow solid precipitate. This precipitate was filtered, washed twice with DMF, twice with acetone, and dried in vacuo. The yellow powder was then dissolved in 5 mL of water and the I^- ions exchanged with Cl^- on a 15 cm long, 2 cm diameter Biorad AG2-X4 column, using deionized water as eluent. The solution of the chloride was used as such.

Quartenized and nonquartenized POs^+NH_2: 4-aminostyrene (1g), 4-vinylpyridine (9.3g) and 200 mg AIBN were refluxed in 20 ml of methanol for 4 hrs under

N_2. After the solution was cooled to ambient temperature, toluene was added to precipitate the copolymer. The yellowish copolymer was filtered, washed twice with 100 ml of toluene and dried in vacuo to yield 10g of poly(4-vinylpyridine-co-4-aminostyrene). $Os(bpy)_2Cl_2$ (1g) and poly(4-vinylpyridine-co-4-aminostyrene) (1g) were dissolved in 25 ml of ethylene glycol and heated to reflux (190°C) for 15 minutes. After cooling to 150°C, 25 ml of DMF was added, followed by 5 ml of methyl iodide. The solution was allowed to reflux for 30 minutes, cooled to room temperature, where 50 ml of toluene was added to precipitate the viscous terpolymer. After the supernatant solution was decanted, the polymer was dissolved in 30 ml of water and stirred for 5 minutes with 5g of Biorad AG2-X4 anion exchange resin in the chloride form. The solution was filtered and the solvent evaporated. The residual paste was dissolved in 20 ml of ethanol and the solution poured into 250 ml of acetone. The hygroscopic black powdery precipitate was filtered and dried in vacuo at ambient temperature.

Synthesis of POs^+: The procedure employed to prepare this material was identical to that for POs^+NH_2, except that poly(4-vinylpyridine) MW = 50,000 was used.

Synthesis of P(4,4'-dimethylbpy)Os^+: This synthesis was similar to that of POs^+, except that $Os(bpy)_2Cl_2$ was replaced by $Os(4,4'\text{-dimethylbpy})_2Cl_2$.

Bonding of POs^+NH_2 to glucose oxidase: POs^+NH_2 (0.1g) was dissolved in 2 mL of 0.5M HCl. Concurrently, glucose oxidase (0.1g) was dissolved in a solution of 0.2g $NaHCO_3$ and 0.2g of Na_2CO_3 in 2 mL of water. After both solutions were chilled to 5°C in an ice bath, a solution of 30 mg $NaNO_2$ in 10μL of water was added to the vigorously stirred POs^+NH_2 solution and was held for 10 s. The glucose oxidase solution was then added dropwise, removed from the ice bath, and after 10 min, the $POs^+N = N - GO$ was separated from the reaction mixture by cation exchange chromatography on a Sephadex C-25 column, using NaCl gradient elution. Spectroscopic analysis shows that the ratio (4-vinylpyridine plus N-methyl-4-vinylpyridinium)/Os in the polymer is 6.5 ± 1.

Electrochemical Cells, Instrumentation and Measurements

These were similar to those described in earlier parts of the series. A Pine Instruments AFMSRX Rotator and MSRX Speed Control were used for the rotating disk electrode (RDE) experiments. A schematic of the flow cell used in the time response experiments is shown in Figure 1. All potentials quoted are relative to saturated calomel electrode (SCE) unless otherwise noted.

Preparation of Membrane Electrodes

The electrode structure is shown in Figure 2. A heat-shrinkable polypropylene sleeve was first shrunk on a 6mm diameter graphite electrode. The electrode's tip was then polished with 1μm alumina, sonicated in D.I. water for 1 min and blown dry in a stream of N_2. A drop of the solution of either the enzyme with the covalently bound redox polymer, or of the solution of the enzyme with the mobile mediating redox polymer, was placed on the polished and cleaned tip. The w[illegible] membrane,

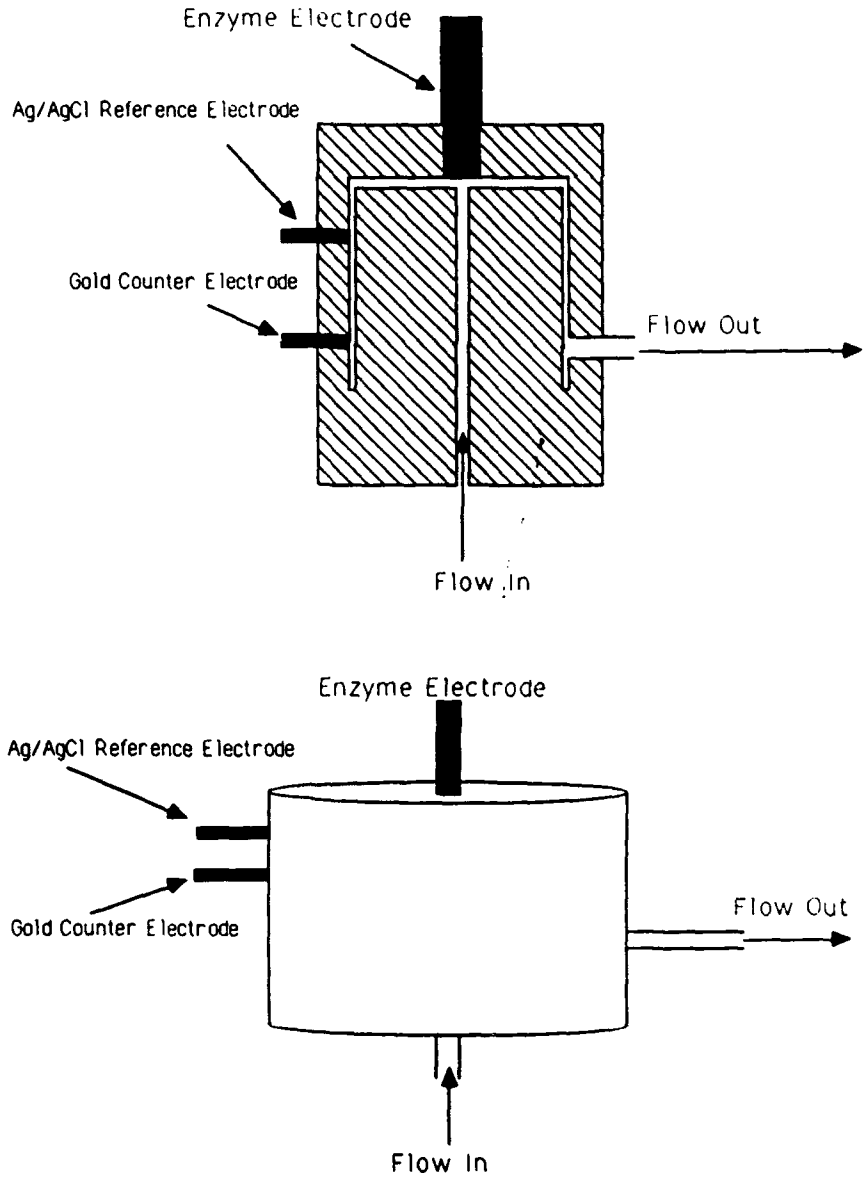

FIGURE 1 Schematic of flow cell.

pre-soaked in 0.1 M phosphate (pH 7) for 5 min, was placed on the enzyme-solution wetted tip and held in place by an O-ring.

Immobilization of Redox Polymer Modified Glucose Oxidase, or Natural Glucose Oxidase and Redox Polymer, Near the Electrode Surface

Two solutions were used in preparing each electrode. One contained 5% glutaraldehyde in water. The second contained either the modified enzyme (50mg/mL) and bovine serum albumin (BSA) (100mg/mL), or the natural enzyme (50mg/mL),

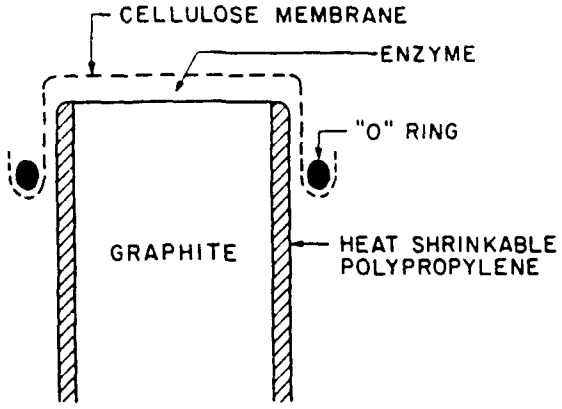

FIGURE 2 Structure of the membrane electrode.

the redox polymer (25–50 mg/mL), and BSA (100 mg/mL). In the latter group, the natural enzyme and/or the BSA was precipitated by some of the polycationic redox polymers. When this was the case, enough NaCl was added to redissolve the precipitate. Typically, 10 μL of the first solution were rapidly mixed with 20 μL of the second, promptly placed on the polished and cleaned graphite electrode tip (see above) and allowed to cure at ambient temperature over a water bath, that prevented drying.

Preparation of Surface-Adsorbed Redox Polymer Electrodes

The electrode structure is shown in Figure 3. A heat-shrinkable polypropylene sleeve was first shrunk on a 0.5 or 0.9 mm diameter graphite or gold electrode. The electrode tip was then polished with 0.3 μm alumina, sonicated in D.I. water

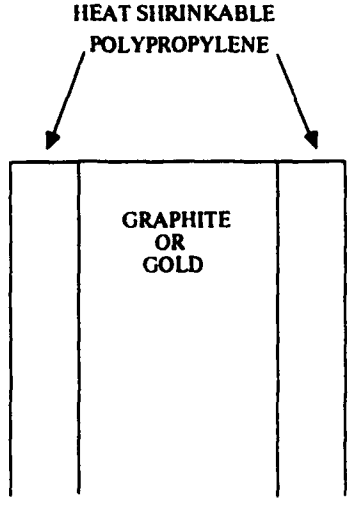

FIGURE 3 Structure of the surface-adsorbed redox polymer electrode.

for 20 seconds and blown dry with a stream of N_2. A drop (4 μL) of quaternized for nonquaternized POs'NH_2 solution (2.6 mg/mL solvent) was applied to the electrode tip, allowed to stand for 4 minutes and then washed off with D.I. water in the case of the quaternized polymer or with ethanol in the case of the nonquaternized polymer. Different levels of quaternization were produced by exposing the nonquaternized surface adsorbed polymer to methyl iodide vapor at ambient temperature for time periods of up to 35 minutes, then exchanging the iodide with chloride through repeated washings in 1 M NaCl. Electrodes for the RDE experiments were polished and modified with redox polymer in a similar manner.

RESULTS

Effect of the Copolymer's Charge on the Electron Transfer Kinetics

Copolymers of vinylferrocene and anionic, neutral and cationic monomers were investigated by cyclic voltammetry as oxidants for reduced glucose oxidase (Table I). The experiments were carried out with glassy carbon electrodes (without membranes or enzyme immobilization) in quiescent solutions under N_2. At the scan rate employed (1 mV/s) all of the redox polymers showed diffusion controlled and reversible one-electron transfer voltammograms (Figure 4, curve a). In the absence of a redox polymer, or of an electron relay bound to the enzyme, glucose oxidase did not exhibit any observable electrochemistry. One observes, however, when both a redox polymer and glucose oxidase are present, the electrochemical oxidation of the reduced enzyme. The reaction sequence in this case is:

$$\text{glucose oxidase-FAD} + \text{glucose} \rightarrow \text{glucose oxidase-FADH}_2 + \text{gluconolactone} \quad (1)$$

$$\text{glucose oxidase-FADH}_2 + RP^n \rightarrow \text{glucose oxidase-FAD} + RP^{(n-2)+} \quad (2)$$

$$RP^{(n-2)+} \rightarrow RP^{n+} + 2e^- \quad (3)$$

In reaction 2 two ferrocinium centers of the redox polymer (RP) transfer electrons to the reduced enzyme in apparently single electron transfer steps (Figure 4, curve b).

TABLE I

Co-monomer/vinylferrocene ratios for the anionic, neutral and cationic co-polymers of polyvinylferrocinium chloride

Copolymer of polyvinylferrocene	Co-monomer/vinylferrocene ratio
sodium polyacrylate	32
polyacrylamide	300
poly-N-vinylpyrrolidone	62
poly-N-methyl-4-pyridinium chloride	200

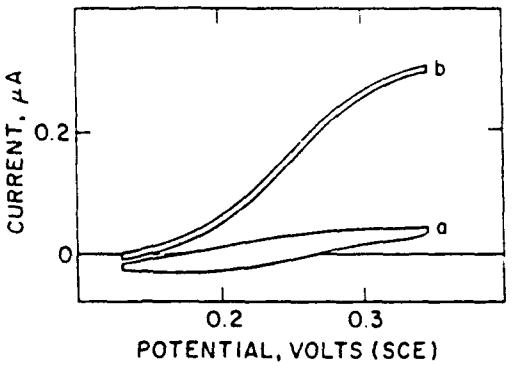

FIGURE 4 Cyclic voltammograms obtained with a solution containing glucose oxidase and poly(vinylferrocene-co-N-methylpyridinium chloride) without glucose (curve a) and with 30mM glucose (curve b). 3mm diameter glassy carbon disk electrode; scan rate 1mV/s.

Containability of the Water-Soluble Redox Polymers in Membranes

Nonpolymeric redox couples, including ferrocene derivatives, diffuse readily through cellulosic membranes such as Spectra/por 6. Their transport is readily observed, for example, by increase in absorption at wavelengths characteristic of the redox mediator in the electrolyte outside the membrane-enclosed compartments. Their diffusion is somewhat, but never fully retarded when the membrane and the nonpolymeric mediator are both anionic or cationic. Thus, the diffusion of ferrocene carboxylate is slowed by cellulosic membranes with sulfonate groups. The water-soluble polymeric redox couples are, in contrast, easy to contain. No transport of the ferrocene-containing redox polymers through the standard membranes employed was detected by absorption spectroscopy.

Electron Transfer from Reduced Glucose Oxidase to POs^+

Complexes of osmium, including $[Os(bpy)_2(py)Cl]^{2+/3+}$ (where bpy is 2,2'-bipyridine or one of its derivatives and py is pyridine or one of its derivatives) are exceptionally effective mediators in the electro-oxidation of reduced glucose oxidase. Complexing of the $Os(bpy)_2^{+}$ with high molecular weight poly(vinylpyridine) makes this mediator membrane containable. The complex formed with poly(vinylpyridine), that is partially methylated to form the water soluble N-methylpyridinium polymer POs^+, is an effective acceptor of electrons from glucose oxidase. Figure 5, curve a shows that voltammogram of POs^+ in 0.15M NaCl with 0.1 M phosphate buffer. The separation between the reduction and the oxidation peaks is about 20 mV, indicating that the polymer is strongly adsorbed on the graphite electrode. When glucose oxidase (10μM) and glucose (50mM) are added, enhanced electro-oxidation of the enzyme-reduced POs^+ is observed (Figure 5, curve b). Addition of 0.5M NaCl, i.e. increase of the NaCl concentration from 0.15M to 0.65M stops the reduction of POs^+ by glucose oxidase (Figure 5, curve c). No glucose concentration dependent current is seen and the only electrochemistry observed is that of strongly adsorbed POs^+.

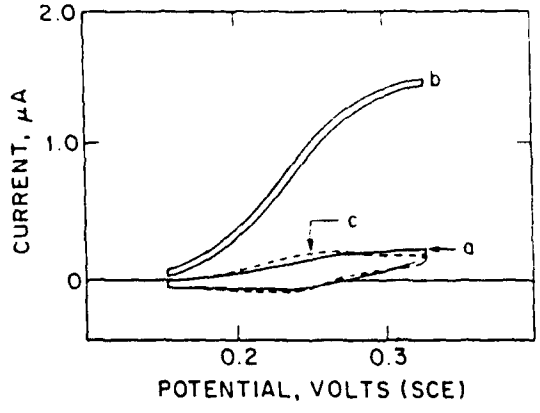

FIGURE 5 Cyclic voltammograms obtained with a 0.1M pH 7 phosphate buffer solution of glucose oxidase and POs$^+$ without glucose and with 0.15M NaCl (curve a); with 50 mM glucose and 0.15M NaCl (curve b); and with 50mM glucose and 0.65M NaCl (curve c). 3mm diameter glassy carbon disk electrode; scan rate 1mV/s.

Electron Transfer to P(4,4'-Dimethylbpy)Os$^+$

The electrochemistry of this redox polymer differs from that of POs$^+$ in two ways. In the absence of glucose oxidase and glucose (Figure 6, curve a) the separation of the reduction and oxidation peaks is about 60 mV suggesting weaker adsorption on graphite; and the polymer's redox potential is shifted from 0.25 V (SCE) for POs$^+$ to 0.15 V (SCE) for P(4,4'-dimethylbpy)Os$^+$. In the presence of glucose oxidase (Figure 6, curve b) the glucose dependent current reaches a level similar to that seen for POs$^+$ (Figure 5, curve b).

Electron Transfer to Go – N = N – POs$^+$

Bonding of the osmium-containing redox polymer to glucose oxidase by one or more azo-bonds has two beneficial effects: it increases the rate of electron transfer from the reduced enzyme to the polymer and it allows the electro-oxidation to

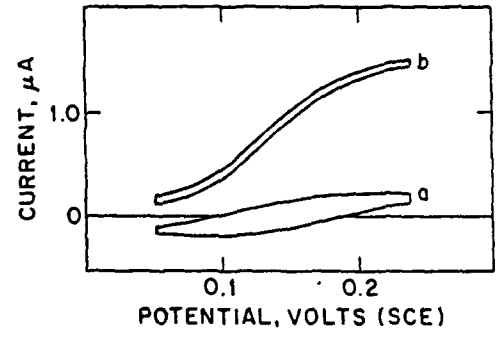

FIGURE 6 Cyclic voltammograms obtained with a 0.15M NaCl, 0.1M pH 7 phosphate buffer solution of glucose oxidase and P(4,4'-dimethylbpy)Os$^+$ without glucose (curve a); and with 50mM glucose (curve b). 3mm diameter glassy carbon disk electrode; scan rate 1mV/s.

persist even in 1M NaCl solutions, where the unbound POs$^+$ glucose oxidase system shows no observable glucose concentration dependent electrochemistry. The voltammogram of the chemically modified enzyme, in the absence of glucose, is seen in Figure 7, curve a. While for unbound POs$^+$ the separation of the reduction and oxidation peaks is approximately 20 mV, the separation for the modified enzyme is 60 mV, suggesting normal diffusion dependence. When glucose is added to the 0.15M NaCl 0.1M phosphate buffer solution containing 10μM of the modified enzyme, electro-oxidation of the modified enzyme is observed (Figure 7, curve b). The oxidation current attained at sufficiently oxidizing potentials is about fourfold higher than for the native enzyme and unbound POs$^+$. While addition of 0.85M NaCl decreases the current by a factor of approximately 4 (Figure 7, curve c), electro-oxidation of the modified enzyme persists. Figure 8 shows a calibration curve for a glucose selective electrode made with the GO – N = N – POs$^+$ enzyme and with a 3500 MW cutoff Spectro/por 6 membrane. At 0.32 V (SCE) the current increases linearly with glucose concentration up to approximately 10 mM.

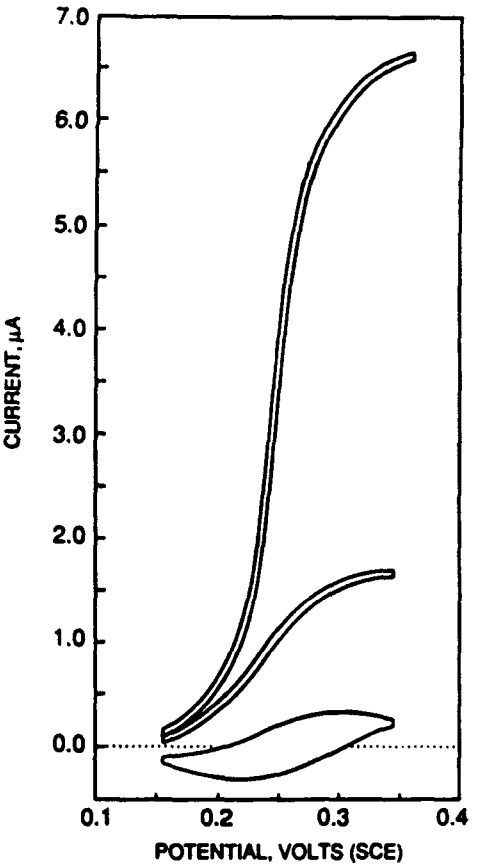

FIGURE 7 Cyclic voltammograms obtained with GO – N = N – POs$^+$ in 0.1M pH 7 phosphate buffer without glucose and with 0.15M NaCl (curve a); with 50mM glucose and 0.15M NaCl (curve b); and with 50mM glucose and 0.65M NaCl (curve c). 3mm glassy carbon disk electrode; scan rate 2mV/s.

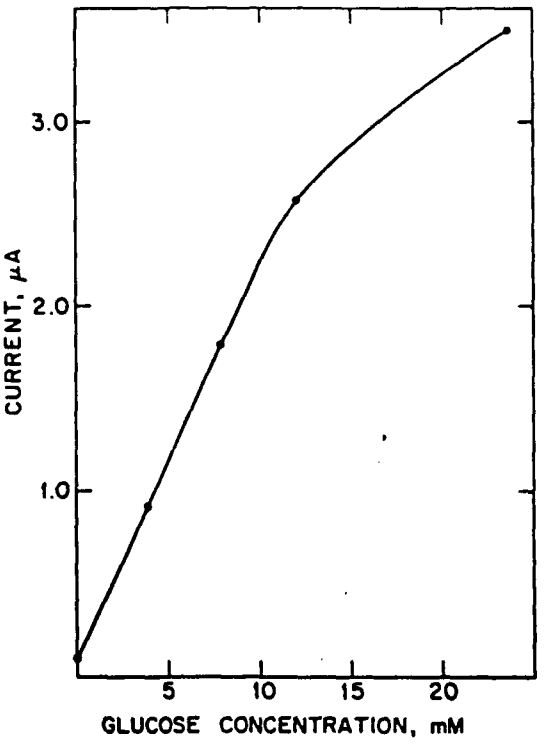

FIGURE 8 Glucose concentration dependence of the current at 0.32V (SCE) for the GO – N = N – POs$^+$ membrane electrode.

Voltammetry of Adsorbed POs$^+$NH$_2$

The behavior of nonquaternized and quaternized POs$^+$NH$_2$ (E° = 0.25 V) adsorbed on carbon and gold electrodes was investigated by cyclic voltammetry (Figures 9a, 9b, 10a, 10b). The experiments were carried out in a quiescent solution of 0.15 M NaHEPES titrated to pH 7 with 10 M HCl (final ionic strength 0.27 M). The electrodes were allowed to cycle for approximately 15 minutes to allow the polymer films to swell or shrink before scans were recorded. Scan rates from 2 mV/s to 200 mV/s were employed. Integration of the cyclic voltammograms at low scan rates (2–5 mV/s) showed that approximately 1.0×10^{-8} moles/cm^2 of nonquaternized POs$^+$NH$_2$ are electroactive on abraded graphite electrodes and 1.0×10^{-9} moles/cm^2 on gold electrodes. For the quaternized polymer, 1.0×10^{-9} moles/cm^2 are electroactive when adsorbed on abraded graphite and 5.0×10^{-10} moles/cm^2 when on gold. Rotating disk electrode experiments revealed that the polymer does not desorb even at high rotation rates (2000 rpm). Furthermore, coulometry showed that less than 10% of the polymer desorbed from the electrodes upon storage for 30 days in a stirred water bath. An increase in chloride concentration of the electrolyte caused the peaks to be shifted negatively (Figures 11a and 11b). For the nonquaternized polymer, increasing [Cl$^-$] from 0.15 M to 1.36 M shifted the peaks 45 mV negative. For the quaternized redox polymer, the peaks shifted

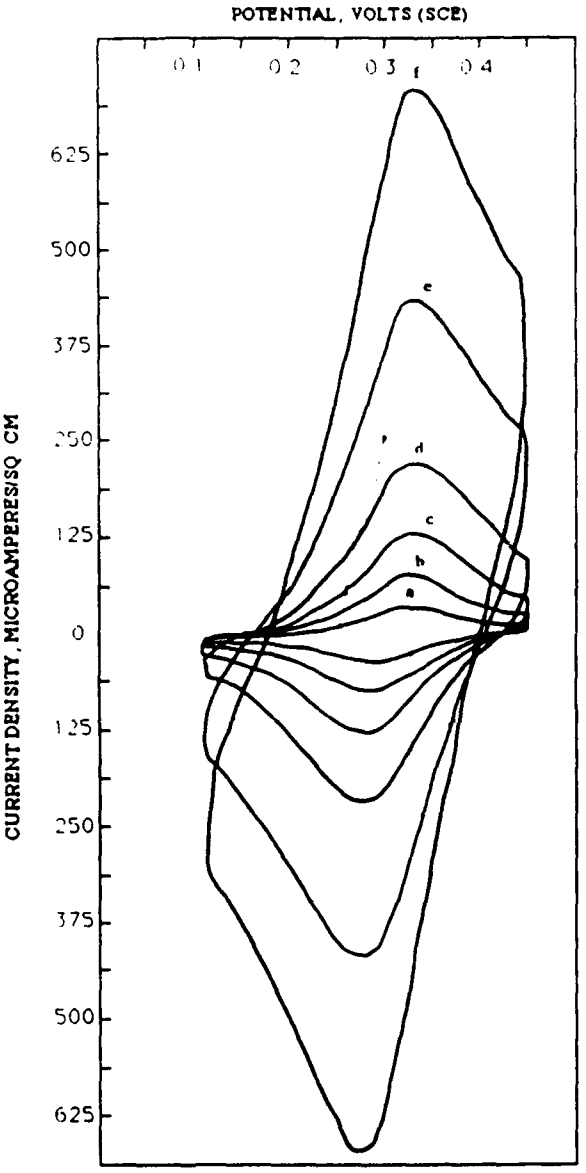

FIGURE 9 (a) Cyclic voltammograms at different scan rates for nonquaternized POs · NH_2 adsorbed on abraded graphite (electrode surface area 0.008 cm^2). Scan rates: a) 2 mV/s, b) 5 mV/s, c) 10 mV/s, d) 20 mV/s, e) 50 mV/s, and f) 100 mV/s. 0.15 M NaHEPES, pH 7. (b) Cyclic voltammograms at different scan rates for nonquaternized POs · NH_2 adsorbed on gold (electrode surface area 0.002 cm^2). Scan rates: a) 5 mV/s, b) 10 mV/s, c) 20 m V/s, d) 50 mV/s, e) 100 mV/s, and f) 200 mV/s. 0.15 M NaHEPES, pH 7.

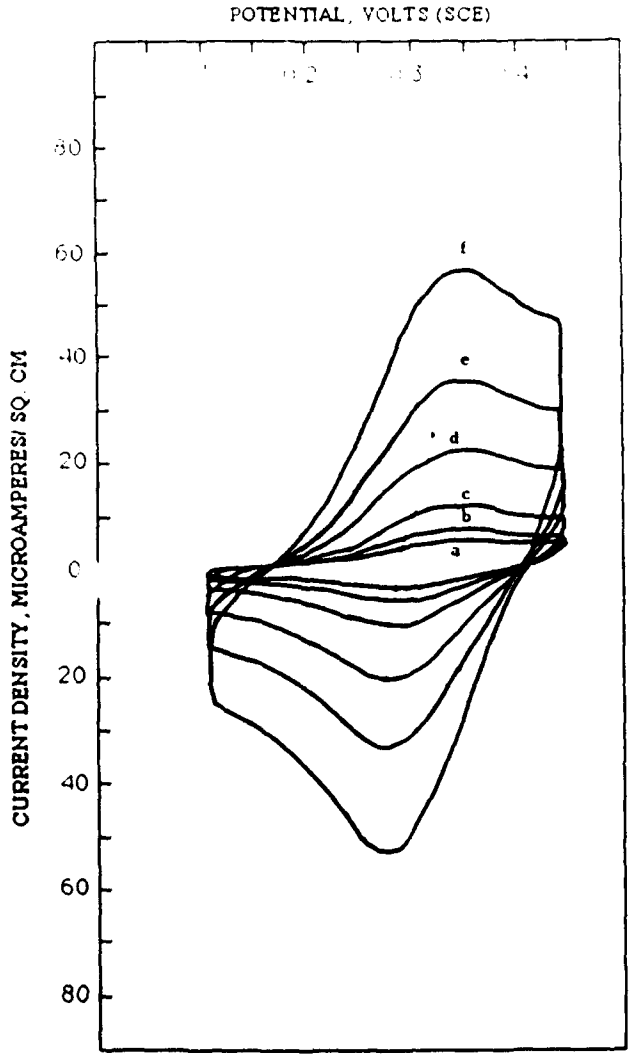

FIGURE 9 continued

50 mV negative for an increase from $[Cl^-]$ = 0.12 M to $[Cl^-]$ = 1.0 M. Decreasing $[Cl^-]$ to 0.27 M shifted the peaks back to their original positions. The formation of the enzyme-polymer complex also shifted the peaks 40 mV negative.

Glucose Response of the Enzyme-Polymer Complex Adsorbed on the Electrode Surface

The oxidation of glucose by the glucose oxidase-POs^+NH_2 surface adsorbed complex was studied by cyclic voltammetry. Electrodes were produced by adsorbing quaternized POs^+NH_2 on the surface of a graphite electrode. This surface layer was examined by cyclic voltammetry, washed with D.I. water and then dried in a stream of N_2. A 4 μL droplet of glucose oxidase solution (4.5 mg/mL) was placed

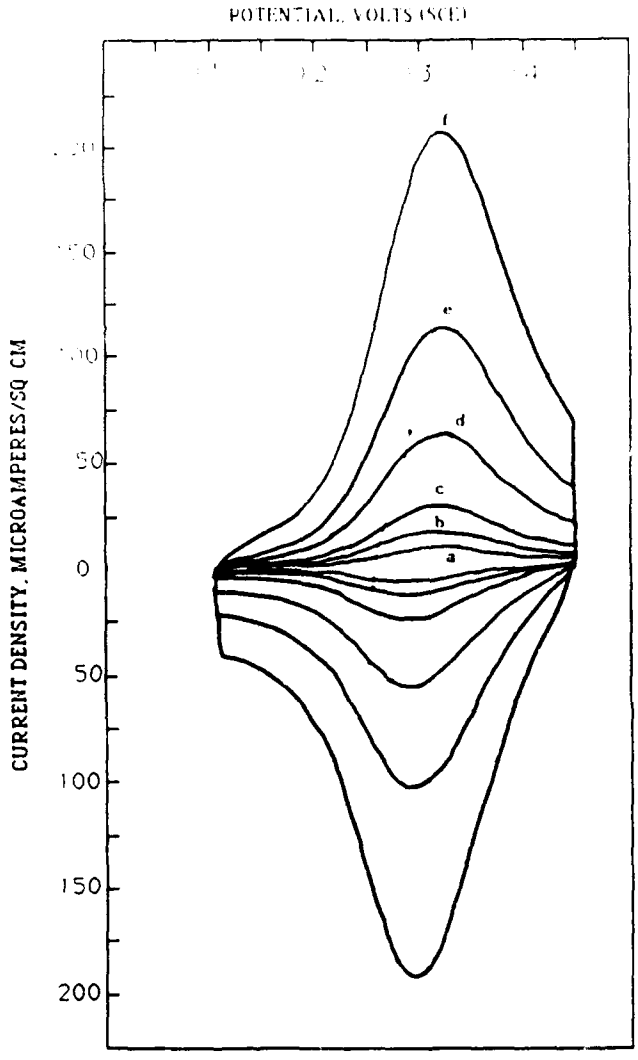

FIGURE 10 (a) Cyclic voltammograms at different scan rates for quaternized POs·NH_2 adsorbed on abraded graphite (electrode surface area 0.002 cm^2). Scan rates: a) 5 mV/s, b) 10 mV/s, c) 20 mV/s, d) 50 mV/s, e) 100 mV/s, and f) 200 mV/s. 0.15 M NaHEPES, pH 7. (b) Cyclic voltammograms at different scan rates for quaternized POs·NH_2 adsorbed on gold (electrode surface area 0.002 cm^2). Scan rates: a) 5 mV/s, b) 10 mV/s, c) 20 mV/s, d) 50 mV/s, e) 100 mV/s, and f) 200 mV/s. 0.15 M NaHEPES, pH 7.

on the electrode surface, contacted for 10 minutes and then rinsed in a stream of D.I. water. The glucose response of the electrodes was tested in 60 mM glucose/0.15 M NaHEPES solutions at pH 7. No containment membrane was used. The cyclic voltammograms for the oxidation of glucose by the enzyme-polymer complex are shown in Figure 12 and the steady state response at a constant potential of 0.45 V is shown in Figure 13 for both a 0.5 mm graphite electrode in a quiescent solution and a 4 mm pyrolytic carbon disk electrode rotating at 20 rpm. Similar results were obtained for electrodes using gold. Chronoamperometric measurements taken in

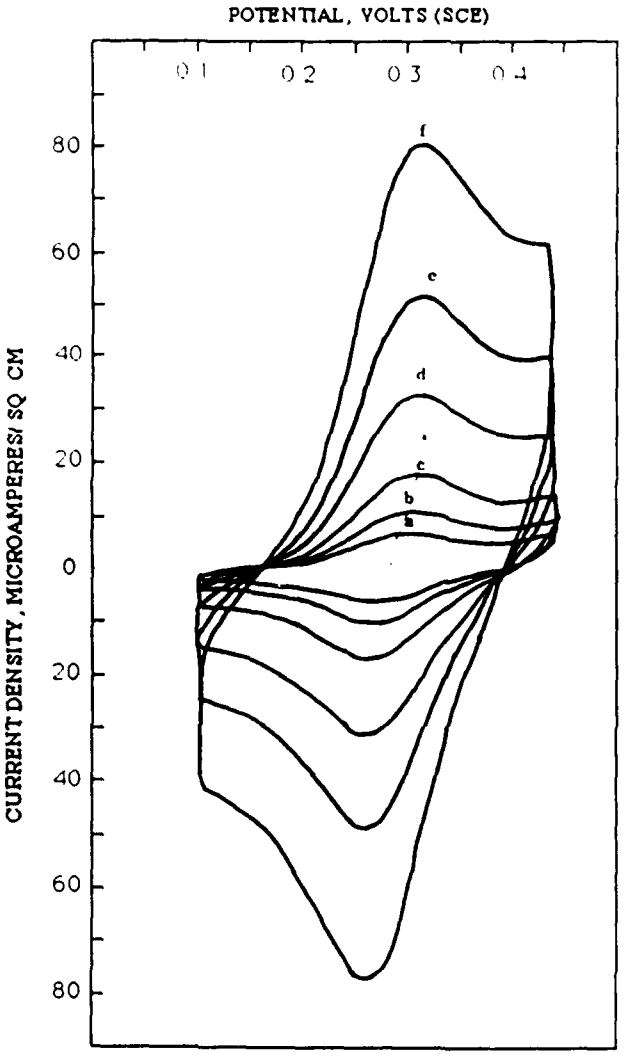

FIGURE 10 continued

the flow cell show that the response time to a change in glucose concentration of the enzyme/quaternized polymer/electrode system is less than 1 s (Figure 14). (The definition of response time for this purpose is the time necessary to reach ½ maximum response). Response times for different flow rates are shown in Figure 15. The glucose concentration dependence of the current at 0.45 V for the enzyme/quaternized polymer/electrode system is shown in Figure 16. Only a background current is present at zero glucose concentration.

Effect of Degree of Quaternization on Glucose Response

The effect of the degree of quaternization on electron transfer between the polymer-enzyme complex adsorbed on a graphite electrode was studied by cyclic voltam-

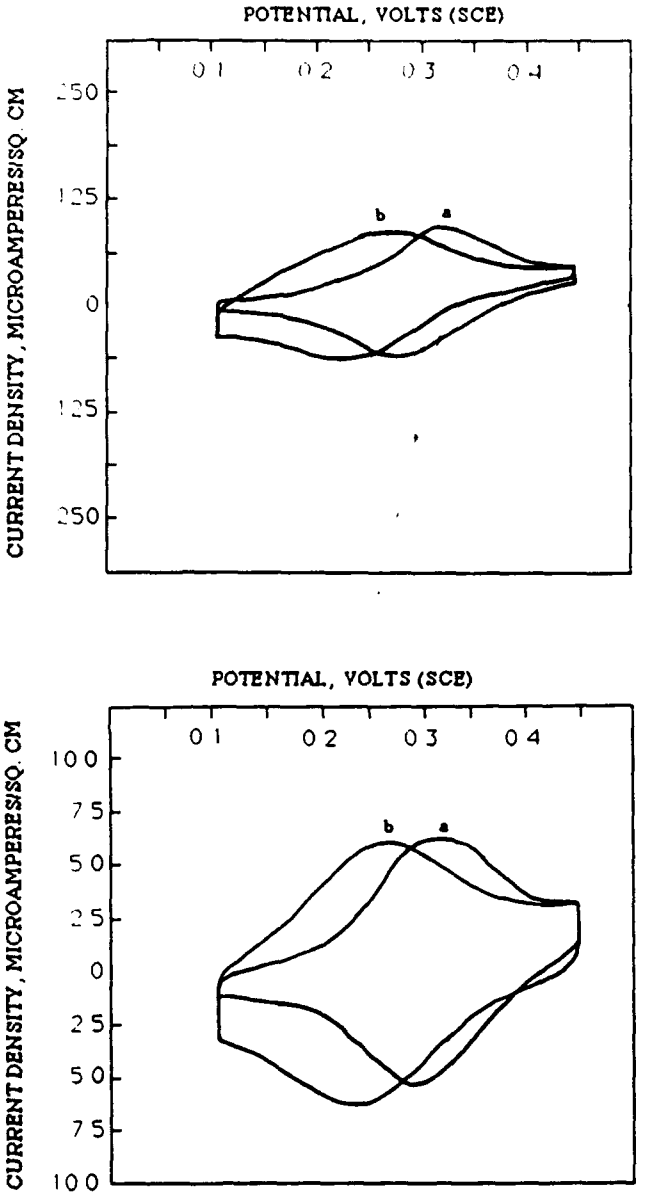

FIGURE 11 (a) Cyclic voltammograms for nonquaternized $POs^{+}NH_2$ at different sodium chloride concentrations: a) $[Cl^-] = 0.15$ M and b) $[Cl^-] = 1.36$ M. Scan rate: 5 mV/s. (b) Cyclic voltammograms for quaternized $POs^{+}NH_2$ at different sodium chloride concentrations: a) $[Cl^-] = 0.12$ M and b) $[Cl^-] = 1.00$ M. Scan rate: 5 mV/s.

metry. Electrodes were tested in 60 mM glucose/0.15 M NaHEPES solutions at pH 7. Increasing the degree of quaternization (i.e. exposure time to methyl iodide vapors) produced no substantial increase in current density per mol of $POs^{+}NH_2$ adsorbed on the electrode surface. The degree of quaternization did, however, have a substantial effect on the hysteresis of the cyclic voltammograms (Figure 17).

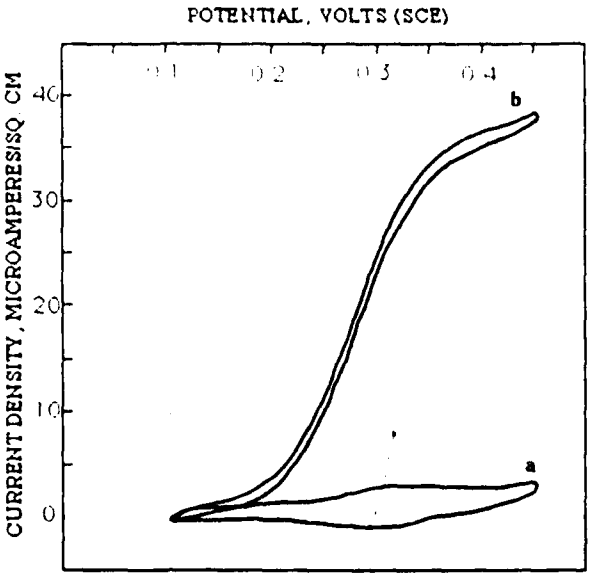

FIGURE 12 Cyclic voltammogram of the quaternized POs·NH_2/enzyme complex in 60 mM glucose, 9.9 units/mL catalase, 0.15 M NaHEPES at pH 7. Scan rate: 5 mV/s a) no glucose, b) 60 mM glucose.

Electrodes produced with the nonquaternized redox polymer exhibited large hysteresis. Increasing quaternization decreased substantially the hysteresis.

Adsorption and the Effect of Ionic Strength on the Surface Adsorbed Enzyme/ Polymer Complex

Adsorption and the effect of ionic strength on glucose oxidase adsorbed on graphite electrode surfaces modified with POs·NH_2 (quaternized) were studied by cyclic voltammetry and chronoamperometry. The electrodes were placed in 4 mL solutions of 60 mM glucose/0.15 M NaHEPES at pH 7, degassed with N_2. 0.9 μg of catalase (44,000 units/ mg protein) were added to prevent the deactivation of glucose oxidase by evolved H_2O_2. Approximately 10 μL of 4 mg/ml solution of glucose oxidase was slowly injected (final glucose oxidase concentration: 10 μg/mL) into the electrochemical cell. The potential was then stepped from 0 V to 0.45 V. The response of the electrode is shown in Figure 18. A similar result was obtained from cyclic voltammetry. As was reported earlier,[6] electron transfer in the enzyme-polymer complex stops in 0.65 M NaCl. In a similar adsorption experiment performed at 0.65 M NaCl no glucose response was observed. An inactivation experiment was performed using an electrode with adsorbed polymer and enzyme, then increasing the ionic strength to 0.65 M by injection of 1 M NaCl/60 mM glucose solution into a stirred cell or in a cell using a pyrolytic carbon disk electrode rotating at 20 rpm. Figure 19 shows the glucose response rapidly decreasing. Only a background current, unrelated to the glucose level, remains at an ionic strength of 0.65 M. The electrode was then removed from the high ionic strength solution, rinsed with copious amounts of D.I. water and placed into a solution of low ionic

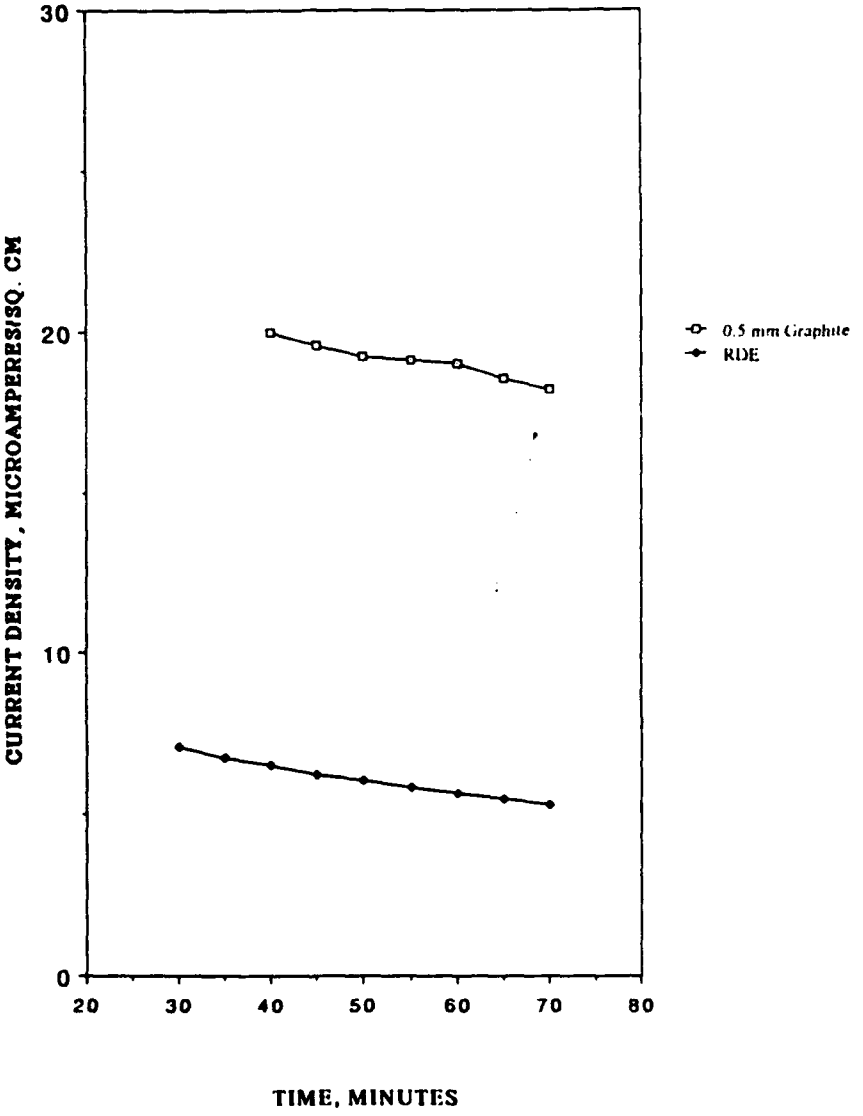

FIGURE 13 Steady state glucose response of glucose oxidase adsorbed on a POs · NH_2 (quaternized) surface modified electrode in 60 mM glucose, 9.9 units/mL catalase, 0.15 M NaHEPES at pH 7.

strength. After a period of approximately 2 hours the electrode regained 75% of its initial response.

DISCUSSION

Mediation of Electro-Oxidation of Glucose Oxidase by Redox Polymers

The advantage of polymeric redox mediators in the enzyme electrode based sensor applications is that they are membrane containable. While low molecular weight

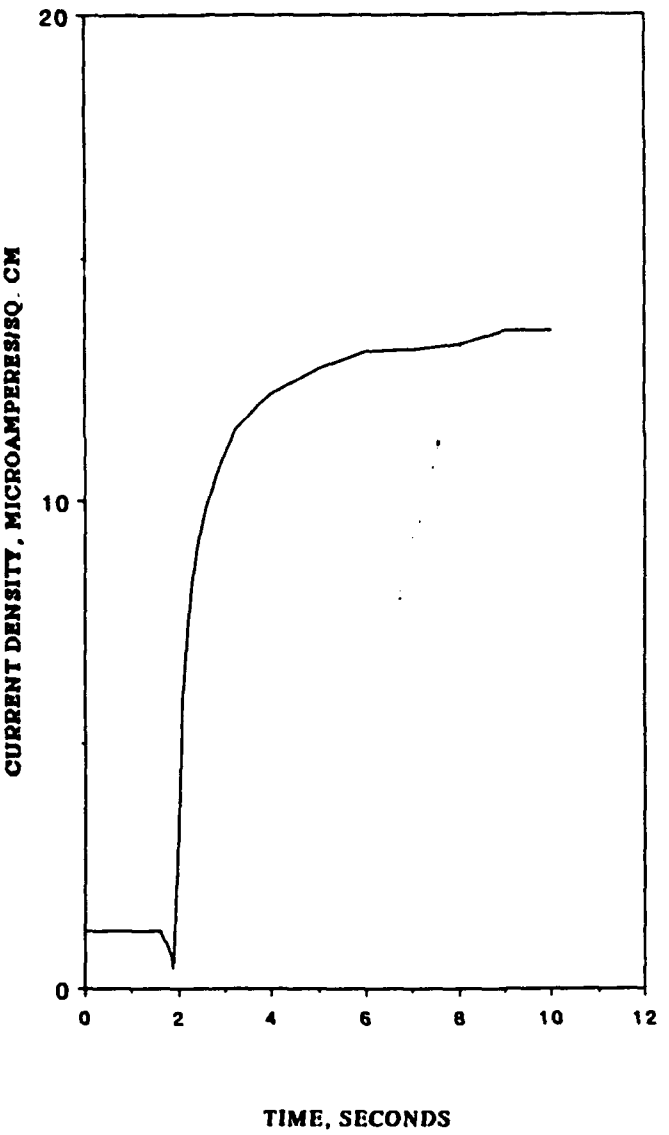

FIGURE 14 Electrode response to a change in glucose concentration from 0 to 50 mM glucose in 0.15 M NaHEPES at pH 7, 9.9 units/mL catalase. Flow rate: 91 mL/min.

redox couples diffuse through membranes that transport reaction substrates and products, polymeric redox couples do not. Thus, for example, simple cellulosic membranes of 3500 MW cutoff effectively contain both the redox polymers and glucose oxidase in the enclosure near an electrode. Such containment is of relevance to the design of mediator-based *in vivo* enzyme electrodes when the redox mediator is toxic or if there is uncertainty about the effect of releasing the mediator into the tissue.

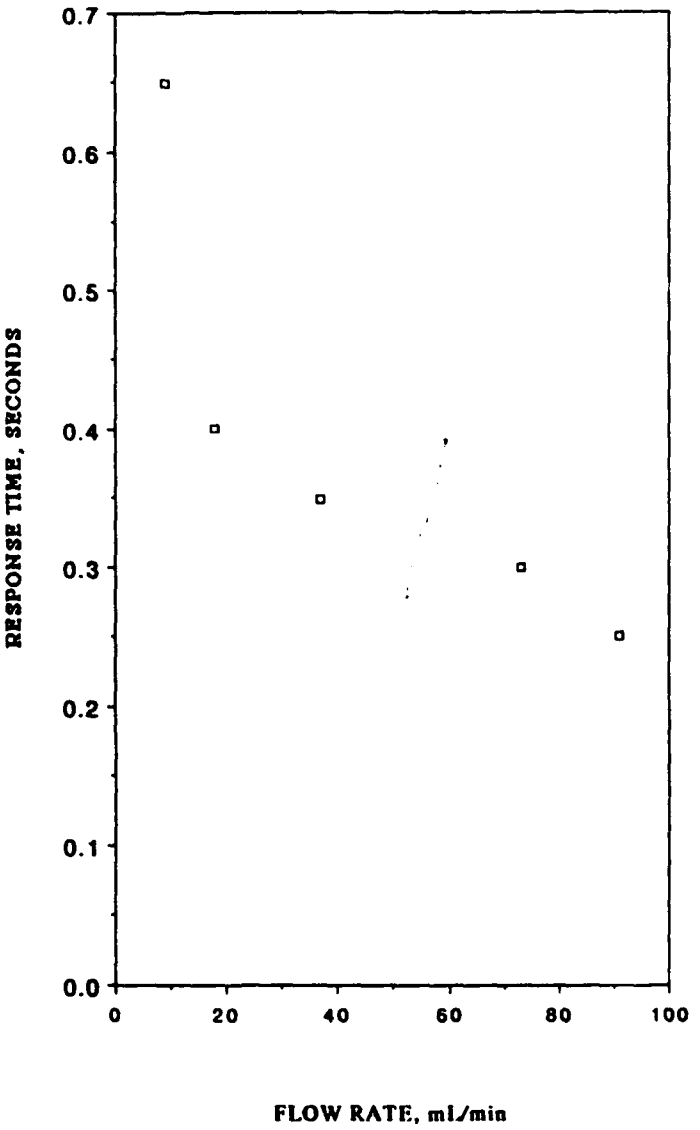

FIGURE 15 Electrode response times at varying flow rates for a change in glucose from 0 to 50 mM.

Effectiveness of Polycationic Redox Polymers as Mediators

In agreement with results of Kulys, Cenas and their coworkers,[10] polycationic redox polymers are shown to be effective electron shuttles. We find that the polycationic polymers shuttle electrons from reduced glucose oxidase to graphite electrodes more rapidly than neutral or weakly cationic redox polymers, and that the latter do so faster than polyanionic redox polymers. This suggests that electrostatic bonding of the polycationic polymer to the negatively charged enzyme creates a transient

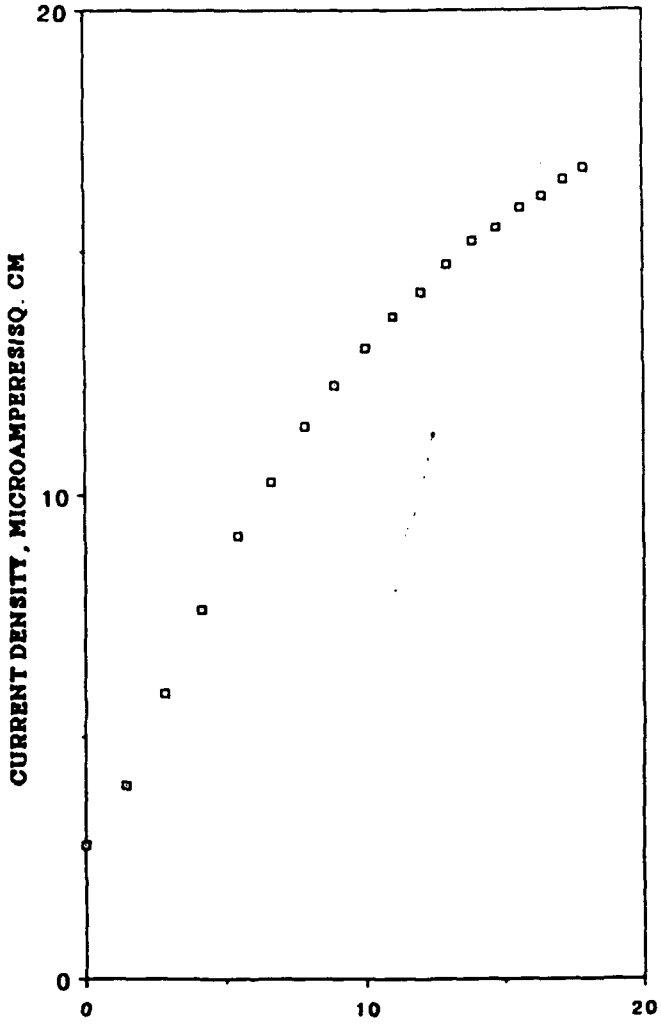

FIGURE 16 Glucose concentration dependence of the current density at 0.45 V for the glucose oxidase/quaternized POs^{+} NH_2/graphite electrode system in 0.15 M NaHEPES at pH 7, 9.9 units/mL catalase.

complex where the electron transfer distance is reduced. That the relevant bonding in the transient adduct is electrostatic in nature is evident also from the effect of the NaCl concentration on the rate of electron transfer from reduced glucose oxidase to the polycationic redox polymer POs^{+}. The decrease in the rate of electron transfer is reflected in the voltammograms of Figure 5. While at 0.15M NaCl one observes only the mediated electro-oxidation of glucose, no such electro-oxidation is seen in 1M NaCl: the only electrochemistry seen is that of the redox polymer. Evidently, at low electrolyte concentrations the polyanionic enzyme and the polycationic redox polymer electrostatically bind each other, while at high NaCl concentrations the redox polymer coils,[18] increasing the electron transfer distance

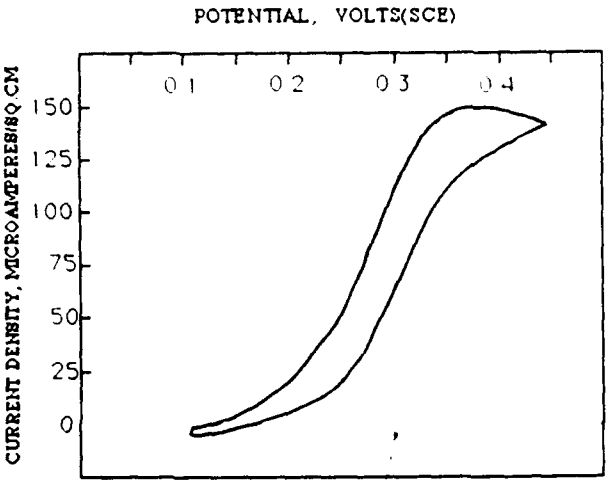

FIGURE 17 Cyclic voltammogram of the nonquaternized $POs^{+}NH_2$/enzyme complex in 60 mM glucose, 0.15 M NaHEPES at pH 7. Scan rate: 1 mV/s.

and thus preventing electron transfer from the enzyme to the polymer. Because the entropy of mixing of the macromolecules is small, transient electron transferring complexes are not formed at high NaCl concentrations.

Electron Transfer from Reduced Glucose Oxidase to Polycationic Osmium Complexes

The redox potentials of several osmium$(bpy)_x(py)_y$ complexes are positive of glucose oxidase.[11] Meyer and his group have shown[12] that osmium complexes of bipyridine, pyridine and related heterocyclics are also fast redox couples, and that their redox potentials can be tailored over a broad range. The redox potential of $Os(bpy)_2(py)Cl$ is approximately 0.3 V (SCE), appropriate for oxidation of reduced glucose oxidase. When its complexing pyridine is replaced by poly(vinylpyridine), the redox potential drops to 0.25 V (SCE) (Figure 5). The potential is further reduced to 0.15 V (SCE) and thus brought closer to the redox potential of the enzyme upon replacing the bipyridine with 4,4'-dimethyl-bipyridine (Figure 6). The osmium complexes that were investigated accept electrons from the $FADH_2$ centers of glucose oxidase rapidly. Consequently, they are effective mediators of the electrochemical oxidation of the enzyme on conventional electrodes (Figure 5, 6).

Electrical Communication between Glucose Oxidase and Electrode Surfaces via Covalently Bound Polycationic Redox Polymer Relays

The polycationic copolymer $POs^{+}NH_2$, that contains aminostyrene in addition to the Os-complexing 4-vinylpyridine functions, can be covalently bound to glucose oxidase by forming its diazonium salt and reacting it with tyrosine or tryptophane residues of the enzyme.

The systems with the enzyme bound polycationic redox polymers differ from the unbound ones in their electron transfer characteristics and therefore, in their electrochemical characteristics. In the unbound redox polymer/enzyme system the rate

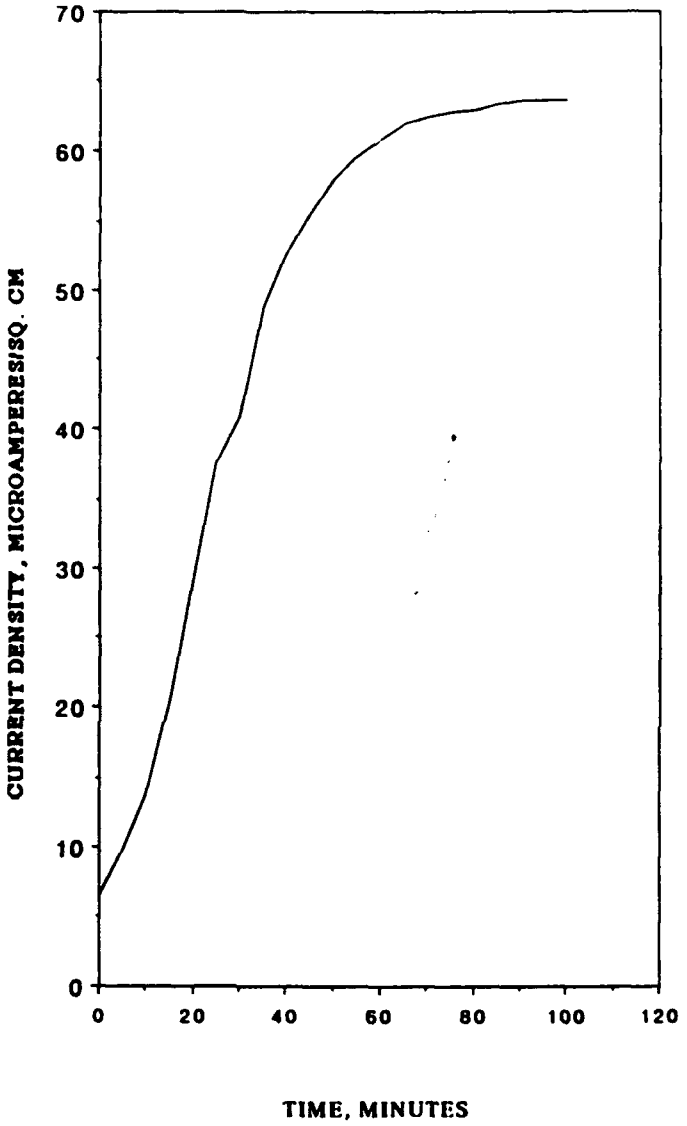

FIGURE 18 Chronoamperometric response of quaternized POs · NH_2/graphite electrode in 10 μg/mL glucose oxidase, 60 mM glucose, 0.15 M NaHEPES at pH 7.

of electron transfer declines rapidly when the electrolyte concentration is increased, becoming vanishingly small at 1M NaCl, when coiling of the polycationic redox polymer increases the electron transfer distance between the polymer's redox centers and the $FADH_2$ centers of the enzyme. In the covalently bound system the decline is less significant and electron transfer persists even in 1M NaCl, showing that the polycationic redox polymer is held within electron transfer distance of the enzyme's $FADH_2$ centers by the covalent bond.

The electron transfer characteristics of the polycationic electron-relay modified glucose oxidase translate to advantageous characteristics in the glucose electrode

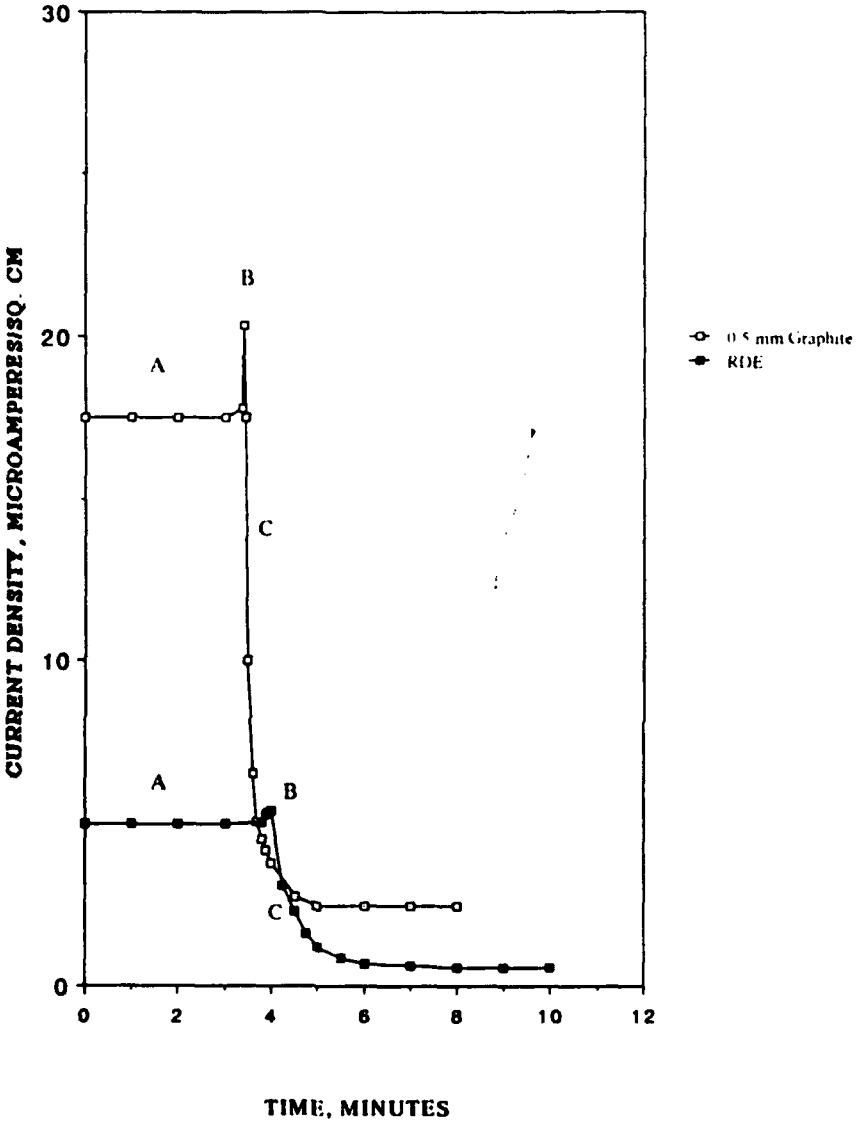

FIGURE 19 Chronoamperometric response of quaternized POs·NH_2/glucose oxidase complex adsorbed on graphite to increased ionic strength. Region A: Steady state glucose response. Region B: Turbulent effects of the solution injection cause a temporarily increased glucose flux to the surface. Region C: Electrode response to the increase in ionic strength from 0.27 M to 0.65 M.

made with this modified enzyme (Figure 7). The bound system leads to a fourfold increase in current (Figures 5 and 7) and the electro-oxidation of glucose persists even at high NaCl concentrations.

Adsorption of Poly(vinylpyridine) Complexes of $Os(bpy)_2Cl^{+2/+3}$

Voltammetric results for both the nonquaternized and quaternized POs·NH_2 polymers show that these are strongly adsorbed on abraded graphite surfaces. This is

evident from the reduced peak splitting (Figures 9 and 10), from the steady performance of the electrode rotated at 2000 rpm and from the small loss of polymer after storing 30 days in a stirred water bath.

Adsorption of Glucose Oxidase on POs$^+$NH$_2$ Coated Electrodes

That glucose oxidase is strongly adsorbed on POs$^+$NH$_2$ coated electrodes and that its redox centers are electro-oxidized by these is seen in Figures 13, 14, and 17. Chronoamperometry shows that even at high enzyme dilution the enzyme builds up on the PVP-Os(bpy)$_2$Cl^{+2} coated surfaces (Figure 17).

Oxidation of Glucose by Surface Adsorbed Enzyme-Redox Polymer Complexes

Electrodes first dipped in a quaternized or nonquaternized POs$^+$NH$_2$ solution, rinsed, then dipped in a glucose oxidase solution and again rinsed, can be used as glucose sensors (Figures 12, 13, and 17). Electrons are transferred from the reduced enzyme, via the polymer, to the electrodes. One advantage of surface adsorbed enzyme-redox polymer complexes in enzyme-electrode based sensor applications is that they do not require a membrane or other form of containment. Unbound redox mediators and enzymes require containment (i.e. membranes and gels) to prevent them from diffusing away from the electrode. Because glucose must diffuse *through the membrane* or gel, such containment lengthens the time response of enzyme-electrode sensors to a sudden change in glucose concentration. Strongly adsorbed surface complexes require no containment to prevent out-diffusion of the enzyme from the electrode. Thus, the response of the electrode is only limited by the transport of glucose through the solution. In a flow system, the time response is less than 1 s (Figure 15), faster than has been reported for sensors employing membranes.[13]

Redox Properties of the Surface Adsorbed Redox Polymer

The small values for ΔEp indicate that both the nonquaternized and quaternized polymers are strongly adsorbed. Increased peak splitting has been attributed to poor electron transfer between the polymer film and the electrode surface, slow diffusion of counter ions into the polymer film,[14] or film (or solution) resistance effects.[15] Peak splitting on carbon is lower than on gold for both polymers, suggesting either faster electron transfer to carbon, or a more open polymer morphology, which may allow faster counter ion transport. The penetration of counter ions into the film and film morphology have been shown to significantly affect the electrochemical response of adsorbed poly(4-vinylpyridine)^{2} and plasma polymerized vinyl ferrocene films.[16] The mid-height peak widths for both polymers are quite broad, suggesting either heterogeneity in the electrode surfaces or a low degree of order in the polymer film.[15] Since peak widths on polished gold are nearly as broad as those on carbon, the latter explanation seems more likely. The shift in peak position caused by increased [Cl$^-$] is attributed to differential ion pairing of [Os(bpy)$_2$Cl]$^{+3}$ and [Os(bpy)$_2$Cl]$^{+2}$ with chloride. Strong ion pairing by the oxidized form of the redox couple is expected to produce a negative shift. Differ-

ential ion pairing has been observed in poly(4-vinyl pyridine)/$[Fe(CN)_6]_n$ films[5] and cyctochromes.[17]

Electrostatic Complexing between the Redox Polymer and the Enzyme

Both nonquaternized and quaternized POs$^+NH_2$ have been shown to effectively relay electrons from glucose oxidase to the electrode surface. Quaternized POs$^+NH_2$ is preferred because of the absence of hysteresis shown in cyclic voltammograms and the fast electron transfer indicated by surface voltammetry experiments. At increased ionic strength, electron transfer ceases in the electrostatic enzyme/polymer complex, with enzyme related changes accounting for a very minor fraction of the loss.[6] We have shown here that the enzyme and the redox polymer remains, nevertheless, on the electrode surface. We attribute loss in glucose response to coiling of the polycationic redox polymer at high ionic strength.[18] The coiled polymer no longer folds along the protein.

Conclusions

Glucose oxidase, an enzyme having a hydrodynamic diameter of 86Å[19] and two deeply buried FAD/$FADH_2$ redox centers, does not exchange electrons with conventional electrodes because the distance between the FAD/$FADH_2$ centers and the electrode surface is excessive for electron transfer even upon adsorption of the enzyme. At low electrolyte concentrations transient electrostatic complexes are formed between glucose oxidase and polycationic redox polymers. These polymers penetrate the negatively charge enzyme sufficiently to allow electron transfer to occur between the $FADH_2$ centers and the Os centers of the polymer. Electrons are then transferred by the redox polymer to the electrode surface. At high electrolyte concentrations the transient enzyme-redox polymer complexes do not form because of coiling by the polymer. As a result, glucose is not electro-oxidized at high electrolyte concentrations.

Polycationic osmium complexes emerge as particularly effective acceptors and thus as useful mediators in the electro-oxidation of glucose. Covalent bonding of a polycationic redox polymer to the enzyme results in a structure wherein the distance between the $FADH_2$ centers and the redox centers of the polymer is sufficiently short to allow rapid electron transfer. Electrons transferred from the $FADH_2$ centers may then percolate along the redox polymer chains and transfer to the electrode. In contrast with electrodes made with the unbound redox polymers that become inactive at high electrolyte concentrations, electrodes made with the enzyme covalently bond to the redox polymer continue to electro-oxidized glucose at high electrolyte concentrations. Evidently the bound polycationic redox polymer cannot coil to the degree that electron transfer from the enzyme ceases.

The electrostatic complex of polyanionic glucose oxidase and polycationic POs$^+NH_2$ is strongly adsorbed, at physiological ionic strength, onto a graphite electrode surfaces. The adsorbed polycationic redox polymer serves as an effective electron transfer relay between the $FADH_2$ centers of glucose oxidase and the electrode. This electrostatic complex forms the basis for a glucose electrode with a fast response time that does not require a membrane or a diffusing electron carrier.

Acknowledgments

We wish to thank Prof. Thomas J. Meyer for a most useful discussion on the properties of osmium complexes and for providing a preprint on this subject. We also wish to thank Goran Svensk for the molecular weight determination of $POs(NH_3)$. The work of the authors is supported in part by the Office of Naval Research and the Robert A. Welch Foundation.

References

1. (a) C. C. Liu, E. J. Lahoda, R. T. Galasco and R. B. Wingard, *Biotechnol. Bioeng.*, 1975, **17**, 1695. (b) L. B. Wingard, Jr., J. G. Schiller, S. K. Wolfson, Jr., C. C. Lin, A. L. Drash and S. J. Yao, *J. Biomed. Mater. Res.*, 1979, **13**, 921–935. (c) C. Bourdillon, J. P. Bourgeois and D. Thomas, *J. Amer. Chem. Soc.*, 1980, **102**, 4231–4235. (d) R. Kamin and G. Wilson, *Anal. Chem.*, 1980, **52**, 1198. (e) R. M. Ianniello and A. M. Yacynych, *Anal. Chem.*, 1981, **53**, 2090–2094. (f) R. M. Ianniello, T. J. Lindsay and A. M. Yacynych, *Anal. Chim. Acta*, 1982, **141**, 23–32. (g) J. F. Caster and L. B. Wingard, Jr., *Biochemistry*, 1984, **23**, 2203–2210. (h) H. J. Wieck, G. H. Hieder and A. M. Yacynych, *Anal. Chim. Acta*, 1984, **158**, 137–141. (i) I. Ikeda, I. Katasho, M. Kamei and M. Senda, *Agric. Biol. Chem.*, 1984, **48(8)**, 1969–1976. (j) K. Narasimhan and L. B. Wingard, Jr., *Enzyme Microb. Technol.*, 1985, **7**, 283–286. (k) J. A. Osborn, A. M. Yacynych and D. C. Roberts, *Anal. Chim. Acta*, 1986, **183**, 287–292. (l) J. V. Twork and A. M. Yacynych, *Biotechnol. Prog.*, 1986, **2**, 67–72. (m) G. Palleschi, M. A. N. Rahni, G. J. Lubrano, J. N. Ngwainbi and G. G. Guilbault, *Anal. Biochem.*, 1986, **159**, 114–121. (n) M. A. N. Rahni, G. G. Guilbault and G. N. de Oliveira, *Anal. Chim. Acta*, 1986, **181**, 219–25. (o) K. Narasimhan and L. B. Wingard, Jr., *Anal. Chem.*, 1986, **58**, 2984–2987. (p) P. N. Bartlett and R. G. Whitaker, *J. Electroanal. Chem.*, 1987, **224**, 27–35.
2. (a) N. Oyama and F. C. Anson, *J. Am. Chem. Soc.*, 1979, **101**, 739. (b) N. Oyama and F. C. Anson, *J. Am. Chem. Soc.*, 1979, **101**, 3450. (c) K. Shigehara, N. Oyama and F. C. Anson, *Inorg. Chem.*, 1980, **20**, 518. (d) N. Oyama and F. C. Anson, *J. Electrochem. Soc.*, 1980, **127**, 247. (e) N. Oyama and F. C. Anson, *J. Electrochem. Soc.*, 1980, **127**, 640. (f) N. Oyama, T. Shimomura, K. Shigehara and F. C. Anson, *J. Electroanal. Chem.*, 1980, **112**, 271. (g) N. S. Scott, N. Oyama and F. C. Anson, *J. Electroanal. Chem.*, 1980, **110**, 303. (h) T. Shimomura, N. Oyama and F. C. Anson, *J. Electroanal. Chem.*, 1980, **112**, 265. (i) K. Shigehara, N. Oyama and F. C. Anson, *J. Am. Chem. Soc.*, 1981, **103**, 2552. (j) N. Oyama, S. Yamaguchi, Y. Nishita, K. Tokida, H. Matsuda and F. C. Anson, *J. Electroanal. Chem.*, 1982, **139**, 371.
3. (a) P. Denisovich, H. D. Abruna, C. R. Leidner, T. J. Meyer and R. W. Murray, *Inorg. Chem.*, 1982, **21**, 2153. (b) J. M. Calvert and T. J. Meyer, *Inorg. Chem.*, 1982, **21**, 3978. (c) E. M. Kober, B. P. Sullivan, W. J. Dressiale, J. W. Caspar and T. J. Meyer, *J. Am. Chem. Soc.*, 1980, **102**, 7387. (d) J. S. Facci, R. H. Schmehl and R. W. Murray, *J. Am. Chem. Soc.*, 1982, **104**, 4959. (e) J. S. Facci and R. W. Murray, *Anal. Chem.*, 1982, **54**, 7721. (f) R. W. Murray, *Ann. Rev. Mat. Sci.*, 1984, **14**, 145. (g) R. W. Murray, *Philos. Trans. R. Soc. London*, 1981, **A302**, 253.
4. (a) P. Yeh and T. Kuwana, *Chem. Lett.*, 1977, 1145. (b) E. F. Bowden, F. M. Hawkridge and H. N. Blount, *J. Electroanal. Chem.* 1984, **161**, 355. (c) D. E. Reed and F. M. Hawkridge, *Anal. Chem.*, 1987, **59**, 2334. (d) J. L. Willit and E. F. Bowden, *J. Electroanal. Chem.*, 1987, **221**, 265. (e) K. B. Koller and F. M. Hawkridge, *J. Electroanal. Chem.*, 1988, **239**, 291. (f) E. F. Bowden, F. M. Hawkridge and H. N. Blount, "Electrochemical Aspects of Bioenergetics" in *Comprehensive Treatment of Electrochemistry*, Vol. 10, S. Srinavasan *et al.* (Eds.), Plenum, 1985, pp. 297–346. (g) J. E. Frew and H. A. O. Hill, *Phil. Trans. Royal Soc. Lond.*, 1987, **B316**, 95–106. (h) H. A. O. Hill, *Pure & Appl. Chem.*, 1987, 743. (i) F. A. Armstrong, H. A. O. Hill and N. J. Walton, *Acc. Chem. Res.*, 1988, **21**, 407. (j) M. J. Eddowes and H. A. O. Hill, *J. Chem. Soc., Chem. Commun.*, 1977, 771. (k) M. J. Eddowes, H. A. O. Hill and K. Uosaki, *J. Am. Chem. Soc.*, 1979, **101**, 4461. (l) M. J. Eddowes, H. A. O. Hill and K. Uosaki, *Bioelectrochem. Bioenerg.*, 1980, **7**, 527. (m) A. E. G. Cass, M. J. Eddowes, H. A. O. Hill, K. Uosaki, R. C. Hammond, I. J. Higgins and E. Plotkin, *Nature*, 1980, **285**, 673. (n) K. Uosaki and H. A. O. Hill, *J. Electroanal. Chem.*, 1981, **122**, 321. (o) W. J. Albery, M. J. Eddowes, H. A. O. Hill and A. R. Hillman, *J. Am. Chem. Soc.*, 1981, **103**, 3904. (p) M. J. Eddowes, H. A. O. Hill and K. Uosaki, *J. Am. Chem. Soc.*, 1979, **101**, 7113.
5. (a) E. F. Bowden and H. Assefa, *Biochem. Biophys. Res. Comm.*, 1986, **139**, 1003.
6. (a) Y. Degani and A. Heller, *J. Phys. Chem.*, 1987, **91**, 1285. (b) Y. Degani and A. Heller, *J Am. Chem. Soc.*, 1988, **110**, 2615. (c) A. Heller and Y. Degani In *Proceedings of the Third*

International Symposium on Redox Mechanism and Interfacial Properties of Molecules of Biological Importance, G. Dryhurst and K. Niki, Eds., Honolulu, HI, Plenum Publ. Corp., New York, 1988, p. 151. (d) P. N. Bartlett, R. G. Whitaker, M. J. Green and J. Frew, *J. Chem. Soc., Chem. Commun.*, 1987, 1603.
7. Y. Degani and A. Heller, *J. Amer. Chem. Soc.*, 1989, **111**, 2357.
8. M. V. Pishko, I. Katakis, S.-E. Lindquist, L. Ye, B. A. Gregg and A. Heller, *Angewandte Chemie*, 1990, **29**(1), 82–84.
9. (a) D. A. Buckingham, F. P. Dwyer, H. A. Goodwin and A. M. Sargeson, *Aust. J. Chem.*, 1964, **17**, 325. (b) P. A. Lay, A. M. Sargeson and H. Taube, *Inorg. Syn.*, 1986, **24**, 291–306.
10. (a) N. Cenas, A. Pocius and J. Kulys, U.S.S.R. Patent, SU 1,016,306 A1, 7 May, 1983; Chem. Abs., 1983, **99**, 140649. (b) A. Pocius, N. Cenas, J. Kulys and Liet, *TSR Moksla. Akad. Darb. Ser. B*, 1984, **3**, 37; Chem. Abs., 1985, **102**, 25153.
11. D. A. Buckingham, F. P. Dwyer and A. M. Sargeson, *Inorg. Chem.*, 1966, **5**, 1243.
12. E. M. Kober, J. V. Casper, P. B. Sullivan and T. J. Meyer, *Inorg. Chem.*, 1988, **27**, 4587–4598.
13. B. A. Petersson, *Anal. Chim. Acta*, 1988, **209**, 231.
14. E. Laviron, *J. Electroanal. Chem.*, 1980, **112**, 1; *J. Electroanal. Chem.*, 1980, **112**, 11; *J. Electroanal. Chem.*, 1981, **122**, 37.
15. P. J. Peerce and A. J. Bard, *J. Electroanal. Chem.*, 1980, **114**, 89.
16. P. Daum, J. R. Lenhard, D. Rolison and R. W. Murray, *J. Amer. Chem. Soc.*, 1980, **102**, 4649.
17. P. Nicholls, *Biochim. Biophys. Acta*, 1979, **346**, 261.
18. (a) I. Nagata and H. Morawetz, *Macromolecules*, 1981, **14**, 87. (b) A. Katchalsky, *Pure Appl. Chem.*, 1971, **26**, 327. (c) H. Eisenberg, *Biological Macromolecules and Polyelectrolytes in Solution*, Clarendon Press: Oxford, 1976. (d) S. L. Carnie, G. A. Christos and T. P. Creamer, *J. Chem. Phys.*, 1988, **89**, 6484.
19. S. Nakamura, S. Hayashi and H. Koga, *Biophys. Acta*, 1976, **445**, 294.

Reprinted from Analytical Chemistry, 1993, 65.

Miniaturized Flexible Amperometric Lactate Probe

Dan Li Wang and Adam Heller*

Department of Chemical Engineering, The University of Texas at Austin, Austin, Texas 78712-1062

A flexible lactate electrode was made of 400 ± 100 7-μm-diameter carbon fibers, epoxy embedded in a 0.3-mm-diameter polyimide tubing. The electrode was modified by precipitating on it the relatively insoluble complex formed between 1100 kDa partially *N*-ethylamine quaternized poly[(vinylpyridine)-Os(bipyridine)$_2$Cl]Cl (POs-EA) and lactate oxidase. The steady-state lactate electrooxidation current, at 2 mM lactate concentration and at 22 °C, was 400 nA. The 50 ± 10 μAc cm^{-2} current density and the 20 mA cm^{-2} M^{-1} sensitivity decreased only by 5% when the partial pressure of oxygen was increased from 0.0 to 0.2 atm. The electrode retains its sensitivity after dry storage at 4 °C for 4 months in air but loses half of its sensitivity in 7 h at 37 °C through polymer desorption when operated at 0.4 V (SCE). To eliminate interference by species that are electrooxidized at 0.4 V (SCE), the lactate-sensing probe was (a) electrically insulated with an epoxy made of poly(vinylimidazole) cross-linked with ethylene glycol diglycidyl ether and (b) coated with an immobilized horseradish peroxidase (HRP)/glucose oxidase (GOX) film. The latter film was formed by coimmobilizing the two enzymes through periodate oxidation of their oligosaccharides to aldehydes and forming Schiff bases between the polyaldehydes and the enzymes' lysyl amines. In the presence of 1 mM glucose and in air, the interfering electrooxidation of 0.1 mM ascorbate was reduced by a factor of 20. This reduction results from formation of hydrogen peroxide in the glucose-catalyzed reaction and H_2O_2 oxidation of the ascorbate in a reaction catalyzed by HRP.

INTRODUCTION

Simple glucose electrodes have been made by adsorbing a poly[(vinylpyridine)Os(bipyridine)$_2$Cl]Cl (POs-EA) derivative on graphite, rinsing, and then complexing glucose oxidase to the adsorbed polymer.[1] Upon complexing, the adsorbed redox polymer binds and penetrates the enzyme and establishes electrical contact between the redox centers of the enzyme and a graphite electrode.[2] Here we apply such a complexing process to forming lactate electrodes on flexible bundles of epoxy-embedded, polyimide tubing-contained, carbon fibers. The electrodes are coated with an interferant-eliminating layer, containing coimmobilized horseradish peroxidase (HRP) and glucose oxidase (GOX). In an aerated glucose solution, H_2O_2 is generated within the film through the GOX-catalyzed reaction. The H_2O_2 oxidizes the interferants, but not lactate, in the HRP-catalyzed reaction. The interference elimination process is built on that described for glucose electrodes, where lactate oxidase has been used to generate H_2O_2 in a lactate-containing aerated solution.[3]

Lactate oxidase from *Pediococcus sp.* commonly used in amperometric lactate sensors,[4] has been used throughout this work. The enzyme catalyzes reaction 1 and also the oxidation of the $FADH_2$ by O_2, whereby H_2O_2 is formed. Amperometric

$$\text{LOX–FAD} + \text{lactate} \rightarrow \text{pyruvate} + \text{LOX–FADH}_2 \quad (1)$$

lactate sensors have been based on this reaction combined with reactions 2 and 3, where M_{ox} and M_{re} are the oxidized

$$\text{LOX–FADH}_2 + 2M_{ox} \rightarrow \text{LOX–FAD} + 2M_{re} \quad (2)$$

$$M_{re} \rightarrow M_{ox} + 2\,e^- \quad (3)$$

and the reduced forms of a diffusional mediator, such as O_2/H_2O_2 or Fc^+/Fc (where Fc is a ferrocene derivative).[5-10] FAD/$FADH_2$ centers of LOX were also nondiffusionally electrically connected to electrodes through a three-dimensional redox epoxy-based electron-relaying network.[4,6]

Lactate monooxygenase from *Mycobacterium smegmatis*, having an FMN cofactor, has also been applied in lactate sensors. This enzyme catalyzes the oxidation of lactate by oxygen to acetic acid and carbon dioxide.[11] However, the enzyme is inhibited by phosphate,[12] an ion present in blood and other tissues, whereas lactate oxidase from *Pediococcus sp.* is not inhibited by phosphate. Because the sensor is to be used in phosphate-containing physiological solutions, the *Pediococcus* enzyme was used in this work.

In vivo measurement of lactate is of clinical interest in monitoring shock, respiratory insufficiency, and heart failure.[13] Miniaturization and flexibility of sensors is relevant to lactate monitoring at a specific site or in an organ where tissue damage upon electrode insertion must be avoided. Miniature glucose sensors[14-18] based on glucose oxidase, an enzyme of higher specific activity than that of lactate oxidase (LOX), have been reported.[14-18] One limit imposed on miniaturization is defined by the achievable current

(1) Piahko, M. V.; Katakis, I.; Lindquist, S.-L.; Ling, Y.; Gregg, B. A.; Heller, A. *Angew. Chem., Int. Ed. Engl.* **1990**, *29*, 82–4.
(2) Heller, A. *J. Phys. Chem.* **1992**, *96*, 3579–87.
(3) Maidan, R.; Heller, A. *J. Am. Chem. Soc.* **1991**, *113*, 9003–4.
(4) Katakis, I.; Heller, A. *Anal. Chem.* **1992**, *64*, 1008–13.
(5) Wandrug, J.; Tvede, K.; Grinsted, J.; Jordening, H. *Clin. Chem.* **1989**, *35/8*, 1740–3.
(6) Hajizadeh, K.; Halsall, H. B.; Heineman, W. *Talanta* **1991**, *38*, 17–47.
(7) Sechaud, F.; Peguin, S.; Coulet, P. R.; Bardeletti, G.: *Process Biochem.* **1989**, *24* (Feb), 33–8.
(8) Cass, A. E.; Davis, G.; Francis, G. D.; Hill, H. A. O.; Aston, W. J.; Higgins, I. J.; Plotkin, E. V.; Scott, L. D.; Turner, A. P. F. *Anal. Chem.* **1984**, *56*, 667–71.
(9) Schuhmann, W.; Loffler, U.; Wohlschlager, H.; Lammert, R.; Schmidt, H.-L.; Wiemhofer, H. D.; Gopel, W. *Sens. Actuators* **1990**, *B1*, 571–5.
(10) Loffler, U.; Wiemhofer, H. D.; Gopel, W. *Biosens. Bioelectron.* **1991**, *6*, 343–8.
(11) Lockridge, O.; Massey, V.; Sullivan, P. A. *J. Biol. Chem.* **1972**, *247*, 8097–160.
(12) Takemori, S.; Nakai, Y.; Katakiri, M.; Nakamura, T. *FEBS Lett.* **1969**, *3*, 214–6.
(13) Mascini, M.; Moscone, D.; Palleschi, G. *Anal. Chim. Acta* **1984**, *157*, 45–51.
(14) Piahko, M. V.; Heller, A. *Anal. Chem.* **1991**, *63*, 2268–72.
(15) Yokoyama, K.; Sode, K.; Tamiya, E.; Karube, I. *Anal. Chim. Acta* **1989**, *218*, 137–42.
(16) Suzuki, H.; Tamiya, E.; Karube, I. *Anal. Chem.* **1988**, *60*, 1078–80.
(17) Tamiya, E.; Karube, I.; Hattori, S.; Suzuki, M.; Yokoyama, K. *Sens. Actuators* **1989**, *18*, 297–307.
(18) Gernet, S.; Koudelka, M.; De Rooij, N. F. *Sens. Actuators* **1989**, *17*, 537–40.

0003-2700/93/0365-1069$04.00/0

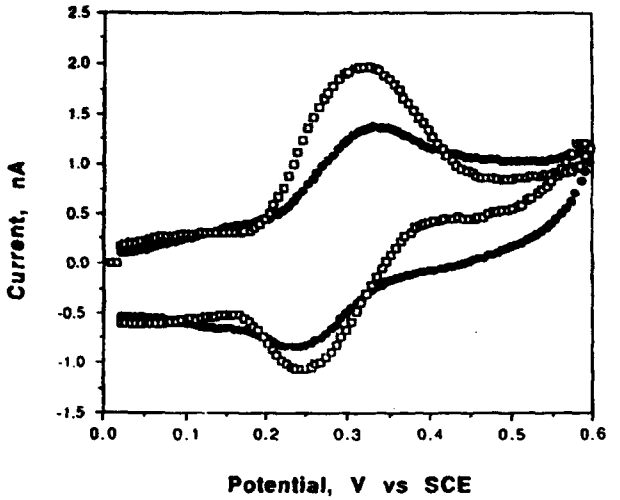

Figure 2. Cyclic voltammograms of 0.5 mM *cis*-bis(2,2′(4-methylamino)bipyridine-*N*,*N*′)dichloroosmium(II) on a carbon fiber-bundle electrode in pH 7.13 phosphate buffer with 0.1 M NaCl at 10V/s scan rate: (●) without Triton X-100 treatment of the electrode; (□) with Triton X-100 treatment of the electrode.

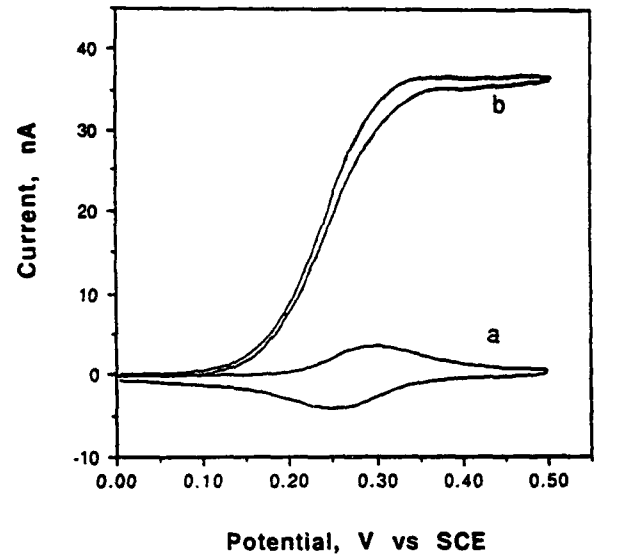

Figure 3. Cyclic voltammograms of the lactate electrode in pH 7.13 phosphate buffer with 0.1 M NaCl, under air: scan rate, 2 mV/s; (a) no lactate, (b) 2.0 mM lactate.

enzyme and redox polymer containing gel.[14] Such characteristics are obviously not realized in the fiber bundle.

Figure 2 shows the doubling of i_p in peaks of the cyclic voltammogram [of a *cis*-bis(2,2′(4-methylamino)bipyridine-*N*,*N*′)dichloroosmium(II) solution] upon Triton-X-100 treatment of the electrode. Evidently adsorption of the nonionic detergent Triton X100 inproves the wetting of the surface by the solution.

Figure 3 shows cyclic voltammograms of the carbon fiber-bundle electrode without lactate and with 2 mM lactate. In the absence of lactate, the separation of the anodic and the cathodic peaks is 40 ± 20 mV. An increase in peak separation with scan rate is observed in thicker films, produced by cross-linking the enzyme polymer complex with polyethylene glycol diglycidyl ether.[20] For a fast, strongly adsorbed redox couple the separation would have been nil, while for a nonadsorbed fast redox couple the separation would have been 59 mV. Maintenance of the electrode at +0.4 V (SCE) for a prolonged period leads to loss of non-cross-linked redox polymer. This is evident from the reduction in the coulometrically measured charge associated with electroreduction and electrooxidation

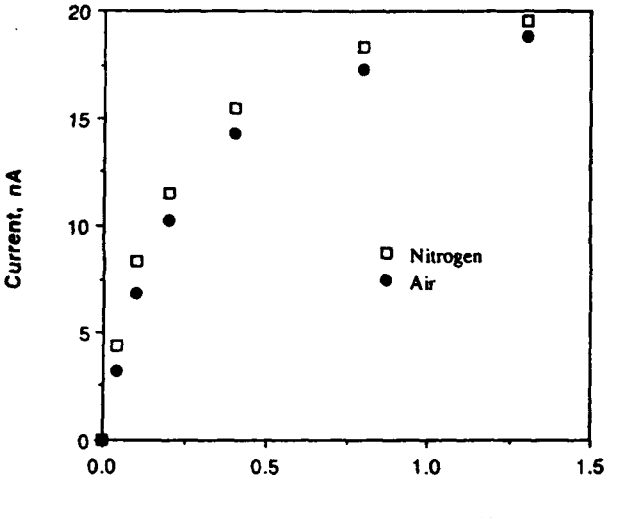

Figure 4. Steady-state lactate response of the electrode at 0.4 V (SCE): under nitrogen or air, in 0.02 M phosphate with 0.1 M NaCl, pH 7.13 at room temperature. Film composition: POs-EA:LOX = 3.1 (weight ratio).

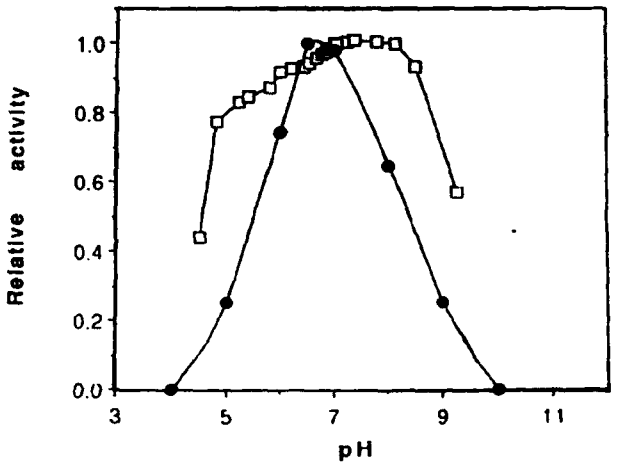

Figure 5. pH dependence of LOX's activity: (●) LOX in solution, H_2O_2 generation,[27] and (□) current of LOX immobilized on the electrode; 1 mM lactate, 0.02 M phosphate with 0.1 M NaCl, in air, room temperature.

of the polymer. When 2 mM lactate is added to the solution, only an electrocatalytic oxidation current is observed at scan rates below 5 mV/s. In the absence of a cross-linker the POs-EA/LOX layer thickness, estimated by $Os^{2+/3+}$ coulometry, is 0.5 ± 0.2 μm (assuming that the molecular weight of each Os-containing segment is 1100 and that the polymer's density is near 1 g/cm³). When the POs-EA complexes the enzyme, precipitation is observed at 1:1 and 1:3 polymer to enzyme ratios.[26] Thus, the film formed on the fiber-bundle electrode contains a precipitate. Measurement of the oxygen sensitivity of the lactate fiber-bundle electrode made with a 1:1 polymer/enzyme weight ratio film (Figure 4) shows that the steady-state electrocatalytic current in air is only 3.6% below that in nitrogen at the physiologically relevant 1.5 mM lactate concentration.

The 10–90% rise time of the steady-state electrocatalytic current in a flow system at a 4 cm/s linear flow velocity (for an increase in lactate concentration from 0 to 2, 0 to 3, or 0 to 4 mM) is 12 s.

The pH dependence of the electrocatalytic current was measured in air at 1 mM lactate concentration and at a POs-

(26) Katakis, I.; Davidson, L.; Heller, A., unpublished results.

Table I. Storage Stability at 4 °C in Air

days	current (nA) at 2 mM lactate
0	11.1
30	10.5
62	11.6
77	10.1
120	11.9

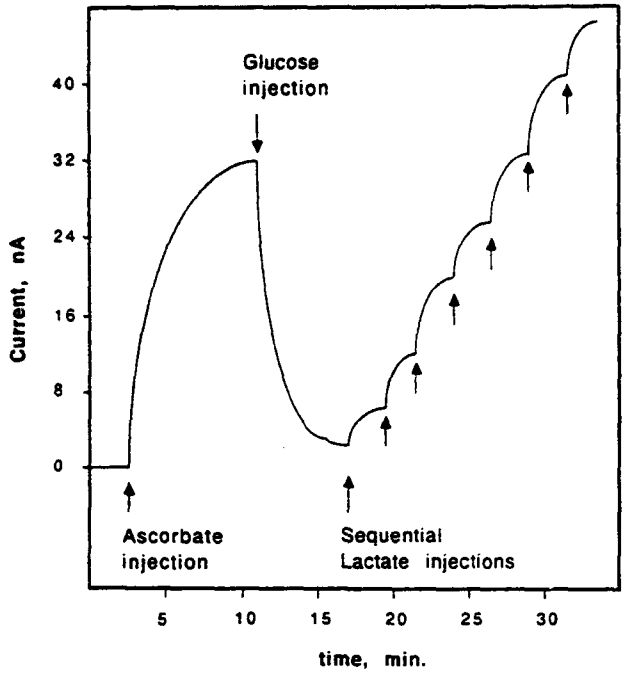

Figure 6. Reduction of ascorbate current by an HRP/GOX film. Conditions as in Figure 4, air.

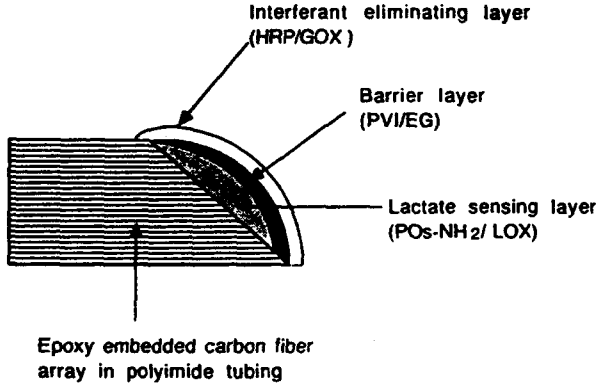

Figure 7. Schematic drawing of the lactate sensor showing the insulating barrier and the interferant-eliminating overlayer.

EA/LOX 3:1 weight ratio. The current is constant within ±7% when the pH is varied between 6.4 and 8.5, the maximum being near pH 7.4 (Figure 5). The pH dependence of the current exhibits a broader pH optimum and a shift to higher pH relative to the natural reaction of the enzyme producing H_2O_2 by O_2 reduction. In an earlier reported macroelectrode with cross-linked lactate oxidase/redox polymer network,[4] the current was also within 20% of its maximum through the same 6.4–8.5 pH range. The current maximum was, however, at pH 8, not 7.4. This small but significant difference suggests that the precipitated POs-EA/LOX film and the diepoxide cross-linked film do not provide identical enzyme microenvironments.

As seen in Table I, an electrode stored at 4 °C for 4 months did not lose activity. In continuous operation of the lactate electrode at 0.45 V (SCE) and at 25 °C, the current drops in

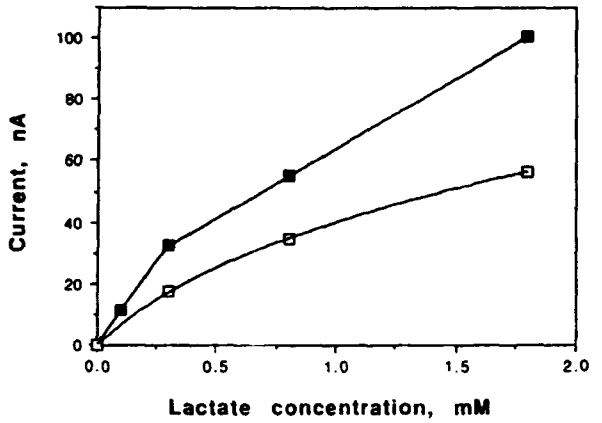

Figure 8. Steady-state lactate response curves for electrodes without (■) and with (□) barrier layers. Conditions as in Figure 4, air.

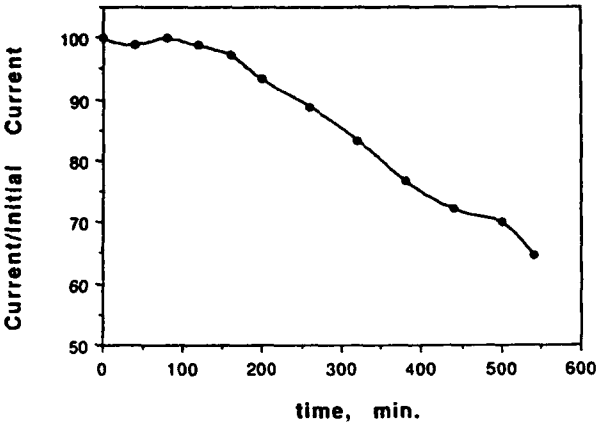

Figure 9. Decay of the steady-state current of the electrode coated with POs-EA/LOX (1:1 weight ratio): 2 mM lactate; conditions as in Figure 4, air.

6 h to 75% of its initial value (Figure 6), primarily because of polymer desorption at positive potentials, where the polycation is highly charged. This desorption is evidenced by the reduced coulometrically measured charge upon electroreduction or electrooxidation of the adsorbate in the absence of lactate.

Figure 7 illustrates the electrode structure with lactate-sensing and interference-eliminating layers. As in glucose sensors, oxidizable species present in physiological samples (serum or blood), such as ascorbate, urate, or acetaminophen (Tylenol) interfere with the sensing of lactate. An interferant-eliminating layer preoxidizes the interferants on their way to the sensing layer through reactions 4 and 5.[2] In eq 5, HA is

$$\text{glucose} + O_2 \xrightarrow{\text{GOX}} \beta\text{-gluconolactone} + H_2O_2 \qquad (4)$$

$$H_2O_2 + 2HA \xrightarrow{\text{HRP}} 2A + 2H_2O \qquad (5)$$

an interfering hydrogen donor. The physiological glucose concentration in serum or in blood (3–10 mM) generates enough hydrogen peroxide to preoxidize all interferants in the presence of HRP, and the enzyme-catalyzed preoxidation of interfering hydrogen donors is fast enough to prevent the interferants from reaching the lactate-sensing layer.[2] In the structure shown in Figure 7, an electrically insulating barrier layer prevented electron transfer to oxidized HRP from the LOX-wiring redox polymer. The insulating layer was thick enough to prevent electrical communication between the sensing and the interferant-eliminating layers, yet thin enough

so as not to hinder substrate or product diffusion.[27]

Figure 8 shows calibration curves for HRP/GOX-coated interference-eliminating electrodes made with and without electrically insulating PVI/EG barrier layers between the sensing and interference-eliminating layers. The barrier layer reduced the current by ~40% and increased the 10–90% rise time from 12 s to ~1 min. The left side of Figure 9 shows the reduction of interference by ascorbate (0.1 mM). When glucose (1 mM) was added, ~95% of the ascorbate-related current was eliminated. The right side of the figure shows the increase in current upon increasing stepwise the lactate concentration from 0 to 2 mM. Because lactate was not oxidized by H_2O_2/HRP, the electrode continued to respond normally to lactate. Figure 10 shows lactate calibration curves with and without 0.1 mM ascorbate. The current measured with 0.1 mM ascorbate was ~7.5% higher than that with no ascorbate. Part of the increase resulted from the reduction in oxygen partial pressure caused by consumption of oxygen in the oxidation of glucose in the outer layer. The observed 7.5% current increase was, however, characteristic only of the 3:1 enzyme/polymer film electrode, where oxygen competition was greater than in the 1:1 electrode. In the 1:1 electrode, oxygen competition suppressed the current by only 3.6% and the ascorbate elmination related current increase was correspondingly smaller. Earlier we showed that in glucose sensors the combination of all interferants (ascorbate, urate, and acetaminophen) at their physiological levels was preoxidized in interference-eliminating LOX/HRP films. The physiological lactate concentrations (1–3 mM) are lower than physiological glucose concentrations (3–10 mM), and glucose oxidase activity is higher than lactate oxidase activity in the films. Therefore, we project that at physiological glucose concentrations the entire group of electrooxidizable interferants with lactate measurements will be effectively preoxidized.

(27) Maidan, R.; Heller, A. *Anal. Chem.*, in press.

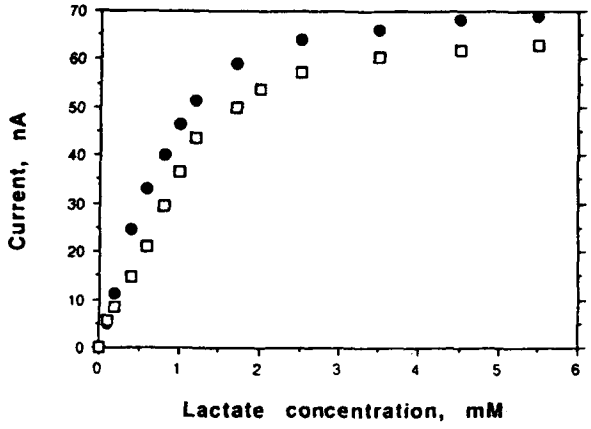

Figure 10. Steady-state lactate current without (□) and with (●) 0.1 mM ascorbate in the solution. Conditions as in Figure 4, air.

After immobilizing its components and overcoating with a bioinert film, the electrode should be practical for whole-blood lactate assay and for implantation.

ACKNOWLEDGMENT

Parts of the work were supported by the Office of Naval Research, the National Institutes of Health under Grant 1RO1 DK42015-01A1, the National Science Foundation, and the Robert A. Welch Foundation.

RECEIVED for review October 1, 1992. Accepted January 12, 1993.

Reprinted from Analytical Chemistry, 1992, 64.

Elimination of Electrooxidizable Interferant-Produced Currents in Amperometric Biosensors

Ruben Maidan and Adam Heller*

Department of Chemical Engineering, The University of Texas at Austin, Austin, Texas 78712-1062

Electrooxidizable ascorbate, urate, and acetaminophen that interfere with amperometric glucose assays are completely and rapidly oxidized by hydrogen peroxide in a multilayer electrode. The multilayer electrode is composed of an immobilized, but not electrically "wired", horseradish peroxidase (HRP) film coated onto a film of electrically "wired" glucose oxidase (GO). The "wired" enzyme is connected by a redox epoxy network to a vitreous carbon electrode. The current from the electrooxidizable interferants is decreased by their peroxidase-catalyzed preoxidation by a factor of 2500, and the glucose/interferant current ratio is increased 10^3-fold. Undesired electroreduction of hydrogen peroxide can result when HRP is also "wired" to the electrode. Such unwanted "wiring" is prevented by incorporating an electrically insulating barrier layer between the wired GO film and the HRP film. The hydrogen peroxide necessary for elimination of interferants can be added externally, or when this is not possible, it can be generated in situ by means of a coupled enzyme reaction.

INTRODUCTION

Electrooxidizable biological fluid constituents, such as ascorbate, urate, and acetaminophen, interfere with the amperometric assay of glucose. Interference is not restricted to a particular type of glucose sensing anode. It is encountered in electrodes diffusionally mediated by O_2/H_2O_2 or ferrocene derivatives and in electrodes with redox polymers that relay electrons from $FADH_2$ centers of glucose oxidase to electrodes.[1-5] In the latter, interferants are electrooxidized both at the electrode surface and by the redox polymer that is directly electrically connected to the electrode.

In hydrogen peroxide type electrodes the selectivity can be improved by electrode coatings that increase the overpotential of interferant electrooxidation, but not that of H_2O_2 oxidation;[6] by membranes that exclude the interferants by size or charge; and by preoxidation of interferants at a separate flow-through electrode. Yacynych et al.[7,8] showed that electropolymerized diaminobenzene and resorcinol form on electrodes charge and size-excluding films that are H_2O_2 permeable, but effectively exclude interferants in H_2O_2 type glucose sensors. Using low (100) molecular weight cutoff membranes, Guilbault et al. excluded from surfaces interferants other than acetaminophen.[9] Lobel and Rishpon[10] and Beh et al.[11] used cellulose acetate as an exclusion membrane. Harrison et al.[12] and Bindra and Wilson[13] used Nafion-type, sulfonated perfluorinated polymers for exclusion of anionic interferants, while Gorton et al. used other sulfonated polymers for their exclusion.[14] Ikeda et al. preelectrooxidized ascorbate and urate on a gold minigrid,[15] while Yao et al.,[16] as well as Okawa et al.,[17] used flow-through electrolytic oxidation columns. Yao[18] used an oxidizing cupric complex containing precolumn. Ascorbate was also eliminated through its ascorbate oxidase catalyzed oxidation by Nagy et al.[19] and by Wang et al.[20]

Here we discuss horseradish peroxidase (HRP) catalyzed preoxidation of interferants. After HRP is oxidized by H_2O_2 it rapidly oxidizes both neutral and charged interferants. It does not oxidize, however, either glucose or lactate at an appreciable rate. Peroxidases are well-known catalysts for oxidation of hydrogen donors (HA) by H_2O_2, accepting electrons from phenols, amino acids, benzidines, ascorbate,

(1) Scheller, F. W., Pfeiffer, D.; Schubert, F.; Renneberg, R.; Kirstein, D. In *Biosensors Fundamentals and Applications*; Turner, A. P. F., Karube, I., Wilson, G. S., Eds.; Oxford University Press: Oxford, 1987; pp 315-346.
(2) Coury, L. A., Jr.; Huber, E. W.; Heineman, W. R. In *Applied Biosensors*; Wise, D. L., Ed.; Butterworths: Boston, 1989; pp 1-37.
(3) Hill, H. A. O.; Sanghera, G. S. In *Biosensors, A Practical Approach*; Cass, A. E. G., Ed.; Oxford University Press: Oxford, 1990; pp 19-46.
(4) (a) Heller, A. *Acc. Chem. Res.* **1990**, *23*, 128-134. (b) Heller, A. *J. Phys. Chem.* **1992**, *96*, 3579-3587.
(5) Cass, A. E. G.; Davis, G.; Francis, G. D.; Hill, H. A. O.; Aston, W. J.; Higgins, I. J.; Plotkin, E. V.; Scott, D. L.; Turner, A. P. F. *Anal. Chem.* **1984**, *56*, 667-671.
(6) Falat, L.; Cheng, H.-Y. *Anal. Chem.* **1982**, *54*, 2108-2111.
(7) Sasso, S. V.; Pierce, R. J.; Walla, R.; Yacynych, A. M. *Anal. Chem.* **1990**, *62*, 1111-1117.
(8) Geise, R. J.; Adams, J. M.; Barone, N. J.; Yacynych, A. M. *Biosens. Bioelectron.* **1991**, *6*, 151-160.
(9) Palleschi, G.; Nabi Rahni, M. A.; Lubrano, G. J.; Ngwainbi, J. N.; Guilbault, G. G. *Anal. Biochem.* **1986**, *159*, 114-121.
(10) Lobel, E.; Rishpon, J. *Anal. Chem.* **1981**, *53*, 51-53.
(11) Beh, S. K.; Moody, G. J.; Thomas, J. D. R. *Analyst* **1991**, *116*, 459-462.
(12) Harrison, D. J.; Turner, R. F. B.; Baltes, H. P. *Anal. Chem.* **1988**, *60*, 2002-2007.
(13) Bindra, D. S.; Wilson, G. S. *Anal. Chem.* **1989**, *61*, 2566-2570.
(14) Gorton, L.; Karan, H. I.; Hale, P. D.; Inagaki, T.; Okamoto, Y.; Skotheim, T. A. *Anal. Chim. Acta* **1990**, *228*, 23-30.
(15) Ikeda, T.; Katasho, I.; Senda, M. *Anal. Sci.* **1985**, *1*, 455-457.
(16) Yao, T.; Kobayashi, Y.; Sato, M. *Anal. Chim. Acta* **1983**, *153*, 337-340.
(17) Okawa, Y.; Kobayashi, H.; Ohno, T. *Chem. Lett.* **1991**, 849-852.
(18) Yao, T. *Anal. Chim. Acta* **1983**, *153*, 175-180.
(19) Nagy, G.; Rice, M. E.; Adams, R. N. *Life Sci.* **1982**, *31*, 2611-2616.
(20) Wang, J.; Naser, N.; Ozsoz, M. *Anal. Chim. Acta* **1990**, *234*, 315-320.

0003-2700/92/0364-2889$03.00/0

urate, and NADH.[21,22] The HRP-catalyzed reaction is

$$2HA + H_2O_2 \xrightarrow{HRP} 2A + 2H_2O \quad (1)$$

In an earlier communication[23] we showed that HRP films on glucose electrodes eliminate interferant-electrooxidation caused currents. Here we describe processes for forming the HRP-based interferant-eliminating films; analyze the parameters affecting the activity of these films; consider their unwanted interaction with glucose sensing layers, based on electrical connection of glucose oxidase redox centers to electrodes through electron-relaying redox polymer networks; describe methods of internal generation of H_2O_2 within HRP films; discuss the interfering peroxide electroreduction reaction;[24-28] and describe methods for making electrodes that are more selective for glucose.

EXPERIMENTAL SECTION

Materials. The glucose-sensing electrodes were made with our earlier described glucose oxidase "wiring" cross-linkable polymer, abbreviated as POs–EA. The polymer has a poly(vinylpyridine) backbone with part of the pyridines complexed to $[Os(bpy)_2Cl]^{+/2+}$ and with part of the pyridines quaternized with ethylamine.[29] Poly(vinylimidazole) (PVI) was prepared according to a published procedure.[30] Glucose oxidase, GO (EC 1.1.3.4, type X, 128 units/mg), horseradish peroxidase, HRP (EC 1.11.1.7, type I, 85 units/mg or type VI, 260 units/mg), and catalase (EC 1.11.1.6, 2600 units/mg) were purchased from Sigma. Lactate oxidase, LOD (from pediococcus sp., 33 units/mg), was supplied by Finnsugar. Poly(ethylene glycol) diglycidyl ether (MW 400) was purchased from Polysciences. All other chemicals were of the purest available commercial grade. Glutaraldehyde stock solutions were prepared using "grade I" solutions and kept frozen. Fresh stock solutions of ascorbate, urate, and acetaminophen were prepared *daily* because of their gradual decomposition. Stock solutions of glucose were allowed to mutarotate at room temperature for 24 h before use and were kept refrigerated. Stock solutions of hydrogen peroxide were prepared by diluting a 30% solution. The H_2O_2 solutions were normalized with potassium permanganate.[31]

The working electrodes were 3-mm-diameter glassy carbon rods (Atomergic V-10 grade) sealed in Teflon or glass tubes with epoxy resin. The electrodes were pretreated by sequentially polishing with 5.0-, 1.0-, and 0.3-μm alumina powder on a cloth felt, sonicated, rinsed with deionized water, and dried under nitrogen.

Glucose-sensing electrodes were prepared using a solution containing 2 mg/mL POs–EA, 0.12 mg/mL poly(ethylene glycol) diglycidyl ether, and 1 mg/mL glucose oxidase in a 5 mM pH 7.8 HEPES buffer solution. The polished electrode was coated with a 2-μL droplet of this mixture. The coating was cured for 48 h under vacuum at about 10 Torr.

To make the otherwise large pore size glucose-sensing redox polymer network impermeable to peroxidase, the electrode with the sensing layer was further cross-linked by dipping in a 0.25% glutaraldehyde solution for 5 s and then rinsed with a phosphate buffer solution. The barrier layer between the sensing and interferant-eliminating layers was made of a solution containing 10 mg/mL PVI and 2 mg/mL ethylene glycol diglycidyl ether. A 2-μL droplet of this solution was applied to the glucose-sensing layer and was cured for 48 h under vacuum.

Electrodes were made with HRP films immobilized (a) directly on the polished electrode surface, (b) on the sensing layer covered electrode after making the sensing layer impermeable to HRP with glutaraldehyde, and (c) on the electrode surface, coated first with the sensing and then with the barrier layer. The HRP was immobilized by one of two methods: one using glutaraldehyde,[32] the other involving $NaIO_4$ oxidation.[33] When glutaraldehyde was used, 5 μL of an HRP (type I) solution (100 mg/mL in a 0.1 M pH 7.3 phosphate buffer containing 5 mg/mL glutaraldehyde) was applied and left to air-dry and cure for 2 h. When the periodate method was used, 50 μL of a 12 mg/mL $NaIO_4$ solution was added to 100 μL of an HRP (type VI) solution (20 mg/mL in 0.1 M sodium bicarbonate) and incubated in the dark, at room temperature, for 2 h. After incubation, 10 μL of the oxidized enzyme solution was spread on the surface of the electrode and allowed to dry and cure for 2 h.

LOD containing HRP layers were prepared by co-immobilizing LOD with HRP using the above glutaraldehyde method except that the HRP solution now contained also 100 mg/mL LOD.

Measurements. Electrochemical experiments were performed with a Princeton Applied Research Model 273 potentiostat/galvanostat. Rotating disk electrode experiments were performed with a Pine Instruments AFMSRX rotator with an MSRS speed controller. The three-electrode cell contained 0.1 M NaCl buffered with phosphate (0.1 M, pH 7.2) coated as needed. Saturated calomel reference (SCE) and platinum wire auxiliary electrodes were used. All measurements were under air and at room temperature. The working electrode was rotated at 1000 rpm unless otherwise specified. In the constant potential experiments, the working electrode was poised at 0.4 V (SCE).

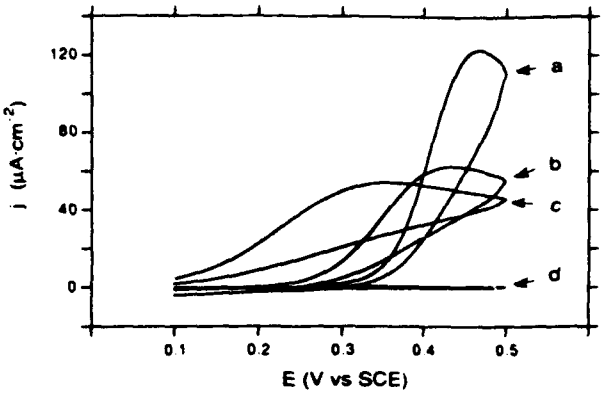

Figure 1. Cyclic voltammograms of an HRP-coated glassy carbon electrode in 1.0 mM interferant-containing solution in the absence of H_2O_2 and (a) acetaminophen; (b) urate; (c) ascorbate; (d) in the presence of 1.0 mM H_2O_2 and urate. Scan rate 10 mV/s.

RESULTS AND DISCUSSION

HRP Catalysis of Oxidation of Interferants by H_2O_2. Figure 1 shows cyclic voltammograms of the HRP film coated glassy carbon electrode in solutions with 10^{-3} M acetaminophen (a), urate (b), or ascorbate (c) but no H_2O_2, and also in a 10^{-3} M urate and 10^{-3} M H_2O_2 containing solution. The electrooxidation of urate, as well as that of the other interferants (not shown), is completely suppressed: the interferant electrooxidation currents reversibly reappear/disappear in solutions without/with H_2O_2. In controls, where the HRP is replaced by albumin in the immobilized film, the electrooxidation currents do not decrease upon addition of H_2O_2. In experiments with HRP-coated electrodes, decomposition of the peroxide by a small amount of catalase causes reappearance of the interferant electrooxidation waves as does addition of azide, a peroxidase inhibitor. We conclude from

(21) Mashly, A. C. *Methods Enzymol.* **1955**, *2*, 801–813.
(22) Dunford, H. B.; Stillman, J. S. *Coord. Chem. Rev.* **1976**, *19*, 187–251.
(23) Maidan, R.; Heller, A. *J. Am. Chem. Soc.* **1991**, *113*, 9003–9004.
(24) Kulys, J. J.; Laurinavicius, V.-S. A.; Pesliakiene, M. V.; Gureviciene, V. V. *Anal. Chim. Acta* **1983**, *148*, 13–18.
(25) Kulys, J.; Schmid, R. D. *Biosens. Bioelectron.* **1991**, *6*, 43–48.
(26) Tatsuma, T.; Watanabe, T. *Anal. Chim. Acta* **1991**, *242*, 85–89.
(27) Bourdillon, C.; Beley, M. *Nouv. J. Chim.* **1983**, *7*, 521–526.
(28) Durliat, H.; Couteix, A.; Comtat, M. *Bioelectrochem. Bioenerg.* **1980**, *22*, 197–209.
(29) Gregg, B. A.; Heller, A. *J. Phys. Chem.* **1991**, *95*, 5970–5975.
(30) Chapiro, A.; Mankowski, Z. *Eur. Polym. J.* **1988**, *24*, 1019–1028.
(31) Schumb, W. C.; Satterfield, C. N.; Wentworth, R. L. *Hydrogen Peroxide*; Reinhold: New York, 1955; Chapter 10.
(32) Wold, F. *Methods Enzymol.* **1972**, *25*, 623–651.
(33) Tijssen, P.; Kurstak, E. *Anal. Biochem.* **1984**, *136*, 451–457.

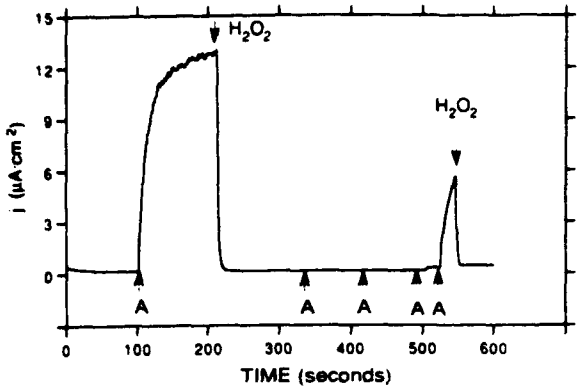

Figure 2. Elimination of the ascorbate electrooxidation current in an HRP-coated glassy carbon electrode. "A" denotes injection of ascorbate, each injection increasing its concentration by 0.1 mM; H_2O_2 denotes injection of hydrogen peroxide, each injection increasing its concentration by 0.2 mM. Glassy carbon electrode 0.4 V (SCE).

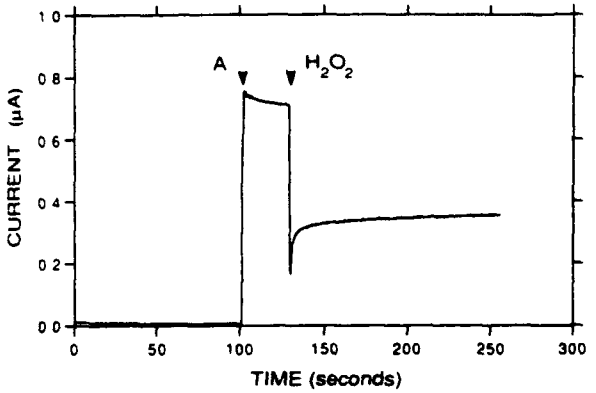

Figure 3. Partial elimination of ascorbate with a lightly loaded (60 units/cm^2) HRP electrode. "A" denotes injection of ascorbate (0.1 mM final concentration); "H_2O_2" denotes injection of H_2O_2 (0.2 mM final concentration). Glassy carbon electrode, 0.4 V (SCE).

these experiments that elimination of the interferants requires both HRP and peroxide.

Because our purpose was to improve the selectivity of glucose electrodes made by wiring glucose oxidase to a three-dimensional POs–EA bound redox epoxy,[34] most of our measurements were at 0.4 V (SCE), the plateau potential of these electrodes. Figure 2 shows the steady-state current of the HRP film coated electrode poised at this potential. Injection of ascorbate ("A") causes the appearance of an oxidation current that disappears upon addition of excess H_2O_2. Further ascorbate additions have no effect on the current as long as the peroxide is not exhausted. The experiment of Figure 2 was performed with an electrode heavily loaded with HRP. In this electrode interferant elimination was not controlled by the amount of enzyme, but by the ratio H_2O_2 to interferant. At low HRP loadings, the elimination reaction is controlled by the HRP activity of the film and/or by mass transport of the reactants.

To examine the effect of HRP loading, a series of electrodes with increasing HRP loadings was prepared. The loadings were chosen to be sufficiently light to allow only partial elimination of the ascorbate even in the presence of excess H_2O_2. Figure 3 shows that an electrode loaded with only 60 units/cm^2 HRP does not completely eliminate interference by 0.1 mM ascorbate. Results obtained for a series of electrodes with HRP loadings between 0 and 180 units/cm^{-2} are summarized in Table I. Loading of 180 units/cm^{-2} is, as seen, necessary to completely eliminate interference by 0.1 mM ascorbate. From Table I it is also evident that as the HRP layer thickness increases the electrooxidation current of ascorbate decreases even in the absence of H_2O_2 for the obvious reason that transport of ascorbate to the electrode is reduced. As expected, when the elimination is HRP-loading limited, increasing the hydrogen peroxide concentration does not decrease the interferant electrooxidation current. On the contrary, because HRP is inhibited by excessive H_2O_2 concentrations, the interferant oxidation current increases rather than decreases at high H_2O_2 concentrations. As a consequence, and as seen in Figure 3, when the electrode is HRP-limited, injection of a large excess of H_2O_2 causes first a drop, then an increase, in the interference current. This increase results from the buildup of the H_2O_2 concentration to an inhibiting level after the ascorbate has been depleted.

Table I. Effect of HRP Loading on the Effectiveness of Elimination of Ascorbate

HRP (units/cm^2)	I_A[a] (μA)	I_{AP}[b] (μA)	% elimination
0	3.48	3.48	0
15	1.67	1.39	16
30	1.22	0.78	23
45	0.89	0.47	44
60	0.74	0.34	52
90	0.66	0.16	74
150	0.55	0.08	86
180	0.48	0.00	100

[a] I_A, current measured for 0.1 mM ascorbate. [b] I_{AP}, current measured for 0.1 mM ascorbate and 0.2 mM H_2O_2.

Table II. Effect of Rotation Rate on the Effectiveness of Elimination of Ascorbate

ω (rpm)	I_A[a] (μA)	I_{AP}[b] (μA)	% elimination
0	0.27	0.09	68
10	0.52	0.32	39
20	0.65	0.42	36
50	0.86	0.60	30
70	0.95	0.67	29
100	1.04	0.76	27
200	1.23	0.94	23
500	1.47	1.20	18
700	1.56	1.30	17
1000	1.67	1.39	16
2000	1.89	1.59	15
4000	1.98	1.73	13

[a] I_A, current measured for 0.1 mM ascorbate. [b] I_{AP}, current measured for 0.1 mM ascorbate and 0.2 mM H_2O_2.

The extent of the ascorbate elimination is mass transfer dependent in HRP-loading limited (15 units/cm^{-2}) electrodes (Table II). An increase in electrode rotation rate now results in an increase in the ascorbate oxidation current both in the absence and in the presence of H_2O_2. At higher rotation rates the electrode, limited by its enzyme loading, copes only with a decreasing fraction of the arriving ascorbate.

As seen in Figures 2 and 3 the ascorbate electrooxidation current appears noisy, even though our system is not. The noise suggests that the electrooxidation of ascorbate might be chaotic or oscillatory.[35] Elimination of ascorbate by peroxide causes disappearance of the "noise".

Figure 4 shows a family of "titration" curves of ascorbate by H_2O_2. Elimination of interference by increasing concentrations of ascorbate requires increasing concentrations of peroxide. Because complete elimination of ascorbate at concentrations exceeding 8 mM requires H_2O_2 concentrations above HRP inhibiting levels, it cannot be accomplished using HRP, though noninhibited peroxidases are likely to eliminate

(34) Gregg, B. A.; Heller, A. *J. Phys. Chem.* **1991**, *95*, 5976–5980.

(35) Labuda, Ya.; Yatsimirskii, K. B. *Teor. Eksp. Khim.* **1991**, *27*, 39–45.

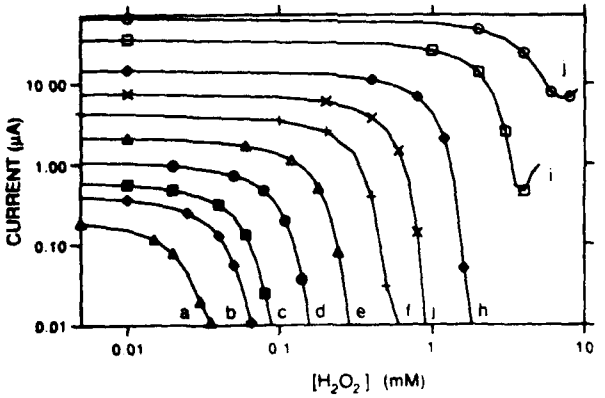

Figure 4. Titration of ascorbate by hydrogen peroxide using a HRP-coated electrode (250 units/cm²). Initial ascorbate concentrations: (a) 0.1 mM; (b) 0.2 mM; (c) 0.3 mM; (d) 0.5 mM; (e) 1.0 mM; (f) 2.0 mM; (g) 4.0 mM; (h) 8.0 mM; (i) 20.0 mM; (j) 40.0 mM.

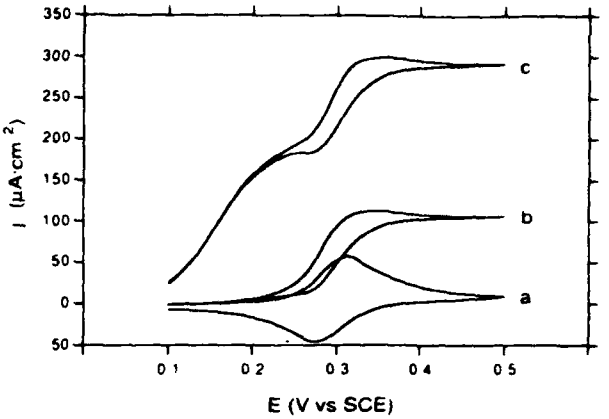

Figure 5. Cyclic voltammograms (a) in phosphate buffer; (b) with added 5.0 mM glucose; (c) with 5.0 mM glucose and 0.5 mM ascorbate. POs–EA/GO electrode; scan rate 2 mV/s.

concentrated interferants. Interference by ascorbate concentrations below 8 mM is completely eliminated with HRP films. Because only the interferant/H_2O_2 ratio in the solution is known, and the critical interferant/H_2O_2 ratio in the film is not, we observe variations between electrodes having different mass transfer characteristics.

In order to determine the upper limit of the interferant elimination capacity of HRP films, an electrode with a high loading of enzyme was prepared. In this electrode addition of H_2O_2 decreased the ascorbate electrooxidation current by a factor of >2500.

Processes for HRP Immobilization in Films. With the objective of simultaneously optimizing specific activity, permeability, and mechanical ruggedness, while not harming the underlying glucose-sensing layer, we evaluated several processes for making HRP films. After a preliminary survey we narrowed the immobilization processes to (a) cross-linking with glutaraldehyde; (b) periodate oxidation of HRP oligosaccharides to aldehydes and coupling with polyacrylamide hydrazide;[36,37] and (c) self-cross-linking of the periodate-oxidized HRP through formation of Schiff bases between the HRP–oligosaccharide-derived aldehydes and HRP–amines, such as lysylamines. The second and third method yielded smoother and better films. Glutaraldehyde cross-linking, though widely practiced, causes a greater loss in enzyme activity than periodate oxidation to HRP polyaldehyde, followed by formation of either poly(acrylhydrazones) or lysyl–Schiff bases. The films made of the HRP polyaldehyde adhered well to both uncoated and variously polymer coated electrodes and, unlike the glutaraldehyde films, did not crack during their drying and curing. The periodate process yielded the best films for HRP type VI, while with the glutaraldehyde process, the best results were obtained for HRP type I. The difference might be associated with differences in the amount or distribution of oligosaccharides in the various HRPs.

Interaction between the Glucose-Sensing and the Interferant-Eliminating Layers. Figure 5 shows cyclic voltammograms for an electrode modified with a glucose-sensing film consisting of a three-dimensional redox epoxy gel, formed of POs–EA and glucose oxidase upon cross-linking with PEGDE.[34] It is seen that in the 0.4–0.5 V (SCE) plateau and under the conditions of the experiment, the current increment associated with 5 mM glucose can be exceeded by that associated with 0.5 mM ascorbate. This is also the case for acetaminophen and for urate. Evidently electrooxidation of the three interferants takes place not only at the carbon

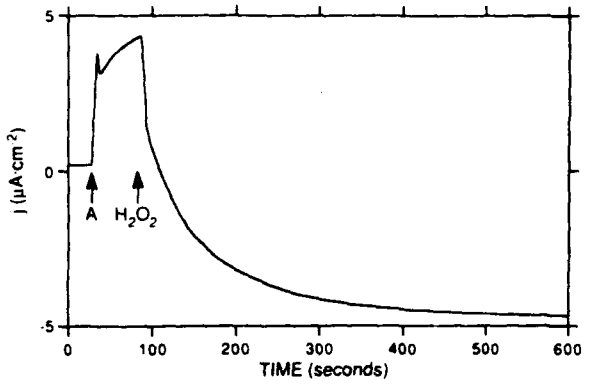

Figure 6. Current reversal upon adding H_2O_2 in an electrode having a POs–EA/GO-sensing layer coated with an HRP layer. "A" denotes injection of ascorbate (0.1 mM final concentration); "H_2O_2" denotes injection of hydrogen peroxide (0.2 mM final concentration). 0.4 V (SCE).

surface, but also in the electron-relaying glucose-sensing layer. While the rate of electrooxidation of glucose can be limited by the rate of electron transfer between enzyme $FADH_2$ centers and that fraction of the osmium centers that are in their proximity, electrooxidation of the interferants proceeds at any of the osmium centers. Therefore, its rate can be high. This, combined with the higher concentration of anionic interferants in the polycationic polymer,[38] aggravates the problem of interference. Fortunately the interference is completely eliminated in HRP film coated electrodes, as will be seen.

When an arbitrary HRP film is coated on the glucose-sensing electrode and the current associated with electrooxidation of ascorbate is measured (Figure 6), addition of H_2O_2 not only suppresses the anodic ascorbate current but reverses it, producing a cathodic current. Thus, interference through electrooxidation of ascorbate is now replaced by interference through electroreduction of H_2O_2. The H_2O_2 electroreduction current is seen also in the absence of ascorbate, but not in the absence of either the HRP or a redox-polymer network. Furthermore, HRP film mediated electroreduction of H_2O_2 takes place whether the HRP and the redox epoxy films are mixed or separated, as long as the two contact each other. Even loosely adsorbed HRP on the redox polymer produces a cathodic H_2O_2 electroreduction current. Dipping of the POs–EA redox epoxy-modified electrode in an HRP solution for a few minutes and rinsing also produces an electrode showing a cathodic current. We thus conclude that the HRP

(36) Nakane, P. K.; Kawaoi, A. *J. Histochem. Cytochem.* **1974**, *22*, 1084–1091.
(37) O'Shannessy, D. J.; Wilchek, M. *Anal. Biochem.* **1990**, *191*, 1–8.
(38) Wang, J.; Golden, T.; Tuzhi, P. *Anal. Chem.* **1987**, *59*, 740–744.

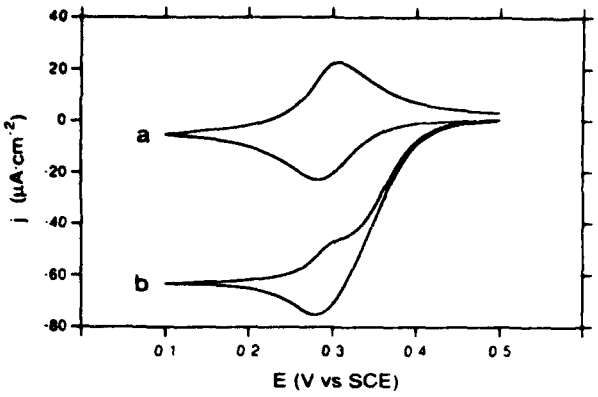

Figure 7. Reduction of hydrogen peroxide on a two-layer electrode having a POs–EA/GO-sensing layer coated with an HRP layer. Cyclic voltammograms (a) in a phosphate buffer solution; (b) with added H_2O_2 (0.1 mM). Scan rate 2 mV/s.

molecule (MW 40 000) can permeate into pores of the redox epoxy network when these are sufficiently large.

Permeation of the HRP into POs–EA is suggested by the following comparative experiments. Two five-electrode batches of thick-layer POs–EA electrodes were prepared (a) with HRP and (b) with bovine serum albumin (BSA). The BSA electrodes were then dipped in an HRP containing solution for 3 h. The peroxide response of the two batches became similar. In a control experiment two thick-layer POs–EA electrodes were prepared (a) with GO and (b) with BSA. The BSA electrode was dipped in a GO-containing solution for 24 h. The glucose response of the BSA electrode was still an order of magnitude smaller than that of the GO electrode. The difference between the first and second set of experiments is explained by the difference in the size of HRP and GO. GO being a larger enzyme (MW 160 000) permeates less into the POs–EA network when the BSA electrode is dipped in the GO-containing solution. It is adsorbed only on the outer surface of the POs–EA layer and is thus poorly "wired". HRP, being a relatively small enzyme (MW 40 000), permeates into the POs–EA network when the BSA electrode is dipped in a HRP-containing solution. The enzyme penetrates into the POs–EA film and is well "wired". The permeability of POs–EA films to HRP was also seen in experiments where the usual diepoxide cross-linker PEGDGE, with nine ethylene glycol units, was replaced by a short analog, MEGDGE, *mono*ethylene glycol diglycidyl ether. Similar electrodes were prepared with POs–EA, BSA, and either MEGDGE or PEGDGE. The electrodes were cured, exposed to HRP, and then poised at 400 mV in the presence of H_2O_2. The cathodic H_2O_2 reduction current of the electrode with the long cross-linker was 5 times higher than that of the short cross-linker. These results suggest that the more tightly cross-linked redox gel obtained with the short cross-linker is less permeable to the HRP.[11]

Figure 7 shows cyclic voltammograms of the POs–EA redox epoxy modified electrode coated with an electrically contacting HRP film in the absence of hydrogen peroxide (a) and in its presence (b). H_2O_2 electroreduction commences at +0.45 V (SCE) and reaches its plateau already at a potential as positive as +0.3 V (SCE). This obviously electrocatalytic reduction of H_2O_2 involves multiple steps, summarized by reactions 2 and 3.

$$2Os^{2+} + H_2O_2 + 2H^+ \xrightarrow{HRP} 2Os^{3+} + 2H_2O \qquad (2)$$

$$Os^{3+} + e^- \rightarrow Os^{2+} \qquad (3)$$

Diffusional redox-couple mediation of the reduction of hydrogen peroxide by peroxidases is well established and

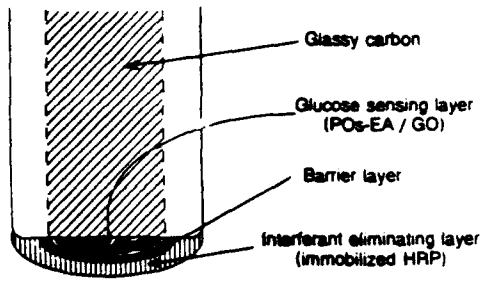

Figure 8. Three layers electrode for interferant elimination. A barrier layer electrically insulates the glucose-sensing layer from the interferant-eliminating layer.

forms the basis of peroxide-reducing electrodes.[39,40] Here the redox polymer network catalyzed electroreduction interferes with the assay glucose, lowering the glucose electrooxidation current.

We overcome the electroreduction of H_2O_2 by either electrically insulating the HRP film from the GO-redox polymer film or by poising the electrode (and thus the electrically connected network of the glucose sensing film) at a sufficiently oxidizing potential, where H_2O_2 is no longer catalytically reduced. This potential is near 0.5 V (SCE) (Figure 7). Because 0.5 V (SCE) is also near the threshold for electrooxidation of H_2O_2, electrical insulation by a barrier film is preferred for the most accurate glucose assays of biological fluids. In less demanding assays, poising the electrodes at 0.5 V (SCE) is, however, simple and adequate.

An electrode with an insulating barrier layer is shown schematically in Figure 8. Ideally, the insulating barrier layer will fully cover the surface of the sensing redox matrix, but will not be thick enough to substantially slow glucose transport to the sensing layer. Insulating films made of cellulose acetate, Nafion, and polypyrrole formed respectively by spin coating, casting, or electropolymerization were tested. These did not perform well: the H_2O_2 reduction current was only partially suppressed and the glucose current was considerably diminished. A good barrier layer was, however, prepared by cross-linking poly(vinylimidazole) with ethylene glycol diglycidyl ether. The resulting gel effectively prevented electrical contact between the sensing layer and did not excessively reduce the catalytic glucose electrooxidation current.

Another method of avoiding the electrical contact between the glucose-sensing layer and the HRP film involves making the redox polymer containing layer impermeable to HRP. When a POs–EA/GO/PEGDGE electrode was additionally cross-linked with glutaraldehyde, the electrode, when poised at 0.4 V (SCE), did not show a cathodic current in the presence of H_2O_2 after exposure to HRP. Evidently direct electrical communication between the redox polymer and HRP requires proximity of segments of the two. Exposure of the Os redox polymer to glutaraldehyde cross-links the matrix sufficiently to prevent diffusion of the 40 kDa HRP into the three-dimensional epoxy matrix.[39]

Interferant-Insensitive Glucose Electrodes. The just described results show the feasibility of three types of interferant eliminating electrodes that do not electroreduce H_2O_2: (a) two-layer electrodes poised at 0.4 V (SCE) with the sensing layer cross-linked and made HRP-impermeable by glutaraldehyde; (b) two-layer electrodes poised at 0.5 V (SCE); and (c) three-layer electrodes with a PVI-based electrically insulating barrier. The glucose response of a two-layer electrode of the second type is shown in Figure 9. In the

(39) Tatsuma, T.; Okawa, Y.; Watanabe, T. *Anal. Chem.* **1989**, *61*, 2352–2355.

(40) Frew, J. E.; Harmer, M. H.; Hill, H. A. O.; Libor, S. I. *J. Electroanal. Chem. Interfacial Electrochem.* **1986**, *201*, 1–10.

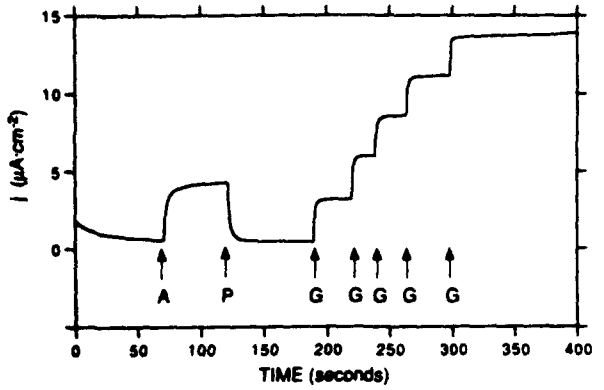

Figure 9. Elimination of interferants in a two-layer electrode. "A" denotes injection of ascorbate (0.1 mM final concentration); "P" denotes injection of hydrogen peroxide (0.2 mM final concentration); "G" denotes injection of glucose, increasing its concentration in 1.0 mM steps. 0.5 V (SCE).

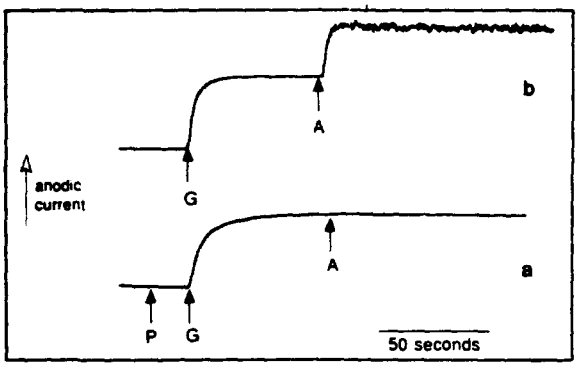

Figure 10. Effect of adding hydrogen peroxide on the current of a three layers electrode: additions of glucose (5 mM final concentration) "G" and ascorbate (0.1 mM final concentration) "A" (a) in the presence of and (b) in the absence of H_2O_2 ("P"). 0.4 V (SCE).

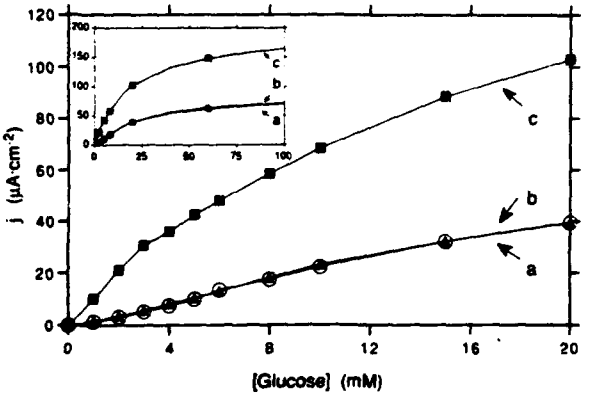

Figure 11. Dependence of the electrocatalytic glucose oxidation current density on glucose concentration: (a) bilayer electrode in the presence of hydrogen peroxide (0.5 mM) and physiological levels of interferants: [ascorbate] = 0.1 mM, [urate] = 0.5 mM, [acetaminophen] = 0.1 mM; (b) bilayer electrode, no interferants; (c) uncoated electrode, no interferants. The insert shows the dependence for a wider concentration range. 0.5 V (SCE).

presence of H_2O_2 no ascorbate related current is seen while the risetime is fast. Figure 10 shows results obtained with an electrode of the first type, having a glutaraldehyde-treated sensing layer, coated with an HRP film. In the presence of H_2O_2 only glucose is electrooxidized, and the measured current is dependent only on its concentration. In the absence of H_2O_2 both glucose and ascorbate are electrooxidized, and the measured current reflects the combined electrooxidation of glucose and ascorbate. Similar results were obtained for urate and acetaminophen.

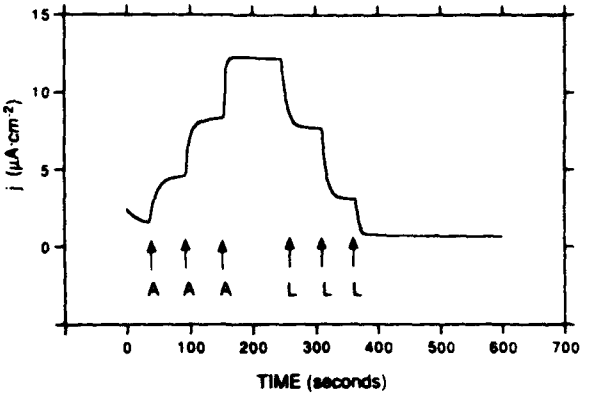

Figure 12. Elimination of ascorbate through in situ production of lactate in a three-layer electrode having an interferant eliminating layer with both HRP and LOD. "A" denotes an injection of ascorbate to increase its concentration by 0.1 mM steps; "L" denotes an injection of lactate to increase its concentration by 0.1 mM. 0.4 V (SCE).

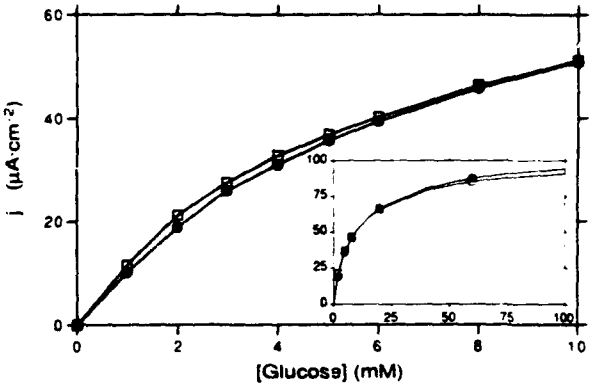

Figure 13. Dependence of the electrocatalytic oxidation current density on glucose concentration in an HRP/LOD-coated electrode: (a) (□) in the presence of lactate (0.5 mM) and physiological levels of three interferants: [ascorbate] = 0.1 mM, [urate] = 0.5 mM, [acetaminophen] = 0.1 mM; (b) (●) in the absence of interferants.

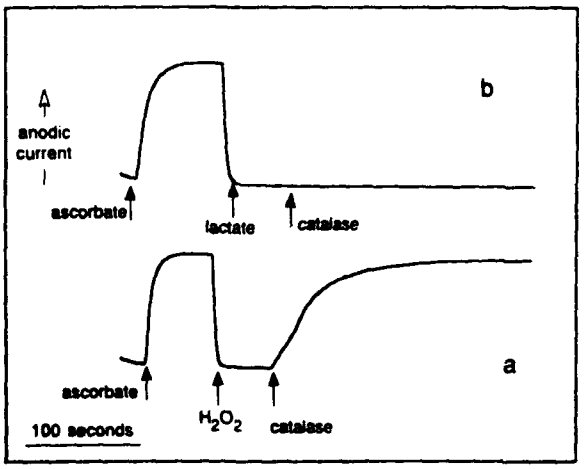

Figure 14. Effect of catalase on the elimination of ascorbate by an interferant eliminating layer containing HRP co-immobilized with LOD: (a) externally added H_2O_2 and (b) internally generated H_2O_2 through lactate oxidase catalyzed oxidation of lactate by O_2.

Figure 11a shows the glucose response of a two-layer electrode in the presence of all three interferants (ascorbate, urate, and acetaminophen) at their physiological levels. Comparison of this response curve with that obtained in the absence of interferants (Figure 11b) shows that the electrode is totally insensitive to these common electrooxidizable interferants. The presence or absence of H_2O_2 does not affect the glucose current itself, proving that glucose is not oxidized

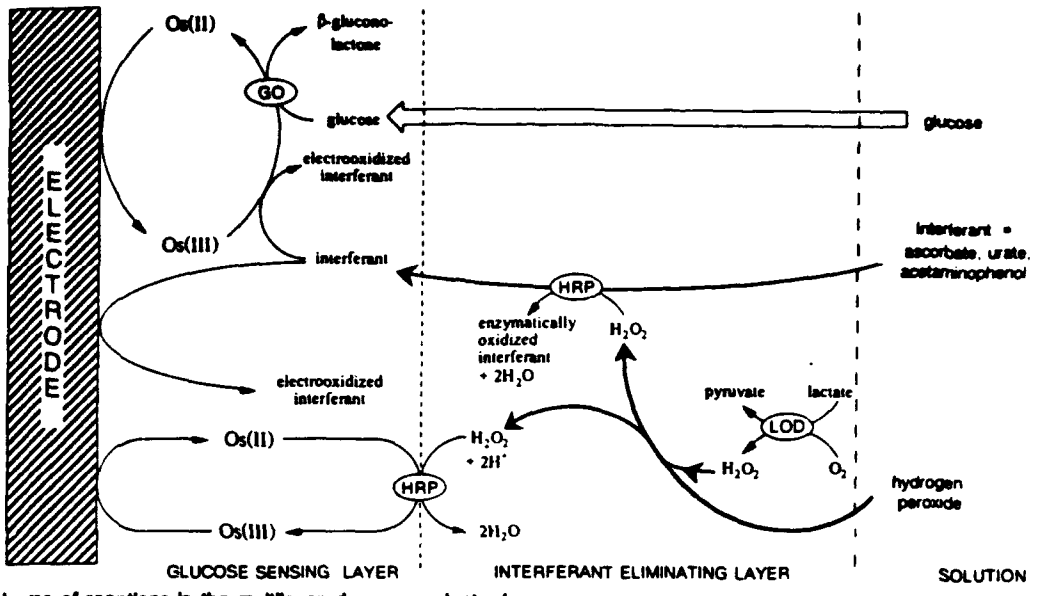

Figure 15. Scheme of reactions in the multilayered enzyme electrode.

at an appreciable rate by H_2O_2 in the HRP film. Figure 11c shows the glucose response of the Figure 11a electrode before it was coated with the peroxidase layer. The HRP layer slows the diffusion and decreases the current response. As a result, the apparent Michaelis constant[34] of the electrode (K_m) increases from 18 mM for the uncoated electrode to 25 mM for the coated one. Optimization of the thickness of the HRP layer thus involves a compromise between completeness of interferant elimination, requiring thicker films, and fast response, requiring thinner ones.

Stability. The interferant-elimination capability of HRP-coated electrodes remains unchanged for 2 months of repeated use when the electrode is stored in air at room temperature between the measurements. The stability is attributed to the initial excess HRP activity of the films. Because the initial activity is higher than essential for eliminating the interferants, the HRP films retain adequate activity even after their partial deactivation.

Built-In Sources of H_2O_2. While addition of H_2O_2 is feasible in clinical and laboratory analyzers, it is inappropriate for either disposable sensors or in sensors operating in vivo. These require a built-in source of peroxide.

Hydrogen peroxide is the oxidation product of oxidase-catalyzed reactions of molecular oxygen and substrates, e.g. lactate. Thus, lactate oxidase (LOD) mediates the oxidation of lactate by oxygen, the products being pyruvate and H_2O_2 (eq 4). The in situ generated H_2O_2 is adequate for eliminating interferants. At the concentration of lactate in physiological fluids (0.6–1.8 mM),[41] enough H_2O_2 is produced to oxidize all the interferants at their physiological concentrations.

$$2CH_3CH(OH)COO^- + O_2 \xrightarrow{LOD} 2CH_3COCOO^- + H_2O_2 \quad (4)$$

Figure 12 shows the results obtained with an electrode similar to the one used in the experiment of Figure 10 but having LOD co-immobilized with HRP in its outer film. Successive additions of lactate ("L") eliminate equivalent amounts of ascorbate ("A"). When this electrode was used in a solution containing physiological levels of the interferants (0.1 mM ascorbate, 0.5 mM urate, 0.1 mM acetaminophen), as well as physiological levels of lactate (0.5 mM) and glucose, the measured current was proportional to the glucose concentration only, i.e., was that measured in the absence of any of the interferants (Figure 13).

The simultaneous presence of several enzymes and of different reaction pathways employing common reagents creates, at least in principle, the possibility of new interfering or competing reactions. Lactate oxidase has been wired by the osmium-based redox polymer, and its films have been used in determining lactate concentration.[42] Thus, the direct electrooxidation of lactate must be prevented, i.e., the barrier layer must also isolate the LOD from the electron relays. The earlier discussed physical isolation methods are adequate for this purpose. No lactate-associated currents are observed in electrodes that do not electroreduce H_2O_2. A secondary cause of interference can be the change in oxygen partial pressure, through the oxygen being consumed by lactate (eq 4) and the Os(III) centers and O_2 competing for glucose oxidase–$FADH_2$ electrons (eq 5). We find, however, that the redox epoxy wired glucose oxidase electrode is insensitive to changes in oxygen partial pressure or lactate concentration. Raising the lactate concentration to 1.5 mM changes the electrocatalytic oxidation current of glucose (5.0 mM) by less than 2%.

$$GO\text{–}FADH_2 + O_2 \rightarrow GO\text{–}FAD + H_2O_2 \quad (5)$$

As seen in Figure 14 the initially generated H_2O_2 is not decomposed by external catalase, a common enzyme in physiological samples. The figure shows that the LOD–HRP film coated electrode rejects ascorbate either upon injecting H_2O_2 (a) or lactate (b). But the subsequent addition of catalase (100 units) affects the ascorbate rejection only when H_2O_2 is externally added (a), not when it is internally generated (b). When ascorbate is rejected by adding lactate, the addition of catalase does not cause a change in the current. However, when ascorbate is eliminated by adding H_2O_2, addition of catalase results in a gradual recovery of the oxidation current, until it eventually stabilizes at the level observed prior to the addition of H_2O_2. The slow current increase results from the gradual decrease in H_2O_2 concentration in the bulk of the solution (eq 6). With the HRP–LOD film the oxidation of interferants is not impaired by external catalase, because the H_2O_2 is generated and utilized

(41) Ganong, W. F. *Review of Medical Physiology*; Appleton & Lange: Norwalk, 1989.

(42) Katakis, I.; Heller, A. *Anal. Chem.* **1992**, *64*, 1008–1013.

in the bienzyme layer itself.

$$2H_2O_2 \xrightarrow{\text{catalase}} O_2 + 2H_2O \quad (6)$$

CONCLUSIONS

Horseradish peroxidase (HRP) based interferant eliminating layers provide practically absolute selectivity to amperometric glucose sensors. In the presence of the enzyme, H_2O_2 preoxidizes all the common electrooxidizable interferants. Figure 15 summarizes the relevant reactions in multilayered electrodes discussed in this work. In the glucose electrode, electrons from the substrate are transferred to the glucose oxidase (GO) and are relayed, via nondiffusing osmium redox centers, to the electrode. The analyzed solution contains electrooxidizable ascorbate, urate, and acetaminophen. These species may be oxidized directly at the electrode surface or through electron relays of the enzyme-wiring redox polymer network. Their electrooxidation increases the anodic current. To prevent their interference, the sensing layer is coated with a layer of immobilized peroxidase, which catalyzes the oxidation of the interferants by H_2O_2. Such oxidation destroys the interferants prior to their reaching the wired glucose oxidase, where they would otherwise be electrooxidized. The H_2O_2 can be either externally supplied or produced in situ through an oxidase-catalyzed O_2 oxidation of a second solute such as lactate. Electrical contact between the HRP and the osmium redox centers must and can readily be prevented, for example by inserting an electrically insulating barrier film between the glucose sensing layer and the HRP layer or by further cross-linking the sensing layer, or by operating the electrode at 0.5 V (SCE).

ACKNOWLEDGMENT

R.M. gratefully acknowledges his Chaim Weizmann postdoctoral fellowship. This work was supported in part by the Office of Naval Research, the National Science Foundation, and the Welch Foundation and NIH under Grant No. 1R01 DK42015-01A1.

RECEIVED for review May 1, 1992. Accepted September 14, 1992.

Reprinted from The Journal of Physical Chemistry, 1992, 96.

Electrical Connection of Enzyme Redox Centers to Electrodes

Adam Heller

Department of Chemical Engineering, The University of Texas at Austin, Austin, Texas 78712-1062
(Received: October 9, 1991; In Final Form: January 13, 1992)

Electrically insulating proteins can be made redox conducting through incorporation of a high density of electron relaying redox centers. Electrons diffuse in the resulting redox conductors by self-exchange between identical and electron transfer between different relaying centers. When the self-exchange rate of the relays and their density are high the flux of electrons through a 1-μm-thick film of a three-dimensional macromolecular network can match or exceed the rate of supply of electrons to or from the ensemble of enzyme molecules covalently bound to it. The network now molecularly "wires" the enzyme molecules to the electrode, and the current measures the turnover of the "wired" enzyme molecules. When the enzyme turnover is substrate flux, i.e., concentration limited, the current increases with the concentration of the substrate. The resulting amperometric biosensors have current densities as high as 10^{-3} A cm^{-2} and sensitivities reaching 1 A cm^{-2} M^{-1}. Because currents as small as 10^{-13} A are measurable with standard electrochemical instruments, the biosensors can be miniaturized to <10-μm dimensions. A practical example of enzyme "wiring" involves (a) forming a macromolecular complex between glucose oxidase and a water-soluble 10^2-kDa $[Os(bpy)_2Cl]^{+/2+}$-containing redox polyamine and (b) cross-linking the complex with a water-soluble diepoxide to form a hydrophilic, substrate and product permeable ~1-μm-thick redox epoxy film. In redox epoxy film based glucose sensors interference by electrooxidizable ascorbate, urate, and acetaminophen is avoided through their peroxidase-catalyzed preoxidation in an H_2O_2 generating surface layer. The novel microelectrodes have no leachable components.

Drug Administration and Biosensors

The objective of administering a drug is achievement of an optimal physiological response. The more frequently and accurately the response and drug concentration are measured, the closer one may get to optimal treatment. The frequency and accuracy of measurements have been limited in the past by the portability and cost of sensing systems. Today, sensing systems can be miniaturized and their electronics or optics produced at a cost that is consistent with the cost of treatment of many diseases. Progress in the development of low-cost microsensors for ex vivo use is likely to allow fine-tuning the administration of drugs. Furthermore, already at the present capabilities and cost of microcontrollers and microvalves, one might start planning for feedback loop-controlled drug delivery. The feedback loops will have three essential components: a drug containing and delivering unit; a sensor, measuring the drug concentration in the target organ or the affected physiological function; and a microcontroller or microprocessor calculating the dose and timing the delivery. Thus, in case of breathing difficulty caused by asthma, treated by drugs such as theophyllin or albuterol, the drug concentration in blood, the volume of air per inhalation, and the blood oxygen concentration would be sensed and fed into a controller or processor; the latter will, in turn, increase or decrease the amount of theophyllin leaked through a microvalve or of albuterol sprayed into the inhaled air until breathing is normal, and the blood is well oxygenated. The concept of therapeutic feedback loops has been around for a good number of years, particularly in the context of control of blood glucose levels in brittle, insulin-dependent diabetics. Although operation of a chemical or biotechnological manufacturing plant without control loops consisting of sensors and electronic controllers or processors connected to flow and temperature controlling valves is no longer conceivable, the use of such loops is only now coming of age in medicine, for example in pacemakers responding to oxygen demand.

The expanded use of microsensors, followed by introduction of medical feedback loops, will allow the pharmaceutical industry to expand its range of drug delivery methods. Today's primary delivery methods are those that allow accurate dosage, particularly infusion, injection, and ingestion. Other methods like inhalation and iontophoretic transdermal transport have been investigated but are not frequently used, even though they have advantages, such as rapid uptake in the case of inhalation (derived of the large lung surface area) and continuous, noninvasive administration, in the case of iontophoresis. The use of these methods is limited by difficulty of accurate and reproducible dosing. Feedback loops will allow the use of these and other delivery methods, as the concentration of the drug in the target organ, or a physiological function affected by the drug, will be frequently or continuously sensed and the microcontroller or processor will correct for any deviation from a desired drug concentration or unwanted change in physiological function. Thus, as long as the drug will be administered in small incremental doses, spaced so as to allow sensing of the drug's concentration in the target organ and of the affected physiological response, alternative delivery methods will become safe.

The pace of introduction of frequent monitoring of a physiological response or of a drug level in a targeted organ, as well as the evolution of therapeutic feedback loops, is now limited by the availability of appropriate miniature biosensors, the focus of our research and the subject of this article. The family of biosensors includes electrochemical (amperometric and potentiometric), optical, and electromechanical devices as well combinations of these. This article focuses on direct, i.e., not diffusionally mediated, amperometric sensors based on direct electrical connection of redox centers of enzymes to electrodes. First, however, it is necessary to consider the diffusional sensors.

Diffusionally Mediated Amperometric Biosensors

In diffusionally mediated amperometric biosensors,[1-4] a substrate, such as glucose, transfers a pair of electrons to the active

(1) Updike, S. J.; Hicks, G. P. *Nature* **1967**, *214*, 986–988.
(2) Silverman, H. P.; Brake, J. M. Method of Determining Microbial Populations, Enzyme Activities and Substrate Concentrations by Electrochemical Analysis. U.S. Patent 3,506,544, April 14, 1970.
(3) Guilbault, G. G. In *Enzyme Electrodes in Analytical Chemistry*; Svehla, G., Eds.; Elsevier: Amsterdam, 1977; Vol. VIII, Chapter 1, pp 1–70.
(4) (a) Mell, L. D.; Malloy, J. T. *Anal. Chem.* **1975**, *47*, 299–307. (b) Rishpon, J. *Biotechnol. Bioeng.* **1987**, *29*, 204–214.

0022-3654/92/2096-3579$03.00/0

redox center of an enzyme, glucose oxidase; the enzyme then unloads the excess electrons onto the oxidizing member of a fast redox couple.[2,5-22] For such electron transfer to take place, the oxidizing species must first diffuse into the protein or glycoprotein shell surrounding the enzyme's reactive center, because the rate of electron transfer, a phonon-assisted tunneling process,[23] declines exponentially with the electron-transfer distance.[24-26] The distance in this case is that between the donor, e.g., a reduced flavin adenine dinucleotide center of glucose oxidase, and the acceptor, the oxidized member of the diffusing couple. After electron transfer, the now reduced member of the couple diffuses out of the enzyme, reaching eventually the proximity of the anode of the cell where, in a second electron-transfer step that is also distance dependent and requires close approach of the electrode, it unloads its electron. Though numerous effective molecular, ionic, and polyionic diffusional mediators are known,[2,5-22] the currently preferred ones are monomeric ferrocenes,[6,27] quinones,[7,15] and osmium bipyridine complexes. All have redox potentials about 0.3–0.6 V positive of the redox potential of the enzyme. At such an overpotential the free energy of activation of the Marcus equation may balance the reorganization energy. A small reorganization energy combined with an appropriate overpotential increases the maximum distance at which a given rate of electron transfer can be maintained or can, alternatively, increase the rate of transfer for a fixed electron-transfer distance. For efficient current collection it is of importance that the rate of electron transfer from the enzyme to the diffusing mediator equal or exceed the rate of electron transfer from the substrate to the enzyme.

Diffusionally mediated amperometric biosensors are of both scientific and technological interest. Products such as analytical instruments and systems for self-monitoring of glucose levels by diabetics in withdrawn samples of blood are in use. Diffusionally mediated biosensors are, however, not likely to be used in feedback loops involving implanted sensors, because of the danger of escape of the diffusing mediator into the body fluid. Such escape would cause the equivalent of an electrical short in delicately orchestrated and interconnected biological electron-transfer routes. Toxicity among fast redox couples that are diffusing mediators is common.

While most diffusing couples are toxic, the natural O_2/H_2O_2 couple is safe, because people are abundantly equipped with catalase, an enzyme that decomposes H_2O_2 to water and dioxygen. This couple mediates by O_2 diffusing to reactive sites in enzymes where it is reduced to H_2O_2, which is amperometrically monitored through its anodic reoxidation to dioxygen.[1] Alternatively, the rate of oxygen consumption can also be amperometrically monitored.[28] O_2/H_2O_2-based amperometric sensors require sophisticated structures for circumventing the intrinsic O_2 partial pressure dependence of their response.[29-31] This makes their miniaturization to micrometer dimensions difficult, though submillimeter structures have been built.[32] The sensors are nevertheless appropriate for in vivo glucose monitoring.[33-37]

Nondiffusional Relaying of Electrons: Electrical Connection of Enzyme Redox Centers to Electrodes

The need for diffusional mediators is altogether avoided if the electrically insulated redox centers of the enzyme are directly electrically connected to the electrode.[38] In this case electrons transferred from the substrate to the enzyme are directly relayed to an external circuit. In a well-connected system the current flowing through the external circuit represents the actual turnover rate of the enzyme. Unless the maximum turnover rate is approached, the turnover and the current increase monotonically with the diffusional flux of substrate and therefore with substrate concentration. Thus, the concentration of the substrate is transduced into and measured as an electrical current.

We shall pause now to estimate the current that flows from a monolayer of an enzyme covering a 1-cm^2 electrode, with each enzyme molecule oxidizing 10^3 substrate molecules per second, when two electrons are transferred from the substrate during its oxidation. For an enzyme having a diameter of 10^2 Å that is densely packed on the surface, there are 1.3×10^{12} enzyme molecules per cm^2. Thus, 2.6×10^{15} electrons are transferred per second and the current density is 4×10^{-4} A cm^{-2}. This is a substantial current density considering that currents of 10^{-13} A are measured in many laboratories, including our own. In the unlikely event that all enzyme molecules remain intact during their

(5) Kulys, J. J.; Samalius, A. S.; Svirmickas, G. J. S. *FEBS Lett.* **1980**, *114*, 7–10.
(6) Cass, A. E. G.; Davis, G.; Francis, G. D.; Hill, H. A. O.; Aston, W. J.; Higgins, I. J.; Plotkin, E. V.; Scott, L. D. L.; Turner, A. P. F. *Anal. Chem.* **1984**, *56*, 667–671.
(7) Ikeda, T.; Katasho, I.; Kamei, M.; Senda, M. *Agric. Biol. Chem.* **1984**, *48*, 1969–1976.
(8) Cass, A. E. G.; Davis, G.; Green, M. J.; Hill, H. A. O. *J. Electroanal. Chem.* **1985**, *190*, 117–127.
(9) Green, M. J.; Hill, H. A. O. *J. Chem. Soc., Faraday Trans.* **1986**, *82*, 1237–1243.
(10) Crumbliss, A. L.; Hill, H. A. O.; Page, D. J. *J. Electroanal. Chem.* **1986**, *206*, 327–331.
(11) Twork, J. V.; Yacynych, A. M. *Biotechnol. Prog.* **1986**, *2*, 67–72.
(12) Talbott, J.; Jordan, J. *Microchem. J.* **1988**, *37*, 5–12.
(13) Taniguchi, I.; Miyamoto, S.; Tomimura, S.; Hawkridge, F. M. *J. Electroanal. Chem.* **1988**, *240*, 333–339.
(14) Turner, A. P. F. Amperometric Biosensors Based on Mediator-Modified Electrodes. In *Methods in Enzymology*; Mosbach, K. D., Ed.; Academic Press: San Diego, 1988; Vol. 137, Part D, pp 90–103.
(15) Senda, M.; Ikeda, T. Bioelectrocatalysis at Enzyme Modified Electrodes. In *Macromolecular Complexes—Dynamic Interactions and Electronic Properties*; Tsuchida, E., Ed.; VCH: New York, 1991; Chapter 10, pp 229–247.
(16) Kulys, J.; Fresenius, Z. *Anal. Chem.* **1989**, *335*, 86–91.
(17) Yokoyama, K.; Tamiya, E.; Karube, I. *J. Electroanal. Chem.* **1989**, *273*, 107–117.
(18) Jönsson, G.; Gorton, L.; Pettersson, L. *Electroanalysis* **1989**, *1*, 49–55.
(19) Bourdillon, C.; Majda, M. *J. Am. Chem. Soc.* **1990**, *112*, 1795–1799.
(20) Liaudet, E.; Battaglini, F.; Calvo, E. J. *J. Electroanal. Chem.* **1990**, *293*, 55–68.
(21) (a) Coury, L. A., Jr.; Oliver, B. N.; Egekeze, J. O.; Sosnoff, C. S.; Brumfield, J. C.; Buck, R. P.; Murray, R. W. *Anal. Chem.* **1990**, *62*, 452–458. (b) Coury, L. A.; Murray, R. W.; Johnson, J. L.; Rajagopalan, J. L. *J. Phys. Chem.* **1991**, *95*, 6034–6040.
(22) Kajiya, Y.; Tsuda, R.; Yoneyama, H. *J. Electroanal. Chem.* **1991**, *301*, 155–164.
(23) DeVault, D. *Quantum Mechanical Tunneling in Biological Systems*, 2nd ed.; Cambridge University Press: Cambridge, 1984.
(24) Sutin, N.; Brunschweig, B. S. *Adv. Chem. Ser.* **1990**, *No. 226*, 65–88.
(25) (a) Beratan, D. N.; Onuchic, J. N.; Betts, J. N.; Bowler, B. E.; Gray, H. B. *J. Am. Chem. Soc.* **1990**, *112*, 7915–7921. (b) Cowan, J. A.; Gray, H. B. *Chem. Scr.* **1988**, *28A*, 21–26.
(26) Cusanovich, M. A. Intracomplex and Intramolecular Electron Transfer in Macromolecules. In *Macromolecular Complexes—Dynamic Interactions and Electronic Properties*; Tsuchida, E., Ed.; VCH: New York, 1991; Chapter 9, pp 213–227.
(27) Yeh, P.; Kuwana, T. *Chem. Lett.* **1977**, 1145–1148.
(28) Clark, L. C.; Lyons, C. *Ann. N.Y. Acad. Sci.* **1962**, *102*, 29–45.
(29) Armour, J. C.; Lucisano, J. Y.; McKean, B. D.; Gough, D. A. *Diabetes* **1990**, *39*, 1519–1526.
(30) Gough, D. A.; Lucisano, J. Y.; Tse, P. H. S. *Anal. Chem.* **1985**, *57*, 2351–2357.
(31) Lucisano, J. Y.; Gough, D. A.; Armour, J. C. *Anal. Chem.* **1987**, *59*, 736–739.
(32) Mastrototaro, J. J.; Johnson, K. W.; Morff, R. J.; Lipson, D.; Andrew, C. C.; Heller, J. W. *Proceedings of the 3rd International Meeting on Chemical Sensors, Cleveland, Sept 24–26, 1990*; The Edison Sensor Technology Center, Case Western University: Cleveland, OH, 1990; pp 300–302.
(33) Kerner, W.; Zier, H.; Steinbach, G.; Brückel, J.; Pfeiffer, E.; Weiss, T.; Cammann, K.; Planck, H. A Potentially Implantable Enzyme Electrode for Amperometric Measurement of Glucose. In *Implantable Glucose Sensors—The State of the Art*; Georg Thieme Verlag: Stuttgart, 1988; pp 8–13.
(34) Sternberg, R.; Barrow, M. B.; Gangiotti, L.; Thévenot, D. R.; Bindra, D. S.; Wilson, G. S.; Velho, G.; Froguel, P.; Reach, G. *Biosensors* **1988**, *4*, 27–40.
(35) Abel, P.; Müller, A.; Fischer, U. *Biomed. Biochim. Acta* **1984**, *43*, 577–584.
(36) (a) Clark, L. C.; Duggan, C. A. *Diabetes Care* **1982**, *4*, 174–180. (b) Clark, L. C.; Spokane, R. B.; Sudan, R.; Stroup, T. L. *Trans.—Am. Soc. Artif. Intern. Organs* **1987**, *33*, 323–328.
(37) Koudelka, M.; Rohner-Jeanrenaud, F.; Terrattaz, J.; Bobbioni-Harsch, E.; de Rooij, N. F.; Jeanrenaud, B. *Biosensors Bioelectron.* **1991**, *6*, 31–36.
(38) Heller, A. *Acc. Chem. Res.* **1990**, *23*, 128–134.

electrical connection to the electrode and their packing is theoretically dense, then, at 10^{-13}-A current measuring capability, the area of the electrode can be reduced to 2.5×10^{-9} cm^2, corresponding to a circular electrode having a diameter of 0.28 μm. This is about the dimension of the smallest feature on an advanced integrated circuit now under development but not yet in production. Another perspective is provided by calculating the minimum number of electrically connected enzyme molecules that can be sensed. In the case of an enzyme (e.g., glucose oxidase) turning over 10^3 times per second, each molecule delivers a current of 3.2×10^{-16} A. One thus observes, when measuring a current of 10^{-13} A, about 300 enzyme molecules. This is the actual number of electrically "wired" glucose oxidase molecules functioning in our 7-μm-diameter glucose microsensors.[39]

Electrical Communication between Redox Enzymes and Electrodes

For convenience of considering electrical connection of enzymes to electrodes (not because the demarcation lines are well defined), we shall divide the redox enzymes into three groups. In the first we include enzymes having NADH/NAD$^+$ or NADPH/NADP$^+$ redox centers. These centers are often weakly bound to the protein of their enzyme. They can act as diffusional carriers of electrons, shuttling between different redox biomolecules, for example, between those of different reductases or dehydrogenases. Being themselves redox mediators, they can be amperometrically assayed. There are three problems that need to be addressed in the design of amperometric NAD$^+$/NADH or NADP$^+$/NADPH biosensors. First, the electrodes need to be designed for two-electron transfer; i.e., the rate of the two-electron-transfer reaction must be faster than the rate of any single-electron-transfer reaction, whereby an irreversibly reacting free-radical intermediate is formed. The relevant time within which the two electrons must be "simultaneously" transferred is defined by the time it takes the radical to irreversibly react. Second, if the biosensor is to be used for an extended period, loss of NADH/NAD$^+$ or NADPH/NADP$^+$ by out-diffusing of the enzyme-containing volume near the electrode surface must be prevented, e.g., through covalent attachment of the NADH/NAD$^+$ to the enzyme's protein via a flexible spacer chain. This chain must be long enough to allow the back-and-forth movement of the centers between their site in the enzyme and the surface of the electrode. Third, the overpotential for the two-electron-transfer reaction at the electrode must be small enough to allow the maintenance of the specificity that is sought and achieved through the use of the enzyme.

Relatively stable two-electron-accepting diffusionally mediated electrodes have been designed. These operate at potentials where their selectivity is adequate.[40,41] Recently, NAD$^+$ has been covalently bound via designed chains to genetically engineered glucose dehydrogenase,[42] so as to shuttle in and out of the enzyme. This and other dehydrogenases can be used in conjunction with NADH oxidizing mediated electrodes to form O_2-insensitive amperometric biosensors.

In a second group of enzymes at least part of the redox centers, usually porphyrin derivatives, are found at or near the periphery of the protein shell. These enzymes are built to transfer or accept electrons on contact and thus directly electrically communicate with electrodes. Their rate of electroreduction/oxidation varies, however, with their orientation on the electrode surface.[26,43] It can be increased through bonding to the electrode surface functions that interact with a specific protein region, so as to properly orient the enzyme for electron transfer. Because highly selective routing of electrons is of essence in biological systems (otherwise the biological system would become equipotential and life could not exist), enzymes that transfer to and accept electrons from randomly contacted redox proteins or electrodes are few, making this family the smallest of the three.

The third family encompasses enzymes having strongly bound redox centers deeply buried in an insulating protein or glycoprotein shell. When adsorbed on an electrode, their redox centers cannot be oxidized or reduced at potentials survived by the enzyme. The rate of electron transfer across the distance between their redox centers and the periphery of their protein or glycoprotein shell, which defines the closest approach of the redox center to an electrode surface, is negligibly slow relative to the turnover rate of these enzymes. Careful studies of the distance dependence of the rate of electron transfer in cytochrome *c* and myoglobin (that are redox proteins, not enzymes) show that the rate drops by a factor of *e* for each 0.91-Å increase in distance.[44] It is, however, incorrect to assume that this distance dependence holds also for other redox proteins. Because of system to system differences in reorganization energy, redox potential difference, amino acid sequence, and folding of the protein defining the electron route, as well as spatial orientation of the centers involved in the electron-transfer steps, the constant of the exponential decay of the electron-transfer rate with distance will vary from case to case. The basic concepts of electron-transfer theory, particularly the relationships defining the dependence of the rate on the free energy of activation (and thereby on the potential difference between the donor and the acceptor) and on the reorganization energy, are nevertheless of practical value in the design of direct amperometric enzyme electrodes.

Glucose Electrodes

Among the amperometric biosensors, glucose sensors, based on the enzyme glucose oxidase, have received more attention in both the scientific and the patent literature than all others combined. The interest in glucose electrodes derives from a coincidence of need—the frequency of glucose analyses exceeding that of any other biochemical, because of the large number of blood glucose assays (in excess of 1 billion in the U.S.) by self-monitoring diabetics and of ruggedness—glucose oxidase withstanding abuse by students and physical chemists.

The enzyme is a glycoprotein of MW 160000 having two FAD/FADH$_2$ redox centers and a hydrodynamic radius of 86 Å.[45] The enzymatic oxidation of glucose involves the reactions

$$\text{glucose} + \text{GO(FAD)} \rightarrow \text{gluconolactone} + \text{GO(FADH}_2\text{)} \quad (1)$$

$$\text{FADH}_2 + \text{O}_2 \rightarrow \text{FAD} + \text{H}_2\text{O}_2 \quad (2)$$

Colorimetric glucose assays are based on peroxidase-catalyzed reactions of H_2O_2 with leuco dyes; amperometric assays are based on electrooxidation of either H_2O_2

$$\text{H}_2\text{O}_2 \rightarrow 2\text{H}^+ + \text{O}_2 + 2\text{e}^- \quad (3)$$

or of another enzyme-reduced diffusional mediator such as a ferrocene derivative Fc (reactions 4 and 5)[8,27] or a heterocyclic quinoid:[46]

$$\text{GO(FADH}_2\text{)} + 2\text{Fc}^+ \rightarrow \text{GO(FAD)} + 2\text{Fc} + 2\text{H}^+ \quad (4)$$

$$2\text{Fc} \rightarrow 2\text{Fc}^+ + 2\text{e}^- \quad (5)$$

The electrically insulating glycoprotein shell surrounding the FAD/FADH$_2$ centers is thick enough to prevent random electron transfer at biologically relevant rates. A novel genetically engineered glucose oxidase has a thicker insulating shell, with more

(39) Pishko, M. V.; Michael, A. C.; Heller, A. *Anal. Chem.* **1991**, *63*, 2268–2272.
(40) Persson, B.; Gorton, L. *J. Electroanal. Chem.* **1990**, *292*, 115–138.
(41) Bremle, G.; Persson, B.; Gorton, L. *Electroanalysis* **1991**, *3*, 77–86.
(42) Persson, M.; Mansson, M. O.; Bülow, L.; Mosbach, K. *Bio/Technology* **1991**, *9*, 280–284.
(43) (a) Guo, L. H.; Hill, H. A. O. *Adv. Inorg. Chem.* **1991**, *36*, 341. (b) Ikeda, T.; Fushimi, F.; Miki, K.; Senda, M. *Agric. Biol. Chem.* **1988**, *52*, 2655–2658. (c) Assefa, H.; Bowden, E. F. *Biochem. Biophys. Res. Commun.* **1986**, *139*, 1003–1008. (d) Armstrong, F. A.; Lannon, A. M. *Biochem. Soc. Trans.* **1988**, *16*, 842–843.
(44) Lieber, C. M.; Karas, J. L.; Mayo, S. L.; Albin, M.; Gray, H. B. Long range Electron Transfer in Proteins. In *Design of Enzymes and Enzyme Models*; Proceedings of the Robert A. Welch Foundation Conferences on Chemical Research; The Welch Foundation: Houston, 1987; pp 9–24.
(45) Nakamura, S.; Hayashi, S.; Koga, K. *Biochim. Biophys. Acta* **1976**, *445*, 294–308.
(46) Albery, W. J.; Bartlett, P. N.; Craston, D. H. *J. Electroanal. Chem. Interfacial Electrochem.* **1985**, *194*, 223–235.

peripheral oligosaccharide, which makes it uniquely stable at 37 °C.[47]

Direct Electrooxidation of Glucose Oxidase

In our initial work, Yinon Degani and I coupled, using a water-soluble carbodiimide, ferrocenecarboxylic acid to lysine amines of glucose oxidase.[48,49] We argued that electrons will be transferred by phonon- or field-assisted tunneling, via such nondiffusing relays, to electrodes, if at least one of the relays binds to a lysine or other amine deep in the insulating glycoprotein shell of the enzyme. We considered it statistically probable to find between one of the two $FAD/FADH_2$ centers and the periphery of the enzyme (representing the surface of closest approach to a metal electrode) such an amide-forming function and proceeded with the enzyme modification experiments. Using modified enzymes, we searched for anodic glucose oxidation currents in electrodes built with dialysis membranes that contained the modified enzymes in the proximity of a graphite electrode. We were driven to this work by the challenge of chemically making a direct electrical connection between an active center of an enzyme and an external circuit and demonstrating that tunneling paths can be built into biomolecules and by foreseeing a more effective interfacing of enzymes and microcircuits than could be done in CHEMFETS. We expected, and later confirmed, that electron collection efficiencies and thus current densities can be higher than in most diffusionally mediated systems; and we saw a way to medical sensors and sensors for the food and beverage industries from which no toxic mediator could be leached.

We observed the expected nondiffusionally mediated electrooxidation of glucose in our very first experiments. As is, however, so common in science, we also found ourselves embarked on a roller coaster. When we checked the directly electron transferring modified enzyme for protein-adsorbed low-molecular-weight diffusional mediators by gel permeation chromatography, i.e., for conventional mediators not covalently bound to the "modified" enzyme, we found that the "relays" that we assumed to be covalently bound could be separated. Thus, the current was flowing not through bound relays but was carried by diffusing mediator ions. Later, reading a patent application on immunosensors and trying to repeat an experiment aimed at covalently binding redox centers to an immunolabeling enzyme, we found that we were not alone in our initial erroneous interpretation of results.[50] Fortunately, because we did not rush to publish, we had no paper to withdraw. After a period in which we obtained results that we could not always reproduce, but that nevertheless kept our hopes alive, we eventually succeeded in establishing the direct electrical communication that we sought. To properly bind the electron relays to the proteins, we first partially unfolded these using 2 M urea, so as to chemically access regions that are normally not accessible to reagents.[48,49] Through such unfolding we were able to reproducibly react 12–14 amines of the enzyme, which has 15 lysyl amines. The relays were bound as amides, produced through reacting the protein amines and an *o*-acylisourea. The latter was formed of a water-soluble carbodiimide and ferrocenecarboxylic acid. Subsequently, connections were made also with ferroceneacetic acid to form ferrocene acetamides of the enzyme protein.[51-53] Recently, jointly with Wolfgang W. Schuhmann and Hanns-Ludwig Schmidt of the Technical University of Munich, we also modified the oligosaccharide periphery of glucose oxidase with flexible spacer chains, carrying at their termini electron relays. When the spacer chains were long, the peripherally attached relays penetrated the enzyme sufficiently deeply to establish direct electrical communication between its redox centers and electrodes.[54]

Attachment of Relay-Modified Enzymes to Electrodes

In the modified enzymes electrons transferred from the substrate to the enzyme's redox center through reaction 1 were subsequently transferred from this center, via protein or oligosaccharide-bound ferrocene relays, to the electrode. As expected, the current at or above the redox potential of the relays was glucose concentration dependent. The modified enzyme functioned, however, only when free in solution, i.e., when contained by a membrane in a thin compartment in the vicinity of the electrode and not when electrode-surface bound. Upon binding of the modified enzyme to a graphite surface through cross-linking, the current dropped to a negligible fraction of the original. The experiment suggested that communication was restricted to electron-transfer routes within the protein, involving fast electron transfer between an $FAD/FADH_2$ redox center and one of the relays and from that relay either directly, or through other relays, to the electrode. For the latter step to be rapid it was of essence that the distance between the critical relay and the electrode be short, i.e., that the enzyme tumble freely so as to transiently minimize the distance. When the enzyme was randomly cross-linked and could not tumble, the overwhelming majority of its potential electron-transfer routes were inoperative because of excessive electron-transfer distances. As a result, our first directly communicating glucose electrodes required membranes to contain the freely tumbling enzyme in a small volume near the electrode. With the membrane slowing down the diffusional glucose transport to the interior fluid and with diffusional transport of the enzyme to the electrode remaining of essence, we were unable to realize two objectives: prompt electron collection, i.e., fast response, and efficient electron collection, i.e., a current density representing the actual turnover rate of the enzyme. On the practical side, the membrane requirement also made the low-cost manufacture of biosensors difficult.

Electrical Wiring of Enzymes

To eliminate the membrane, we had to electrically connect the redox centers so that unique orientation or tumbling would not be necessary for discharge of eletrons from the modified enzyme to the electrode. We did so by molecular "wiring" of the enzyme to the electrode, the "wire" being a redox macromolecule designed to (a) complex the enzyme protein, (b) electrically connect the redox center of the enzyme to the electrode, and (c) physically attach the enzyme to the electrode surface, all without deactivating the enzyme.

Redox macromolecules have been used earlier as diffusional mediators of electron transfer between enzymes and electrodes and for enzyme entrapment. In 1980 Nakamura, Nankai, Iijima, and Fukuda described electron mediation between an enzyme and an electrode through organic redox polymers, particularly quinone and quinoid heterocyclics such as thionine, riboflavin, or gallocyanine.[55] Foulds and Lowe[56] and Umana and Waller[57] entrapped glucose oxidase in polypyrrole, a degenerate semiconducting polymer. The polymer, in the presence of traces of platinum, offers a high surface area on which H_2O_2 generated through reaction 2 is electrooxidized. Polypyrroles were used also by several other groups[58-61] in the oxidation of hydrogen peroxide, as were poly-

(47) DeBaetseller, A.; Vasavada, A.; Dohet, P.; Ha-Thi, V.; DeBeukelaer, M.; Erpicum, T.; DeClerck, L.; Hanotier, J.; Rosenberg, S. *Bio/Technology* **1991**, *9*, 559–561.

(48) Degani, Y.; Heller, A. *J. Phys. Chem.* **1987**, *91*, 1285–1289.

(49) Degani, Y.; Heller, A. *J. Am. Chem. Soc.* **1988**, *110*, 2615–2620.

(50) Hill, H. A. O. European Patent Application 84303090.0 filed Aug 5, 1984.

(51) Bartlett, P. N.; Whitaker, R. G. *J. Chem. Soc., Chem. Commun.* **1987**, 1603–1604.

(52) Bartlett, P. N.; Bradford, V. Q.; Whitaker, R. G. *Talanta* **1991**, *38*, 57–63.

(53) Heller, A.; Degani, Y. Direct Electrical Communication Between Chemically Modified Enzymes and Metal Electrodes: III. Electron Transfer Relay Modified Glucose Oxidase and D-Amino-Acid Oxidase. In *Redox Chemistry and Interfacial Behavior of Biological Molecules*; Dryhurst, G., Niki, K., Eds.; Plenum: New York, 1988; pp 151–170.

(54) Schuhmann, W.; Ohara, T. J.; Schmidt, H.-L.; Heller, A. *J. Am. Chem. Soc.* **1991**, *113*, 1394–1397.

(55) Nakamura, K.; Nankai, S.; Iijima, T.; Fukuda, M. U.S. Patent 4,224,125, Sept 23, 1980.

(56) Foulds, N. C.; Lowe, C. R. *J. Chem. Soc., Faraday Trans.* **1986**, 1259–1264.

(57) Umana, M.; Waller, J. *Anal. Chem.* **1986**, *38*, 2979–2983.

(58) Belanger, D.; Nadrean, J.; Fortier, J. *J. Electroanal. Chem.* **1989**, *274*, 143–155.

aniline,[62-64] poly(*o*-phenylenediamine),[65] and polyindole.[66] Ferrocene-modified polypyrrole was subsequently used to immobilize glucose oxidase.[67,68]

Highly flexible ferrocene-modified siloxanes and polyethylene oxides were also used as mediators, carrying electrons between glucose oxidase and other enzymes and high surface area carbon pastes that adsorb the enzyme and the redox polymer.[69-74] In most of these redox polymer systems, the polymers, often of low molecular weight (20 kDa or less), acted as diffusional mediators. For example, in the case of glucose sensors based on electropolymerized [(ferrocenyl)amidopropyl]pyrrole[67] or ferrocene-modified polysiloxanes or polypyrroles,[69-74] oxidation of the ferrocenes to ferricinium cations increases the solubility sufficiently to allow such diffusional mediation, even though precipitation of the mediator that is insoluble in its reduced form reduces the rate of its escape into the solution. Because in electropolymerized polypyrrole the chains are short, the ferrocene-modified polypyrrole probably acts as a special kind of a diffusional mediator, the polymer becoming more water-soluble when oxidized, i.e., when the short polymer chain acquires positive charge through oxidation of neutral ferrocene segments.

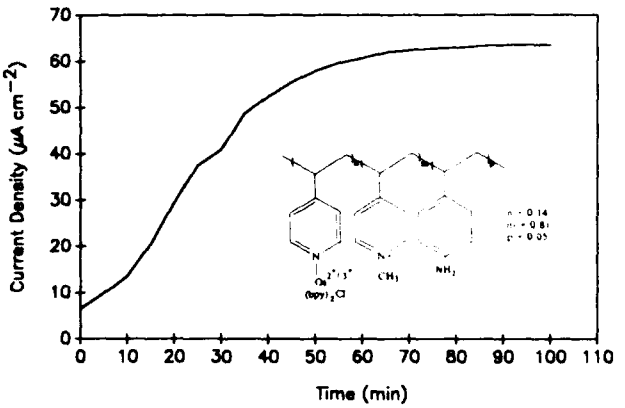

Figure 1. The electrode-surface-adsorbed redox macromolecule shown in the insert "catches" and irreversibly complexes (from a $\sim 10^7$ M solution) glucose oxidase molecules. The time dependence of the glucose current reflects the diffusional flux of enzyme molecules to the electrode surface. If the enzyme concentration is raised, the rate of increase in glucose current becomes correspondingly faster. From ref 76.

Principles of Wire Design

Our objectives in the design of stable redox macromolecules for electrical wiring of redox centers of enzymes to electrodes were the following: first, to assure that the wiring redox macromolecule will complex the enzyme and penetrate its protein so as to enable electron transfer from the buried redox center to the periphery of the enzyme. This required that the redox polymer be adequately soluble in water and that it have hydrophobic, charged, or hydrogen-bonding domains to adequately bind domains of the enzyme protein.[75] Our next objective was to assure that *only* a small fraction of the segments of the molecular wire be bound at any moment to the electrode surface, with most segments remaining unadsorbed, i.e., dangling in water, and thus available to complex and penetrate the enzyme.[76] Our third objective was to form of the enzyme complexing wires a three-dimensional network incorporating in its volume, through covalent bonding, a large number of enzyme molecules.[77-79] This network had to allow rapid in and out diffusion of the substrate and the product, as well as fast electron diffusion.

To meet these objectives, we used high molecular weight ($\sim 10^5$ Da) redox polyelectrolytes, with one-third to one-sixth of the component units having a bound redox center.[76-79] Segments of the polyelectrolyte were designed either to hydrophobically interact with the enzyme protein, to hydrogen-bond to the enzyme protein, or to electrostatically interact with oppositely charged domains of the enzyme protein. Upon such interaction they deeply penetrated the peripheral protein or glycoprotein surface, i.e., the surface defining the closest approach of the enzyme's redox center to an electrode. Through such deep penetration the electron-transfer distances between a redox center of the enzyme and at least one redox center of the wiring redox polyelectrolyte were sufficiently reduced for electrons to be transferred from the enzyme to the wire at a rate equaling or exceeding the turnover rate of the enzyme. The transferred electrons then propagated by diffusing between the relaying redox centers along the wire, occasionally crossing between undulating segments of the wires as their relaying redox centers approached each other.

Attachment of Wires to Electrodes

Attachment of segments of the wires to the electrode surfaces was assured by making the wires long enough. Adsorption of practically any macromolecule, even a highly water-soluble polyelectrolyte, to a surface can be made irreversible (except through displacement by a more strongly adsorbed solution species), by making its molecular weight high enough. The essence of the statistical argument behind this is the following: let there be a weakly adsorbed macromolecule having, say, only one of its repeating units per thousand adsorbed on the surface at any instant, each unit spending 99.9% of the time in the solution, off the electrode surface. If the chains have about 10^3 units, the probability of desorption, i.e., of the event that no segment is in contact with the surface, is high. If, however, the macromolecule consists of 10^6 units, there are about 10^3 units adsorbed at any instant, and the likelihood of their simultaneous lifting off is negligibly small. Thus, in contrast with other investigators of enzyme–redox polymer systems, we did not use strongly adsorbed water-insoluble polymers of low molecular weight, but used instead highly water-soluble redox polymers of high molecular weight. Even with the great majority of their segments being off the surface and available for interaction with the enzyme's protein, these were not desorbed because of their high molecular weight.

Redox macromolecules with excessively strongly electrode-adsorbed segments, such as polypyrroles, make poor wires because their chains do not extend sufficiently into the solutions, and when they do their segments are too rigid to fold along protein chains. In contrast, the better wiring redox macromolecules are long, their individual segments are poorly adsorbed, spending most of their

(59) Tamiya, G.; Karube, I. *Sens. Actuators* **1989**, *18*, 297.
(60) Yabuki, S.; Shinohara, H.; Aizawa, M. *J. Chem. Soc., Chem. Commun.* **1989**, 945–946.
(61) Trojanavicz, M.; Matuszewski, W.; Podsiadla, *Biosensors Bioelectron.* **1990**, *5*, 149–156.
(62) Bartlett, P. N.; Whitaker, R. G. *Biosensors* **1987/8**, *3*, 359–379.
(63) Shinohara, M.; Chiba, T.; Aizawa, M. *Sens. Actuators* **1987**, *13*, 79–84.
(64) Shaolin, M.; Huaiguo, X.; Bidong, Q. *J. Electroanal. Chem.* **1991**, *304*, 7–16.
(65) Malitesta, C.; Palmisano, F.; Torsi, L.; Zambonin, P. G. *Anal. Chem.* **1990**, *62*, 2735–2740.
(66) Pandey, P. C. *J. Chem. Soc., Faraday Trans. 1* **1988**, *84*, 2259–2265.
(67) Foulds, N. C.; Lowe, C. R. *Anal. Chem.* **1988**, *60*, 2473–2478.
(68) Dicks, J. M.; Hattori, S.; Karube, I.; Turner, A. P. F.; Yokozawa, T. *Ann. Biol. Clin.* **1989**, *47*, 607–619.
(69) Hale, P. D.; Boguslavsky, L. I.; Inazaki, T.; Karan, H. I.; Lee, H. S.; Skotheim, T. A. *Anal. Chem.* **1991**, *63*, 677–682.
(70) Hale, P. D.; Inagaki, T.; Karan, H. I.; Okamoto, Y.; Skotheim, T. *J. Am. Chem. Soc.* **1989**, *111*, 3482–3484.
(71) Inagaki, T.; Lee, H. S.; Hale, P. D.; Skotheim, T. A.; Okamoto, Y. *Macromolecules* **1989**, *22*, 4641–4643.
(72) Inagaki, T.; Lee, H. S.; Skotheim, T. A.; Okamoto, Y. *J. Chem. Soc., Chem. Commun.* **1989**, 1181–1183.
(73) Hale, P. D.; Inagaki, T.; Lee, H. S.; Karan, H. I.; Okamoto, Y.; Skotheim. T. A. *Anal. Chim. Acta* **1990**, *228*, 31–37.
(74) Gorton, L.; Karan, H. I.; Hale, P. D.; Inagaki, T.; Okamoto, Y.; Skotheim, T. A. *Anal. Chim. Acta* **1990**, *228*, 23–30.
(75) Degani, Y.; Heller, A. *J. Am. Chem. Soc.* **1989**, *111*, 2537–2358.
(76) Pishko, M. V.; Katakis, I.; Lindquist, S. E.; Ye, L.; Gregg, B. A.; Heller, A. *Angew. Chem., Int. Ed. Engl.* **1990**, *29*, 82–84.
(77) Gregg, B. A.; Heller, A. *Anal. Chem.* **1990**, *62*, 258–263.
(78) Gregg, B. A.; Heller, A. *J. Phys. Chem.* **1991**, *95*, 5970–5975.
(79) Gregg, B. A.; Heller, A. *J. Phys. Chem.* **1991**, *95*, 5976–5980.

time floating off the electrode rather than anchored to it; and while floating, they catch enzymes through their built-in protein-complexing functions.

Capture of Enzymes by Wiring Redox Macromolecule-Coated Surfaces

Figure 1 shows in slow motion a graphite-adsorbed redox polymer capturing and electrically connecting glucose oxidase molecules as they diffuse to the surface on which the redox polyelectrolyte is adsorbed. It also shows the simplest of our methods of making glucose electrodes.[76] In order to observe the evolution of the electrocatalytic glucose oxidation current as a function of time, we slowed the diffusional enzyme transport by using only a 10^{-7} M enzyme concentration. The complex between the electrode-adsorbed redox macromolecule and the enzyme is so strong that it forms even at this low enzyme concentration and in the absence of free redox polymer from the solution. This simplest of the wiring polymers is a 20:1 copolymer of 4-vinylpyridine and 4-aminostyrene, with about one-seventh of the pyridines complexed to $[Os(bpy)_2(py)Cl]^{+/2+}$ and with the residual uncomplexed pyridines N-methylated to add positive charge to the chains. The positive charge increases the solubility of the polymers in water and their electrostatic interaction with anionic regions of the enzyme protein. The osmium bis- and tris(bipyridine) complexes, including $[Os(bpy)_2(py)Cl]^{+/2+}$, are fast and stable redox couples.[80] The electron diffusion coefficient in $[Os(bpy)_2Cl]^{+/2+}$ complexed poly(vinylpyridine) exceeds 10^{-9} cm^2 s^{-1}.[78,81,82] The potential of the redox polymer is 0.27 V (SCE), well positive of that of the enzyme-bound $FAD/FADH_2$ center, near −0.38 V (SCE) at pH 7.

The response time of this simple electrode is faster than 0.5 s, and its current density at high glucose concentrations is 35 μA cm^{-2},[76] about one-tenth of that estimated for a well-packed monolayer of the enzyme.

Effect of the Ionic Strength on the Enzyme–Redox Polymer Complex: Partial Chain Separation at High Ionic Strength

Because in these simplest electrodes the redox polymers are complexed to the enzyme proteins, both the folding of the polycationic redox polymers and their interaction with regions of the enzyme are sensitive to ionic strength. At high ionic strength the charges on the interacting macromolecules are screened by anions in the solution, causing the polyelectrolytes that are stretched by electrostatic repulsion at low ionic strength to ball up. As a result, even though the complex does not fully dissociate, segments of the polymer no longer penetrate the enzyme and electron transfer from the enzyme to the polymer becomes ineffective. Nevertheless, because the complex does not dissociate even at high ionic strength, electron transfer from the enzyme to the complexing redox macromolecule becomes again effective when the same electrode is placed in a solution of reduced ionic strength. The usually unwanted sensitivity of the electrical communication between the enzyme and the electrode to ionic strength can be limited by covalently bonding segments of the redox macromolecule to the enzyme after their complex is formed.[75]

Three-Dimensional Enzyme Wiring Networks

The current densities are greatly increased upon wiring multiple layers of an enzyme to an electrode through a three-dimensional network of interconnecting redox macromolecules.[77-79] To avoid limiting of the in-diffusion of the substrate and the out-diffusion of the product, it is of essence that these networks form open and hydrophilic structures. Our process of forming such enzyme-wiring networks requires a redox macromolecule having the discussed enzyme-complexing, enzyme-penetrating, and electrode-binding

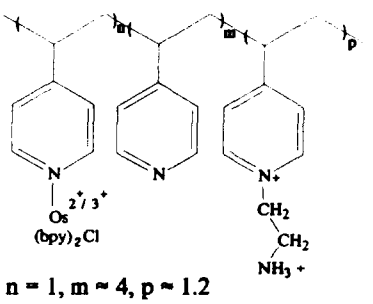

Figure 2. Structure of an enzyme complexing redox polyamine designed for cross-linking with a water-soluble diepoxide to form a three-dimensional wired enzyme network.[78]

features and, in addition, also covalently cross-linkable centers. For the enzyme to be covalently bound to the network in a simple one-step process, the cross-linkable groups of the wire should be similar to cross-linkable groups found in the enzyme. The first step in forming the network is complexing a cross-linkable, but not yet cross-linked, wire with the enzyme in a fast homogeneous solution reaction. In the next step, the enzyme–redox polyelectrolyte complexes are cross-linked to form the network. While the enzyme complexing water-soluble wires have high molecular weight, the cross-linkers are smaller water-soluble macromolecules that do not complex strongly either the enzyme or the redox macromolecule and thus do not break up their complex. Their molecular weight is low, so that they will not excessively adsorb on the electrodes and thereby interfere with the electrical contact between the electrode and the enzyme–redox polymer complex. When the aqueous solution of the cross-linker is mixed with the aqueous solution of the complex, and the mixed solution is concentrated, the three-dimensional structure, relaying electrons between the enzyme and the electrode, forms. Usually this curing is done on the electrode surface itself.

Enzyme Wiring Epoxy Cements

Three-dimensional redox polyelectrolyte networks that electrically connect enzyme redox centers to electrodes have been formed in different systems,[77-79] of which enzyme-wiring hydrophilic epoxy cements are an example.[78,79] Our recipe for making wired enzyme electrodes resembles instructions on tubings of household epoxy cements: "on a clean gold or carbon surface thoroughly mix one drop of the liquid in the blue container with one drop of the liquid in the red container, apply to the surface and allow to cure for 3 hours". In our case the "red" component is an aqueous solution of the complex formed of two polyamines: the enzyme, having lysine amines (and other epoxy-bondable functions), and the wiring redox polymer, now modified to a polyamine of the type shown in Figure 2. The polymer again has a poly(vinylpyridine) backbone with about one-third to one-fifth of the pyridines complexed to $[Os(bpy)(2)Cl]^{+/2+}$ and about half the pyridines reacted with 2-bromoethylamine, so as to form pyridinium-*N*-ethylamine polycationic domains that make the polymer well soluble in water and that readily react with epoxides. This MW 130 000 redox polyelectrolyte complexes enzyme proteins and wires their redox centers also without cross-linking, as seen in the isoelectric focusing experiment of Figure 3. The composition of the complex is 7:3 (w/w) polymer to glucose oxidase. Note that the polyanionic enzyme moves to the anode until reaching its isoelectric pH domain. The polymer, a polycation at any pH, smears to the cathode without focusing at a particular pH. The 7:3 complex formed between the two is immobile at pH 6.5. The polyamine of Figure 2 also complexes and penetrates the protein shell of lactate oxidase,[84] glycero-3-phosphate oxidase,[84] and cellobiose oxidase,[85] wiring these enzymes. Both the redox polyelectrolyte, having several hundred cross-linkable amines, and glucose oxidase, with 15 lysine amines, react with the diepoxide. The cross-linking diepoxide is a MW 400–600

(80) Kober, E. M.; Caspar, J. V.; Sullivan, B. P.; Meyer, T. J. *Inorg. Chem.* **1988**, *27*, 4587.
(81) Forster, R. J.; Kelly, A. J.; Vos, J. G.; Lyons, M. E. G. *J. Electroanal. Chem.* **1989**, *270*, 365–379.
(82) Oh, S. M.; Faulkner, L. R. *J. Electroanal. Chem.* **1989**, *111*, 5613–5618.
(83) Pishko, M. V.; Heller, A. Unpublished results.
(84) Katakis, I.; Heller, A. *Anal. Chem.* **1992**, *64*, 1008–1013.
(85) Elmgren, M.; Lindquist, S.-E. Private communication.

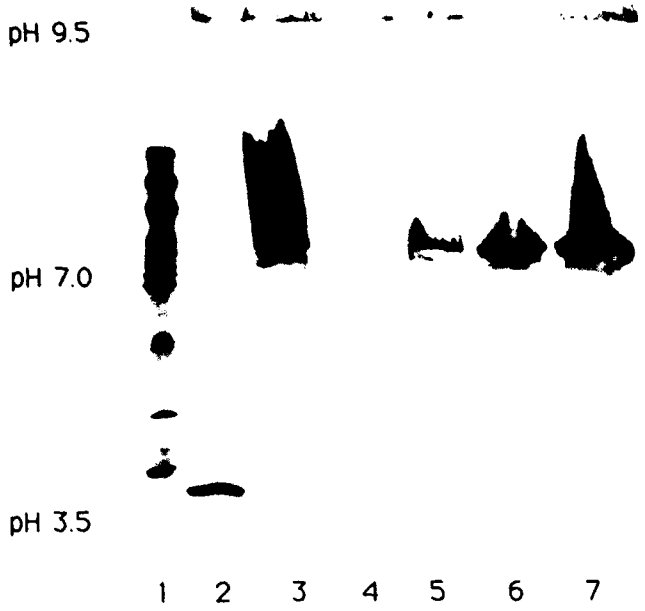

Figure 3. Isoelectric focusing experiment showing formation of a 1:1 (w/w) complex between the polycationic redox polyamine of Figure 2 and glucose oxidase: 1, isoelectric focusing pI standard; 2, glucose oxidase; 3, redox polymer; 4, 3:7 polymer/enzyme (w/w) ratio; 5, 1:1 polymer/enzyme (w/w) ratio; 6, 4:6 polymer/enzyme (w/w) ratio; 7, 7:3 polymer/enzyme (w/w) ratio. At 3:7 polymer to enzyme ratio (4) the complex precipitated, preventing its transfer to the gel.

poly(ethylene glycol) diglycidyl ether, of ~40-Å length when fully stretched, having 7–12 ethylene oxide units between its terminal epoxides. It has been chosen because it is water-soluble and because it interacts less with proteins than other polymers.

The Challenge of Analyzing the Kinetics of Three-Dimensionally Wired Enzyme Electrodes

Electrooxidation of a substrate like glucose at an electrode coated with the three-dimensional wired enzyme network involves a sequence of coupled processes: diffusion of the substrate to the surface of the hydrogel and the product away from it; diffusion of the substrate into the hydrogel and out-diffusion of the product; oxidation of the substrate and reduction of the enzyme's redox center according to eq 1; electron transfer from the enzyme's redox center to a nearby redox center of the complexing macromolecule; diffusion of the electron to the electrode, through percolative electron transfer within and between redox macromolecules; and electron transfer from a contacting macromolecule to an electrode. In the strongly hydrophilic open networks, substrate and product diffusion are not greatly different from those in water. Unless the substrate concentration is low enough to make the reaction mass transport limited also in the absence of the network, this process will not be rate limiting.[78] Electron transfer to the electrode from a nearby redox center of the redox macromolecule is also fast (simply because the centers are redox couples known to be fast). The rate-limiting process is tentatively perceived as the "spreading" of the charge from the reduced enzyme center through the wiring network.[79]

The redox polyelectrolyte-to-enzyme ratio must be high enough to wire most of the enzyme molecules; furthermore, because the conductance of the network increases upon increasing the redox polymer-to-enzyme ratio, whereby the average electron-transfer distance is reduced, a high polymer-to-enzyme ratio is of essence for efficient current collection when the turnover rate of the enzyme is high. The capacity of the network to carry current by multiple self-exchange reactions within and between its segments must equal or exceed the capacity of the incorporated enzyme molecules to deliver electrons.

The rate of electron diffusion through the redox polymer itself can be increased also by reducing the electron-transfer distances, through increasing the loading of the polymer with redox [Os-

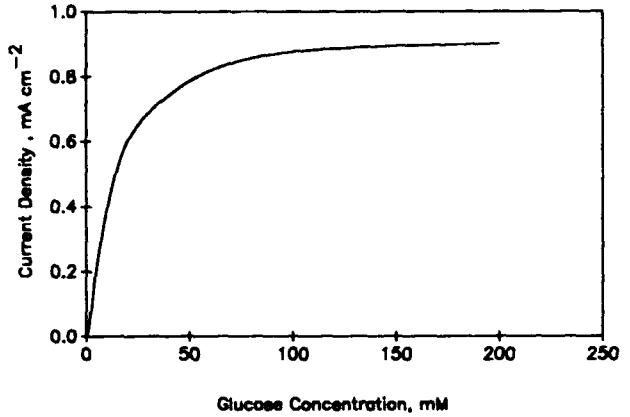

Figure 4. Dependence of the steady-state current density on the glucose concentration in an electrode made with a three-dimensional redox epoxy network wiring glucose oxidase: polished vitreous carbon; air-saturated physiological buffer; 0.4 V vs SCE; 1000 rpm.[88]

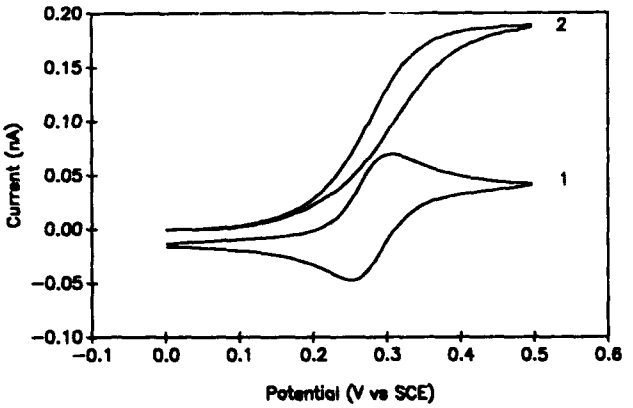

Figure 5. Current–voltage characteristics of a 7-μm-diameter glucose microelectrode at physiological (5 mM) glucose concentration. The electrode is an epoxy-embedded graphite fiber in a glass capillary. Physiological buffer; scan rate 5 mV s^{-1}. 1: no glucose; 2: 5 mM glucose.[39]

$(bpy)_2Cl]^{+/2+}$ centers. When heavily redox center loaded networks are used, enzymes like glucose oxidase are well connected at 10:1 polymer-to-enzyme ratio even in ~1-μm-thick films, and electrons are collected by the electrode faster than by the natural oxidant of the enzyme, molecular oxygen. The current collection efficiency, reflecting the relative rates of electron transfer via the wiring network to the electrode and electron transfer to oxygen, can be tracked using calibrated rotating ring-disk electrodes. Here the gold disk is coated with the wired enzyme; the ring is made of platinum, a catalyst for oxidation of the H_2O_2 generated through oxidation of the enzyme by reaction 2. In the absence of a disk potential sufficient to oxidize the wiring network, the enzyme in the network on the disk produces only hydrogen peroxide, the flux of which is observed as a ring electrooxidation current when the ring is poised at 0.7 V (SCE). The fraction of the enzyme electrically well connected to the electrode can be estimated from the loss in ring current when the oxidizing disk potential is turned on, i.e., when the wiring network and oxygen compete for electrons from the enzyme $FADH_2$ centers.

Wired Enzyme Network Based Microelectrodes

In semiinfinite electrodes and in concentrated glucose solutions, the steady-state current density reaches 0.8 mA cm^{-2} (Figure 4). In microelectrodes the current densities are even higher, reaching 2 mA cm^{-2}, because electrons diffuse now radially to the electrode surface.[39] In microelectrodes made with 7-μm-diameter epoxy embedded graphite fibers in glass capillaries of 20-μm o.d., we observe at physiological 5 mM glucose concentration an easy to measure 0.2-nA current (Figure 5) and, at limiting glucose concentration, a current of 1 nA. In these microelectrodes, electron transfer to the wiring network competes effectively with electron

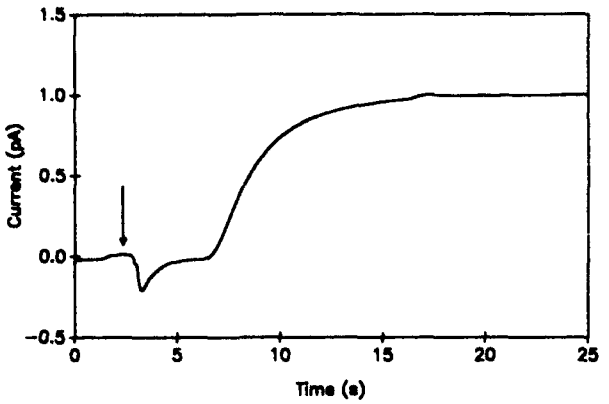

Figure 6. Response of the glucose microsensor of Figure 5 in a flow system to a glucose injection (5 mM glucose) as indicated by the arrow.[39]

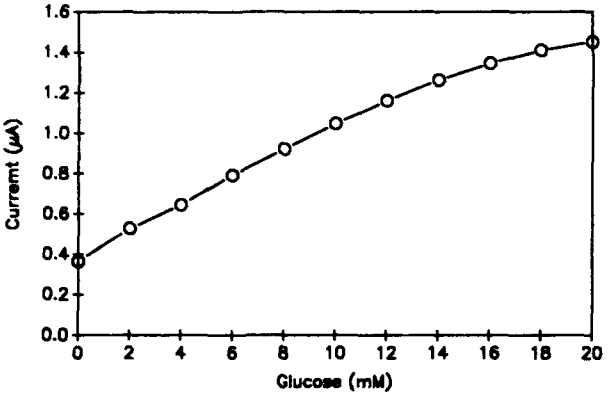

Figure 7. Dependence of the steady-state current on the glucose concentration in a redox–epoxy wired glucose electrode made with glucose oxidase genetically engineered for improved thermal and pH stability (3-mm-diameter vitreous carbon electrode, stirred aerated physiological buffer, 0.5 V vs SCE).[83]

transfer to oxygen. When the glucose solutions are air-saturated, the current is only 3% higher than in deaerated solutions under nitrogen (Figure 6).[39]

Stability of Wired Enzymes

Electrodes made with three-dimensionally wired epoxy networks can be stored at 25 °C either in air or in buffer solutions near pH 7 without substantial change for at least a month. It is possible that electrodes made with glucose oxidase, genetically engineered for improved thermal and pH stability,[47] will be even more stable upon storage. In the engineered thermostable enzyme the oligosaccharide-to-protein ratio is greatly increased, resulting in lower specific activity[47] and in a thicker insulating shell around the redox centers. We were, nevertheless, able to connect the redox centers of the thermostable enzyme to electrodes using epoxy cements (Figure 7).[83] Because the redox polymer network excludes proteolytic enzymes, the network-embedded enzyme appears stable to their attack. With the potential applied, the electrodes made with the standard enzyme from *Aspergillus niger* operate at ambient temperature in an aqueous buffered glucose solution with a ~2% loss of current per day.[83] The rate of current decay is faster at 37 °C, and the electrodes require more frequent recalibration. Interestingly, when used in blood plasma,[86] the current of the electrodes drops drastically but reversibly; the current is restored when the electrodes are removed from blood and are retested in glucose-containing buffer.

Initial in Vivo Experiments

Even with the substantial reversible current loss in blood, we were able to observe in experiments involving subcutaneously inserted needle-type redox polymer wired glucose electrodes current

(86) Kerner, W.; Pishko, M. V.; Heller, A. Unpublished results.

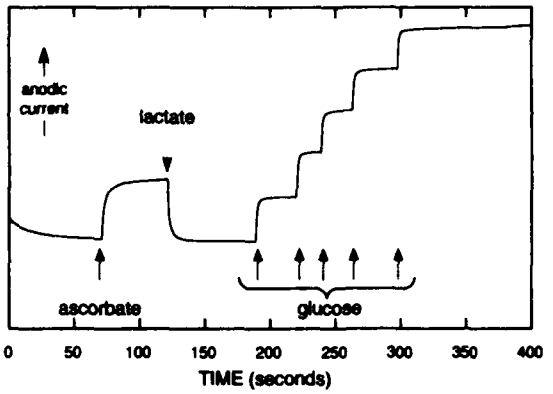

Figure 8. Suppression of the ascorbate electrooxidation current upon injection of lactate in a wired glucose oxidase electrode coated with immobilized peroxidase and lactate oxidase. Lactate and oxygen react in the presence of lactate oxidase to form pyruvate and hydrogen peroxide. Hydrogen peroxide oxidizes ascorbate in the presence of horseradish peroxidase.[87]

changes paralleling independently measured blood glucose levels. Because the current in these needle-type macroelectrodes was mass transport, i.e. glucose diffusion, limited and because their response was fast, the electrodes were sensitive to movement. To reduce movement sensitivity, our in vivo assays involve now coincidence measurements made with pairs of subcutaneous electrodes. The coincidence measurements allow rejection of current transients resulting from the movement of one limb of a pair with implanted subcutaneous sensors. Either such coincidence measurements or microelectrode arrays, where the current is not mass transport limited, are likely to allow reduction of electrode-movement-related noise.

Elimination of Currents from Electrooxidizable Interferants

The electrodes, when used as biosensors, can be quite sensitive to electrooxidizable constituents other than the substrate of the wired enzyme. Common interferants in amperometric blood glucose assays include ascorbate (vitamin C), urate, and acetaminophen, known in the U.S. as Tylenol. These compounds are electrooxidized on the Os-complex loaded electrodes. We eliminate their interference by preoxidizing the samples at peroxidase films applied to our electrode surfaces.[87] While glucose is immune to rapid oxidation by hydrogen peroxide in the presence of a peroxidase, the interferants are promptly oxidized. The peroxide required to make the electrodes highly glucose specific is, of course, not externally added in implanted electrodes but generated in situ using an oxidase of a serum constituent such as lactate. An example of the suppression of the effects of interferants in a wired glucose oxidase electrode through an added layer of lactate oxidase and peroxidase is seen in Figure 8. Here blood lactate and oxygen react to form pyruvate and hydrogen peroxide; the peroxide oxidizes peroxidase, and the oxidized peroxidase then oxidizes and thus eliminates the interferants.[88]

A View of the Status of Amperometric Biosensors for in Vivo Applications and Feedback Loops

Solutions are now in hand to some of the problems associated with building in vivo biosensors, including solution to the problem of building biosensors where all components are bound in a single giant three-dimensional structure, i.e., without components that might leach into the blood;[79] to the problem of eliminating interferants, common in the blood, that affect the accuracy of the readings;[87] and to the problem of high enough current densities to allow miniaturization to dimensions characteristic of components in microelectronic devices.[39] Problems that remain, and on which colleagues worldwide and we are working, are stabilization of the response of the sensors in order to extend the period between their required recalibration or replacement; exclusion of the blood

(87) Maidan, R.; Heller, A. *J. Am. Chem. Soc.* **1991**, *113*, 9003–9004.
(88) Ye, L.; Heller, A. Unpublished results.

component that reversibly suppresses the current; attachment, by covalent bonding, of poly(ethylene oxide) or other nonfouling blood compatible membranes to the surface of the electrodes; and further reduction in sensitivity to motion. While these problems are real, all can be addressed by applying already existing knowledge.

Acknowledgment. Our work is supported in part by the Office of Naval Research, the National Science Foundation, The Welch Foundation, and the Texas Advanced Research Program. I thank Chiron Corp. for a gift of genetically engineered thermostable glucose oxidase and Barry Miller for reading the manuscript.

Reprinted from The Journal of Physical Chemistry, 1991, 95.

Redox Polymer Films Containing Enzymes. 1. A Redox-Conducting Epoxy Cement: Synthesis, Characterization, and Electrocatalytic Oxidation of Hydroquinone

Brian A. Gregg*,† and Adam Heller*

Department of Chemical Engineering, University of Texas at Austin, Austin, Texas 78712
(Received: October 30, 1990; In Final Form: April 1, 1991)

A two-component redox-conducting epoxy cement has been prepared and electrochemically characterized. The redox epoxy, designed for use in enzyme electrodes (see following paper), is formed by reacting two water-soluble components (a poly(vinylpyridine) complex of $Os(bpy)_2Cl$ and a diepoxide) under near-physiological conditions. The resulting films are hydrophilic, strongly bound to gold and carbon electrode surfaces, and highly permeable to water-soluble molecules and ions. The electron "diffusion coefficient", D_e, of such films at 25 °C, pH 7 is approximately (2–4) × 10^{-9} cm^2/s and shows an activation energy of 60 ± 2 kJ/mol. D_e increases with increasing ionic strength and with decreasing pH. Measurement of the characteristic current densities for electron "diffusion" and for the electrocatalytic oxidation of hydroquinone in the redox polymer shows that a substantial portion of the film is electroactive.

Introduction

Our interest[1-6] in enzyme electrodes[7-12] has led us to develop a novel method for making cross-linked redox polymers that resemble hydrophilic epoxy cements. Binding an enzyme covalently into a polymer film on an electrode surface demands a hydrophilic and enzyme-binding reaction that can occur under near-physiological conditions and that results in a polymer matrix that promotes the stability of the enzyme. Further desirable characteristics in such polymers include fast diffusion of substrate and product through the polymer film, rapid electron self-exchange in the redox polymer, and facile electrical communication with the active site of the oxidoreductase. We previously reported[6] a redox polymer based on a poly(vinylpyridine) complex of osmium bis(bipyridine) chloride that was cross-linked by the reaction between pendant *N*-hydroxysuccinimide groups and lysines on the enzyme surface. However, competition between the desired aminolysis of the *N*-hydroxysuccinimide groups and their spontaneous hydrolysis resulted in unsatisfactory variations from film to film. Here we report an improved and simplified polymer and a process that employs a classical cross-linking reaction and results in durable and reproducible polymer films. The cross-linking process consists of the reaction between a commercially available, water-soluble diepoxide and the primary amino functions both on the enzyme surface and pendant on the polymer. We describe the synthesis of the polymer and examine the effects of cross-linker concentration, ionic strength, pH, and temperature on its electrochemical behavior. The permeability of these redox polymer films to a test compound, *p*-benzoquinone, is described as is the electrocatalytic oxidation of hydroquinone. These results allow us to characterize the kinetics of substrate permeability, electron "diffusion", and electrocatalysis in these films and compare them to known redox polymers. The following paper describes the electrochemical characteristics of these redox polymer films containing covalently bound glucose oxidase.

Experimental Section

Chemicals. 2-Bromoethylamine hydrobromide (Aldrich), poly(ethylene glycol) diglycidyl ether (Polysciences, PEG 400, cat. no. 08210), K_2OsCl_6 (Johnson Matthey), and Na–HEPES (sodium 4-(2-hydroxyethyl)-1-piperazineethanesulfonate) (Aldrich) were used as received. Poly(4-vinylpyridine) (PVP, Polysciences, MW 50,000) was purified three times by dissolution in methanol, filtration, and precipitation with ether. Unless otherwise noted, all experiments were performed at room temperature in a standard aqueous buffer solution containing 100 mM NaCl and 20 mM phosphate at pH 7.1.

Redox Polymer, POs–EA. *cis*-bis(2,2′-bipyridine-*N*,*N*′)dichloroosmium(II)[13] (0.494 g, 0.864 mmol) and poly(4-vinyl-

† Present address: Solar Energy Research Institute, 1617 Cole Blvd., Golden, CO 80401-3393.

(1) Degani, Y.; Heller, A. *J. Phys. Chem.* **1987**, *91*, 1285–1289.
(2) Degani, Y.; Heller, A. In *Redox Chemistry and Interfacial Behavior of Biological Molecules*; Dryhurst, G., Niki, K., Eds.; Plenum Press: New York, 1987.
(3) Degani, Y.; Heller, A. *J. Am. Chem. Soc.* **1988**, *110*, 2615–2620.
(4) Degani, Y.; Heller, A. *J. Am. Chem. Soc.* **1989**, *111*, 2357–2358.
(5) Pishko, M. V.; Katakis, I.; Lindquist, S.-L.; Ye, L.; Gregg, B. A.; Heller, A. *Angew. Chem., Int. Ed. Engl.* **1990**, *29*, 82–84.
(6) Gregg, B. A.; Heller, A. *Anal. Chem.* **1990**, *62*, 258–263.
(7) Wise, D. L., Ed. *Applied Biosensors*, Butterworth: Boston, 1989.
(8) Luong, J. H. T.; Mulchandani, A.; Guilbault, G. G. *Trends Biochem.* **1988**, *6*, 310–316.
(9) Higgins, I. J. *Biotec* **1988**, *2*, 3–8.
(10) Bartlett, P. N.; Whitaker, R. G. *Biosensors* **1987/1988**, *3*, 359–379.
(11) Foulds, N. C.; Lowe, C. R. *Anal. Chem.* **1988**, *60*, 2473–2478.
(12) Hale, P. D.; Inagaki, T.; Karan, H. I.; Okamoto, Y.; Skotheim, T. A. *J. Am. Chem. Soc.* **1989**, *111*, 3482–3484.

0022-3654/91/2095-5970$02.50/0

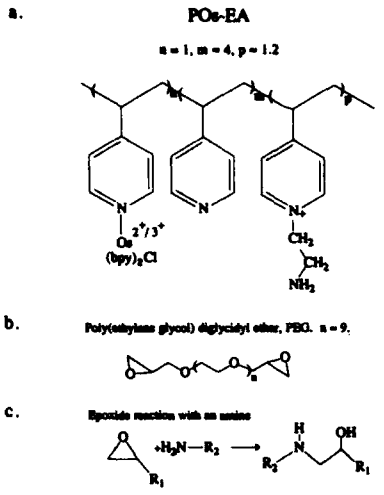

Figure 1. (a) Approximate chemical structure of the osmium-containing redox polymer backbone, POs–EA; bpy is 2,2'-bipyridine. (b) Chemical structure of the diepoxide cross-linking agent. (c) General reaction of an epoxide with an amine.

pyridine) (0.430 g, 4.09 mequiv) were heated under nitrogen at reflux in 18 mL of ethylene glycol for 2 h. After the solution was cooled to room temperature, 30 mL of DMF and 1.5 g of 2-bromoethylamine hydrobromide (7.3 mmol) were added, and the solution was stirred at 45 °C overnight. The crude polymer was precipitated by pouring the solution into rapidly stirred acetone. The hygroscopic precipitate was collected, dissolved in H_2O, filtered, and precipitated as the PF_6^- salt by addition of a solution of NH_4PF_6. The dry PF_6^- salt (0.49 g) was then dissolved in 20 mL of acetonitrile, diluted with 50 mL of H_2O, and stirred over 5.2 g of anion exchange beads (Bio-Rad AG1-X4, chloride form) for 2 h. This solution was filtered and evaporated under vacuum to ca. 10 mL. Concentrated HCl was then added to pH 2, and the solution was dripped into rapidly stirred acetonitrile. The precipitate was filtered and dried in a vacuum desiccator.

Both hexafluorophosphate and chloride forms of the polymer were analyzed by elemental analysis (Galbraith) and by visible absorption spectrophotometry. The approximate structure of the polymer (hereinafter referred to as POs–EA) at pH 7 is shown in Figure 1. The estimated molar mass of the polymer repeat unit, as precipitated at pH 2, is 1510 g/equiv.

Electrodes. A representative electrode film was prepared as follows: a vitreous carbon rotating-disk electrode (3 mm diameter) was polished on a polishing cloth sequentially with alumina of decreasing particle size (1 μm, 0.3 μm, 0.05 μm), sonicated, rinsed with water after every polish, and then dried in air. A 50-μL portion of a stock solution of POs–EA (4 mg/mL in 10 mM HEPES, pH 8.2) was added to 10 μL of a stock solution of poly(ethylene glycol) diglycidyl ether (PEG, 2.3 mg/mL in H_2O). Of the resulting mixture, 2 μL was applied to the vitreous carbon disk and allowed to dry and set up at 37.5 °C for 48 h. The electrodes were then rinsed in H_2O for 10 min to remove any salts and unreacted species and dried at 37.5 °C for one more hour before use.

Deactivated gold-disk electrodes for the electrocatalysis experiments were prepared by polishing with alumina, as above, but on a tissue (Kimwipe) surface. This treatment reproducibly decreased the electron-transfer kinetics for gold electrodes, although the mechanism for this decrease is uncertain.

Equipment. Electrochemical measurements were performed with a Princeton Applied Research 175 universal programmer, a Model 173 potentiostat and a Model 179 digital coulometer. The signal was recorded on a Kipp and Zonen X-Y-Y' recorder. A single-compartment, water-jacketed electrochemical cell was used with an aqueous saturated calomel (SCE) reference electrode and a platinum counter electrode. All potentials are reported vs SCE. The rotating-disk experiments utilized a Pine Instruments AFMSRX rotator and MSRS speed control.

Chronoamperometry. These measurements were performed with a Princeton Applied Research Model 273 potentiostat. The potential was initially held at 0.0 V vs SCE for 15 s, then stepped to 0.60 V for 0.3 s before stepping back to 0.0 V. The slopes of the resulting i vs $t^{-1/2}$ plots were unaffected by extending the range of the potential step (−0.2 V to 0.7 V) or by varying the residence time (0.2–0.5 s). Three hundred data points were recorded. The reported results are averages of four or five measurements. The temperature-resolved experiments began with the water-jacketed cell and electrolyte solution at ca. 5 °C. The cell was slowly warmed (~40 °/h) with a heat gun while the temperature was measured with a thermometer close to the electrode. The electrode was rotated at 500 rpm to promote mixing and prevent temperature gradients.

Results and Discussion

Redox Polymer, POs–EA. The immobilization of enzymes in inert polymers has been the subject of extensive research.[14,15] POs–EA (Figure 1) is a variation on our previously reported osmium-containing polymer[6] in which cross-linking is now achieved via the reaction of a commercially available, water-soluble diepoxide with the pendant amine functions on the polymer as well as with amine functions (e.g., lysines) on the enzyme surface. This material is synthetically simpler than the previous polymer and stable in aqueous solution for at least 1 month. The reaction between epoxide and amine proceeds very slowly in neutral aqueous solution. Thus, a solution of POs–EA containing the diepoxide (PEG), with or without enzyme, can be prepared that remains essentially unreacted for at least 48 h. The reaction between epoxide and amine takes place to a significant extent only after the solution has been dried onto a surface. This greatly enhances the simplicity and reproducibility of the electrode-making process relative to the previous polymer[6] which contained N-hydroxysuccinimide groups capable of reacting *both* with primary amines *and* with water. The reaction between the diepoxide and POs–EA (see Figure 1) does not change the charge density on the polymer; it simply transforms a pendant primary amine group into a secondary amine when it reacts with one epoxide, or to a tertiary amine when it reacts with two epoxides.

Both POs–EA and PEG are highly water soluble. The hydrophilicity of the two components of the redox polymer, and the use of a long cross-linking agent (PEG is approximately 40 Å long when extended), were expected to result in a highly swollen, gel-like redox polymer structure that would promote facile permeation of the films by substrate and product molecules. We show below that these films are indeed highly permeable to solution species. The epoxy–amine network-forming reaction yields tough, hydrophilic redox-conducting epoxy cements that are strongly adsorbed to platinum, gold, ITO, graphite, or vitreous carbon electrode surfaces.

Typical cyclic voltammograms of POs–EA cross-linked with 5.9 wt % PEG on a vitreous-carbon-disk electrode in the standard aqueous buffer solution at pH 7.1 are shown in Figure 2. At low scan rates (Figure 2a) the voltammograms exhibit the classical symmetric shape,[16] showing the reversible oxidation and reduction of a surface bound species with an apparent standard potential of 0.28 V vs SCE. Faster scan rates (Figure 2b) lead to a splitting of the oxidation and reduction peaks and to a tailing of the waves characteristic of a diffusion-limited process.

Effects of Cross-linker Concentration on Peak Potential and Peak Width. A series of eight electrodes were made with concentrations of the cross-linking agent (PEG) varying from 2% to 21% of the total film weight. The highest concentration corresponds to about one molecule of PEG per 3.8 reactive sites on the polymer (i.e., per 1.9 amines, each of which can react twice).

(13) Lay, P. A.; Sargeson, A. M.; Taube, H. *Inorg. Syn.* **1986**, *24*, 291–306.

(14) Mosbach, K., Ed. *Methods in Enzymology*; Academic Press: New York, 1987; Vols. 135–137.

(15) Trevan, M. D. *Immobilized Enzymes*; Wiley: New York, 1980.

(16) Murray, R. W. In *Electroanalytical Chemistry*; Bard, A. J., Ed.; Marcel Dekker: New York, 1984; pp 191–368.

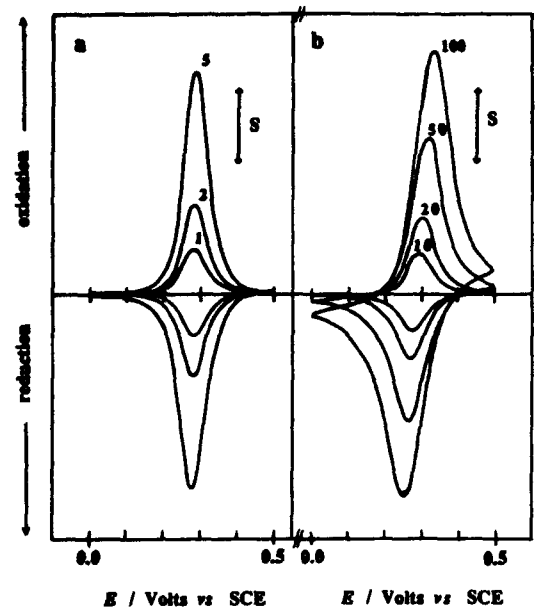

Figure 2. Cyclic voltammograms of POs–EA crosslinked with 5.9 wt % PEG, $\Gamma = 2.2 \times 10^{-8}$ mol/cm^2, in the standard buffer at pH 7.1. The numbers on the curves give the scan rate in mV/s. (a) $S = 56.6$ μA/cm^2. (b) $S = 566$ μA/cm^2.

Approximately the same total weight of POs–EA plus PEG, 5μg, was applied to each electrode (geometrical area = 0.071 cm^2). The amount of polymer that remained bound to the electrode surface was found to be independent of cross-linker concentration. After the 48-h reaction time, 86% ± 6% of the POs–EA originally applied to the electrode surface was electroactive, as measured by integrating the current under a cyclic voltammogram at a slow scan rate (1 mV/s). When the reaction time was extended to 3 days, an average of 90% remained bound to the surface. Thus, even lightly cross-linked films are almost quantitatively secured to the electrode surface.

Increasing the concentration of cross-linker in the polymer films shifts the apparent standard potential, E°, of the osmium couple to more positive values and increases the peak width at half-height, E_{whm}, of both oxidation and reduction waves (Figure 3). Most redox polymer films exhibit an E_{whm} greater than the theoretical value of 90.6 mV,[16] although narrower peaks have also been observed. The POs–EA films exhibit peak widths as low as 68 mV at low cross-linker concentration (2% by weight) and increase up to approximately the theoretical value at high PEG concentration (21% by weight). The oxidation peaks were always slightly narrower than the reduction peaks (Figure 3).

"Diffusion Coefficients" for Charge Propagation. Potential step chronoamperometry[16] leads to the determination of the product $D_e^{1/2}C_p$, where D_e is the "diffusion coefficient" for the diffusion-like propagation of charge through the polymer film and C_p is the concentration of redox centers in the film. Thus, if C_p or, equivalently, the film thickness is known, D_e may be calculated. Since the film thickness under experimental conditions is usually not known precisely, the value of $D_eC_p^2$ (or its square root) is often reported. Chronoamperometry in the standard buffer solution at room temperature of the eight electrodes with varying cross-linker concentration led to the values of $D_eC_p^2$ shown in Figure 4. Within the accuracy of these measurements (±50%), $D_eC_p^2$ does not exhibit any obvious trend with concentration of cross-linker; the variations between electrodes are seemingly random. The average value and standard deviation of $D_eC_p^2$ for the eight electrodes is $(6.4 \pm 0.9) \times 10^{-16}$ mol^2 cm^{-4} s^{-1}. This compares well with literature results for similar polymers.[17-19] As an

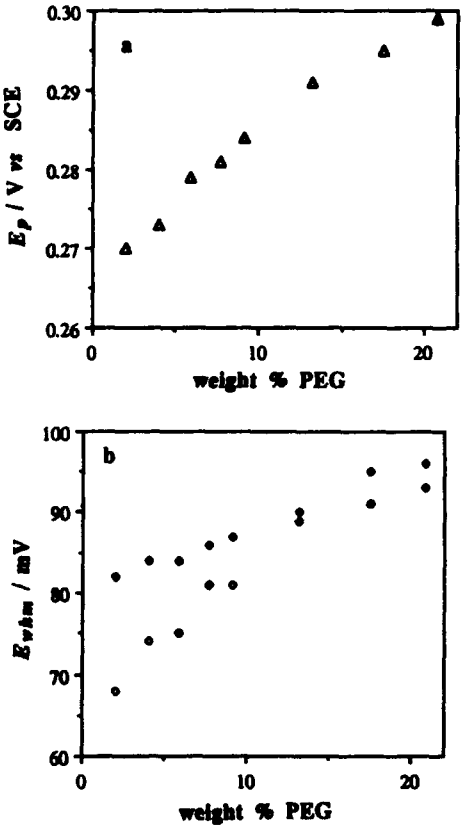

Figure 3. (a) Change in the peak potential of POs–EA with increasing wt % cross-linker. Average electroactive surface coverage is $\Gamma = (3.7 \pm 0.3) \times 10^{-8}$ mol/cm^2. (b) Change in peak width at half-height, E_{whm}, with increasing wt % cross-linker for oxidation peaks (◊) and reduction peaks (♦) measured at 5 mV/s.

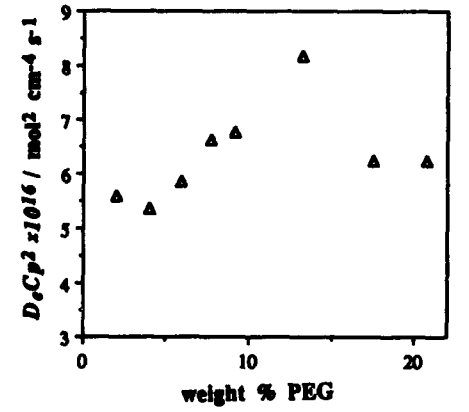

Figure 4. Change in chronocoulometric response, shown as $D_eC_p^2$, with increasing wt % cross-linker for electrodes described in Figure 3.

illustration of the magnitude of the electron "diffusion coefficient": if the concentration of redox sites in the polymer, C_p, were 6.5 $\times 10^{-4}$ mol/cm^3 (corresponding to a dry film at pH 7 with 9% by weight cross-linker and a density of 1.0 gm/cm^3), then $D_e \approx (1.5 \pm 0.2) \times 10^{-9}$ cm^2/s. If C_p were 5.0×10^{-4} mol/cm^3 (corresponding to a partially solvent-swollen film), then $D_e \approx (2.6 \pm 0.4) \times 10^{-9}$ cm^2/s.

Interpretation of D_e as the "diffusion coefficient" for charge propagation through the polymer film requires that charge propagation be the rate-limiting step in the chronoamperometric response, rather than, for example, the flow of charge-compensating counterions. A steady-state method of measuring D_e that eliminates interferences from other possible rate-limiting processes and that does not require knowledge of C_p has been described.[20]

(17) Andrieux, C. P.; Haas, O.; Saveant, J.-M. *J. Am. Chem. Soc.* **1986**, *108*, 8175–8182.
(18) Forster, R. J.; Kelly, A. J.; Vos, J. G.; Lyons, M. E. G. *J. Electroanal. Chem.* **1989**, *270*, 365–379.
(19) Oh, S.-M.; Faulkner, L. R. *J. Am. Chem. Soc.* **1989**, *111*, 5613–5618.
(20) Chen, X.; He, P.; Faulkner, L. R. *J. Electroanal. Chem.* **1987**, *222*, 223–242.

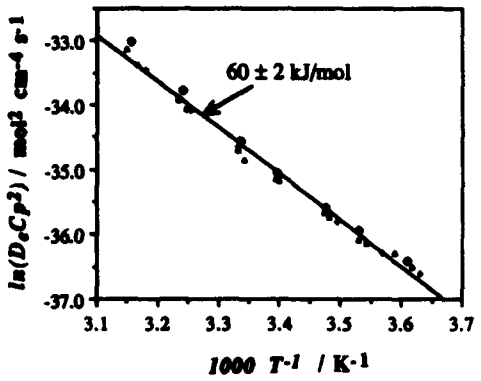

Figure 5. Arrhenius plot of chronocoulometric response, $D_eC_p^2$, as a function of temperature for four electrodes with cross-linker concentrations ranging from 2% to 21% by weight.

We applied this technique to corroborate our values of $D_eC_p^2$ obtained from chronoamperometry. A relatively thick layer of POs–EA was deposited over both ring and disk of a ring-disk electrode and the steady-state disk current was measured with both ring and disk biased at 0.50 V (polymer in the Os^{III} state) and with the disk at 0.50 V and the ring at 0.00 V (Os^{II} state, i.e. electrons flowing from ring to disk). From the difference in the two steady-state currents and a knowledge of the dimensions of the ring and the disk, an apparent value of $D_e \approx 4 \times 10^{-9}$ cm²/s was estimated.[20] The uncertainty in this experiment is large because of the small signal-to-noise ratio; nevertheless, the approximate agreement with the chronamperometric results lends confidence to our interpretation that these measurements reflect the "diffusion coefficient" for electrons.

For descriptions of electrocatalytic reactions, the measurement of $D_eC_p^2$ can be combined with the experimentally measured electroactive surface coverage, Γ_p, to calculate the limiting current density for electron "diffusion", j_e, through the polymer film[17,21,22] according to

$$j_e = FD_eC_p^2/\Gamma_p \quad (1)$$

where F is Faraday's constant. j_e expresses the maximum steady-state current density for an electrocatalytic reaction occurring only at the polymer/solution interface, eq 1 being simply the Fick's Law expression for electron "diffusion" through a completely concentration-polarized film of thickness $d = \Gamma_p/C_p$. If the electrocatalytic reaction occurs throughout the bulk of the polymer film, or primarily in a zone close to the electrode surface, current densities substantially higher than j_e may be attained.[22,23] The average electron-"diffusion"-limited current density for the electrodes shown in Figure 4 is $j_e = 1.7 \pm 0.3$ mA/cm².

Activation Energy for Charge Transfer. The chronoamperometric responses of four electrodes (wt % PEG: 2.0, 5.9, 9.1, and 21) were measured as a function of temperature, Figure 5. The activation energies for electron "diffusion" of these electrodes were identical within experimental error: $E_{act} \approx 60 \pm 2$ kJ/mol. Thus, a single line is fitted to the data for these four electrodes in Figure 5. Forster et al.[18] reported activation energies for a similar, but noncross-linked, osmium-containing polymer that varied from 16 to 122 kJ/mol depending on the type of electrolyte and the ionic strength, while Lyons et al.[24] reported that E_{act} ranged from 32 to 43 kJ/mol for a similar, but noncross-linked, ruthenium-containing polymer. The lack of a dependence of E_{act} on cross-linker concentration contrasts with the results of Oh and Faulkner,[19] who observed an almost linear increase in the activation energy of D_e with increasing cross-linker concentration, from about 25 kJ/mol at 4% cross-linker to about 59 kJ/mol at 12% cross-linker.

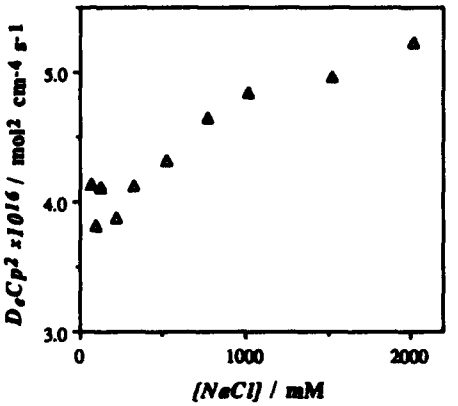

Figure 6. Change in chronoamperometric response, $D_eC_p^2$, with concentration of sodium chloride for a vitreous carbon electrode coated with POs–EA, $\Gamma = 2.7 \times 10^{-8}$ mol/cm², 4.0 wt % PEG.

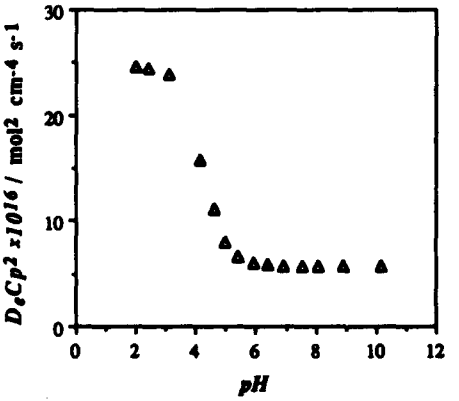

Figure 7. Change in chronoamperometric response, $D_eC_p^2$, with pH for a vitreous carbon electrode coated with POs–EA, $\Gamma = 2.2 \times 10^{-8}$ mol/cm², 5.9 wt % PEG.

Their result was interpreted as implying that electron "diffusion" was controlled by segmental motions of the polymer; i.e., the electron would hop between redox sites only after random fluctuations of the polymer brought the two sites together. Increasing the degree of cross-linking restricted polymer chain motion and thus increased E_{act}. The discrepant behavior of POs–EA/PEG may be explained by our use of a very long cross-linker; the length from pyridine to pyridine along the (extended) PEG chain is about 48 Å, i.e. much greater than the average osmium complex to osmium complex distance along the polymer backbone (≈15 Å). Hence, PEG probably does not greatly restrict the short-range polymer segmental motion, which presumably controls the electron-transfer process.

Effect of Ionic Strength and pH on Charge Transfer. The kinetics of charge transfer through the polymer film, as expressed by $D_eC_p^2$, is a function of both the ionic strength of the solution and of the pH. Figure 6 shows the change in $D_eC_p^2$ for a vitreous carbon electrode coated with POs–EA ($\Gamma = 2.7 \times 10^{-8}$ mol/cm², 4.0 wt % PEG) as NaCl is added to a solution of 10 mM phosphate buffer at pH 7.1. Such an increase in $D_eC_p^2$ with ionic strength has been observed previously.[18] This may be caused by the increased self-association of the polymer at high ionic strengths, as is often observed in solution,[25,26] i.e. by an increase in C_p rather than D_e. The tendency for polyelectrolytes to self-associate, or coil, with increasing ionic strength has been held responsible for the decrease in efficiency of noncross-linked, redox polymer-mediated oxidation of glucose oxidase at high ionic strength.[4,5] This decrease in efficiency is still evident, but substantially alleviated, in glucose oxidase containing films of POs–EA/PEG,[27]

(21) Andrieux, C. P.; Saveant, J. M. *J. Electroanal. Chem.* **1982**, *134*, 163–166.
(22) Andrieux, C. P.; Dumas-Bouchiat, J. M.; Saveant, J. M. *J. Electroanal. Chem.* **1982**, *131*, 1–35.
(23) Buttry, D. A.; Anson, F. C. *J. Am. Chem. Soc.* **1984**, *106*, 59–64.
(24) Lyons, M. E. G.; Fay, H. G.; Vos, J. G.; Kelly, A. J. *J. Electroanal. Chem.* **1988**, *250*, 207–211.
(25) Katchalsky, A. *Pure Appl. Chem.* **1971**, *26*, 327–373.
(26) Eisenberg, H. *Biological Macromolecules and Polyelectrolytes in Solution*; Clarendon Press: Oxford, 1976.
(27) Gregg, B. A.; Heller, A. Unpublished results.

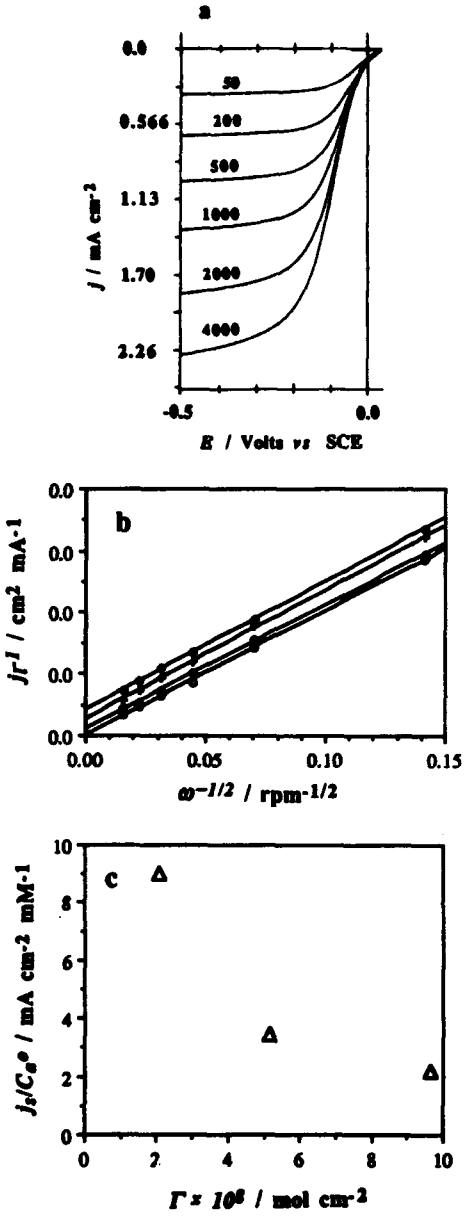

Figure 8. (a) Reduction of 1.1 mM benzoquinone on a POs–EA/PEG-coated gold-disk electrode at 5 mV/s. Electrode area is 0.071 cm^2, surface coverage is $\Gamma = 2.1 \times 10^{-8}$ mol/cm^2. The numbers on the curves give the rotation rate in rpm. (b) Koutecky–Levich plots of benzoquinone reduction current at −0.5 V at POs–EA/PEG-coated electrodes as a function of surface coverage: (○) bare gold electrode; (♦) $\Gamma = 2.1 \times 10^{-8}$ mol/cm^2; (+) $\Gamma = 5.2 \times 10^{-8}$ mol/cm^2; (◇) $\Gamma = 9.7 \times 10^{-8}$ mol/cm^2. (c) Benzoquinone permeation current density per millimolar concentration as a function of surface coverage.

suggesting that cross-linking results in a reduced tendency to alter conformation with changing ionic strength.

The change in $D_eC_p^2$ with pH is shown in Figure 7. A 200 mM solution of NaCl and HCl, pH 2.3, was titrated with 200 mM NaOH while the chronoamperometric response was measured. A marked change in $D_eC_p^2$ occurred around pH 4, close to the reported pK_a of poly(vinylpyridine) (p$K_a \approx 3.3$).[18] An increase of $D_eC_p^2$ in a similar polymer with decreasing pH has recently been reported,[18] where, however, only the range from pH 1 to pH 0.3 was examined. The protonation of the polymer occurring near its pK_a is expected to cause at least some swelling of the film as the charge density and counterion concentration increase; thus, C_p will probably decrease. Thus, it appears that the increase in $D_eC_p^2$ is caused by an increase in D_e. This interpretation is, however, tentative and requires further corroboration.

Permeability. The permeability of redox polymer films to solution species is of importance for biosensor and electrocatalytic applications. Thus, the reduction of a model compound, *p*-benzoquinone, as a function of film thickness and cross-linker concentration was investigated. The reduction of *p*-benzoquinone occurs at a potential approximately 0.25–0.30 V negative than that of the osmium(III/II) couple. Thus, catalytic reduction on the osmium polymer can be neglected. The electroreduction of benzoquinone at a POs–EA/PEG-coated gold-disk electrode is shown in Figure 8a at different rotation rates.

The limiting current density, j_l, for a substrate that partitions into a film and diffuses through it to the electrode is described by[28-30]

$$1/j_l = d/FC_s^\circ \kappa D_s + 1/0.62FC_s^\circ D^{2/3}\nu^{-1/6}\omega^{1/2} \qquad (2)$$

where d is the film thickness, C_s° is the bulk concentration of substrate, κ is the partition coefficient of substrate into the polymer film, D_s is the diffusion coefficient of substrate inside the polymer film, D is the diffusion coefficient of substrate in solution, ν is the kinematic viscosity, and ω is the angular velocity of the rotating electrode. In the kinetic treatment of redox polymer electrodes given by Saveant and co-workers,[17,21,22,31,32] a characteristic current density for substrate diffusion through polymer-modified electrodes is formulated[21] as

$$j_s = FC_s^\circ \kappa D_s/d \qquad (3)$$

thus, the intercept of a plot of j_l^{-1} vs $\omega^{-1/2}$ gives j_s. Figure 8b shows such plots for a bare gold electrode and for three gold electrodes coated with different thicknesses of POs–EA/PEG. The resulting characteristic current densities for substrate diffusion through the polymer films show the expected decrease with increasing film thickness (Figure 8c). Similar measurements demonstrated that the permeability was independent of cross-linker concentration in the range 2–21 wt % PEG. The data shown in Figure 8 establish that POs–EA films are highly permeable to benzoquinone, showing permeation current densities, j_s, of greater than 2 mA/cm^2 per millimolar concentration of substrate, even for quite thick polymer films. The decrease in benzoquinone reduction current between a bare gold electrode and one coated with a ca. 1.5-μm (dry thickness) film of POs–EA/PEG is less than 15% at 50 rpm. Hence, in biosensor or electrocatalytic applications, such electrodes are not expected to be limited by the permeability of small, uncharged substrates through the redox polymer film.

Electrocatalytic Oxidation of Hydroquinone. The oxidation of hydroquinone on a deactivated gold surface at pH 7.1 is kinetically slow, allowing observation of its catalytic oxidation on a POs–EA-coated gold electrode, Figure 9. The formal potential of the hydroquinone/benzoquinone couple at pH 7.1 is 0.04 V vs SCE;[33] thus, its oxidation by the osmium complex of POs–EA ($E_p \approx 0.28$ V) is essentially irreversible. Figure 9 shows the sluggish oxidation of a 3.1 mM hydroquinone solution on the deactivated[34] gold surface (shown at $\omega = 2000$ rpm), while on the polymer-coated

(28) Gough, D. A.; Leypoldt, J. K. *Anal. Chem.* **1979**, *51*, 439.
(29) Leddy, J.; Bard, A. J. *J. Electroanal. Chem.* **1983**, *153*, 223–242.
(30) Oh, S. M.; Faulkner, L. R. *J. Electroanal. Chem.* **1989**, *269*, 77–97.
(31) Andrieux, C. P.; Dumas-Bouchiat, J. M.; Saveant, J. M. *J. Electroanal. Chem.* **1984**, *169*, 9–21.
(32) Leddy, J.; Bard, A. J.; Maloy, J. T.; Saveant, J. M. *J. Electroanal. Chem.* **1985**, *187*, 205–227.
(33) Bard, A. J.; Faulkner, L. R. *Electrochemical Methods*; Wiley: New York, 1980.
(34) On nondeactivated gold electrodes (i.e., polished with aluminum on a polishing cloth rather than on a Kimwipe), the oxidation of H_2Q leads to a higher current (by about a factor of 4) than on deactivated electrodes, but the shape of the wave is similar to that shown in Figure 9; i.e., no current plateau is reached in the accessible potential range (up to 0.55 V vs SCE). On nondeactivated, POs–EA-coated gold electrodes, waves attributable to oxidation of H_2Q on both the gold substrate and on the POs–EA were observed, but the current reached a distinct plateau on the film-covered electrodes and was substantially higher than on the bare electrodes. The catalytic current onset was shifted negative of the POs–EA onset potential. At low rotation rates a wave caused by the oxidation and rereduction of the redox polymer appeared on top of the electrocatalytic current. These differences between POs–EA-coated deactivated and nondeactivated electrodes show that the deactivation process survived the application of the redox polymer; e.g., the current onset in Figure 9 occurs at the POs–EA onset potential and a rereduction wave for the redox polymer is not observed.

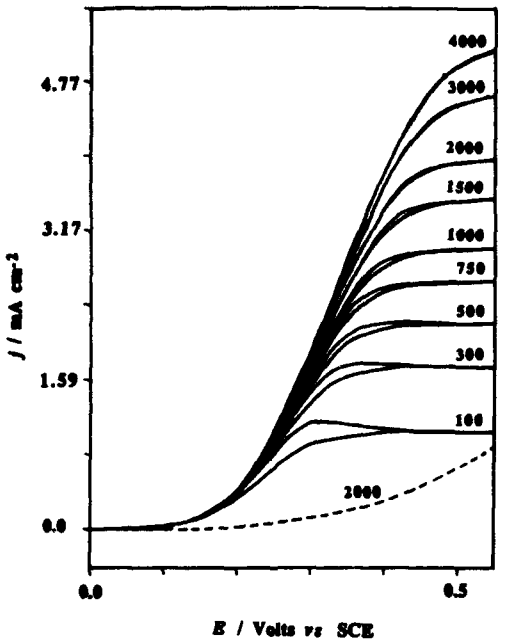

Figure 9. Catalytic oxidation of 3.1 mM hydroquinone at a POs–EA/PEG-coated gold-disk electrode. $A = 0.126$ cm^2, $\Gamma = 1.3 \times 10^{-8}$ mol/cm^2, $v = 20$ mV/s. The numbers on the curves give the rotation rate in rpm. The dashed line shows the response of the bare gold electrode.

electrode, oxidation of the redox polymer leads to a catalytic current plateau proportional to the square root of the rotation rate. There is no evidence for an upward curvature in the plateau region (Figure 9), at least for the lower rotation rates, that would indicate some contribution to the catalytic current from the gold substrate. That is, in the plateau region, the POs–EA efficiently oxidizes the H_2Q before it arrives at the gold electrode, thus the background current under our experimental conditions is negligible.

Extrapolation of the plateau currents in Figure 9 (in a Kautecky–Levich plot) to $\omega^{-1/2} = 0$ leads to a limiting catalytic oxidation current density of $j_k = 21.1$ mA/cm^2 for a film of surface coverage, $\Gamma_p = 1.34 \times 10^{-8}$ mol/cm^2. j_k decreases monotonically with increasing surface coverage, reaching $j_k = 3.8$ mA/cm^2 for $\Gamma_p = 9.65 \times 10^{-8}$ mol/cm^2. The expected limiting current density for electron "diffusion" through such a polymer film ($\Gamma_p = 1.34 \times 10^{-8}$ mol/cm^2, $D_eC_p^2 \approx 6.4 \times 10^{-16}$ mol^2 cm^{-4} s^{-1}) if the reaction took place only at the outer surface of the electrode, is $j_e \approx 4.6$ mA/cm^2. The observation that the measured limiting catalytic current density, j_k, is substantially higher than the maximum rate that electrons can diffuse to the electrode from the outer film surface, j_e, demonstrates that much of the reaction must be occurring inside the film, i.e. in a "reaction layer" predominantly near the electrode surface.[22,23] The decrease in j_k with increasing film thickness is consistent with this interpretation. This illustrates again that the polymer films are highly permeable to solution species, allowing reaction throughout a substantial portion of the bulk redox polymer. This behavior contrasts with that of a number of redox polymer films in which the catalytic reaction is essentially confined to the polymer/solution interface because of insufficient penetration of the substrate into the polymer film.[35-39] The results also demonstrate that the POs–EA/PEG redox polymer films are capable of supporting large catalytic current densities. Such information on the permeability and catalytic properties of these redox polymers will contribute to the characterization of the enzyme-containing polymer films.[40]

Conclusions

A two-component redox epoxy resin has been developed using poly(ethylene glycol) diglycidyl ether as cross-linker for an osmium-containing redox polymer with a poly(vinylpyridine) backbone. The resulting redox-conducting epoxy cements strongly bind to gold, vitreous carbon, graphite, and other electrode surfaces. Films of the redox epoxies are highly permeable to solution species and are able to support large catalytic currents for the oxidation of hydroquinone, substantial portions of the film being electroactive. The activation energy for electron "diffusion" through the polymer film is independent of the extent of cross-linking, suggesting that the motion of the polymer backbone is not greatly restricted by the long-chain cross-linking reagent. The permeability and hydrophilicity of these films, as well as the occurrence of the cross-linking reaction under near-physiological conditions, make these epoxies attractive for enzyme electrode applications.

Acknowledgment. Support of this work by the Office of Naval Research and by the Welch Foundation is gratefully acknowledged.

Registry No. PEG diglycidyl ether, 26403-72-5; hydroquinone, 123-31-9; carbon, 7440-44-0.

(35) Rocklin, R. D.; Murray, R. M. *J. Phys. Chem.* **1981**, *85*, 2104–2112.
(36) Ikeda, T.; Leidner, C. R.; Murray, R. W. *J. Am. Chem. Soc.* **1981**, *103*, 7422–7425.
(37) Schmehl, R. H.; Murray, R. W. *J. Electroanal. Chem.* **1983**, *152*, 97.
(38) Krishnan, M.; Zhang, X.; Bard, A. J. *J. Am. Chem. Soc.* **1984**, *106*, 7371–7380.
(39) Anson, F. C.; Tsou, Y. M.; Saveant, J. M. *J. Electroanal. Chem.* **1984**, *178*, 113.
(40) Gregg, B. A.; Heller, A. Following paper in this journal.

High Current Density "Wired" Quinoprotein Glucose Dehydrogenase Electrode

Ling Ye,*,† Martin Hämmerle,‡ Arjen J. J. Olsthoorn,§ Wolfgang Schuhmann,‡ Hans-Ludwig Schmidt,‡ Johannis A. Duine,§ and Adam Heller†

Department of Chemical Engineering, University of Texas at Austin, Austin, Texas 78712, Lehrstuhl für Allgemeine Chemie und Biochemie, Technische Universität München, D-8050 Freising-Weihenstephan, Germany, and Department of Microbiology and Enzymology, Delft University of Technology, 2628 BC Delft, The Netherlands

Glucose electrodes were prepared by "wiring" quinoprotein glucose dehydrogenase, GDH (EC 1.1.99.17) to glassy carbon with an osmium complex containing redox-conducting epoxy network. Their current density at 70 mM glucose concentration reached 1.8 mA cm^{-2} when 15 μg cm^{-2} of the enzyme having an activity of 250 units mg^{-1} was applied to the electrode. Under the same conditions, electrodes made with glucose oxidase (GOX) of similar activity (250 units mg^{-1}) had a maximum current density of 0.66 mA cm^{-2}. The maximum current density was reached with 8 % GDH in the redox polymer film. The current density was almost flat through the 6.3–8.8 pH range and was not altered when the solution was either aerated or argon purged. It decreased at 25 °C to half its initial value in 8 h.

INTRODUCTION

Many quinoproteins (enzymes containing a quinone cofactor) have been isolated and characterized in recent years.[1] These enzymes have either pyrroloquinoline quinone (PQQ), topaquinone (TPQ), or tryptophanyltryptophanquinone (TTQ) as cofactor.[2] Glucose dehydrogenase belongs to the group of PQQ-containing quinoproteins.[3] Two quite different types of quinoprotein glucose dehydrogenase exist, one soluble and the other membrane-bound.[4] The soluble type has so far only been detected in *Acinetobacter calcoaceticus* strains, while the membrane-bound one is widely distributed among Gram-negative bacteria, including *A. calcoaceticus*.[5] The soluble type enzyme, used in the here described investigations has been characterized by several research groups[6-8] and it is referred to here as GDH (EC 1.1.99.17). Its gene has been cloned[9] and an efficient expression of the apo-enzyme was obtained in a recombinant *Escherichia coli* strain.[10] Reconstitution of apo- to holo-enzyme requires the presence of PQQ[3] and Ca^{2+}.[11] The latter two are firmly bound to the protein, in contrast to other PQQ-containing enzymes where dialysis against EDTA-containing buffers easily removes them.[12] The enzyme has a very high catalytic activity: approximately 8 mmol of glucose is oxidized per minute per milligram of protein with Wurster's blue[7] and approximately 3 with 2,6-dichlorophenol indophenol.[6] Taking the latter value, this is up to 20 times the activity of pure glucose oxidase. In contrast, the rates obtained with the presumed natural electron acceptor of this GDH,[13] cytochrome b_{562}, are rather low.

Redox centers of flavoprotein enzymes such as glucose oxidase (GOX) have been electrically connected to glassy carbon, graphite, and gold electrodes through a 3-dimensional redox conducting network, to which the enzyme is covalently bound. One of these networks is made of a water-soluble osmium complex containing redox polymer POs-EA[14,15] (Figure 1) that binds the protein moiety of enzymes, such as GOX, forming a redox polymer/enzyme complex.[16] Ethylamine functions of POs-EA and lysylamines of GOX are cross-linked with a water-soluble diepoxide, poly(ethylene glycol diglycidyl ether) (PEGDE). The cross-linking, i.e. epoxy-curing reaction, can be carried out on the electrode surface itself. The cured film, though insoluble in water, is highly hydrophilic and is permeable to water-soluble ions and molecules. Because the enzyme in the film is electrically connected to the electrode and because the film is permeable to glucose and gluconate, a catalytic glucose electrooxidation current density of 0.8 mA cm^{-2} is obtained in 3-mm-diameter electrodes at a 1:1 polymer to enzyme (weight/weight) ratio[16] and 2 mA cm^{-2} in 7-μm-diameter microelectrodes.[17] POs-EA-based epoxies also connect redox centers of other flavoprotein oxidases to electrodes.[18]

Amperometric GDH sensors that are O_2 insensitive have been reported.[19,20] These sensors employed diffusional redox shuttles, such as the 1,1'-dimethylferricinium cation, with which ca. 60 μA cm^{-2} current density was reached. Here we report that O_2-insensitive glucose electrodes reaching a 1.8 mA cm^{-2} current density can be made with GDH connected through the PEGDE cross-linked redox epoxy POs-EA.

MATERIALS AND METHODS

Glucose oxidase (EC 1.1.3.4, from *Aspergillus niger*) purchased from Boehringer and gluconic acid purchased from Sigma were

† University of Texas at Austin.
‡ Technische Universitat Munchen.
§ Delft University of Technology.

(1) Duine, J. A.; Frank, J.; Jongejan, J. A. *Adv. Enzymol.* **1987**, *59*, 169–212.
(2) Duine, J. A. *Eur. J. Biochem.* **1991**, *200*, 271–284.
(3) Duine, J. A.; Frank, J.; Van Zeeland, J. K. *FEBS Lett.* **1979**, *108*, 443–446.
(4) Matsushita, K.; Shinagawa, E.; Adachi, O.; Ameyama, M. *FEBS Microbiol. Lett.* **1988**, *55*, 55–59.
(5) Duine, J. A. Energy generation and the glucose dehydrogenase pathway in Acinetobacter. In *The Biology of Acinetobacter*; Tower, K. J., Ed.; Plenum Press: New York, 1991; pp 295–312.
(6) Hauge, J. *J. Biol. Chem.* **1964**, *239*, 3630–3639.
(7) Dokter, P.; Frank, J.; Duine, J. A. *Biochem. J.* **1986**, *239*, 163–167.
(8) Geiger, O.; Goerisch, H. *Biochemistry* **1986**, *25*, 6043–6048.
(9) Cleton-Jansen, A. M.; Groen, N.; Vink, K., Van de Putte, P. *Mol. Gen. Genet.* **1989**, *217*, 430–434.
(10) Van der Meer, R. A.; Groen, B. W.; Van Kleef, M. A. G.; Frank, J.; Jongejan, J. A.; Duine, J. A. *Methods Enzymol.* **1990**, *188*, 260–283.
(11) Geiger, O.; Goerisch, H. *Biochem. J.* **1989**, *261*, 415–421.
(12) Duine, J. A.; Frank, J.; Jongejan, J. A. *Anal. Biochem.* **1983**, *133*, 239–245.
(13) Dokter, P.; Van Wielink, J. E.; Van Kleef, M. A. G.; Duine, J. A. *Biochem. J.* **1988**, *254*, 131–138.
(14) Gregg, B. A.; Heller, A. *J. Phys. Chem.* **1991**, *95*, 5970–5975.
(15) Gregg, B. A.; Heller, A. *J. Phys. Chem.* **1991**, *95*, 5976–5980.
(16) Heller, A. *J. Phys. Chem.* **1992**, *96*, 3579–3587.
(17) Pishko, M. V.; Michael, A. C.; Heller, A. *Anal. Chem.* **1991**, *63*, 2268.
(18) Katakis, I.; Heller, A. *Anal. Chem.* **1992**, *64*, 1008–1013.
(19) D'Costa, E. J.; Higgins, I. J.; Turner, A. P. F. *Biosensors* **1986**, *2*, 71–87.
(20) Yokoyama, K.; Sode, K.; Tamiya, E.; Karube, I. *Anal. Chim. Acta* **1989**, *218*, 137–142.

0003-2700/93/0365-0238$04.00/0

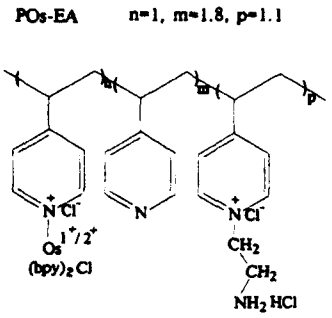

Figure 1. Structure of the osmium complex containing redox polymer POs-EA.

used as received. Glucose (1 M) (from Merck, Darmstadt, FRG) stock solution was made with deionized water, allowed to mutarotate for more than 24 h at room temperature and was stored at 4 °C. Poly(ethylene glycol 400 diglycidyl ether) (PEGDE) was purchased from Polysciences and was used as received. The other chemicals were reagent or better grade. A pH 7.3 phosphate buffer solution (PBS), containing 0.15 M NaCl and 20 mM Na_2HPO_4, was used for all electrochemical measurements, unless otherwise indicated. When used in the flow system, the carrier buffer was partially degassed by reducing the pressure above it with a water aspirator for ca. 20 min. Deionized water, filtered with a hollow fiber microfiltration capsule (0.2 μm, MICROGON, Laguna Hills, CA, was used throughout the experiments. Potassium hexachloroosmate was purchased from Strem Chemicals and used as received.

The redox polymer was poly(vinylpyridine) partially N-complexed with [osmium bis(bipyridine) chloride]$^{+/2+}$ and quaternized with bromoethylamine (POs-EA, Figure 1). The synthesis procedure was similar to that described by Gregg and Heller.[14] *cis*-bis(2,2′-bipyridine-*N*,*N*′)dichloroosmium(II) (0.6 g, 1.05 mmol) and poly(4-vinylpyridine) (0.33 g, 3.15 mequiv of monomer units) were heated under nitrogen to reflux in 18 mL of ethylene glycol for 3 h. The intermediate polymer was collected by dripping the reaction mixture into rapidly stirred ethyl acetate (400 mL). The sticky polymer was redissolved in a minimum amount of methanol. The intermediate polymer was precipitated from the methanol solution by adding the methanol solution dropwise to 800 mL of rapidly stirred ether and then filtered and dried. The intermediate polymer (0.3 g), bromide (2.418 g, 7.5 mmol) were dissolved in 15 mL of ethylene glycol/DMF (1:1) and heated for 24 h at 100 °C under nitrogen with stirring. After being precipitated from acetone, the crude polymer was dissolved with a small amount of water and passed through a Sephadex column (G-50, Pharmacia) with 0.2 M NaCl as the eluant. The collected solution was stirred with 12 g of Bio-Red AG1-X4 ion-exchange resin (Cl form) for 24 h, filtered, and desalted by ultrafiltration. The final polymer product was obtained by evaporating the water in a vacuum oven at 80 °C. The elemental analysis and UV–vis spectroscopy showed that the repeating unit of the polymer had 1.1 ethylamine pendant functions and 1.8 unsubstituted pyridine rings per osmium complexed pyridine.

GDH apo-enzyme and PQQ were obtained as described by Van der Meer.[10] Wurster's blue was synthesized according to the procedure of Michaelis and Grannick.[21] The apo-enzyme (2 mg mL^{-1}) was dissolved in 10 mM HEPES buffer, pH 8.0. PQQ (6.6 mg mL^{-1}) was dissolved in 10 mM HEPES (pH 8.0) with 3 mM $CaCl_2$. A 10-μL aliquot of the PQQ solution was then added to 100 μL of the enzyme solution and mixed thoroughly. The mixture was incubated at room temperature for 15 min; then the enzymatic activity of the reconstituted holo-enzyme was assayed spectrophotometrically by monitoring the decoloration of Wurster's blue.[7] The measured activity was 250 units mg^{-1}. The PQQ–GDH solution was stored at 4 °C. The reconstituted GDH can be stored at 4 °C for more than 2 months without measurable loss of activity.

Rotating disk electrodes were made by press fitting 3-mm-diameter glassy carbon rods into Teflon housing. Stationary disk electrodes were prepared by sealing the glassy carbon rods into glass tubings with a fast curing epoxy. The surfaces of the electrodes were polished with rough, then increasingly fine, sandpaper, then with 5-, 1-, and 0.3-μm alumina to a mirror finish. The electrodes were sonicated for ca. 5 min and rinsed with deionized (DI) water after each polishing step. The enzyme electrodes were prepared by applying sequentially 1 μL of the polymer PVPOs-EA (10 mg mL^{-1} in DI H_2O), 0.5 μL of GDH (2 mg mL^{-1} in the reconstituted solution) or GOX (2 mg mL^{-1} in 10 mM HEPES, pH 8), and 0.5 μL of PEGDE 400 (3 mg mL^{-1} in DI H_2O) to the electrode surface. The components were mixed, allowed to dry, and then cured for more than 24 h at room temperature. Before the electrochemical measurements, the electrodes were soaked in phosphate buffer solution (PBS) for 30 min and rinsed with DI water.

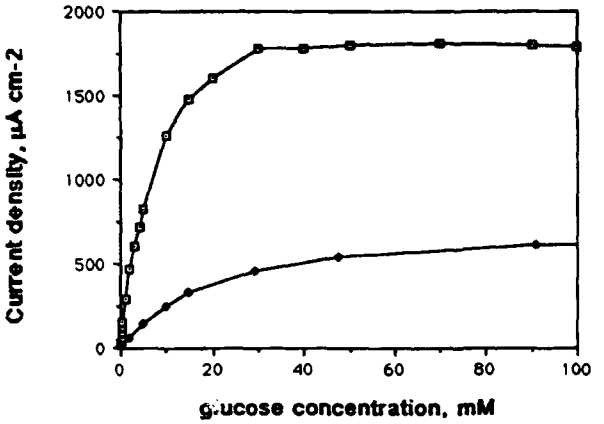

Figure 2. Comparison of the current output and the sensitivity for GDH and GOX electrodes: (open square) GDH electrode; (solid diamonds) GOX electrode. Conditions: 0.4 V vs SCE; 1000 rpm; air atmosphere.

The electrochemical measurements were carried out either in a conventional electrochemical cell or in a flow injection analysis system.[22] A Model 400 bipotentiostat from EG&G Princeton Applied Research was used for the amperometric measurements, and a KIPP & ZONEN BD41 strip chart recorder was used to record the data. The rotator used was a Model ASR 2 analytical rotator from Pine Instruments. All steady-state currents were measured at 0.4 V vs SCE.

RESULTS AND DISCUSSION

Current Response. The variation of the current density with glucose concentration of POs-EA/PEGDE-wired GDH and GOX electrodes is seen in Figure 2. When the electroactive film contains 8% of the enzyme, the current density of the GDH electrode substantially exceeds that of the GOX electrode at 0–12 mM glucose and levels off at 1.8 mA cm^{-2} at near 70 mM glucose. This current density is about 3 times that reached with GOX. The sensitivity of the wired GDH electrode at 5 mM glucose is 165 μA cm^{-2} M^{-1}. The higher current density of the GDH electrode, relative to that of the GOX electrode, derives from the faster rate of electron transfer from the $PQQH_2$ centers than from $FADH_2$ centers to the osmium complex in the redox polymer/enzyme network. The rate constant for the electron transfer to diffusional shuttles from reduced GDH is also much faster than from reduced GOX.[19,23] The rate constant for the electron transfer from reduced GDH to ferrocenemonocarboxylic acid is 96.0×10^5 L mol^{-1} s^{-1}, while it is only 2.01×10^5 L mol^{-1} s^{-1} from reduced GOX.[23] That the 3-dimensional redox network is effective in collecting from GDH and transferring them to the surface of the electrode is seen from the magnitude of the increase in current density relative to that with electron shuttling with 1,1′-dimethylferrocene. For the latter, D'Costa, Higgins,

(21) Michaelis, L.; Grannick, S. *J. Am. Chem. Soc.* **1943**, *65*, 1747–1755.

(22) Schuhmann, W. *Sens. Actuators B* **1991**, *4*, 41–49.
(23) Davis, G. *Biosensors* **1985**, *1*, 161–178.

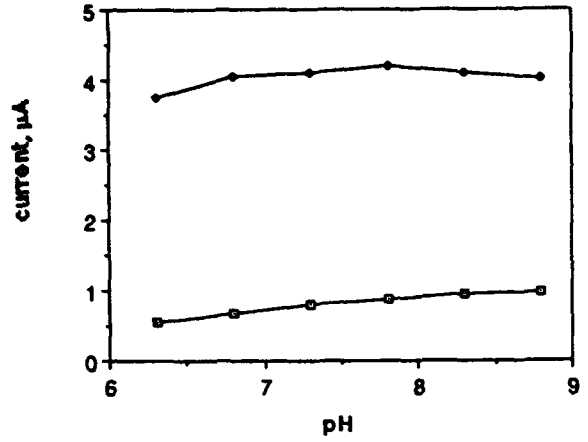

Figure 3. Effect of pH on the current output of the GDH and GOX electrodes. Solution of 0.15 M NaCl, 20 mM Na_2PO_4, and 1 mM glucose was titrated to the desired pH with HCl.

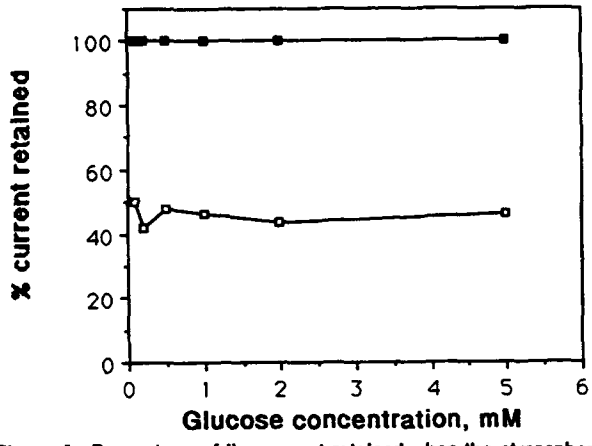

Figure 4. Percentage of the current retained when the atmosphere is changed from argon to oxygen: (solid square) GDH electrode; (open square) GOX electrode.

and Turner,[19] using a porous graphite electrode, observed 54 $\mu A\ cm^{-2}$ at 4 mM glucose and reached a limiting current density near 5.3 mM glucose. In comparison, the wired GDH electrode has a current density of 724 $\mu A\ cm^{-2}$ at 4 mM glucose and a limiting current density of 1.817 $\mu A\ cm^{-2}$ near 70 mM glucose. It is thus evident that the redox network effectively connects not only $FADH_2/FAD$ centers[14-18] but also the PQQ centers to the electrodes. The enhanced limiting current density implies that in the PEGDE cross-linked POs-EA wired GOX electrodes the current density is not limited by electron transfer through the redox polymer but by the electron transfer from the enzyme redox centers to the polymer. This transfer is faster for PQQ–GDH than for FAD–GOX.

pH Dependence. The pH dependence of the current densities for the GDH and the GOX electrodes is shown in Figure 3. The optimal activity of free GDH is at pH 9 when Wurster's blue is used as the electron acceptor.[7] However, when the electron acceptor is oxidized phenazine methosulfate, the pH optimum is 7.[24] Thus the current of the GDH electrode changes relatively little from pH 6.3 to 8.8.

Absence of Current Suppression by Oxygen. The current of the GDH electrode is not suppressed by dissolved O_2 (Figure 4). Comparison of stationary GDH and GOX electrodes by testing in the same solution, with a bipotentiostat holding their potentials at 0.4 V vs SCE and a mechanical stirrer operating at 500 rpm to facilitate even mass transfer to both electrodes, showed that only the current of the GOX electrode decreased as the atmosphere was changed from argon to oxygen.

(24) Olsthoorn, A. J. J.; Duine, J. A. Unpublished results.

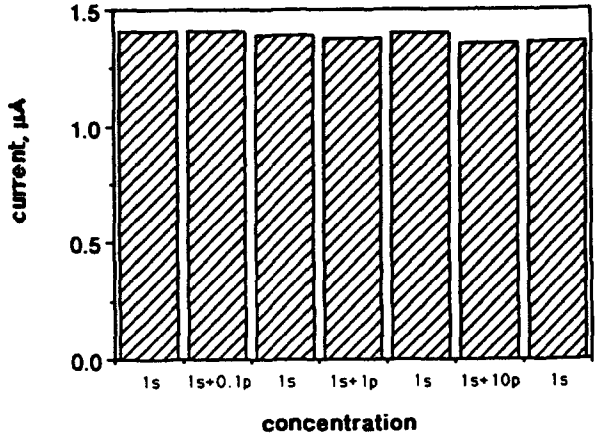

1s= 1 mM glucose
1p= 1 mM gluconate

Figure 5. Response of GDH electrodes to pulses of 1 mM glucose with different concentrations of gluconic acid added, measured in a flow injection system.

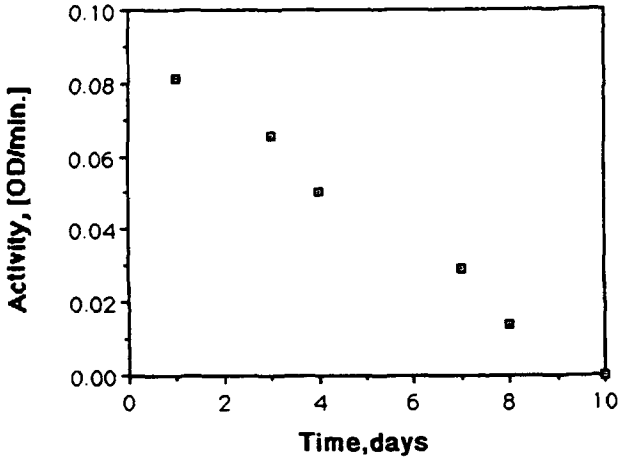

Figure 6. Stability of reconstituted GDH in solution at room temperature. The activity of the enzyme was assayed spectroscopically.

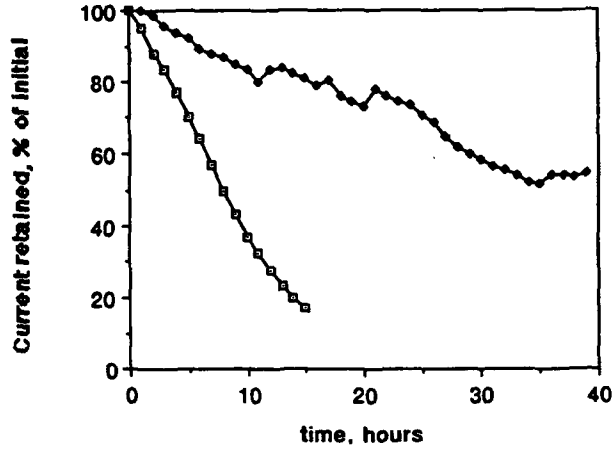

Figure 7. Comparison of the stability of the GDH electrodes. Continuous operation was in a 10 mM glucose solution in a conventional electrochemical cell (open squares) and in a flow injection analyzer where 15 μL of 10 mM glucose pulses was injected once per hour (solid diamonds). Electrodes were at 0.4 V vs SCE.

Product Inhibition. Product inhibition of the electrode was studied in the flow injection analysis system by periodically injecting samples of 1 mM glucose to which increasing

concentrations of gluconate were added. The current of the GDH electrode is not affected by gluconate (Figure 5).

Stability. The half-life of the dissolved enzyme in 10 mM HEPES buffer (pH 7.3) at room temperature, determined by periodic spectrophotometric assay of its activity (Figure 6), is 5 days. However, the decay of the current of the GDH electrodes was faster when tested continuously in 10 mM glucose at 25 °C, pH 7.3 (Figure 7, open squares). The current dropped to its initial value in about 8 h.

The operational stability of the "wired" GDH electrode is glucose concentration dependent, the output declining more rapidly at higher glucose concentrations. Figure 7 shows the rates of decline for GDH electrodes in a conventional electrochemical cell where the glucose concentration was held at 10 mM and in a flow injection analyzer where a computer-controlled injection system injected fixed volumes of 10 mM glucose once every 60 min. Under the conditions of the experiment, it took less than 3 min for the sample to pass through the cell; i.e., the electrode was in 10 mM glucose for only 3 min each hour. The rate of current loss is thus related to the amount of glucose electrooxidized (Figure 7).

We conclude that PQQ–glucose dehydrogenase is effectively electrically wired through an osmium complex based redox polymer to glassy carbon. The extraordinarily high limiting current density, 1.8 mA cm^{-2}, suggests fast electron transfer from PQQ to the osmium complex centers of the polymer.

ACKNOWLEDGMENT

The work at the University of Texas was supported by the Office of Naval Research, the Welch Foundation, and the National Science Foundation. The work at the Technische Universität München was supported by the Bundesministerium für Forschung und Technologie (BMFT), Projektträger BEO.

RECEIVED for review June 25, 1992. Accepted October 29, 1992.

Electroanalysis, 5(1993) 825-831

Bienzyme Sensors Based on "Electrically Wired" Peroxidase*

T. J. Ohara, M. S. Vreeke, F. Battaglini,[1] and A. Heller[2]
Department of Chemical Engineering, University of Texas at Austin, Austin, Texas 78712-1062, USA
Received April 26, 1993.

ABSTRACT

Single-layer and bilayer bienzyme electrodes based on the combination of a three-dimensional (3-D) redox epoxy network that electrically connects redox centers of bound horseradish peroxidase (HRP) to electrodes with a hydrogen peroxide generating enzyme, the redox centers of which are not connected to the redox-epoxy network, are described. In the single-layer electrodes, H_2O_2 generated by the first enzyme oxidizes the second enzyme HRP, which oxidizes the redox polymer network that is electrochemically reduced at 0 mV saturated calomel electrode (SCE). When the redox centers of the H_2O_2 generating enzyme are also electrically connected to the redox-epoxy network, the substrate reduced redox centers are oxidized by the redox polymer network, thus lowering the cathodic current. Such attenuation is avoided in bilayer electrodes, where the H_2O_2 producing enzyme and the redox-epoxy-HRP network are not electrically connected.

The single-layer bienzyme electrodes extend the range of amperometric biosensors based on directly redox-epoxy "wired" enzymes to enzymes that are difficult to electrically connect to redox polymer networks and whose preferred or only cosubstrate is oxygen. For the difficult to wire enzyme-choline oxidase, the cathodic current density in the single-layer peroxidase and choline oxidase containing electrode is 80 $\mu A\ cm^{-2}$ at 10 mM choline concentration, while the anodic current density of the directly wired enzyme is only 5 $\mu A\ cm^{-2}$. Alcohol oxidase is not electrically connected to the wiring 3-D redox-epoxy network. The anodic current density of its redox-epoxy wired electrodes is close to nil, while the cathodic current density, observed in alcohol oxidase and wired peroxidase containing single-layer electrodes at 10 mM ethanol, is 5 $\mu A\ cm^{-2}$. When well-wired enzymes, such as glucose oxidase or lactate oxidase, are utilized in single-layer electrodes, limiting cathodic current densities of 60 $\mu A\ cm^{-2}$ are observed for both enzymes. These currents are much lower than those observed in the directly wired enzyme anodes.

KEY WORDS: Biosensors, Peroxidase, Electrical wiring.

INTRODUCTION

In order to circumvent the problems associated with the high (0.7 V vs the saturated calomel electrode (SCE)) operating potential of H_2O_2 monitoring amperometric biosensors, Kulys et al. [1] introduced in 1981 the concept of peroxidase containing bienzyme electrodes. The electrodes had a film of horseradish peroxidase (HRP), glucose oxidase (GOX), and bovine serum albumin (BSA) coimmobilized through glutaraldehyde crosslinking. The hydrogen peroxide formed in the GOX catalyzed reaction of glucose and oxygen, oxidized HRP which, in turn, oxidized dissolved $Fe(CN)_6^{4-}$ to $Fe(CN)_6^{3-}$. The latter ion was electroreduced in the amperometric assay. The resulting glucose sensing cathode was less sensitive to electrooxidizable interferants and to fouling, caused by the formation of insoluble films upon electrooxidation of biomolecules. A residual problem of the single-layer $Fe(CN)_6^{4-/3-}$ bilayer electrode has been the competing reverse reaction of reduction of $Fe(CN)_6^{3-}$ to $Fe(CN)_6^{4-}$ by glucose reduced glucose oxidase $FADH_2$ centers. Such reduction diminishes the cathodic current.

Subsequently, Tatsuma and Watanabe [2] immobilized HRP on SnO_2 electrodes using a silane as a coupler, then glutaraldehyde crosslinked GOX on the immobilized HRP film, and used ferrocene monocarboxylate to mediate electron transport. Though the two enzymes were separated, the ferricinium carboxylate formed from

*Dedicated to the memory of Prof. W. Simon.
[1]Present Address: Department of Chemistry and Biochemistry, Concordia University, 1455 Maisonneuve Blvd West, Montreal, Quebec H3G1M8, Canada.
[2]To whom correspondence should be addressed.

1040-0397/93/$5.00 + .25

ferrocene carboxylate upon electron transfer to oxidized HRP, was partly electroreduced by the GOX-$FADH_2$ centers. This parasitic reduction diminished the cathodic current. The problem was partially overcome by Kulys et al. [3,4] who built bienzyme electrodes without mediators, relying on the direct electroreduction of oxidized HRP on graphite electrodes. Because HRP multilayers cannot be effectively electroreduced in this case, only the actual electrode surface contacting HRP molecules is electroreduced. Therefore, the current densities are low (45 $\mu A\ cm^{-2}$) and the dynamic range is narrow (0.27 to 2.46 μM).

Gorton et al. followed a similar approach using surface adsorbed peroxidase to measure H_2O_2 produced in a variety of oxidases. They improved on the original Kulys design by using macroporous graphite [5] and carbon paste electrodes [6] to increase the surface area.

Boguslavsky et al. recently alleviated the problem of the electrooxidation of enzyme $FADH_2$ centers by mediators through using carbon-adsorbed, and thus less diffusionally mobile, ferrocene based redox macromolecules. Their electrodes were built by immobilizing cholesterol oxidase on carbon pastes with macromolecule-bound ferrocenes [7].

Here, we describe bienzyme electrodes made with H_2O_2 producing redox enzymes that are poorly or not at all connected to electrodes by a 3-dimensional (3-D) redox-epoxy network. These networks, however, effectively connect HRP to the electrode. We show that effective cathodes can be built by coimmobilizing in a single-layer electrode the 3-D redox-epoxy network, that electrically connects HRP, together with H_2O_2 producing choline oxidase (ChOX), alcohol oxidase (AOX), or D-amino acid oxidase-(D-AAOX). These are superior in current density, sensitivity, and dynamic range to anodes based on direct "wiring" of these enzymes.

In this context, we also analyze well "wired" enzymes: GOX and lactate oxidase (LOX). We point to limitations of single-layer wired HRP bienzyme cathodes with GOX and LOX, where the $FADH_2$ centers of the oxidase are directly and efficiently oxidized by the redox epoxy networks and, as a result, produce less H_2O_2 in the presence of oxygen.

EXPERIMENTAL

Reagents

The redox polymer (POs-EA) used was poly(4-vinylpyridine) modified by partial complexing of pyridines with $Os(bpy)_2Cl^{+/2+}$ and partial quaternization of the residual pyridines with bromoethyl amine, to facilitate crosslinking. Preparation of the redox polymer POs-EA has been described earlier [8]. Glucose oxidase (E.C. 1.1.3.4, type X-S from Aspergillus niger, 198 units/mg solid), HRP (E.C. 1.11.1.7, type VI from horseradish, 288 units/mg), AOX (E.C. 1.1.3.13 from Pichia pastoris, 33 units/mg protein), D-amino acid oxidase (D-AAOX) (E.C. 1.4.3.3 from porcine kidney, 9.9 units/mg), and choline oxidase (ChOX) (E.C. 1.1.3.17, from alchaligenes species, 11 units/mg solid) were from Sigma. Lactate oxidase (from pediococcus sp., 312 units/mg) was purchased from Genzyme. Polyethylene glycol diglycidyl ether (PEGDGE) MW 400 (PEGDGE 400) was purchased from Polysciences. All others chemicals were of the best available commercial grade. Glutaraldehyde stock solutions were prepared using grade I solutions and kept frozen. Stock solutions of glucose were left to mutarotate at room temperature for 24 hours before use and then kept refrigerated. Stock solutions of L-lactate was prepared daily.

Electrode Construction and Preparation

Rotating disk electrodes were made of 1-cm length of 3-mm diameter vitreous carbon rods from Atomergic Chemicals Corp. These were press-fitted into one end of a Teflon sleeve. The opposite end of the sleeve had a press-fitted stainless steel rod threaded to match a Pine Instruments rotator. Electrical contact between the vitreous carbon and stainless steel rod was made with a silver epoxy (Epo-tek H2Oe from Epoxy Technology Inc). The electrodes were polished first with 6 μm then with 1 μm diamond suspension followed by 0.3 μm alumina (purchased from Buehler). After each polishing step, the electrodes were sonicated 3 to 6 minutes in deionized water.

Bilayer Electrodes

The inner hydrogen peroxide sensing layer was prepared using a 20 mg/mL HRP type VI solution in 0.1 M $NaHCO_3$. A 100 μL of the HRP solution was reacted with 50 μL of 12 mg/mL $NaIO_4$ and incubated for 2 hours in the dark at room temperature. The $NaIO_4$ treatment forms aldehyde functions by oxidation of sugar residues at the enzyme surface. Next, 10 μL of the oxidized HRP was added to 50 μL of 10 mg/mL POs-EA and 60 μL of 0.5 mg/mL PEGDGE 400. The polished electrode was coated with 3 μL of this mixture, and the film on the electrode was cured for 48 hours in a vacuum desiccator.

The preparation of the outer layer depended on the enzyme that was being immobilized. For a typical alcohol oxidase electrode, 10 μL of 0.52% enzyme solution was mixed with 10 μL of 20% BSA and 5 μL of 2.5% glutaraldehyde. An electrode already coated with a layer of redox-epoxy cemented HRP was treated with 5 μL of the oxidase-containing mixture and cured for a least 2 hours. ChOX electrodes were prepared similarly to the AOX electrodes, except that different amounts of the enzyme were used. Lactate oxidase electrodes were made by applying 10 μL of a mixture containing 60 μg/mL glutaraldehyde, 10 mg/mL LOX, and 5 mg/mL BSA onto the electrode. D-amino acid oxidase electrodes were prepared by using a solution containing 2.9 mg/mL D-AAOX and 0.77% glutaraldehyde. A 10 μL aliquot of this mixture was put on the electrode and incubated for at least 2 hours. For glucose oxidase electrodes, 100 μL (20 mg/mL, 10 mM HEPES, pH = 8) GOX was reacted with 50 μL (12 mg/mL $NaIO_4$) and incubated for 2 hours in the dark at room temperature. After incubation, 2 μL of

oxidized enzyme would typically be spread on the electrode and allowed to incubate for at least 2 hours.

Single-layer Electrodes

These were prepared in a manner similar to the preparation of the H_2O_2 sensing inner layer of the bilayer system, except that a defined quantity of an oxidase was also added to the mixture containing POs-EA, PEGDGE 400, and oxidized HRP. Typically, 3 μL of the resulting solution was coated on the electrode and allowed to cure for at least 48 hours.

Measurements

Electrochemical measurements were performed with a Princeton Applied Research model 173 potentiostat/galvanostat. The disk electrodes were rotated with a Pine Instruments model AFMSRX rotator and model MSRS speed controller. The standard three electrode cells had an SCE reference electrode and a platinum wire auxiliary electrode. All measurements were performed in an open cell under air and at room temperature. All constant potential experiments were performed with a rotating disk electrode at 1000 rpm. The working electrode was typically poised at 0 V (SCE), and the resulting current was measured as a function of time.

Flow Injection Analysis

These experiments were performed in a wall jet cell, using 1-mm-diameter glassy carbon electrodes (Cypress System, Lawrence, KS). Injection valve and sample loops were from Rheodyne Co. (Cotati, CA). The electrodes were poised at 0 V (SCE). The carrier was a pH 7.5 phosphate buffer solution.

RESULTS AND DISCUSSION

Single-Layer Bienzyme Cathodes

The dynamic range for five single-layer bienzyme electrodes, where both HRP and the hydrogen peroxide generating enzyme are bound within the 3-D PolyOs-NH_2-PEDGE redox-epoxy network [9], are shown in Figure 1. The electrodes were made with AOX, ChOX, LOX, D-AAOX, and GOX. The substrate concentration dependence of their steady-state cathodic current densities was measured at 0 V (SCE). Figure 2 shows corresponding data for the dependence of their anodic current densities, measured at 0.5 V (SCE). No curve is shown for AOX because the current was nil in the absence of O_2 i.e., when H_2O_2 was not generated. As seen in Figure 2, the anodic currents resulting from electron transfer from enzyme $FADH_2$ centers to the redox polymer network increase in the order AOX < D-AAOX < ChOX < LOX < GOX. The H_2O_2 concentrations in these films and thus the cathodic currents are reduced through partial electrooxidation of $FADH_2$ centers by the redox polymer. Because an $FADH_2$ electrooxidation current is not observed for AOX and is very small for ChOX and D-AAOX, single-layer bienzyme electrodes are appropriate for the

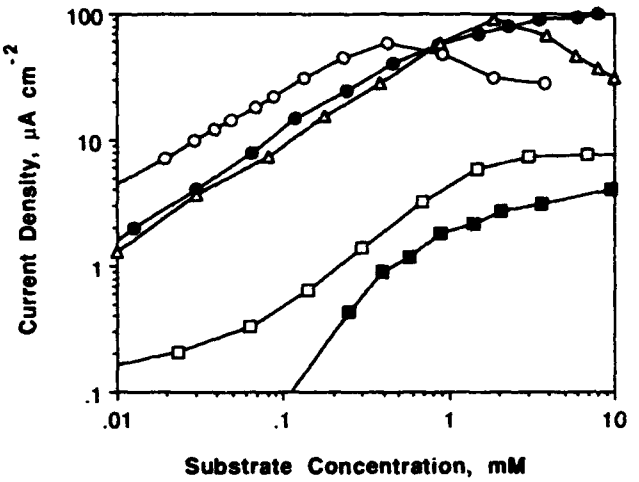

FIGURE 1. Dependence of the current density on concentration of the substrate for single-layer cathodes. Each cathode has 10 μg redox polymer, 1 μg crosslinker, and one of the following: 14 μg AOX with ethanol substrate (closed squares), 20 μg ChOX with choline substrate (closed circles), 24 μg LOX with lactate substrate (open circles), 42 μg D-AAOX with D-alanine substrate (open squares), and 15μg GOX with glucose substrate (triangles). pH 7.4, 0.0 mV versus SCE, 1000 rpm.

FIGURE 2. Dependence of the current density on the concentration of the substrate for single-layer anodes. Each anode has 10 μg redox polymer, 1 μg crosslinker, and one of the following: 20 μg ChOX with choline substrate (closed circles), 24 μg LOX with lactate substrate (open circles), 20 μg D-AAOX with D-alanine substrate (open squares), and 20μg GOX with glucose substrate (triangles). pH 7.4, 500 mV versus SCE, 1000 rpm.

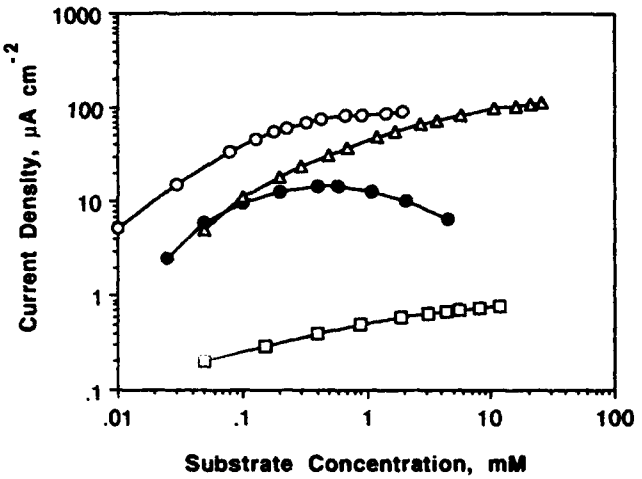

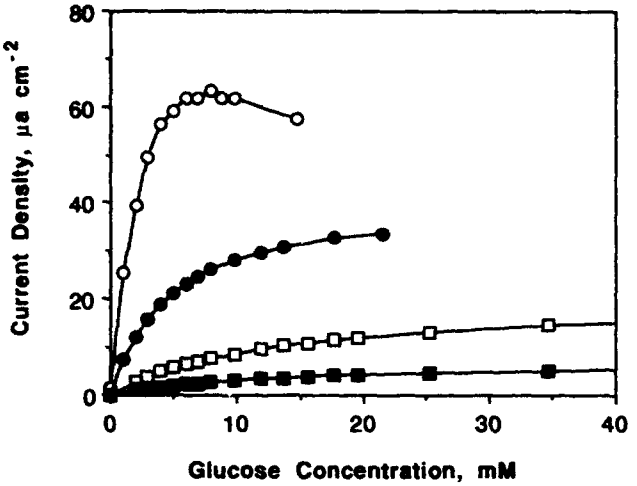

FIGURE 3. Dependence of the current density on glucose concentration for a single-layer glucose cathode made with 0.25 μg (closed squares), 0.5 μg (open squares), 2.5 μg (closed circles), and 5 μg (open circles) glucose oxidase loadings. pH 7.4, 0.0 mV versus SCE, 1000 rpm.

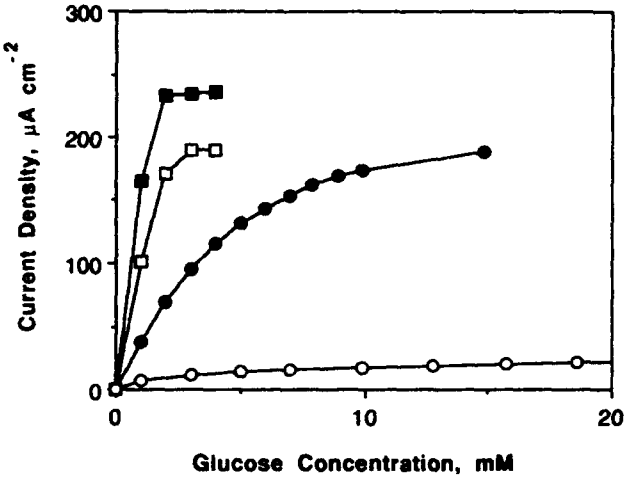

FIGURE 5. Dependence of current density on glucose concentration for a glucose oxidase bilayer cathode. The glucose oxidase loadings in the outer layer are 131 μg (closed squares), 26 μg (open squares), 2.6 μg (closed circles), and 1.3 μg (open circles). pH 7.4, 0.0 mV versus SCE, 1000 rpm.

assay of alcohols, choline, and D-amino acids. Lactate and glucose can also be cathodically assayed with single-layer cathodes, but interpretation of the relationship between the current density and the concentration of the substrate is difficult. It is particularly so in the case of GOX where, at high GOX loading, the current increases with substrate concentration up to 8 mM glucose and then decreases at higher concentrations (Figure 3). The decrease is attributed to the short circuiting of the dic current by the directly wired oxidase. In the c on between electrooxidation of GOX-$FADH_2$ centers and their reaction with O_2, the first is favored at high glucose concentrations, where the system is O_2 depleted and the second at low glucose concentrations, where O_2 is abundant.

Bilayer Bienzyme Cathodes

In electrodes made with separate redox-epoxy wired HRP and oxidase layers, there is no electrical contact between the two as long as interdiffusion of the two layers is pre-

FIGURE 4. Dependence of the current density on lactate concentration for a lactate oxidase bilayer cathode. The lactate oxidase loading in the outer layer is 100 μg. pH 7.4, 0.0 mV versus SCE, 1000 rpm.

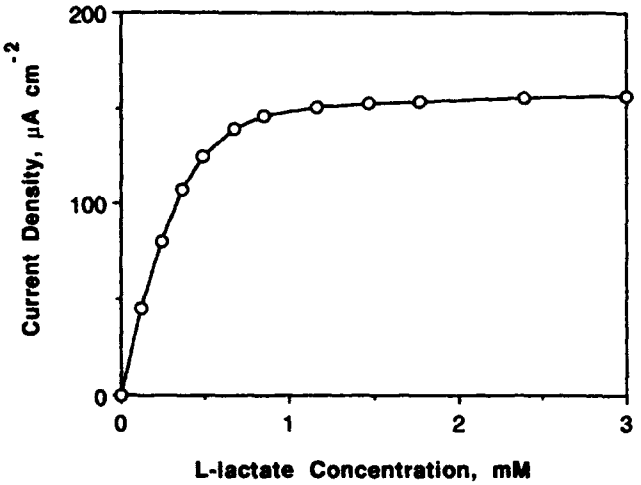

FIGURE 6. Dependence of the current density on the D-alanine (squares) and D-tyrosine (circles) concentrations for a D-AAOX bilayer cathode. The D-AAOX loadings in the outer layer are 24 μg for alanine and 133 μg for tyrosine. pH 7.4, 0.0 mV versus SCE, 1000 rpm.

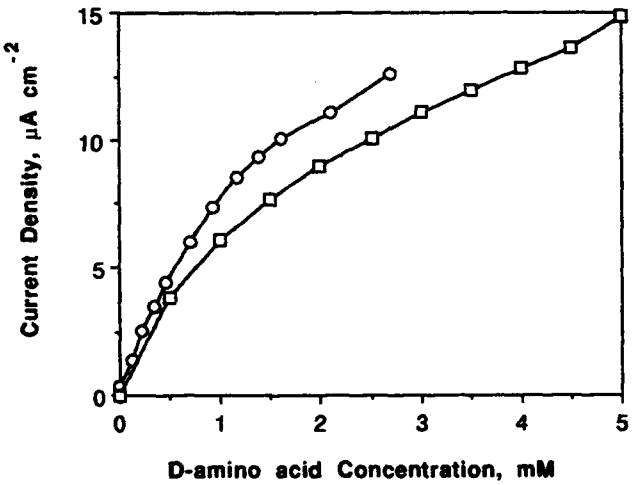

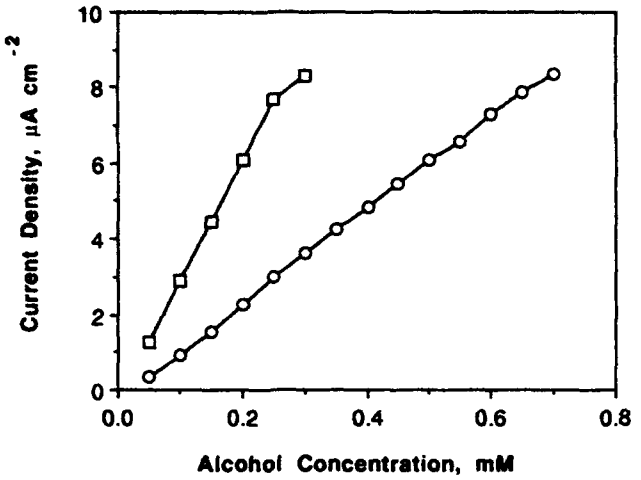

FIGURE 7. Dependence of the current density on the methanol (squares) and ethanol (circles) concentrations for an alcohol oxidase bilayer cathode. The alcohol oxidase loading in the outer layer is 200 μg. pH 7.4, 0.0 mV versus SCE, 1000 rpm.

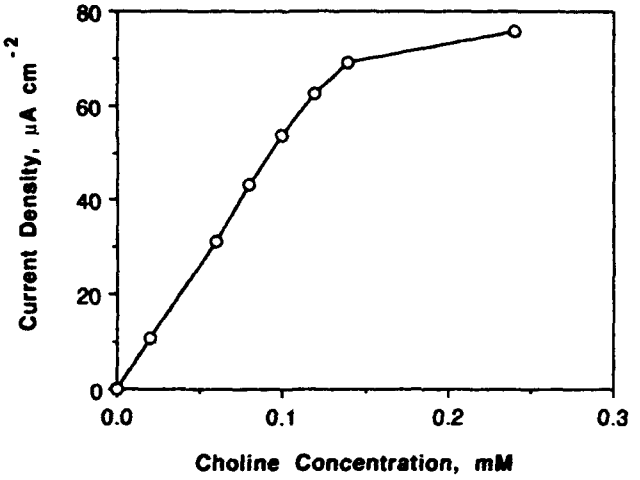

FIGURE 8. Dependence of the current density on the choline concentration for a choline oxidase bilayer cathode. The choline oxidase loading in the outer layer is 400 μg. pH 7.4, 0.0 mV versus SCE, 1000 rpm.

vented. Here the flow of electrons from oxidase $FADH_2$ centers to the peroxidase-wiring redox epoxy network is negligible. Thus, catalytic electroreduction of the network by the substrate, e.g., glucose, does not compete with electrooxidation of the redox hydrogel by oxidized HRP even in the case of the well-wired enzymes, such as GOX and LOX. In the absence of direct electrooxidation through a wiring polymer network the cathodic currents, for these easy to wire enzymes, are higher in the bilayer cathodes than in single-layer cathodes (Figures 4 and 5). Unlike the single-layer cathodes, the bilayer cathodes do not exhibit a current decrease at high substrate concentrations.

The single-layer electrodes differ from the bilayer electrodes also in their weight fraction of electrically insulating protein and thus in their electron transport characteristics. When the fraction of (electrically insulating) enzyme protein in the hydrogel is excessively high, electron transport is poor and the H_2O_2 electroreduction by HRP is limited by the flux of electrons from the electrode via the redox hydrogel to the incorporated HRP molecules. Therefore, enzymes, such as D-AAOX, ChOX, and AOX, that have a relatively low specific activity, are expected to reach higher current densities with bilayer electrodes which can be more heavily oxidase loaded. Indeed, both bilayer cathodes with D-AAOX and AOX show higher current densities than single-layer electrodes (Figures 6 and 7). The current density of the bilayer ChOX cathode is nevertheless similar to that of the single-layer cathode, even though this enzyme has a low specific activity (Figure 8). This anomaly may reflect the better H_2O_2 collection efficiency in the single-layer sys-

FIGURE 9. Redox cycles for bilayer and single-layer cathodes. Single-layer cathodes have an electrically wired HRP, and H_2O_2 diffuses within the film. Bilayer cathodes have an electrically wired HRP inner layer and a nonwired oxidase outer layer. H_2O_2 diffuses between the layers.

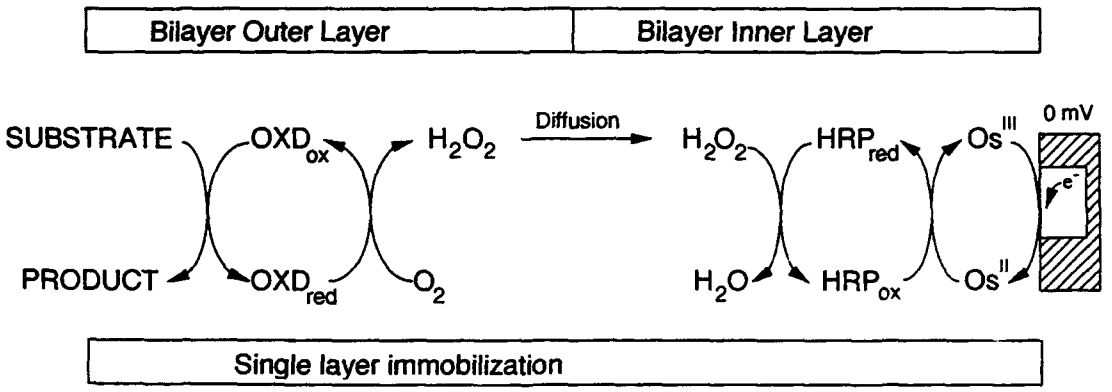

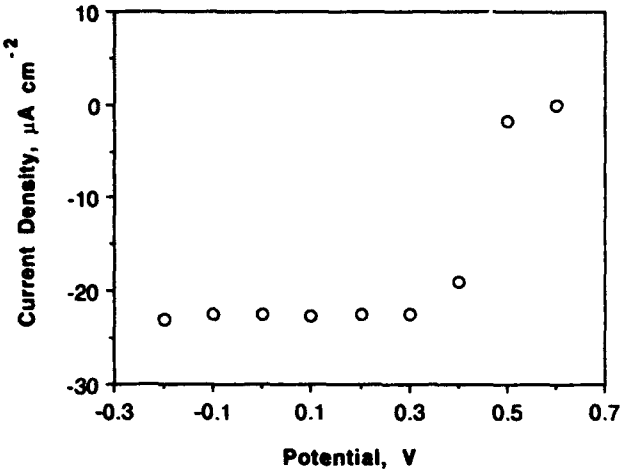

FIGURE 10. Potential dependence of the steady state current for a lactate bilayer electrode made with 100 μg lactate oxidase in the outer layer. pH 7.4, 1000 rpm, 0.2 mM lactate.

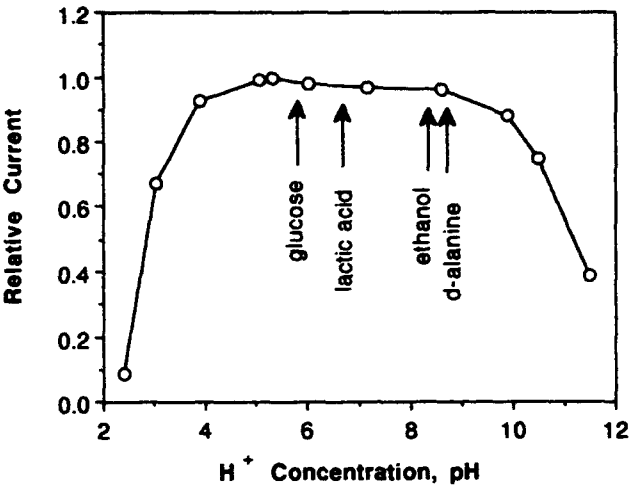

FIGURE 12. Dependence of the maximum current on the D-alanine concentration for a D-amino acid oxidase bilayer cathode operated in a flow system. Flow rates 0.75 mL min^{-1} (circles), 1.5 mL min^{-1} (squares), and 2.1 mL min^{-1} (triangles); carrier pH 7.5 phosphate buffer solution. The D-amino acid oxidase loading in the outer layer is 15 μg.

tem, where the H_2O_2 need not diffuse from layer to layer to be sensed. The proposed redox cycle sequence in bilayer and single-layer electrodes is shown schematically in Figure 9.

Potential and pH Dependence of the Current Density of the Bilayer Cathodes

The potential dependence of the cathodic current of the lactate bilayer electrode is shown in Figure 10. It is similar to that of the H_2O_2 electrode itself [9]. The cathodic current reaches its plateau already at +0.3 V (SCE) and does not change substantially at least to −0.2 V (SCE).

The pH dependence of the currents for the single-layer and bilayer cathodes is similar to the pH dependence of the oxidase's activity in solution. The pH dependence of the current for wired HRP cathodes is nearly flat between pH 4 and 9. It straddles the pH optima of the five oxidases studied (Figure 11).

FIGURE 11. pH dependence of the cathodic current for the standard inner layer H_2O_2 sensor at 0.01 mM H_2O_2. The pH was adjusted with HCl or NaOH in a universal buffer containing 0.02 KH_2PO_4 M of one of the following: sodium citrate, boric acid, KH2PO4 and sodium barbital. The pH optima for bilayer cathodes are indicated. 0.0 mV versus SCE and 1000 rpm.

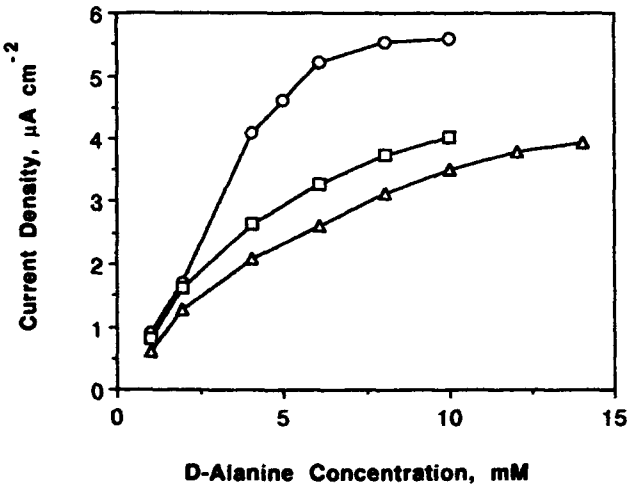

Flow Injection Analysis

In flow injection analysis it is not necessary to reach a steady-state current in order to assay the analyte. This is an advantage in bilayer electrodes where it takes, in some

TABLE 1 Operational Half-Lives of Single-Layer and Bilayer Cathodes at 0.0 V (SCE) at 25 °C in Air-Saturated Solution

	Half-Life In Continuous Operation	
Hours Enzyme	*Single-Layer*	*Bilayer*
Alcohol oxidase	4	7
Glucose oxidase	>15[a]	>40
Lactate oxidase	6	>30
Choline oxidase	23	>30
D-Amino acid oxidase	48	>30

[a]The current initially increased and then declined.

cases, ca. 5 minutes to reach a steady-state current. Furthermore, through varying the flow rate of the carrier, the sensitivity and dynamic range can be adjusted to the desired range. Working at a linear flow rate of 1.1 mL min^{-1} and a loop sample of 50 μL, a bilayer lactate electrode (20 μg of enzyme) exhibits a linear current increase with lactate concentration from 0.2 to 1.8 mM (20 μg LOX, 1.1 mL min^{-1} flow rate; phosphate buffer carrier, not shown). This may be compared with steady-state rotating disk experiments where the current is linear only to 0.6 mM lactate. The FIA is completed in less than 90 seconds. The same effect is noted for alcohol oxidase, where the linear region is increased to 2 mM.

The effect of increasing the flow rates in FIA experiments is shown in figure 12 for a D-AAOX bilayer cathode. When the flow rate is increased, the contact time with the substrate is reduced and a lower H_2O_2 concentration is reached. As a result, sensitivity is lost, but the current still increases at high substrate concentrations where, at lesser flow rates, it would have saturated.

Long-Term Stability

Table 1 shows the half-life time for different types of electrodes. The bilayer electrodes are in general more stable than the single-layer electrodes, because they are made with a substantial excess of enzyme. Thus, even when the enzyme's activity decays, the sensors remain substrate flux, not enzyme turnover, limited.

CONCLUSIONS

Substrates of H_2O_2 generating enzymes that are difficult to electrically connect to electrodes by 3-D redox-polymer networks can be readily assayed with bienzyme electrodes at 0.0 V (SCE). This advantage is gained, however, at the expense of having to operate the electrodes in aerated solutions.

ACKNOWLEDGMENTS

The work described was supported by the Office of Naval Research, by the National Science Foundation, and by the Welch Foundation.

REFERENCES

1. J. J. Kulys, M. V. Pesliakinene, and A. S. Samalius, *Bioelectrochem. Bioeng. 8* (1981) 81.
2. T. Tatsuma and T. Watanabe, *Anal. Chem. 61* (1989) 2352.
3. J. Kulys, and R. D. Schmid, *Bioelectrochem. Bioenerg. 24* (1990) 305–311.
4. J. Kulys, U. Bilitewski, and R. D. Schmid, *Sensors and Actuators B3*(1991) 227.
5. G. Jönsson and L. Gorton, *Electroanalysis 1* (1989) 465.
6. L. Gorton, G. Jönsson-Pettersson, E. Csöregi, K. Johansson, E. Dominguez, and G. Marko-Varga, *Analyst 117* (1992) 1235.
7. L. I. Boguslavsky, P. D. Hale, H. S. Skotheim, and H. S. Lee, *Biosensors '92*, Proc. 2nd World Congress on Biosnsors, May 20–22, 1992, Geneva, Switzerland, 1992, p. 104.
8. B. G. Gregg and A. Heller, *J. Phys. Chem. 95* (1991) 5970.
9. M. Vreeke and A. Heller, *Anal. Chem. 64* (1992) 3084.

Reprinted from Analytical Chemistry, 1990, 62, 258.

Cross-Linked Redox Gels Containing Glucose Oxidase for Amperometric Biosensor Applications

Brian A. Gregg and Adam Heller*

Department of Chemical Engineering, University of Texas at Austin, Austin, Texas 78712

Oxidoreductases, such as glucose oxidase, can be electrically "wired" to electrodes by electrostatic complexing or by covalent binding of redox polymers so that the electrons flow from the enzyme, through the polymer, to the electrode. We describe two materials for amperometric biosensors based on a cross-linkable poly(vinylpyridine) complex of $[Os(bpy)_2Cl]^{+/2+}$ that communicates electrically with flavin adenine dinucleotide redox centers of enzymes such as glucose oxidase. The uncomplexed pyridines of the poly(vinylpyridine) are quaternized with two types of groups, one promoting hydrophilicity (2-bromoethanol or 3-bromopropionic acid), the other containing an active ester (*N*-hydroxysuccinimide) that forms amide bonds with both lysines on the enzyme surface and with an added polyamine cross-linking agent (triethylenetetraamine, trien). In the presence of glucose oxidase and trien this polymer forms rugged, cross-linked, electroactive films on the surface of electrodes, thereby eliminating the requirement for a membrane for containing the enzyme and redox couple. The glucose response time of the resulting electrodes is less than 10 s. The glucose response under N_2 shows an apparent Michaelis constant, $K_m' = 7.3$ mM, and limiting current densities, j_{max}, between 100 and 800 $\mu A/cm^2$. Currents are decreased by 30–50% in air-saturated solutions because of competition between O_2 and the Os(III) complex for electrons from the reduced enzyme. Rotating ring disk experments in air-saturated solutions containing 10 mM glucose show that about 20% of the active enzyme is electrooxidized via the Os(III) complex, while the rest is oxidized by O_2. These results suggest that only part of the active enzyme is in electrical contact with the electrode.

INTRODUCTION

Enzyme-based biosensors are being used in an increasing number of clinical, environmental, agricultural, and biotechnological applications (*1–4*). Ideally, the high selectivity of enzymes, when coupled with modern electrode technology, should result in an electrochemical sensor capable of detecting the concentration of a single biochemical species in a medium containing a diverse mixture of other compounds. Amperometric enzyme electrodes (*5*) require some form of electrical communication between the electrode and the active site of the redox enzyme. However, the measurement of a current proportional to the concentration of the enzyme substrate is complicated by the fact that the active site is often located deep inside an insulating protein shell. Thus, redox enzymes such as glucose oxidase do not exchange electrons with simple metal electrodes (*6–9*). Historically, electrical communication between enzyme and electrode has been achieved through the use of diffusing mediators. The first mediator employed for flavin adenine dinucleotide (FAD)–enzyme electrodes was the natural substrate of the flavin-linked oxidases, O_2 (*10–15*). For example, the reaction of glucose oxidase (GO) is

$$\text{GO–FAD} + \text{glucose} \rightarrow \text{GO–FADH}_2 + \text{gluconolactone} \quad (1)$$

$$\text{GO–FADH}_2 + O_2 \rightarrow \text{GO–FAD} + H_2O_2 \quad (2)$$

and the first commercial amperometric glucose sensors measured either the decrease in O_2 concentration at an oxygen electrode (*15*) or the increase in H_2O_2 concentration at a platinum electrode. The H_2O_2 formed in such sensors degrades the enzyme (*16*). Nature alleviates this problem through the use of the highly active enzyme catalase, which catalyzes the disproportionation of the H_2O_2 to water and oxygen. Furthermore, the electrode current depends on the concentration of *both* enzyme substrates, i.e., glucose *and* O_2. Measurement of the H_2O_2 concentration requires both a highly catalytic electrode (e.g., Pt) and a potential (ca. 0.7 V vs SCE) substantially positive of the reversible potential for the $FAD/FADH_2$ couple ($E^\circ \approx -0.4$ V vs SCE) (*17*). This may result in large spurious currents due to a number of easily oxidized species in the system to be measured. Because of this problem, selective membranes were required to maintain the specificity of the enzyme electrode.

The more recent devices have employed small diffusing electron mediators (Ox/Red) such as ferrocenes (*18, 19*), quinones (*20*), ruthenium amines (*21*), components of organic metals (*22–27*), and octacyanotungstates (*28*). In such electrodes, reaction 1 above is followed by

$$\text{GO–FADH}_2 + 2\text{Ox} \rightarrow \text{GO–FAD} + 2\text{Red} + 2H^+ \quad (3)$$

where the reduced form of the mediator (Red) is subsequently electrooxidized. Catalase can be added to such a system to protect the enzyme from H_2O_2. The potential at which these electrodes operate is only slightly positive of the formal potential of the mediator, and a highly active noble metal electrode is not required for the reaction. Thus, spurious currents due to competing species may be reduced. Still, in an oxygen-containing medium, there is a competition between the oxidized form of the mediator (Ox) and oxygen for the reduced form of the enzyme (GO–FADH_2) (eqs 2 and 3). Thus, the electrode current is independent of the oxygen concentration only insofar as the mediator competes effectively with O_2.

Many enzyme electrodes require that the enzyme be confined to the proximity of the electrode surface by a membrane. Diffusion of substrate and product through such a membrane controls the (usually slow) response time of these electrodes. The required membrane seal also increases the cost of these electrodes. Furthermore, the small mediators commonly employed in the recent devices eventually diffuse through the membranes and are lost. Recently, a polymeric redox "wire" based on the poly(vinylpyridine) (PVP) complex of $Os(bpy)_2Cl$ (abbreviated POs^+) has been introduced (*29*). The "wire" electrically connects the enzyme to the electrode yet, by virtue of its molecular size, remains confined behind the membrane. This polycationic redox polymer forms electrostatic complexes with the polyanionic glucose oxidase in a manner mimicking the natural attraction of some redox proteins for enzymes, e.g., cytochrome *c* for cytochrome *c* oxidase (*30*). We report here a method for bonding a similar redox polymer to the enzyme and immobilizing the enzyme/polymer compound on an electrode in one step. The need for a membrane is eliminated in the resulting electrode. To simultaneously "wire" and immobilize the enzyme, we quaternize the PVP backbone with either the bromoacetic or bromopropionic acid ester of *N*-hydroxysuccinimide (NHS). The NHS esters react rapidly with primary amines, e.g., lysines on the enzyme surface, to

0003-2700/90/0362-0258$02.50/0

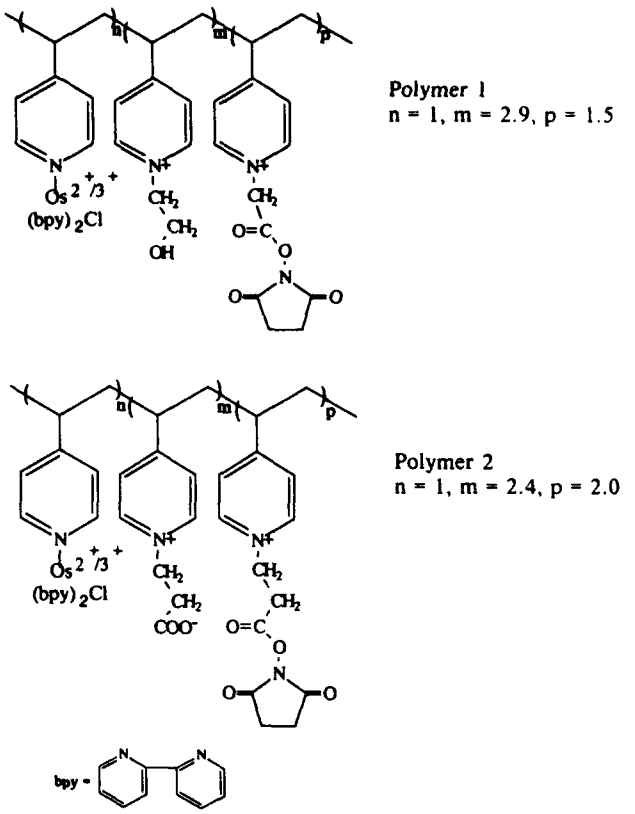

Figure 1. Structures of the two cross-linkable, redox gel-forming polymers.

form amide bonds (*31*). In the presence of an enzyme and a cross-linking agent (triethylenetetraamine, trien) this polymer forms, on the surface of an electrode, an insoluble, cross-linked film containing covalently bound enzyme. The resulting electrode is simple to make, fast, and rugged. We report the synthesis of two derivatives of this polymer and the electrochemical characterization of several polymer/glucose oxidase electrodes as a function of temperature and the concentrations of glucose, other sugars, and oxygen. We also describe a convenient method for quantifying the relative rates of eqs 2 and 3 in our system by rotating ring disk voltammetry.

EXPERIMENTAL SECTION

Chemicals. Glucose oxidase [EC 1.1.3.4] from *Aspergillus niger* (Sigma, catalog no. G-8135), catalase [EC 1.11.1.6] (Sigma, catalog no. C-100), Na-HEPES (sodium 4-(2-hydroxyethyl)-1-piperazineethanesulfonate) (Aldrich), and K_2OsCl_6 (Johnson Matthey) were used as received. Poly(vinylpyridine) (PVP, Polysciences, MW 50 000) was purified 3× by dissolution in methanol, filtration, and precipitation with ether.

Polymers. The structure of the polymers reported here is shown in Figure 1. The poly(vinylpyridine) complex of the $Os(bpy)_2Cl_2$ was synthesized as previously reported (*32*) and purified by precipitation from ethyl acetate. The resulting polymer was quaternized in warm (ca. 60 °C) dimethyl formamide (DMF) under N_2 with either bromoethanol (Aldrich) or a mixture containing equimolar amounts of triethylamine and 3-bromopropionic acid (Aldrich) for 2 h. (The polymer compositions shown in Figure 1 assume that these materials reacted quantitatively with the poly(vinylpyridine) backbone.) After the initial partial quaternization, a slight excess of either the bromoacetic or bromopropionic acid ester of *N*-hydroxysuccinimide (NHS) (synthesized from the respective acid chloride and NHS essentially by the method of Pollak et al. (*33*)) was added, and the solution was further warmed for ca. 2 h. The resulting solution was then cooled and poured into rapidly stirred acetone, and the precipitate was filtered, washed with acetone, and stored in a desiccator.

The polymer quaternized with bromoethanol and the bromoacetic acid ester of NHS (polymer 1, POs^+–EtOH–C_2NHS) has a formula weight of 1878 g/repeat unit, assuming the composition shown in Figure 1. This corresponds to ca. 0.8 μmol of active ester groups per milligram of polymer. The polymer quaternized with bromopropionic acid and the bromopropionic acid ester of NHS (polymer 2, POs^+–$EtCOO^-$–C_3NHS) has approximately 1.0 μmol of active ester groups per milligram of polymer.

Electrodes. A representative electrode film was prepared as follows: An electrode consisting of a gold disk, 4.7 mm in diameter, surrounded by a platinum ring, was polished first with 0.3-μm alumina and then with 0.05-μm alumina, sonicated, rinsed with water, and dried in air. Aliquots (4 μL each) of the following solutions were then applied to the gold disk: 10 mg/mL glucose oxidase solution in 10 mM HEPES buffer, pH 7.2; 8 mM trien in the same buffer solution; and a freshly made solution of 10 mg/mL polymer 2 in H_2O. The solutions were briefly mixed on the electrode surface; the electrode was then dried in a vacuum dessicator containing a beaker of H_2O for at least 30 min. Similar films were made on glassy carbon, graphite, and platinum electrodes of various sizes.

Equipment. Electrochemical measurements were performed with a Princeton Applied Research 175 universal programmer, a Model 173 potentiostat, and a Model 179 digital coulometer. The signal was recorded on a Kipp and Zonen X-Y-Y′ recorder. A conventional single-compartment electrochemical cell was used with an aqueous saturated calomel reference electrode (SCE) (0.226 V vs a normal hydrogen electrode (NHE)) and a platinum counter electrode. The rotating ring disk experiments were performed with a Pine Instruments AFMSRX rotator, MSRS speed control and RDE4 bipotentiostat, and either a glassy carbon disk/platinum ring electrode (GC/Pt RRDE) or a gold disk/platinum ring electrode (Au/Pt RRDE), both from Pine Instrument Co.

RESULTS AND DISCUSSION

Enzyme Immobilization and Film Formation. The immobilization of enzymes has been the subject of extensive recent work (*2*, *34*, *35*) because heterogeneous catalysis has advantages over homogeneous catalysis and also because, in some cases, enzymes are stabilized by immobilization (*36–39*). The observed stabilization has been attributed both to the protection against attack by proteases that is afforded by the polymeric support and to the physical confinement of the enzyme's peptide chains that can retard thermal denaturation. Polymers containing *N*-hydroxysuccinimide (NHS) esters have been commonly used as coupling agents for affinity chromatography (*40*) and for the immobilization of a number of enzymes (*33*).

Recently, Foulds and Lowe (*41*) have reported the entrapment of glucose oxidase in films of ferrocene-containing polypyrrole. In these electrodes both direct current and indirect (O_2-mediated) current were observed. Hale et al. (*42*) described a biosensor based on the adsorption of glucose oxidase onto a mixture of carbon paste and a ferrocene-containing siloxane polymer. Here we report the covalent binding of glucose oxidase in an electrically conducting, hydrophilic, cross-linked redox gel on the surface of an electrode. The NHS ester chemistry was incorporated in the previously developed PVP-based polycationic redox polymer (POs^+) (*29*, *32*) by quaternizing some of the uncomplexed pyridines of POs^+ with bromoacetic or bromopropionic acid esters of NHS. To provide solubility in water to the resulting polymer, the remaining free pyridines were quaternized with either 2-bromoethanol or 3-bromopropionic acid (Figure 1).

Active NHS esters are highly specific for primary amines; they also slowly hydrolyze in aqueous solution (*33*). Thus, the two reactions of importance are the aminolysis and the hydrolysis of these active ester groups on the polymer chain. The cross-linked polymer is formed on the surface of the electrode by the addition of a few microliters of a fresh solution of the polymer to a solution of the enzyme and the cross-linking agent (trien) followed by evaporation of the solvent. It is feasible to use the enzyme as the only cross-linking agent.

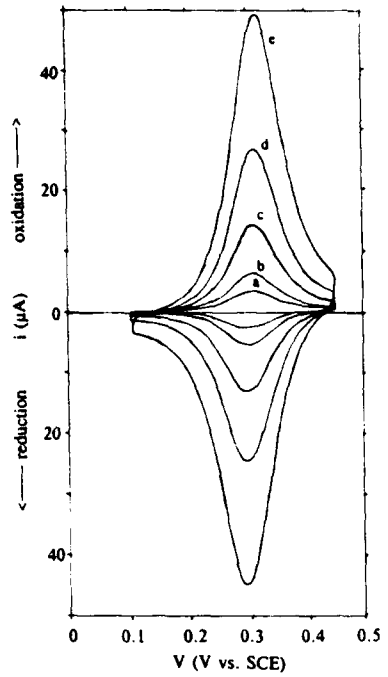

Figure 2. Cyclic voltammograms of a cross-linked film consisting of polymer 2, glucose oxidase, and triethylenetetraamine on glassy carbon in the absence of glucose: 0.1 M HEPES buffer at pH 7.1; scan rates (mV/s), (a) 10, (b) 20, (c) 50, (d) 100, (e) 200.

This requires, however, a high concentration of enzyme and results in an electrode exhibiting slow charge-transfer kinetics. Polymer/GO/trien films have been prepared on glassy carbon, graphite, gold, and platinum electrodes; the electrode characteristics were not noticeably affected by the nature of the conducting substrates. In systems where the enzyme is free to diffuse, platinum or glassy carbon electrodes often cause irreversible adsorption or denaturation of the enzyme (*43*). Apparently the enzyme in the cross-linked polymer films is protected from the deactivating influence of the electrode surface.

Electrochemical Characterization of the Polymer/Enzyme Film. In the absence of glucose oxidase in the polymer film, the current density resulting from direct electrooxidation of glucose (30 mM) is less than the background current (<10 nA/cm^2) in the range 0–0.5 V vs SCE. Cyclic voltammetric waves at different scan rates of a thin layer of polymer 2/GO/trien on a glassy carbon electrode are shown in Figure 2 in a solution containing 0.1 M HEPES buffer titrated to pH 7.1 with HCl (ionic strength, 0.17 M). In the absence of glucose, the enzyme gives no response and only the polymer electrochemistry is observed. The electrode exhibits the classical features of a kinetically fast redox couple strongly bound to an electrode surface (*44*). At a scan rate of 200 mV/s the difference in the reduction and the oxidation peak potentials is less than 20 mV, showing that charge transfer and counterion movement through the film, as well as charge transfer from the film to the electrode, are rapid (*44*). Integration of the charge passed on either reduction or oxidation of the polymer leads to a value of $\Gamma \approx 10^{-9}$ mol/cm^2 of redox active centers on the surface. The symmetrical surface waves and fast kinetics seen in Figure 2 show that the presence of the enzyme does not appreciably affect the electrochemistry of the osmium polymer film. Later results will show that, conversely, the presence of the polymer does not appreciably affect the specificity or the activity of the enzyme.

Catalytic Oxidation of Glucose with Polymer/Enzyme Films. Upon addition of glucose (40 mM) to the solution, a catalytic oxidation wave is observed and the reduction peak is eliminated (Figure 3). Thus, glucose oxidase is reduced

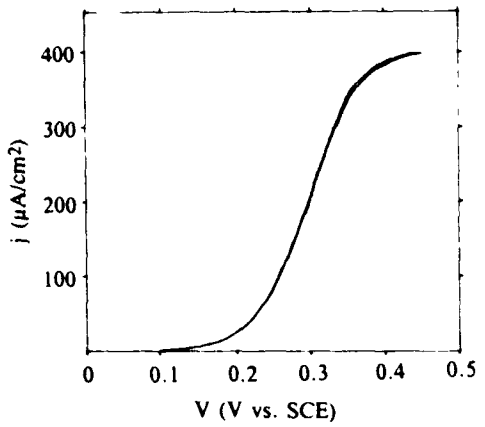

Figure 3. Cyclic voltammogram of the film shown in Figure 2 under N_2 after addition of 40 mM glucose: scan rate, 5 mV/s; rotation rate, 1000 rpm.

by the glucose penetrating the gel (eq 1), electrons are transferred from the reduced enzyme to the Os(III) sites (eq 3), and the electrons are then transferred through the osmium polymer film to the electrode surface. The absence of a reduction wave shows that, at this scan rate (5 mV/s), the film is homogeneously maintained in the reduced state by the transfer of electrons from GO–FADH$_2$ to the Os(III) complex (eq 3). This is also evidenced by the almost complete lack of hysteresis between the forward and the reverse scans. At faster scan rates (data not shown) a hysteresis appears and, eventually, a reduction wave is also observed. Thus, at fast scan rates, the film is no longer completely reduced by enzyme-mediated electron transfer from glucose in the time required for the scan. The appearance of the hysteresis and the reduction wave is a function of substrate concentration, scan rate, film composition and thickness, and ionic strength.

The temperature dependence of a film of polymer 2/GO/trien was investigated from 14 to 40 °C in a solution containing 0.1 M HEPES, catalase, and 30 mM glucose under a nitrogen atmosphere. Thirty millimolar glucose is many times the apparent Michaelis constant of the electrode (see below) and is close to the saturation level for substrate. The electrode was rotated at 500 rpm (the results were independent of rotation rate above ca. 300 rpm), and the potential was held at 0.35 V vs SCE. Over this range, the current exhibits a smooth exponential increase with temperature. An Arrhenius plot of this data (Figure 4) gives an activation energy for the rate-determining step in these films under such conditions of 11.1 kcal/mol.

Glucose Response and Apparent Michaelis Constant of the Enzyme Electrodes. The glucose response curves of films on rotating disk electrodes were measured at 2000 rpm (fast rotation rates were required to prevent concentration polarization at low glucose concentration) and 0.45 V vs SCE. Aliquots of a 1 M solution of glucose were injected into the cell (solution volume 100 mL) while the current was monitored. The current stabilized in ca. 10 s, i.e., in the time required to reach a uniform glucose concentration throughout the cell. Thus, an upper limit on the response time of these enzyme electrodes is 10 s.

The glucose response curves measured under N_2 are consistent with those expected for Michaelis–Menten kinetics. Castner and Wingard (*45*) have shown that enzymes immobilized on rotating disk electrodes, under conditions where the enzymatic reaction is rate controlling, follow the Eadie–Hofstee form of the Michaelis–Menten equation:

$$j_{ss} = j_{max} - K_m'(j_{ss}/C^*) \qquad (4)$$

where j_{ss} is the steady-state current density, j_{max} is the maximum current density under saturating substrate conditions

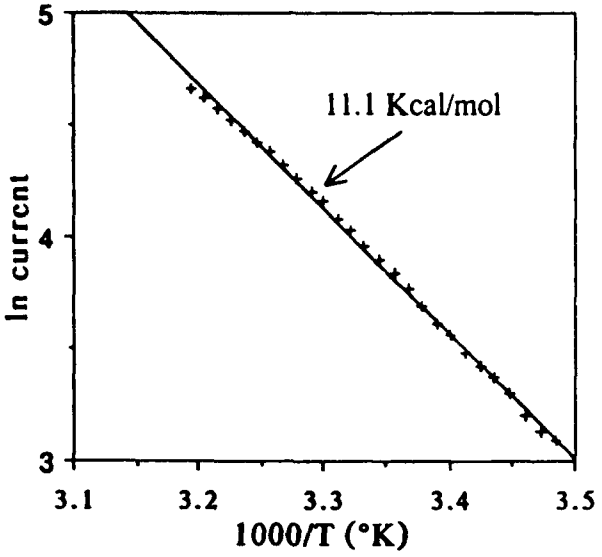

Figure 4. Arrhenius plot of the steady-state catalytic current of a polymer 2/glucose oxidase/trien film on a gold disk electrode: 0.1 M HEPES at pH 7.1, 30 mM glucose, N_2 atmosphere, catalase added to solution. The electrode was rotated at 500 rpm and held at 0.35 V vs SCE.

(this is related to the V_{max} measured in homogeneous solution), K_m' is the apparent Michaelis constant (which can differ substantially from that measured in homogeneous solution and is not an intrinsic property of the enzyme, but of the system), and C^* is the concentration of glucose in solution. The glucose response data (Figure 5a) were plotted in an Eadie–Hofstee type plot (Figure 5b) giving a straight line with a slope equal to the negative of the apparent Michaelis constant (K_m' = 7.3 mM) and an intercept equal to $j_{max} \approx 565$ $\mu A/cm^2$. The K_m' measured for a number of films varied only slightly; j_{max}, however, varied from ca. 100 to 800 $\mu A/cm^2$ depending on film thickness, composition, and temperature. The apparent Michaelis constant, K_m', characterizes the enzyme electrode, not the enzyme itself. It is a measure of the substrate concentration range over which the electrode response is approximately linear. Castner and Wingard (*45*) obtained values of K_m' for glucose oxidase electrodes of 6, 14, and 36 mM for glucose oxidase immobilized with derivatized albumin, allylamine, and a silane, respectively.

Competition between Oxygen and the Redox Polymer. A comparison of glucose response curves measured under N_2 and under air is shown in Figure 6. There was no catalase present in either the film or the solution. The decrease in catalytic current density in air-saturated solutions can be explained by the competition between O_2 and the Os(III) complex for electrons from the reduced enzyme (eqs 2 and 3). Thus, the response of the present polymer/enzyme electrode is still dependent on the oxygen concentration, although this dependence is less than that for an electrode measuring either O_2 or H_2O_2. Improvements in the redox polymer would be expected to further decrease the oxygen sensitivity of these electrodes.

When O_2 is competing with the redox couple for the oxidation of the enzyme, it is important to quantify the relative rates of the two competing reactions (eqs 2 and 3). This was achieved by rotating ring disk voltammetry. The enzyme-containing polymer film was deposited only on the disk of a rotating ring disk electrode (RRDE). The disk electrode was either Au or glassy carbon, i.e., a material with a high overpotential for oxidation of H_2O_2, while the ring was Pt, a good catalyst for the oxidation of H_2O_2. The measurement was conducted by placing the electrode in a HEPES solution through which air was being continuously bubbled and that

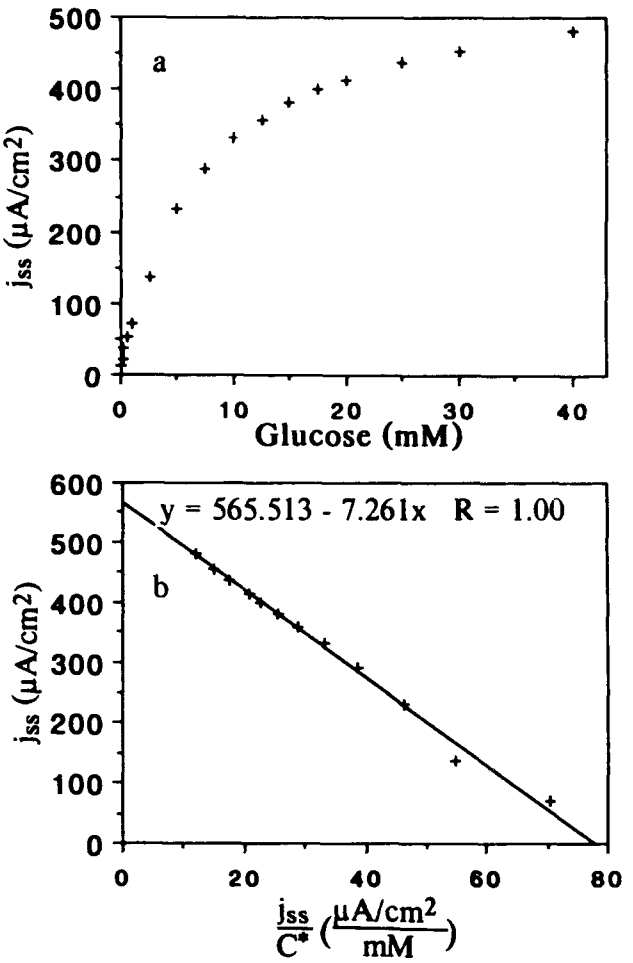

Figure 5. (a) Steady-state glucose response curve of the film shown in Figure 4 under N_2 at 37.5° C: ω = 2000 rpm, V = 0.45 V vs SCE. (b) Eadie–Hofstee type plot of the data in a. The best fit equation is shown.

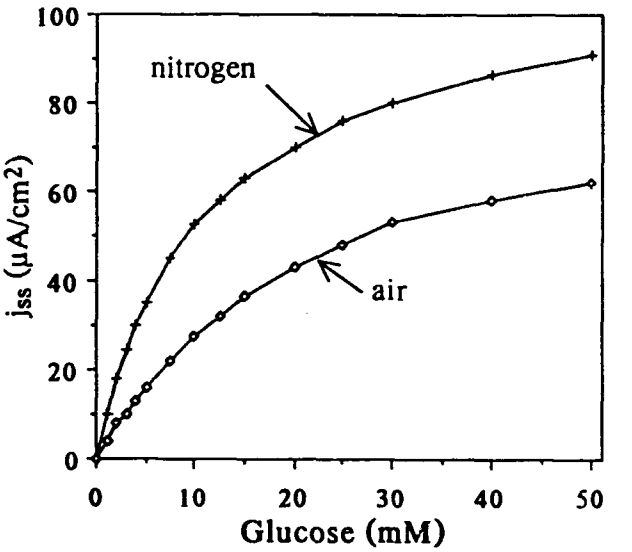

Figure 6. Steady-state glucose response curves under N_2 and under air of a film composed of polymer 1/glucose oxidase/trien: no catalase in the film or in solution, T = 23 °C, ω = 2000 rpm, V = 0.45 V vs SCE.

contained at first, no sugar. There was no catalase either in the film or in solution. The electrode was rotated at 1000 rpm while the ring was biased at 0.7 V vs SCE. After stabilization of the background current (ca. 10 min), the disk potential was stepped from 0.1 V (polymer in the Os(II) state) to 0.45 V

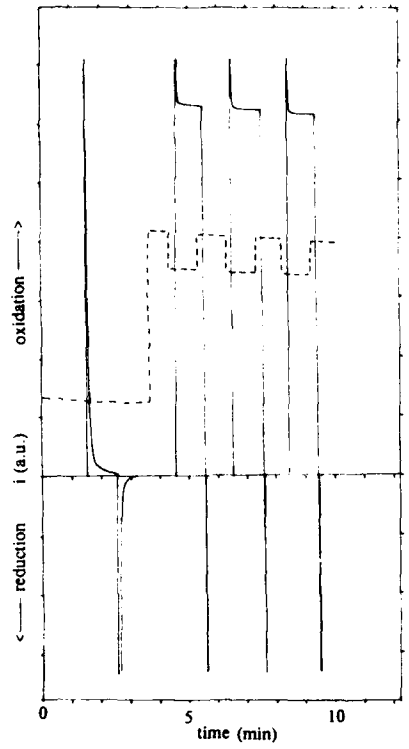

Figure 7. Rotating ring disk experiment with a polymer 2/glucose oxidase/trien film on a glassy carbon disk surrounded by an uncoated platinum ring. The solid line is the disk current (disk potential was either 0.1 or 0.45 V), and the dashed line (offset by ca. 0.2 min) is the ring current (ring potential was 0.7 V). Conditions: air-saturated HEPES buffer (0.1 M) at pH 7.1; no catalase in the film or in solution. At $t \approx$ 1.5 min the disk potential was stepped from 0.1 to 0.45 V; at $t \approx 2.5$ min it was stepped back to 0.1 V. At $t \approx 4$ min glucose was injected to a concentration of 10 mM. At $t \approx 4.5$ min the disk voltage was stepped from 0.1 to 0.45 V; at $t \approx 5.5$ min it was stepped back to 0.1 V. The cycle was repeated twice more.

(polymer in the Os(III) state) and then back (Figure 7). The disk showed only charging current; i.e., no steady-state current was observed. Furthermore, the ring current, as expected, showed no change upon stepping the potential of the disk. Upon addition of 10 mM glucose (i.e., a value close to K_m', in the normal operational range of the electrode), the ring current increased because of the oxidation of H_2O_2 formed by the enzyme bound to the disk. The increase in ring current upon addition of glucose (while the polymer is in its inactive, Os(II), state) is a measure of the activity of the enzyme immobilized in the redox polymer. This mode of operation is similar to that of a peroxide-measuring glucose sensor. Stepping the disk potential from 0.1 to 0.45 V now resulted in a steady-state disk current and a substantial and reversible (upon stepping back to 0.1 V) decrease in the ring current. Thus, the increase in the polymer-mediated oxidation of glucose (disk current) resulted in the decrease of the oxygen-mediated oxidation of glucose (ring current). After subtraction of the background, this decrease in ring current upon oxidation of the polymer was measured to be ca. 20% of the total. Since the percentage of the total H_2O_2 that is collected at the ring is a function only of the geometry of the derivatized RRDE, the 20% decrease in ring current upon oxidation of the polymer corresponds to the percentage of the active enzyme that is directly oxidized by the polymer rather than by the competing O_2.

Selectivity and Stability of the Enzyme Electrode. The selectivity of these enzyme electrodes was briefly examined by holding the potential at 0.45 V while fructose, galactose, and ethylene glycol were added sequentially at concentrations of 10 mM. These substances, individually or collectively, had no measurable effect on the electrode current (i.e., less than 1 nA). Addition of 10 mM glucose led to a current of 9.3 μA. These results, and the high activity of the immobilized enzyme (as seen from the large j_{max}), suggest that the glucose oxidase covalently bound in these redox polymer films retains much of its native selectivity and activity.

Preliminary tests of these electrodes in solutions containing ascorbate (a common interferent) have shown that the current due to ascorbate oxidation is apparently inversely proportional to the surface coverage of the polymer film. Thus, the redox polymer is an advantageously poor electrocatalyst for the oxidation of ascorbate. When stored dry, without precautions, in the laboratory ambient, the electrodes showed no deterioration over the course of 3 weeks. Longer tests are in progress.

CONCLUSIONS

A simple and effective method for immobilizing redox enzymes on electrodes while simultaneously electrically connecting them to the electrode is described. The resulting cross-linked, enzyme-containing films are stable, selective, and highy active for the catalytic oxidation of glucose. Although the glucose-related current density from these electrodes is high, O_2 can still competitively oxidize a significant fraction of the enzymes. This technique for immobilization and electrical connection of redox enzymes appears to be promising for a number of enzyme electrode applications.

LITERATURE CITED

(1) Wise, D. L., Ed. *Applied Biosensors*; Butterworths: Boston, 1989.
(2) Mosbach, K., Ed. *Methods in Enzymology*; Academic Press: New York, 1987; Vol. 137.
(3) Luong, J. H. T.; Mulchandani, A.; Guilbault, G. G. *Trends Biochem.* **1988**, *6*, 310–316.
(4) Higgins, I. J. *Biotec* **1988**, *2*, 3–8.
(5) Bartlett, P. N.; Whitaker, R. G. *Biosensors* **1987/1988**, *3*, 359–379.
(6) Hill, H. A. O. *Pure Appl. Chem.* **1987**, *59*, 743–748.
(7) Degani, Y.; Heller, A. *J. Phys. Chem.* **1987**, *91*, 1285–1289.
(8) Degani, Y.; Heller, A. *J. Am. Chem. Soc.* **1988**, *110*, 2615–2620.
(9) Degani, Y.; Heller, A. In *Redox Chemistry and Interfacial Behavior of Biological Molecules*; Dryhurst, G., Niki, K., Eds.; Plenum Press: New York, 1987.
(10) Clark, L. C., Jr.; Lyons, C. *Ann. N.Y. Acad. Sci.* **1962**, *102*, 29–45.
(11) Clark, L. C., Jr.; Spokane, R. B.; Homan, M. M.; Sudan, R.; Miller, M. *Trans. Am. Soc. Artif. Intern. Organs* **1988**, *34*, 259–265.
(12) Jönsson, G.; Gorton, L. *Anal. Lett.* **1987**, *20*, 839–855.
(13) Ianniello, R. M.; Yacynych, A. M. *Anal. Chem.* **1981**, *53*, 2090–2095.
(14) Mason, M. *Biotec* **1988**, *2*, 49–53.
(15) Updike, S. J.; Hicks, G. P. *Nature* **1967**, *214*, 986–988.
(16) Tse, P. H. S.; Gough, D. A. *Biotechnol. Bioeng.* **1987**, *29*, 705–713.
(17) Stankovich, M. T.; Schopfer, L. M.; Massey, V. *J. Biol. Chem.* **1978**, *253*, 4971.
(18) Green, M. J.; Hill, H. A. O. *J. Chem. Soc., Faraday Trans. 1* **1986**, *82*, 1237–1243.
(19) Cass, A. E. G.; Davis, G.; Green, M. J.; Hill, H. A. O. *J. Electroanal. Chem. Interfacial Electrochem.* **1985**, *190*, 117–127.
(20) Kulys, J. J.; Cénas, N. K. *Biochim. Biophys. Acta* **1983**, *744*, 57–63.
(21) Crumbliss, A. L.; Hill, H. A. O.; Page, D. J. *J. Electroanal. Chem. Interfacial Electrochem.* **1986**, *206*, 327.
(22) Kulys, J. J.; Samalius, A. S.; Swirmickas, J. S. *FEBS Lett.* **1980**, *114*, 7.
(23) Cénas, N. K.; Kulys, J. J. *Bioelectrochem. Bioenergy* **1981**, *8*, 103.
(24) Kulys, J. J.; Cénas, N. K. *Biochim. Biophys. Acta* **1983**, *744*, 57.
(25) Albery, W. J.; Bartlett, P. N.; Cass, A. E. G.; Craston, D. H.; Haggett, B. G. D. *J. Chem. Soc., Faraday Trans. 1* **1986**, *82*, 1033.
(26) Albery, W. J.; Bartlett, P. N. *J. Elctroanal. Chem. Interfacial Electrochem.* **1985**, *194*, 211.
(27) Albery, W. J.; Bartlett, P. N.; Craston, D. H. *J. Electroanal. Chem. Interfacial Electrochem.* **1985**, *194*, 223.
(28) Taniguchi, I.; Miyamoto, S.; Tomimura, S.; Hawkridge, F. M. *J. Electroanal. Chem. Interfacial Electrochem.* **1988**, *240*, 33.
(29) Degani, Y.; Heller, A. *J. Am. Chem. Soc.* **1989**, *111*, 2357–2358.
(30) Hazzard, J. T.; Moench, S. J.; Erman, J. E.; Satterlee, J. D.; Tollin, G. *Biochemistry* **1988**, *27*, 2002–2008.
(31) Anderson, G. W.; Zimmerman, J. E.; Callahan, F. M. *J. Am. Chem. Soc.* **1964**, *86*, 1839–1842.
(32) Pishko, M. V.; Katakis, I.; Lindquist, S.-E.; Ye, L.; Gregg, B. A.; Heller, A. *Angew. Chem.*, in press.
(33) Pollak, A.; Blumenfeld, H.; Wax, M.; Baughn, R. L.; Whitesides, G. M. *J. Am. Chem. Soc.* **1980**, *102*, 6324–6336.
(34) Mosbach, K., Ed. *Methods in Enzymology*; Academic Press: New York, 1987; Vol. 135 and 136.
(35) Trevan, M. D. *Immobilized Enzymes*; Wiley and Sons: New York, 1980.
(36) Klibanov, A. M. *Anal. Biochem.* **1979**, *93*, 1–25.

(37) Martinek, K.; Klibanov, A. M.; Goldmacher, V. S.; Berezin, I. V. *Biochim. Biophys. Acta* **1977**, *485*, 1–12.
(38) Martinek, K.; Klibanov, A. M.; Goldmacher, V. S.; Tchernysheva, A. V.; Mozhaev, V. V.; Berezin, I. V.; Glotov, B. O. *Biochim. Biophys. Acta* **1977**, *485*, 13–28.
(39) Torchilin, V. P.; Maksimenko, A. V.; Smirnov, V. N.; Berezin, I. V.; Klibanov, A. M.; Martinek, K. *Biochim. Biophys. Acta* **1978**, *522*, 277–283.
(40) Schnaar, R. L.; Lee, Y. C. *Biochemistry* **1975**, *14*, 1535–1541.
(41) Foulds, N. C.; Lowe, C. R. *Anal. Chem.* **1988**, *60*, 2473–2478.
(42) Hale, P. D.; Inagaki, T.; Karan, H. I.; Okamoto, Y.; Skotheim, T. A. *J. Am. Chem. Soc.* **1989**, *111*, 3482–3484.
(43) Bowden, E. F.; Hawkridge, F. M.; Blount, H. N. In *Comprehensive Treatise of Electrochemistry*; Srinivasan, S., et al., Eds.; Plenum: New York, 1985; Vol. 10.
(44) Murray, R. W. *Electroanal. Chem.* **1984**, *13*, 191–368.
(45) Castner, J. F.; Wingard, L. B., Jr. *Biochemistry* **1984**, *23*, 2203–2210.

RECEIVED for review June 19, 1989. Accepted November 7, 1989. We gratefully acknowledge the financial support for this research from the Office of Naval Research, Contract No. N0014-88-K-0401, the Texas Advanced Research Program, and the Robert A. Welch Foundation.

ANGEWANDTE CHEMIE
Volume 29 Number 1
January 1990
Pages 82-84
International Edition in English
Reprint

Direct Electrical Communication between Graphite Electrodes and Surface Adsorbed Glucose Oxidase/Redox Polymer Complexes

By *Michael V. Pishko, Ioanis Katakis, Sten-Eric Lindquist, Ling Ye, Brian A. Gregg*, and *Adam Heller**

The redox centers of glucose oxidase, like those of most oxidoreductases, are electrically insulated by a protein (glycoprotein) shell. Because of this shell, the enzyme cannot be oxidized or reduced at an electrode at any potential. In an earlier communication it was shown that in homogeneous solutions, water-soluble polycationic poly(vinylpyridine) complexes of $[Os(bpy)_2Cl]^{2\oplus}$ bind to and accept electrons from reduced glucose oxidase, a polyanion.[1] Here we show that the same polycationic redox polymers are strongly adsorbed on graphite; that these modified surfaces adsorb strongly the enzyme; and that the surface adsorbed enzyme/polymer complexes communicate electrically with the electrodes. Electrodes containing these adsorbed complexes are faster and easier to construct than commercially available glucose electrodes.

Poly(4-vinylpyridine) (PVP), as well as *N*-methylated PVP, were shown earlier to be strongly adsorbed on pyrolytic graphite and to yield, with diffusing redox species, long-lived reproducible electrodes.[2, 3] Their electrochemistry is consistent with the physisorption of segments of the macromolecules providing a three-dimensional network into and out of which ions diffuse. Earlier studies of the electrochemistry of small redox proteins that do not have thick insulating shells around their redox centers, (such as cytochrome c, myoglobin, ferredoxin and phycocyanin) have also shown that, even though these proteins are directly electrooxidized reduced on electrodes, their rates of electron transfer can be enhanced by adsorbed "promoters" (e.g. bipyridine, methyl viologen) that bind and orient the proteins, but do not participate in the redox processes.[4] We now find that pyrolytic carbon and graphite electrode surfaces can be modified with adsorbed polycationic redox polymers that complex glucose oxidase. In these structures, electrons are vectorially transferred from enzyme-bound glucose to the electrode via the redox centers of the enzyme and those of the redox polymer.

Strong adsorption of the redox polymer **1** on graphite is seen in the cyclic voltammetry of the terpolymer of poly(*N*-methyl-4-vinyl pyridinium chloride), 4-aminostyrene, and the PVP complex of $[Os(bpy)_2Cl_2]$ (see Scheme 1); at scan rates from 2 to 200 $mV s^{-1}$, the peak separation is 30 mV or less. Integration of the cyclic voltammograms at low scan rates ($2-5\,mV s^{-1}$) shows that approximately 1.0×10^{-9} moles cm^{-2} of **1** are electroactive. The polymer does not desorb from rotating disk electrodes even at high angular velocities (2000 rpm), and coulometry shows that less than 10% of the polymer is desorbed from the electrodes after 30 days of storage in a stirred water bath. The polycationic adsorbed polymer **1** strongly binds glucose oxidase. Cyclic voltammograms for the oxidation of glucose by the enzyme–polymer complex are shown in Figure 1. The current response at a constant potential of 0.45 V (vs. SCE) persists for more than 10 hours when electrodes are rotated at 20 rpm in physiological salt solutions that do not contain

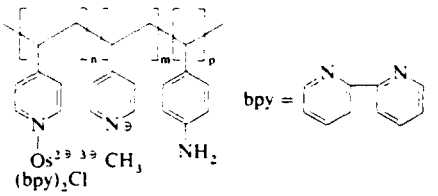

1, n = 0.14, m = 0.81, p = 0.05

Scheme 1. Structure of the quaternized redox terpolymer **1**.

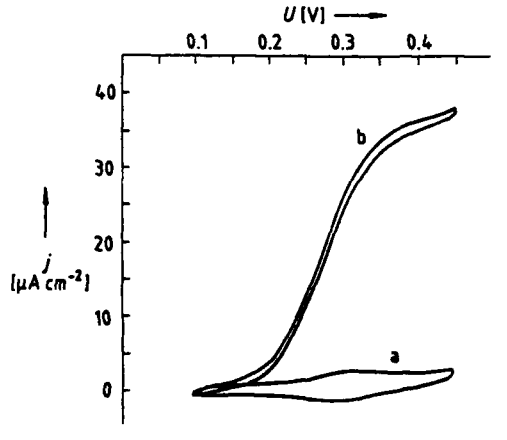

Fig. 1. Cyclic voltammogram of the **1** glucose oxidase complex in 60 mM glucose, 9.9 units catalase mL^{-1}, 0.15 M sodium (4-(2-hydroxymethyl)-1-piperazineethanesulfonate (NaHEPES) at pH 7. Scan rate: $5\,mV s^{-1}$ a) no glucose, b) 60 mM glucose. Potential Cl vs. SCE; glucose oxidase **1** graphite electrode.

[*] Prof. Dr. A. Heller, M. V. Pishko, I. Katakis, Dr. S.-E. Lindquist, L. Ye, Dr. B. A. Gregg
Department of Chemical Engineering, University of Texas at Austin
Austin, TX 78712 (USA)

[**] We wish to thank *Yinon Degani* for his valuable advice on the synthesis of the polymers and *Goran Svensk* for the molar mass determination of the Osmium-containing redox-polymer **1**. This work was supported in part by the Office of Naval Research and the Robert A. Welch Foundation.

any enzyme or polymer, declining approximately 10% over the first hour and 70% after 10 hours. The electrodes were stored in air at room temperature for 30 days with negligible loss in activity. Chronoamperometric measurements in a flow cell show that the current responds to an increase in glucose concentration in less than 1 s (Fig. 2). Response

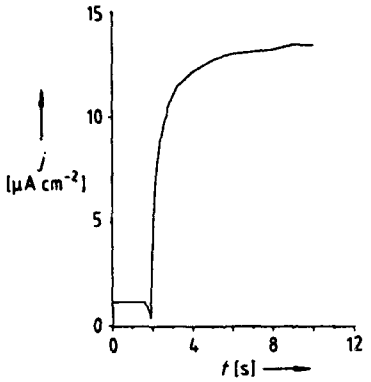

Fig. 2. Electrode response to a change in glucose concentration from 0 to 50 mM glucose in 0.15 M NaHEPES at pH 7.9 units catalase mL^{-1}. Flow rate: 193 $cm\,s^{-1}$. Glucose oxidase/1 graphite electrode.

times for different flow rates vary from 0.4 s at a linear flow rate of 42 $cm\,s^{-1}$ to 0.2 s at a flow rate of 210 $cm\,s^{-1}$. The glucose concentration dependence of the current at 0.45 V (SCE) is shown in Figure 3. A background current persists at zero glucose concentration. Because the electrodes are simple to construct and the materials cost little, they are likely to be appropriate for use in fast, disposable glucose sensing tips.

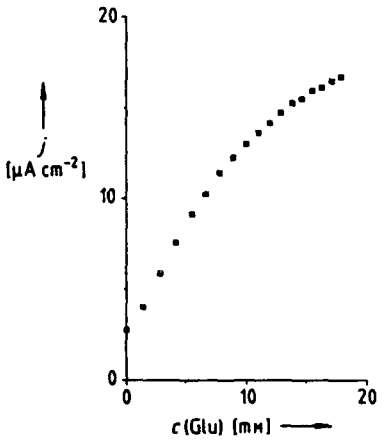

Fig. 3. Glucose concentration dependence of the current density at 0.45 V for the glucose oxidase/1/graphite electrode system in 0.15 M NaHEPES at pH 7 and 9.9 units catalase mL^{-1}.

The rate of glucose oxidase adsorption on redox-polymer 1 modified graphite electrode was studied by chronoamperometry. Electrodes were placed in 4 mL solutions of 60 mM glucose and 0.15 M NaHEPES at pH 7 and kept under N_2. 0.9 μg of catalase (44000 units per mg protein) was added to prevent the deactivation of glucose oxidase by evolved H_2O_2. Approximately 10 μL of a 4 mg mL^{-1} solution of glucose oxidase was slowly injected into the electrochemical cell to yield a final glucose oxidase concentration of 10 μg mL^{-1}. The potential was then stepped from 0 V to 0.45 V (SCE). The rise in current upon enzyme-complexing by the redox polymer coating of the electrode is shown in Figure 4.

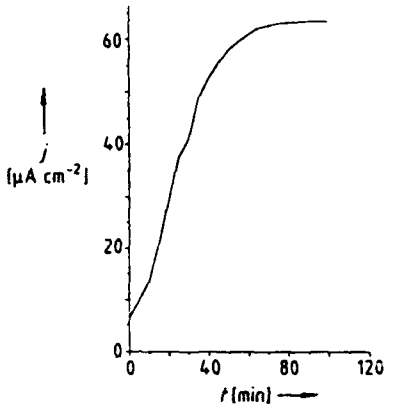

Fig. 4. Chronoamperometric response of a 1 graphite electrode in 10 μg mL^{-1} glucose oxidase, 60 mM glucose, 0.15 M NaHEPES at pH 7 with no catalase present.

Investigation of the effect of increasing salt concentration shows that electron transfer ceases at high (> 0.5 M) salt concentration in solutions containing only NaCl and buffer (no enzyme) but recovers upon dilution (to 0.15 M). This indicates that appropriate electrostatic bonding is critical for electron transfer not only in solution,[1] but also in adsorbed layers. The recovery of the current when the ionic strength is decreased shows that even at increased ionic strength, the complex does not dissociate. The loss in current response to glucose at high ionic strength is apparently caused by coiling of the polycationic redox polymer 1.[1, 5] The coiled polymer no longer penetrates the protein, wherefore electron transfer cannot take place. At physiological ionic strength, the complex of polyanionic glucose oxidase and polycationic redox polymer 1 is, however, an effective electron relay between the enzyme bound substrate and the conductor.

Experimental Procedure

Glucose oxidase (E.C. 1.1.3.4) type X, catalase (E.C. 1.11.1.6) and NaHEPES were purchased from Sigma. $[Os(bpy)_2Cl_2]$ was prepared from K_2OsCl_6 (Aldrich) following a reported procedure. [6] 4-aminostyrene was purchased from Polysciences. Azobisisobutyronitrile (AIBN) and 4-vinylpyridine were purchased from Aldrich. Synthesis of the redox terpolymer 1 was prepared as reported [1]. Graphite (HB pencil leads 0.5 or 0.9 mm diameter) and pyrolytic carbon disks (4 mm diameter) were used as electrodes.

A Pine Instruments AFMSRX Rotator and an MSRX Speed Control were used for the rotating disk electrode (RDE) experiments. The flow cell was similar in design to a reported wall jet system [7].

The electrodes were insulated with a heat-shrinkable polypropylene sleeve. Their tips were then polished with 0.3 μm alumina, sonicated in deionized water for 20 s and blown dry with a stream of N_2. A drop (4 μL) of a solution of 1 (2.6 mg mL^{-1} solvent) was applied to the electrode tip, allowed to stand for 4 min and then washed off with deionized water. The enzyme was adsorbed on the terpolymer coated surfaces by placing a 4 μL droplet of glucose oxidase solution (4.5 mg mL^{-1}) on the electrode surface, contacting for 10 min and rinsing. No containment membrane was used. Electrodes for the RDE experiments were polished and modified with a redox polymer in a similar manner.

Received: August 7, 1989;
supplemented: October 2, 1989 [Z 3485 IE]
German version: *Angew. Chem. 102* (1990) 109

[1] Y. Degani, A. Heller, *J. Am. Chem. Soc. 111* (1989) 2357.
[2] N. Oyama, F. C. Anson, *J. Am. Chem. Soc. 101* (1979) 739, 3450; K. Shigehara, N. Oyama, F. C. Anson, *Inorg. Chem. 20* (1981) 518; N. Oyama, F. C.

Anson, *J. Electrochem. Soc. 127* (1980) 247, 640; N. Oyama, T. Shimomura, K. Shigehara, F. C. Anson, *J. Electroanal. Chem. 112* (1980) 271; N. Scott, N. Oyama, F. C. Anson, *ibid. 110* (1980) 303; T. Shimomura, N. Oyama, F. C. Anson, *ibid. 112* (1980) 265; *J. Am. Chem. Soc. 103* (1981) 2552; N. Oyama, S. Yamaguchi, Y. Nishita, K. Tokuda, H. Matsuda, F. C. Anson, *J. Electroanal. Chem. 139* (1982) 371.

[3] J. Jernigan, N. Surridge, M. Zvanut, M. Silver, R. Murray, *J. Phys. Chem. 93* (1989) 4620; P. Denisovich, H. Abruna, C. Leidner, T. Meyer, R. Murray, *Inorg. Chem. 21* (1982) 2153; J. Calvert, T. Meyer *ibid. 21* (1982) 3978; E. Kober, B. Sullivan, W. Dressiale, J. Caspar, T. Meyer, *J. Am. Chem. Soc. 102* (1980) 7387; J. Facci, R. Schmehl, R. Murray, *ibid. 104* (1982) 4959; J. Facci, R. Murray, *Anal. Chem. 54* (1982) 7721; R. Murray, *Annu. Rev. Mater. Sci. 14* (1984) 145; *Philos. Trans. R. Soc. London A 302* (1981) 253.

[4] P. Yeh, T. Kuwana, *Chem. Lett. 1977*, 1145; E. Bowden, F. Hawkridge, H. Blount, *J. Electroanal. Chem. 161* (1984) 355; D. Reed, F. Hawkridge, *Anal. Chem. 59* (1987) 2334; J. Willit, E. Bowden, *J. Electroanal. Chem. 221* (1987) 265; K. Koller, F. Hawkridge, *ibid. 239* (1988) 291; E. Bowden, F. Hawkridge, H. Blount: "Electrochemical Aspects of Bioenergetics" in S. Srinivasan, Y. Chizmadzhev, J. Bockris, B. Conway, E. Yeager (Eds.): *Comprehensive Treatment of Electrochemistry, Vol. 10*, Plenum, New York 1985, S. 297–346; J. Frew, H. Hill, *Philos. Trans. R. Soc. London B 316* (1987) 95–106; H. Hill, *Pure Appl. Chem. 59* (1987) 743; F. Armstrong, H. Hill, N. Walton, *Acc. Chem. Res. 21* (1988) 407; M. Eddowes, H. Hill, *J. Chem. Soc. Chem. Commun. 1977*, 771; M. Eddowes, H. Hill, K. Uosaki, *J. Am. Chem. Soc. 101* (1979) 4461; *Bioelectrochem. Bioenerg. 7* (1980) 527; A. Cass, M. Eddowes, H. Hill, K. Uosaki, R. Hammond, I. Higgins, E. Plotkin, *Nature (London) 285* (1980) 673; K. Uosaki, H. Hill, *J. Electroanal. Chem. 122* (1981) 321; W. Albery, M. Eddowes, H. Hill, A. Hillman, *J. Am. Chem. Soc. 103* (1981) 3904; M. Eddowes, H. Hill, K. Uosaki, *ibid. 101* (1979) 7113.

[5] I. Nagata, H. Morawetz, *Macromolecules 14* (1981) 87; A. Katchalsky, *Pure Appl. Chem. 26* (1971) 327; H. Eisenberg: *Biological Macromolecules and Polyelectrolytes in Solution*, Clarendon Press, Oxford 1976; S. Carnie, G. Christos, T. Creamer, *J. Chem. Phys. 89* (1988) 6484.

[6] D. Buckingham, F. Dwyer, H. Goodwin, A. Sargeson, *Aust. J. Chem. 17* (1964) 325; P. Lay, A. Sargeson, H. Taube, *Inorg. Synth. 24* (1986) 291–306.

[7] W. Albery, P. Bartlett, A. Cass, D. Creston, B. Haggett, *J. Chem. Soc. Faraday Trans. 1 82* (1986) 1033–1050.